ATTACHMENT A – 1

ERDC MODELING REPORT

ERDC LR-DRAFT

Engineer Research and Development Center

US Army Corps of Engineers®
Engineer Research and Development Center

ERDC
INNOVATIVE SOLUTIONS for a safer, better world

Three Dimensional Hydrodynamic, Water Quality, and Sediment Transport Modeling of Mobile Bay

Barry Bunch, Earl Hayter, Sung-Chan Kim, Elizabeth Godsey and Ray Chapman

June 2018

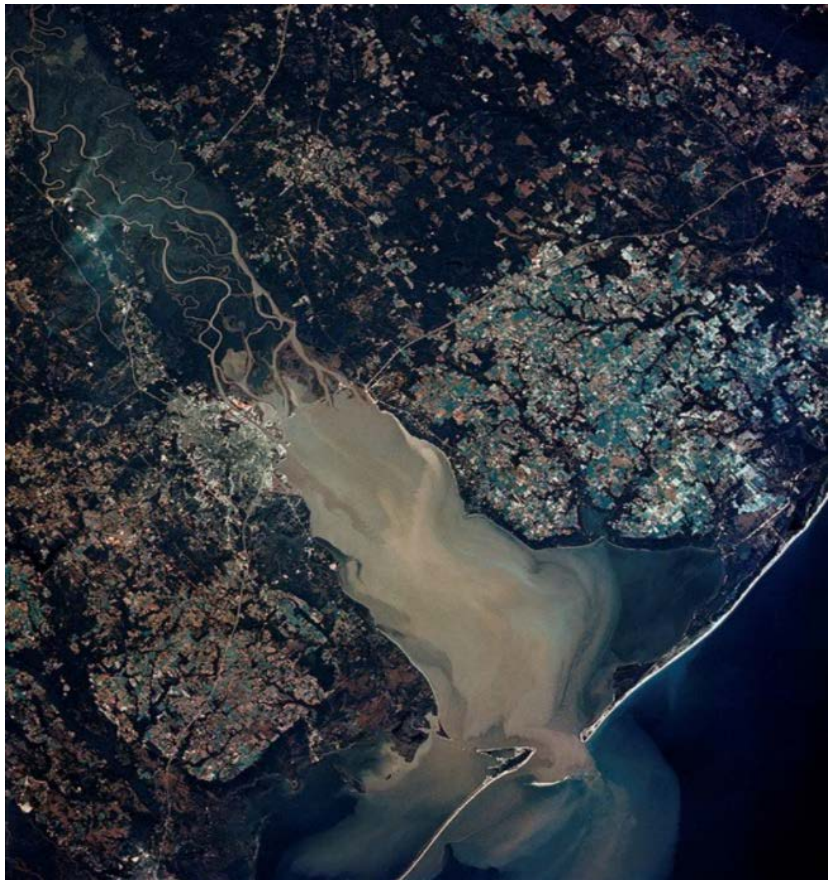

The U.S. Army Engineer Research and Development Center (ERDC) solves the nation's toughest engineering and environmental challenges. ERDC develops innovative solutions in civil and military engineering, geospatial sciences, water resources, and environmental sciences for the Army, the Department of Defense, civilian agencies, and our nation's public good. Find out more at www.erdc.usace.army.mil.

To search for other technical reports published by ERDC, visit the ERDC online library at http://acwc.sdp.sirsi.net/client/default.

Three Dimensional Hydrodynamic, Water Quality, and Sediment Transport Modeling of Mobile Bay

Barry Bunch, Earl Hayter

Environmental Laboratory
U.S. Army Engineer Research and Development Center
3909 Halls Ferry Road
Vicksburg, MS 39180

Sung-Chan Kim

Coastal and Hydraulics Laboratory
U.S. Army Engineer Research and Development Center
3909 Halls Ferry Road
Vicksburg, MS 39180

Elizabeth Godsey

U.S. Army Corps of Engineers, Mobile District
109 St. Joseph Street
Mobile, AL 36602

Ray Chapman

Ray Chapman & Associates
1725 MacArthur Place
Vicksburg, MS 39180

Formerly of the Coastal and Hydraulics Laboratory

Final report

Prepared for: U.S. Army Corps of Engineers, Mobile District
Mobile, AL 36602

Abstract

A hydrodynamic, water quality and sediment transport modeling study of Mobile Bay was performed to determine the impact of a harbor design plan that would enable Mobile Harbor to better accommodate deep draft containerships and bulk carriers on water quality and sedimentation in the bay. The central elements of the plan include deepening the Bar and Bay segments of ship channel, widening a segment of the Bay channel for two-way traffic, easing two bends in the Bar channel and expanding the Choctaw turning basin.

The water quality modeling study examined the potential impacts on the following state variables: dissolved oxygen, salinity, temperature, total suspended solids, nutrients and chlorophyll-*a* ("Chl-a"). The 3D water quality model CE-QUAL-ICM was calibrated for calendar year 2010, and then used to evaluate the following four sets of conditions:; Existing (No Project), with-Project, future without project (Existing with Sea Level Rise), and Project with Sea Level Rise. Comparison of results between the following pairs of model simulations were performed: Existing and with-Project, and future without project (Existing with SLR) and Project with SLR. These comparisons showed that no alteration in the behavior of any water quality constituent evaluated was evident. In most cases the differences in constituent behavior were undetectable over the one-year model simulations.

The sediment transport modeling study evaluated 1) sedimentation in the navigation channel, 2) bathymetric changes due to net erosion and/or deposition in the potential beneficial use sites on the east side of the bay, and 3) bathymetric changes due to net erosion and/or deposition in the existing along channel deposal sites. The specific objectives and findings from the sediment transport modeling study were the following:

- Potential project impacts on sedimentation in the navigation channel from the proposed channel modifications: The average annual shoaling rate in the navigation channel increased from 5 to 15 percent.

- Potential erosion of the dredged material placed in six potential Beneficial Use (BU) areas: Analysis of the bathymetric change in the six BU areas showed less than $\pm$ 8 cm change in the bed elevation during the one-year simulation in all grid cells. That is, the change in bed elevations varied from less than 8 cm of net erosion to 8 cm of net deposition as compared to the bed

elevation changes in those grid cells during a sediment transport simulation of the channel improvements in the bay without the potential BU areas.

- Potential erosion of dredged material placed in the existing open water along channel placement sites: The results from the one-year model simulation with channel improvements showed less than $\pm$ 9 cm change in the bed elevations in every grid cell within these placement areas from that of the existing condition simulation.

- Impact of an o.5 m rise in sea level on sedimentation in the navigation channel: The simulation of Project Channel Depths with sea level rise showed less than a 0.5 percent increase in shoaling rates from those with existing conditions in every section of the navigation channel.

Contents

Abstract ii

Figures and Tables iv

Unit Conversion Factors vviiiii

Introduction 1

Hydrodynamic Modeling 4

Coastal Storm Modeling System (CSTORM-MS) 6
GSMB Multi-Block Hydrodynamic Modeling 9
49 and 59 Multi-Block System Comparison 18
Existing and With Project Simulations 29
Multi-Block ICM Linkage and Hydrodynamic Forcing 44
Ship Simulations Support Modeling 44

Water Quality Modeling 54

CEQUAL-ICM Water Quality Model 54
Calibration 63
Scenario Results and Discussion 78
Existing (No Project) and Project Comparisons 79
SLR Existing and Project Comparisons 82
Conclusions 94

Estuarine Sediment Transport Modeling 95

Description of Sediment Transport Model 95
Setup of MB-SEDZLJ 104
Sediment Transport Model Calibration 111
Sediment Transport Model Simulations 120
Conclusions 123

Conclusions 125

References 127

Addendum: Screening Level Storm Tide Comparison between Existing and With-Project Conditions 134

Appendix A: CEQUAL-ICM Input Decks 139

Figures and Tables

Figures

1 Mobile Harbor Federal Navigation Project Limits and Dimensions 3
2 Multi-Block Geophysical Scale Hydrodynamic, Sediment and Water Quality Transport Modeling System (GSMB)....4
3 ADCIRC domain boundary, Red, and STWAVE boundary, Blue....7
4 Project view of the STWAVE grid boundary 7
5 Color contours of ADCIRC element edge size in meters 8
6 Color contours of ADCIRC higher resolution element edge size 8
7 Time series of comparison of observed and modeled water surface elevations at Dauphin Island, AL, April 2010 10
8 Mobile Bay 49 Block System 10
9 Upper Bay and Single Block Delta 11
10 Grid Block Delta System....12
11 Unresolved Tidal Constituent Forcing....13
12 January Dauphin Island Water Surface Elevation Comparison 14
13 June Dauphin Island Water Surface Elevation Comparison 14
14 December Dauphin Island Water Surface Elevation Comparison....15
15 December Coast Guard Sector Water Surface Elevation Comparison....15
16 December Meaher State Park Water Surface Elevation Comparison....16
17 WIS and Dauphin Island Observed Wind Speed 17
18 WIS and Dauphin Island Observed Wind Direction 17
19 Univ of South Alabama CTD cast stations for 2009-2010....18
20 Observed and Model Salinity Profiles at Dauphin Island....19
21 Observed and Model Salinity Profiles at Site M2 19
22 Observed and Model Salinity Profiles at Site M4 20
23 Observed and Model Salinity Profiles at Dauphin Island....20
24 Observed and Model Salinity Profiles at Site M2 21
25 Observed and Model Salinity Profiles at Site M4 21
26 Observed and Model Salinity Profiles at Dauphin Island....22
27 Observed and Model Salinity Profiles at Site M2 22
28 Observed and Model Salinity Profiles at Site M4 23
29 USACE Delta survey stations for 2016-2017 in Upper Bay....24
30 TR-01 Near Bottom Salinity Comparison of 49 and 59 Block Simulations 25
31 AR@CW Near Bottom Salinity Comparison of 49 and 59 Block Simulations 25
32 MR-01 Near Bottom Salinity Comparison of 49 and 59 Block Simulations 26
33 CO-01 Near Bottom Salinity Comparison of 49 and 59 Block Simulations....26
34 MR-09 Near Bottom Salinity Comparison of 49 and 59 Block Simulations....27
35 September 13-14, 2016 Observed and Model Salinity Profiles MR-01....27
36 September 13-14, 2016 Observed and Model Salinity Profiles CO-01 28
37 September 13-14, 2016 Observed and Model Salinity Profiles MR-09 28
38 September 13-14, 2016 Observed and Model Salinity Profiles TR-03....29
39 September 13-14, 2016 Observed and Model Salinity Profiles AR@CW....29
40 Turning Basin Extension Design and Grid Modification 30
41 Turning Basin Extension Grid Modification 31
42 Bend Easing Design at the Mobile Bay Entrance 32
43 Bend Easing Grid Modification Mobile Bay Entrance....33
44 Channel Widening – Passing Lane Design 34
45 Channel Widening – Passing Lane Grid Modification 35

46 NOAA NEP stations 36
47 Time Series Comparison at MR-01 37
48 Time Series Comparison at MR-09 37
49 Time Series Comparison at TR-03 38
50 Time Series Comparison at TR@CW 38
51 Time Series Comparison at AR@CW 39
52 Time Series Comparison at Dauphin Island 39
53 Time Series Comparison at Bon Secour 40
54 Time Series Comparison at Cedar Point 40
55 Time Series Comparison at Middle Bay Light 41
56 Time Series Comparison at MR-01 41
57 Time Series Comparison at AR@CW 42
58 Time Series Comparison at Cedar Point 42
59 Sea Level Rise Time Series Comparison at Bon Secour 43
60 Mean Surface and Bottom Salinity: July – September 2010 43
61 Differences in Surface and Bottom Salinity: July – September 2010 44
62 Maximum BEPL SE Flood Current Velocities 46
63 Maximum BEPL SE Flood Current Difference 47
64 Maximum TB SE Flood Current Velocities 48
65 Maximum TB SE Flood Current Difference 49
66 Maximum BEPL N Ebb Current Velocities 50
67 Maximum BEPL N Ebb Current Difference 51
68 Maximum TB N Ebb Current Velocities 52
69 Maximum TB N Ebb Current Difference 53
70 Study Domain for all Simulations 59
71 Hydrodynamic and Water Quality Model in Mobile Bay Estuary 59
72 Stations used for Model Calibration 65
73 Comparison of Simulated and Measured Temperatures 66
74 Comparison of Simulated and Measured Surface Salinities 67
75 Comparison of Simulated and Measured Bottom Salinities 68
76 Comparison of Simulated and Measured Surface DO values 70
77 Comparison of Simulated and Measured Bottom DO values 71
78 Comparison of Simulated and Measured Surface Ammonium values 73
79 Comparison of Simulated and Measured Surface Nitrate values 74
80 Comparison of Simulated and Measured Surface DIP values 75
81 Comparison of Simulated and Measured Surface Chl-a values 76
82 Comparison of Simulated and Measured Surface TSS values 77
83 Comparison of Existing and with-Project Surface Temperatures 80
84 Comparison of Existing and with-Project Bottom Temperatures 81
85 Comparison of Existing and with-Project Surface Salinities 83
86 Comparison of Existing and with-Project Bottom Salinities 84
87 Comparison of Existing and with-Project Surface Dissolved Oxygen 85
88 Comparison of Existing and with-Project Bottom Dissolved Oxygen 86
89 Comparison of Existing and with-Project with SLR Surface Temperature 88
90 Comparison of Existing and with-Project with SLR Bottom Temperature 89
91 Comparison of Surface Salinity for Existing and with-Project with SLR 90
92 Comparison of Bottom Salinity for Existing and with-Project with SLR 91
93 Comparison of Surface DO for Existing and with-Project with SLR 92
94 Comparison of Bottom DO for Existing and with-Project with SLR 93
95 Sediment transport processes simulated in GSMB-SEDZLJ 99
96 Multi-Bed Layer Model used in GSMB-SEDZLJ 99
97 Schematic of Active Layer used in GSMB-SEDZLJ 100

98 Stations show location of SEDFLUME cores collected during the thin layer placement study. 107
99 Beneficial Use areas A – F to the east of the navigation channel..... 109
100 Placement Areas (black quadrilaterals) along the navigation channel 110
101 Seven measurement stations in the Upper Delta 112
102 SSC versus discharge time series measured at the North Tensaw River Station..... 113
103 Aerial photo of turbid water in Mobile Bay..... 114
104 Dynamic channel morphology is evident in this bathymetric survey of the upper navigation channel that depicts spatially (intra-channel) varying sedimentation patterns in the channel from August 2010 to January 2011 115
105 Grid resolution in proximity to the Mobile Theodore intersection with the navigation channel south of Gaillard Island 116
106 Grid resolution across the navigation channel..... 117
107 Dredged volumes calculated from the dredging records between August 2010 and January 2011..... 118
108 Sediment transport model calibration results showing the percentage difference between measured and simulated sedimentation rates..... 119
109 Simulated increases in annual shoaling vary from 5 to 15 % along channel with-Project depths. Four channel stations are shown in red to the east side of the channel..... 122
A-1 Color contour map of maximum existing condition storm tide water levels for Hurricane Katrina 136
A-2 Difference in Project – Existing, maximum storm tide water levels for Hurricane Katrina 136
A-3 Difference in Project – Existing, maximum storm tide water levels for Hurricane Katrina near the Port of Mobile 137
A-4 Color contour map of maximum existing condition storm tide water levels for Hurricane Ike 137
A-5 Difference in Project – Existing, maximum storm tide water levels for Hurricane Ike near the Port of Mobile..... 138
A-6 Difference in Project – Existing, maximum storm tide water levels for Hurricane Ike near the Port of Mobile..... 138

Tables

1. USGS Long Term Discharge and 2010 Monthly Mean Discharge: USGS Gage 2471019 Tensaw River..... 5
2. Ship Simulation Forcing..... 45
3. Water Quality Model State Variables. 57
4. Active Water Quality Model State Variables. 58
5. Water Quality Grid Characteristics 60
6. Surficial Sediment Composition of 14 SEDFLUME Cores 106
7. Simulated Percentage Increases in Annual Shoaling Along Channel with-Project depths from North End (CS 1) to South End (CS 13) of Channel Shown in Figure 109..... 122

Unit Conversion Factors

Multiply	By	To Obtain
acres	4,046.873	square meters
acre-feet	1,233.5	cubic meters
cubic feet	0.02831685	cubic meters
cubic yards	0.7645549	cubic meters
degrees (angle)	0.01745329	radians
degrees Fahrenheit	(F-32)/1.8	degrees Celsius
feet	0.3048	meters
gallons (U.S. liquid)	3.785412 E-03	cubic meters
inches	0.0254	meters
knots	0.5144444	meters per second
microns	1.0 E-06	meters
miles (nautical)	1,852	meters
miles (U.S. statute)	1,609.347	meters
miles per hour	0.44704	meters per second
pounds (force)	4.448222	Newtons
square feet	0.09290304	square meters
square miles	2.589998 E+06	square meters
square yards	0.8361274	square meters
yards	0.9144	meters

Introduction

Mobile Harbor, Alabama, is located in the southwestern part of the state, at the junction of the Mobile River with the head of Mobile Bay. The port is about 28 nautical miles north of the Bay entrance from the Gulf of Mexico and 170 nautical miles east of New Orleans, Louisiana. The current dimensions of the existing navigation channel are: 47 feet deep by 600 feet wide across Mobile Bar and 45 feet deep by 400 feet wide in the bay and 45 feet deep by 730 feet wide in the Mobile River to a point about 1 mile below the Interstate 10 highway tunnels. The channel then becomes 40 feet deep and proceeds north over the Interstate 10 and U.S. 90 highway tunnels to the Cochrane/Africatown Bridge. The Mobile River, on which the ASPA facilities are located, is formed some 45 miles north of the city with the joining of the Alabama and Black Warrior/Tombigbee Rivers. The Mobile River also serves as the gateway to international commerce for the Tennessee/Tombigbee Waterway. In the southern region of Mobile Bay, access can be gained to the Gulf Intracoastal Waterway which stretches from St. Marks, Florida, to Brownsville, Texas. Figure 1 shows the authorized dimensions and geographic limits of the Mobile Harbor Federal Navigation Channel.

The current principal navigation problems are that larger vessels are experiencing transportation delays and inefficiencies due to insufficient channel depth and width. Specifically, vessels are carrying less cargo tons than maximum capacity because of sailing draft constraints (*i.e.*, channel depth) and delays are occurring as a result of one-way traffic patterns for vessels over a certain size. In addition, increased vessel size and traffic congestion has led to safety concerns.

In a response to these problems, the Mobile District of the U.S. Army Corps of Engineers and the Alabama State Port Authority have proposed a harbor design plan that would enable the Port to better accommodate deep containerships and bulk carriers. The central elements of the plan include deepening the Bar and Bay segments of ship channel, widening a segment of the Bay channel for two-way traffic, easing two bends in the Bar channel and expanding the Choctaw turning basin.

The major elements of the plan evaluated in this study include:

- Deepen the existing Bar, Bay, and River Channels (below Station 226+16) by 5 feet to project depths of 52, 50, and 50 feet, respectively, with an additional 2 feet for advanced maintenance plus 2 feet of allowable overdepth for dredging (total depths of 56, 54, and 54 feet, respectively).

- Incorporate minor bend easing at the double bends (at Stations 1857+00 and 1775+26) in the Bar Channel approach to the Bay Channel.

- Widen the Bar Channel to 500 feet from the mouth of Mobile Bay northward for 5 nautical miles to provide a two-way traffic area for passing.

- Expand the Choctaw Pass Turning Basin to the south to better accommodate safe turning of the design vessel and other large vessels.

To evaluate the potential effects of channel deepening and widening, the U.S. Army Corps of Engineers, Mobile District requested the support of the Engineering Research and Development Center (ERDC) in conducting numerical modeling of waves, currents, water quality and sediment transport for the Mobile Harbor General Reevaluation Report (GRR). A numerical modeling approach was implemented using the Geophysical Scale Transport Modeling System (GSMB) to quantify the relative changes in hydrodynamics, water quality and sediment transport processes within Mobile Bay and lower delta resulting from the proposed modifications to the channel. The components of GSMB include the two-dimensional (2D) deep water wave model WAM (http://wis.usace.army.mil), STWAVE nearshore wave model (Smith *et al.* 1999) and the large scale unstructured 2D ADCIRC hydrodynamic model (http://www.adcirc.org). These components make up the Coastal Storm Modeling System, CSTORM-MS (Massey *et al.* 2015). In addition, the three-dimensional models CH3D-MB (Luong and Chapman 2009), which is the multi-block (MB) version of CH3D-WES (Chapman *et al.* 1996, Chapman *et al.* 2007), MB CH3D-SEDZLJ sediment transport model (Hayter *et al.* 2012 and 2015, Gailani *et al.* 2014), and CE-QUAL-ICM water quality model (Bunch *et al.* 2003, and Cerco and Cole 1994) were applied. Simulations changes under existing and future conditions accounting for a 0.5

m rise in sea level, with and without modifications to the navigation channel were made. Each scenario was simulated for the 2010 time period with the exception of the storm surge modeling which was evaluated using two historic storms (Hurricane Katrina 2005 and Hurricane Ike 2008).

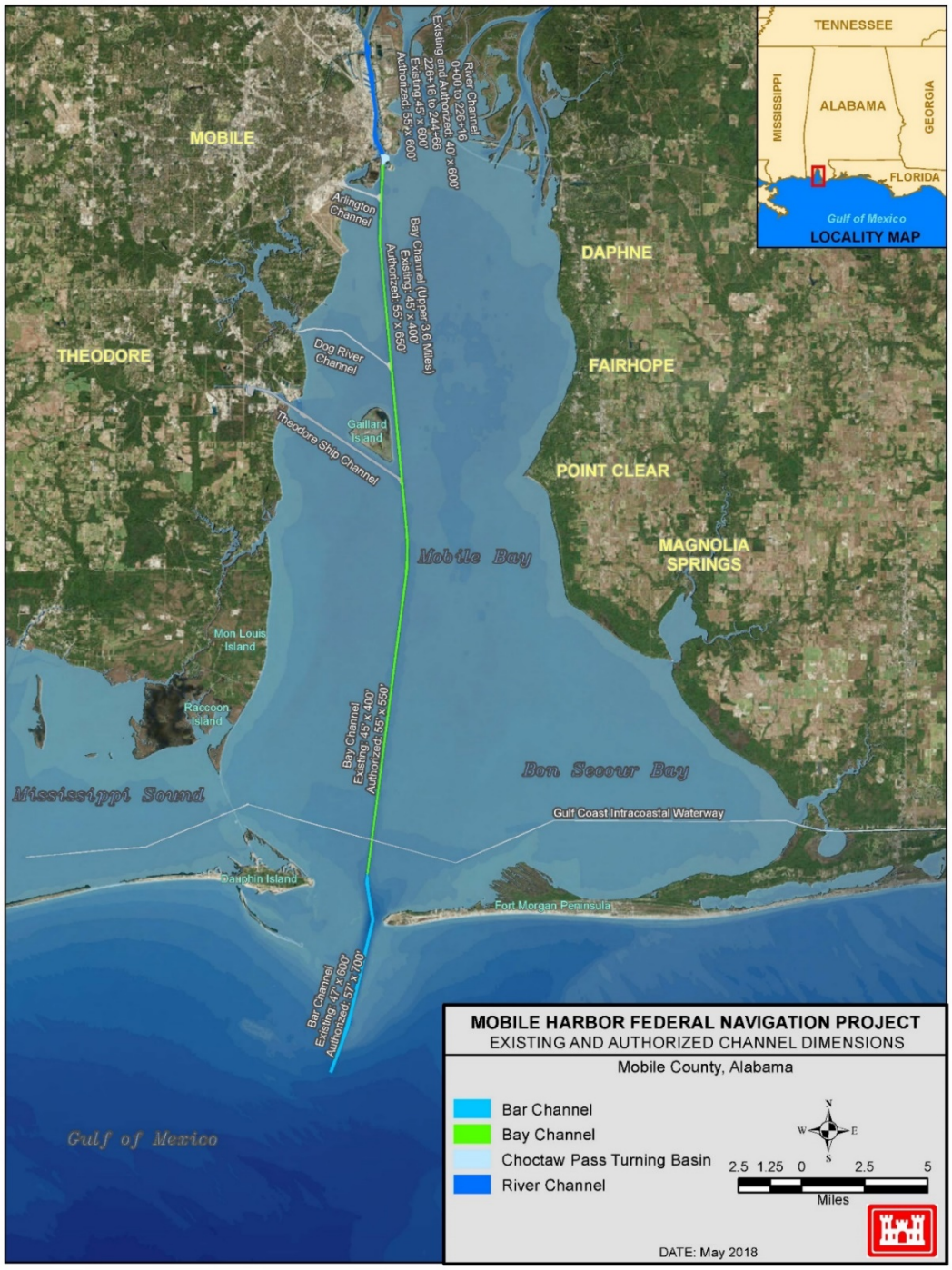

Figure 1. Mobile Harbor Federal Navigation Project Limits and Dimensions

Hydrodynamic Modeling

ERDC-EL and ERDC-CHL have completed a number of large scale hydrodynamic, sediment and water quality transport model studies. These studies utilized the Geophysical Scale Transport Modeling System (GSMB). The model framework of GSMB is shown in Figure 2, where it is seen that USACE accepted wave, hydrodynamic, sediment and water quality transport models are both directly and indirectly linked.

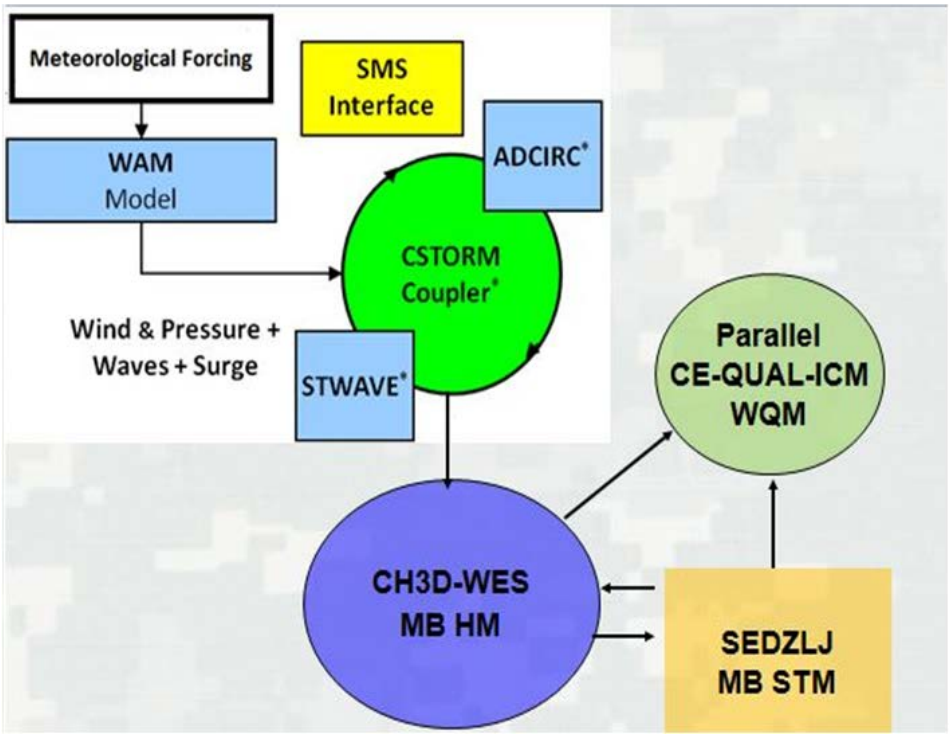

Figure 2. Multi-Block Geophysical Scale Hydrodynamic, Sediment and Water Quality Transport Modeling System (GSMB)

The components of GSMB shown above are the two-dimensional (2D) deep water wave model WAM (http://wis.usace.army.mil), STWAVE nearshore wave model (Smith *et al.* 1999) and the large scale unstructured 2D ADCIRC hydrodynamic model (http://www.adcirc.org). These components make up the Coastal Storm Modeling System, CSTORM-MS (Massey *et al.* 2015). In addition, the three-dimensional (3D) models CH3D-MB (Luong and Chapman 2009), which is the multi-block (MB) version of CH3D-WES (Chapman *et al.* 1996, Chapman *et al.* 2009), MB CH3D-SEDZLJ sediment transport model (Hayter *et al.* 2012 and 2015, Gailani *et al.* 2014) and CE-QUAL-ICM water quality model (Bunch *et al.* 2003, and Cerco and Cole 1994). The parallel

versions of ADCIRC and STWAVE coupled via the CSTORM-MS framework (Massey *et al.* 2011) provides the offshore water surface elevation tidal boundary, wave height, period, direction and radiation stress gradient forcing to the GSMB hydrodynamic MB-CH3D-WES and sediment transport, MB-SEDZLJ, modules. In addition, the hydrodynamic module provides the static geometry and time varying vertical eddy diffusivity, flow and cell column volume to the CE-QUAL-ICM water quality model.

The time period selected for GSMB hydrodynamic, sediment and water quality modeling of Mobile Bay was January through December of 2010. This time period represented an average hydrologic year, as seen in Table 1. In

Table 1. USGS Long Term Discharge and 2010 Monthly Mean Discharge: USGS Gage 2471019 Tensaw River

Month	Long Term Discharge (m^3/s)			2010 Mean
	Mean	Maximum	Minimum	
January	907	1252	255	1134
February	1024	1478	407	1283
March	1061	1548	421	1199
April	725	1330	255	658
May	632	1273	124	931
June	420	979	117	425
July	354	1048	95	211
August	264	547	96	168
September	337	756	92	114
October	385	1273	124	134
November	520	1207	134	200
December	813	1583	142	318

addition, observed vertical salinity profile (Dzwonkowski *et al.* 2011) and water quality data was available throughout the year and sediment transport results from a previous SAM project, Gailani *et al.* 2014, which used 2010 forcing, could be used for comparison.

Coastal Storm Modeling System (CSTORM-MS)

The 2D numerical models applied within CSTORM are the Advanced Circulation (ADCIRC) model (ADCIRC 2017, Luettich *et al*. 1992, Kolar *et al*. 1994) and the Steady-state Wave, STWAVE, model (Smith *et al*. 1999 and 2001, Massey *et al*. 2011). The CSTORM coupling framework (Massey *et al*. 2011) controls two-way passing of data between the ADCIRC and STWAVE. Specifically, ADCIRC passes updated depth-integrated currents and water surface elevations along with wind forcing to STWAVE, and in turn, STWAVE provides ADCIRC wave radiation stress gradient forcing. This dynamic interaction between the surge/circulation and wave fields has, in previous research and projects, been demonstrated to improve modeling capabilities.

The ADCIRC and STWAVE grid domains are shown in Figure 3, with a project view of the STWAVE domain for Mobile Bay in Figure 4. The ADCIRC grid has more than 176,000 nodes and 331,000 triangular elements. The element edge size ranges from 20 kilometers far offshore in the Atlantic Ocean to less than 20 meters nearshore, as seen Figure 5 and 6. Water depths ranged from almost 8,000 meters in the Atlantic to 0.1 meters at the shoreline.

The STWAVE grid has uniform square cells of 200.0 meters with 759 cells in the x-coordinate, (I) direction and 734 cells in the y-coordinate, (J) direction. The grid is rotated 90.0 degrees with x-coordinate to the North and y-coordinate to the West. The full-plane mode simulations used 28 frequency and 72 directional bins. Bathymetry interpolated to the grids was developed from three sources. For regions outside of Mississippi Sound and Mobile Bay, depths are based on contour lines and soundings extracted from the National Geospatial-Intelligence Agency Digital Nautical Charts (https://dnc.nga.mil/) and NOAA National Centers for Environmental Information (NCEI, https://www.ngdc.noaa.gov/) databases. Mississippi Sound, Mobile Bay and Mobile-Tensaw Delta bathymetry was a composite of recent bathymetric surveys, which was provided by CESAM. These data sets were either delivered or converted to NAD83 Alabama State Plane West (0102) meters. Mean-Low-Water (MLW) and Mean-Lower-Low–Water (MLLW) vertical datum were adjusted to Mean-Tide-Level meters (MTL).

Figure 3. ADCIRC domain boundary, Red, and STWAVE boundary, Blue.

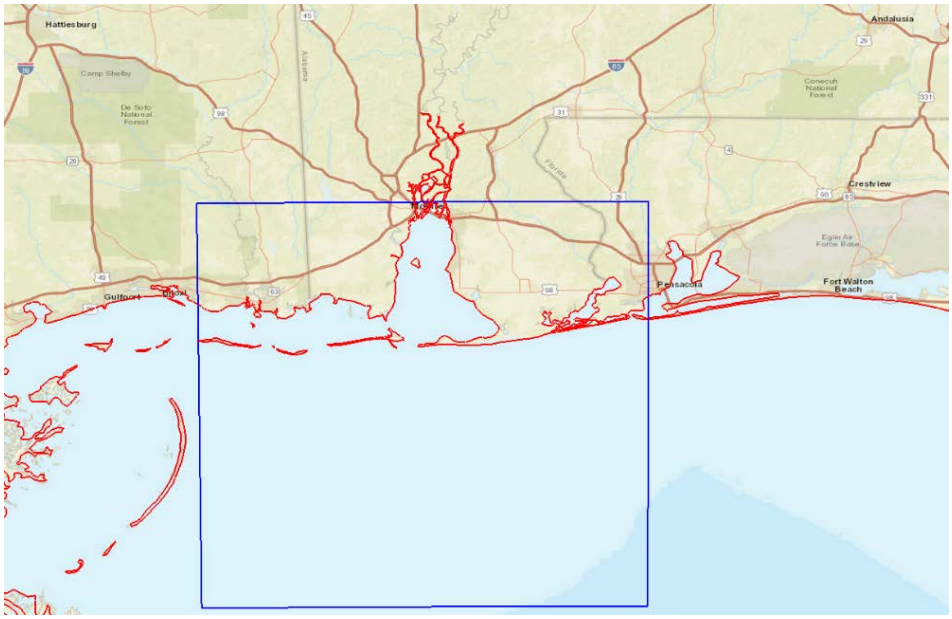

Figure 4. Project view of the STWAVE grid boundary

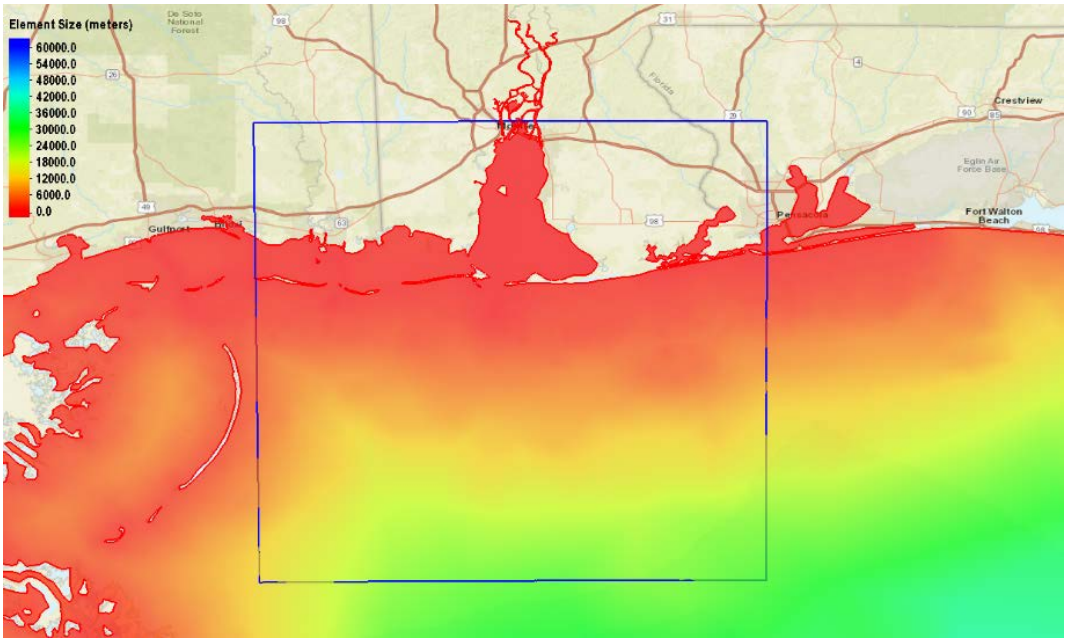

Figure 5. Color contours of ADCIRC element edge size in meters

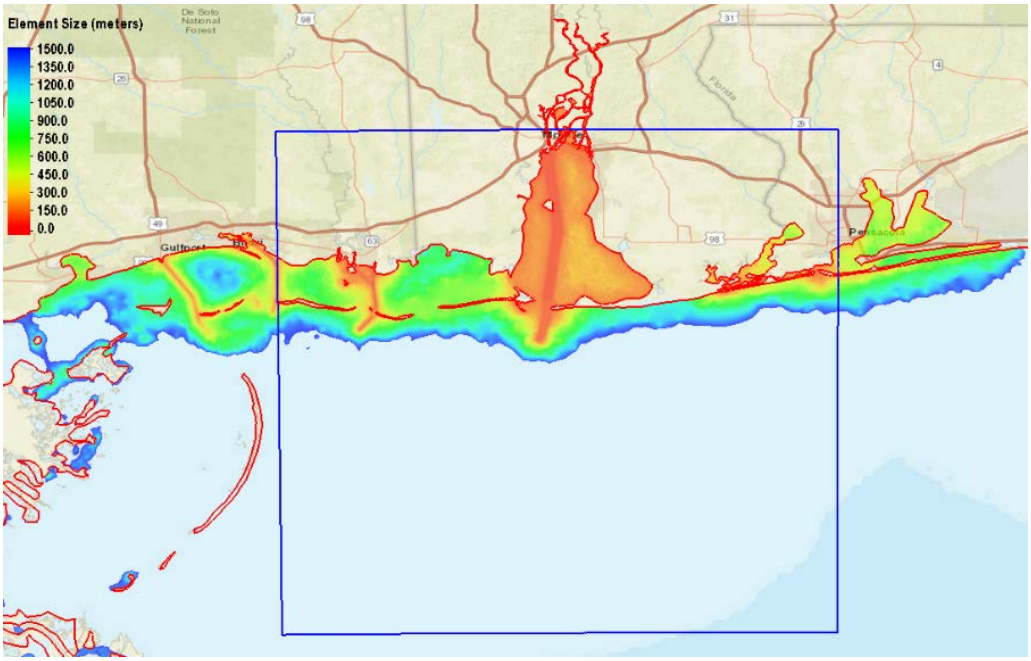

Figure 6. Color contours of ADCIRC higher resolution element edge size

Monthly 2010 CSTORM simulations generated GSMB wave and offshore tidal forcing. Meteorological forcing obtained from the ERDC Wave Information Study (WIS), Oceanweather, Inc. (OWI) (2011). The OWI

products include hourly wind components and atmospheric pressure at 0.25-deg spacing for the entire Gulf of Mexico. ADCIRC tidal forcing utilized 8 tidal constituents (M2, S2, N2, K1, O1, Q1, P1 and K2). Offshore boundary wave energy spectra forcing for STWAVE was derived from the Wave Information Study (WIS 2018) database save point WIS Station ID 73350 located at 87.90° W, 29.35° N. An example of the CSTORM coupled model result is presented in Figure 7, which shows an April 2010 time series comparison of modeled and observed water surface elevation at Dauphin Island, NOAA NOS CO-OPS Station 8735180. The phasing of the water levels is represented well and the amplitudes of the water levels are within about 5 cm.

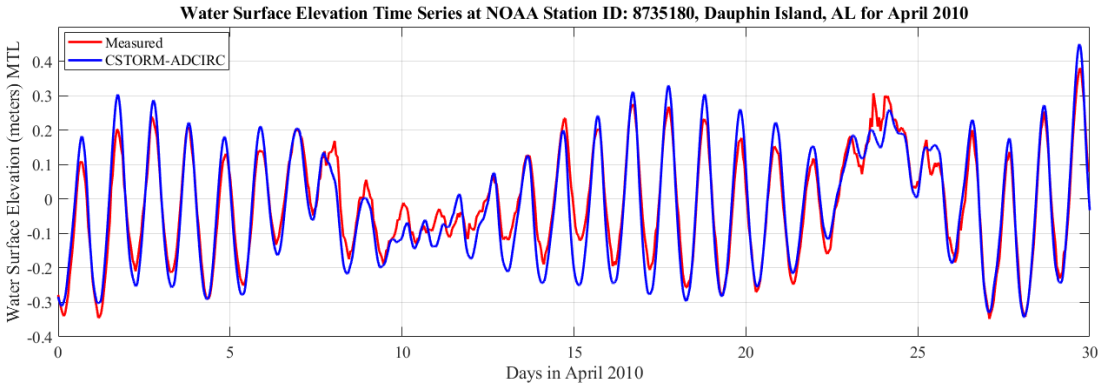

Figure 7. Time series of comparison of observed and modeled water surface elevations at Dauphin Island, AL, April 2010

Addition information on CSTORM is included in an addendum at the end of this report, which describes a screening level comparison that was performed between the existing and with-Project conditions simulations using ADCIRC.

GSMB Multi-Block Hydrodynamic Modeling

The primary purpose of hydrodynamic modeling in this study is the support of sediment and water quality transport. To this end, an existing MB grid system previously developed, validated and applied to a number of CESAM projects (Chapman *et al.* 2006, 2009, 2011, 2012 and Gailani *et al.* 2014) was updated. Two versions of the MB system were utilized. The 49 block system, which was used for both the 2010 sediment and water quality transport tasks, is shown in (Figures 8 and 9). The green lines in these figures shows the overlapping or communication cells for each block. A 59 block system that divided the single block that represented the delta was subdivided into nine additional blocks Figure 10). This system was used to investigate the

influence of minor tributaries and additional channel connections on the distribution of salinity throughout the Delta.

The bathymetry interpolated to the multi-block grids and meteorological forcing is that used in the CSTORM simulations, as described above. River flow forcing for December 2009 to December 2010 model simulation time period was obtained from the USGS Alabama website, (https://waterdata.usgs.gov/al/nwis/dv/?referred_module=sw).

As previously stated, CSTORM provided the offshore water surface elevation (WSE) forcing, as well as the wave height, period, direction and radiation stress gradient forcing. The ADCIRC simulations used to produce the offshore WSE boundary forcing used 8 harmonic constituents (M_2, S_2, N_2, K_1, O_1, Q_1, P_1, and K_2), of which the K_1 and O_1 are primary and have amplitudes of about 0.14m. The Solar Semiannual and Solar Annual tidal constituents have amplitudes of 0.05 and 0.08m, respectively, which cannot be dismissed

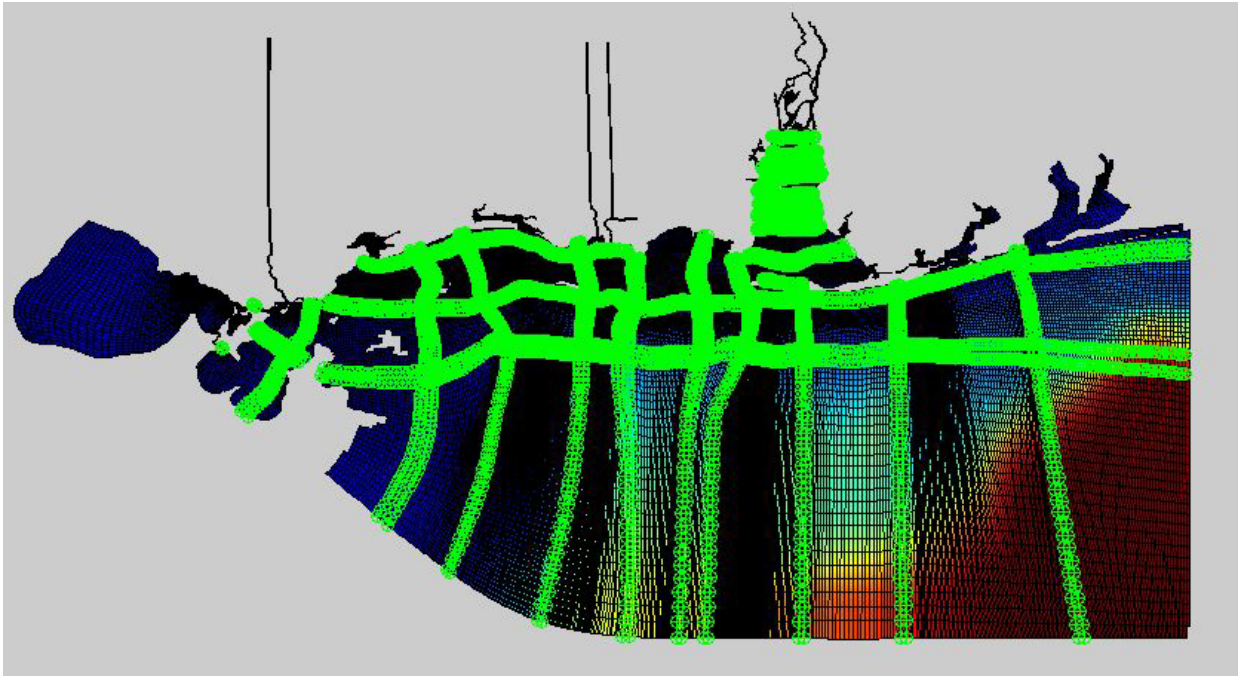

Figure 8. Mobile Bay 49 Block System

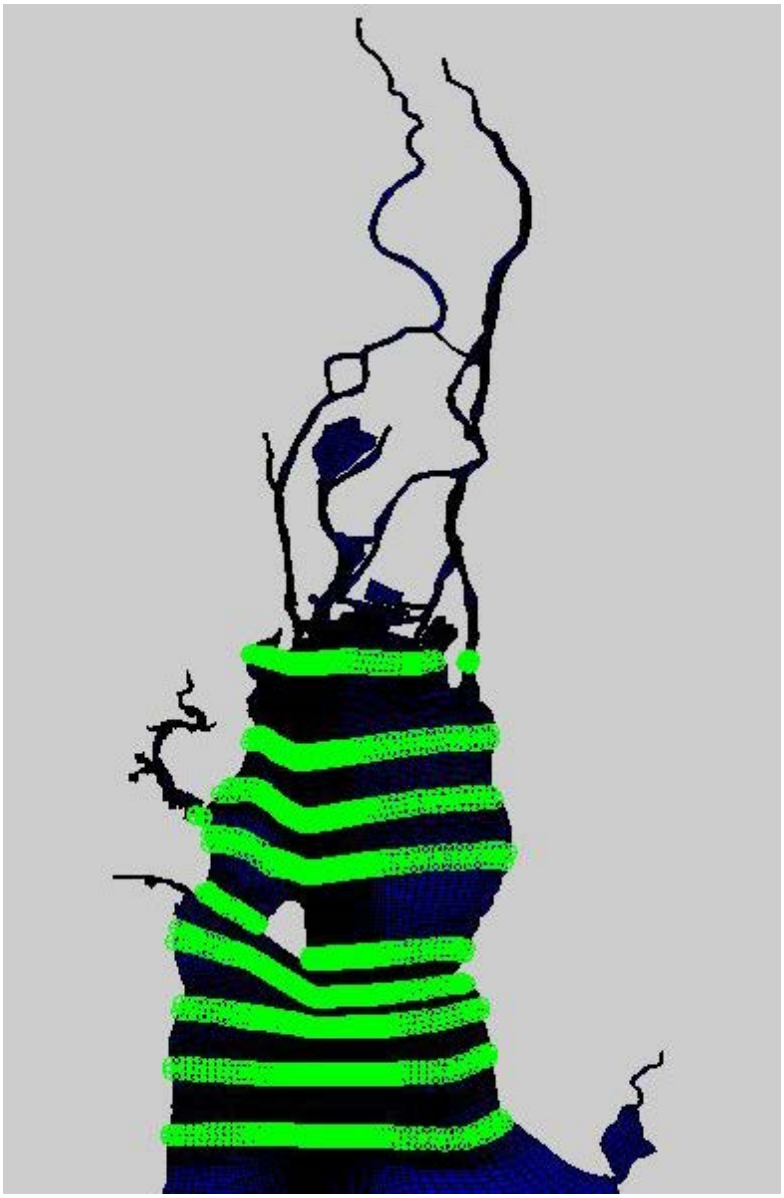

Figure 9. Upper Bay and Single Block Delta System

when developing offshore forcing for GSMB. To account for the unresolved tidal constituent forcing, the NOAA predicted tide signal at Dauphin Island gage (8735180) was filtered to remove the tidal and atmospherically forced WSE response. The resulting filtered signal, which is added to the offshore WSE boundary forcing, is shown in Figure 11.

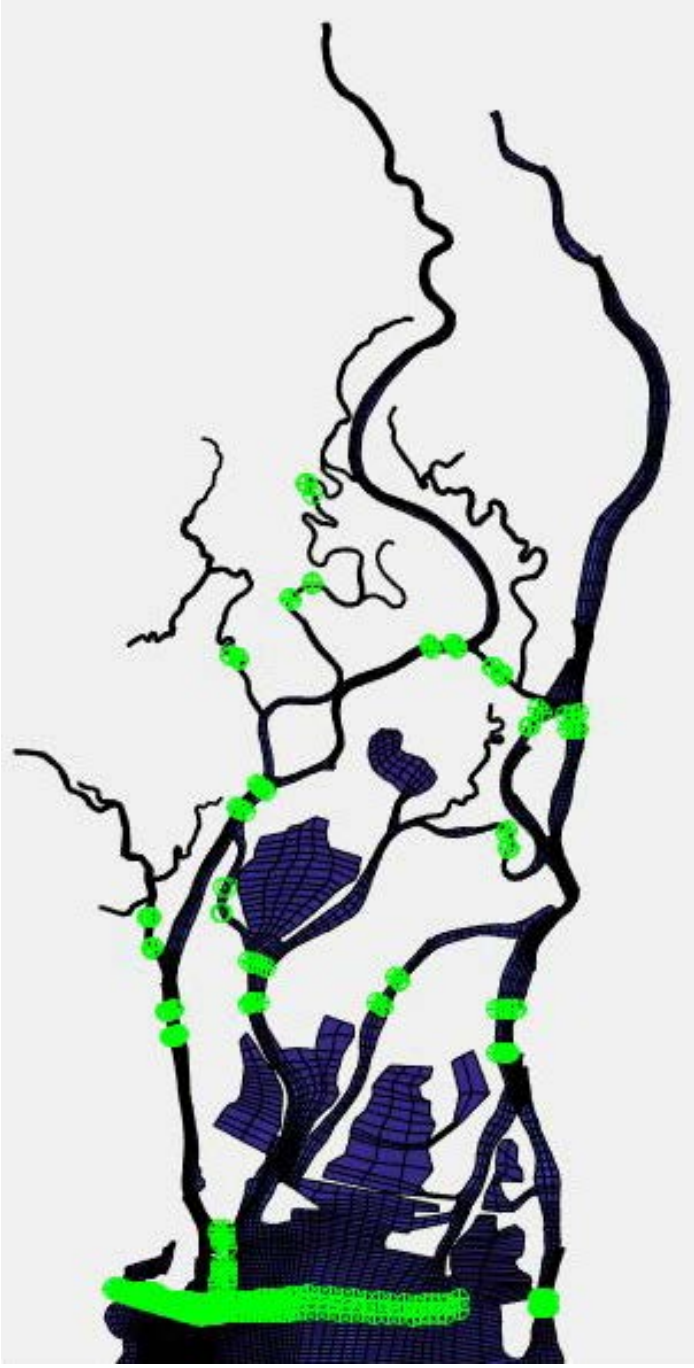

Figure 10. Grid Block Delta System

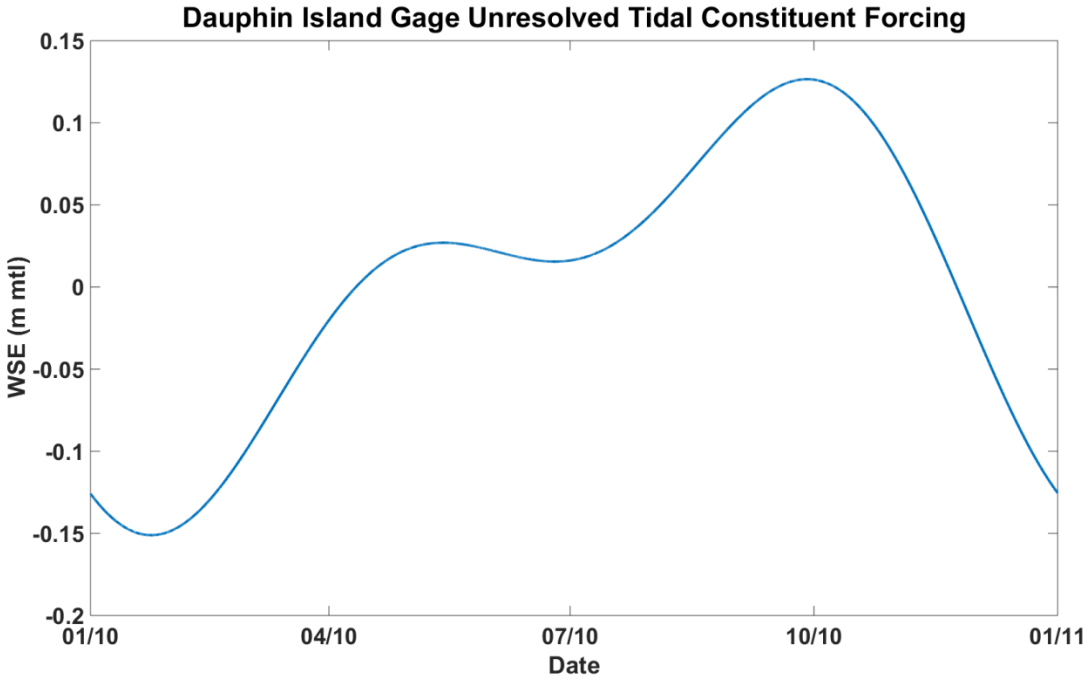

Figure 11. Unresolved Tidal Constituent Forcing

The influence of the filtered signal contribution is easily seen in a comparison of modeled and observed WSE at the Dauphin Island NOAA gage. Figures 12-14 presents comparisons during the months of January, June and September. Similar comparisons for December at the Coast Guard Sector and Meaher State Park are shown in Figures 15 and 16, respectively. It is seen in these comparisons that there is good agreement between the modeled and observed tidal variation with minor differences in the meteorological response.

The primary reason for the differences in meteorological response is seen in Figures 17 and 18, which compare the OWI model wind speed and direction to those observed at Dauphin Island during January of the 2010 simulation period. Although the day to day nature of the WIS winds are comparable to the observed, peak wind speed associated with fast moving fronts are not captured. Irrespective, the tidal and meteorological forced variation in WSE throughout the Bay is well represented during the simulation year.

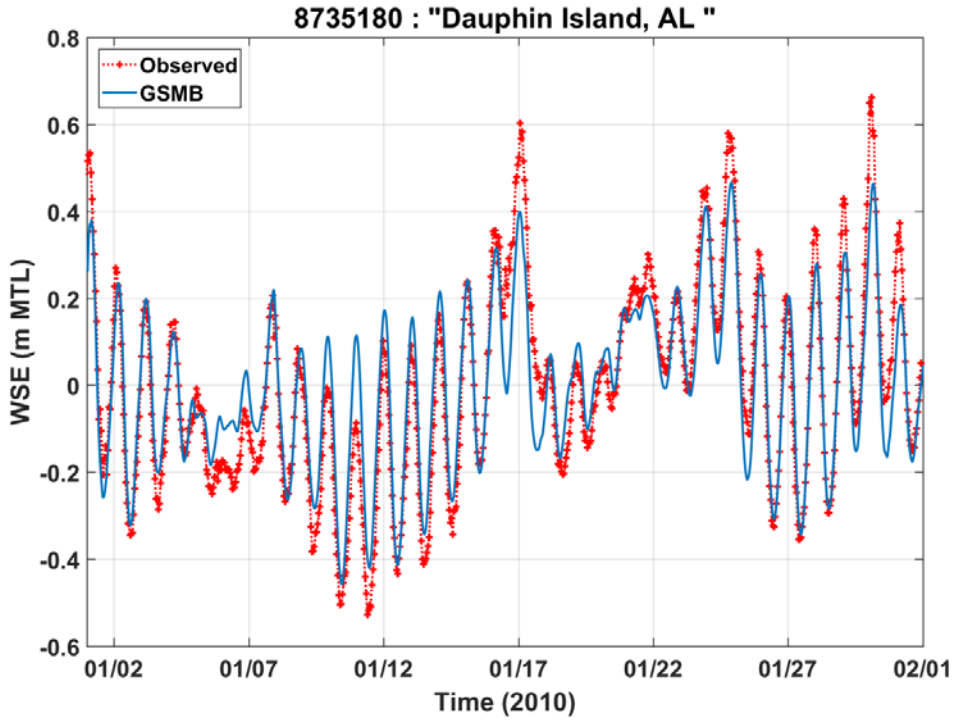

Figure 12. January Dauphin Island Water Surface Elevation Comparison

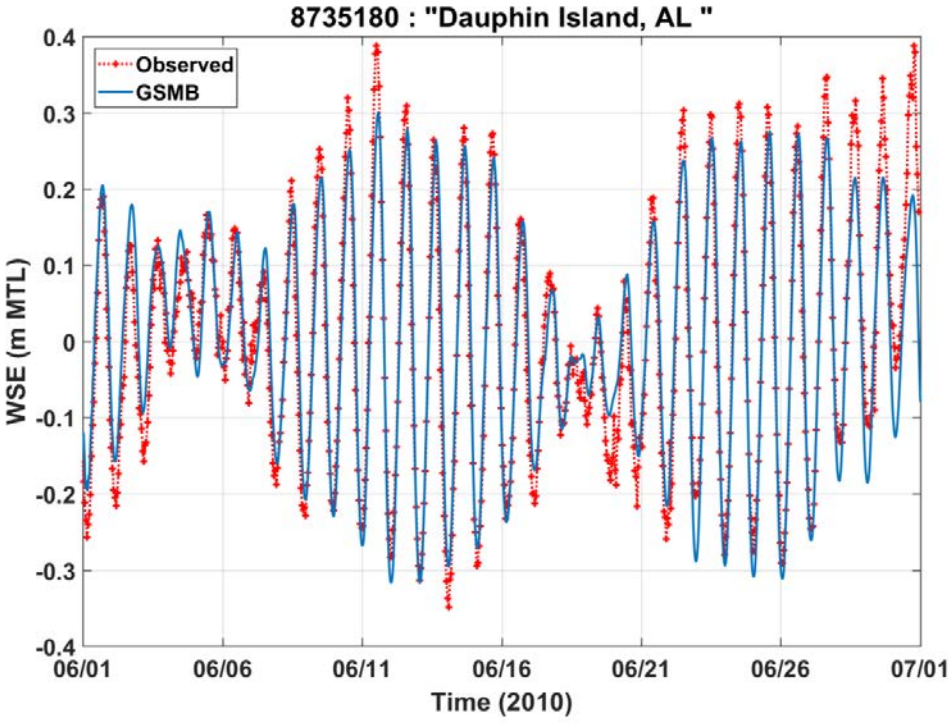

Figure 13. June Dauphin Island Water Surface Elevation Comparison

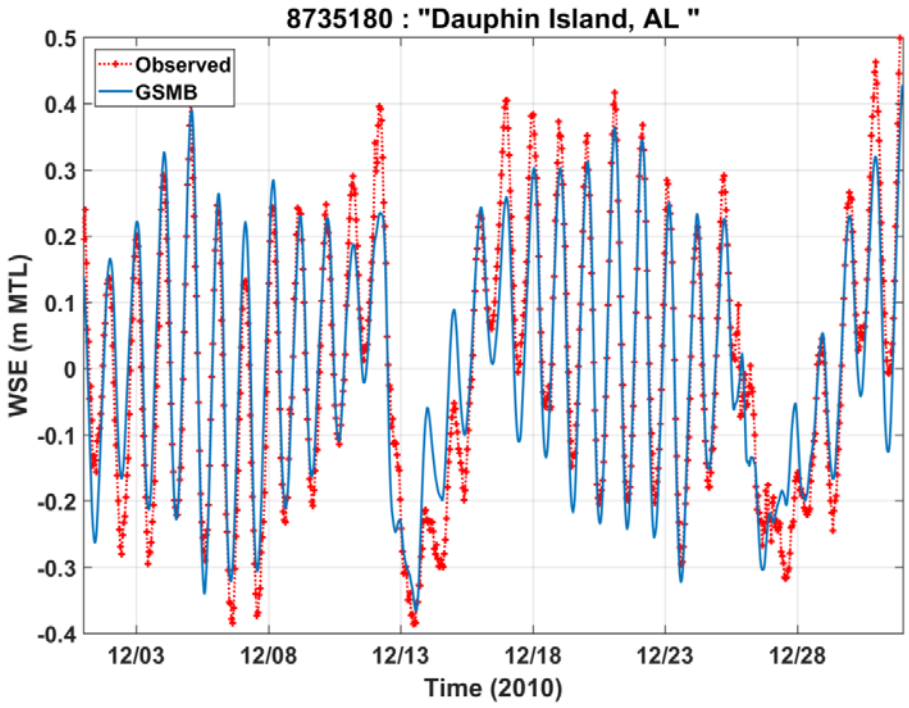

Figure 14. December Dauphin Island Water Surface Elevation Comparison

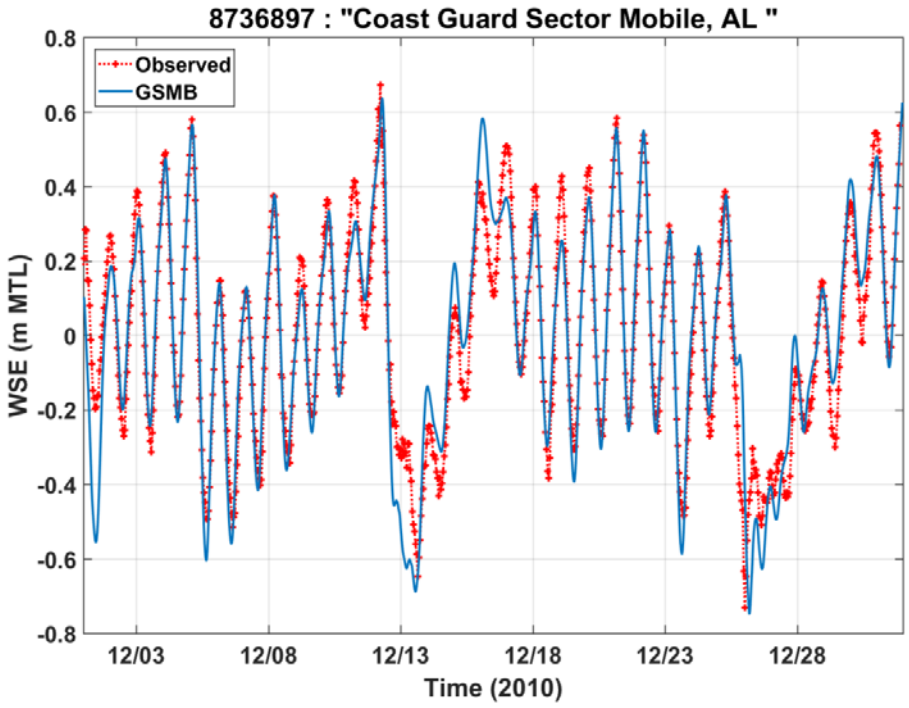

Figure 15. December Coast Guard Sector Water Surface Elevation Comparison

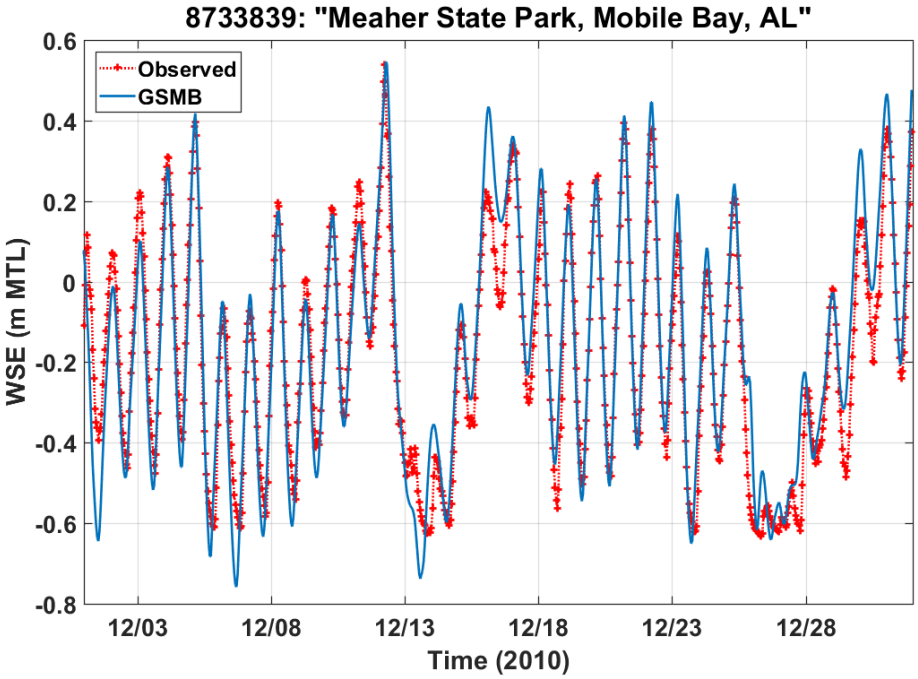

Figure 16. December Meaher State Park Water Surface Elevation Comparison

To demonstrate that transport is properly represented, it is important that the vertical distribution of salt or stratification is capture well and the model simulations are volume and mass conservative. The transport validation presented is an extension of that performed during the ERDC Flooding and Coastal Systems Research task "Initial Assessment of ADH-3D Hydrodynamic and Salinity Transport: Mobile Bay" (Chapman *et al.* 2014). The purpose of that unpublished research task was to determine if it was appropriate to recommend the application of ADH as a complementary approach or replacement of GSMB to USACE Districts. The results of this research demonstrated that ADH does not conserve volume/mass, the required grid resolution is inefficient and it fails to satisfy vertical direction continuity boundary conditions. As a result, it was concluded that it should not be recommended for application to USACE projects requiring defensible transport of salt, temperature, sediment and water quality constituents. In addition, this research reinforced the fact that volume and mass conservative transport can only be achieved by control volume based models such as GSMB.

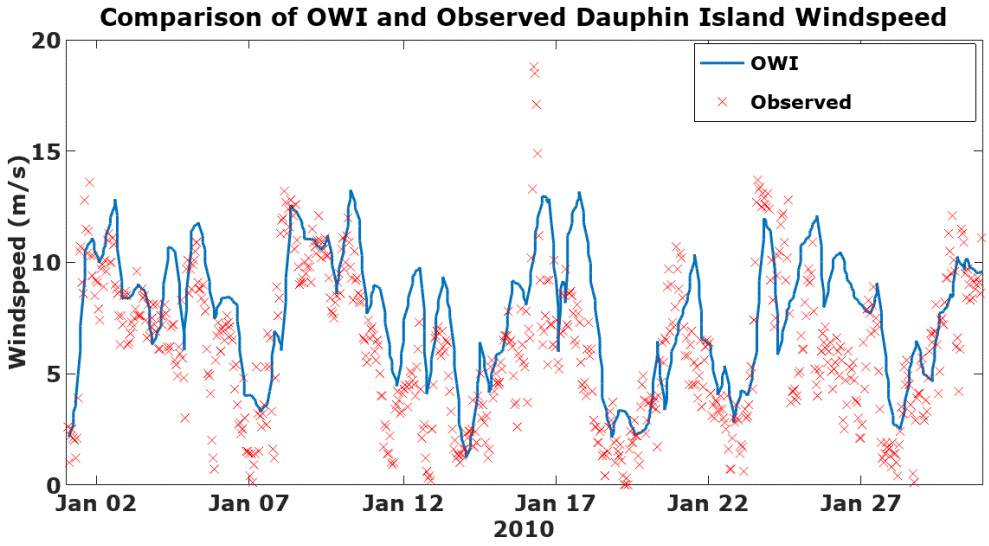

Figure 17. WIS and Dauphin Island Observed Windspeed

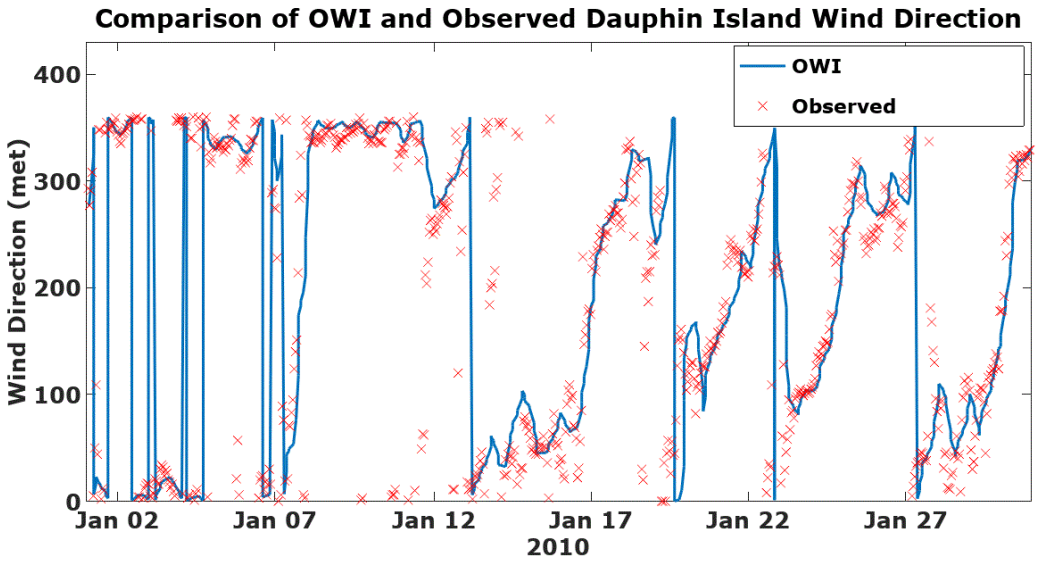

Figure 18. WIS and Dauphin Island Observed Wind Direction

Transport validation was achieved through comparison of predicted vertical salinity profiles with observed data. Figure 19 shows the sites sampled during a University of South Alabama (USLA) field study (Dzwonkowski *et al.* 2011). Figures 20 - 28 present comparisons of observed vertical salinity profiles with model results. The DI, M2 and M4 sample sites are shown for 30 March, 2 June and 19 October of the 2010 simulation time period. In these plots, the observed data are red crosses with the model results presented as

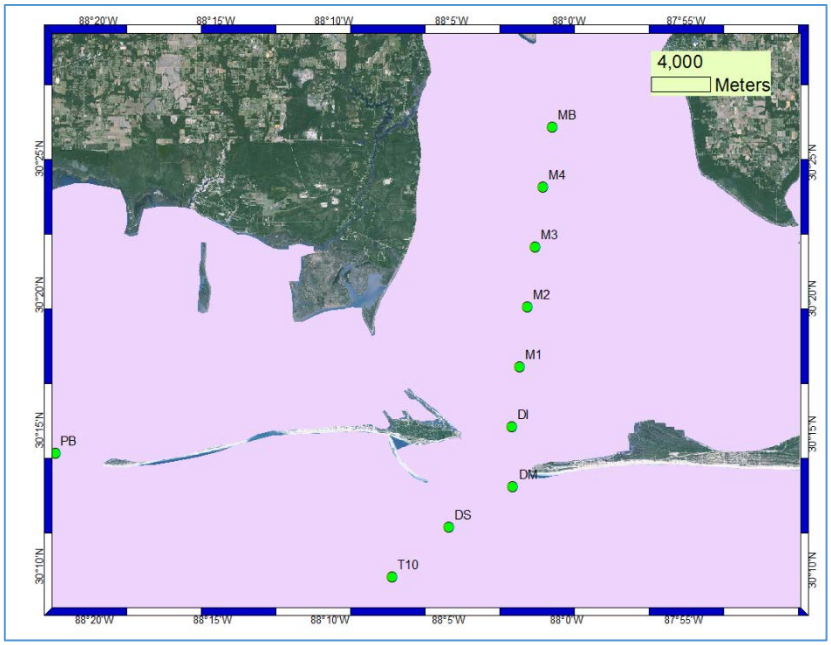

Figure 19. Univ of South Alabama CTD cast stations for 2009-2010.

green lines depicting hourly snapshots spanning plus or minus 6 hours of the sampling time. The blue line is the arithmetic mean of the model profile snapshots. Differences in the observed and model profiles are can again be attributed to inaccuracies of meteorological, riverine and tidal forcing. In all cases, the observed and modeled profiles agree well, capturing the degree and variability of stratification throughout the year.

49 and 59 Multi-Block System Comparison

As previously stated, 49 and 59 block multi-block systems were developed and employed in this study. The 49 block system was applied for both the 2010 sediment and water quality transport tasks and the 59 block system was used to investigate the influence of minor tributaries and additional channel connections on the distribution of salinity throughout the Delta. To ensure consistency between the 49 and 59 block system simulations, a comparison of salinity profiles and time series was undertaken utilizing the SAM 2016 data collection (Allen 2016) sites shown in Figure 29. In this figure, the data collection sites are abbreviations as follows; AR, Apalachee River; BR, Blakeley River; CO, Mobile-Tensaw Cut-Off Channel; CW, Causeway; MR, Mobile River; TR, Tensaw River.

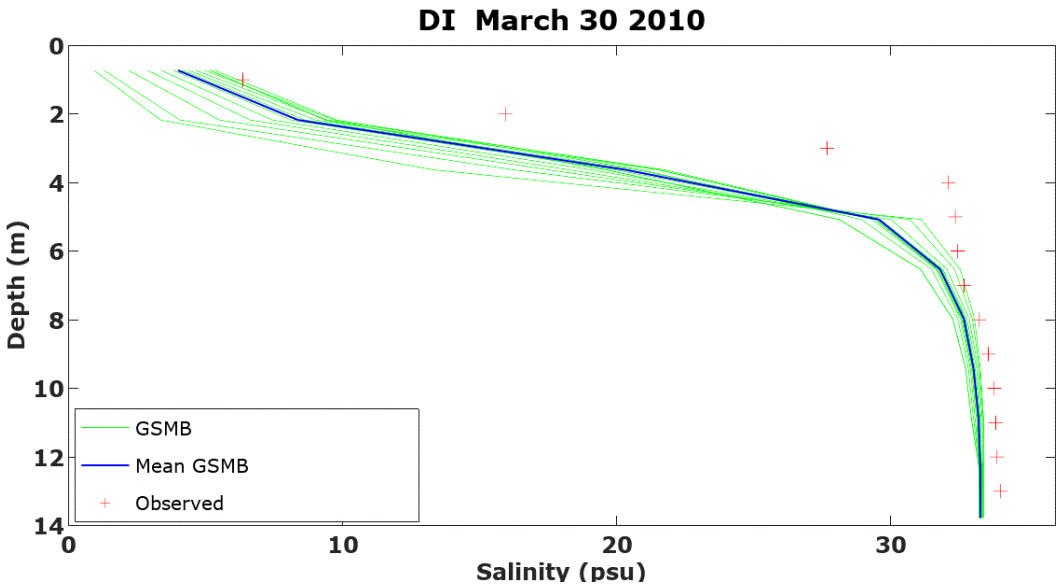

Figure 20. Observed and Model Salinity Profiles at Dauphin Island

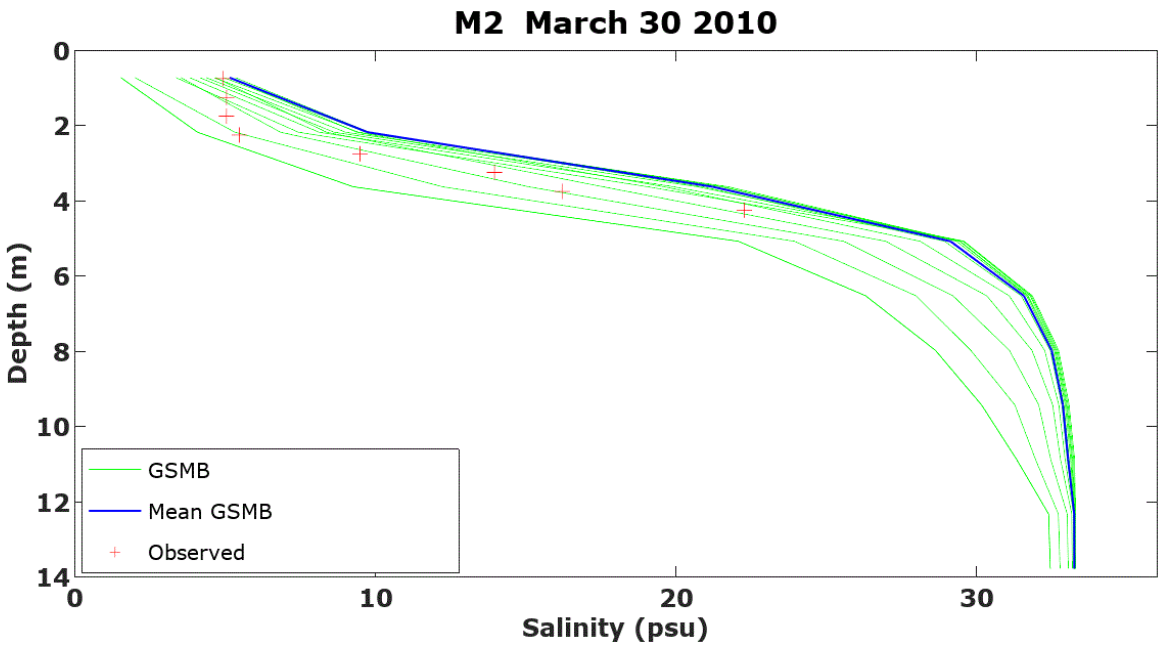

Figure 21. Observed and Model Salinity Profiles at Site M2

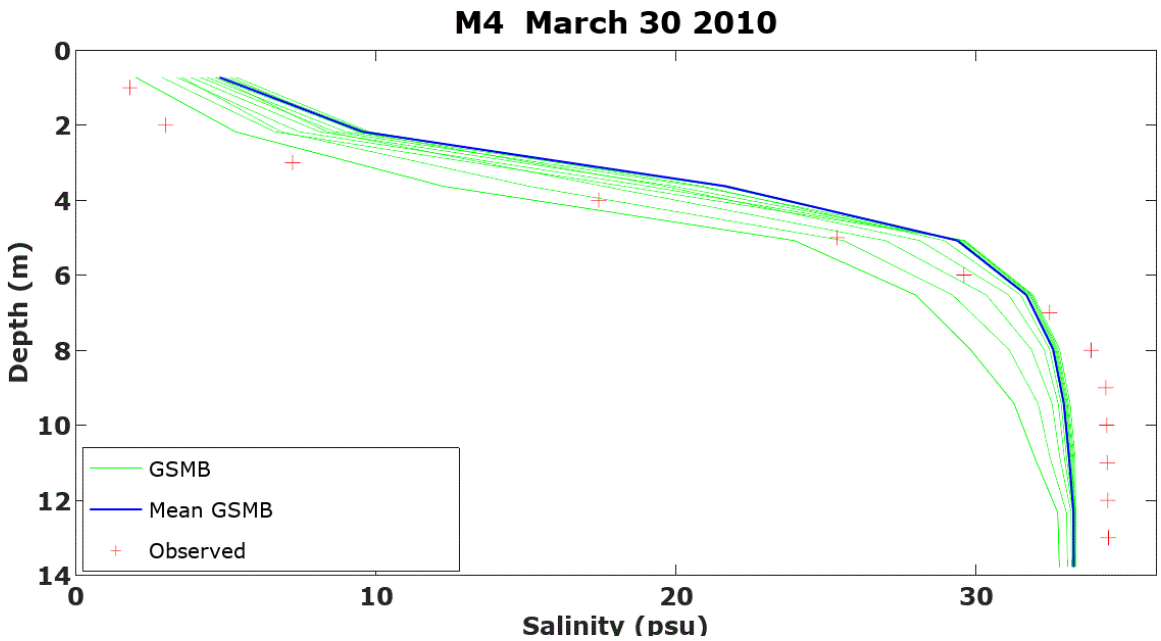

Figure 22. Observed and Model Salinity Profiles at Site M4

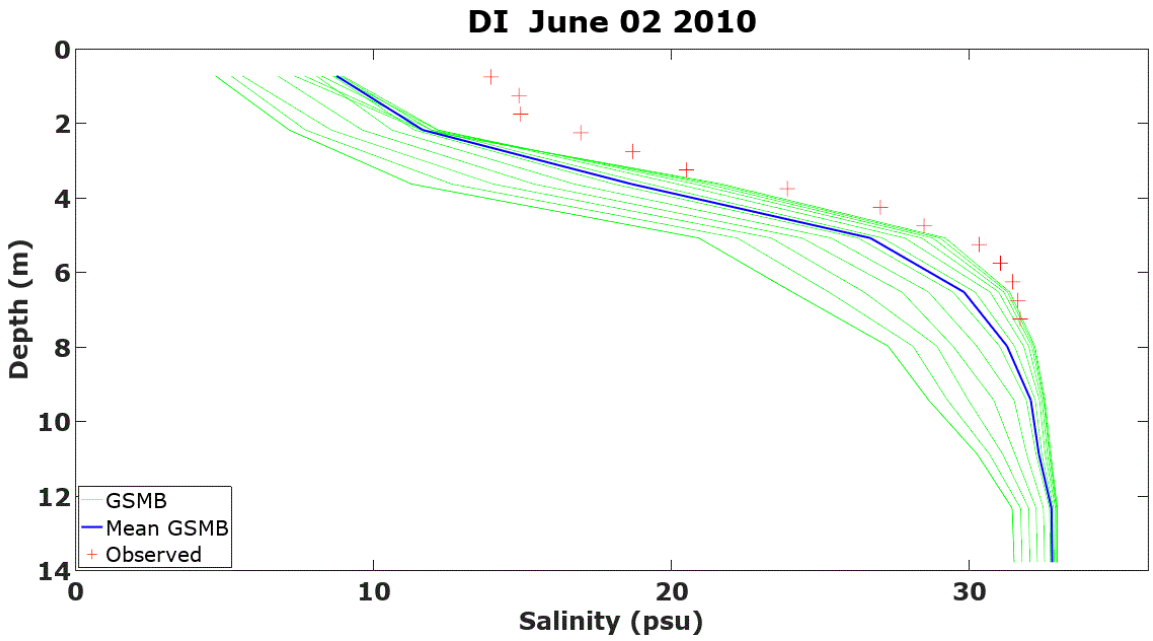

Figure 23. Observed and Model Salinity Profiles at Dauphin Island

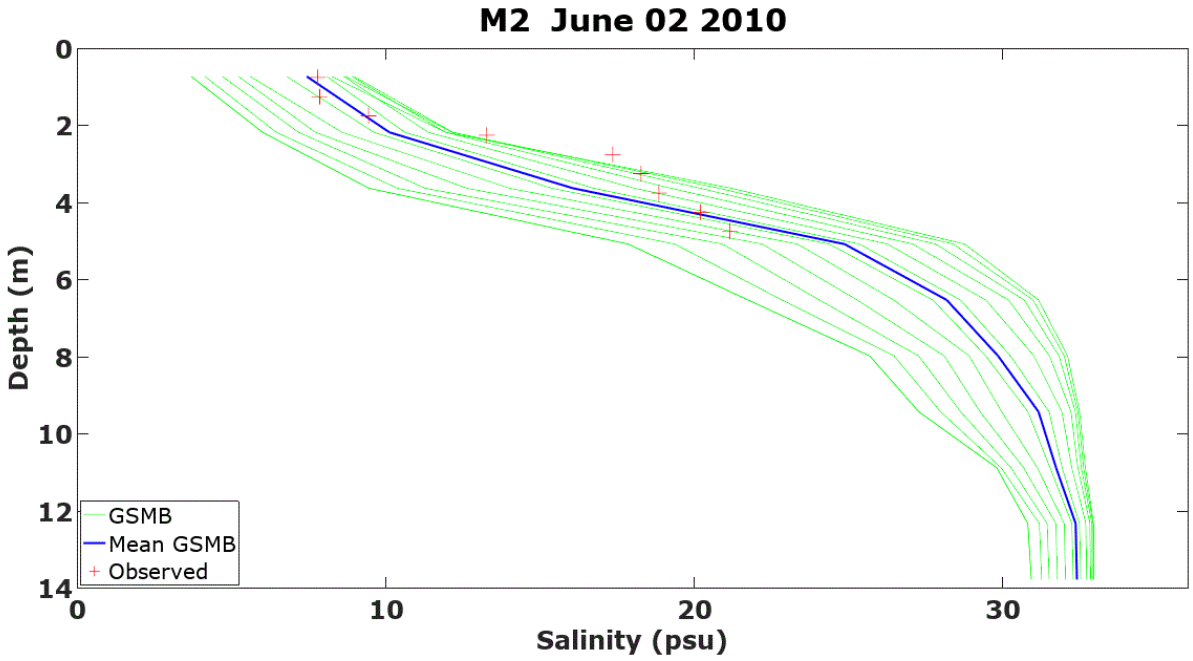

Figure 24. Observed and Model Salinity Profiles at Site M2

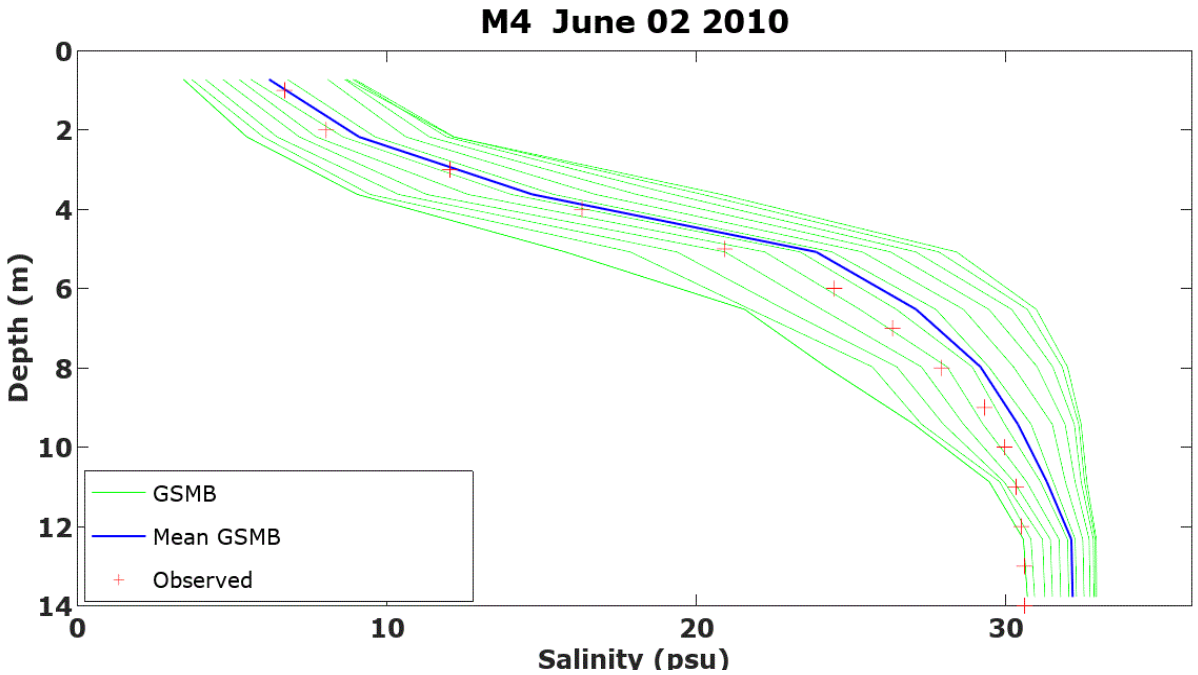

Figure 25. Observed and Model Salinity Profiles at Site M4

Figure 26. Observed and Model Salinity Profiles at Dauphin Island

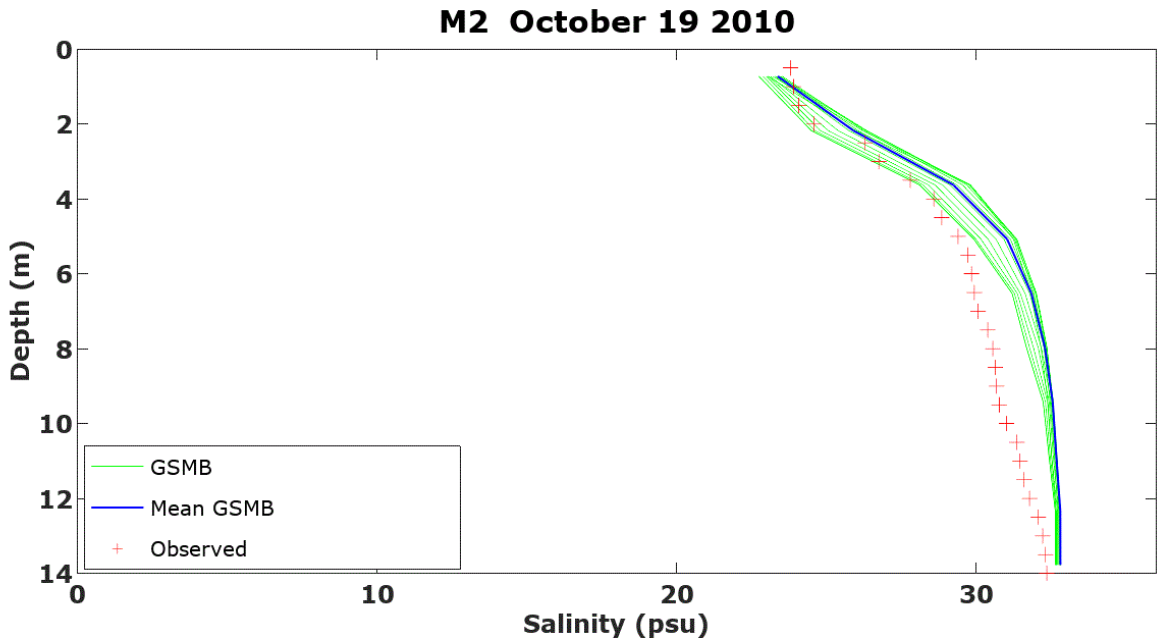

Figure 27. Observed and Model Salinity Profiles at Site M2

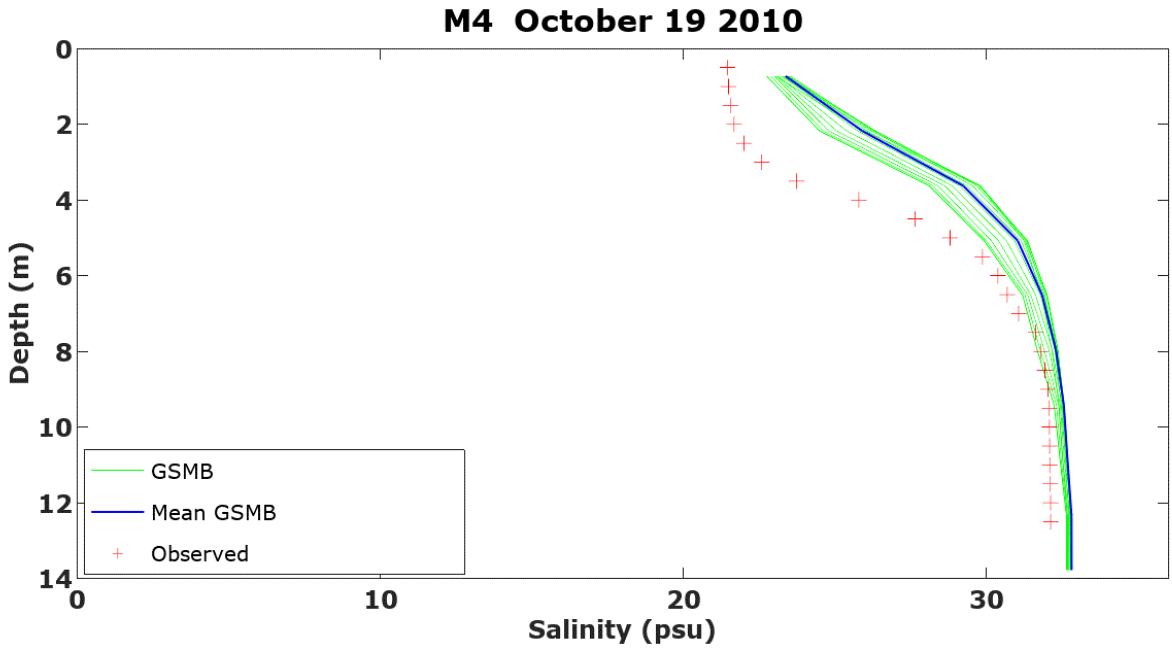

Figure 28. Observed and Model Salinity Profiles at Site M4

Time series comparisons of near bottom salinity from the 49 and 59 block simulations are presented in Figure 30-34. It is seen in Figures 30 and 31 that the Tensaw side of the Delta is relatively fresh during the 2016 measurement time with near bottom salinity values of about 5 psu at the northern (TR-01) and southern (AR@CW) data collection sites. In addition, it is seen that nearly identical simulation results are provided by the 49 and 59 block systems. Similarly comparable results for the two grid systems are shown for the more saline (> 20 psu) Mobile side of the Delta at sites MR-01, CO-01 and MR-09 in Figures 32 - 34, respectively. Figures 35 – 39 present comparisons of observed vertical salinity profiles collected during 13 – 14 September 2016 with the 49 and 59 grid block system simulation results. It is seen in Figures 35 – 39 that the degree of stratification at MR-1, CO-01 and MR -09 is well represented by both the 49 and 50 block systems as compared to data collected at different times during the tide cycle. Although the profile sample depth at MR-09 is significantly less than that of the model, the difference between surface and bottom salinity is comparable. As expected, the sample sites from the East side of the delta show fresher salinity distribution at both TR-03 and the Apalachee causeway site.

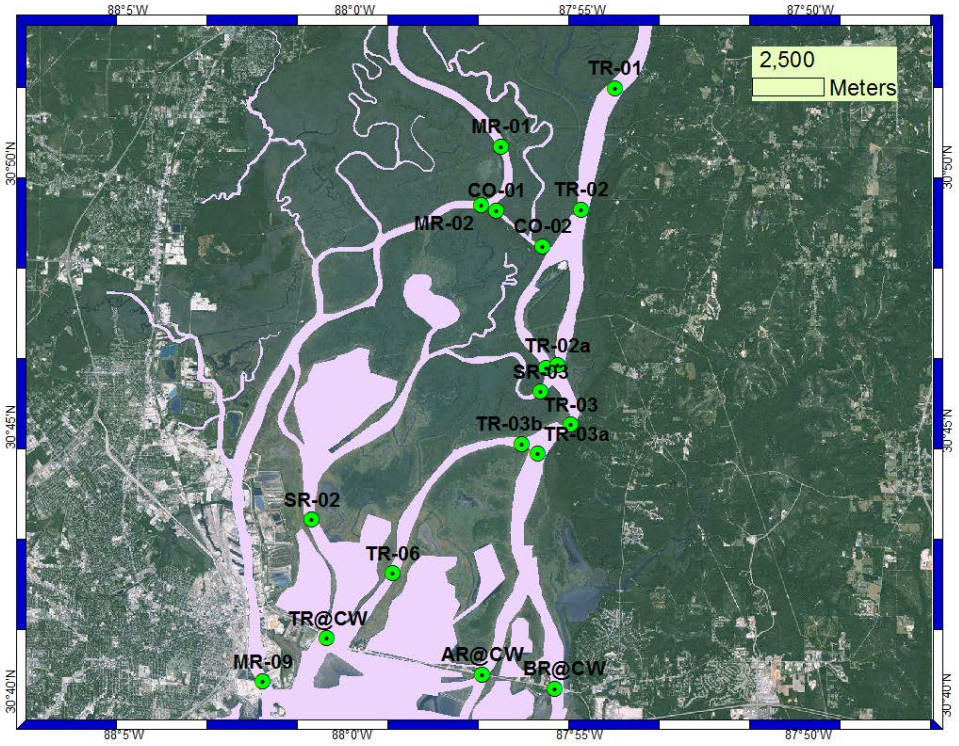

Figure 29. USACE Delta survey stations for 2016-2017 in Upper Bay.

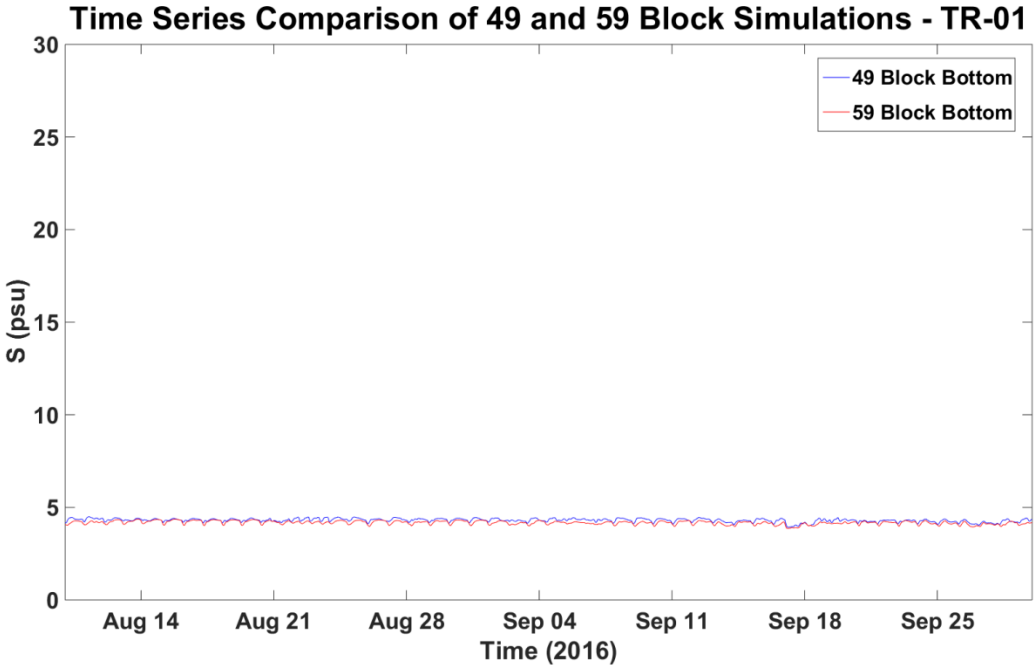

Figure 30. TR-01 Near Bottom Salinity Comparison of 49 and 59 Block Simulations

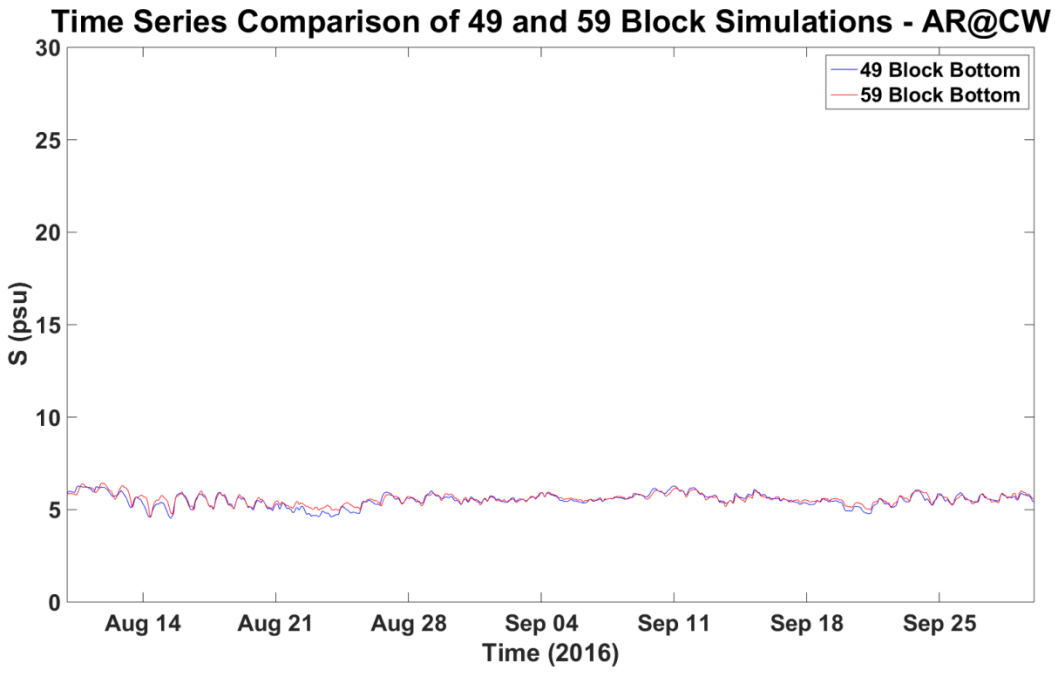

Figure 31. AR@CW Near Bottom Salinity Comparison of 49 and 59 Block Simulations

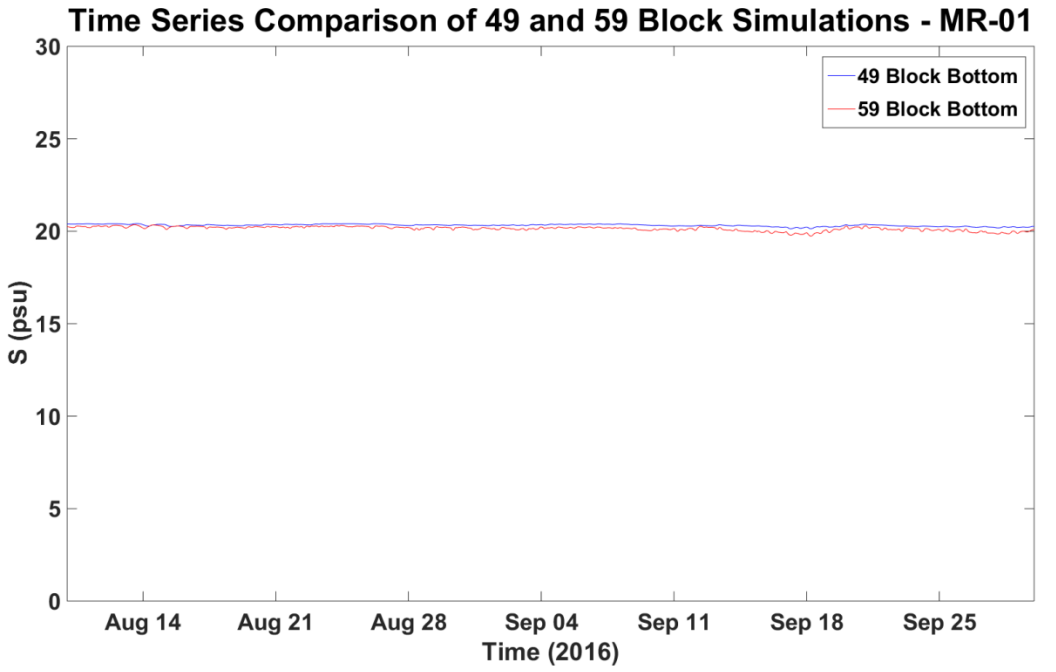

Figure 32. MR-01 Near Bottom Salinity Comparison of 49 and 59 Block Simulations

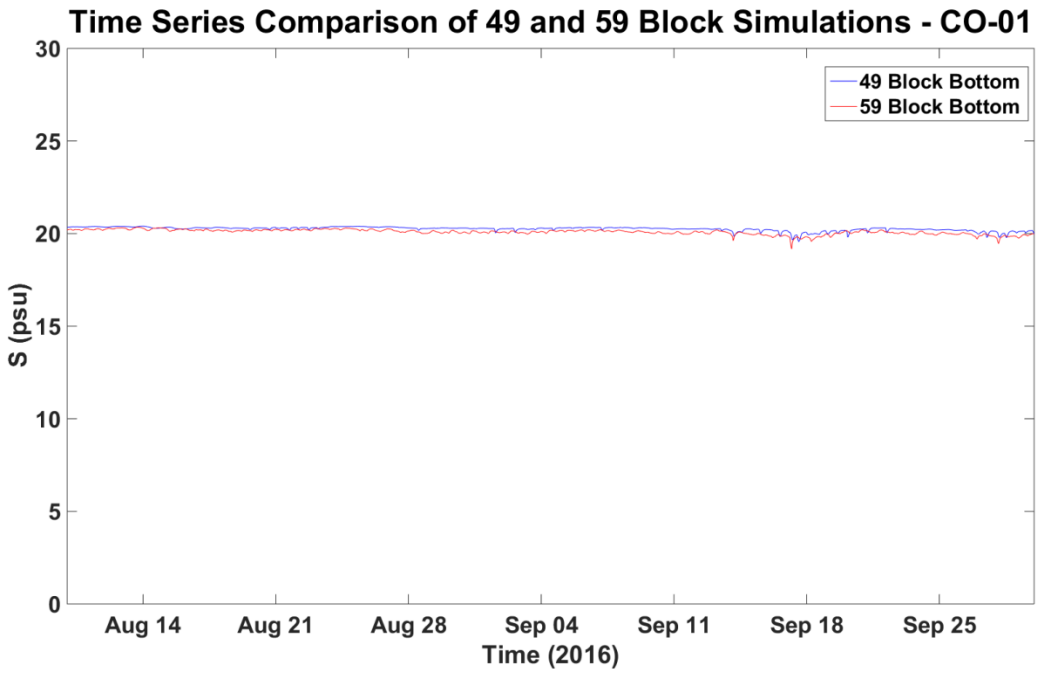

Figure 33. CO-01 Near Bottom Salinity Comparison of 49 and 59 Block Simulations

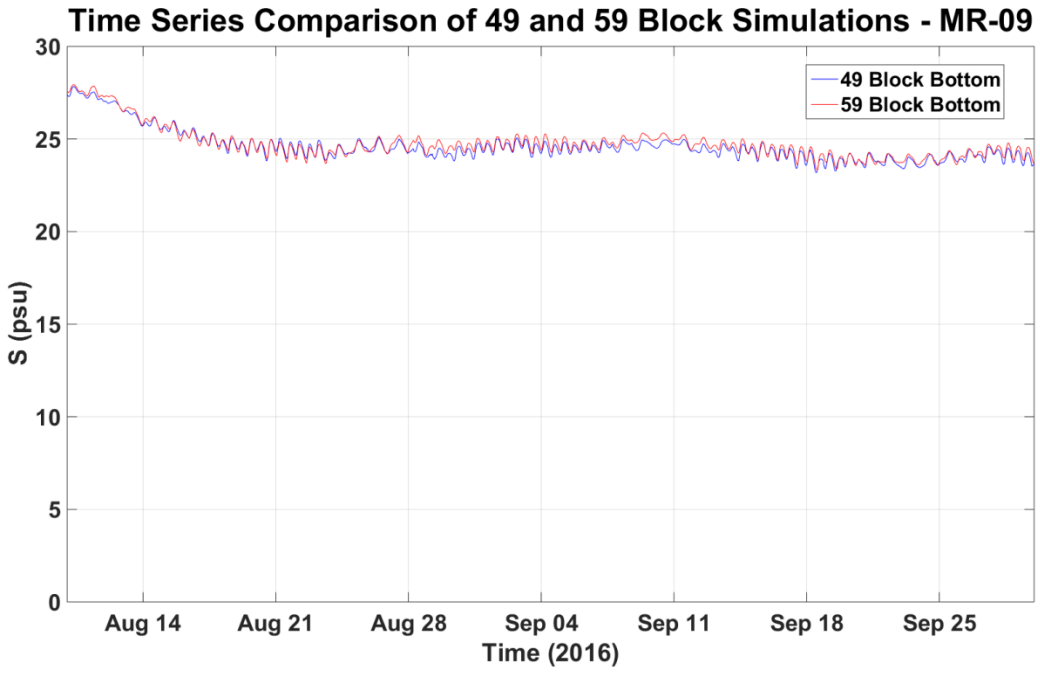

Figure 34. MR-09 Near Bottom Salinity Comparison of 49 and 59 Block Simulations

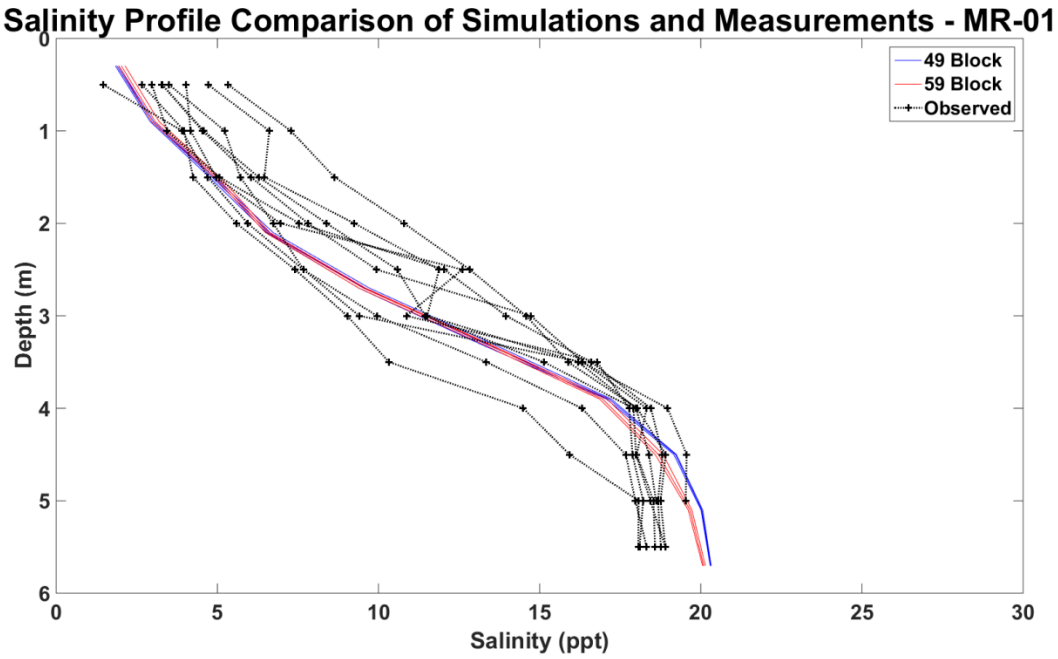

Figure 35. September 13-14, 2016 Observed and Model Salinity Profiles MR-01

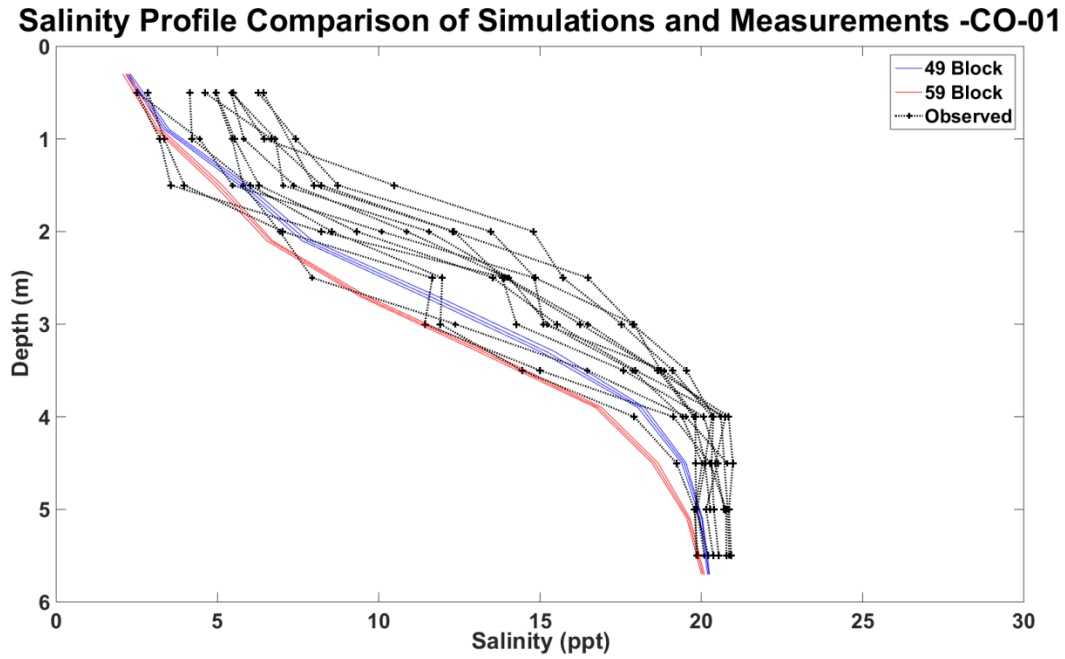

Figure 36. September 13-14, 2016 Observed and Model Salinity Profiles CO-01

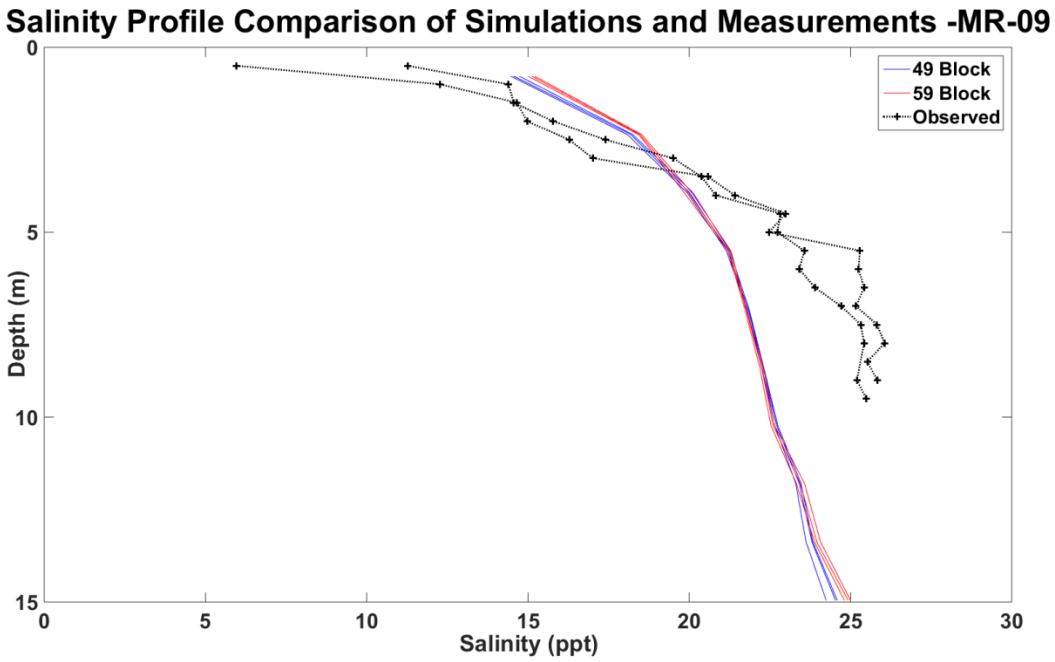

Figure 37. September 13-14, 2016 Observed and Model Salinity Profiles MR-09

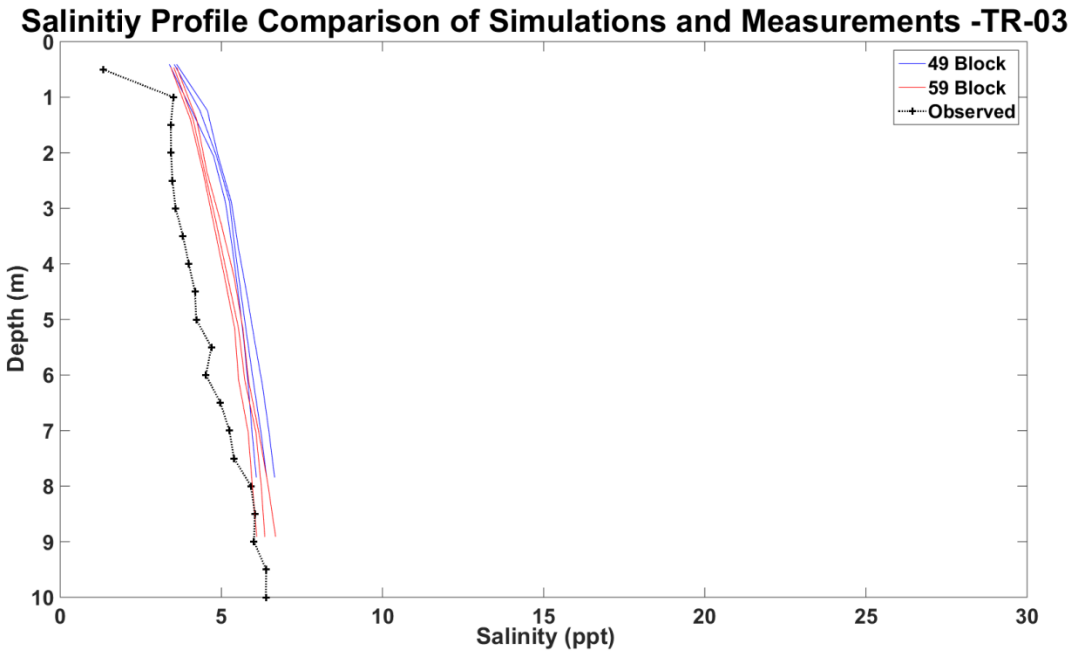

Figure 38. September 13-14, 2016 Observed and Model Salinity Profiles TR-03

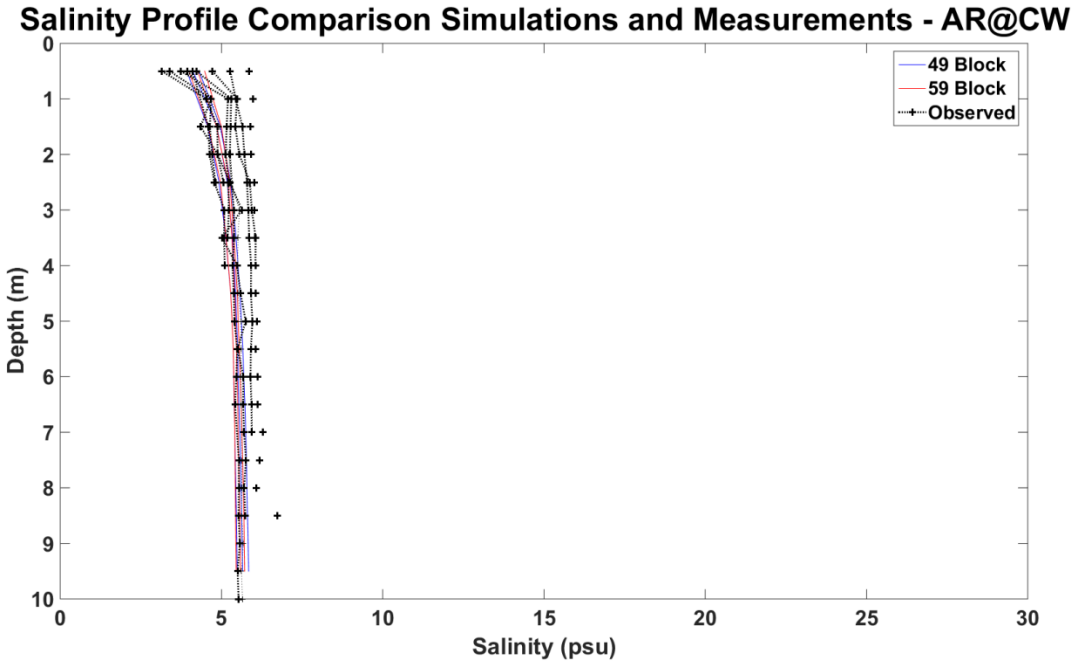

Figure 39. September 13 - 14, 2016 Observed and Model Salinity Profiles AR@CW

Existing and With-Project Simulations

The primary purpose of the hydrodynamic modeling task was to support the investigation of potential project impacts on sedimentation and water quality. The existing channel configuration specified a 45 foot mllw existing depth with 2 feet of advanced maintenance and overdepth, resulting in a simulated depth of 49 feet mllw. Similarly, the 47 foot mllw entranced channel was increased to 51 feet mllw. The existing turning basin was specified to be 45 feet mllw with a total of 6 feet advanced maintenance and overdepth, resulting in a depth of 51 feet mllw.

The project Bay channel design specified a simulated depth of 50 feet with 2 feet of advanced maintenance and overdepth, resulting in a simulated depth of 54 feet mllw. The entrance channel and turning basin project depths were increased to 56 feet mllw. In addition, the model grid was modified to include the 250 foot extension on the South side of the tuning shown it Figure 40 and the grid modification, Figure 41. Further modification to the project grids included the bend easing at the entrance channel, Figure 42, along with

the corresponding grid modification shown in Figure 43. Channel widening for a passing lane, shown in Figure 44 and the grid modification, Figure 45.

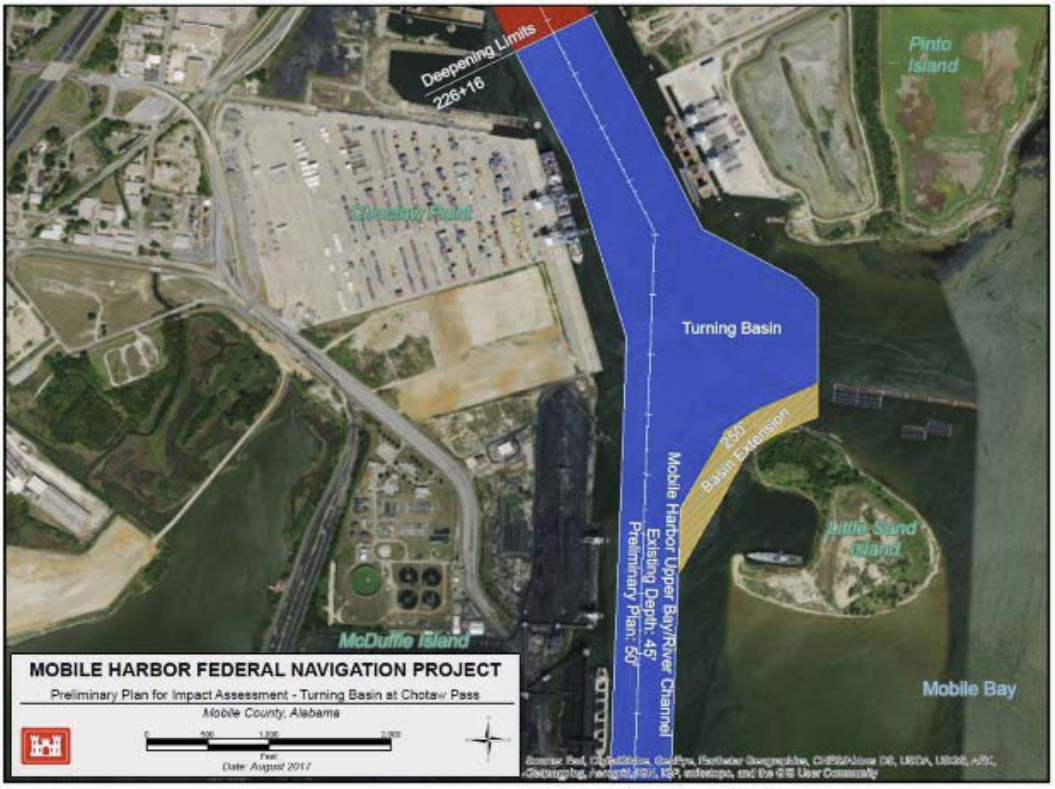

Figure 40. Turning Basin Extension Design and Grid Modification

The sensitivity of the Mobile Bay and Delta salinity distribution to project impacts was examined by comparisons of surface and bottoms time series at five Delta stations described in the previous section (MR-01, MR-09, TR-03, TR@CW, AR@CW, Figure 28) and four Bay stations (Dauphin Island, Bon Secour, Cedar Point, Middle Bay Light, Figure 46). Figures 47 – 51 present time series comparisons of surface and bottom salinity with and without project at the Delta Sites and Figure 52 – 55 at sites within the Bay. It is seen in the plots that the maximum change in salinity is less than 2 ppt.

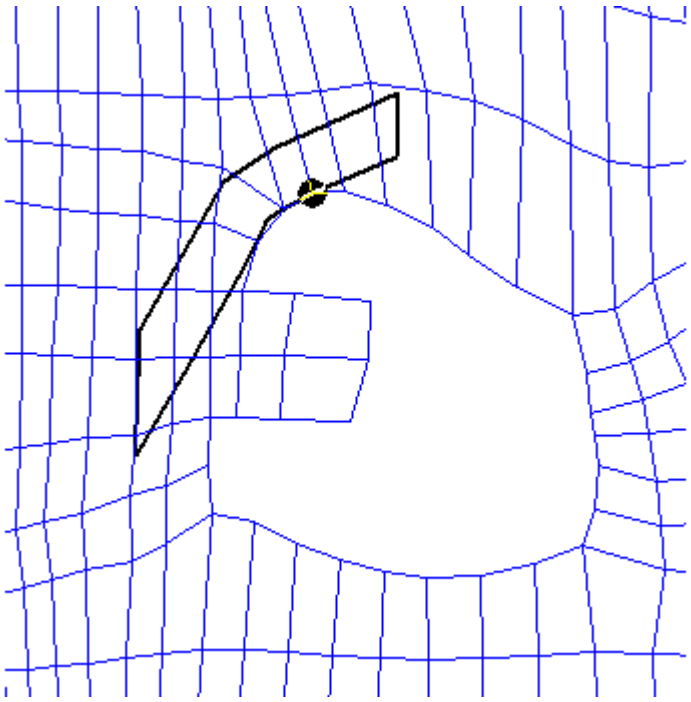

Figure 41. Turning Basin Extension Grid Modification

Figures 56 – 59 present similar plots for the “Sea Level Rise” alternative simulations at MR-01, AR@CW, Cedar Point and Bon Secour where it is again seen that the maximum change in salinity is less than 2 ppt.

An overall view of bay wide salinity variation is presented in Figure 60, in which it is seen that the range of salinity in the surface and bottom layers exceeds 30 ppt during a relatively low flow time period. A sense of the project impact is presented in Figure 61 where the salinity differences are again seen to be less than 2 ppt.

Figure 42. Bend Easing Design at the Mobile Bay Entrance

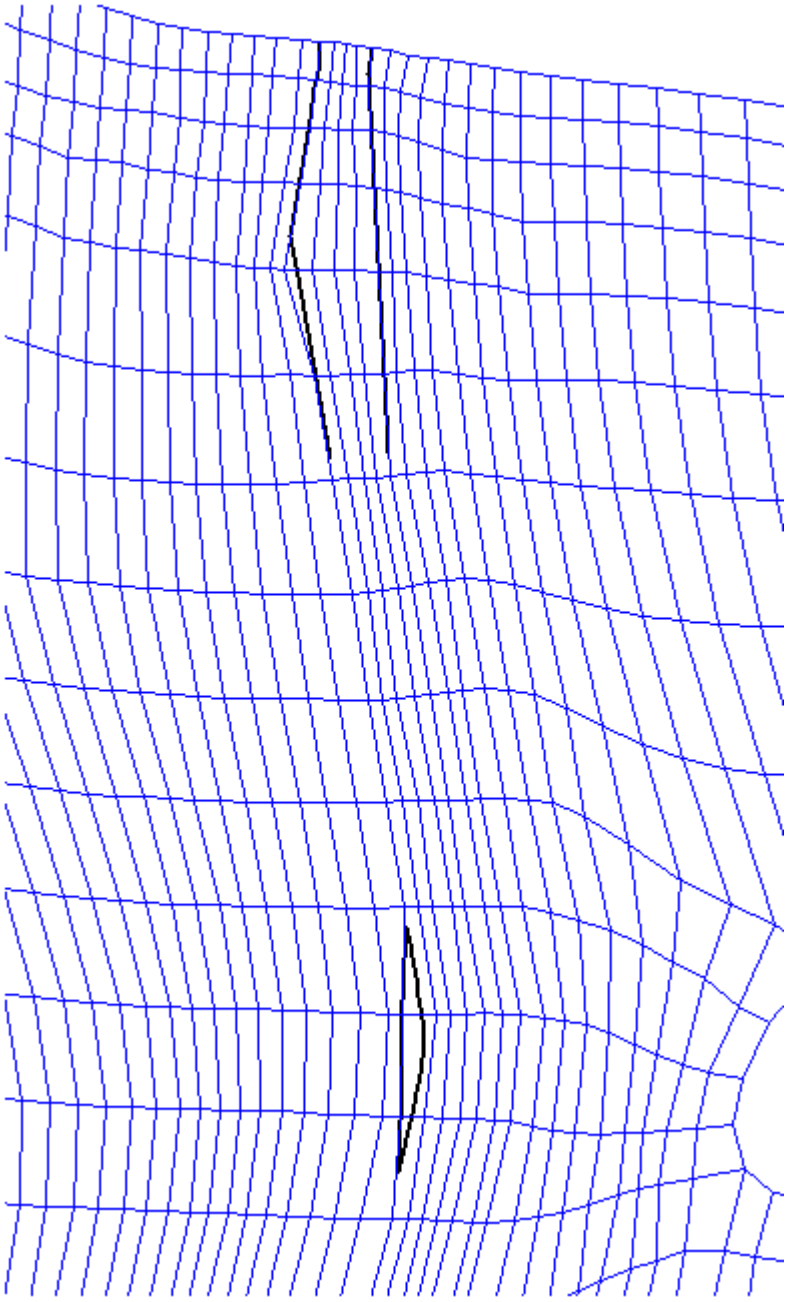

Figure 43. Bend Easing Grid Modification Mobile Bay Entrance

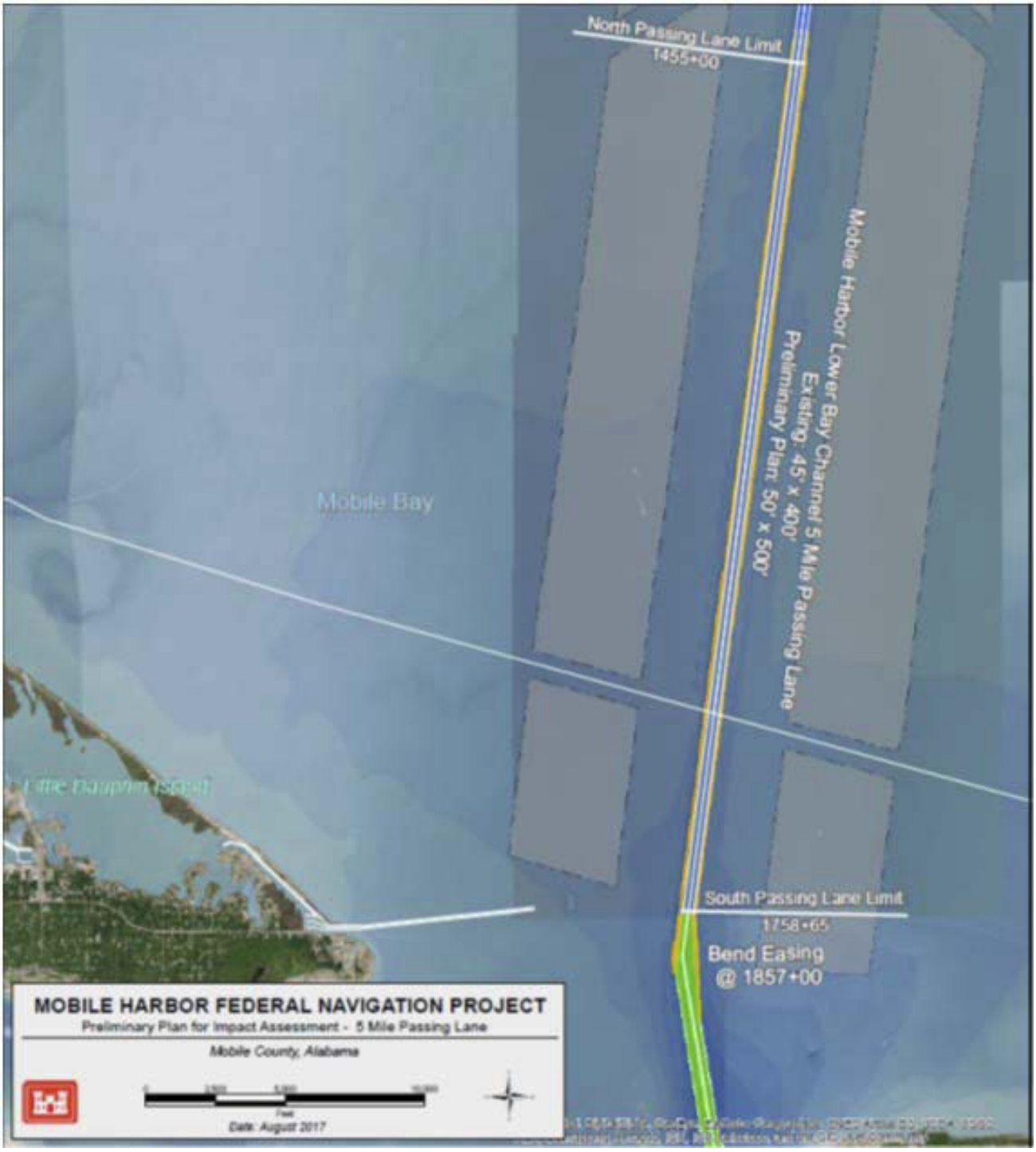

Figure 44. Channel Widening - Passing Lane Design

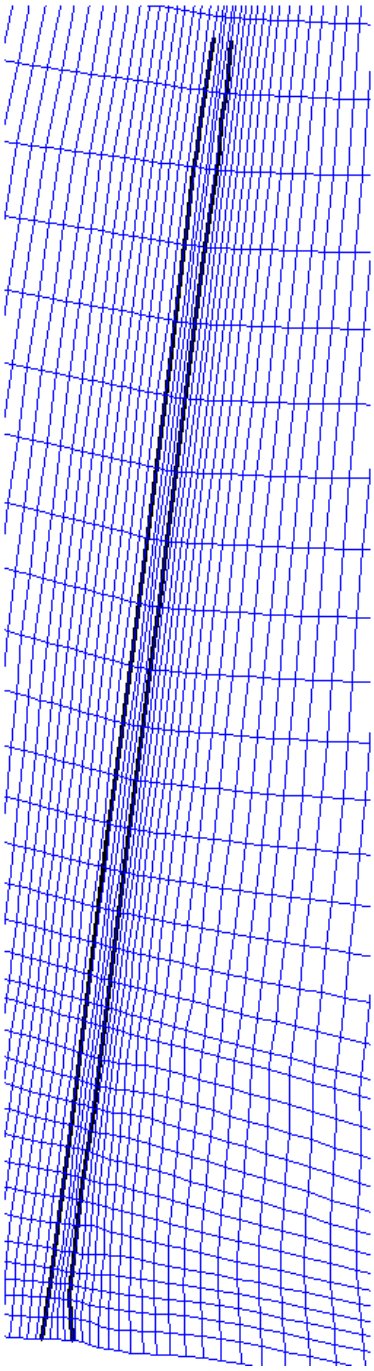

Figure 45. Channel Widening - Passing Lane Grid Modification

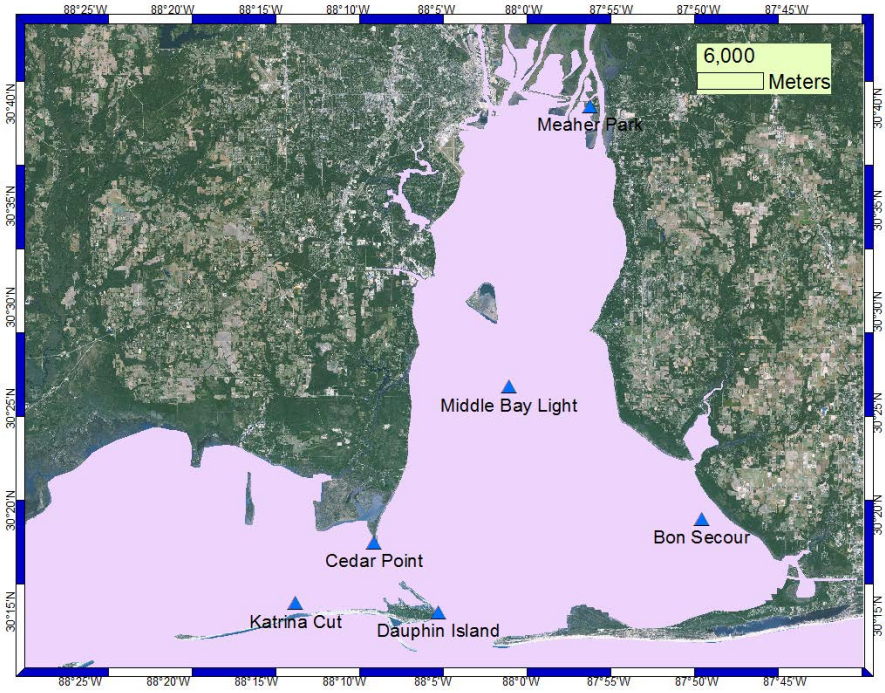

Figure 46. NOAA NEP stations

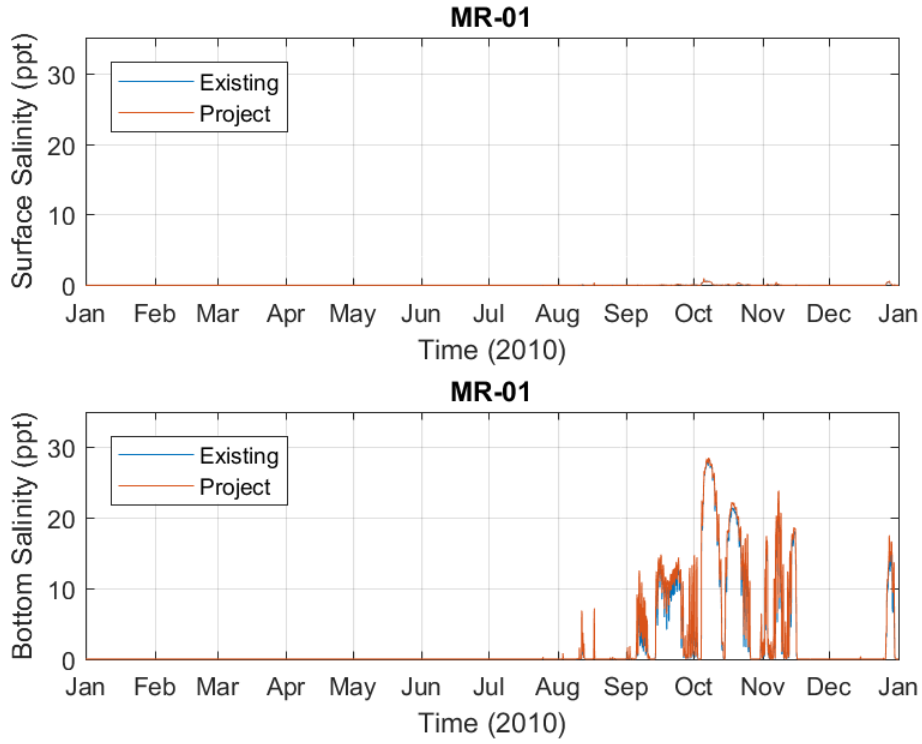

Figure 47. Time Series Comparison at MR-01

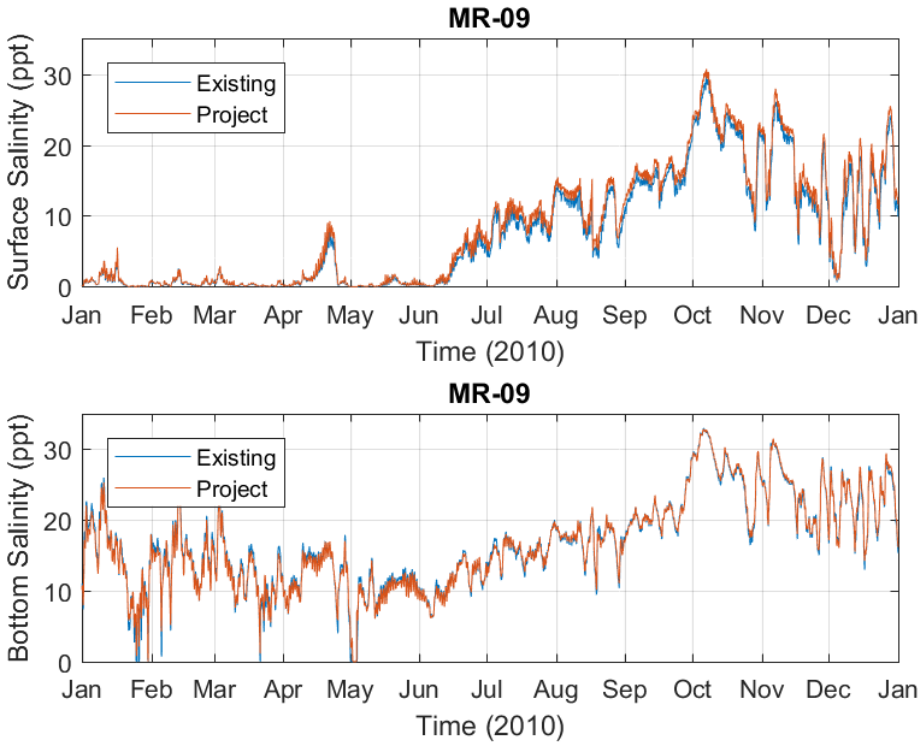

Figure 48. Time Series Comparison at MR-09

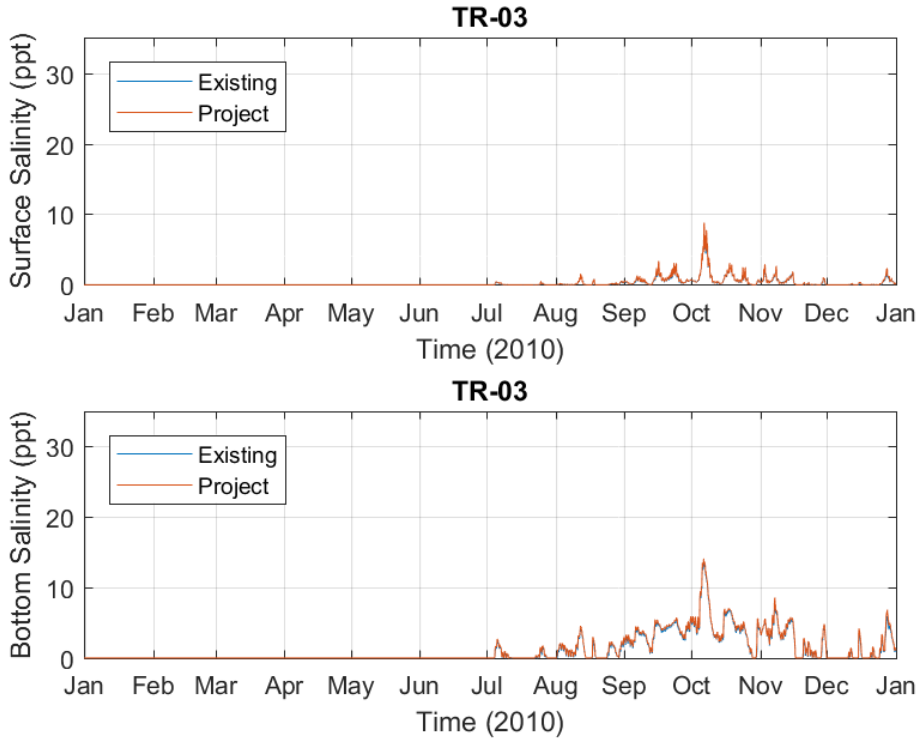

Figure 49. Time Series Comparison at TR-03

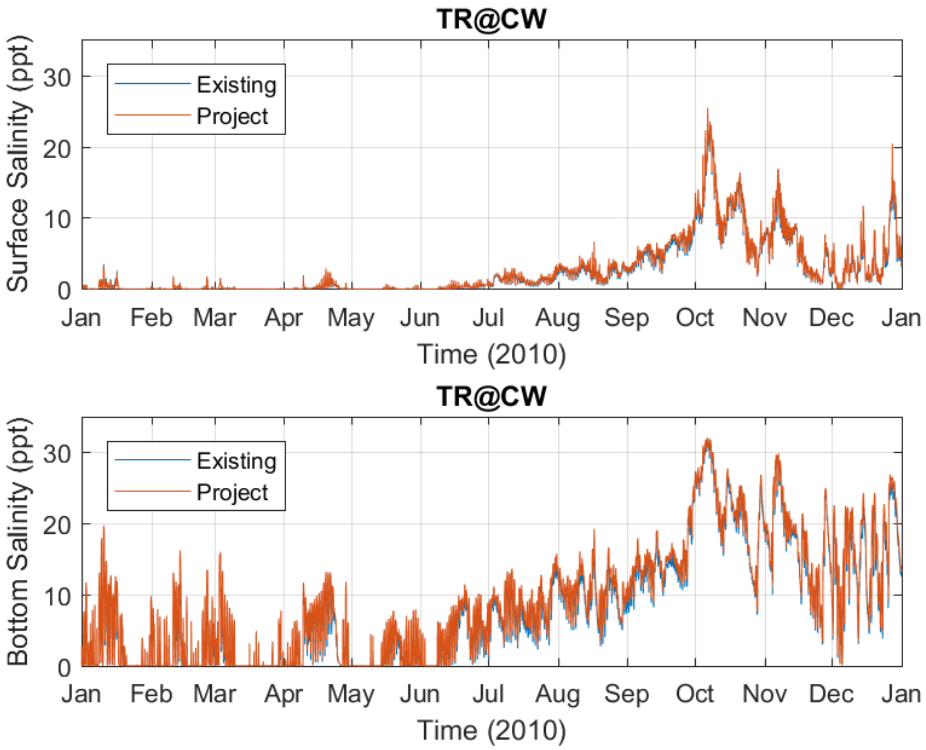

Figure 50. Time Series Comparison at TR@CW

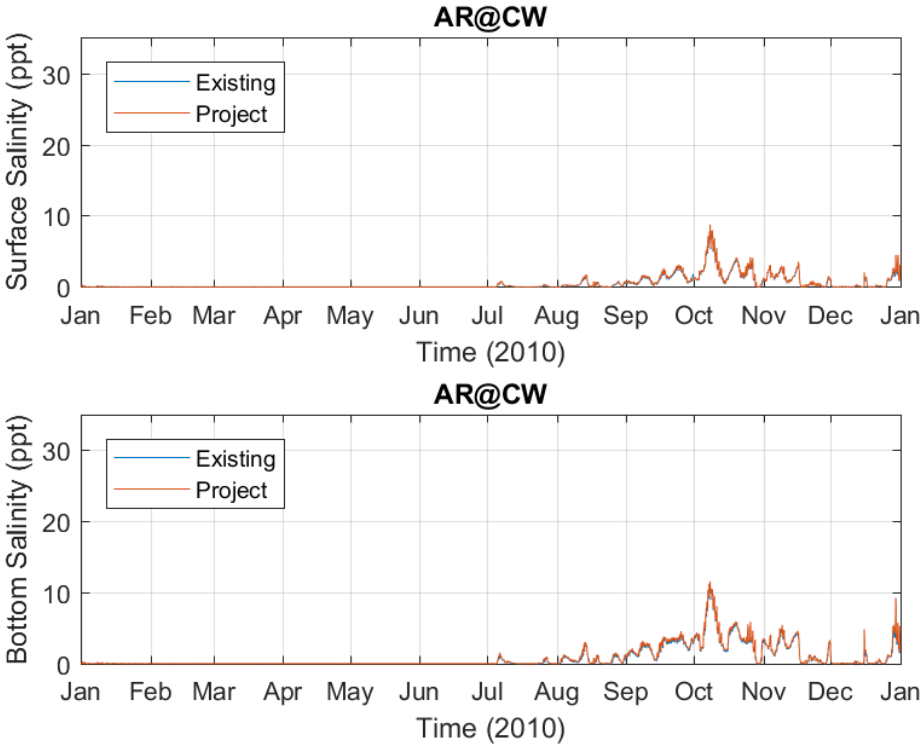

Figure 51. Time Series Comparison at AR@CW

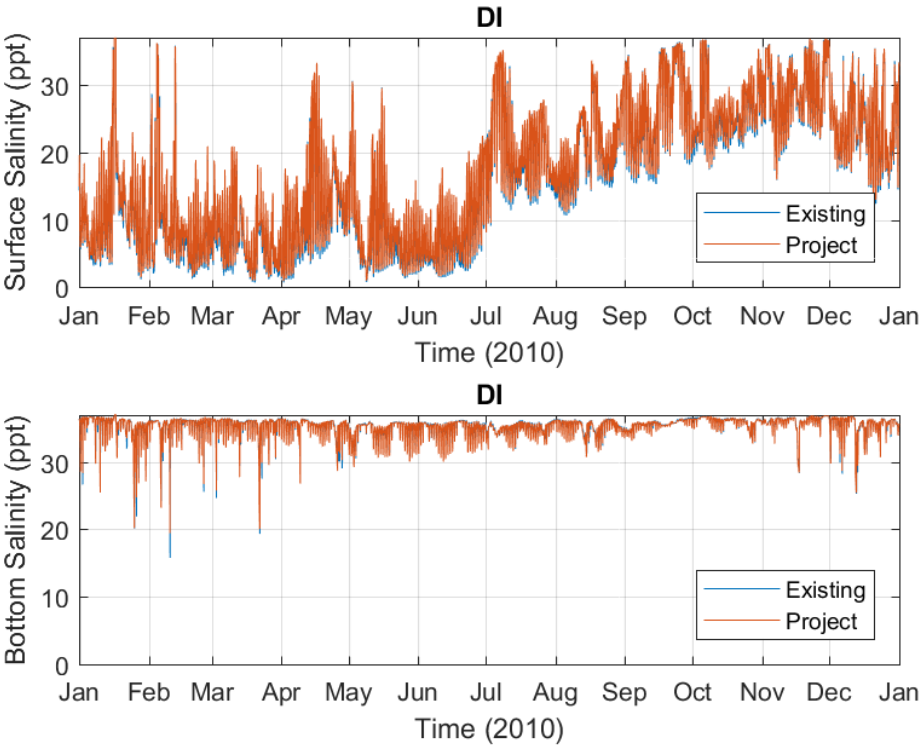

Figure 52. Time Series Comparison at Dauphin Island

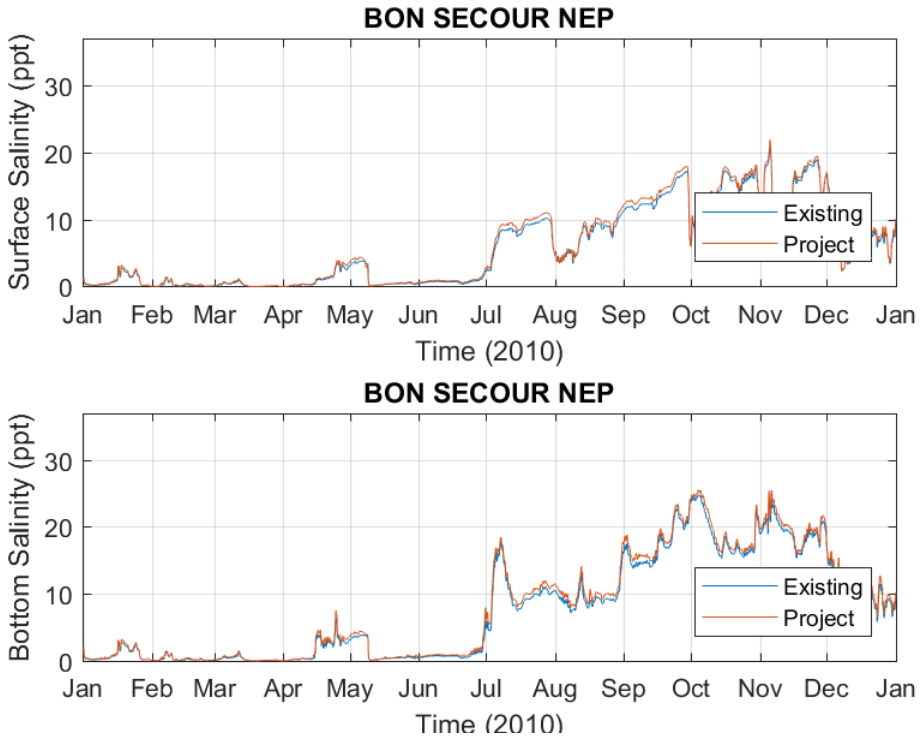

Figure 53. Time Series Comparison at Bon Secour

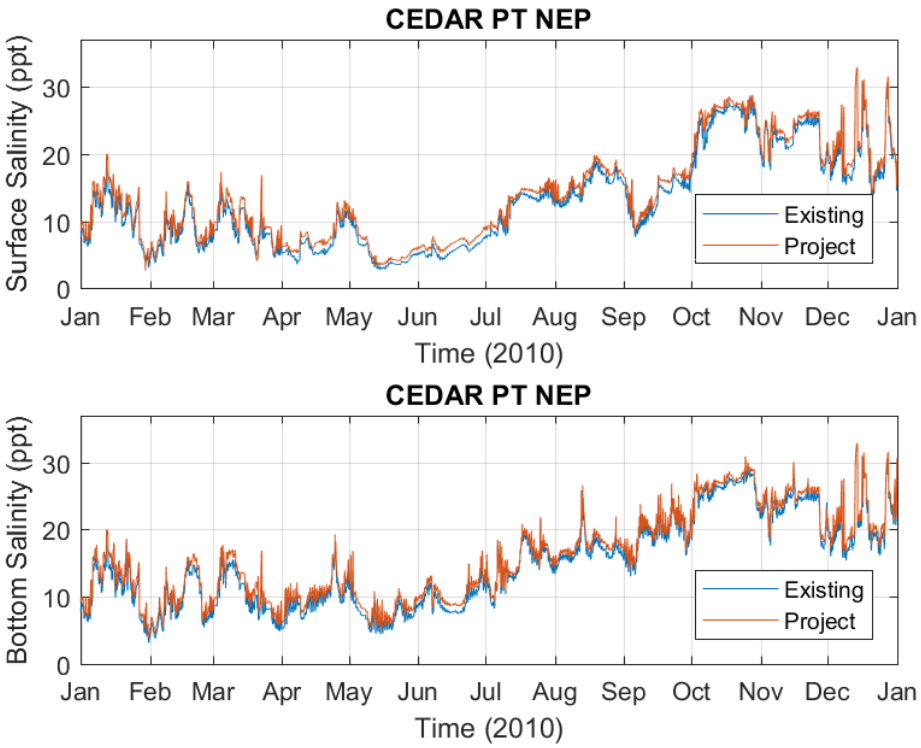

Figure 54. Time Series Comparison at Cedar Point

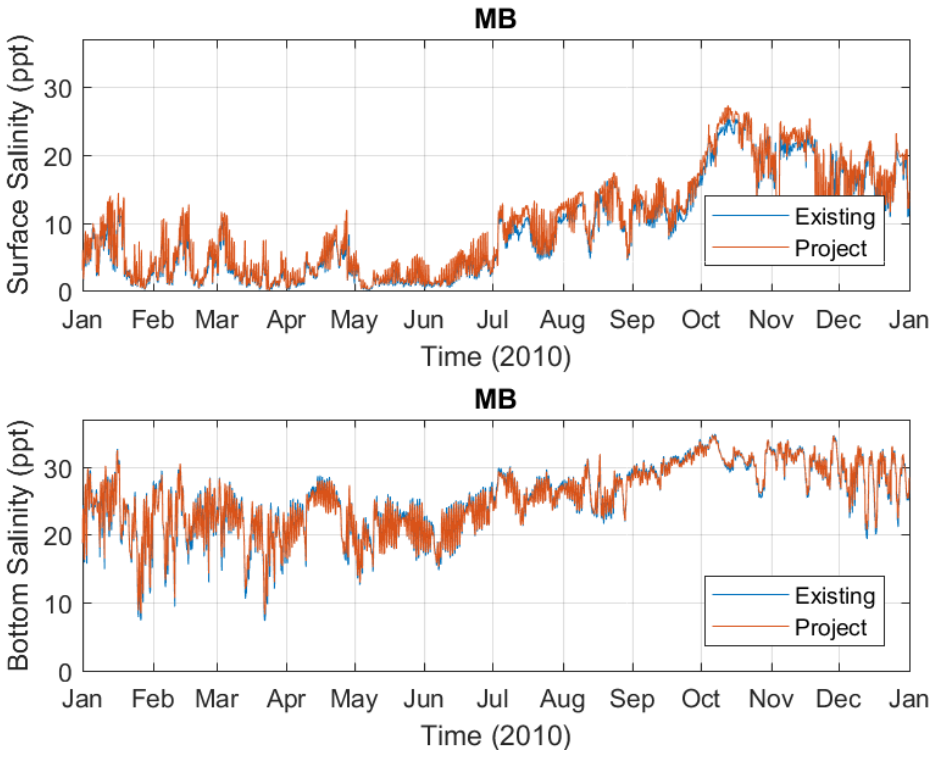

Figure 55. Time Series Comparison at Middle Bay Light

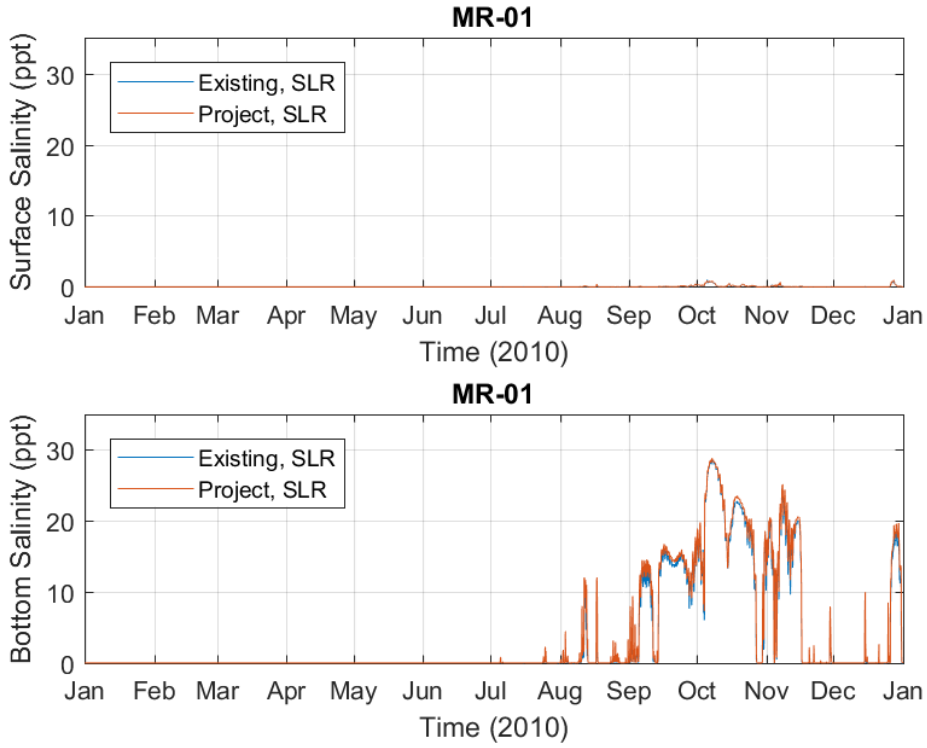

Figure 56. Sea Level Rise Time Series Comparison at MR-01

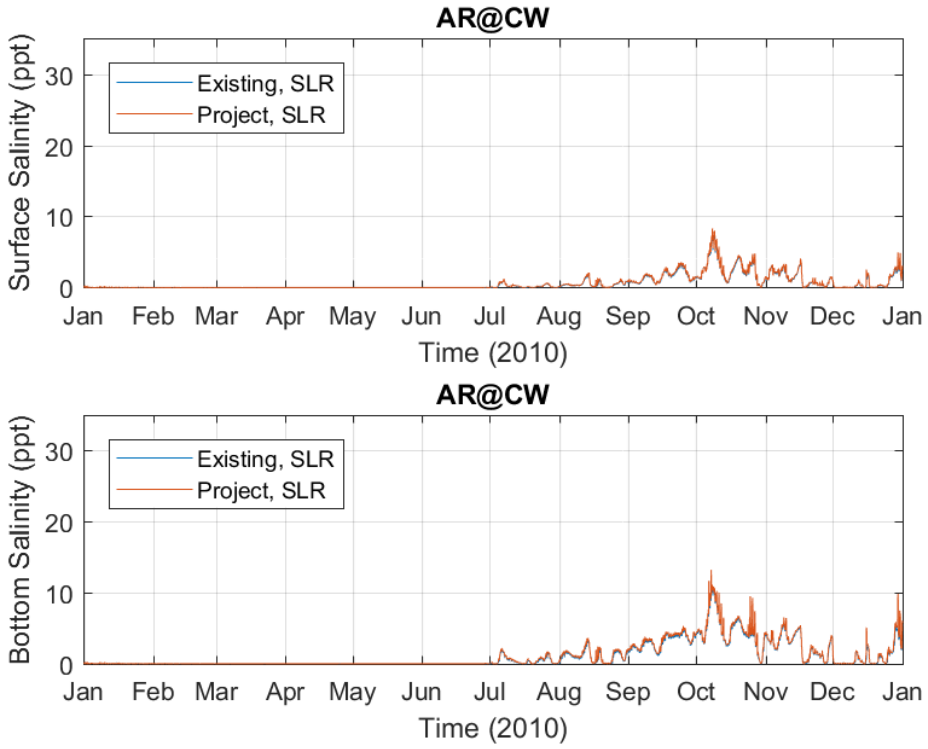

Figure 57. Sea Level Rise Time Series Comparison at AR@CW

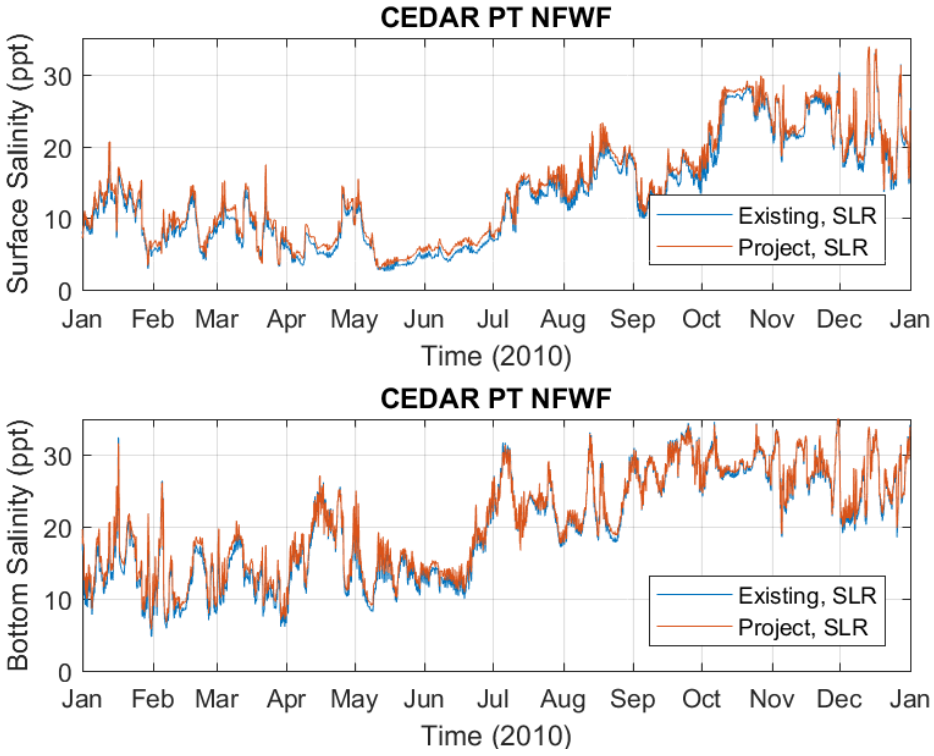

Figure 58. Sea Level Rise Time Series Comparison at Cedar Point

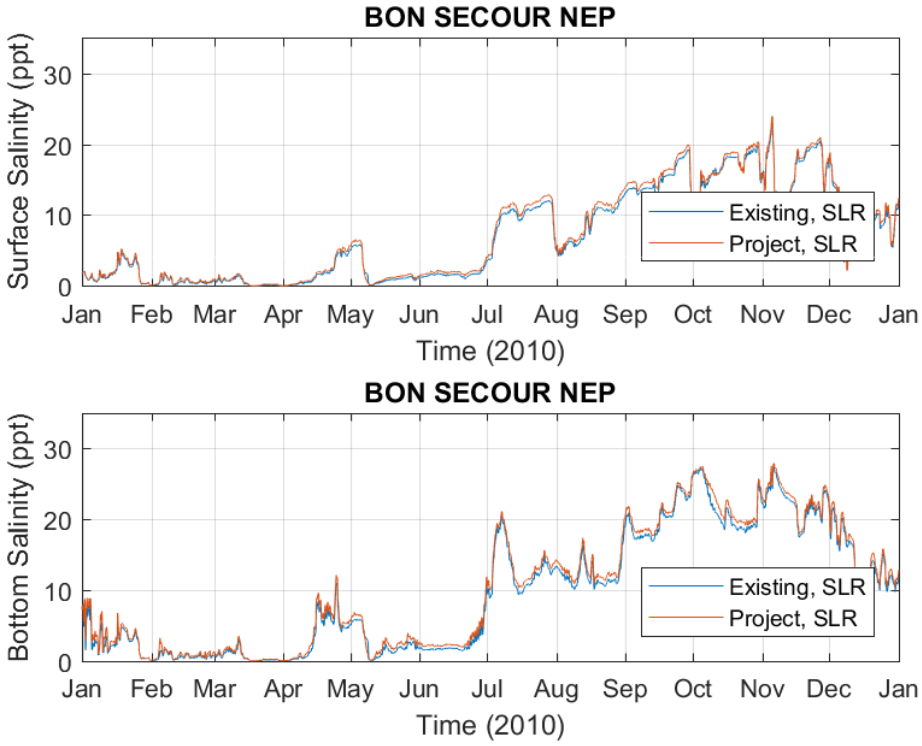

Figure 59. Sea Level Rise Time Series Comparison at Bon Secour

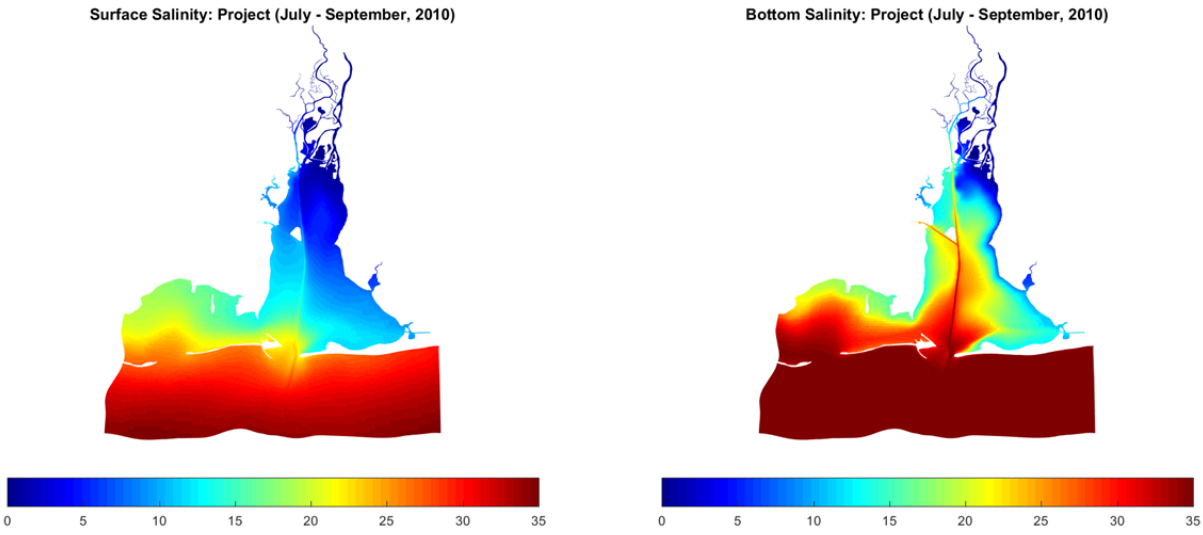

Figure 60. Mean Surface and Bottom Salinity: July – September 2010

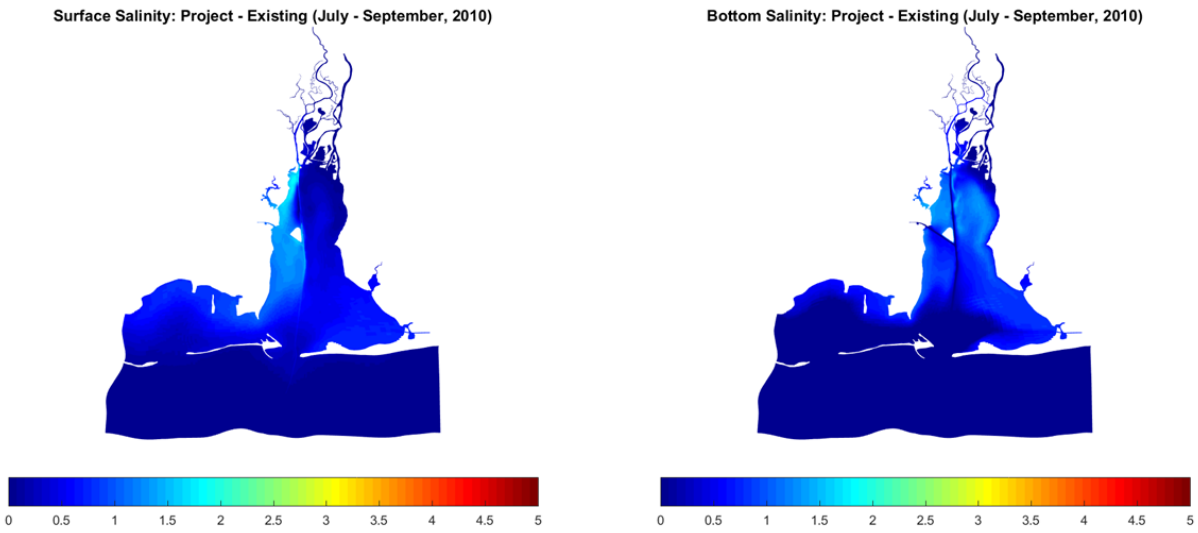

Figure 61. Differences in Surface and Bottom Salinity: July – September 2010

Multi-Block ICM Linkage and Hydrodynamic Forcing

In order to supply hydrodynamic forcing to ICM, linkage files that relate the 49 block system to a single or global water quality grid must be constructed. These linkage files provide a three dimensional mapping of multi-block grid geometry and hydrodynamics to ICM cells and flow faces. Details of the linkage process can be found in Chapman *et al.* (1997), Kim (2007) and Melendez *et al.* (2009). Hydrodynamic forcing files were provided to ICM and test simulations preformed to ensure consistent volume/mass conservation and salinity transport results. Subsequent to model testing, 2010 model simulations were performed and ICM hydrodynamic forcing generated for updated existing and project systems. Sea level rise simulations, consisting of a 0.5 m water level increase applied to the tidal forcing, were performed utilizing the existing and project systems.

Ship Simulator Support Modeling

Hydrodynamic model simulations to support the Ship Simulator Task were undertaken using the ADCIRC model described in the CSTORM-MS section above. A series of simulation generated snapshots of the hydrodynamic fields for two sub-regions of the computational domain. These sub-regions covered 1) the turning basin (TB) and approach and 2) the combined bend easing and passing lane (BEPL) previously shown. These simulations were performed with existing depths of 45 feet mllw in the Bay

and 47 feet mllw for the Bay entrance. Alternative design simulation were performed with increased depths of 51 feet mllw in the Bay and 53 feet mllw at the Bay entrance, in addition to two passing lane widening scenarios of 500 and 550 feet mllw. Combinations of a constant wind speed of 20 knots (10.2 m/s), wind directions of North, East, Southeast and West, maximum Spring tide flood and ebb tide with low flow conditions of 5000 ft^3/s (142 m^3/s) and high flow of 60,000 ft^3/s (1,700 m^3/s) were specified for both the existing and project conditions. A list of ship simulation hydrodynamic forcing is provided in Table 2.

Table 2. Ship Simulation Forcing

Wind Direction	Tide	Flow
N	Ebb	High
E	Ebb	High
W	Ebb	High
SE	Ebb	High
N	Flood	Low
E	Flood	Low
W	Flood	Low
SE	Flood	Low

Example scenario of existing condition velocity magnitude and difference plots of existing maximum current velocities subtracted from project maximum current velocities are shown in Figures 62 – 69. Figures 62 – 65 present the SE Flood maximum current velocity and difference plot for the BEPL and TB, respectively. Figures 66 – 69 present the N-Ebb maximum current velocity and difference plot for the BEPL and TB, respectively.

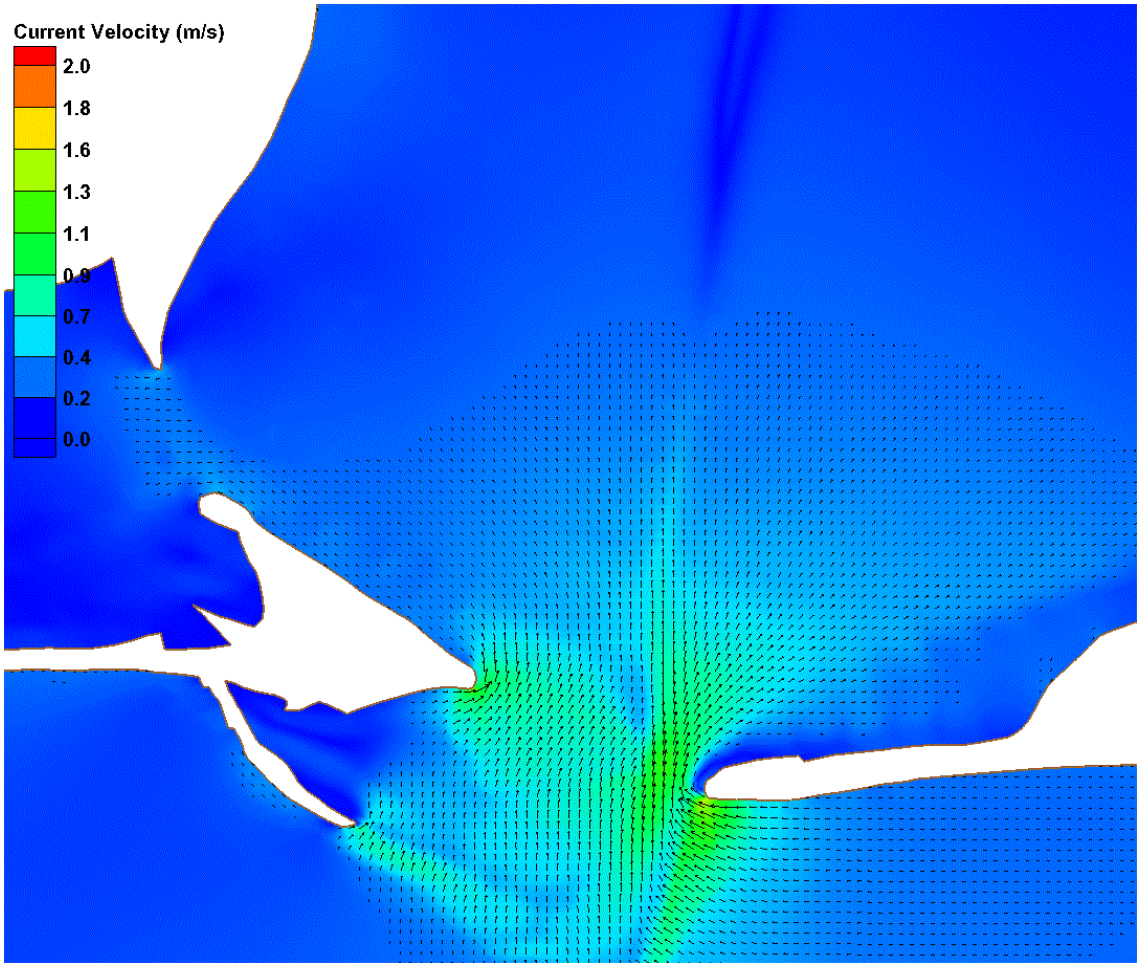

Figure 62. Maximum BEPL SE Flood Current Velocities

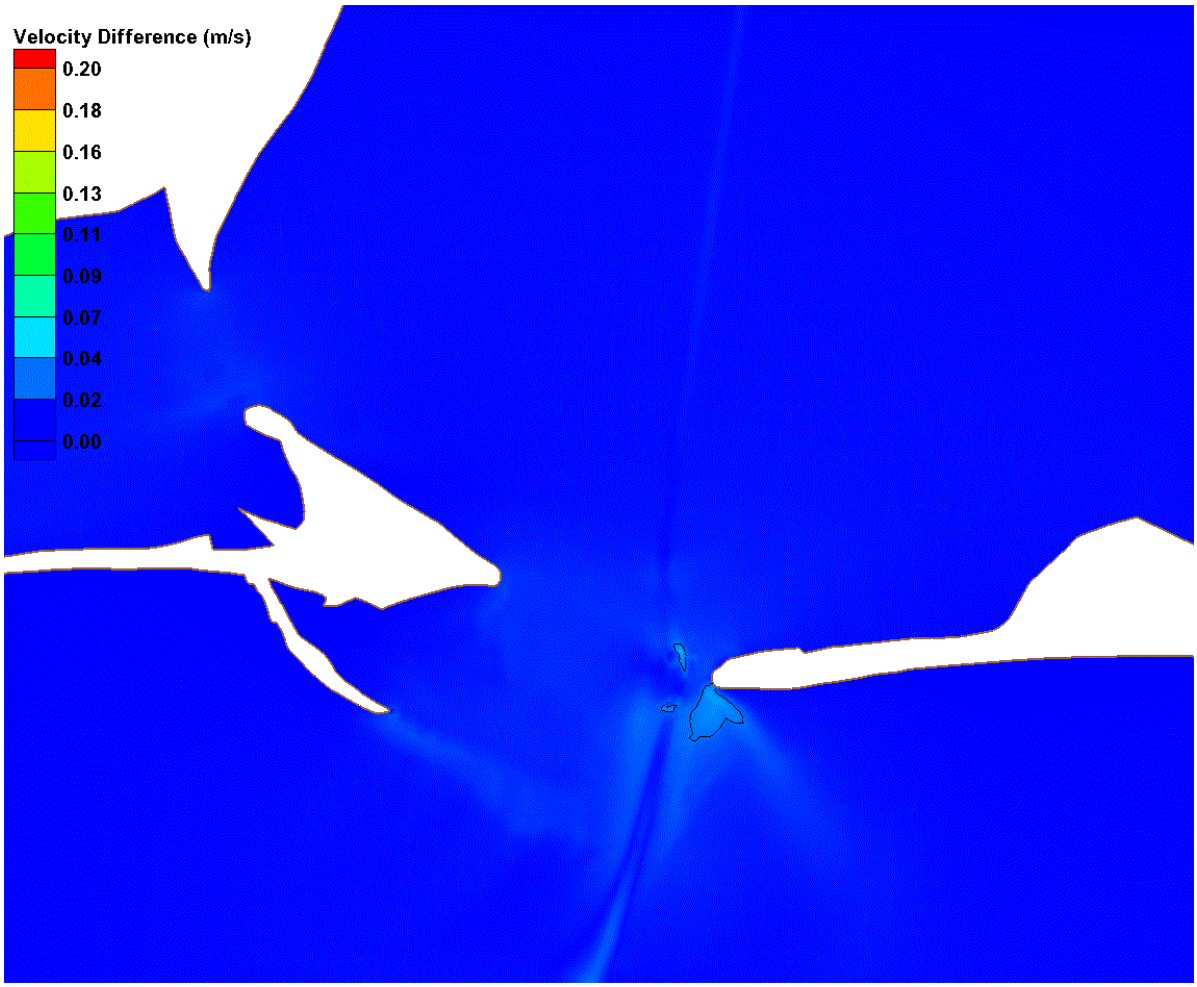

Figure 63. Maximum BEPL SE Flood Current Difference

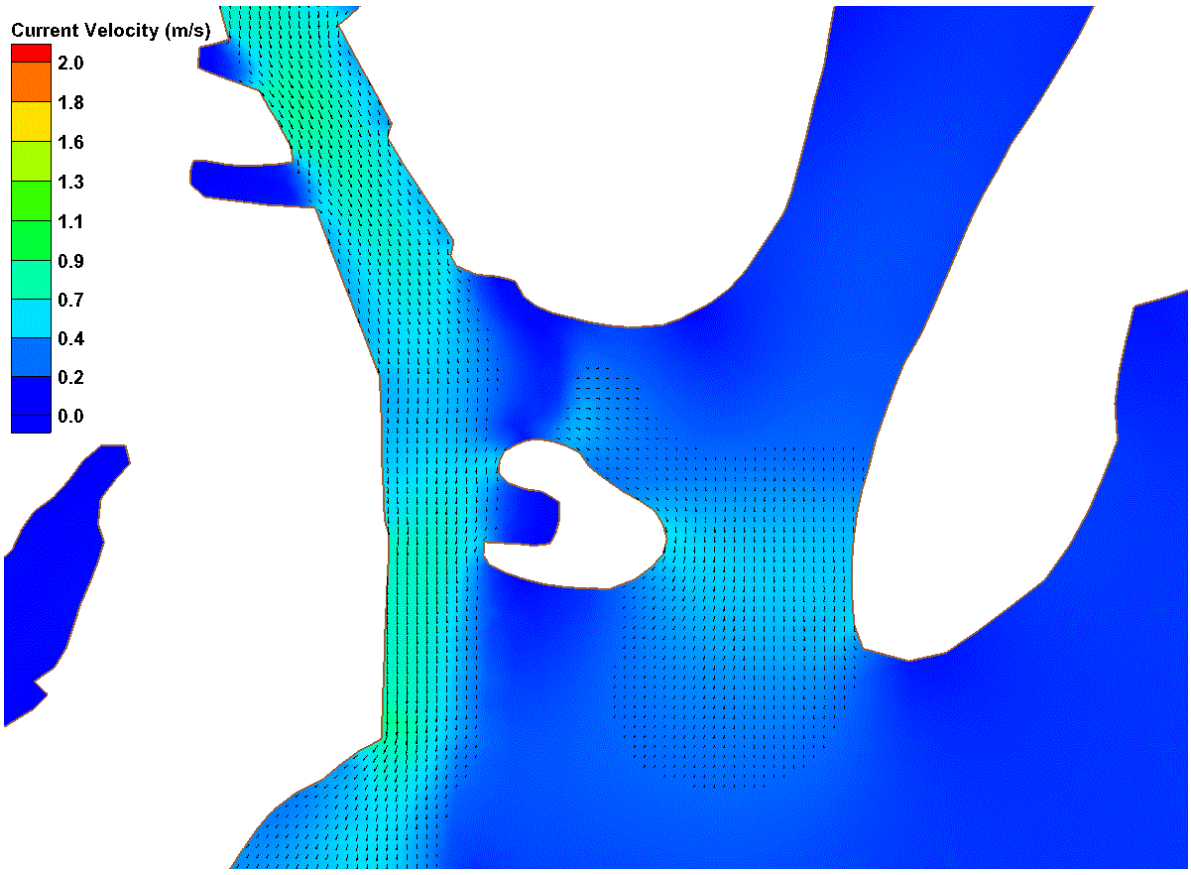

Figure 64. Maximum TB SE Flood Current Velocities

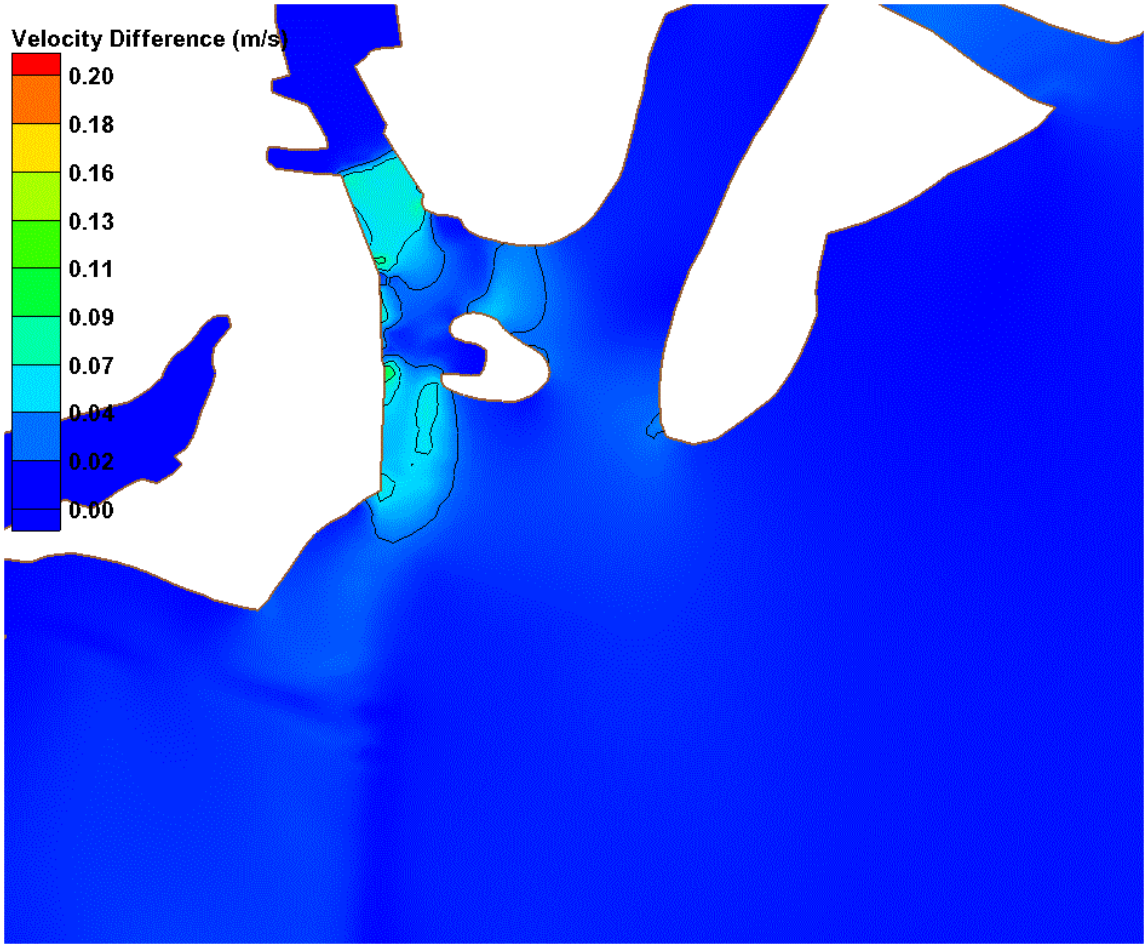

Figure 65. Maximum TB SE Flood Current Difference

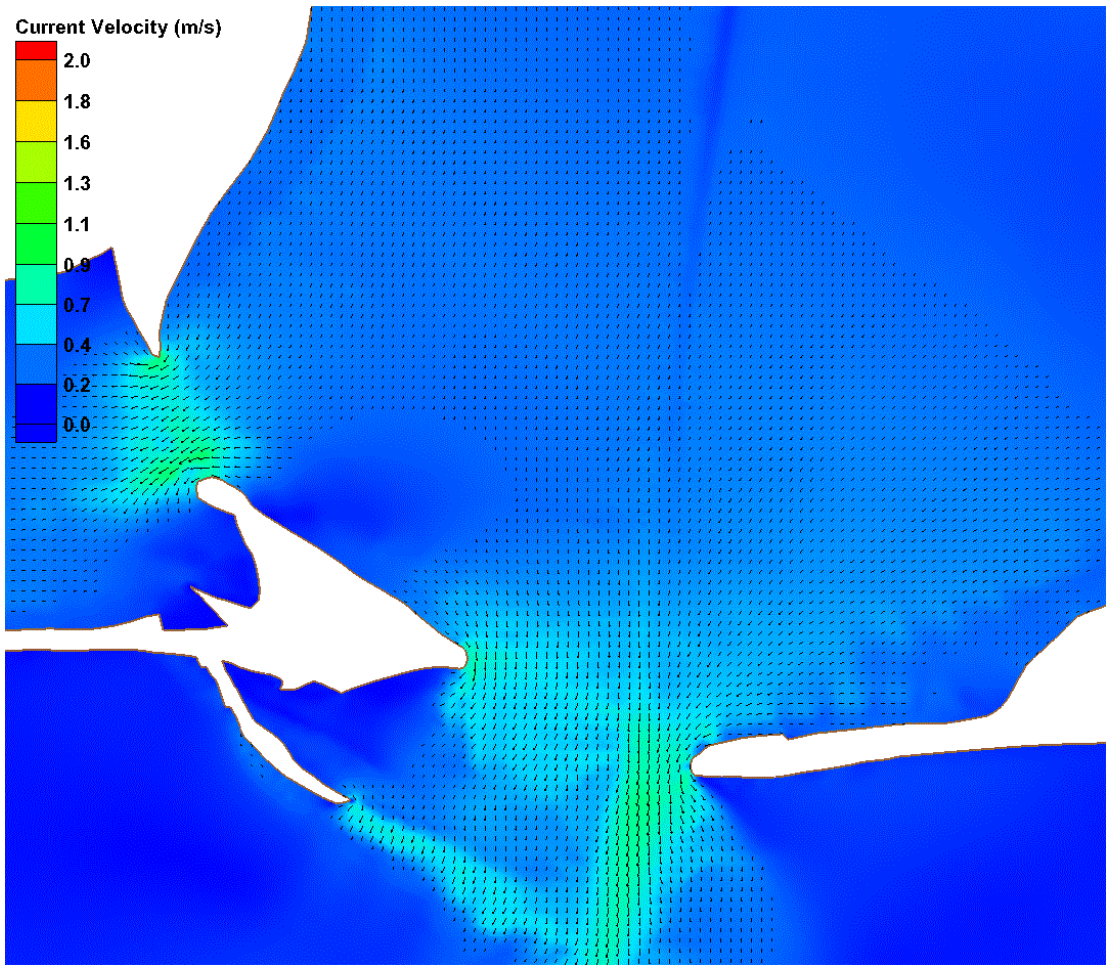

Figure 66. Maximum BEPL N Ebb Current Velocities

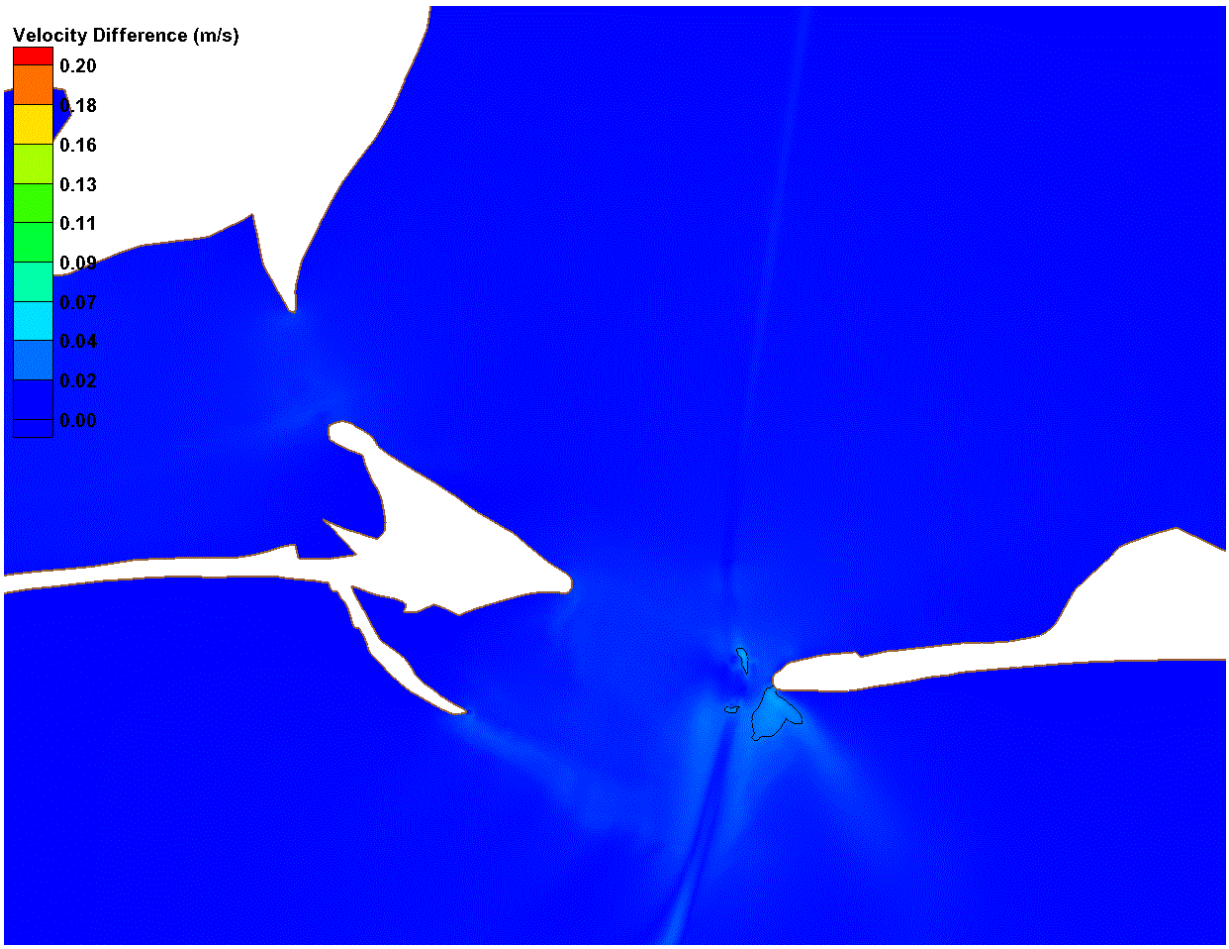

Figure 67. Maximum BEPL N Ebb Current Difference

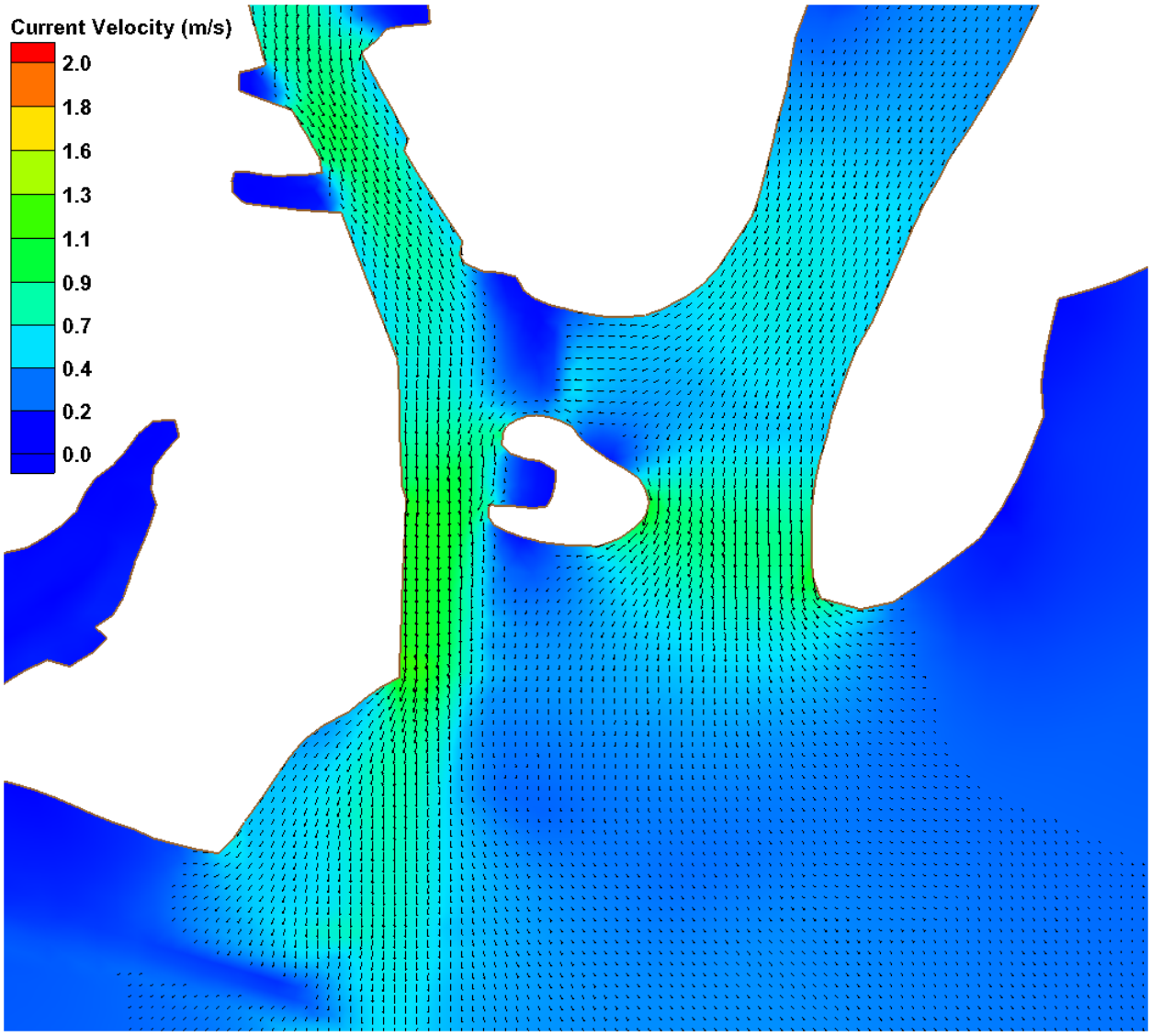

Figure 68. Maximum TB N Ebb Current Velocities

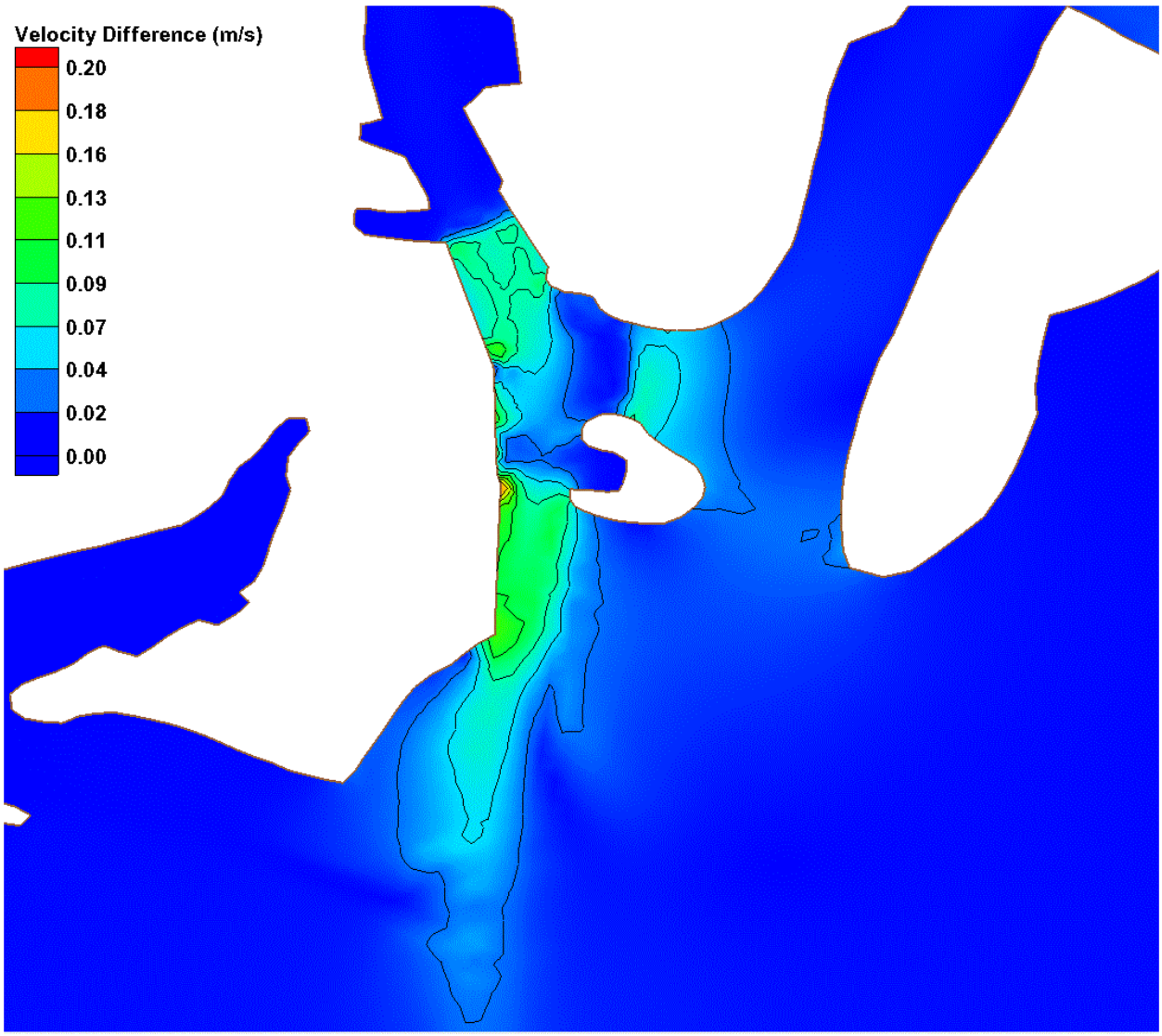

Figure 69. Maximum TB N Ebb Current Difference

Water Quality Modeling

The focus of the water quality effort was to understand the existing water quality within the waters of Mobile Bay estuary and quantify relative water quality changes resulting from proposed Mobile Harbor Federal Navigation channel modifications. A 3D water quality model was applied in concert with the hydrodynamic model GSMB. Three dimensional modeling was required to capture vertical temperature and salinity structure of existing deep-draft channels and adjoining waters. The numerical model CEQUAL-ICM was applied to quantify dissolved oxygen, salinity, temperature, total suspended solids, nutrients and chlorophyll-*a* ("Chl-a") for existing and alternatives selected. Calibration of CEQUAL-ICM was conducted through comparison to existing data. A total of four conditions were evaluated: Existing (No Project), with-Project (Existing conditions with channel modifications), No Project with-Projected future Sea Level Rise, and Project with-Projected future Sea Level Rise. When evaluating impacts the No Project and Project results were compared and the No Project with-Projected future Sea Level Rise and Project with-Projected future Sea Level Rise results were compared.

CEQUAL-ICM Water Quality Model

CEQUAL-ICM (ICM) is a flexible, widely applicable, state-of the-art eutrophication model. Initial application was to Chesapeake Bay (Cerco and Cole 1994). Since the initial Chesapeake Bay study, the ICM model code has been generalized with minor corrections and model improvements. Subsequent additional applications of ICM included the Delaware Inland Bays (Cerco et al. 1994), Newark Bay (Cerco and Bunch 1997), the San Juan Estuary (Bunch et al. 2000), Florida Bay (Cerco *et al*. 2000), St. Johns River (Tillman *et al*. 2004) and Port of Los Angeles (Bunch *et al*. 2003a and 2003b, Martin *et al*. 2008, and Tillman *et al*. 2008), Mississippi Sound (Wamsley *et al*. 2013). Each model application employed a different combination of model features and required addition of system-specific capabilities.

General features of ICM include:

Operational in one-, two-, or three-dimensional configurations

Thirty-six state variables including physical properties.

Sediment-water oxygen and nutrient fluxes may be computed in a predictive sub-model or specified with observed sediment-oxygen demand rates (SOD)

State variable may be individually activated or deactivated.

Internal averaging of model output over arbitrary intervals.

Computation and reporting of concentrations, mass transport, kinetics transformations, and mass balances.

Debugging aids include ability to activate and deactivate model features, diagnostic output, volumetric and mass balances.

Operates on a variety of computer platforms. Coded in ANSI Standard FORTRAN F77.

ICM is limited by not computing the hydrodynamics of the modeled system. Hydrodynamic information (*i.e.*, flows, diffusion coefficients, and volumes) must be specified externally and read into the model. Hydrodynamics may be specified in binary or ASCII format and are usually obtained from a hydrodynamic model such as the GSMB.

Conservation of Mass Equation

The foundation of CEQUAL-ICM is the solution to the three-dimensional mass-conservation equation for a control volume. Control volumes correspond to cells on the model grid. CEQUAL-ICM solves, for each volume and for each state variable, the equation:

$$\frac{\delta V_j C_j}{\delta t} = \sum_{k=1}^{n} Q_k C_k + \sum_{k=1}^{n} A_k D_k \frac{\delta C}{\delta x_l} + \Sigma S_j \quad (1)$$

in which:

V_j = volume of jth control volume (m^3)
C_j = concentration in jth control volume (g m^{-3})
t, x = temporal and spatial coordinates
n = number of flow faces attached to jth control volume

Q_k = volumetric flow across flow face k of j^{th} control volume ($m^3\ s^{-1}$)
C_k = concentration in flow across face k ($g\ m^{-3}$)
A_k = area of flow face k (m^2)
D_k = diffusion coefficient at flow face k ($m^2\ s^{-1}$)
S_j = external loads and kinetic sources and sinks in j^{th} control volume ($g\ s^{-1}$)

Solution of Eq. 1 requires discretization of the continuous derivatives and specification of parameter values. The equation is solved explicitly using upwind differencing or the QUICKEST algorithm (Leonard 1979) to represent C_k. The time step, determined by stability requirements, is dependent upon the grid resolution and system energy. For systems with coarser resolution under quiescent conditions time steps can be five to fifteen minutes. In the case of this system, the combination of fine resolution in the channel and rivers results in a shorted time step on the order of 15 to 30 seconds. For notational simplicity, the transport terms are dropped in the reporting of kinetics formulations. The parallel version of ICM was used for improved computational efficiency. The combination of a large number of cells, low average time steps, and long run times necessitates using a version of the model capable of operating on multiple processors in order to reduce the required "clock time" to perform simulations.

State Variables

CEQUAL-ICM incorporates 36 state variables in the water column including physical variables, multiple algal groups, and multiple forms of carbon, nitrogen, phosphorus and silica (Table 3). Two zooplankton groups, micro-zooplankton and meso-zooplankton, are available and can be activated when desired.

Of the state variables listed in Table 3, 14 variables were used in this modeling study. These were chosen based on the availability of observed data and the need to represent relevant water quality processes. Variables activated are listed in Table 4. Initial values (initial conditions) and values for inflowing waters (boundary conditions) were required for the period simulated. Where possible boundary conditions are based on observed data from sampling stations close to the physical boundary locations. Conditions for the initial simulation were uniform throughout the water column. Concentrations and other water quality conditions from the end of the first simulation were output and used as initial conditions for subsequent simulations. This output

represented a spatially varied data set. Repeating this approach repeatedly resulted in spatially distributed set of initial conditions that are reflective of the boundary conditions and processes occurring in the system.

Table 3. Water Quality Model State Variables

Temperature	Salinity
Fixed Solids	Cyanobacteria
Diatoms	Other Phytoplankton
Zooplankton 1	Zooplankton 2
Labile Dissolved Organic Carbon (DOC)	Refractory Dissolved Organic Carbon
Labile Particulate Organic Carbon	Refractory Particulate Organic Carbon
Ammonium (NH4)	Nitrate + Nitrite Nitrogen (NO3)
Urea	Labile Dissolved Organic Nitrogen (DON)
Refractory Dissolved Organic Nitrogen	Labile Particulate Organic Nitrogen
Refractory Particulate Organic Nitrogen	Total Phosphate (TP)
Labile Dissolved Organic Phosphorus (DOP)	Refractory Dissolved Organic Phosphorus (DOP)
Refractory Particulate Organic Phosphorus	Labile Particulate Organic Phosphorus
Particulate Inorganic Phosphorus	Chemical Oxygen Demand (COD)
Dissolved Oxygen (DO)	Particulate Biogenic Silica
Dissolved Silica	Internal Phosphorus Group 1
Internal Phosphorus Group 2	Internal Phosphorus Group 3
Clay	Silt
Sand	Organic Sediments

Table 4. Active Water Quality Model State Variables

Temperature	Salinity
Fixed Solids	Other Phytoplankton
Labile Dissolved Organic Carbon (DOC)	Labile Particulate Organic Carbon (POC)
Nitrate + Nitrite Nitrogen (NO3)	Ammonium (NH4)
Labile Dissolved Organic Nitrogen (DON)	Labile Particulate Organic Nitrogen (PON)
Total Phosphate (TP)	Labile Dissolved Organic Phosphorus (DOP)
Labile Particulate Organic Phosphorus (POP)	Dissolved Oxygen (DO)

CEQUAL-ICM Grid

Mobile GRR study computational grid is shown in Figures 70 and 71. The number of cells was consistent in all conditions evaluated. The only grid changes between the different cases evaluated were water column depth and cell width in the areas of proposed project modifications. These changes were incorporated in the model grid without addition or deletion of cells and maintained the same grid characteristics (number of cells, number of faces) for all cases simulated. Therefore, the characteristics of all grids for the water quality runs were the same and are listed in Table 5. Water quality model grids have the same number of cells as the hydrodynamic grid described earlier except along the ocean boundaries. Cells along the ocean boundary were removed due to differences in how ICM handle at ocean boundaries. GSMB specifies a water surface elevation or head condition at the ocean boundary while ICM requires a flow for the face along the boundary. Not including edge cells along the ocean boundary in the water quality model has no impact upon water quality computations on the interior of the grid.

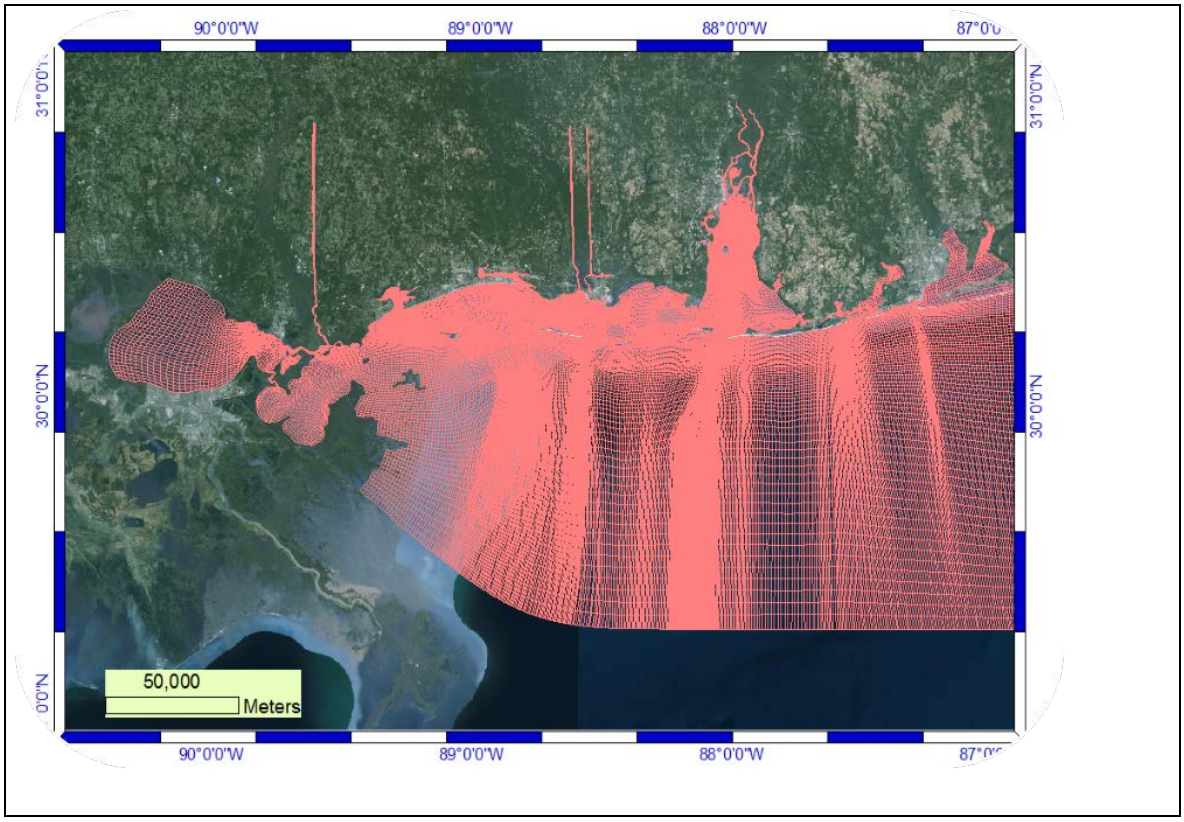

Figure 70. Study Domain for all Simulations

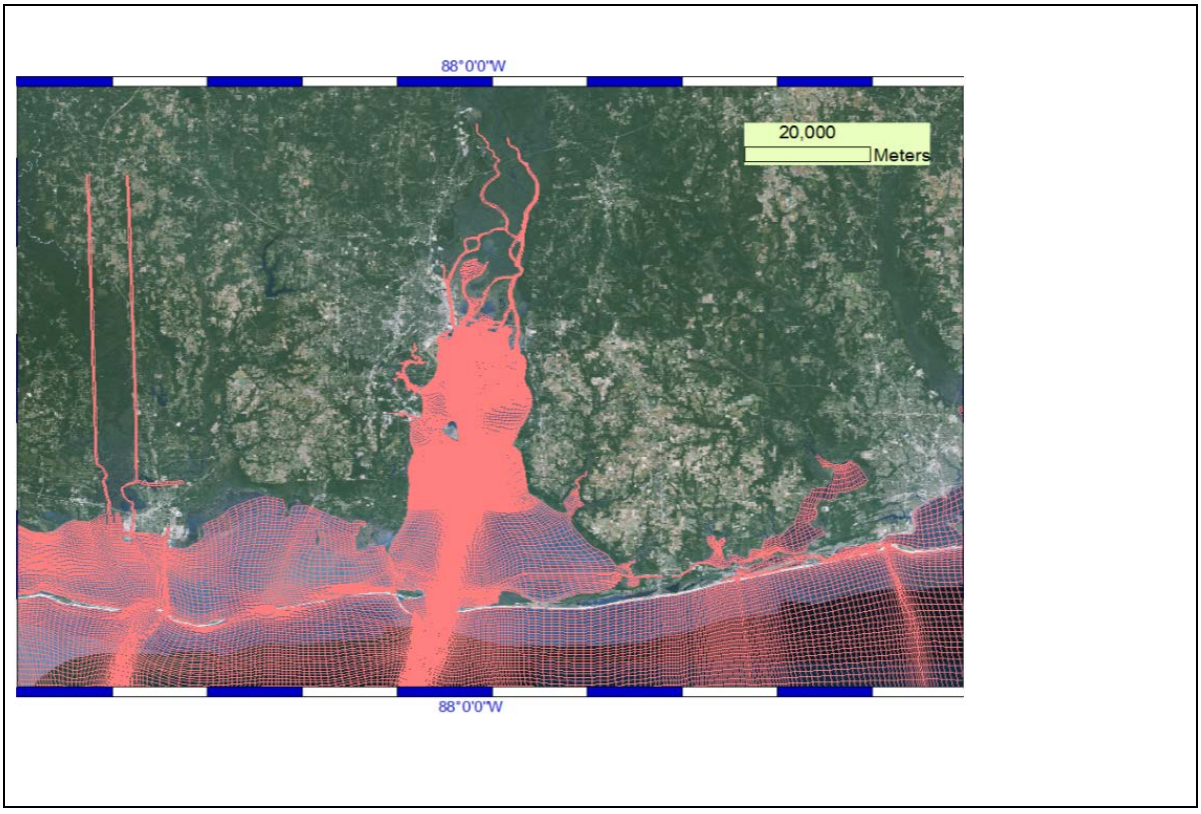

Figure 71. Hydrodynamic and Water Quality Model in Mobile Bay Estuary

Table 5. Water Quality Grid Characteristics

Grid Features	Existing, Project, SLR, Project with SLR
Total Cells	826830
Surface Cells	82683
Total Flow Faces	2370527
Horizontal Flow Faces	1626380
Surface Horizontal Flow Faces	162638

Data Requirements

The following data are required for an application of ICM:

1. Bathymetry
2. Observed data
3. Initial conditions
   a. Temperature
   b. Water quality constituents
4. Boundary conditions
   a. Inflow/outflow
   b. Temperature
   c.Water quality
5. Meteorology

These data initialize conditions at the start of a model run and provide time-varying inputs that drive the model during the course of a simulation. The role of each in the model is described below.

Bathymetry

Bathymetric information described the physical shape (depths, widths) of the waterbody bottom. This information is obtained from the GSMB hydrodynamic and linkage files. Together they define the depth of the water column and the relationship of the individual cells to one another so that the ICM appropriately replicates the actual system structure. ICM uses a single

grid configuration of the GSMB multi-block grids described previously including ten vertical layers.

Observed Data

Information for water quality constituents being simulated are necessary to insure the model reasonably represents the biological, chemical, and physical processes occurring in the system. These data do not need to be continuous but should be of such frequency that it realistically is representative of the changes that occur in the system. Observed data are used for three purposes:

1. Define the initial conditions (concentrations, temperature) in the model.
2. Define the conditions at the edges, or boundary, of the model where inflows occur.
3. Serve as a check on model performance with model predictions being compared to observed data.

A brief discussion of these follows.

Boundary Conditions

Water quality conditions for inflowing waters of rivers to the model domain are specified as boundary conditions. These values change with time and are based on observations at or near those locations. Boundary conditions in this study are varied monthly to reflect the change in inflowing water quality conditions. Data for the year 2010 were used to specify boundary condition data where possible. Data from other periods were used to augment when necessary. Data from Alabama Department Environmental Management (ADEM) and Mississippi Department of Environmental Quality (MDEQ) monitoring stations were used for this purpose. Emphasis was placed on the Mobile and Tensaw rivers based on their proximity to study area.

Offshore boundary conditions were set using the GOM-9 station. Riverine inflows included the Pearl, Jordan, Wolf, Biloxi, West Pascagoula, Fish, Mobile, West Tensaw, East Tensaw, Perdido, Escambia, and Blackwater rivers. Boundary conditions for the West Tensaw were developed using water quality data from MOMB1 station. East Tensaw boundary conditions were based on data from Mobile River at Mount Vernon. Data from the MDEQ station near Kiln were used for the Jourdan boundary and also the Pearl,

Escambia, Perdido, and Blackwater. Wolf River boundary conditions were developed using MDEQ station near Lizana. Wolf boundary values were also used for Biloxi. Escatapwa observations were used to set boundaries for the Fish and West Pascagoula rivers.

Once these boundary inflowing waters are in the model their water quality conditions mix with the waters within the model domain and are affected by the ongoing water quality processes.

Point source loads for the year 2010 were included at two locations. The Clifton Municipal Wastewater Treatment Plant and Kimberly Clark. Loads were updated monthly and distributed over the entire water column at the point of discharge. Benthic fluxes consisted of Sediment Oxygen Demand (SOD). SOD was modeled as 0.25 g/m^2 offshore and 1.0 g/m^2 in estuarine waters.

Initial Conditions

Initial conditions are important to ensure that the model represents the conditions that exist prior to the time period being simulated. A set of uniform initial conditions approximating the expected conditions at the being of the model simulation are applied to the whole model. The model was run for a period of time during which the physical, chemical, and biological processes in the model alter the conditions in the individual cells of the model. When the simulation is complete, the final concentrations and values for all modeled constituents in all cells are output. These values represent a spatially varying concentration and temperature field that was generated by the modeled processes and conditions. This varied field was then used as initial conditions for a subsequent simulation. An advantage of this approach is that the initial condition at a location is more representative of the process in the model than they would be with uniform initial condition values.

Initial conditions for the water column were specified as uniform for all layers based on observed data closest to the simulation start day of January 1, 2010. To provide a more realistic, *i.e.*, spatially varied, initial conditions in the study area, ICM was run for 60 days using the uniform initial conditions discussed above and the concentration field for all constituents output at the end of the simulation. These values were then used as initial conditions for a subsequent simulation. This process was repeated until a spatially varying set of initial conditions that were consistent with observations were obtained.

Comparison Data

Comparison data have no direct effect on model computations but are used to assess model performance. Care must be taken to match the observed data with model output that corresponds to the time and place the data was collected. Model concentration output consists of daily averaged values for all water constituents modeled. Observed data used for comparison are likely one-time instantaneous observations and measurements. As such they are subject to not reflecting changing conditions that are captured in the daily average water quality model output.

Meteorological Data

Meteorological data measured at Mobile Regional Airport for the calibration period (2010) was obtained from the Air Force Combat Climatological Center. Daily values for cloud cover, dry bulb temperature, dew point temperature, and wind speeds were used in the heat exchange program (Eiker 1977) to compute heat exchange coefficients, solar illumination, fractional day length, and equilibrium temperature. These data are contained in Appendix D. Appendix D contains ICM kinetic (the rate of change in a biochemical or other reaction) rates files used in this study. Complete descriptions of the kinetic processes in ICM can be found in Cerco and Noel (2004). Also contained in Appendix D are the settling file for solids and particulates, light extinction file, and a copy of the ICM control file.

Calibration

Calibration was accomplished through an iterative process consisting of running ICM, comparing model output to observed data, and modifying kinetic rates, boundary conditions, and other model inputs and controls until comparisons were acceptable. Model performance was evaluated using visual comparison of model results with observed data. Figure 72 indicates some of the stations that were used for calibration. Emphasis was placed on stations in the Mobile Bay itself. Time-series plots of model output and observed data demonstrate model performance over time and provide indications of interactions between modeled parameters.

Primary assessments of model performance were made using time series plots of model output and observations. In cases for surface conditions or when the water column is completely mixed this approach proved

insightful. Surface DO and temperature are examples throughout the simulation.

ICM model results consisted of daily average values output from the start of simulation for all constituents for all cells in the water quality grid. Model performance was evaluated by comparing model output for cells corresponding to physical locations with observed data. Where depths are indicated for observed data model cells corresponding to that location were used for comparison. Points to consider when viewing the plots are: 1) model output represent cell and daily average concentrations, whereas observed data are instantaneous point measurements and 2) parameters such as dissolved oxygen and salinity show significant daily variations in response to meteorology, diurnal effects, and tidal action.

Calibration Results and Discussion

Time series results for temperature are shown in Figures 73 for selected sites. These time series are for the surface layer for the period January 1, 2010 through December 31, 2010. Together these stations bound the study area and also illustrate conditions at areas of special interest. As in evident in Figure 73, the model performs well in temperature prediction. The seasonal variation in temperature is well captured.

As the simulation progresses for locations further south in the Bay, the impact of the river inflows decreases, resulting in more variation in surface temperature in response to tidal and wind induced circulation and coastal inflows.

Time series for surface and bottom ICM salinities are presented in Figures 74 and 75. The variation of salinity levels seen in these figures is primarily transport and mixing resulting from hydrodynamic forcing. Overall, modeled surface salinity levels agree well with observations. The agreement at the stations in the rivers indicate that the model is performing well for both the surface and bottom salinities. These station's model results transition from the river flow dominated early portion of the simulation to the low flow tidal influenced salt water intrusion period of the later simulation. By capturing this behavior the model indicates that it is suited to capture the impacts that these processes have on water quality over a range of hydrodynamic conditions throughout the year. It also indicates that the model

is suited to quantify issues in the riverine areas resulting from alteration of the salt water intrusion potentially due to changes in channel bathymetry.

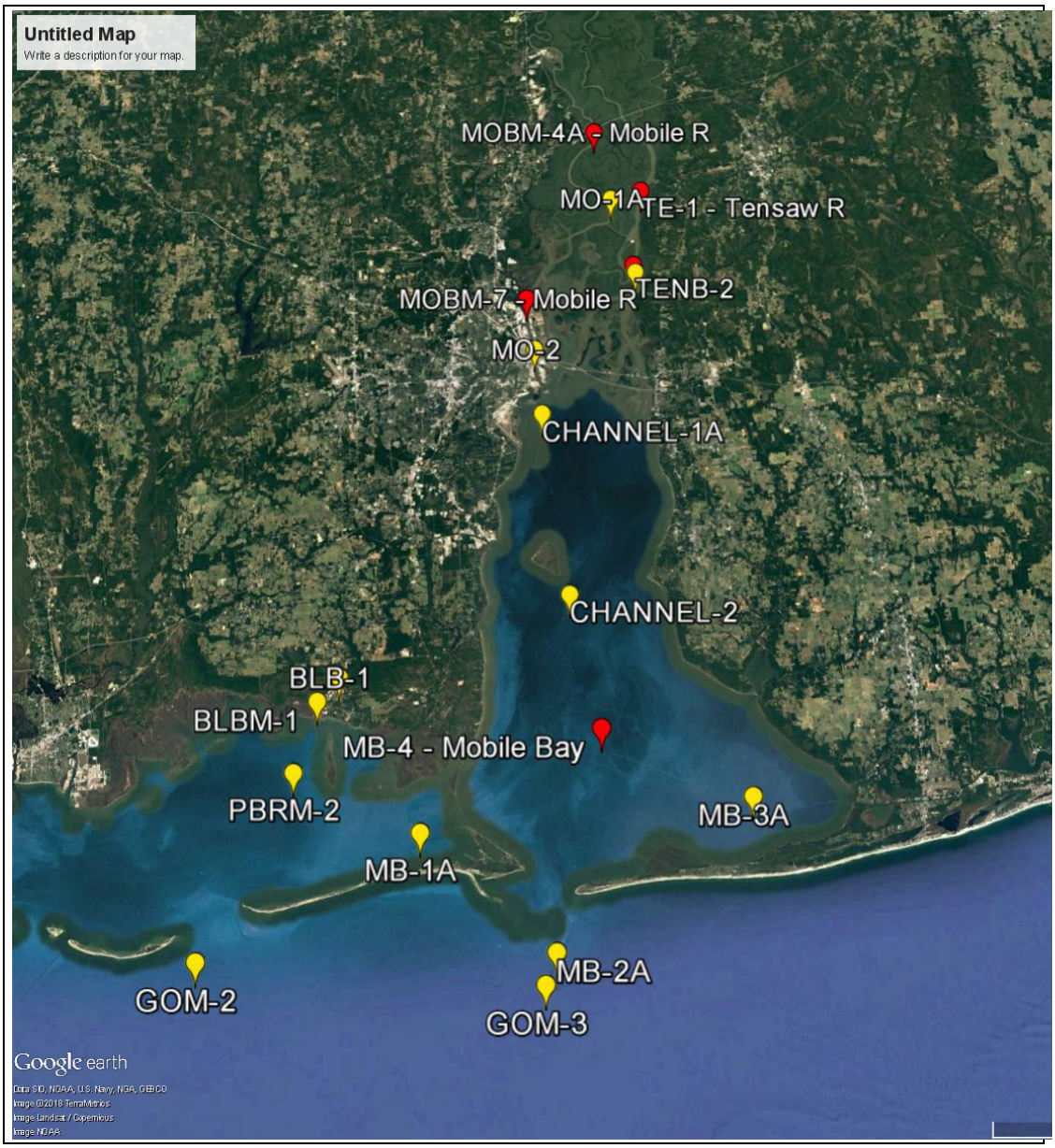

Figure 72. Stations used for Model Calibration

Calibration results for Dissolved Oxygen (DO) indicate model performance for surface DO was reasonable (see Figure 76). Early in the simulation corresponds to cold weather conditions during which oxygen saturation is highest and biological activity is reduced. The water column was generally completely mixed due to higher river inflows. DO levels decreased with time in the first third of the year and the model captured trends in the

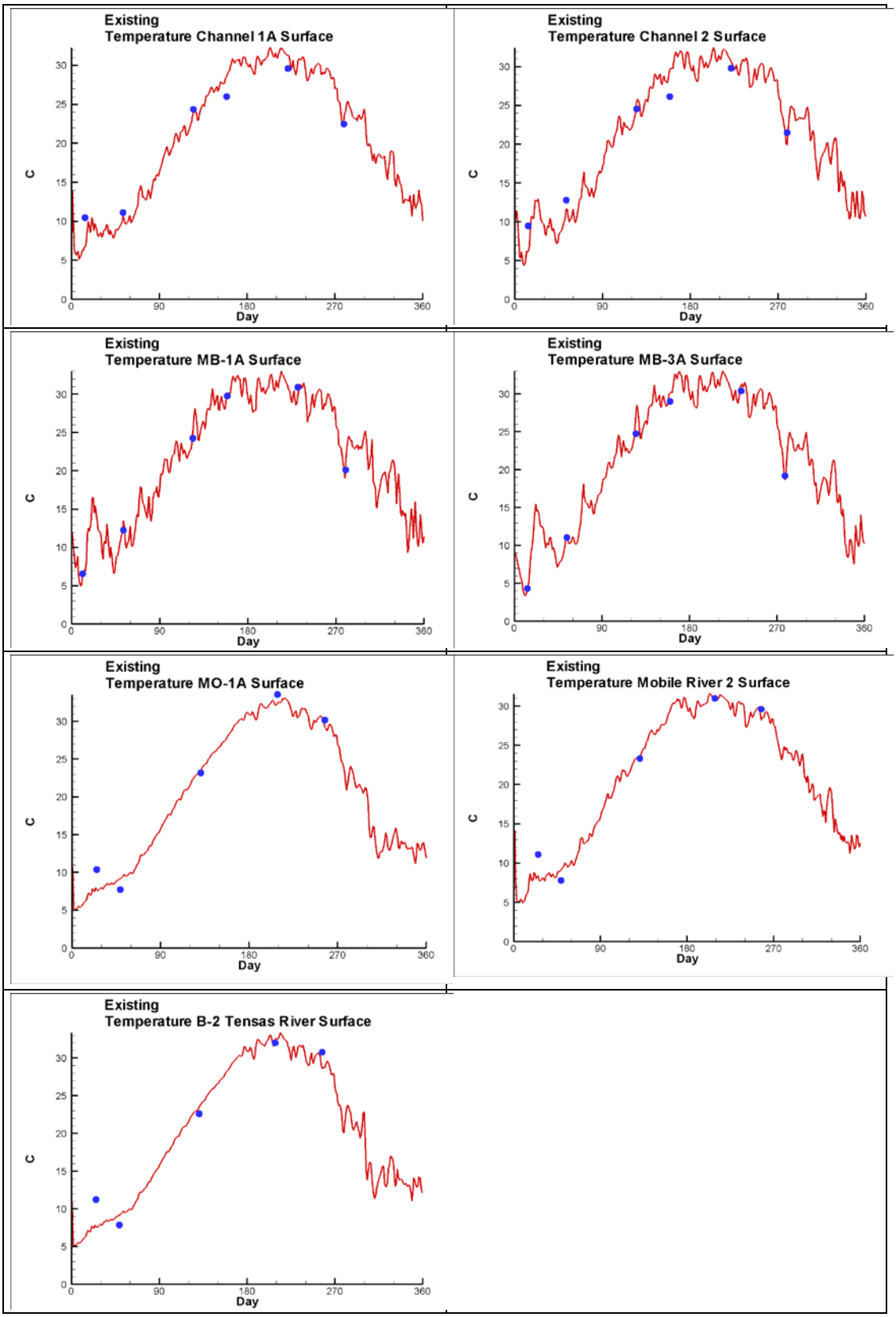

Figure 73. Comparison of Simulated and Measured Temperatures

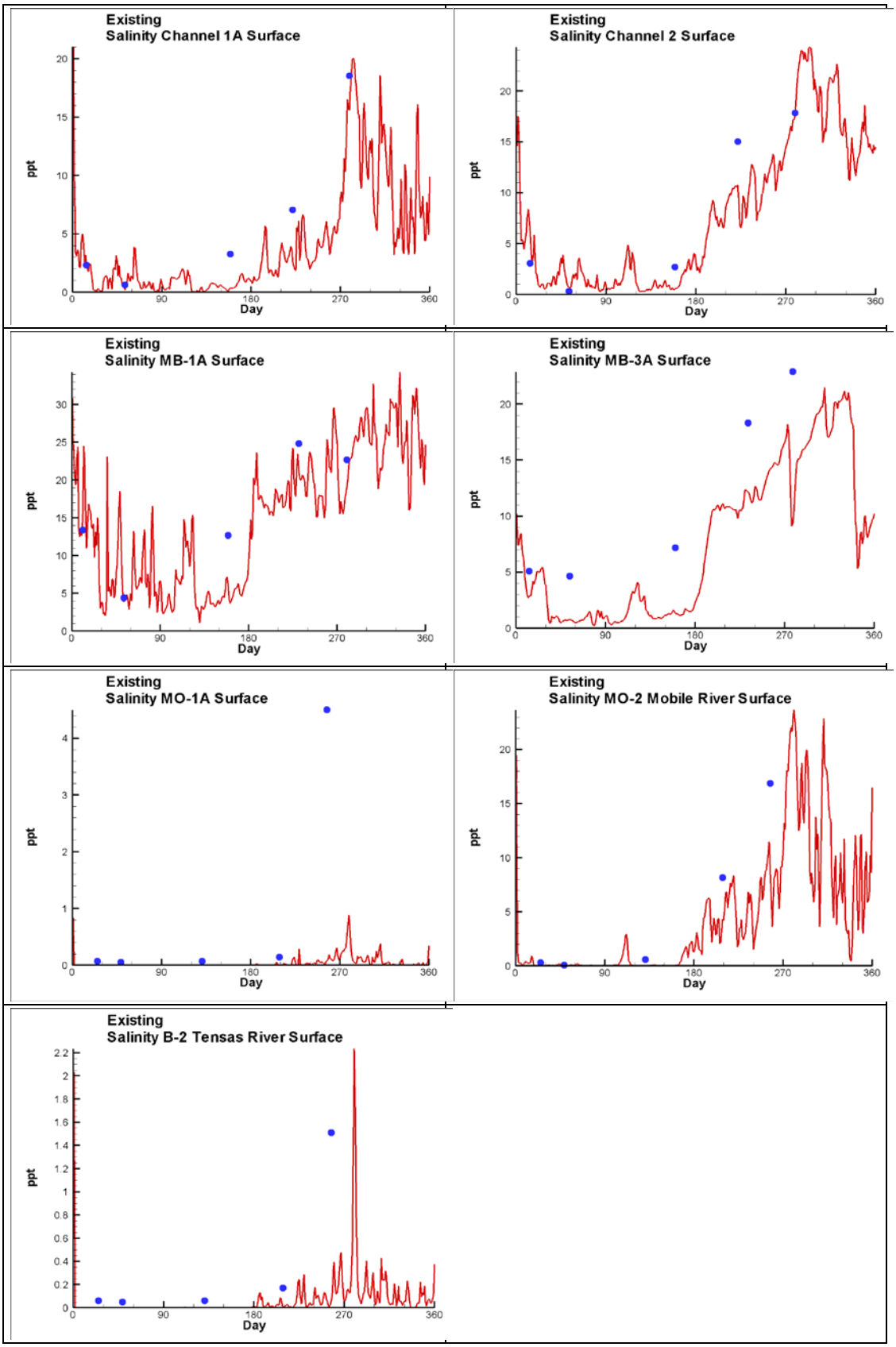

Figure 74. Comparison of Simulated and Measured Surface Salinities

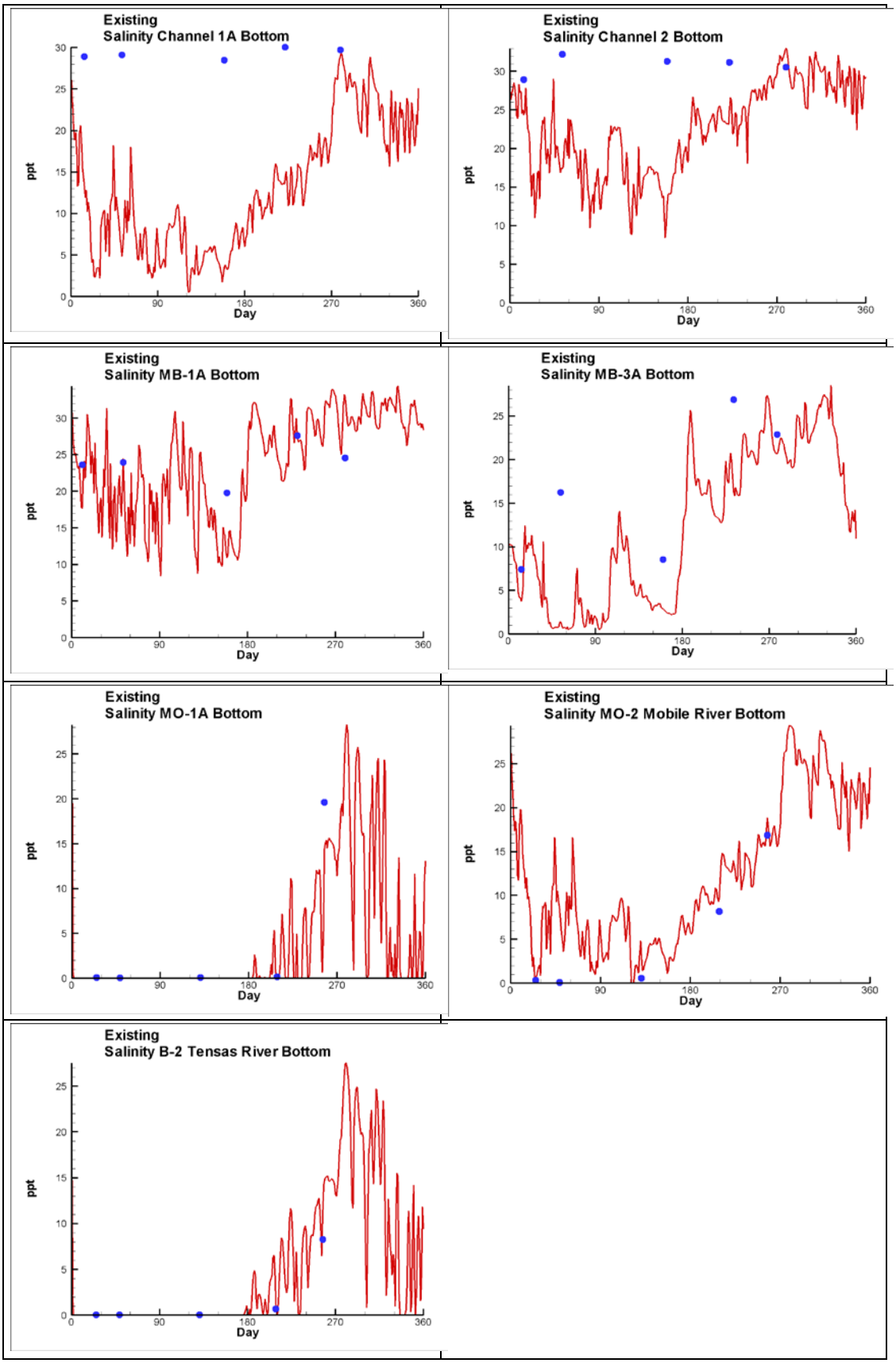

Figure 75. Comparison of Simulated and Measured Bottom Salinities

observed data. Surface DO levels for the Channel 1 and Channel 2 locations indicated that the model captured the observed behavior in DO for the duration of the year-long simulation. In the vicinity of Mobile River mouth, MO-1A and Mobile River 2, ICM performed reasonably for the first half of the simulation but over-predicted surface DO in comparison to the two observed data points between Day 180 and 270. Similar behavior is seen for the Tensaw River B-2 station. This is possibly due to unaccounted for loadings exerting oxygen demands in these locations.

Dissolved Oxygen results for surface waters indicate that the model performed well and was able to capture changes in DO as a result of temperature and circulation influences. In general, during the first period of the year, tributary inflows and their associated water quality played more significant roles in many locations in the system. Stations located in rivers, channels or even the upper Bay were dominated by the riverine flows and riverine water quality. In many instances the waters at these locations were completely mixed with there being little variation from surface to bottom. As the simulation progressed and tributary inflows decreased, tidal flushing and coastal processes dominated flow conditions with offshore waters imparting in larger influences in DO and water quality conditions. With the riverine and tributary flows lower at times more vertical variation was observed in the water column and even the surface. The irregular patterns exhibited at the riverine and channel stations during the later third of the simulation are indications of this. Stations in the lower portion of the Bay, MB-1A and MB-3A also had reasonable model results for surface DO in comparison to data.

Bottom DO results for Station MO-1A on the Mobile River (see Figure 77) indicated that the model captured the bottom DO levels well during the first 6 months. In the latter half of the simulation, DO levels gyrated with frequent swings of several mg/l of daily average DO. DO varied from 8 or greater mg/L to 3 mg/L during this period. Model predictions corresponded well to the two samples during this period of time. These swings were due to fluctuating boundary inflows enabling an influx of Bay waters with high salinities and lower DO. These low river flow-Bay water intrusion periods tended to be more quiescent allowing SOD to exert a greater influence on the bottom of the water column. Further downstream at Mobile River Station 2 model water column bottom DO levels were elevated to near those of the surface level during the first months of the simulation. This is indicative of a completely mixed water column and would be expected with high flow conditions. As the simulation period progressed DO levels decreased in response to a combination of factors including increasing temperature and

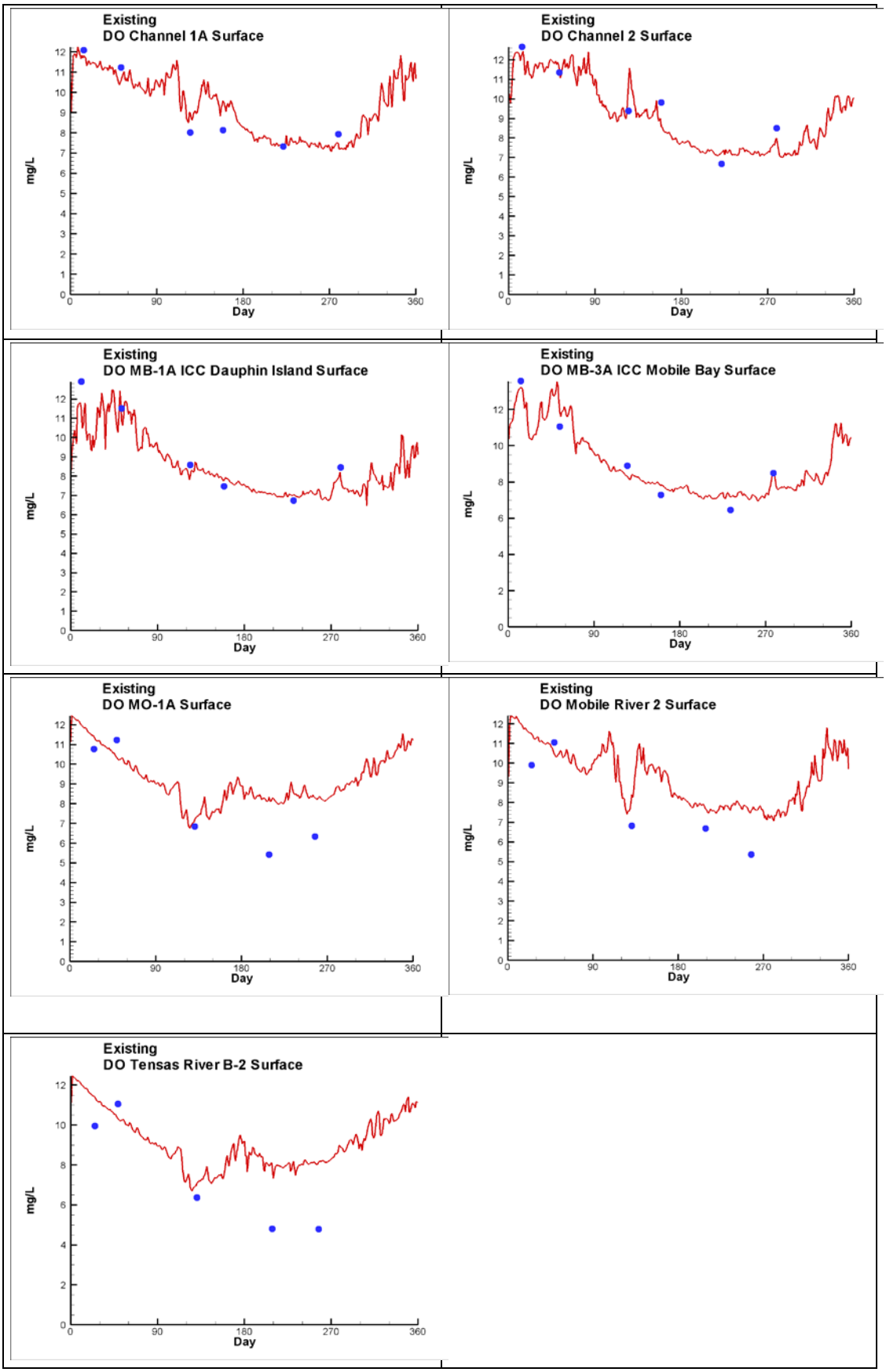

Figure 76. Comparison of Simulated and Measured Surface DO values

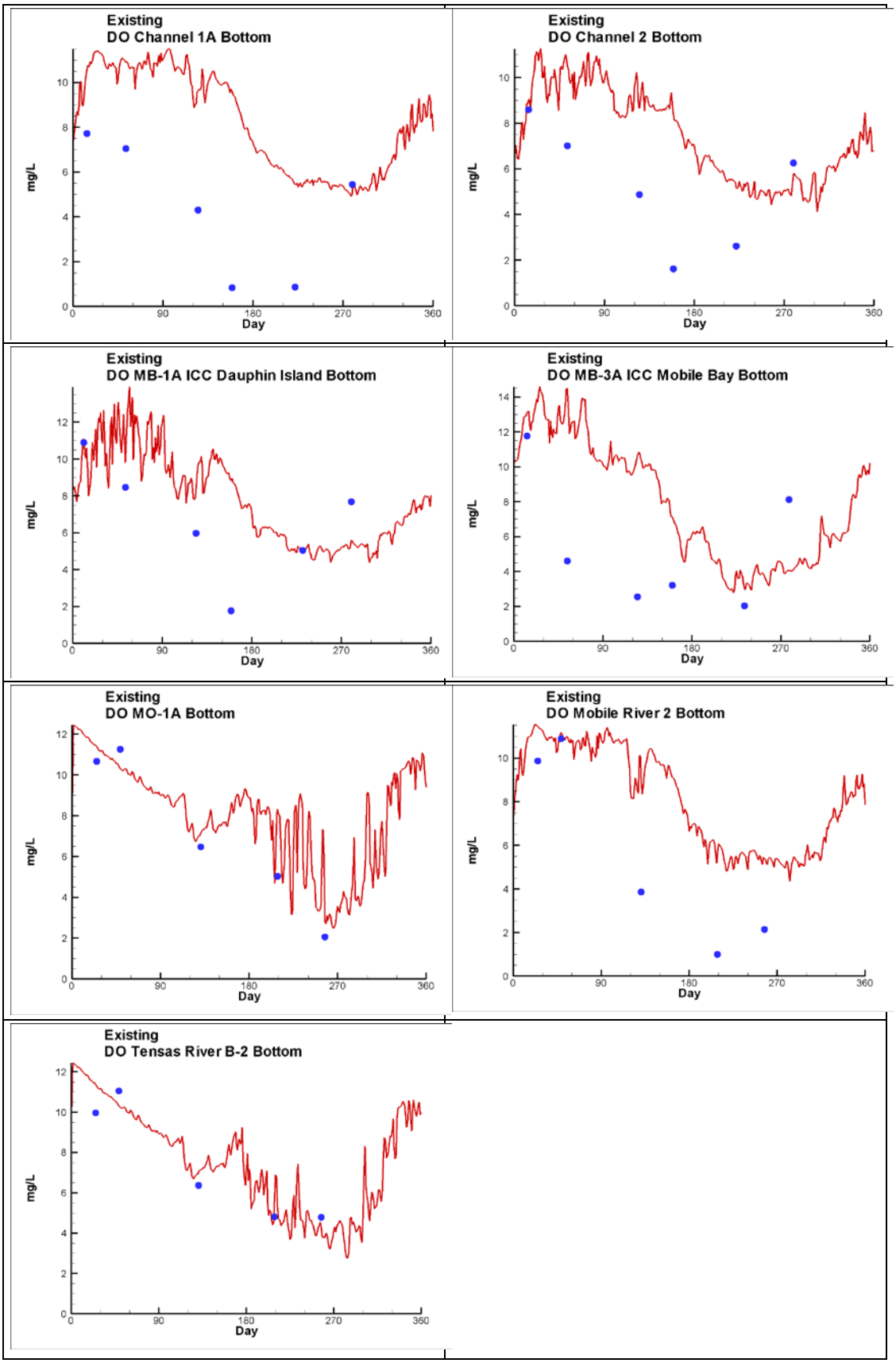

Figure 77. Comparison of Simulated and Measured Bottom DO values

salinity which decreased DO saturation levels. DO results for Tensaw indicated that the model performed well for the bottom waters and was able to capture the behavior at that location. Bottom water model DO for MB1 were higher than observed values for the middle of the simulation while MB3 DO model results corresponded to observation for the first half of the simulation but were slightly lower than observations later.

Simulated DO levels in the bottom waters are sensitive to several issues. Circulation and flushing are primary factors. Water column conditions in regards to oxygen demanding substances, temperature, and salinity all continually impact DO levels in the water column. External impacts include benthic fluxes, sediment oxygen demand, and boundary loads.

During calibration, multiple runs were made to improve water quality model results. Observed data indicate that the water column was completely mixed during portions of the year. These periods corresponded to cooler weather and higher riverine flows. Later in the year, stratification developed. This corresponded to periods of lower tributary flows. Several model modifications were used to address these issues. Boundary conditions were varied with depths for DO for the Mobile and Tensaw Rivers. Benthic fluxes were used to account for sediment releases of nutrients and oxygen demanding substances. Finally, light extinction in the water column was adjusted to decrease the amount of light available throughout the water column for algae.

Nutrient results are shown in Figures 78 to 80. Model predictions for Ammonium and Nitrate are shown in Figures 78 and 79, respectively. Simulated and measured Ammonium observations agreement for the simulation were good. Increases in Ammonium at the mouths of the Mobile and Tensaw River correspond to increases in the specified boundary levels. When very low boundary conditions are specified, Ammonium levels at the river mouths decrease correspondingly. As seen in Figure 79, Nitrate results agreed well with observations. As seen in Figure 80, simulated DIP levels for the riverine stations were representative of observed data at those locations.

Simulated Chlorophyll levels were slightly higher than reported values but still reasonable (see Figure 81). Only one form of algae was modeled which limits the ability of the model to capture different algal species blooms.

As seen in Figure 82, TSS model results are representative of the observed data with one exception. High levels of TSS during the first month of the simulation at MO-1A and Tensaw B-2 were not captured by the model.

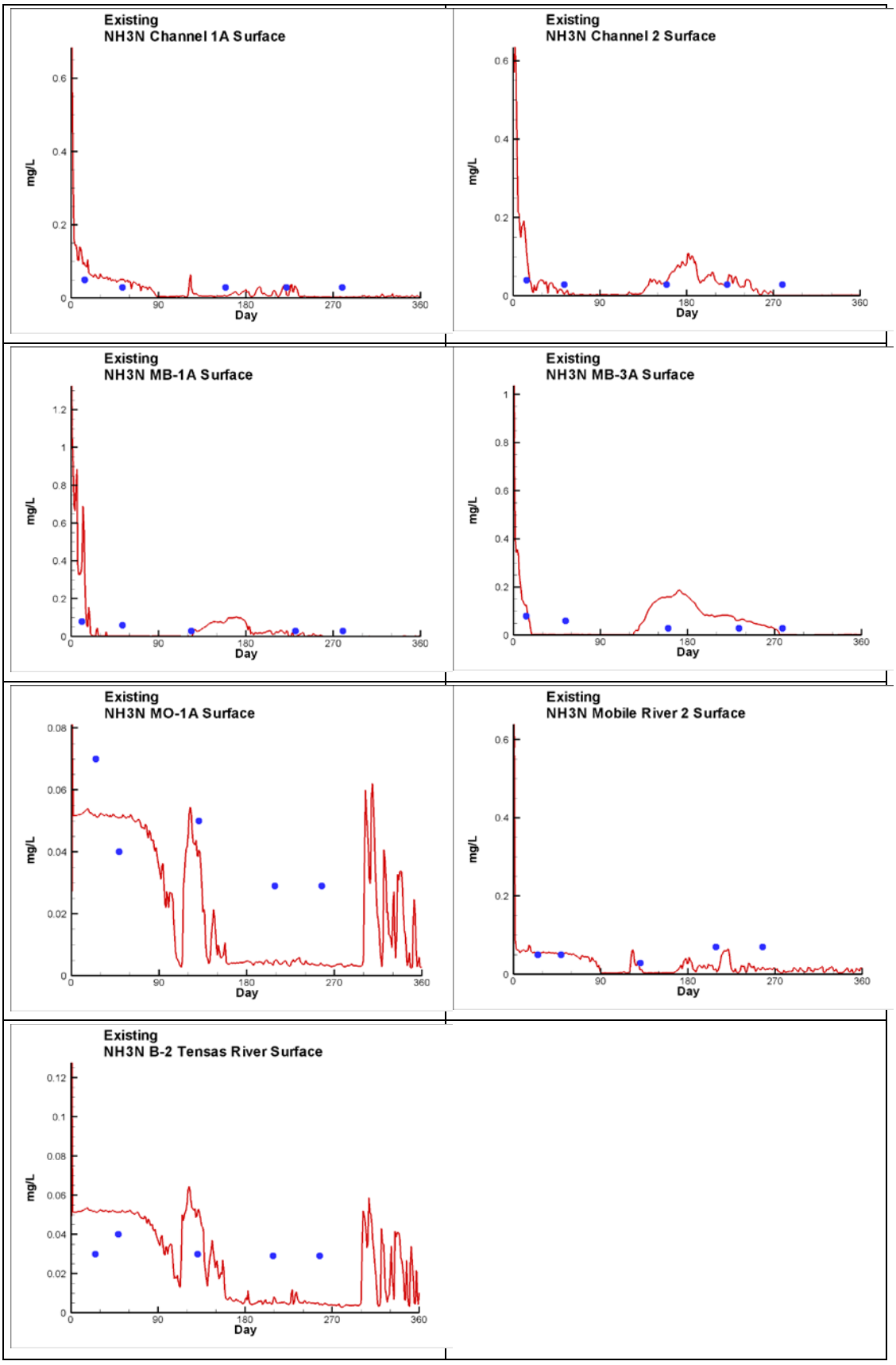

Figure 78. Comparison of Simulated and Measured Surface Ammonium values

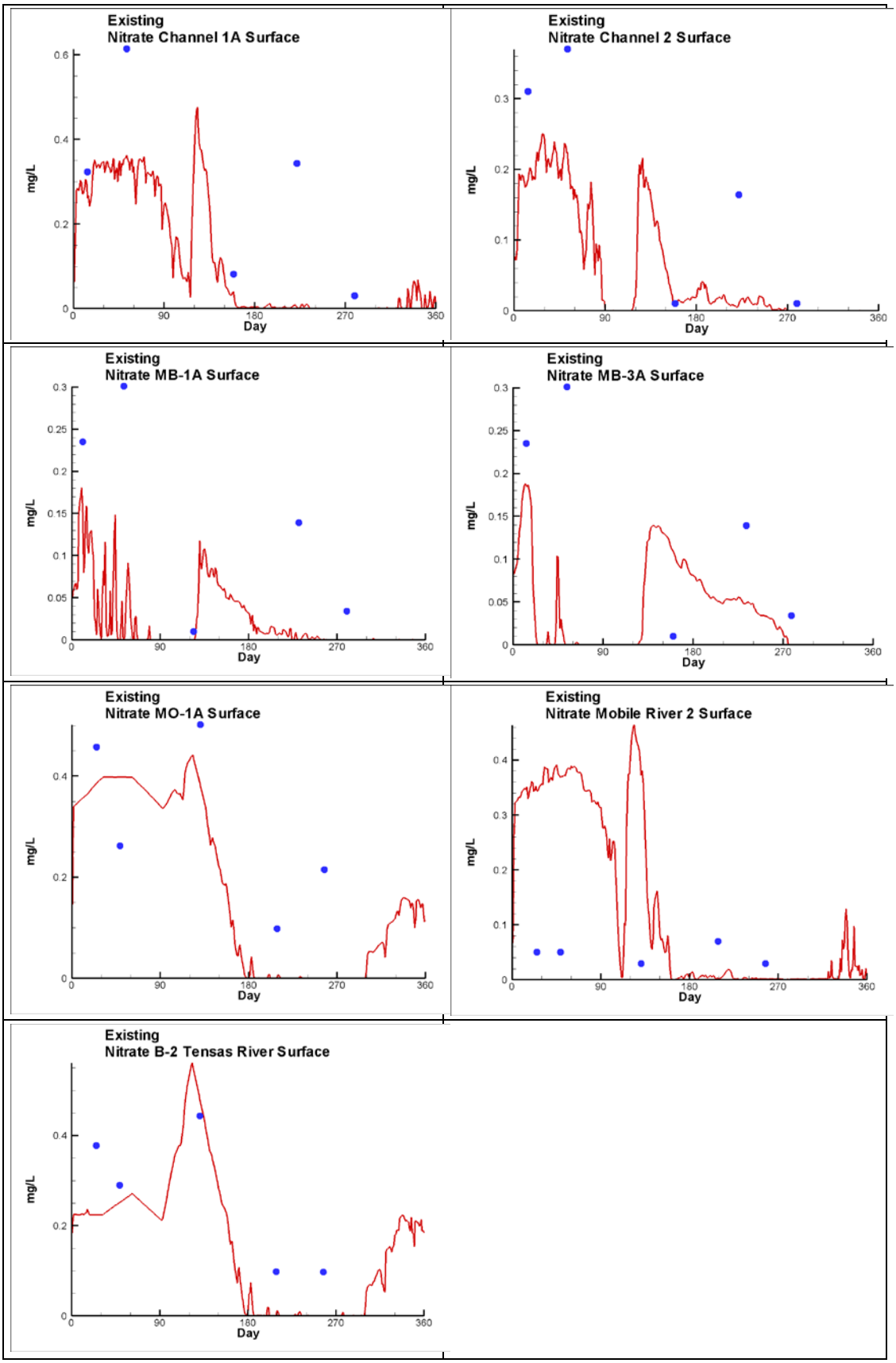

Figure 79. Comparison of Simulated and Measured Surface Nitrate values

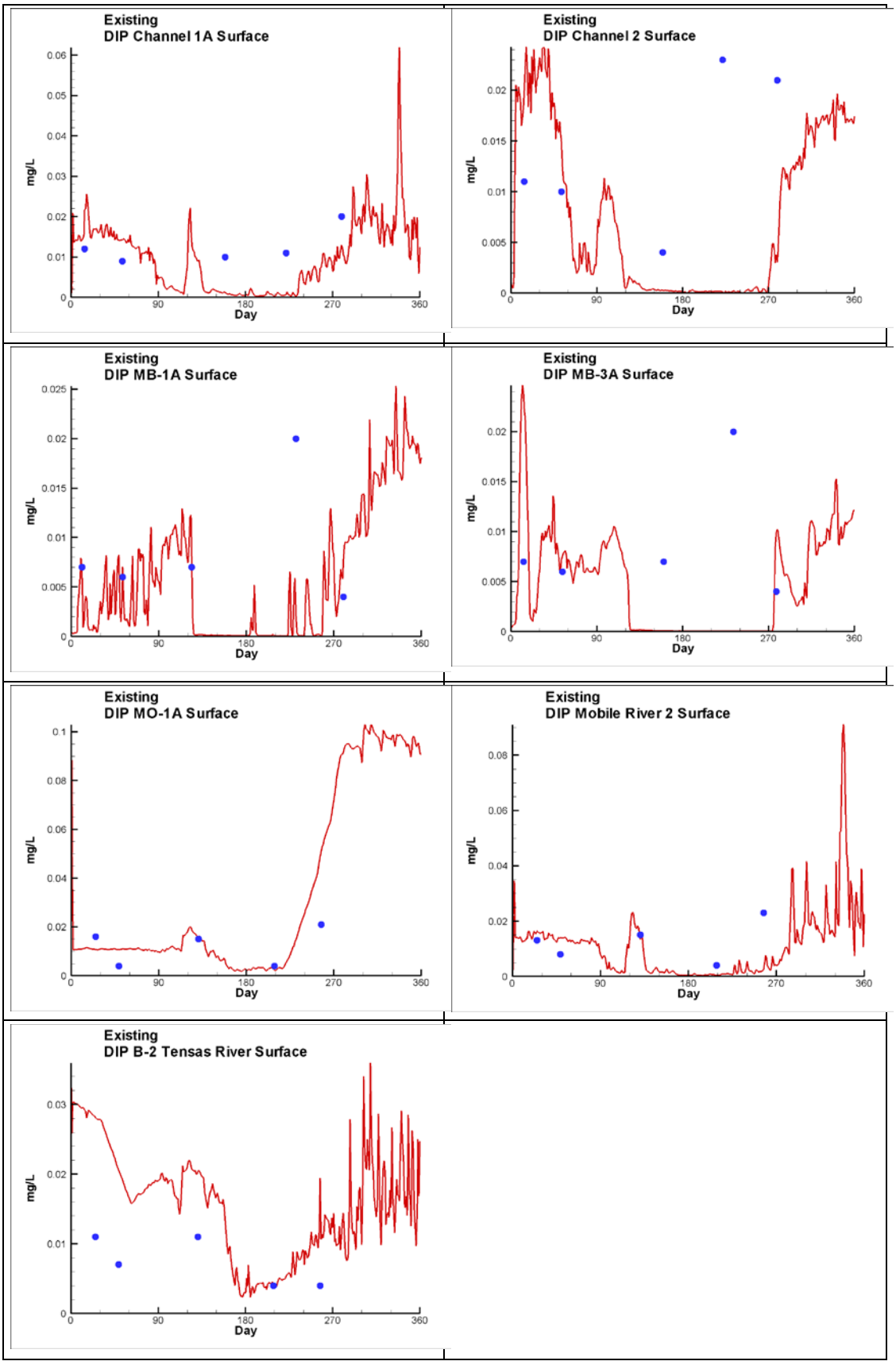

Figure 80. Comparison of Simulated and Measured Surface DIP values

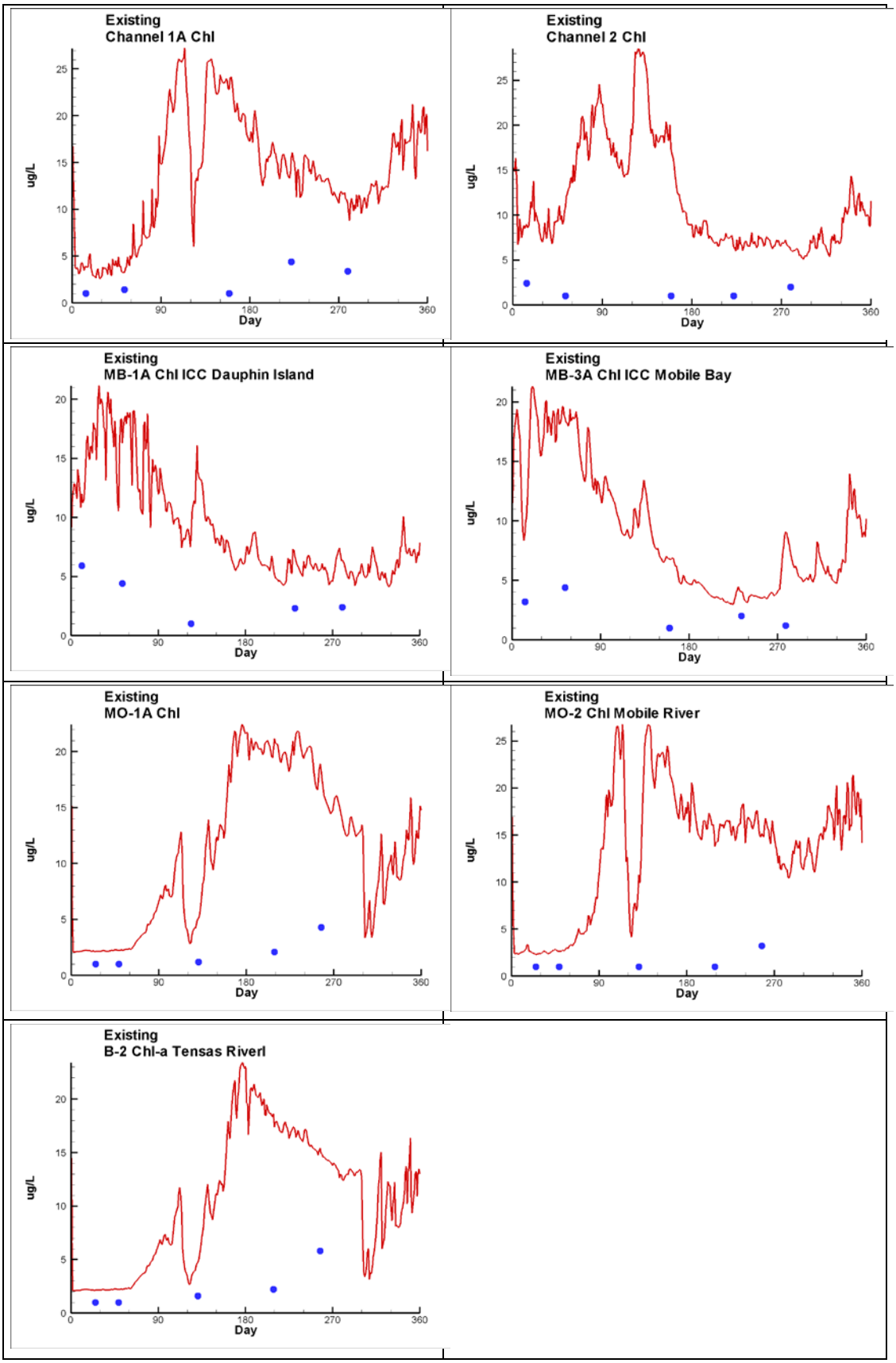

Figure 81. Comparison of Simulated and Measured Surface Chl-a values

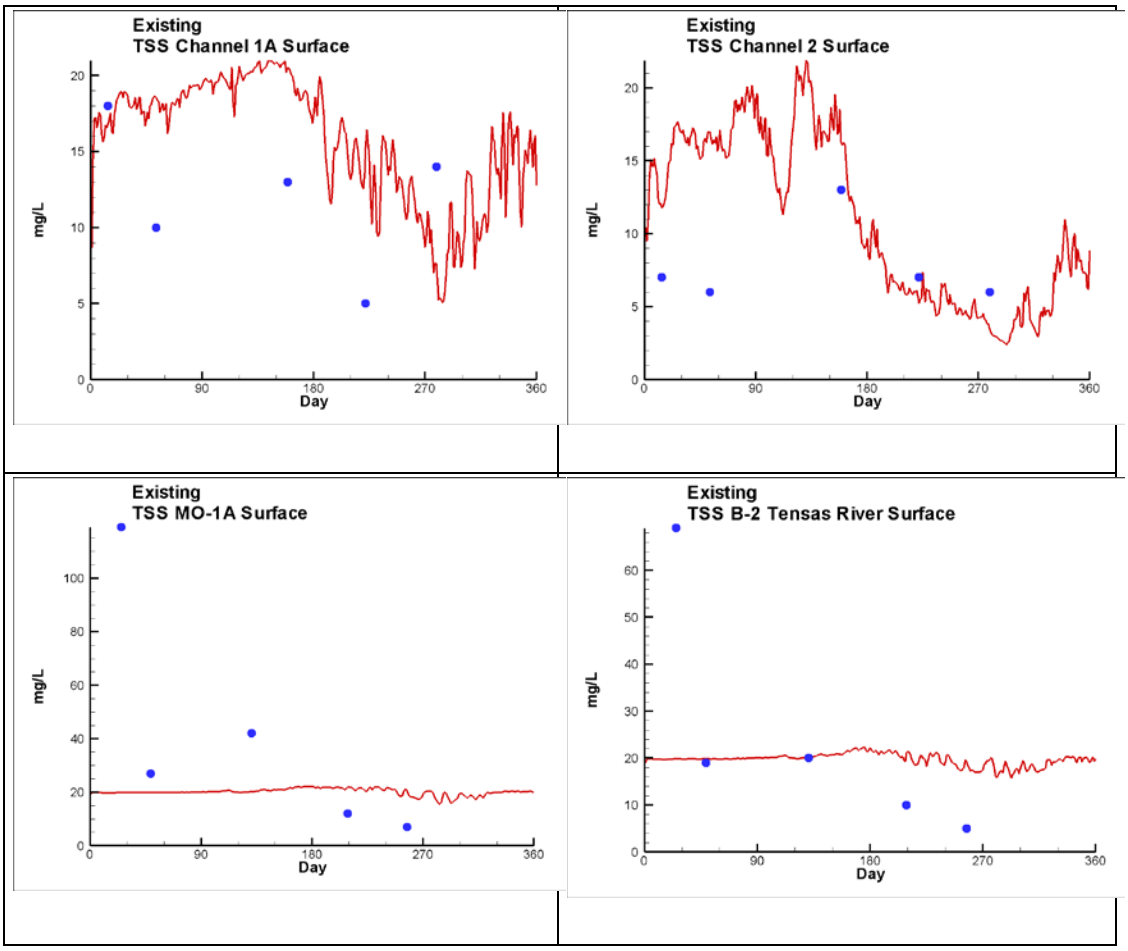

Figure 82. Comparison of Simulated and Measured Surface TSS values

This is likely due to high TSS loads to the rivers that were not captured by the boundary conditions.

The role of calibration in this study was to demonstrate that the water quality model could provide a reasonable assessment of the relative differences in water quality due to differences in hydrodynamic fields. Scenarios to be evaluated differ only in channel geometry and resulting impacts upon flow and volume. No changes in water quality loads, benthic loads, tributary inflows or other input conditions are features of this analysis. If water quality changes are not evident in comparison of two modeled cases, then the implication is that the conditions that exist under one case are the same as the other cases. The differences in conditions modeled were not sufficient to generate meaningful water quality differences and there is no relative impact. CEQUAL-ICM as set up and calibrated for this project is suited to make the assessment of relative water quality impacts.

Scenario Results and Discussion

Presentation and discussion of scenario runs includes model results for four sets of conditions:

1. Existing (No Project) – Current channel configuration and sea level
2. Project – Proposed channel deepening and widening with current sea level.
3. Existing with Sea Level Rise - Current channel configuration with a projected sea level rise incorporated in the initial water levels and ocean boundary elevations.
4. Project with Sea Level Rise - Proposed channel deepening and widening with a projected 0.5 m sea level rise incorporated in initial water levels and ocean boundary elevations.

Existing, or No Project, reflect the current harbor configuration, current channel depths and existing flow conditions. This is the base or reference condition. Project includes all of the existing condition features with the proposed GRR channel modifications implemented. The details of these modification are presented in the "Existing and With-Project Simulations" section in the "GSMB Multi-Block Hydrodynamic Modeling" chapter above. These changes were implement by changing local cell depths and widths where required and could be implemented without adding or removing cells or flow faces. The end result is that the 'with-Project' scenario has the same setup as the Existing case but is run with a set of hydrodynamics that reflects a channel with difference in depth and width. Therefore, any difference in the Existing and with-Project are the result of the changes in the hydrodynamics due to the channel bathymetry modifications.

These two scenarios are repeated with 0.5 meter sea level rise included to reflect theoretical future conditions with and without the channel modifications. The Existing with Sea Level Rise case uses the Existing case channel configuration with water levels that incorporate potential sea level rise conditions. Since the same bathymetry was used as in the Existing case no additional cells were required so the same ICM setup except for hydrodynamics was used as the Existing case. The same is true for with-Project with Sea Level Rise scenario where it was a repeat of the Existing with Sea Level Rise only with a different hydrodynamics set.

When comparing model results for the scenarios 1) the Existing and Project were compared and 2) the Existing with Sea level Rise and Project with Sea Level Rise were compared.

The essence of incorporating Sea Level Rise into the model is that the water column in the model increased by the height of the imposed sea level rise. Depending on the location in the system, this change in water column volume (and corresponding cell volumes) could be noteworthy as in shallow areas or insignificant in deeper waters of channels.

As with the calibration effort time series of water quality conditions at selected locations were used to assess impacts. However, instead of figures comparing model and observed data, one set of model results were compared to another's. Any differences in the two model's output are wholly due to the difference in the hydrodynamic conditions that occurred at that location. Times where there are no differences in the time series at that location indicate that the differences in the two scenarios were insignificant. Times when a difference is evident are an indication that the differences in hydrodynamic conditions impacted water quality conditions. The degree of impact is relative to the existing conditions that occur at that location. Numerous locations were selected for evaluation of project impacts upon water quality resulting from proposed project activities. These locations tended to correspond to sites where observations are made or water quality data are collected.

Existing (No Project) and Project Comparisons

Temperature

Selected time series comparison of Existing and with-Project temperature results for surface and bottom are shown in Figures 83 and 84. In these plots, both the Existing and Project model results are presented. Any differences in the simulation results will appear as separation of the time series lines. The greater the separation in magnitude or timing then the greater the difference in the modeled conditions. A single line indicates that the difference between the Existing and with-Project conditions was negligible.

Negligible temperature changes between Existing and with-Project conditions were expected in surface temperatures and as seen in Figure 83 negligible differences were predicted. All forcings impacting temperature calculations were the same and the only means to alter temperature were changes in circulation due to structural modifications. Based on the temperature results, the relative changes in circulation between the Existing and with-Project conditions was insufficient to have a significant impact on surface temperatures. Theoretically water column bottom waters are more susceptible to changes because the water column depth increased. As shown in Figure 84, bottom water temperature for the Existing and with-Project conditions were

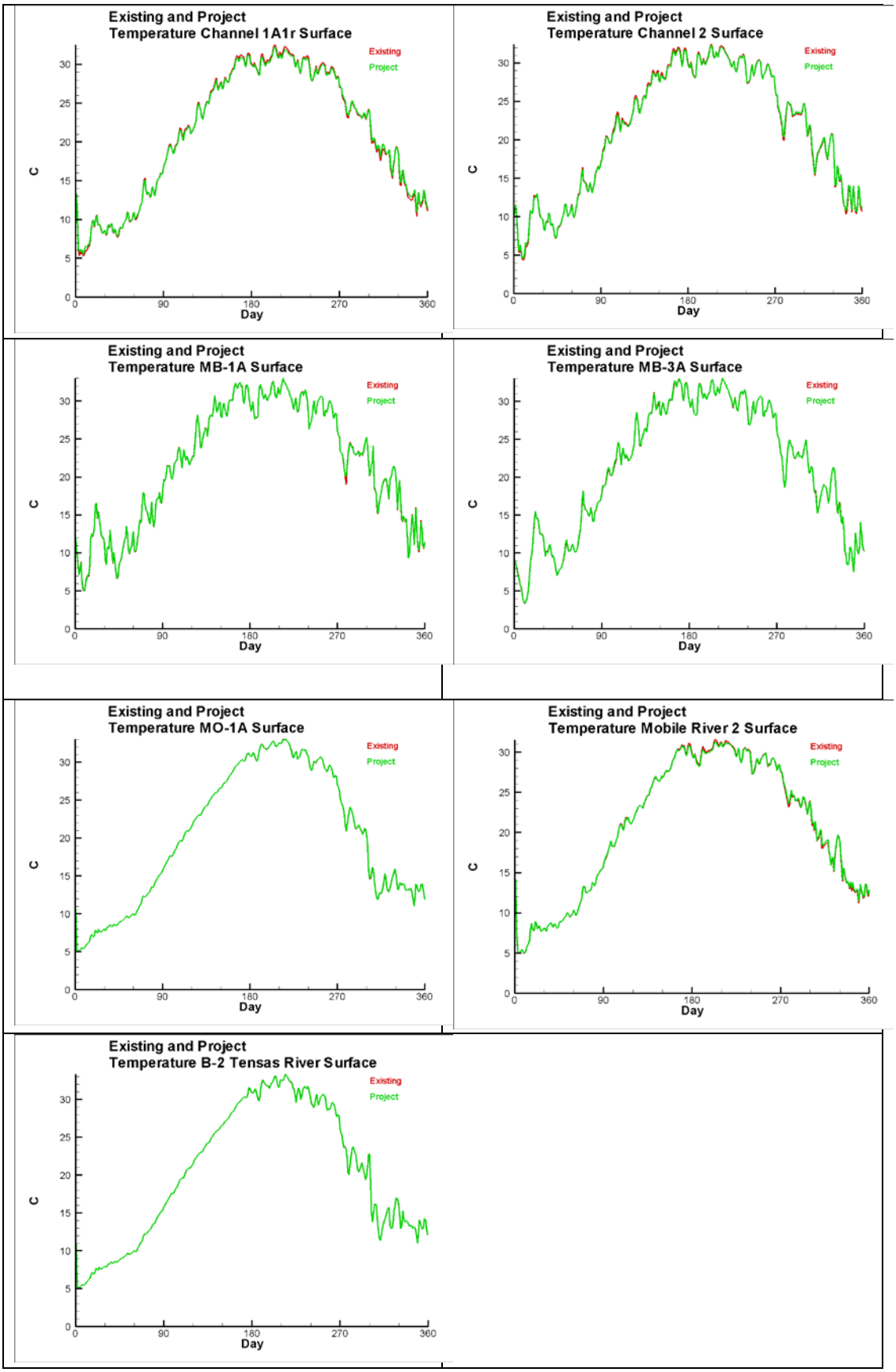

Figure 83. Comparison of Existing and with-Project Surface Temperatures

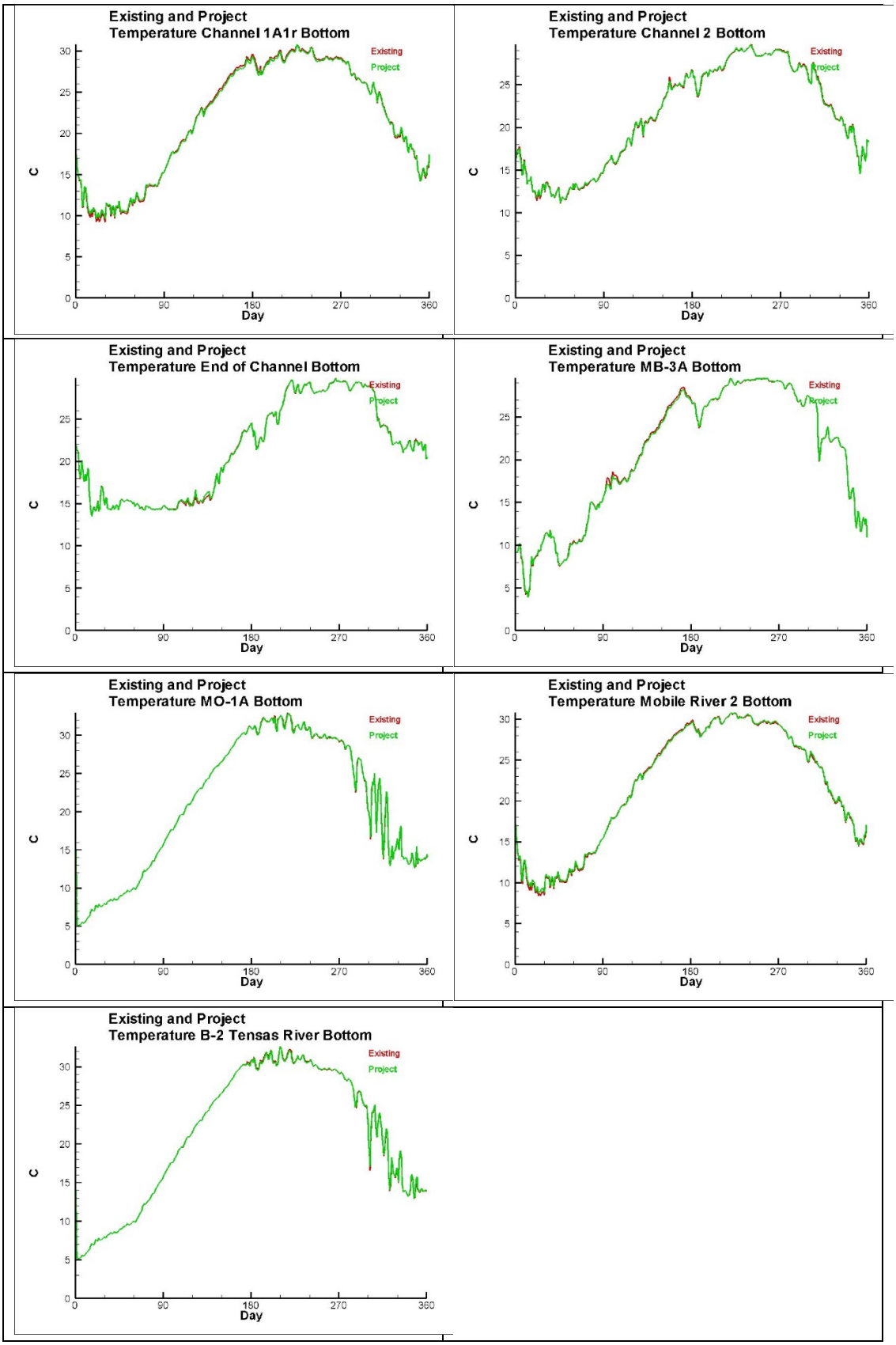

Figure 84. Comparison of Existing and with-Project Bottom Temperatures

unchanged over year long duration of the simulation. That indicates the project will not alter the thermal regime of the system nor have an impact on temperature sensitive biological of chemical process in the system.

Salinity

Figures 85 and 86 contain time series of the daily average surface and bottom salinity for the Existing and with-Project cases. As indicated in the surface, Figure 85, and the bottom, Figure 86, there are very minor differences in the salinity. The same patterns, trends, and behavior exist after the channel widening and deepening are incorporated in the model as occurred before. There are no changes in duration or exposure to any level of salinity in at any of the locations shown.

Dissolved Oxygen

Figures 87 and 88 contain time series of the daily average surface and bottom dissolved oxygen concentrations for the Existing and with-Project cases. As indicated in the surface, Figure 87, and the bottom, Figure 88, there are very minor differences in the DO. The same patterns, trends, and behavior exist after the channel widening and deepening are incorporated as occurred before. There are no changes in duration or exposure to any level of DO in at any of the locations shown. Since DO levels represent the end product of numerous water quality processes then changes in any of those processes can have an impact on DO levels. From the results shown in Figures 87 and 88, no impact from the project is predicted in DO levels in the surface or bottom waters at these locations. Another way to view this is that the daily average DO conditions with-Project are the same as they are without the project.

SLR Existing and Project Comparisons

The same modeling approach and setup was used in the Existing and with- Project to evaluate the potential impact of a proposed sea level rise. For comparison purposes the Existing case was also run using hydrodynamics incorporating sea level rise to generate a future without project condition. Surface and bottom time series comparisons of daily average model output for the same locations used for the Existing and with-Project cases were evaluated for the Existing and with-Project with Sea Level Rise cases.

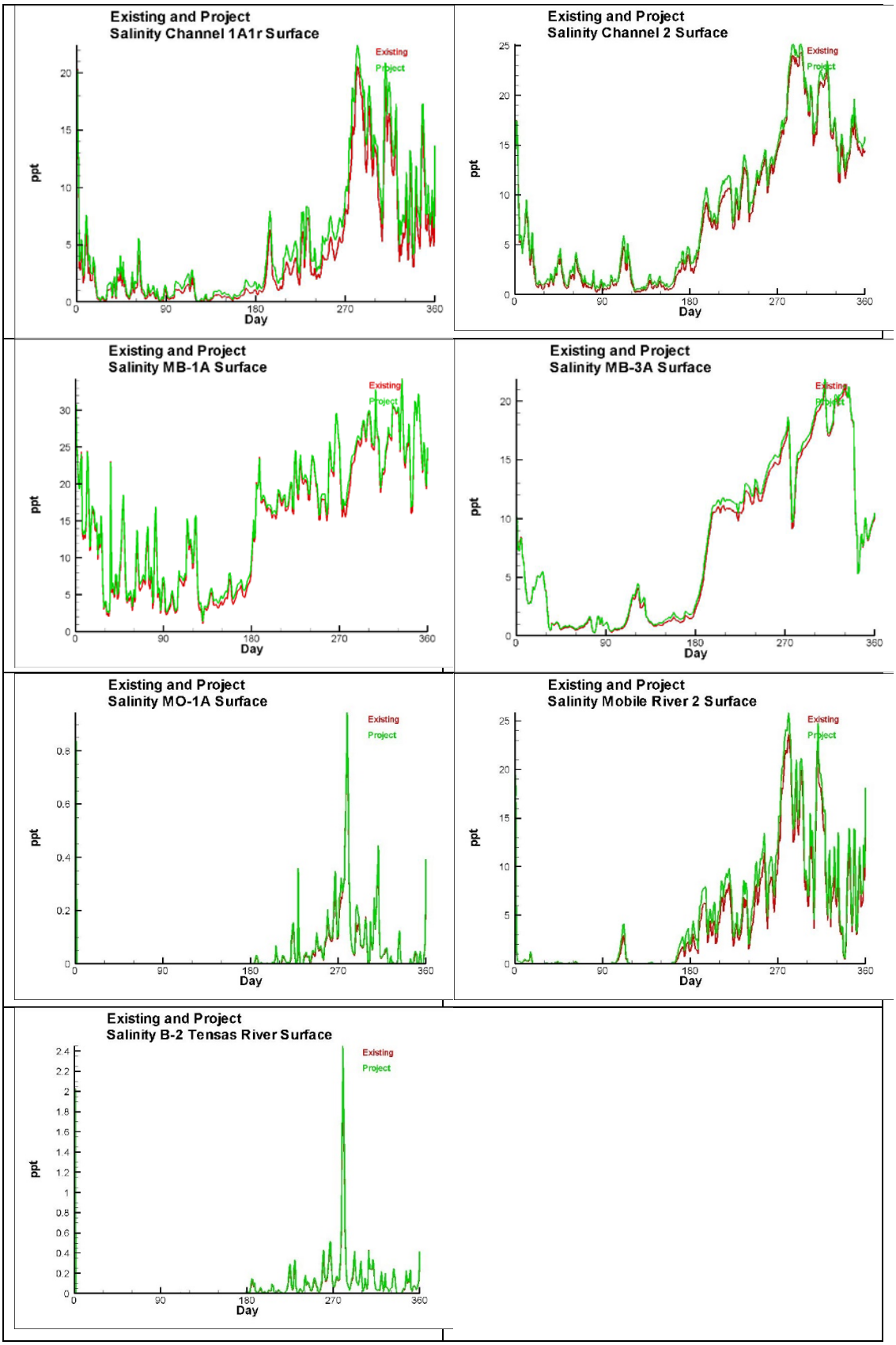

Figure 85. Comparison of Existing and with-Project Surface Salinities

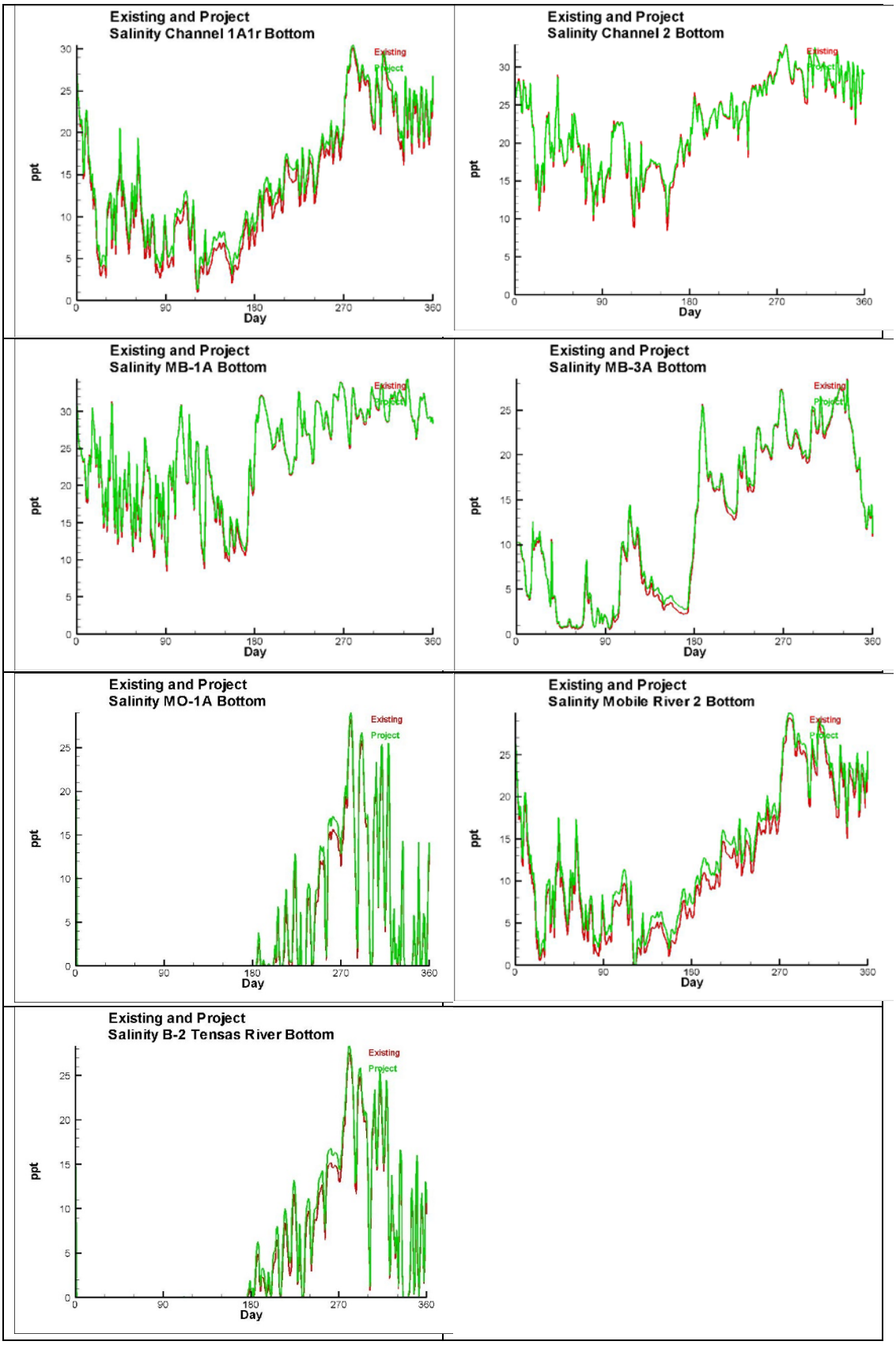

Figure 86. Comparison of Existing and with-Project Bottom Salinities

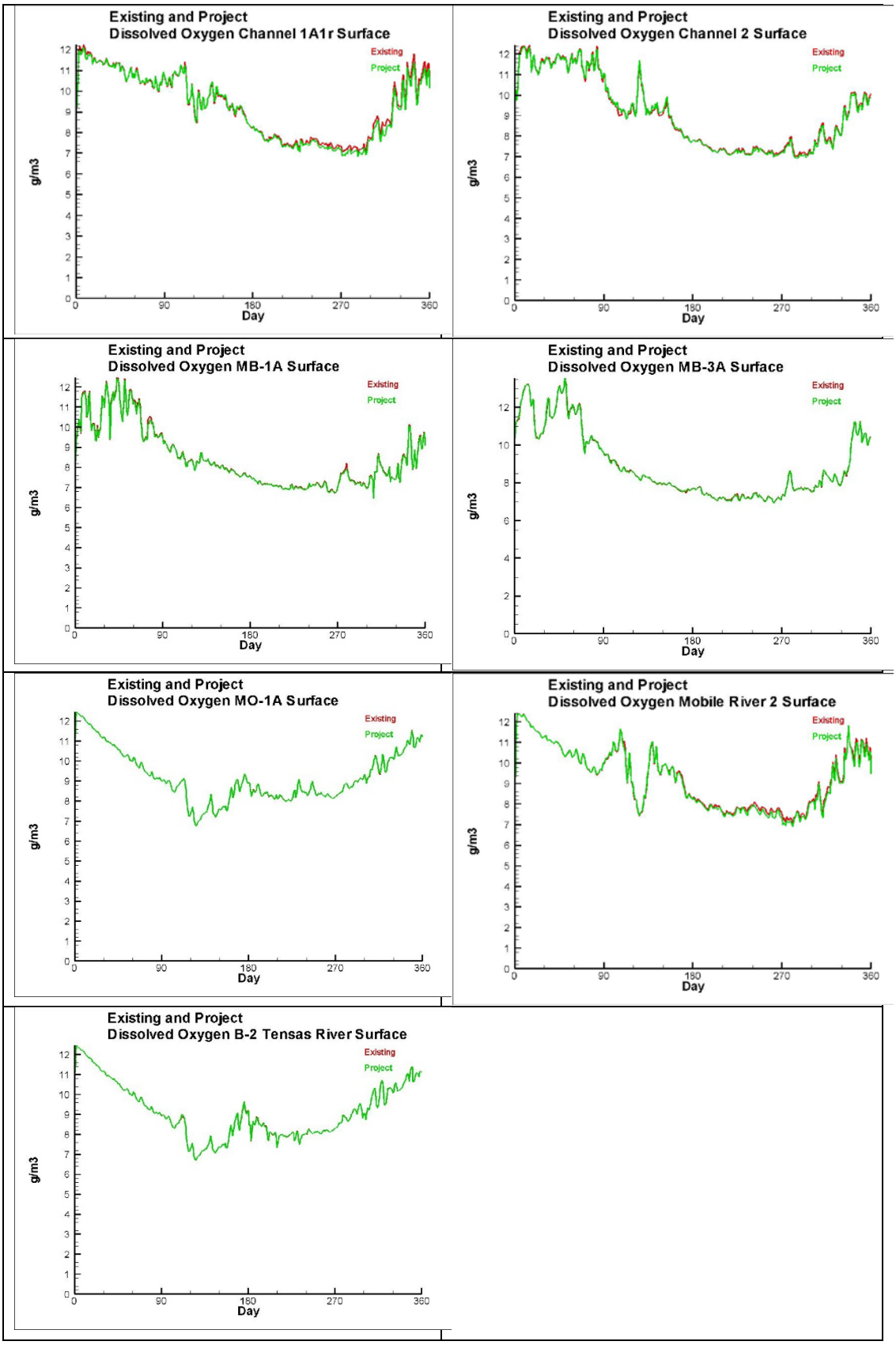

Figure 87. Comparison of Existing and with-Project Surface Dissolved Oxygen

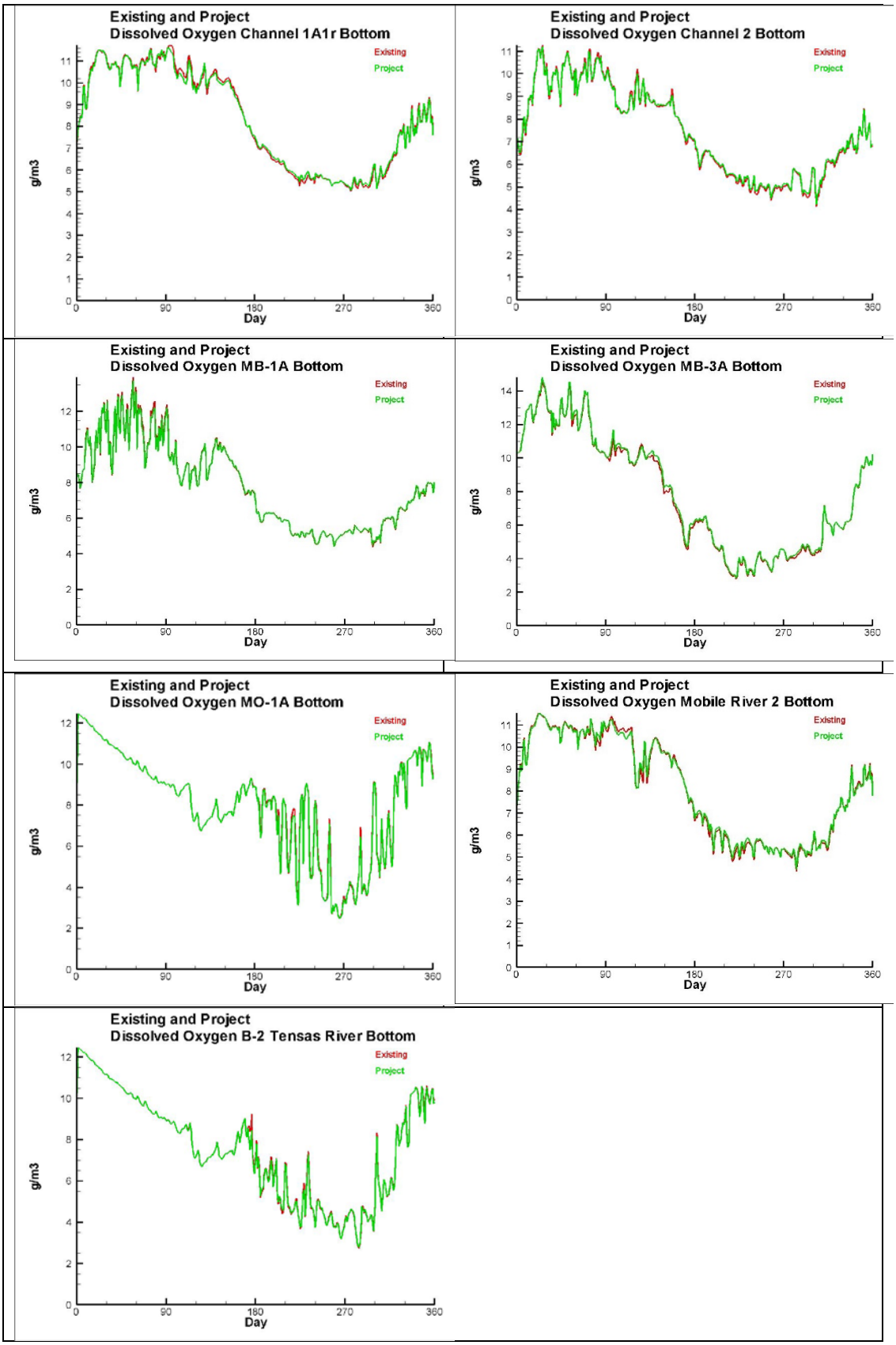

Figure 88. Comparison of Existing and with-Project Bottom Dissolved Oxygen

Temperature

Select time series comparison of Existing with SLR and with-Project with SLR temperature for surface and bottom are shown in Figures 89 and 90. Negligible temperature changes between Existing with SLR and with-Project with SLR conditions were expected in surface temperatures and as seen in Figure 89 negligible differences were predicted. Similar to the non-SLR case, all forcings impacting temperature calculations were the same and the only means to alter temperature were changes in circulation. Based on the temperature results, the relative changes in circulation between the Existing with SLR and with-Project with SLR conditions were insufficient to have a significant impact on surface temperatures. Theoretically bottom waters are more susceptible to changes because the water column got deeper. As indicated in Figure 90, bottom water temperature for the future without project condition with SLR and with-Project conditions were unchanged over the year-long simulation.

Salinity

Figures 91 and 92 contain time series of the daily average salinity for the Existing with SLR and Project with SLR cases. As indicated in the surface, Figure 91, and the bottom, Figure 92, there are very minor differences in the salinity between the two cases. The same patterns, trends, and behavior exist with SLR after the channel widening and deepening are incorporated in the model. There are no changes in duration or exposure to any level of salinity in at any of the locations shown.

Dissolved Oxygen

Figures 93 and 94 contain time series of the daily average dissolved oxygen concentrations for the future without project conditions with SLR and with-Project with SLR cases. As indicated in the surface, Figure 93, and the bottom, Figure 94, there are very minor differences in the DO. The same patterns, trends, and behavior exist after the channel widening and deepening are incorporated in the model. There are no changes in duration or exposure to any level of DO at any of the locations shown. Since DO levels represent the end product of numerous water quality processes then changes in any of those processes can have an impact on DO levels. From the results shown in Figures 93 and 94, no impact from the project is predicted in DO levels in the surface or bottom waters at these locations. This analysis indicates that for these two cases, future without project conditions with SLR and with-Project with SLR there are no DO differences.

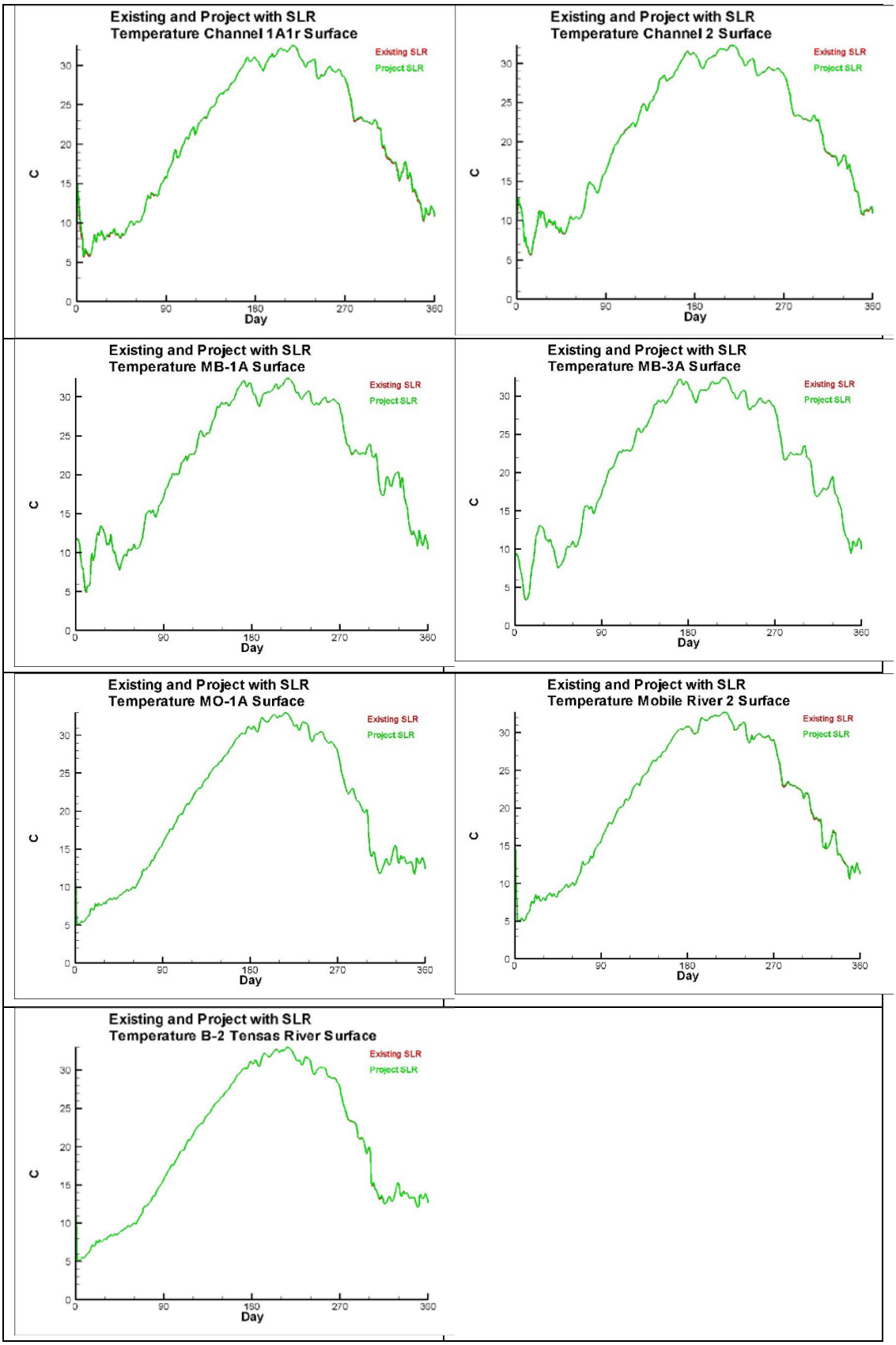

Figure 89. Comparison of Existing and with-Project with SLR Surface Temperature

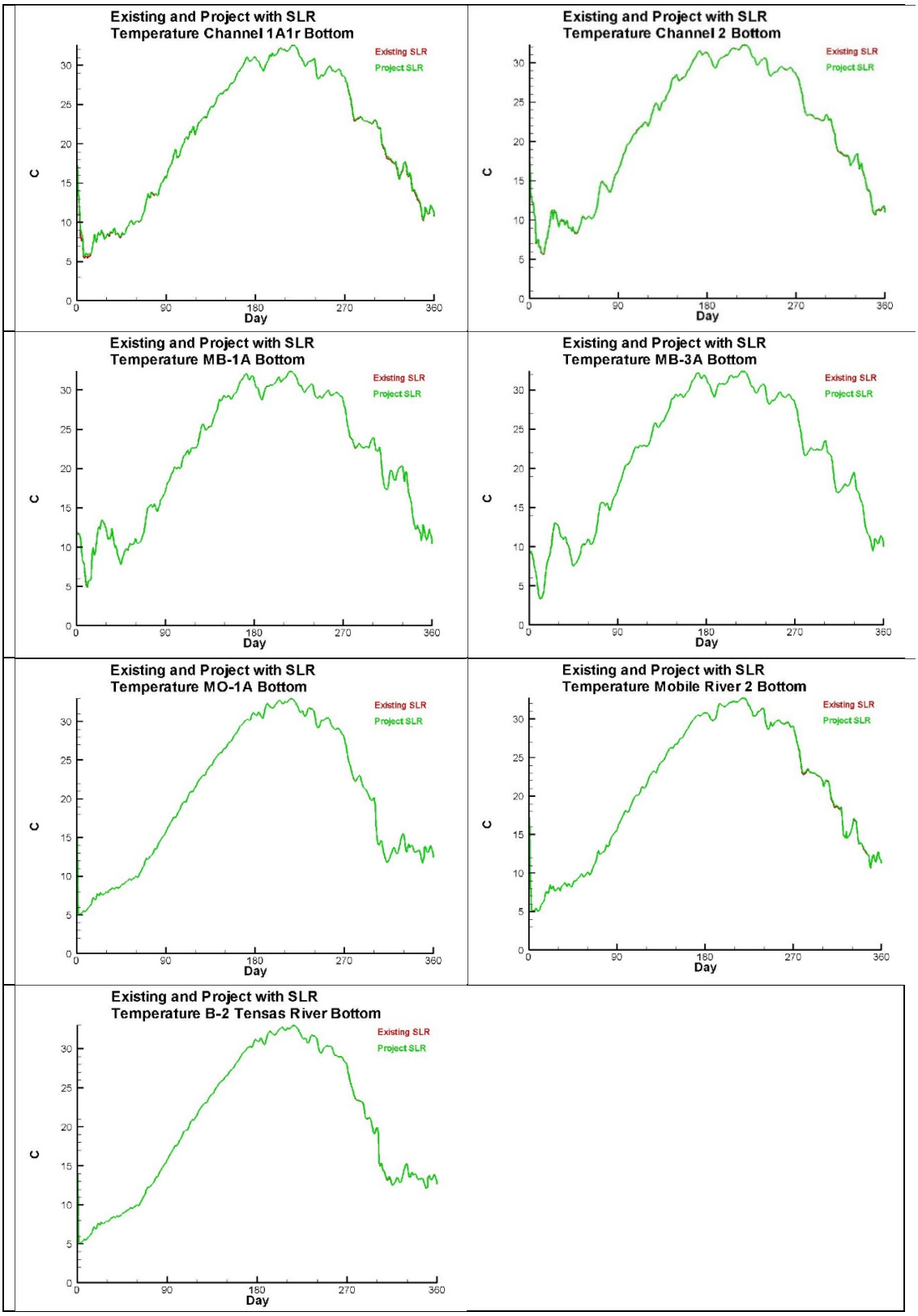

Figure 90. Comparison of Existing and with-Project with SLR Bottom Temperature

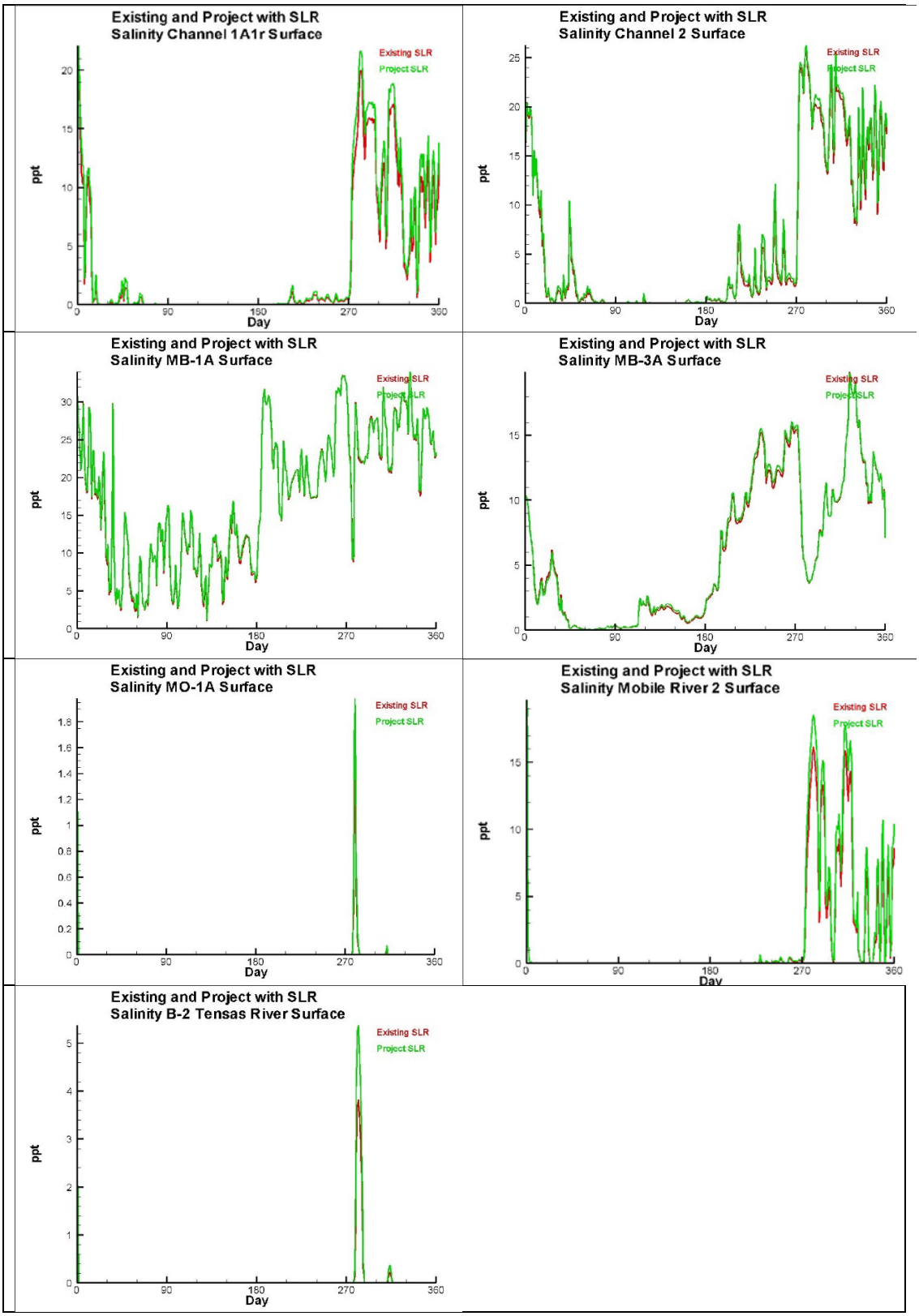

Figure 91. Comparison of Surface Salinity for Existing and with-Project with SLR

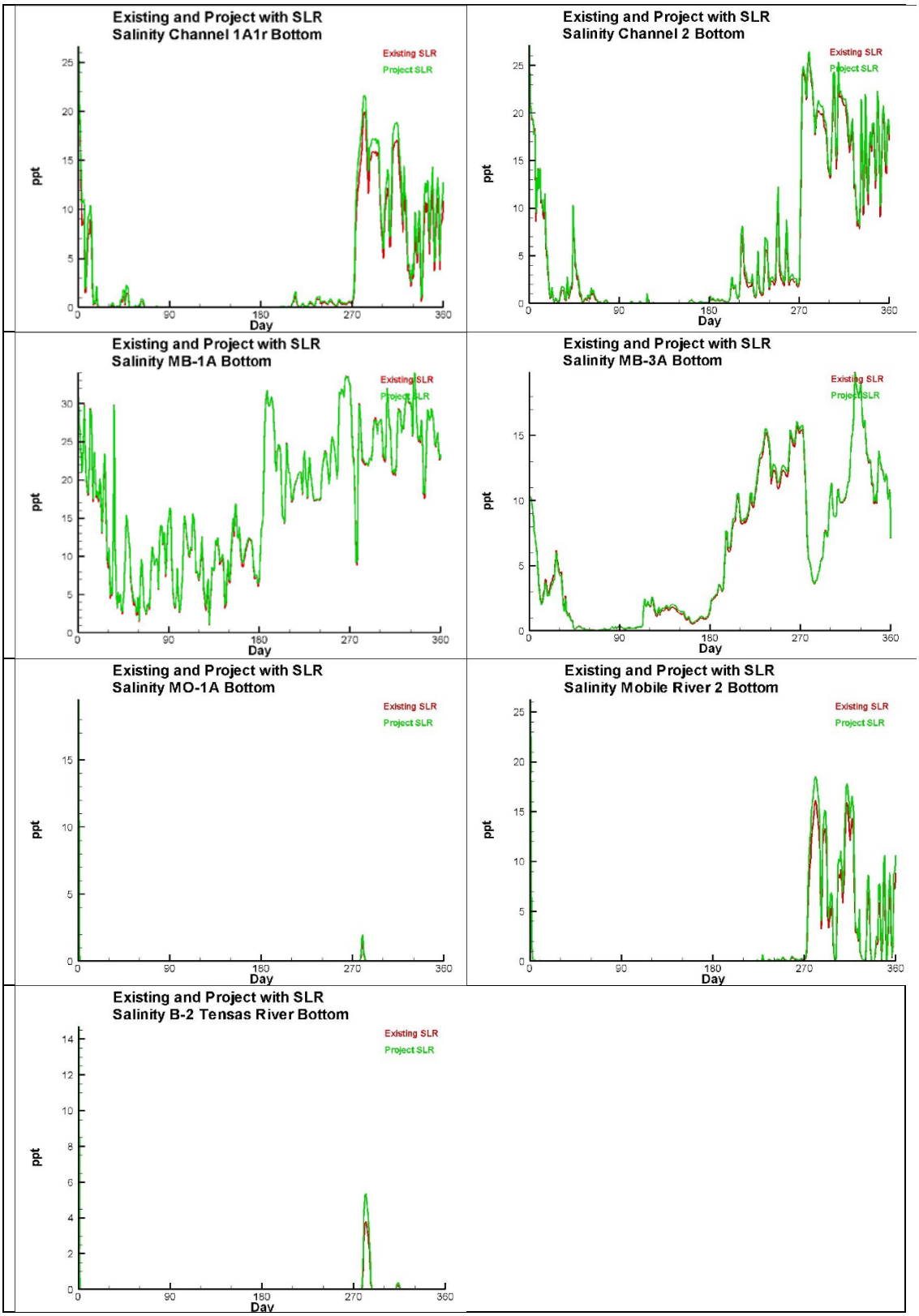

Figure 92. Comparison of Bottom Salinity for Existing and with-Project with SLR

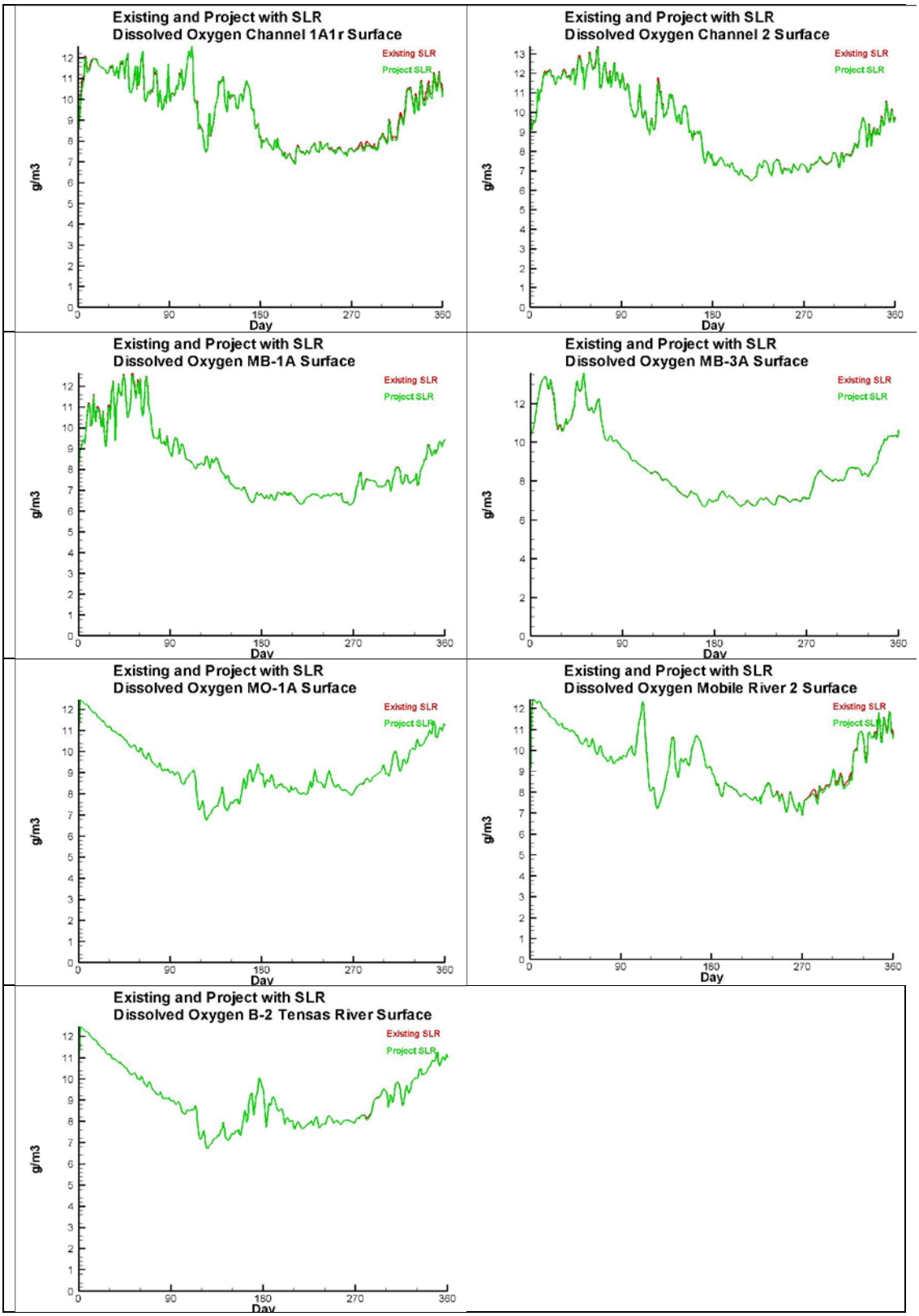

Figure 93. Comparison of Surface DO values for Existing and with-Project with SLR

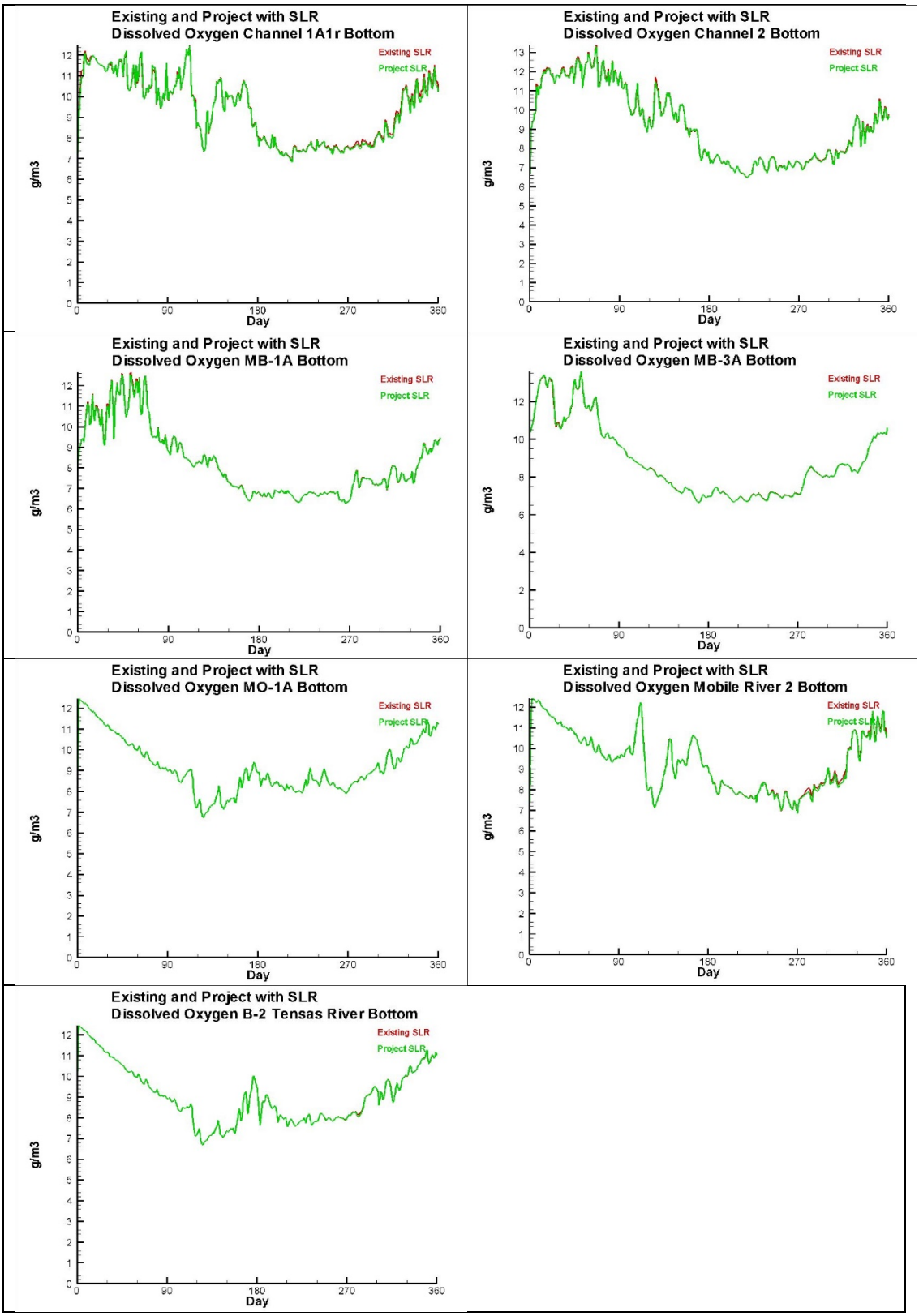

Figure 94. Comparison of Bottom DO values for Existing and with-Project with SLR

Conclusions

This study investigated the water quality impacts arising from widening and deepening the existing navigation channel in Mobile Bay. A 3D water quality model was developed specifically for this task, CEQUAL-ICM. Hydrodynamic information for CEQUAL-ICM was supplied by GSMB. Observed data and reported information was used for setting up the model. CE-QUAL-ICM was calibrated for the calendar year 2010 and then used to evaluate four sets of conditions; Existing (No Project), with-Project, future without project (Existing with Sea Level Rise), and Project with Sea Level Rise. Daily average values for all cells for all water quality constituents were saved during the model simulations and then retrieved for select locations afterwards. Comparison of these results enabled direct comparison of conditions between pairs of different model simulations; Existing and with-Project, and future without project (Existing with SLR) and Project with SLR. The results of the comparisons are that no alteration in the behavior of any water quality constituent evaluated was evident. In most cases the differences in constituent behavior were undetectable.

Estuarine Sediment Transport Modeling

The purpose of the sediment transport modeling was to assess the relative changes in sedimentation rates within the navigation channel, dredged material placement sites, and surrounding areas as a result of channel improvements within the bay. This modeling was performed using the 59-block Mobile Bay model described in the GSMB Hydrodynamic Modeling chapter.

In this section, a description of the sediment transport module that is dynamically linked to GSMB hydrodynamic module is given. Then, a description of how, building upon the sediment transport model used for the thin layer placement site modeling study, existing sediment data, and data collected and analyzed during this study were used to setup the Mobile Bay sediment transport model used in this study is provided, followed by a description of the calibration of the model and the model simulations that were performed. Results of the model simulations are given last.

Description of Sediment Transport Model

The sediment transport module of GSMB is a modified version of the SEDZLJ mixed sediment transport model (Jones and Lick 2001; James *et al.* 2010) that a) includes a three-dimensional representation of the sediment bed, and b) can simulate winnowing and armoring of the surficial layer of the sediment bed. GSMB-SEDZLJ is dynamically linked to GSMB-Hydro in that the hydrodynamics and sediment transport modules are both run during each model time step. This enables simulated changes in morphology to be instantly fed-back to the hydrodynamic model. The modifications that have been made to MB-SEDZLJ are described later in this section.

One of the first steps in performing sediment transport modeling is to use grain size distribution data from sediment samples collected at different locations throughout the model domain to determine how many discrete sediment size classes are needed to adequately represent the full range of sediment sizes. Typically, three to eight size classes are used. For example, for the native sediment throughout the Mobile Bay model domain, two size classes are used to represent sediment in the cohesive sediment size range, i.e., less than 63 μm, and three size classes are used to represent the noncohesive sediment size range, i.e., greater than 63 μm. Three additional sediment size classes are used to represent the dredge material placed in the designated Beneficial Use (BU) areas, two size classes for the cohesive sediment fraction

and one size class for the noncohesive sediment fraction of the BU material. Each sediment size class is represented in SEDZLJ using the mean diameter within that size range. The sediment diameters used for the simulated sediment size classes are given later in this section.

Suspended Load Transport of Sediment

The GSMB-SEDZLJ sediment transport module simulates the transport of each sediment size class to determine the suspension concentration in all computational grid cells. The transport of suspended sediment is determined through the solution of the following 3D advective-dispersive transport equation for each sediment size class:

$$\frac{\partial C_i}{\partial t} + \frac{\partial uC_i}{\partial x} + \frac{\partial vC_i}{\partial y} + \frac{\partial (w - W_{Si})C_i}{\partial z} = \frac{\partial}{\partial x}\left(K_H \frac{\partial C_i}{\partial x} \right) + \frac{\partial}{\partial y}\left(K_H \frac{\partial C_i}{\partial y} \right) + \frac{\partial}{\partial z}\left(K_v \frac{\partial C_i}{\partial z} \right) + S_i \quad (2)$$

where:

C_i = concentration of ith size class of suspended sediment,

(u,v,w) = velocities in the (x,y,z) directions,

t = time,

W_{Si} = settling velocity of *ith* sediment size class,

K_H = horizontal turbulent eddy diffusivity coefficient,

K_V = vertical turbulent eddy diffusivity coefficient, and

S_i = source/sink term for the *ith* sediment size class that accounts for erosion/deposition.

The equation used to calculate S_i is the following:

$$S_i = E_{sus,i} - D_{sus,I} \quad (3)$$

where $E_{sus,i}$ = sediment erosion rate for the *ith* sediment size class that is eroded and entrained into suspension, and $D_{sus,i}$ = sediment deposition rate for the *ith* sediment size class. Expressions for $D_{sus,i}$ and $E_{sus,i}$ are given later in this chapter.

The settling velocities for noncohesive sediments are calculated in SEDZLJ using the following equation (Cheng 1997):

$$W_s = \frac{\mu}{d}\left(\sqrt{25 + 1.2 d_*^2} - 5 \right)^{\frac{3}{2}} \quad (4)$$

where μ = dynamic viscosity of water; d = sediment diameter; and d_* = non-dimensional particle diameter given by:

$$d_* = d\left[\left(\rho_s/\rho_w - 1\right) g/\nu^2\right]^{1/3} \quad (5)$$

where ρ_w = water density, ρ_s = sediment particle density, g = acceleration due to gravity, and ν = kinematic fluid viscosity. Cheng's formula is based on measured settling speeds of sediments. As a result, it produces slower settling speeds than those given by Stokes' Law because real sediments have irregular shapes and thus a greater hydrodynamic resistance than perfect spheres as assumed in Stokes' law.

For the cohesive sediment size classes, the settling velocities are set equal to the mean settling velocities of flocs and eroded bed aggregates determined from the PICS analysis described by Smith and Friedrichs (2010).

The erosion and deposition of each of the sediment size classes, i.e., the source/sink term in the 3D transport equation given above, and the subsequent change in the composition and thickness of the sediment bed, are calculated by GSMB-SEDZLJ in every grid cell at each time step.

Description of MB-SEDZLJ

SEDZLJ is a sediment bed model that represents the dynamic processes of erosion, bedload transport, bed sorting, armoring, consolidation of fine-grain sediment dominated sediment beds, settling of flocculated cohesive sediment, settling of individual noncohesive sediment particles, and deposition. An active layer formulation is used to describe sediment bed interactions during erosion and deposition. The active layer facilitates coarsening during the bed armoring process. The GSMB-SEDZLJ module was designed to directly use the results obtained from a SEDFLUME study (Jones and Lick 2001).

Figure 95 shows the sediment transport processes simulated in GSMB-SEDZLJ. In this figure, U = near bed flow velocity, C = near bed sediment concentration, δ_{bl} = thickness of layer in which bedload transport occurs, U_{bl} = average bedload transport velocity, D_{bl} = sediment deposition rate for the sediment classes transported as bedload, and E_{bl} = sediment erosion rate for the sediment classes transported as bedload. Expressions for D_{bl}, D_{sus}, E_{bl}, and E_{sus} are given later in this chapter. Specific capabilities of GSMB-SEDZLJ are listed below.

- Whereas a hydrodynamic model is calibrated to account for the total bed shear stress, which is the sum of the form drag due to bed forms and other large-scale physical features (*e.g.*, boulder size particles) and the skin friction (also called the surface friction), the correct component of the bed shear stress to use in predicting sediment resuspension and deposition is the skin friction. The skin friction is calculated in GSMB-SEDZLJ as a function of the near-bed current- and wave orbital-velocity and the effective bed roughness. The latter is specified in GSMB-SEDZLJ as a linear function of the mean particle diameter in the active layer.

- Multiple size classes of fine-grained cohesive and noncohesive sediments can be represented in the sediment bed. This capability is necessary in order to simulate coarsening and subsequent armoring of the surficial sediment bed surface during high flow events.

- To reasonably represent the processes of erosion and deposition, the sediment bed in GSMB-SEDZLJ can be divided into multiple layers, some of which are used to represent the existing sediment bed and others that are used to represent new bed layers that form due to deposition during model simulations. Figure 96 shows a schematic diagram of this multiple bed layer structure. The graph on the right hand side of this figure shows the variation in the measured gross erosion rate (in units of cm/s) with depth into the sediment bed as a function of the applied skin friction. A site specific SEDFLUME study (as described in Gailani *et al.* (2014) performed during the thin layer placement modeling study was used to estimate these erosion rates.

- Erosion from both cohesive and noncohesive beds is affected by bed armoring, which is a process that limits the amount of bed erosion that occurs during a high-flow event. Bed armoring occurs in a bed that contains a range of particle sizes (*e.g.*, clay, silt, sand). During a high- flow event when erosion is occurring, finer particles (*i.e.*, clay and silt, and fine sand) tend to be eroded at a faster rate than coarser particles (*i.e.*, medium to coarse sand). The differences in erosion rates of the various sediment particle sizes creates a thin layer at the surface of the sediment bed, referred to as the active layer, that is depleted of finer particles and enriched with coarser particles. This depletion-enrichment process can lead to bed armoring, where the active layer is primarily composed of coarse particles that have limited mobility. The multiple bed model in GSMB-SEDZLJ accounts for the exchange of sediment through and the change in composition of this active layer. The thickness of the active

layer is calculated as a time varying function of the mean sediment particle diameter in the active layer, the critical shear stress for resuspension corresponding to the mean particle diameter, and the bed shear stress.

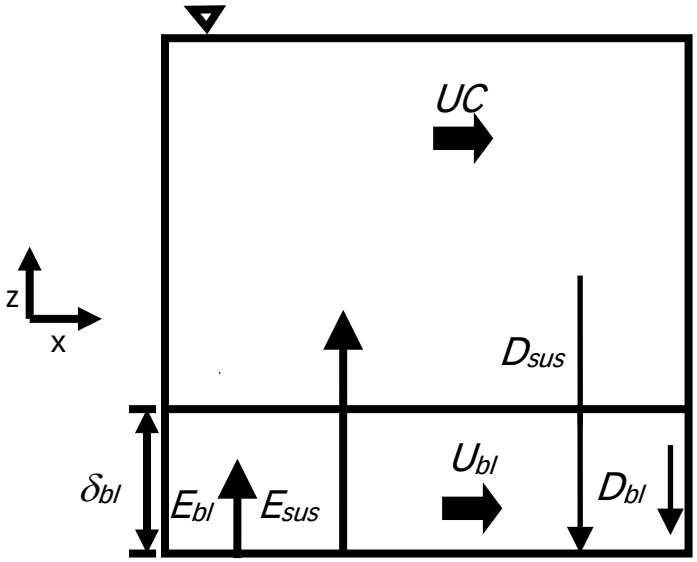

Figure 95. Sediment transport processes simulated in GSMB-SEDZLJ

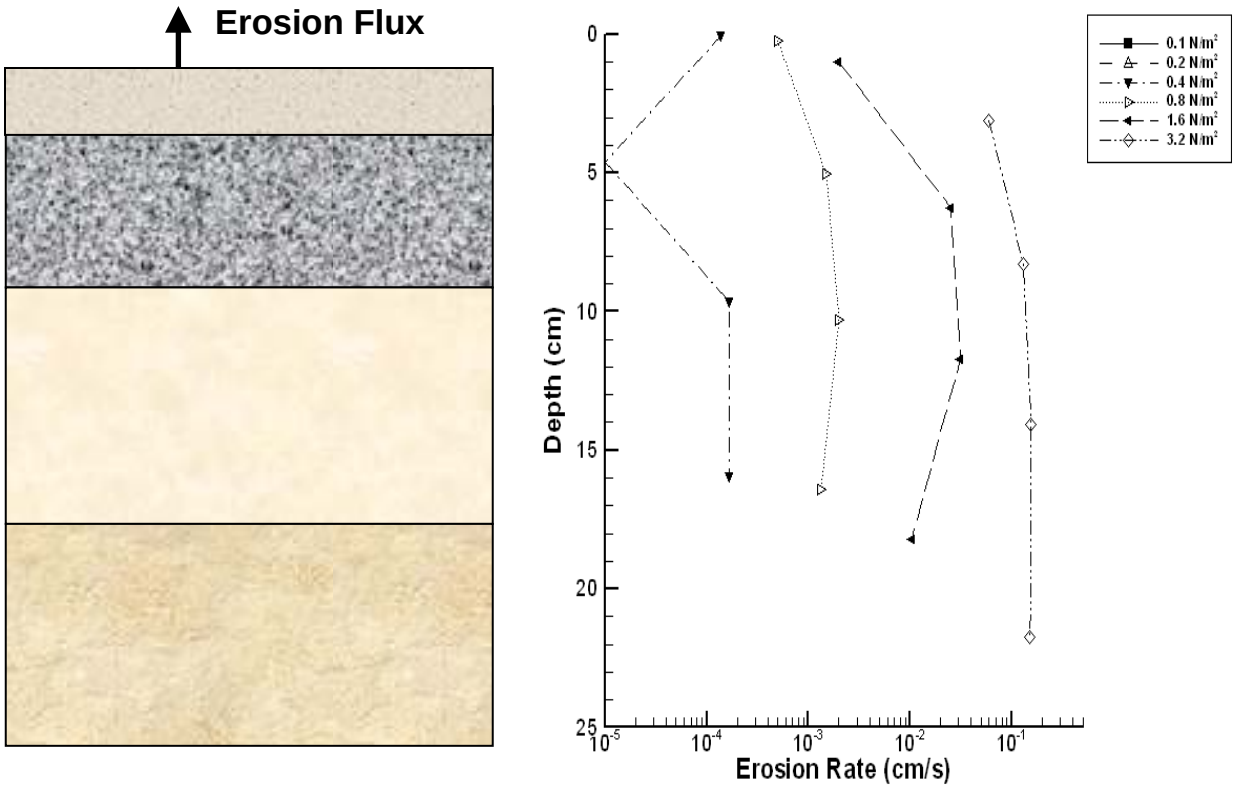

Figure 96. Multi-Bed Layer Model used in GSMB-SEDZLJ

Figure 97 shows a schematic of the active layer at the top of the multi-bed layer model used in GSMB-SEDZLJ.

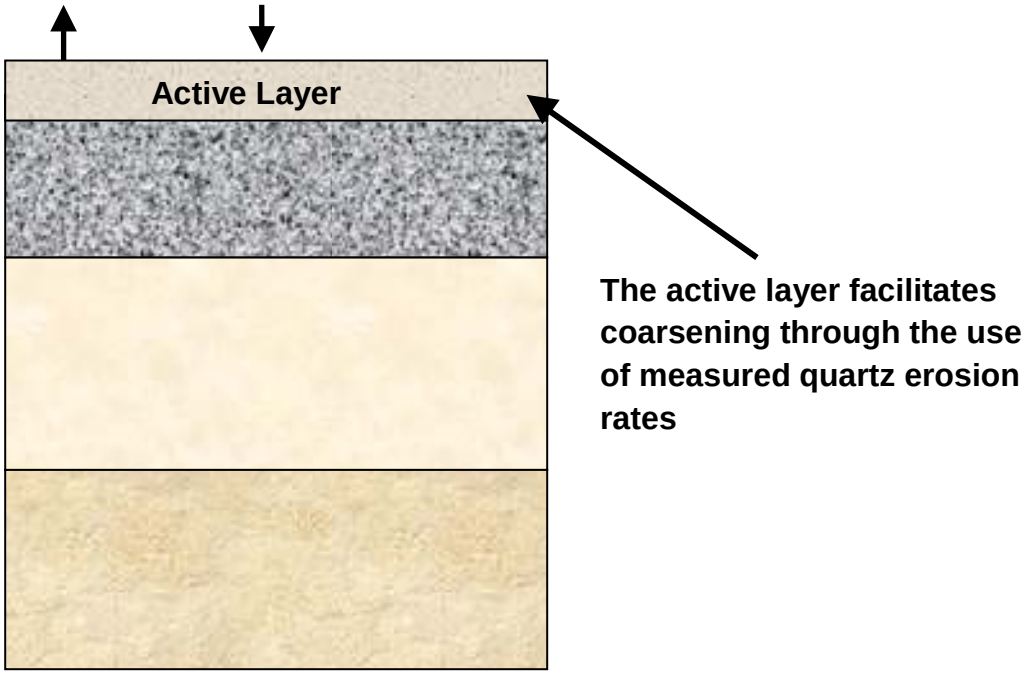

Figure 97. Schematic of Active Layer used in GSMB-SEDZLJ

- GSMB-SEDZLJ can simulate overburden-induced consolidation of cohesive sediments. An empirical algorithm that estimates the process of primary consolidation, which is caused by the expulsion of pore water from the sediment, of a fine-grained, *i.e.*, cohesive, dominated sediment bed is included in MB-SEDZLJ. The consolidation algorithm in GSMB-SEDZLJ accounts for the following changes in two important bed parameters: 1) increase in bed bulk density with time due to the expulsion of pore water, and 2) increase in the bed shear strength (also referred to as the critical shear stress for resuspension) with time. The latter parameter is the minimum value of the bed shear stress at which measurable resuspension of cohesive sediment occurs. As such, the process of consolidation typically results in reduced erosion for a given excess bed shear stress (defined as the difference between the bed shear stress and bed shear strength) due to the increase in the bed shear strength. In addition, the increase in bulk density needs to be represented to reasonably account for the mass of sediment (per unit bed area) that resuspends when the bed surface is subjected to a flow-induced excess bed shear stress. Models that represent primary consolidation range from empirical equations that approximate the increases in bed bulk density and critical shear stress for resuspension due to porewater expulsion (Sanford 2008) to numerical models that solve the non-linear finite strain

consolidation equation that governs primary consolidation in saturated porous media (Arega and Hayter 2008).

An empirical-based consolidation algorithm is included in GSMB-SEDZLJ. Simulation of consolidation requires performing specialized consolidation experiments to quantify the rate of consolidation. However, these experiments were not conducted as a component of this modeling study. As a result, consolidation was not simulated.

- GSMB-SEDZLJ contains a morphologic algorithm that, when enabled by the model user, will adjust the bed elevation to account for erosion and deposition of sediment during each time step in each grid cell. The updated bed elevations are used by the hydrodynamic model in the next time step. In this way, the hydrodynamic and sediment transport models are dynamically coupled. The morphologic routine was activated in this modeling study.

Bedload Transport of Noncohesive Sediment

The approach used by Van Rijn (1984) to simulate bedload transport is used in GSMB-SEDZLJ. The 2D mass balance equation for the concentration of sediment moving as bedload is given by:

$$\frac{\partial\left(\delta_{bl}C_b\right)}{\partial t} = \frac{\partial q_{b,x}}{\partial x} + \frac{\partial q_{b,y}}{\partial y} + Q_b \tag{6}$$

where δ_{bl} = bedload thickness; C_b = bedload concentration; $q_{b,x}$ and $q_{b,y}$ = x- and y-components of the bedload sediment flux, respectively; and Q_b = sediment flux from the bed. Van Rijn (1984) gives the following equation for the thickness of the layer in which bedload is occurring:

$$\delta_{bl} = 0.3dd_*^{0.7}(\Delta\tau)^{0.5} \tag{7}$$

where $\Delta\tau = \tau_b - \tau_{ce}$; τ_b = bed shear stress, and τ_{ce} = critical shear stress for erosion.

The bedload fluxes in the x- and y-directions are given by:

$q_{b,x} = \delta_{bl}\, u_{b,x} C_b$

$q_{b,y} = \delta_{bl}\, u_{b,y} C_b$

where $u_{b,x}$ and $u_{b,y}$ = x- and y-components of the bedload velocity, u_b, which van Rijn (1984) gives as

$$u_b = 1.5\tau_*^{0.6}\left[\left(\frac{\rho_s}{\rho_w}-1\right)gd\right]^{0.5} \quad (8)$$

with the dimensionless parameter τ_* given as

$$\tau_* = \frac{\tau_b - \tau_{ce}}{\tau_{ce}} \quad (9)$$

The *x*- and *y*-components of u_b are calculated as the vector projections of the GSMB-Hydro velocity components.

The sediment flux from the bed due to bedload, Q_b, in Equation 6 is equal to:

$$Q_b = E_{bl} - D_{bl} \quad (10)$$

Deposition of Sediment

In contrast to previous conceptual models, deposition of suspended noncohesive sediment and cohesive flocs is now believed to occur continually, and not just when the bed shear stress is less than a so-called critical shear stress of deposition (Mehta 2013). The rate of deposition of the *ith* sediment size class, $D_{sus,i}$ is given by:

$$D_{sus,i} = -\frac{W_{s,i}C_i}{d} \quad (11)$$

where $W_{s,i}$ is given by Equation 3 for noncohesive sediment and by the PICs measured settling velocities for suspended flocs and bed aggregates, and d = thickness of the bottom water column layer in a three-dimensional grid.

Because of their high settling velocities, noncohesive sediments deposit relatively quickly (in comparison to the deposition of cohesive sediments) under all flows. Due to the settling velocities of flocs being a lot slower than those of noncohesive sediment, the deposition rate of flocs are usually several orders of magnitude smaller.

Deposited cohesive sediments usually form a thin surface layer that is often called a fluff or benthic nepheloid layer that is often less than 1 cm in

thickness. The fluff layer typically forms in estuaries via deposition of suspended flocs during the decelerating phase of tidal flows, in particular immediately before slack water (Krone 1972; Hayter and Mehta 1986; and Hayter *et al.* 2010). The fluff layer is usually easily resuspended by the accelerating currents following slack water in tidal waters.

The rate of deposition of the *ith* noncohesive sediment class moving as bedload is given by (James *et al.* 2010):

$$D_{bl,i} = -P_{bl,i} W_{s,i} C_{bl,i} \tag{12}$$

where $C_{bl,i}$ = mass concentration of the *ith* noncohesive sediment class being transported as bedload, and $P_{bl,i}$ = probability of deposition from bedload transport. The latter parameter is given by:

$$P_{bl,i} = \frac{E_{bl,i}}{W_{s,i} C_{bl,i}^{eq}} \tag{13}$$

where

$$C_{bl,i}^{eq} = \frac{0.18 C_o \tau_b}{d_*} \tag{14}$$

which is the steady-state sediment concentration in bedload that results from a dynamic equilibrium between erosion and deposition, d_* is given by Equation 4, and C_o = 0.65.

Erosion of Sediment

Erosion of a cohesive sediment bed occurs whenever the current and wave-induced bed shear stress is great enough to break the electrochemical interparticle bonds (Partheniades 1965; Paaswell 1973). When this happens erosion takes place by the removal of individual sediment particles or bed aggregates. This type of erosion is time dependent and is defined as surface erosion or resuspension. In contrast, another type of erosion occurs more or less instantaneously by the removal of relatively large pieces of the bed. This process is referred to as mass erosion, and occurs when the bed shear stress exceeds the bed bulk strength along some deep-seated plane that is typically much greater than the bed shear strength of the surficial sediment.

The erosion rate of cohesive sediments is given by Equation 15 where the exponent, coefficient, and critical shear stress for erosion, n, a, and τ_{cr}, respectively, are given in Gailani *et al*. (2014). These values were determined from the SEDFLUME study performed during the thin layer placement modeling study. The erosion rates of the noncohesive sediment size classes were determined as a function of the difference between the bed shear stress and the critical shear stress for erosion using the results obtained by Roberts *et al*. (1998) who measured the erosion rates of quartz particles in a SEDFLUME.

$$E_{coh,i} = a_i \tau_i^n \quad \text{for } \tau_b > \tau_{cr} \tag{15}$$

where τ_b = current- and wave-induced bed shear stress.

The erosion rate of the *ith* noncohesive sediment size class that is transported as bedload, $E_{bl,i}$, is calculated by the following equation in which it is assumed there is dynamic equilibrium between erosion and deposition:

$$E_{bl,i} = P_{bl,i} W_{s,i} C_{bl,i} \tag{16}$$

Modifications made to GSMB-SEDZLJ

The methodology described by Lick (2009) to include the effect of bed slope on erosion rates and bedload transport was added to the original version of SEDZLJ that was implemented in GSMB-SEDZLJ. The bed slopes in both the x- and y-directions are calculated, and scaling factors are applied to the bed shear stress, erosion rate, and bedload transport equations. A maximum adverse bed slope is specified that prevents bedload transport from occurring up too steep an adverse slope.

Also added to the original version of SEDZLJ was the capability to simulate the formation of a fluff layer on top of an existing sediment bed. Being able to represent the resuspension of this layer during the early stages of the accelerating flow following slack water is essential to accurately simulating sediment transport, in particular in stratified estuaries such as Mobile Bay.

Setup of MB-SEDZLJ

The three-dimensional GSMB-SEDZLJ model was setup to simulate sediment transport in the 59-block Mobile Bay model using the following information:

- The mean settling velocities for cohesive flocs and bed aggregates are 0.7 and 1.3 mm/s, respectively, determined by the PICs analyses conducted during the Bayou Casotte project. Bayou Casotte results were used as they gave more representative floc settling velocities than those obtained from the SEDFLUME study conducted in Mobile Bay in January 2013 (Gailani *et al*. 2014).
- SEDFLUME estimates erosion rate versus bed shear stress given by Equation 14 with the cohesive sediment erosion parameterization given elsewhere (Gailani *et al*. 2014).
- Grain size distributions and bed bulk densities with depth in the SEDFLUME cores.
- The usSEABED database developed and supported by the USGS (http://walrus.wr.usgs.gov/usseabed/) provided additional data on surficial sediment types at some locations in the model domain.

Based on an analysis of all these data it was decided that two cohesive sediment classes and three noncohesive sediment classes were needed to adequately represent the measured range of sediment sizes and to represent differences in cohesive sediment transport properties (*e.g*., settling and erosion) for the native sediment and the dredged material placed in the BU areas as well in the along channel placement sites. Five size classes (two cohesive and three noncohesive) were used to represent the native sediment as well as the dredged material placed in the BU areas. The two cohesive size classes represented flocs and eroded bed aggregates. Diameters are specified for the cohesive sediment classes, but they are not used in GSMB-SEDZLJ since cohesive sediments are not treated as individual sediment particles as noncohesive sediments are. The diameters of the three noncohesive sediment size classes used to represent the native sediment were 120 μm (very fine/fine sand), 240 μm (fine sand) and 500 μm (medium sand). It was assumed that the specific gravity of all simulated sediment classes was 2.65. The settling velocities for the three noncohesive sediment classes are calculated in MB-SEDZLJ using Equation 4. The settling speeds for the 120 μm, 240 μm, and 500 μm sediment classes are equal to 8.3, 19.8, and 60.0 mm/s, respectively.

Using the available grain size distribution data from the collected SEDFLUME cores, the data in the usSEABED database as well as the compositions of the dredged material to be placed in the potential BU areas, 14 different sediment compositions were used to represent the various sediment types with spatially varying composition in the Mobile Bay model domain (see Table 1). Each number in this table represents the percentage of each of the

five sediment size classes for the top bed layer in each sediment core, and CS_f and CS_a are the cohesive floc and bed aggregate size classes, respectively. The grain size distributions for six of the 11 SEDFLUME cores collected as part of the Mobile Bay thin layer placement study are shown in Table 6 as cores 2 through 7. The numbers in parentheses to the right of Core 2 through 7 correspond to the station numbers shown in Figure 98. This figure shows where the SEDFLUME cores were collected during the thin layer placement study. The six cores used for BU areas A-F are core numbers 8 to 13, and

Table 6 Surficial Sediment Composition of 14 SEDFLUME Cores

SEDFLUME Cores	Sediment Diameter (*μm*)				
	CS_f	CS_a	120	240	500
Core No. 1 (TLP)	12	79	5	0	4
Core No. 2 (1)	0	0	13	74	13
Core No. 3 (2)	8	72	6	0	14
Core No. 4 (4)	9	86	0	0	5
Core No. 5 (6)	10	83	0	0	7
Core No. 6 (10)	10	82	2	0	6
Core No. 7 (11)	11	83	3	0	3
Core No. 8 (BU-A)	19	32	5	40	4
Core No. 9 (BU-B)	36	25	5	30	4
Core No. 10 (BU-C)	51	21	5	20	3
Core No. 11 (BU-D)	68	22	5	0	5
Core No. 12 (BU-E)	68	32	0	0	0
Core No. 13 (BU-F)	80	20	0	0	0
Nearshore east of MB and the ebb tidal delta	0	0	0	50	50

core number 1 represents the sediment in the areas where thin layer placement of dredged material occurred in 2012.

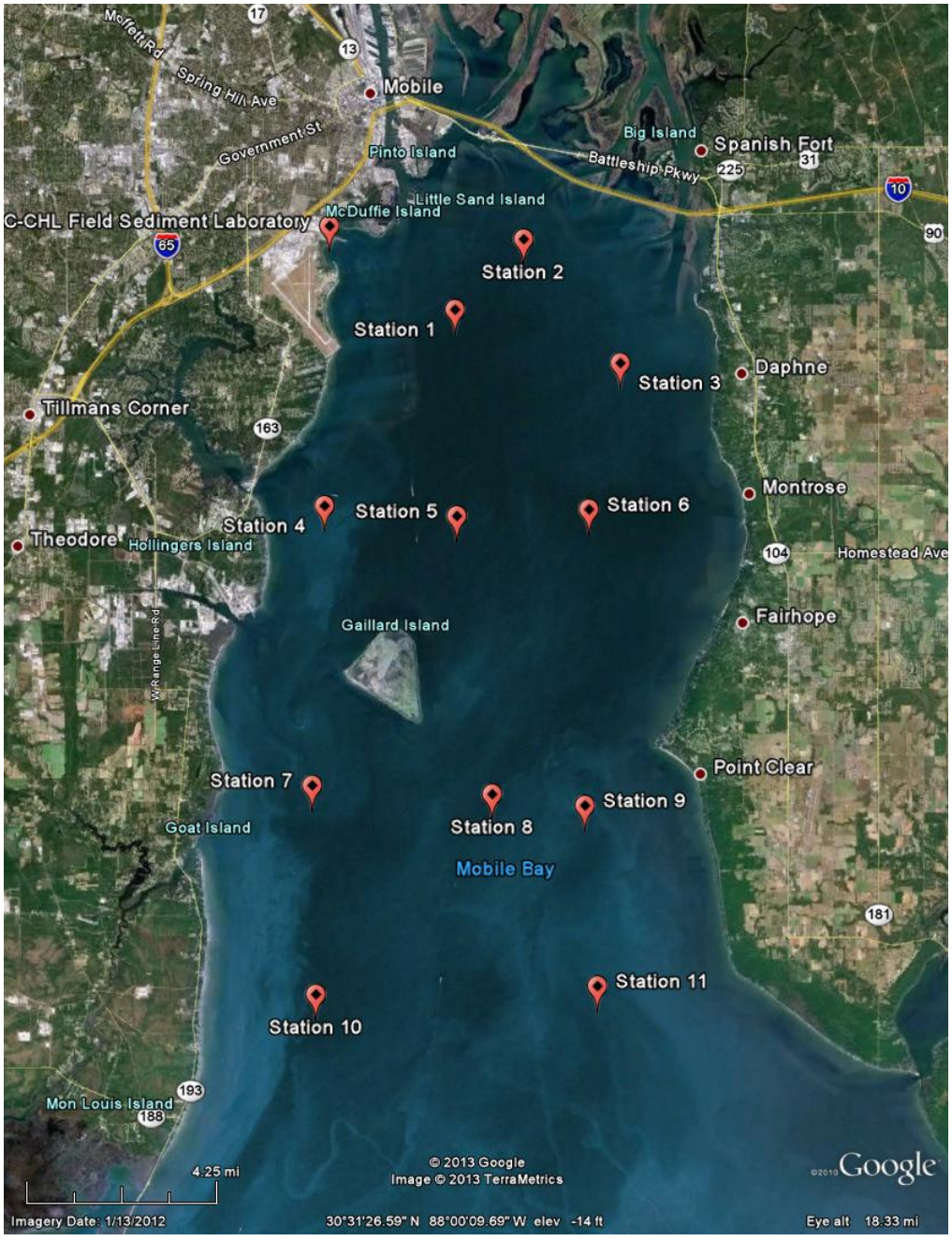

Figure 98. Stations show location of SEDFLUME cores collected during the thin placement layer study.

Six bed layers were used for each SEDFLUME core. The first (top) layer is the active layer through which depositing and eroding sediment passes. The

second layer is the layer in which new sediment deposits are placed. This layer is subdivided into a user-specified number of sublayers that can be used to represent consolidating fine-grain dominated sediment. The third through sixth bed layer are used to represent the existing sediment bed in each grid cell at the start of the model simulation. The grain size distribution in each subsurface bed layer (i.e., third to sixth bed layers) in each SEDFLUME core was set equal to that found from the SEDFLUME analyses, as was the critical shear stress and bed density for each subsurface bed layer.

The white rectangles in Figure 99 are the six potential BU areas evaluated in this study on the east side of the bay. The Mobile Bay navigation channel is divided into different reaches along its length, each of which has a different color. Figure 100 shows the outline (in black) of the placement areas along the navigation channel. The red numbers indicate the placement areas where TLP of dredge material occurred in the summer of 2012. The grid cells inside the numbered placement areas were assigned the sediment characteristics given for the TLP core in Table 6. The other grid cells were assigned one of the 13 other cores given in this table.

Sediment Transport Boundary Conditions

Sediment boundary conditions were prescribed at open water boundary along the Gulf of Mexico and at the upstream boundaries for the Mobile and Tensaw Rivers in Grid-Block 59.

Boundary Condition along the Gulf of Mexico open water tidal boundaries: Because of the unknown suspended sediment concentrations (SSC) at these boundaries, and because of the relatively large distance between this boundary and the predominant area of interest in this modeling study, a zero influx (predominantly during flood tides) of suspended sediment was assumed to occur at these boundaries. In addition, a zero gradient boundary condition was imposed at these boundaries during outgoing (*i.e.*, ebb) tides so that suspended sediment could be advected across these boundaries. Since these open water boundaries are far removed from the area of interest in Mobile Bay, the assumed no influx boundary conditions will not have any measureable impact on the simulation of sediment transport in Mobile Bay.

Figure 99. Beneficial Use areas A – F to the east of the navigation channel.

Figure 100. Placement Areas (black quadrilaterals) along the navigation channel. Number of Placement Area in red.

Boundary conditions at the upstream boundaries for the Mobile and Tensaw Rivers: The USACE Mobile District and ERDC measured SSC and discharges during the field study at the seven stations in the upper bay shown in Figure 101 (Ramirez *et al*. 2018). Figure 102 shows an example of the SSC – discharge measurements made at the North Tensaw River during one of the measurement periods. These measurements were used to adjust the discharge – SSC rating curves used for the Mobile and Tensaw Rivers during the TLP modeling study. The seven stations shown are the North Mobile River, South Mobile River, Tensaw River, Blakely, Apalachee, Tensaw River at the Causeway and the State Docks on the lower Mobile River.

Model Grid

The dynamic nature of the sediment transport in the salinity stratified Mobile Bay is seen in Figures 103 and 104. Figure 103 shows an aerial view of a fairly turbid Mobile Bay, indicative of a high suspended sediment load during high river flows. Figure 104 shows results from a bathymetric survey of the upper navigation channel that depicts spatially (intra-channel) varying sedimentation patterns over the period from August 2010 to January 2011. The dynamic nature of the channel morphology is apparent in this figure. These observations, along with several other studies performed by the USACE, the USGS, the EPA, and the University of South Alabama, support that a finely resolved grid was needed to be able to represent the spatially and temporally varying transport of sediment that occurs in the navigation channel and elsewhere in Mobile Bay. Figure 105 shows the fine grid resolution in proximity of the Mobile Bay and Theodore Ship channel intersection south of Gaillard Island, and Figure 106 shows a zoomed in representative view of the grid across the navigation channel. Twelve cells are used to represent the channel and side slopes. This level of resolution is sufficient to enable simulation of the intra-channel longitudinal and lateral sediment transport, both as bedload and suspended load.

Sediment Transport Model Calibration

The method that was used to calibrate GSMB-SEDZLJ consisted of the following steps.

1. The base case 59-Block Mobile Bay GSMB model was run for 2010. The simulated sedimentation rates in the reaches along the navigation channel were compared to the measured rates. The dredging records from 2009 – 2011 were used to compute the sedimentation rates in the different reaches. Figure 107 shows an example of the calculated dredged volumes between

August 2010 and January 2011. The simulated sedimentation rates in these reaches were calculated by dividing the dredged volumes by the time period between dredging events.

Figure 101. Seven Measurement Stations in the Upper Delta.

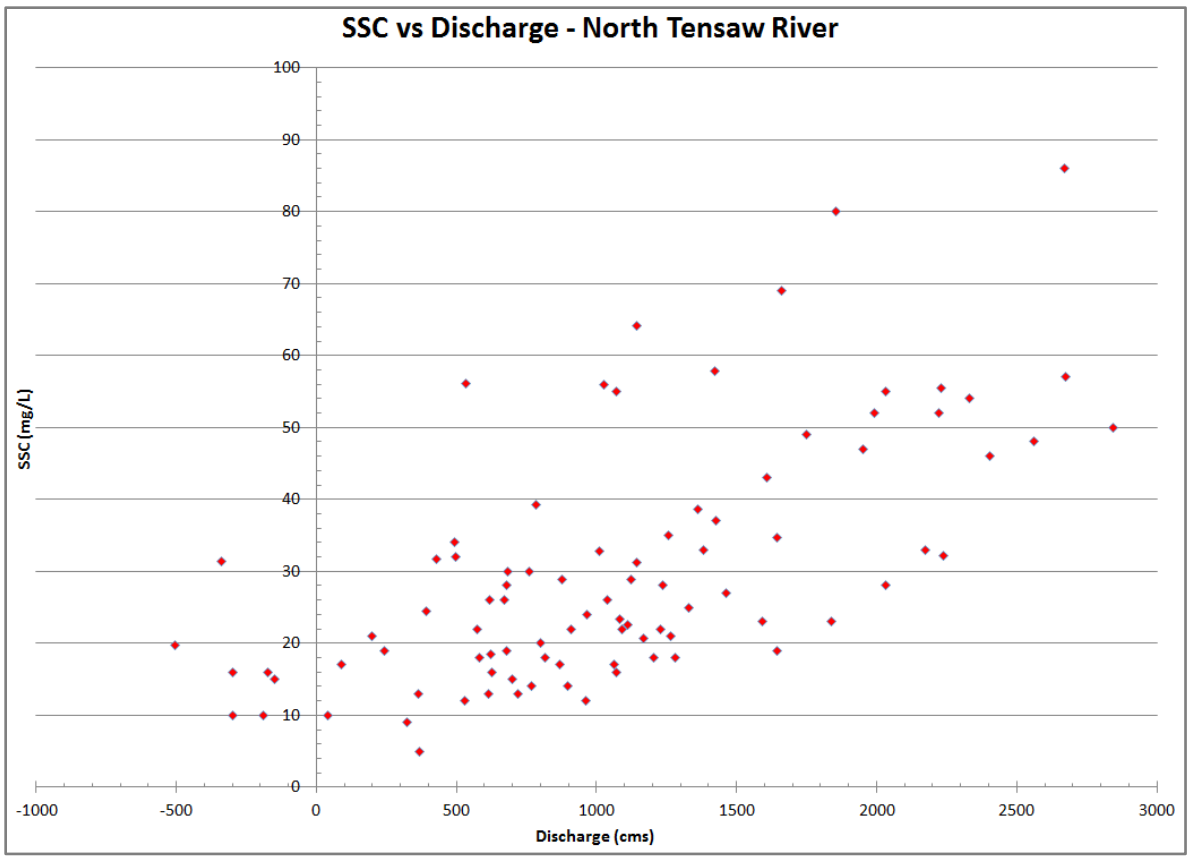

Figure 102. SSC versus Discharge time series measured at the North Tensaw River station.

2. If the simulated sedimentation rates were not within ± 10 percent of the measured rates in the different reaches, adjustments were made to either the settling velocities of the cohesive floc sediment class or to the rating curves at the two upstream boundaries in Grid-Block 59. The ± 10 percent envelope about the measured rates is considered to be the estimated uncertainty envelope for the simulated sediment transport.

The location of the reach where the absolute value of the difference was greater than 10 percent as well as the pattern of differences in the reaches both upstream and downstream of the reach was used to guide the decision as to what adjustments were made.

The results from the sediment transport model calibration are shown in Figure 108. This figure shows the percentage difference between the measured and simulated sedimentation rate, with positive values indicating that the measured rate was higher than the simulated rate. The objective of the sediment transport model calibration was achieved since the difference

between the measured and simulated sedimentation rates did not differ by more than 10 percent as seen in Figure 108. Overall, the simulated channel shoaling volume was 2.5 percent less than the historic dredged volume.

Figure 103. Aerial Photo of Turbid water in Mobile Bay

Figure 104. Dynamic channel morphology is evident in this bathymetric survey of the upper navigation channel that depicts spatially (intra-channel) varying sedimentation patterns in the channel from August 2010 to January 2011.

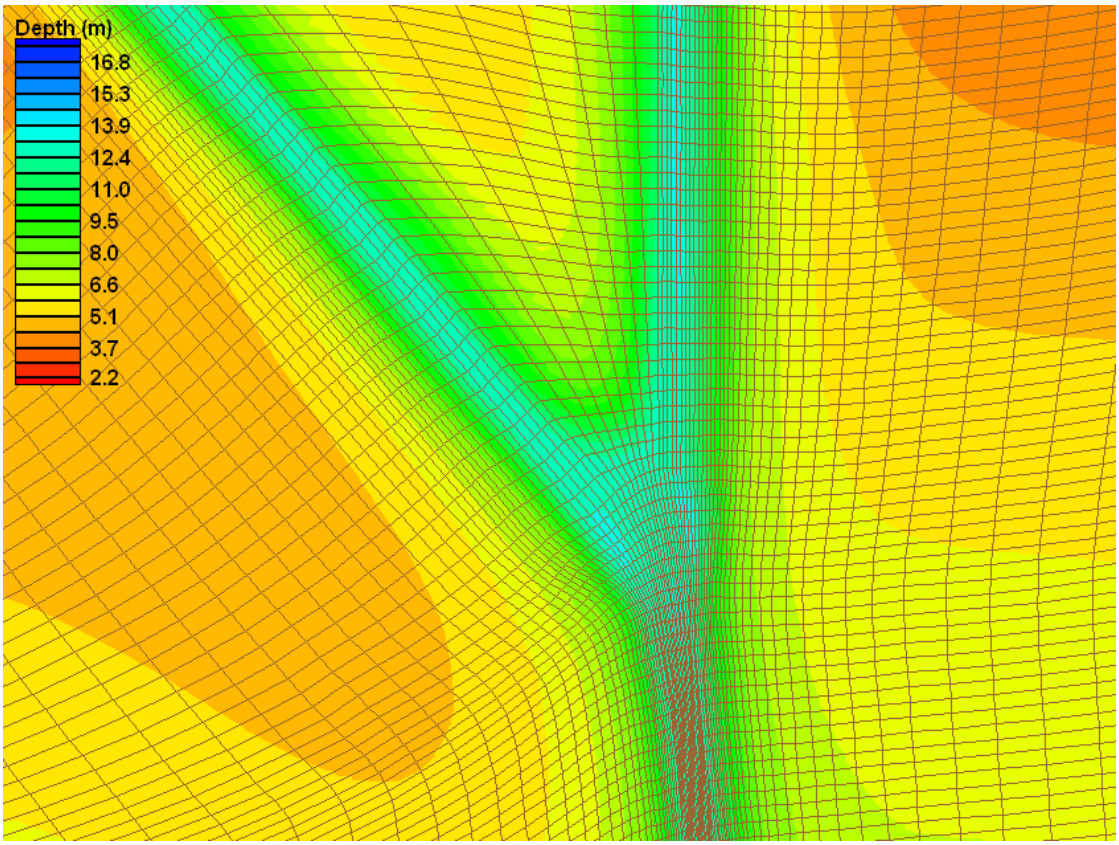

Figure 105. Grid resolution in proximity to the Mobile Theodore intersection with the navigation channel south of Gaillard Island.

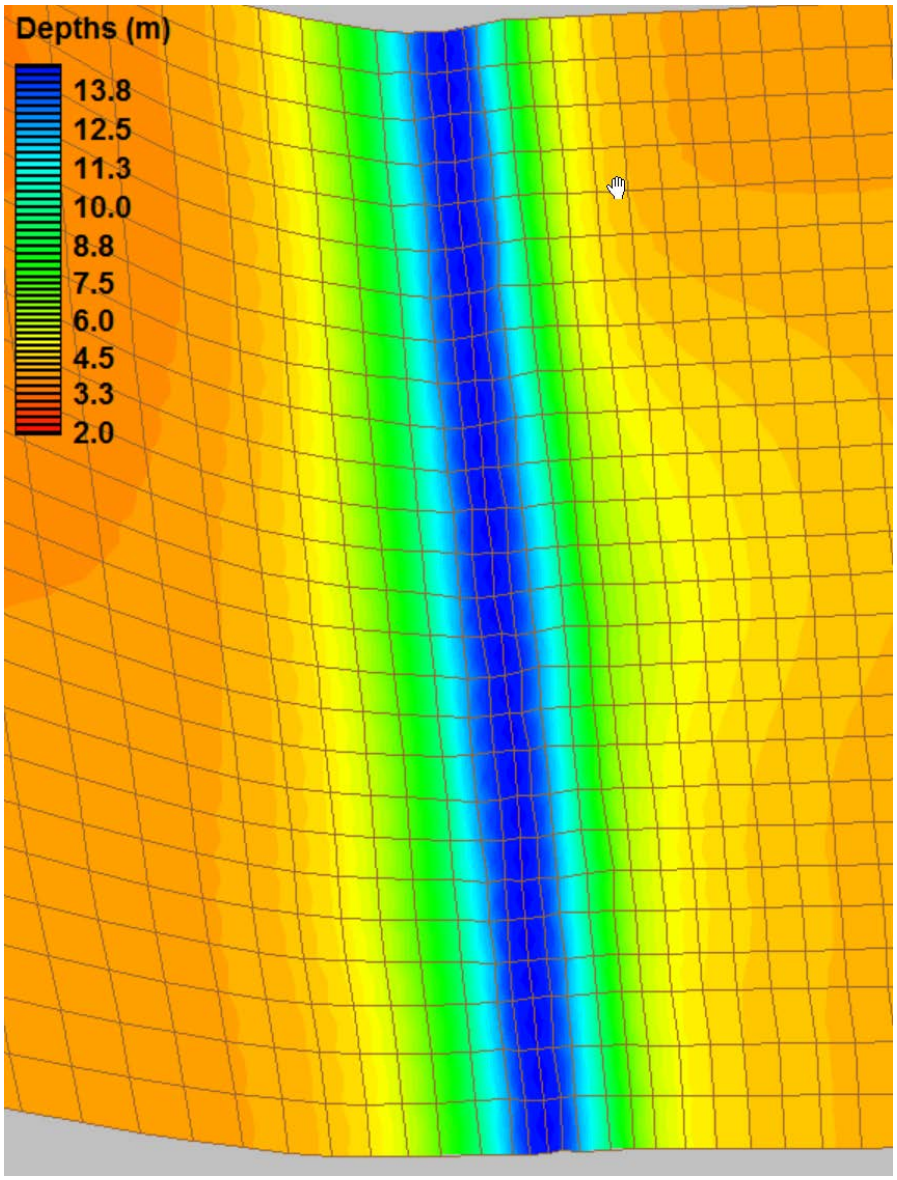

Figure 106. Grid resolution across the navigation channel.

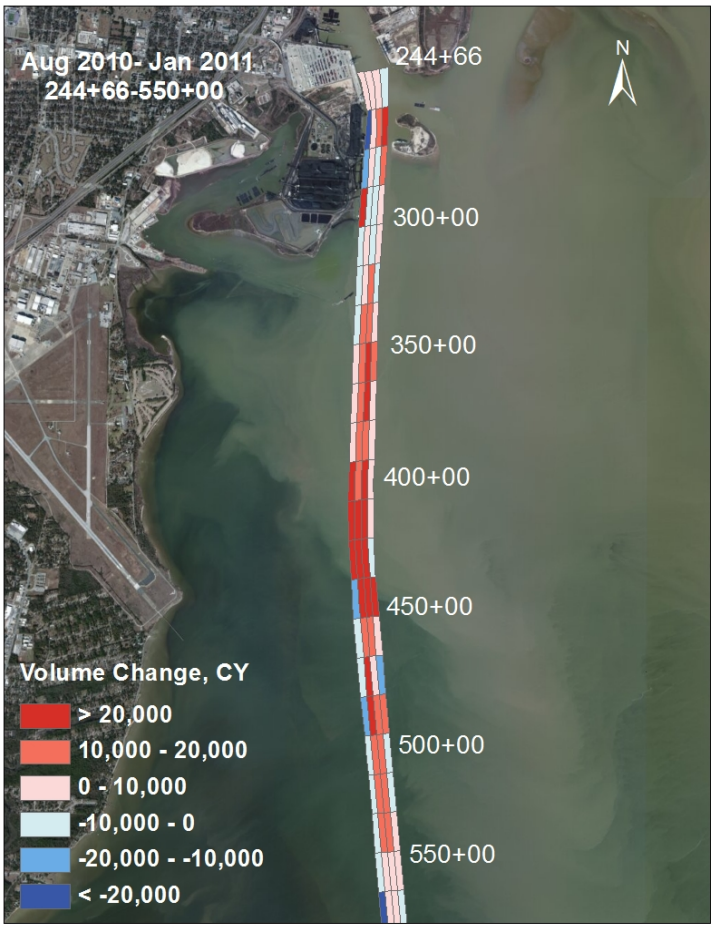

Figure 107. Dredged volumes calculated from the dredging records between August 2010 and January 2011.

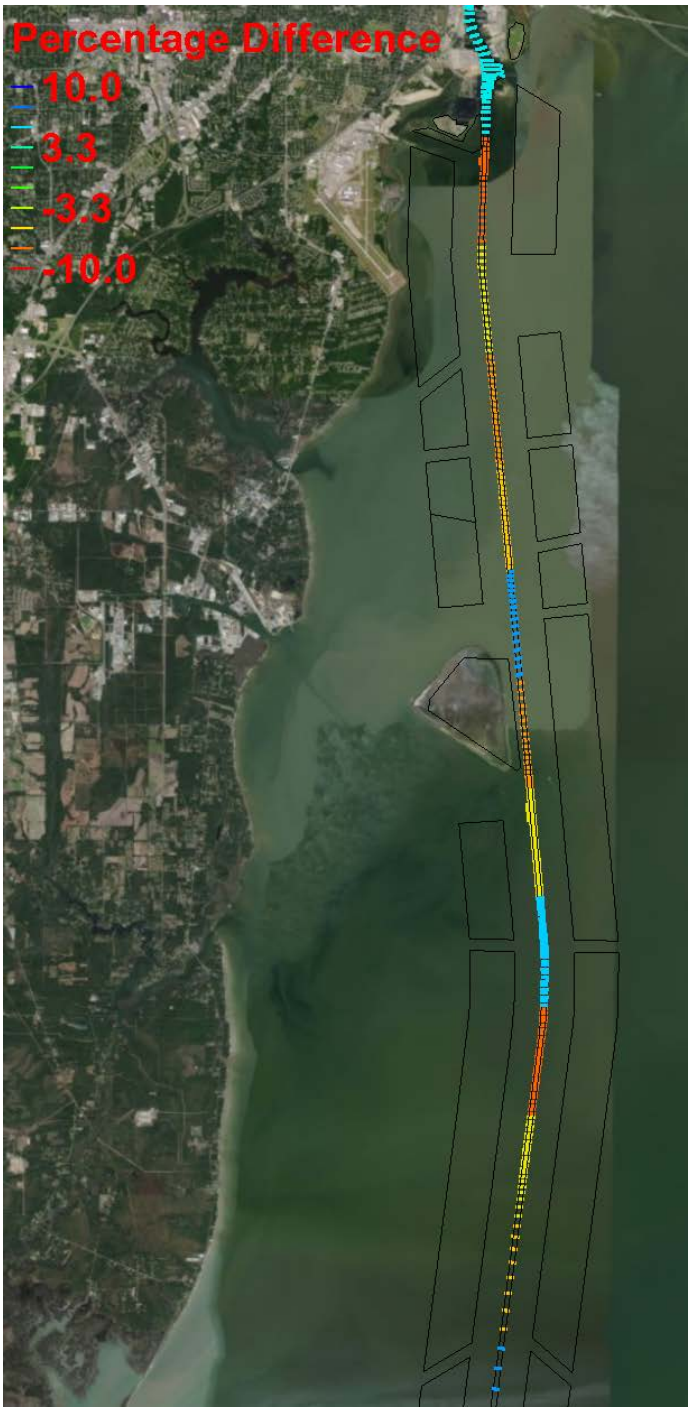

Figure 108. Sediment transport model calibration results showing the percentage difference between measured and simulated sedimentation rates.

Sediment Transport Model Simulations

The purpose of the sediment transport modeling task was to investigate the following:

1) Potential project impacts on sedimentation in the navigation channel from the proposed channel modifications.

2) Potential erosion of the dredged material placed in six potential BU areas that are shown in Figure 99. The water depths in the grid cells within the six BU areas was reduced by 0.9 m (3 feet).

3) Potential erosion of dredged material placed in the Open Water placement sites shown in Figure 100.

4) Impact of an o.5 m rise in sea level on sedimentation in the navigation channel.

Each of these four cases were investigated by running the calibrated GSMB model for one year (January 1 to December 31, 2010). First the MB-hydrodynamic and transport model was cold started and run for December 2009 to spin-up these models. Then the one year sediment transport simulations were hot started using the output files from the one month cold start.

The driving forces included in GSMB for these sediment transport simulations were astronomical tides at the outer open water boundaries of the GSMB model domain; temporally and spatially variable winds and atmospheric pressures; Mobile, Tensaw, Pearl, Pascagoula, Jourdan, Wolf, Biloxi, Perdido, Escambia, Blackwater, and Fish River flows; base flows into the grid-blocks in the Upper Delta; incident shortwave radiation; and locally generated wind waves. The latter were simulated by STWAVE as described in the CSTORM Modeling System sub-section in the Hydrodynamic Modeling section.

Impacts of Project on Sedimentation in the Navigation Channel

Figure 109 shows the simulated increases in average annual shoaling vary from 5 to 15 percent along the navigation channel with-Project Channel Depths. Table 7 shows the percentage difference for each of the channel segments seen in Figure 109. The simulation of Project Channel Depths with SLR showed less than 0.5 percent increase in shoaling from those shown in

Table 7 in every channel section.

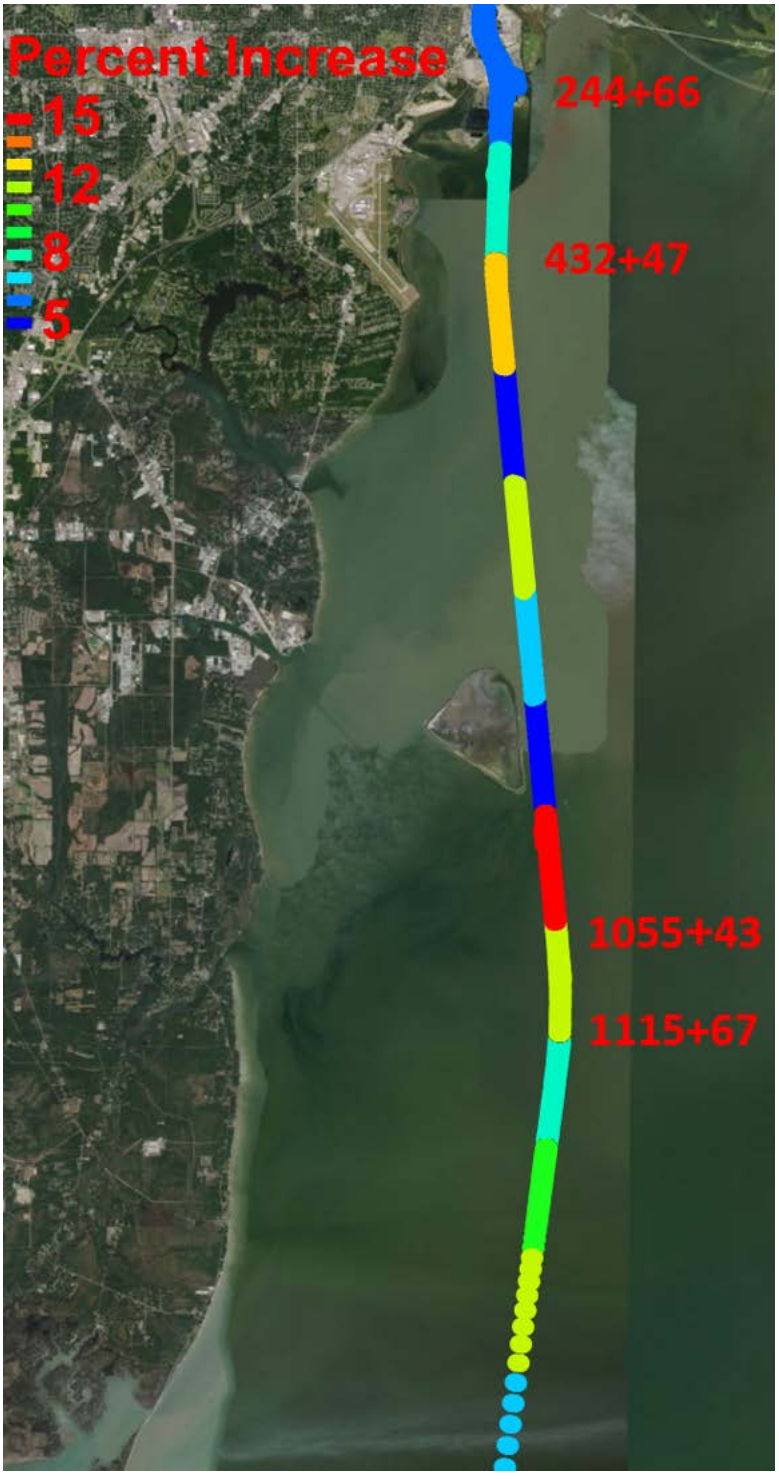

Figure 109. Simulated increases in annual shoaling vary from 5 to 15 % along channel with-Project depths. Four channel stations are shown in red to the east side of the channel.

Table 7. Simulated Percentage Increases in Annual Shoaling Along Channel with-Project Depths from North End (CS 1) to South End (CS13) of Channel Shown in Figure 109.

Channel Section (CS)	% Increase
1	6
2	8
3	13
4	5
5	12
6	7
7	5
8	15
9	12
10	8
11	10
12	12
13	7

Impacts of Project on Sedimentation in the Beneficial Use Areas

The results from the one year model simulation with-Project Channel Depths with the 0.9 m (3 feet) reduced water depths from proposed placement in the grid cells within the six BU areas showed less than $\pm$ 8 cm change in the bed elevation in every grid cell. This means the change in bed elevation varied from less than 8 cm of net erosion to 8 cm of net deposition. This small difference range indicates there was in essence no discernable net erosion or net deposition as this is within the uncertainty of the sediment transport model. In addition, the results from the one year model simulation with-Project Channel Depths with SLR with the 0.9 m (3 feet) of reduced water depths in the grid cells within the six BU areas also showed less than $\pm$ 8 cm change in every grid cell. The base case simulation (Project Channel Depths without the 0.9 m (3 feet) reduced water depths in the grid cells within the six BU areas showed a slightly smaller difference range ($\pm$ 5 cm change in the bed elevation in every grid cell).

Impacts of Project on Sedimentation in the Open Water Placement Areas

The results from the one year model simulation with-Project Conditions showed less than ± 9 cm change in the bed elevation in every grid cell within the Open Water Placement Areas from the results obtained from the one year model simulation with Existing Conditions. This means the change in bed elevation varied from less than 9 cm of net erosion to 9 cm of net deposition over the one year model simulation. This small difference range between the Existing and with-Project simulations indicates the deepening of the proposed channel modifications will have minimal impact on the sediment in the existing Open Water Placement Areas.

Conclusions

The purpose of the sediment transport modeling was to assess the relative changes in sedimentation rates within the navigation channel, dredged material placement sites, and surrounding areas as a result of channel improvements within the bay. The findings from this modeling study were the:

1) Potential project impacts on sedimentation in the navigation channel from the proposed channel modifications.

   As shown in Figure 109, the average annual shoaling rate in the navigation channel increased from 5 to 15 percent.

2) Potential erosion of the dredged material placed in six potential BU areas that are shown in Figure 99. The water depths in the grid cells within the six BU areas was reduced by 0.9 m (3 feet).

   The grid cells in the six BU areas showed less than ± 8 cm change in the bed elevation over a one year simulation in every grid cell. This means the change in bed elevations due to the shallower water depths and different sediment compositions in the BU areas varied from less than 8 cm of net erosion to 8 cm of net deposition as compared to the bed elevation changes in those grid cells during a sediment transport simulation of the channel improvements in the bay without the potential BU areas.

3) Potential erosion of dredged material placed in the Open Water placement sites shown in Figure 100.

The results from the one year model simulation with channel improvements showed less than ± 9 cm change in the bed elevations in every grid cell within the Open Water Placement Areas from the results obtained from the one year model simulation with Existing Conditions.

4) Impact of an o.5 m rise in sea level on sedimentation in the navigation channel.

The simulation of Project Channel Depths with SLR showed less than a 0.5 percent increase in shoaling rates from those given in Table 7 in every channel section.

Conclusions

The purpose of this water quality and sediment transport modeling study of Mobile Bay was to determine the impact of a harbor design plan that would enable Mobile Harbor to better accommodate deep containerships and bulk carriers on water quality and sedimentation in the bay. The central elements of the plan include deepening the Bar and Bay segments of ship channel, widening a segment of the Bay channel for two-way traffic, easing two bends in the Bar channel aestnd expanding the Choctaw turning basin.

The water quality modeling study determined the impact of the proposed changes to Mobile Harbor and the navigation channel on the following state variables: dissolved oxygen, salinity, temperature, total suspended solids, nutrients and chlorophyll-*a* ("Chl-a"). The 3D water quality model CE-QUAL-ICM was calibrated for calendar year 2010, and then used to evaluate the following four sets of conditions:; Existing (No Project), with-Project, future without project (Existing with Sea Level Rise), and Project with Sea Level Rise. Daily average values for all cells for all water quality constituents were saved during the model simulations and then retrieved for select locations afterwards. Comparison of these results enabled direct comparison of conditions between pairs of different model simulations; Existing and with-Project, and future without project (Existing with SLR) and Project with SLR. The results of the comparisons are that no alteration in the behavior of any water quality constituent evaluated was evident. In most cases the differences in constituent behavior were undetectable.

The sediment transport modeling study evaluated 1) sedimentation in the navigation channel, 2) bathymetric changes due to net erosion and/or deposition in the potential beneficial use sites on the east side of the bay, and 3) bathymetric changes due to net erosion and/or deposition in the existing along channel deposal sites. The specific objectives and findings from the sediment transport modeling study were the following:

- Potential project impacts on sedimentation in the navigation channel from the proposed channel modifications: As shown in Figure 109, the average annual shoaling rate in the navigation channel increased from 5 to 15 percent.

- Potential erosion of the dredged material placed in six potential BU areas that are shown in Figure 99: The water depths in the grid cells within the six BU areas was reduced by 0.9 m (3 feet), and then the year-long 2010

simulation was run. Analysis of the bathymetric change in the grid cells in the six BU areas showed less than ± 8 cm change in the bed elevation over a one year simulation in every grid cell. That is, the change in bed elevations due to the shallower water depths and different sediment compositions in the BU areas varied from less than 8 cm of net erosion to 8 cm of net deposition as compared to the bed elevation changes in those grid cells during a sediment transport simulation of the channel improvements in the bay without the potential BU areas.

- Potential erosion of dredged material placed in the Open Water placement sites shown in Figure 100: The results from the one year model simulation with channel improvements showed less than ± 9 cm change in the bed elevations in every grid cell within the Open Water Placement Areas from the results obtained from the one year model simulation with Existing Conditions.

- Impact of an o.5 m rise in sea level on sedimentation in the navigation channel: The simulation of Project Channel Depths with SLR showed less than a 0.5 percent increase in shoaling rates from those given in Table 7 in every channel section.

References

_____, “Bayou Casotte Harbor Channel Improvement Project Field Data Collection and Modeling Appendix, Mobile District, USACE. 2012.

ADCIRC. 2017. ADCIRC Utility Programs, http://adcirc.org/home/related-software/adcirc-utility-programs/, accessed on Aug. 1, 2017.

Allen, R.J. 2016. “Mobile-Tensaw Field Data Report,” U.S. Army District, Mobile, AL.

Allen, R.J. 2017. “Hydrodynamic and Water Quality Field Data Collection in the Mobile-Tensaw Delta: Validation of an Existing 3-Dimensional Hydrodynamic Model,” A presentation. U.S. Army Corps of Engineers, Mobile District, Mobile, AL.

Bunch, B.W., Cerco, C.F., Dortch, M.S., Johnson, B.H., and Kim, K.W. 1999. “Hydrodynamic and Water Quality Modeling Study of San Juan Bay Estuary,” ERDC-TR-00-01, U.S. Army Engineer Research and Development Center, Waterways Experiment Station, Vicksburg, MS.

Bunch, B.W., Tillman, D.H., and Mark, D.J. 2000. “POLA Main Channel Deepening Water Quality and Hydrodynamic Study,” U.S. Army Engineer Research and Development Center, Waterways Experiment Station, Vicksburg, MS.

Bunch, B.W., Tillman, D.H., and Mark, D.J., 2002. “Water Quality and Hydrodynamic Analysis of the Cabrillo Shallow Water Habitat,” U.S. Army Engineer Research and Development Center, Waterways Experiment Station, Vicksburg, MS.

Bunch, B.W., Tillman, D.H., and Mark, D.J. 2002. “Pier 400 Submerged Storage Site Water Quality and Hydrodynamic Modeling Study,” U.S. Army Engineer Research and Development Center, Waterways Experiment Station, Vicksburg, MS.

Bunch, B.W., Tillman, D.H., and Mark, D.J. 2002. “POLA Pier 400 Sensitivity Analysis,” U.S. Army Engineer Research and Development Center, Waterways Experiment Station, Vicksburg, MS.

Bunch, B.W., Channel, M., Corson, W.D., Ebersole, B.A., Lin, L., Mark, D.J., McKinney, J.P., Pranger, S.A., Schroeder, P.R., Smith, S.J., Tillman, D.H., Tracy, B.A., Tubman, M.W., and Welp, T.L. 2003. "Evaluation of Island and Near-Shore Confined Disposal Facility Alternatives, Pascagoula River Harbor Dredged Material Management Plan," Technical Report ERDC-TR-03-3, U.S. Army Engineer Research and Development Center, Waterways Experiment Station, Vicksburg, MS.

Bunch, B.W., Kim, K.W., 2011. "Hydrodynamic and Water Quality Modeling of the widening of Cano Martin Pena, San Juan Bay Estuary, Puerto Rico", Letter Report, U.S. Army Engineer Research and Development Center, Waterways Experiment Station, Vicksburg, MS, Jan 2011.

Cerco, C., and Cole, T. 1993. "Three dimensional eutrophication model of Chesapeake Bay, *Journal of Environmental Engineering*, 119(6), 1006-1025.

Cerco, C., and Cole, T. 1994. "Three-Dimensional Eutrophication Model of Chesapeake Bay," Technical Report EL-94-4, U.S. Army Engineer Waterways Experiment Station, Vicksburg, MS.

Cerco, C.F., Bunch, B.W., Cialone, M.A., and Wang, H. 1993. "Hydrodynamic and Eutrophication Model Study of Indian River-Rehoboth Bay Delaware," TR-EL-94-5, US Army Engineer Waterways Experiment Station, Vicksburg, MS.

Cerco, C.F., and Bunch, B.W. 1997. "Passaic River Tunnel Diversion Model Study, Report 5, Water Quality Modeling." TR-HL-96-2, US Army Engineer Waterways Experiment Station, Vicksburg, MS.

Cerco, C., and Meyers, M. 2000. "Tributary refinements to the Chesapeake Bay model," *Journal of Environmental Engineering*, 126(2), 164-174.

Cerco, C.F., Bunch, B.W., Teeter, A.M., and Dortch, M.S. 2000. "Water Quality Model of Florida Bay," ERDC/EL TR-00-00, U. S. Army Engineer Research and Development Center, Waterways Experiment Station, Vicksburg, MS.

Cerco, C., Johnson, B., and Wang, H. 2001. "Tributary refinements to the Chesapeake Bay model," ERDC-TR-02-4, US Army Engineer Research and Development Center, Vicksburg, MS.

Cerco, C.F., and Moore, K. 2001. "System-wide submerged aquatic vegetation model for Chesapeake Bay," *Estuaries*, 24(4), 522-534.

Cerco, C., and Noel, M. 2004. "The 2002 Chesapeake Bay eutrophication model," draft technical report, US Army Engineer Research and Development Center, Vicksburg, MS.

Chapman, R.S., Johnson, B.H., and Vemulakonda, S.R. 1996. "User Guide for the Sigma Stretched Version of CH3D-WES; A Three-dimensional Numerical Hydrodynamic, Salinity and Temperature Model," Technical Report HL-96-21, U.S. Army Engineer Waterways Experiment Station, Vicksburg, MS.

Chapman, R.S., Cole, T.M., and Gerald, T.K. 1997. "Development of Hydrodynamic Water Quality (POM-IPXMT) Linkage for the Lake Michigan Mass Balance Project," Final Report. U.S. Environmental Protection Agency, Office of Research and Development, ERL-Duluth, Large Lakes Research Station, Grosse Ile, Michigan.

Chapman, R.S., P.V. Luong, and M.W. Tubman. 2006. "Mississippi Sound Hydrodynamic and Salinity Sensitivity Modeling," Final Report prepared for U.S. Army District, Mobile, AL.

Chapman, R., and Bunch, B. 2009. "Hilo Bay Water Circulation and Water Quality Study," Honolulu District for County of Hawaii.

Chapman, R. S., and P.V. Luong. 2009. "Development of a Multi-block CH3D with a Wetting, Drying and CLEAR Linkage Capability," Report prepared for Louisiana Coastal Area (LCA) Ecosystem Restoration Plan S&T Office, Vicksburg, MS.

Chapman, R.S., Grzegorzewski, A.S., Luong, P.V., Smith, E.R., Smith, S.J., and Tubman, M.W. 2011. "The Effects of DA-10 Removal on Circulation and Sediment Transport Potential within the Horn Island Pass and Lower Pascagoula Sound Channels," Final Report prepared for U. S. Army District, Mobile, AL.

Chapman R.S, Hayter, E.J., Smith, S.J., Luong, P.V., Tubman, M., Grzegorzewski, A.S., Gailani, J.Z., Bunch, B.W., and Tillman, D.H. 2012. "Hydrodynamic, Water Quality and Sediment Transport Modeling to Investigate the Impacts of Widening the Pascagoula Lower Sound and Bayou

Casotte Navigation Channels," Final Report prepared for U. S. Army District, Mobile, AL.

Chapman, R.S., Kim, S., Massey, T.C., McAlpin, T.O., and Savant, G. 2014, "Initial Assessment of ADH-3D Hydrodynamic and Salinity Transport: Mobile Bay," ERDC Flooding and Coastal Systems Research Program, U.S. Army Engineer Waterways Experiment Station, Vicksburg, MS.

Cialone, M.A., Massey, T.C., Anderson, M.E., Grzegorzewski, A.S., Jensen, R.E., Cialone, A., Mark, D.J., Pevey, K.C., Gunkel, B.L., McAlpin, T.O. 2015. North Atlantic Coast Comprehensive Study (NACCS) Coastal Storm Model Simulations: Waves and Water Levels. ERDC/CHL TR-15-14. Vicksburg, MS: U.S. Army Engineering Research and Development Center.

Dzwonkowski, B., Park, K., Ha, H.K., Graham, W.M., Hernandez, F.J., and Powers, S.P., 2011. "Hydrographic variability on a coastal shelf directly influenced by estuarine flow," *Continental Shelf Research*, 31, 939-950.

Eiker, E.E. 1977. "Heat Exchange Program," Thermal Simulations of Lakes. Publication No. 65-902, Edison Electric Institute, New York, NY.

FEMA 2006, High Water Mark Collection for Hurricane Katrina in Alabama, FEMA report #1605-DR-AL.

Gailani, J.Z., Hayter, E.J., Chapman, R.S., Anderson, M.E., Cialone, M.A., Luong, P.V., Mark, D.J., Smith, S.J., Taylor, M.B., Perkey, D., Lovelace, N.D., and Godsey, E.S. 2014. "Modeling of Thin Layer Placement of Dredged Material in Mobile Bay," Technical Report prepared for U. S. Army District, Mobile, AL.

Hayter E.J., Chapman, R.S, Luong, P.V., Smith, S.J., and Bryant, D.B. 2012. "Demonstration of Predictive Capabilities for Fine-Scale Sedimentation Patterns within the Port of Anchorage, AK," Letter Report prepared for U. S. Army District, Anchorage, AK.

Hayter E.J., Chapman, R.S., Lin, L., Luong, P.V., Mausolf, G., Perkey, D., Mark, D., and Gailani, J.Z. 2015. "Modeling Sediment Transport in Grand Traverse Bay, Michigan to Determine Effectiveness of Proposed Revetment at Reducing Transport of Stamp Sands onto Buffalo Reef," Letter Report prepared for U. S. Army District, Detroit, MI.

Hayter, E.J., Chapman, R.S., Massey, T.C., and Bryant, M.A. 2018. "Development and Application of a Geophysical Scale Hydrodynamic and Sediment Transport Modeling System (GSMB): Kotzebue - Blossom Point Navigation Channel," Draft Report prepared for the U. S. Army District, Anchorage, AK.

Kim, S.-C. 2007. "Linkage between an Unstructured Water Quality Model, CE-QUAL-ICM, and Structured Three-Dimensional Hydrodynamic Model, CH3D-WES." SWWRRP Technical Note, U.S. Army Engineer Waterways Experiment Station, Vicksburg, MS.

Kolar, R.L., Gray, W.G., Westerink, J.J., and Luettich, R.A. 1994. "Shallow Water Modeling in Spherical Coordinates: Equation Formulation, Numerical Implementation, and Application," *Journal of Hydraulic Research*, 32 (1), 3-24.

Leonard, B.P. 1979. "A Stable and Accurate Convection Modelling Procedure based on Quadratic Upstream Interpolation," *Computer Methods in Applied Mechanics and Engineering*, (19), 59-98.

Luettich, R.A., Jr., Westerink, J.J., and Scheffner, N.W. 1992. ADCIRC: "An Advanced Three-Dimensional Circulation Model for Shelves, Coasts, and Estuaries," Technical Report DRP-92-6, U.S. Army Engineer Research and Development Center, Vicksburg, MS.

Massey, T.C., Anderson, M.E., Smith, J.M., Gomez, J.G., and Jones, R. 2011. "STWAVE: Steady-State Spectral Wave Model User's Manual for STWAVE, Version 6.0," Special Report, SR-11-1, U.S. Army Engineer Research and Development Center, Vicksburg, MS.

Massey, T.C., Wamsley, T.V., and Cialone, M.A. 2011. "Coastal Storm Modeling – System Integration," *Proceedings of the 2011 Solutions to Coastal Disasters Conference*, Anchorage, Alaska, 99-108.

Massey, T.C., Ratcliff, J.J., and Cialone, M.A. 2015. "North Atlantic Coast Comprehensive Study (NACCS) Storm Simulation and Statistical Analysis: Part II – High Performance Semi-Automated Production System," in *Proceedings of Coastal Sediments*, San Diego, CA, May 11-15, 2015; edited by Ping Wang, Julie Rosati, and Jun Cheng; DOI: 10.1142/9789814689977_0218.

Melendez, W., Settles, M., Pauer, P. and Rygwelski, K. 2009. "LM3: A High-Resolution Lake Michigan Mass Balance Water Quality Model," U.S. EPA, Office of Research and Development, National Health and Environmental Effects Research laboratory, Mid-Continent Ecology Division-Duluth, Large Lakes and Rivers Forecasting Research Branch, Large Lakes Research Station, Grosse III, MI.

Oceanweather, Inc. 2011. "Homogeneous Long Term Atmospheric Forcing Gulf of Mexico and North Atlantic for Coastal Modeling," BAA Report to ERDC-Vicksburg, MS.

Ramirez, M., Taylor, M.B., Ganesh, N., and Pratt, T.C. 2018. "Mobile Harbor Study Quantifying Sediment Characteristics and Discharges into Mobile Bay," Draft Technical Report prepared for U.S. Army District, Mobile, AL.

Smith, J.M., Resio, D.T. and Zundel, A. 1999. "STWAVE: Steady-state Spectral Wave Model, Report 1: User's Manual for STWAVE Version 2.0," Coastal and Hydraulics Laboratory Instruction Report CHL-99-1, U.S. Army Engineer Waterways Experiment Station. Vicksburg, MS.

Smith, J.M., Sherlock, A.R., and Resio, D.T. 2001. "STWAVE: Steady-state Spectral Wave Model User's Manual for STWAVE, Version 3.0," ERDC/CHL SR-01-1. U.S. Army Engineer Research and Development Center, Vicksburg, MS.

Smith, S.J., and Friedrichs, C.T. 2010. "Size and settling velocities of cohesive flocs and suspended sediment aggregates in a trailing suction hopper dredge plume," *Continental Shelf Research* (2010), doi:10.1016/j.csr.2010.04.002.

Snir, M., Otto, S., Huss-Lederman, S., Walker, D., and Dongarra, J. 1998. "MPI – The Complete Reference: Volume 1 The MPI Core," MIT Press, Cambridge, MA.

Tillman, D.H., Cerco, C.F., Noel, M.R., Martin, J.L., Hamrick, J. 2004. "Three-dimensional eutrophication modeling of the Lower St. Johns River, Florida," Technical Report TR-04-13, U.S. Army Engineer Research and Development Center, Waterways Experiment Station, Vicksburg, MS.

Tillman, D.H., McAdory, R., Bunch, B.W., Martin, S.K., Briggs, M.J., Carson, F.C., Savant, G., Raphelt, N.K. 2008. "Circulation and Water Quality Modeling in Support of Deepening the Port of Los Angeles: Alternative Disposal Sites,"

Technical Report ERDC TR-08-6, U.S. Army Engineer Research and Development Center, Waterways Experiment Station, Vicksburg, MS.

Wamsley, T.V., Godsey, E.S., Bunch, B. W., Chapman, R.S., Gravens, M.B., Grzegorzewski, A.S., Johnson, B.D., King, D.B, Permenter, R.L., Tillman, D.H., and Tubman, M.W. 2013. "Mississippi Coastal Improvements Program; Evaluation of Barrier Island Restoration Efforts," Technical Report ERDC-TR-13-12, U.S. Army Engineer Research and Development Center, Waterways Experiment Station, Vicksburg, MS.

WIS 2018. Wave Information Study website, http://wis.usace.army.mil.

Addendum

Screening Level Storm Tide Comparison between Existing and With-Project Conditions

A screening level comparison of storm tide levels in Mobile Bay between existing conditions and with-Project conditions was undertaken for two historical hurricanes, Hurricane Katrina 2005 and Hurricane Ike 2008. The ADCIRC model and grid, described in the Coastal Storm Modeling System (CSTORM-MS) section above, was used to perform existing condition simulations for this comparison without wave forcing. The existing conditions grid was then updated to include project conditions as described in the Existing and With-Project Simulations section above. Tide forcing using 8 tidal constituents (M2, S2, N2, K1, O1, Q1, P1 and K2), a six year (2010-2016) August monthly mean river inflow condition of 410 m^3/s representing the Mobile-Tensaw River Complex and Oceanweather Inc. (OWI) reconstructed hindcast winds and pressure fields were applied.

The Hurricane Katrina simulations were 20.5 days with a start date of August 9, 2005 at 1800 GMT and end date of August 30, 2005 at 0600 GMT. The first 14 days of the simulations were for spinning up the model from rest and only included river and tidal forcing. The existing condition simulation produced maximum storm tide water levels of 1.4 m, mtl in the eastern lower bay up to approximately 3.7 m mtl in the northern regions of Grand Bay and Chuckfee Bay, Figure A-1. Peak water levels within the Port of Mobile were approximately 3.2 m mtl, which compares well with observed high water mark data of 3.1 m, mtl, FEMA (2006). The modeled peak water level at Dauphin Island was 2.0 m, mtl, which also compares well with the recorded value of 1.8 m, mtl, at the NOAA gauge. The project condition simulation produced maximum storm tide water levels that were nearly unchanged. The southwestern portion of Mobile Bay showed an increased maximum water level of less than 2 cm, as seen in Figure A-2. Maximum water level differences in the vicinity of the Port were less than 0.5 cm, Figure A-3. It should be kept in mind that water level changes of this magnitude are well within the model grid and forcing uncertainty.

The Hurricane Ike simulations were 22.5 days with a start date of August 22, 2008 at 1800 GMT and end date of September 14, 2008 at 0600 GMT. The first 14 days of the simulations were for spinning up the model from rest and included only river and tidal forcing. The existing condition simulations produced maximum storm tide water levels of 0.7 m mtl in the

eastern lower bay up to 1.2 m mtl within Grand Bay and Chuckfee Bay, Figure A-4. Peak water levels near the Port of Mobile were approximately 1.1 m, mtl, which is similar to the peak recorded value at the NOAA gauge of 1.2 m mtl. Peak simulated water levels near Dauphin Island of 1.0 m, mtl again compare well to the 1.1 m, mtl, reported at the NOAA gauge. Modeled peak water levels at Weeks Bay were approximately 0.8 m, mtl, while the NOAA gauge recorded a peak value of 1.0 m, mtl. As before, project condition simulation resulted in maximum storm tide water levels that were close to the existing condition, with maximum differences less than 0.5 cm over the entire Bay, as seen in Figure A-5 and A-6. It should be kept in mind that water level changes of this magnitude are well within the model grid and forcing uncertainty.

Figure A-1. Color contour map of maximum existing condition storm tide water levels for Hurricane Katrina.

Figure A-2. Difference in Project - Existing, maximum storm tide water levels for Hurricane Katrina.

Figure A-3. Difference in Project – Existing, maximum storm tide water levels for Hurricane Katrina near the Port of Mobile.

Figure A-4. Color contour map of maximum existing condition storm tide water levels for Hurricane Ike.

Figure A-5. Difference in Project - Existing, maximum storm tide water levels for Hurricane Ike.

Figure A-6. Difference in Project – Existing, maximum storm tide water levels for Hurricane Ike near the Port of Mobile.

Appendix A

CEQUAL-ICM Input Decks

In this section are contained copies of some input decks for CEQUAL-ICM.

1. Control File – wqm_con.npt
2. Kinetic rates file – wqm_mrl.npt
3. Settling rates file – wqm_stl.npt
4. Algae rates- wqm_agr.npt
5. Light extinction – wqm_stl.npt
6. Meteorological file – wqm_met.npt

Control File

Control file for WQM

```
TITLE C
.................................TITLE.................................

Mobile Bay and Viciniy 1st run with final real 2010 hydro

real 2010 mobile met AUTOC = ON DLTFN = 0.5  DLTMAX = 120

wqEXIST_5 ico for initial cond, new cbc and BFI apl output every 1
day

Binary Initial conditions BFC,KEI, MRL, AGR consistent with Bayou
Cassottte, MS Sound

GEOM DEFINE   NB     NSB     NQF    NHQF   NSHQF      NL

          826830   82683 2370527 1626380  162638      10

TIME CON  TMSTRT   TMEND

             0.0   360.1

# DLT       NDLT

               1

DLT DAY     DLTD    DLTD    DLTD    DLTD    DLTD    DLTD    DLTD
DLTD    DLTD

             0.0

DLT VAL   DLTVAL  DLTVAL  DLTVAL  DLTVAL  DLTVAL  DLTVAL  DLTVAL
DLTVAL  DLTVAL

            120.

DLT MAX   DLTMAX  DLTMAX  DLTMAX  DLTMAX  DLTMAX  DLTMAX  DLTMAX
DLTMAX  DLTMAX
```

```
            120.

DLT FTN   DLTFTN  DLTFTN  DLTFTN  DLTFTN  DLTFTN  DLTFTN  DLTFTN
DLTFTN  DLTFTN

            0.50

HM DLT    AHMDLT  FILGTH

          1800.0    30.0

SNAPSHOT    SNPC    NSNP

              ON       3

SNAP DAY    SNPD    SNPD    SNPD    SNPD    SNPD    SNPD    SNPD
SNPD    SNPD

             0.0     5.0    30.0

SNAP FRQ    SNPF    SNPF    SNPF    SNPF    SNPF    SNPF    SNPF
SNPF    SNPF

             1.0     5.0    30.0

PLOT        PLTC   QPLTC   SPLTC SAVPLTC    NPLT

             OFF      ON     OFF     OFF       1

PLOT DAY    PLTD    PLTD    PLTD    PLTD    PLTD    PLTD    PLTD
PLTD    PLTD

             0.5

PLOT FREQ   PLTF    PLTF    PLTF    PLTF    PLTF    PLTF    PLTF
PLTF    PLTF

             1.0

AV PLOT    APLTC    NAPL
```

```
              ON       1

AVPLT DAY  APLTD   APLTD   APLTD   APLTD   APLTD   APLTD   APLTD
APLTD   APLTD

             0.0

AVPLT FREQ  APLF    APLF    APLF    APLF    APLF    APLF    APLF
APLF    APLF

            1.00   0.125        0.020833

TRAN FLUX  HTFLC   VTFLC   STFLC    NTFL

             OFF     OFF     OFF       1

FLUX DAY    TFLD    TFLD    TFLD    TFLD    TFLD    TFLD    TFLD
TFLD    TFLD

             0.0

FLUX FREQ   TFLF    TFLF    TFLF    TFLF    TFLF    TFLF    TFLF
TFLF    TFLF

           30.41

KIN FLUX    KFLC    NKFL

             OFF      16

FLUX DAY    KFLD    KFLD    KFLD    KFLD    KFLD    KFLD    KFLD
KFLD    KFLD

             0.0   122.0   274.0   487.0   639.0   852.0  1004.0
1217.0  1369.0

          1582.0  1734.0  1947.0  2099.0  2312.0  2464.0  2555.0

FLUX FREQ   KFLF    KFLF    KFLF    KFLF    KFLF    KFLF    KFLF
KFLF    KFLF
```

```
          365.25  365.25  365.25  365.25  365.25  365.25  365.25
365.25  365.25

          365.25  365.25  365.25  365.25  365.25  365.25  365.25

OXY PLOT    OPLC    NOPL   NOINT

             OFF       1       4

OXY INT     OINT    OINT    OINT    OINT    OINT    OINT    OINT
OINT    OINT

           -10.0   0.211    2.11    5.11

OXY DAY     OPLD    OPLD    OPLD    OPLD    OPLD    OPLD    OPLD
OPLD    OPLD

        .0208333

OXY FREQ    OPLF    OPLF    OPLF    OPLF    OPLF    OPLF    OPLF
OPLF    OPLF

        .0416667

MASS BAL    MBLC    NMBL

              ON       1

MBL DAY     MBLD    MBLD    MBLD    MBLD    MBLD    MBLD    MBLD
MBLD    MBLD

             0.0

MBL FREQ    MBLF    MBLF    MBLF    MBLF    MBLF    MBLF    MBLF
MBLF    MBLF

             5.0

DIAGNSTCS   DIAC    NDIA

              ON       1
```

```
DIA DAY     DIAD    DIAD    DIAD    DIAD    DIAD    DIAD    DIAD
DIAD    DIAD

              0.

DIA FREQ    DIAF    DIAF    DIAF    DIAF    DIAF    DIAF    DIAF
DIAF    DIAF

            0.50

RESTART     RSOC    NRSO    RSIC

             OFF       1     OFF

RST DAY     RSOD    RSOD    RSOD    RSOD    RSOD    RSOD    RSOD
RSOD    RSOD

           360.0

HYD MODEL   HYDC

          BINARY

HYD SOLTN    SLC   CONSC      TH MINSTEP

          UPWIND    MASS    0.55    0.01     1.00    0.01

CONTROLS    SEDC   AUTOC     VBC    BFOC    STLC    ICIC    ICOC
SAVMC

             OFF      ON      ON     OFF      ON  BINARY      ON
OFF

CONTROLS  SUSFDC  DEPFDC   KEIMC  SEDKIN

             OFF     OFF   P_ABS   33-35

DEAD SEA     FLC   XYDFC    ZDFC

              ON      ON      ON
```

```
HDIFF       XYDF  ZDFMUL

             0.5    1.00

CST INPUT    S1C     S2C     S3C     BFC    ATMC   SAVLC   SEDTR

              ON     OFF     OFF      ON     OFF     OFF     OFF

NUTR RED  REDS1C  REDS1N  REDS1P  REDS2C  REDS2N  REDS2P  REDS3C
REDS3N  REDS3P

             1.0     1.0     1.0     1.0     1.0     1.0     1.0
1.0     1.0

NUTR RED  REDCBC  REDCBN  REDCBP

             1.0     1.0     1.0

BOUNDARY   BNDTC

          INTERP

ACT CST      ACC     ACC     ACC     ACC     ACC     ACC     ACC
ACC     ACC

              ON      ON      ON     OFF     OFF      ON     OFF
OFF      ON

             OFF      ON     OFF      ON      ON     OFF      ON
OFF      ON

             OFF      ON      ON     OFF      ON     OFF     OFF
OFF      ON

             OFF     OFF     OFF     OFF     OFF     OFF     OFF
OFF     OFF

# FILES    NHYDF   NTVDF

              13       2
```

```
MAP
FILE.............................MAPFN.........................

        fort.95

GEO
FILE.............................GEOFN.........................

        wqmgeo.inp

ICI
FILE.............................ICIFN.........................

        wqm_ico.mobilewq10_exist_5

AGR
FILE.............................AGRFN.........................

        wqm_agr.mobile_4

ZOO
FILE.............................ZOOFN.........................

        wqm_zoo.run156

SUS
FILE.............................SUSFN.........................

        wqm_sfi.run367

STL
FILE.............................STLFN.........................

        wqm_stl.mobile

MRL
FILE.............................MRLFN.........................

        wqm_mrl.mobile_2
```

```
EXT
FILE.............................EXTFN.........................

        wqm_kei.mobile_5

HYD
FILE.............................HYDFN.........................

        janexisthydro.dat

        febexisthydro.dat

        marexisthydro.dat

        aprexisthydro.dat

        mayexisthydro.dat

        junexisthydro.dat

        julexisthydro.dat

        augexisthydro.dat

        sepexisthydro.dat

        octexisthydro.dat

        novexisthydro.dat

        decexisthydro.dat

        janexisthydro.dat

MET
FILE.............................METFN.........................

        mobile_ap_icm_met_wind_2010.inp

        mobile_ap_icm_met_wind_2010.inp
```

```
S1
FILE.............................S1FN.........................

        wqm_ps_2010.npt

        wqm_ps_2010.npt

S2
FILE.............................S2FN.........................

        wqm_nps.96_031910

        wqm_nps.96_031910

S3
FILE.............................S3FN.........................

        wqm_atm_bank_wet.96_run326

        wqm_atm_bank_wet.96_run326

ATM
FILE.............................ATMFN........................

        wqm_atm.chop_SJ

        wqm_atm.chop_SJ

SVI
FILE.............................SAVFN........................

        wqm_sav.run415

        wqm_sav.run415

CBC
FILE.............................CBCFN........................

        run_5_cbc.npt

        run_5_cbc.npt
```

```
BFI
FILE.............................BFIFN.........................

        wqm_bfi.mobile_uniform_10

        wqm_bfi.mobile_uniform_10

ICO
FILE.............................ICOFN.........................

        wqm_ico.mobilewq10_exist_10

SNP
FILE.............................SNPFN.........................

        wqm_snp.mobilewq10_exist_10

RSO
FILE.............................RSOFN.........................

        wqm_rso.mobilewq10_exist_10

PLT
FILE.............................PLTFN.........................

        wqm_plt.mobilewq10_exist_10

APL
FILE.............................APLFN.........................

        wqm_apl.mobilewq10_exist_10

DIA
FILE.............................DIAFN.........................

        wqm_dia.mobilewq10_exist_10

TFL
FILE.............................TFLFN.........................

        wqm_tfl.mobilewq10_exist_10
```

```
KFL
FILE.............................KFLFN.........................

        wqm_kfl.mobilewq10_exist_10

OPL
FILE.............................OPLFN.........................

        wqm_opl.mobilewq10_exist_10

MBL
FILE.............................MBLFN.........................

        wqm_mbl.mobilewq10_exist_10

ALO
FILE.............................ALOFN.........................

        wqm_alo.mobilewq10_exist_10

ZFO
FILE.............................ZFOFN.........................

        wqm_zfo.mobilewq10_exist_10

BFO
FILE.............................BFOFN.........................

        wqm_bfo.mobilewq10_exist_10

SVO
FILE.............................BFOFN.........................

        wqm_svo.mobilewq10_exist_10

SUD
FILE.............................BFOFN.........................

        wqm_sfo.mobile_wq10_exist_10
```

Kinetic Rates File

Mobile mrl file consistent with what is in Ship Island report. barry 12/18/2017
Direct PO4 settling 1 m/d. Mid Sept - Mid Oct Apr 1, 2009

```
HALF SAT    KHONT    KHNNT   KHOCOD   KHODOC    KHNDN
              3.0      1.0    0.500      0.5      0.1

RATIOS       AOCR     AONT
             2.67     4.33

REF T RESP  TRCOD    TRMNL    TRHDR    TRSUA
             23.0     20.0     20.0     20.0

TEMP EFF    KTCOD    KTMNL    KTHDR    KTSUA
            0.041    0.069    0.069    0.092

NITRIF T    KTNT1    KTNT2     TMNT
            0.090    0.090     30.0

SORPTION   KADPO4    KADSA   JBSPO4   JESPO4
              0.0      0.0    255.0    285.0

MISC         AANOX     ANDC
               0.5    0.933

REAER        AREAR    BREAR    CREAR
             0.156      1.5      1.5

           SPVAR    PRINT
        CONSTANT       NO

            KLDC
          0.0100

           SPVAR    PRINT
        CONSTANT       NO

            KRDC
           0.000

           SPVAR    PRINT
        CONSTANT       NO

            KLPC
           0.020

           SPVAR    PRINT
```

```
CONSTANT      NO

    KRPC
   0.005

   SPVAR   PRINT
CONSTANT      NO

    KLDN
   0.052

   SPVAR   PRINT
CONSTANT      NO

    KRDN
   0.000

   SPVAR   PRINT
CONSTANT      NO

    KLPN
   0.015

   SPVAR   PRINT
CONSTANT      NO

    KRPN
   0.005

   SPVAR   PRINT
CONSTANT      NO

    KLDP
   0.100

   SPVAR   PRINT
CONSTANT      NO

    KRDP
   0.000

   SPVAR   PRINT
CONSTANT      NO

    KLPP
   0.100

   SPVAR   PRINT
CONSTANT      NO
```

```
            KRPP
           0.000   0.000   0.000   0.000   0.000   0.000
0.000   0.000   0.000

           SPVAR   PRINT
         CONSTANT      NO

            KSUA
           0.030   0.100   0.100   0.000   0.000   0.000
0.000   0.000   0.000

           SPVAR   PRINT
         CONSTANT      NO

            KCOD
          20.000  20.000  20.000   0.000   0.000   0.000
0.000   0.000   0.000

           SPVAR   PRINT
         CONSTANT      NO

          KDCALG
           0.000

           SPVAR   PRINT
         CONSTANT      NO

          KLCALG
           0.000

           SPVAR   PRINT
         CONSTANT      NO

          KDNALG
           0.000

           SPVAR   PRINT
         CONSTANT      NO

          KLNALG
           0.000

           SPVAR   PRINT
         CONSTANT      NO

          KDPALG
           0.400   0.400   0.400   0.000   0.000   0.000
0.000   0.000   0.000
```

```
           SPVAR   PRINT
         CONSTANT      NO

           KLPALG
            0.000   0.000   0.000   0.000   0.000   0.000
0.000   0.000   0.000

           SPVAR   PRINT
         CONSTANT      NO

           NTMAX
            0.040   0.040   0.040   0.000   0.000   0.000
0.000   0.000   0.000
```

Settling Rates File

Consistent uniform settling with Ship Island modeling R line 2 Barry Bunch 12/19/2017

```
          SPVARM  PRINTM
        CONSTANT      NO

     BOX     WSS   WSLAB   WSREF     WSC     WSD      WSG
WSPBS   WSPO4
       1   0.100   0.050   0.000   0.000   0.000   0.050
1.000   0.000
```

Algae Rates File

Mar 26, 2009. Increase APC3 a bit to take up a little more P. Increase from 0.02 to 0.022.

```
Title line

Title line

Otherwise the same as wqm_agr.run352

 Mobile_4 run consistent with Ship Island benchmark
wqm_agr_shipisland

PREDATN     TRPR    KTPR

            20.0  0.0320

FRACTN N    FNIP    FNUP   FLNDP   FNRDP    FNLP    FNRP

            0.10    0.00    0.00    0.00   0.550   0.350

FRACTN P    FPIP   FPLDP   FPRDP    FPLP    FPRP

            0.20    0.00    0.50   0.200   0.100

FRACTN C    FDOP   FCLDP   FCRDP    FCLP    FCRP

            0.00   0.700    0.10   0.550   0.350

FRACTN SI   FSAP

             0.0

GROUP 1 1   ANC1    APC1    ASC1    STF1

           0.167  0.0125   0.000    0.30

GROUP 1   CCHLC1

             30.
```

```
GROUP 1 2   KHN1  KHNH41    KHP1    KHS1    KHR1   KHST1
            0.01   0.001 0.00250    0.00    0.50     0.5
GROUP 1 3 ALPHMN   PRSP1   PRPWR
            3.15    0.25     2.0
GROUP 1 4   TMP1     TR1
            29.0   20.00
GROUP 1 5  KTG11   KTG12    KTB1
          0.0050  0.0040  0.0322
GROUP 1 6   FNI1   FNLD1   FNRD1   FNLP1   FNRP1
            0.55    0.20    0.00   0.200   0.050
GROUP 1 7   FPI1   FPLD1   FPRD1   FPLP1   FPRP1
            0.75    0.25    0.00   0.000   0.000
GROUP 1 8  FCLD1   FCRD1   FCLP1   FCRP1
           0.000   0.000   0.000    0.00
GROUP 2 1   ANC2    APC2    ASC2    STF2
           0.167  0.0125   0.300     0.1
GROUP 2   CCHLC2
            75.0
GROUP 2 2   KHN2  KHNH42    KHP2    KHS2    KHR2   KHST2
           0.025   0.001  0.0025    0.03     0.5     2.0
GROUP 2 3 ALPHMN   PRSP2   PRPWR
```

```
             8.00    0.25     2.0

GROUP 2 4   TMP2     TR2

             16.0   20.00

GROUP 2 5  KTG21   KTG22    KTB2

          0.0018  0.0060  0.0322

GROUP 2 6   FNI2   FNLD2   FNRD2   FNLP2   FNRP2

             0.55    0.20    0.00   0.200   0.050

GROUP 2 7   FPI2   FPLD2   FPRD2   FPLP2   FPRP2

             0.75    0.25    0.00   0.000   0.000

GROUP 2 8  FCLD2   FCRD2   FCLP2   FCRP2

            0.100    0.00   0.100   0.000

GROUP 3 1   ANC3    APC3    ASC3    STF3

            0.167  0.0220   0.100    0.00

GROUP 3   CCHLC3

              60.

GROUP 3 2   KHN3  KHNH43    KHP3    KHS3    KHR3   KHST3

            0.020   0.001  0.0025   0.001    0.50    35.0

GROUP 3 3 ALPHMN   PRSP3   PRPWR

            10.00    0.25     2.0

GROUP 3 4   TMP3     TR3

             30.0   20.00
```

```
GROUP 3 5  KTG31   KTG32    KTB3

         0.00400 0.00000  0.0322

GROUP 3 6   FNI3   FNLD3   FNRD3   FNLP3   FNRP3

            0.55    0.20    0.00   0.200   0.050

GROUP 3 7   FPI3   FPLD3   FPRD3   FPLP3   FPRP3

            0.75    0.25    0.00   0.000   0.000

GROUP 3 8  FCLD3   FCRD3   FCLP3   FCRP3

           0.000   0.000   0.000    0.00

GROUP 1   SPVAR1  PRINT1

        CONSTANT      NO

     BOX     PM1    BMR1    BPR1

       1     0.0   0.030   0.000

GROUP 2   SPVAR2  PRINT2

        CONSTANT      NO

     BOX     PM2    BMR2    BPR2

       1   300.0   0.010   0.010

GROUP 3   SPVAR3  PRINT3

        CONSTANT      NO

     BOX     PM3    BMR3    BPR3

       1   450.0   0.010   0.100

PREDATN    TPVAR   PRINT
```

CONSTANT	ALL
DAY	TVPR
1	1.000

Light Extinction File

Linear model ke = a + b * ISS + c * VSS - d * SALT From Run84

Change upper bay, potomac to agree with lower bay, potomac 07/11/16

one supplied modified to be consoistent with Ship Island input. barry 12/18/2017

INTKE	INITKE	KECHL
0.5	0.1	0.02

SPVARKE	PRINTKE
CONSTANT	NO

CELL	KE	KEISS	KEVSS	KEDOC
1	0.7500	0.0800	0.0557	0.0000

Meteorology File

Mobile Meteorological data for Calibration & Scenario runs

JDAY	KT	TE	IO	FD	WS
0.0	23.9	9.7	24.8	0.380	4.24
1.0	18.9	4.9	29.8	0.380	3.90
2.0	16.3	2.3	26.7	0.390	3.54
3.0	16.3	1.0	26.0	0.390	3.69
4.0	17.2	0.1	29.7	0.390	4.00
5.0	10.7	3.6	31.1	0.390	2.01
6.0	14.0	6.2	25.8	0.390	2.53
7.0	27.9	-1.2	17.4	0.390	7.03
8.0	21.8	-1.7	27.4	0.390	5.46
9.0	18.7	-0.4	31.7	0.390	4.44
10.0	9.4	4.3	31.8	0.390	1.54
11.0	14.0	6.2	31.4	0.390	2.65
12.0	12.8	6.0	31.1	0.390	2.38
13.0	10.3	6.9	22.4	0.390	1.28
14.0	15.7	10.4	27.2	0.390	2.55
15.0	35.6	14.5	13.0	0.400	5.27
16.0	30.8	12.3	13.8	0.400	4.92
17.0	13.2	13.8	23.7	0.400	1.78
18.0	12.2	14.0	30.6	0.400	1.16
19.0	21.0	15.1	16.0	0.400	2.81
20.0	41.7	19.1	17.8	0.400	5.14
21.0	18.0	17.0	29.0	0.400	2.33
22.0	24.1	13.3	28.5	0.400	3.70
23.0	48.3	17.1	11.9	0.400	6.52
24.0	22.8	11.8	33.7	0.410	4.00
25.0	18.2	11.5	34.1	0.410	3.20
26.0	13.1	11.3	34.6	0.410	2.15
27.0	11.2	12.7	30.8	0.410	1.11
28.0	21.6	12.3	19.2	0.410	3.43
29.0	28.3	10.5	12.4	0.410	4.76
30.0	22.9	2.9	17.9	0.410	4.98
31.0	10.9	10.6	32.1	0.410	1.48
32.0	16.6	13.3	29.7	0.420	2.51
33.0	19.0	11.4	31.5	0.420	3.19
34.0	24.1	9.9	17.5	0.420	4.17
35.0	31.2	14.7	14.4	0.420	4.53
36.0	23.6	9.1	19.9	0.420	4.26
37.0	21.5	4.5	17.1	0.420	4.44
38.0	16.2	9.2	35.2	0.430	2.83
39.0	27.5	11.0	16.2	0.430	4.61

40.0	22.7	4.1	36.2	0.430	5.12
41.0	14.7	4.8	24.2	0.430	2.88
42.0	20.1	2.6	14.1	0.430	4.15
43.0	17.5	7.0	37.1	0.430	3.38
44.0	13.6	11.8	38.7	0.430	2.16
45.0	23.8	8.7	35.5	0.440	4.61
46.0	16.3	7.2	41.3	0.440	3.25
47.0	13.6	9.5	41.4	0.440	2.36
48.0	12.0	12.1	40.5	0.440	1.89
49.0	11.0	13.1	33.9	0.440	1.52
50.0	11.4	15.3	40.2	0.450	0.86
51.0	18.7	13.8	34.1	0.450	2.88
52.0	22.7	16.6	16.8	0.450	2.99
53.0	26.9	11.2	30.6	0.450	4.70
54.0	24.5	8.4	27.6	0.450	4.72
55.0	17.3	9.0	44.6	0.450	3.42
56.0	11.0	13.1	35.0	0.460	1.19
57.0	17.7	10.6	26.5	0.460	2.99
58.0	15.0	14.8	45.3	0.460	2.31
59.0	16.1	14.6	38.1	0.460	2.38
60.0	32.3	7.1	20.1	0.460	6.38
61.0	21.7	9.0	36.2	0.460	4.17
62.0	17.9	11.4	47.1	0.470	3.23
63.0	12.4	14.7	45.2	0.470	1.89
64.0	13.9	14.7	46.9	0.470	2.24
65.0	11.6	17.6	46.2	0.470	1.03
66.0	12.6	16.7	31.5	0.470	1.69
67.0	30.4	14.3	23.5	0.480	4.71
68.0	42.5	18.7	19.1	0.480	5.44
69.0	37.2	19.9	26.6	0.480	4.54
70.0	26.0	18.8	35.4	0.480	3.45
71.0	23.3	16.0	46.4	0.480	3.72
72.0	18.5	17.0	47.7	0.480	2.73
73.0	24.5	16.0	45.9	0.490	3.81
74.0	20.7	15.4	48.0	0.490	3.23
75.0	16.1	12.1	21.0	0.490	2.46
76.0	17.8	14.4	25.9	0.490	2.63
77.0	13.6	21.6	50.4	0.490	1.63
78.0	24.0	17.4	45.0	0.500	3.41
79.0	37.1	11.9	22.9	0.500	6.37
80.0	18.8	9.1	28.9	0.500	3.45
81.0	15.9	19.9	48.5	0.500	2.01
82.0	19.5	19.2	39.2	0.500	2.45
83.0	31.0	18.7	33.7	0.510	4.00
84.0	25.5	18.0	45.9	0.510	3.60
85.0	24.1	17.8	49.5	0.510	3.43
86.0	29.2	19.9	35.0	0.510	3.75
87.0	31.7	15.5	52.4	0.510	5.25
88.0	16.1	20.7	55.6	0.520	2.14

89.0	20.8	21.4	54.8	0.520	2.61
90.0	21.6	22.0	54.6	0.520	2.59
91.0	28.5	20.2	48.7	0.520	3.66
92.0	35.7	20.7	25.4	0.520	4.22
93.0	23.0	23.0	31.1	0.520	2.40
94.0	22.2	23.7	45.3	0.530	2.40
95.0	27.7	22.2	47.7	0.530	3.23
96.0	38.3	22.6	40.6	0.530	4.28
97.0	40.6	21.0	31.5	0.530	4.89
98.0	21.8	19.8	58.4	0.530	3.13
99.0	17.5	20.4	44.6	0.540	2.27
100.0	21.0	22.0	58.3	0.540	2.68
101.0	22.5	24.2	57.5	0.540	2.55
102.0	21.6	23.2	54.1	0.540	2.53
103.0	26.4	23.3	52.1	0.540	3.02
104.0	29.9	23.5	56.2	0.540	3.41
105.0	20.6	26.6	57.7	0.550	2.01
106.0	18.4	26.0	52.1	0.550	1.82
107.0	24.5	24.1	51.8	0.550	2.68
108.0	22.8	21.5	44.9	0.550	2.98
109.0	20.0	20.7	38.8	0.550	2.51
110.0	16.1	26.1	53.0	0.550	1.46
111.0	22.0	25.1	54.0	0.560	2.31
112.0	42.0	22.9	48.2	0.560	4.71
113.0	74.1	22.5	20.4	0.560	8.06
114.0	42.4	23.9	53.7	0.560	4.71
115.0	31.7	22.9	61.4	0.560	3.92
116.0	24.5	22.0	56.7	0.570	3.13
117.0	19.4	22.3	59.0	0.570	2.49
118.0	25.1	23.1	61.6	0.570	3.00
119.0	44.3	22.9	46.7	0.570	4.95
120.0	64.1	23.7	21.2	0.570	6.55
121.0	82.3	24.3	22.3	0.570	8.31
122.0	51.9	25.1	29.4	0.570	5.10
123.0	31.1	26.8	45.3	0.580	2.91
124.0	20.5	31.4	59.5	0.580	1.33
125.0	21.5	30.6	55.9	0.580	1.69
126.0	34.1	27.4	56.7	0.580	3.17
127.0	37.5	25.9	47.0	0.580	3.66
128.0	27.4	21.1	64.2	0.580	3.66
129.0	30.1	24.8	56.1	0.590	3.54
130.0	46.7	25.2	44.6	0.590	4.71
131.0	48.0	26.3	41.5	0.590	4.48
132.0	44.1	26.5	48.0	0.590	4.15
133.0	31.4	27.8	49.0	0.590	2.81
134.0	32.8	26.7	42.3	0.590	3.04
135.0	27.6	25.1	29.3	0.590	2.59
136.0	19.4	28.6	41.6	0.590	1.50
137.0	24.3	29.9	53.0	0.600	1.97

138.0	19.8	29.5	46.6	0.600	1.48
139.0	33.1	28.9	54.4	0.600	2.82
140.0	38.8	28.6	54.4	0.600	3.37
141.0	27.3	30.5	47.4	0.600	2.12
142.0	22.5	33.1	55.8	0.600	1.40
143.0	24.5	32.3	58.8	0.600	1.85
144.0	31.0	29.3	54.9	0.600	2.63
145.0	23.3	28.5	43.2	0.600	1.95
146.0	26.4	30.3	59.7	0.610	2.18
147.0	23.7	31.3	59.2	0.610	1.89
148.0	24.3	30.7	58.0	0.610	1.93
149.0	25.2	26.5	39.6	0.610	2.28
150.0	26.1	28.7	40.7	0.610	2.14
151.0	22.1	31.5	48.3	0.610	1.54
152.0	26.9	30.6	51.4	0.610	2.08
153.0	30.6	28.9	48.2	0.610	2.55
154.0	36.9	28.6	45.5	0.610	3.08
155.0	46.7	28.2	47.2	0.610	4.01
156.0	31.0	29.2	34.0	0.610	2.43
157.0	29.9	31.6	54.1	0.610	2.25
158.0	25.4	30.9	56.3	0.610	2.06
159.0	31.3	30.9	52.7	0.620	2.42
160.0	35.3	30.7	53.3	0.620	2.75
161.0	36.0	30.6	54.4	0.620	2.83
162.0	23.6	33.2	48.2	0.620	1.56
163.0	23.8	33.6	49.1	0.620	1.14
164.0	24.3	34.0	51.8	0.620	1.58
165.0	22.9	32.3	45.3	0.620	1.22
166.0	22.9	32.4	42.9	0.620	1.42
167.0	23.8	33.9	55.9	0.620	1.25
168.0	23.3	33.3	52.5	0.620	1.48
169.0	25.0	33.5	43.6	0.620	1.69
170.0	26.4	32.0	59.5	0.620	1.97
171.0	30.0	33.0	59.7	0.620	2.14
172.0	36.8	28.7	46.1	0.620	3.10
173.0	36.9	30.1	52.6	0.620	2.96
174.0	27.2	32.8	55.2	0.620	1.93
175.0	23.4	33.8	57.2	0.620	1.41
176.0	26.8	32.9	59.7	0.620	1.93
177.0	27.8	32.0	51.9	0.620	2.04
178.0	32.9	29.6	40.0	0.620	2.59
179.0	26.8	29.7	39.9	0.620	2.08
180.0	33.1	28.4	30.3	0.620	2.70
181.0	24.7	30.4	36.1	0.620	1.81
182.0	25.4	31.1	40.8	0.620	1.85
183.0	44.5	27.9	52.8	0.620	3.98
184.0	36.2	27.7	57.9	0.620	3.45
185.0	41.3	28.4	44.8	0.610	3.51
186.0	41.5	27.9	36.9	0.610	3.54

187.0	39.9	28.9	45.4	0.610	3.30
188.0	23.9	33.9	56.7	0.610	1.50
189.0	23.9	33.8	54.9	0.610	1.43
190.0	23.7	33.5	52.7	0.610	1.60
191.0	25.1	32.1	44.0	0.610	1.76
192.0	36.5	30.9	53.7	0.610	2.81
193.0	42.4	30.3	50.0	0.610	3.32
194.0	35.1	31.6	55.1	0.610	2.64
195.0	27.3	31.5	43.2	0.610	2.01
196.0	35.6	30.0	40.8	0.610	2.74
197.0	29.8	30.6	42.7	0.610	2.24
198.0	22.9	31.9	42.9	0.600	1.64
199.0	22.5	31.6	41.1	0.600	1.37
200.0	28.1	31.9	50.0	0.600	2.04
201.0	27.6	33.4	55.7	0.600	1.87
202.0	24.1	34.2	57.4	0.600	1.54
203.0	24.1	33.6	50.2	0.600	1.33
204.0	23.9	31.9	30.4	0.600	1.35
205.0	31.7	30.5	35.4	0.600	2.31
206.0	32.5	30.9	40.4	0.600	2.40
207.0	28.2	31.9	50.3	0.590	2.06
208.0	23.1	33.3	55.0	0.590	1.50
209.0	34.0	30.9	56.6	0.590	2.66
210.0	36.0	31.2	51.7	0.590	2.74
211.0	30.5	33.3	53.6	0.590	2.10
212.0	27.9	33.4	53.1	0.590	1.94
213.0	26.5	34.2	50.8	0.590	1.71
214.0	25.1	32.5	40.2	0.580	1.69
215.0	26.3	33.4	45.2	0.580	1.71
216.0	25.1	32.0	44.1	0.580	1.78
217.0	23.1	32.3	41.4	0.580	1.63
218.0	33.0	31.4	45.1	0.580	2.44
219.0	27.1	31.6	40.8	0.580	1.93
220.0	35.5	30.5	47.5	0.580	2.72
221.0	39.3	30.7	54.4	0.570	3.08
222.0	39.2	30.2	51.2	0.570	3.13
223.0	44.7	29.0	40.5	0.570	3.69
224.0	46.2	28.8	36.2	0.570	3.74
225.0	26.0	31.2	40.5	0.570	1.84
226.0	28.1	30.8	40.2	0.570	2.06
227.0	38.6	28.5	35.5	0.560	3.17
228.0	56.5	28.0	31.6	0.560	4.69
229.0	52.4	28.9	43.9	0.560	4.27
230.0	27.8	30.9	38.3	0.560	2.00
231.0	23.8	32.6	43.9	0.560	1.56
232.0	30.6	31.5	44.2	0.560	2.18
233.0	31.1	31.8	45.6	0.550	2.22
234.0	28.9	30.4	39.8	0.550	2.20
235.0	25.6	31.8	54.6	0.550	1.90

236.0	21.3	32.2	54.9	0.550	1.54
237.0	26.0	30.2	49.4	0.550	2.08
238.0	24.0	29.1	30.5	0.550	1.83
239.0	43.0	26.1	32.6	0.540	3.91
240.0	43.3	25.3	30.3	0.540	4.09
241.0	39.3	26.8	34.8	0.540	3.50
242.0	34.9	27.0	34.0	0.540	3.08
243.0	32.7	28.5	48.6	0.540	2.80
244.0	21.6	31.5	52.6	0.530	1.56
245.0	21.6	30.5	47.6	0.530	1.70
246.0	29.2	27.6	50.1	0.530	2.70
247.0	20.3	28.1	51.7	0.530	1.89
248.0	21.0	30.9	49.8	0.530	1.63
249.0	28.3	30.5	48.2	0.530	2.16
250.0	24.0	30.7	39.7	0.520	1.77
251.0	22.0	31.4	45.8	0.520	1.21
252.0	22.1	30.9	37.3	0.520	1.58
253.0	26.8	30.8	42.7	0.520	1.97
254.0	32.2	30.3	46.7	0.520	2.51
255.0	32.8	25.6	51.5	0.510	3.50
256.0	18.7	29.2	50.1	0.510	1.64
257.0	31.1	29.0	44.4	0.510	2.55
258.0	26.9	28.1	43.8	0.510	2.33
259.0	26.5	29.4	41.1	0.510	2.12
260.0	20.8	30.6	45.4	0.500	0.95
261.0	21.6	30.9	41.5	0.500	1.35
262.0	24.0	29.6	35.8	0.500	1.89
263.0	23.2	29.3	38.1	0.500	1.85
264.0	31.0	27.9	43.6	0.500	2.68
265.0	33.2	26.8	45.6	0.500	3.08
266.0	30.7	28.1	39.0	0.490	2.59
267.0	23.6	28.8	38.2	0.490	1.89
268.0	24.6	27.8	31.9	0.490	2.01
269.0	28.8	23.1	36.6	0.490	3.10
270.0	16.0	24.9	44.1	0.490	1.64
271.0	20.5	23.6	47.3	0.480	2.27
272.0	28.8	20.2	47.5	0.480	3.85
273.0	25.3	21.8	46.8	0.480	3.10
274.0	22.5	21.6	47.0	0.480	2.83
275.0	30.5	18.8	46.7	0.480	4.35
276.0	27.7	15.7	47.1	0.470	4.54
277.0	26.6	15.6	46.8	0.470	4.37
278.0	22.7	18.0	46.3	0.470	3.41
279.0	13.8	22.3	45.8	0.470	1.65
280.0	14.9	23.9	44.8	0.470	1.01
281.0	15.9	25.6	44.0	0.470	1.56
282.0	19.2	25.2	42.9	0.460	1.93
283.0	25.1	23.6	40.7	0.460	2.65
284.0	23.2	23.5	34.6	0.460	2.40

285.0	20.5	24.0	38.3	0.460	2.10
286.0	23.7	20.9	42.2	0.460	2.91
287.0	15.1	20.0	43.2	0.450	1.99
288.0	14.6	22.0	42.3	0.450	1.69
289.0	14.9	22.8	41.3	0.450	1.14
290.0	15.6	23.4	39.1	0.450	1.20
291.0	18.4	22.9	38.5	0.450	1.97
292.0	23.3	21.4	33.4	0.450	2.70
293.0	14.9	23.1	39.9	0.440	1.24
294.0	16.4	21.7	39.6	0.440	1.91
295.0	18.6	21.7	37.7	0.440	2.10
296.0	33.7	23.1	27.5	0.440	3.49
297.0	42.2	24.2	20.6	0.440	4.13
298.0	59.5	24.4	17.3	0.440	5.85
299.0	53.6	25.3	14.5	0.430	4.98
300.0	30.2	21.7	17.1	0.430	3.38
301.0	26.8	14.1	36.2	0.430	4.52
302.0	14.9	18.2	37.4	0.430	1.91
303.0	15.1	21.3	31.0	0.430	1.28
304.0	15.7	22.4	33.0	0.430	1.36
305.0	29.5	20.5	18.7	0.420	3.34
306.0	38.3	19.4	14.2	0.420	4.61
307.0	39.6	14.6	22.9	0.420	6.28
308.0	23.2	11.1	36.2	0.420	4.24
309.0	16.6	10.4	36.2	0.420	2.96
310.0	15.5	10.8	36.0	0.420	2.70
311.0	11.6	14.4	35.4	0.420	0.53
312.0	12.5	16.6	34.7	0.410	0.73
313.0	12.9	17.0	31.2	0.410	0.56
314.0	13.1	18.0	32.8	0.410	0.85
315.0	13.7	19.1	32.1	0.410	1.56
316.0	13.9	18.6	28.8	0.410	1.43
317.0	15.2	20.0	22.2	0.410	1.52
318.0	19.6	18.3	12.4	0.410	2.24
319.0	30.1	18.6	17.2	0.400	3.72
320.0	15.6	14.5	32.7	0.400	2.26
321.0	12.8	15.9	27.2	0.400	1.19
322.0	24.0	14.7	23.9	0.400	3.54
323.0	19.1	18.2	17.9	0.400	2.31
324.0	22.7	19.8	25.7	0.400	2.64
325.0	31.4	20.7	17.0	0.400	3.51
326.0	28.6	21.8	18.3	0.400	3.02
327.0	23.3	21.9	16.3	0.400	2.40
328.0	38.7	21.0	18.8	0.390	4.40
329.0	34.3	18.2	13.4	0.390	4.26
330.0	23.2	7.0	30.9	0.390	4.65
331.0	12.4	10.4	29.2	0.390	1.91
332.0	26.0	13.8	21.8	0.390	3.95
333.0	49.7	18.6	11.0	0.390	6.28

334.0	17.3	8.0	29.8	0.390	3.20
335.0	10.8	10.5	30.6	0.390	0.36
336.0	11.7	13.1	29.9	0.390	1.41
337.0	20.9	15.3	26.5	0.390	2.91
338.0	28.1	10.0	25.5	0.390	5.14
339.0	20.6	4.0	29.4	0.390	4.46
340.0	12.9	5.6	30.3	0.390	2.42
341.0	12.2	5.1	25.1	0.380	2.18
342.0	10.7	5.8	29.8	0.380	1.84
343.0	10.6	9.0	29.3	0.380	1.26
344.0	23.5	12.4	25.5	0.380	3.73
345.0	33.2	8.8	21.7	0.380	6.49
346.0	22.6	1.1	30.3	0.380	5.56
347.0	11.8	2.8	30.3	0.380	2.38
348.0	17.5	7.0	21.0	0.380	3.30
349.0	44.4	16.3	16.8	0.380	6.39
350.0	21.6	13.6	19.4	0.380	3.16
351.0	23.6	7.4	15.2	0.380	4.44
352.0	18.0	7.1	29.1	0.380	3.47
353.0	11.9	8.6	28.5	0.380	1.94
354.0	22.3	12.9	19.5	0.380	3.38
355.0	26.6	18.2	19.2	0.380	3.31
356.0	26.4	8.9	28.9	0.380	5.12
357.0	13.8	8.6	27.6	0.380	2.33
358.0	22.1	8.8	21.7	0.380	3.85
359.0	30.5	1.2	15.1	0.380	7.29
360.0	15.8	2.8	29.6	0.380	3.33
361.0	9.9	6.5	29.9	0.380	0.93
362.0	17.5	9.0	27.1	0.380	3.02
363.0	29.1	13.9	15.1	0.380	4.35
364.0	50.9	17.8	10.4	0.380	6.62

ATTACHMENT A - 2

USGS MODELING REPORT

USGS
science for a changing world

Prepared in cooperation with the U.S. Army Corps of Engineers

Effects of Proposed Navigation Channel Improvements on Sediment Transport in Mobile Harbor, Alabama

Open-File Report 2018–1123

U.S. Department of the Interior
U.S. Geological Survey

Effects of Proposed Navigation Channel Improvements on Sediment Transport in Mobile Harbor, Alabama

By Davina L. Passeri, Joseph W. Long, Robert L. Jenkins, and David M. Thompson

Prepared in cooperation with the U.S. Army Corps of Engineers

Open-File Report 2018–1123

U.S. Department of the Interior
U.S. Geological Survey

U.S. Department of the Interior
RYAN K. ZINKE, Secretary

U.S. Geological Survey
James F. Reilly II, Director

U.S. Geological Survey, Reston, Virginia: 2018

Suggested citation:
Passeri, D.L., Long, J.W., Jenkins, R.L., and Thompson, D.M., 2018, Effects of proposed navigation channel improvements on sediment transport in Mobile Harbor, Alabama: U.S. Geological Survey Open-File Report 2018–1123, 22 p., https://doi.org/10.3133/ofr20181123.

ISSN 2331-1258 (online)

Acknowledgments

This research was chartered by the U.S. Army Corps of Engineers Mobile District. The authors thank Soupy Dalyander and Elizabeth Godsey for reviewing this publication. Betsy Boynton and Rebekah Davis supported the review, editing, and publishing process.

Contents

Abstract 1
Introduction 1
Modeling Approach 3
Proposed Navigation Channel Modifications 3
Model Description 3
Model Setup 4
Boundary Conditions 5
Morphological Tide 6
Simulations 7
Modeling Results 7
Model Performance 7
Modeled Versus Observed Bed Level Changes 8
2010 Climatology 9
10-Year Climatology 12
Discussion 16
Summary and Conclusions 19
References Cited 21

Figures

1. The Mobile Harbor study area, Alabama, including Mobile Bay and the navigational channel, which consists of the upper bay channel, the lower bay channel, and the entrance channel 2
2. Delft3D model domains and initial elevations, Mobile Harbor, Alabama. 4
3. Observed bed level changes in Mobile Harbor, Alabama. *A*, from 2002 to 2014. *B*, from 2002 to 2015. *C*, from 2009 to 2014 9
4. Modeled bed level change in Mobile Harbor, Alabama. *A*, after 10 years in the 10-year existing condition simulation. *B*, after 5 years in the 10-year existing condition simulation 10
5. Changes in bed level for the 2010 simulations, Mobile Harbor, Alabama. *A*, existing conditions. *B*, with-project conditions. *C*, difference in final bed level between existing and with-project conditions 11
6. Changes in bed level for the 2010 simulations, Mobile Harbor, Alabama. *A*, existing conditions accounting for 0.5 meter of sea level rise. *B*, with-project conditions accounting for 0.5 meter of sea level rise. *C*, difference in final bed level between existing conditions accounting for 0.5 meter of sea level rise and with-project conditions accounting for 0.5 meter of sea level rise ... 12
7. Percent change in the volume of sediment eroded or deposited in the entrance channel, Mobile Harbor, Alabama. *A*, between 2010 existing and 2010 with-project conditions. *B*, between 2010 existing with 0.50 meter of sea level rise and 2010 with-project with 0.50 meter of sea level rise. 14

8. Changes in bed level for the 10-year simulations, Mobile Harbor, Alabama. *A*, existing conditions. *B*, with-project conditions. *C*, difference in final bed level between existing and with-project conditions 15
9. Changes in bed level for the 10-year simulations, Mobile Harbor, Alabama. *A*, existing conditions accounting for 0.5 meter of sea level rise. *B*, with-project conditions accounting for 0.5 meter of sea level rise. *C*, difference in final bed level between existing conditions accounting for 0.5 meter of sea level rise and with-project conditions accounting for 0.5 meter of sea level rise ... 16
10. Percent change in the volume of sediment eroded or deposited in the entrance channel, Mobile Harbor, Alabama. *A*, between the 10-year existing and 10-year with-project conditions. *B*, between the 10-year existing condition with 0.50 meter of sea level rise and 10-year with-project condition with 0.50 meter of sea level rise. 18

Tables

1. Characteristics and percent occurrence of wave conditions for each wave bin for 10-year climatology and 2010 climatology, Mobile Harbor, Alabama 6
2. Coefficients of determination and root mean square error values for through-channel and cross-channel velocity components during flood and ebb tide at inlet, volume flux during flood and ebb tide at inlet and water levels at the Dauphin Island tide gage, Mobile Harbor, Alabama 8
3. Volume of sediment eroded or deposited in the entrance channel at the end of the 2010 simulations, Mobile Harbor, Alabama 13
4. Volume of sediment eroded or deposited in the entrance channel for the 10-year climatology simulations, Mobile Harbor, Alabama 17
5. Shoaling volume in the entrance channel at the end of each year for the 10-year simulations, Mobile Harbor, Alabama 19

Conversion Factors

International System of Units to U.S. customary units

Multiply	By	To obtain
	Length	
meter (m)	3.281	foot (ft)
kilometer (km)	0.6214	mile (mi)
kilometer (km)	0.5400	mile, nautical (nmi)
meter (m)	1.094	yard (yd)
	Volume	
cubic meter (m^3)	6.290	barrel (petroleum, 1 barrel = 42 gal)
cubic meter (m^3)	264.2	gallon (gal)
cubic meter (m^3)	0.0002642	million gallons (Mgal)
cubic meter (m^3)	35.31	cubic foot (ft^3)
cubic meter (m^3)	1.308	cubic yard (yd^3)
cubic meter (m^3)	0.0008107	acre-foot (acre-ft)
	Flow rate	
cubic meter per second (m^3/s)	70.07	acre-foot per day (acre-ft/d)
meter per second (m/s)	3.281	foot per second (ft/s)
cubic meter per second (m^3/s)	35.31	cubic foot per second (ft^3/s)

Datum

Vertical coordinate information is referenced to the North American Vertical Datum of 1988 (NAVD 88).
Elevation, as used in this report, refers to the distance above the vertical datum.

Abbreviations

ADCP	acoustic Doppler current profiler
CoNED	Coastal National Elevation Database
DEM	digital elevation model
ECMWF	European Centre for Medium-Range Weather Forecast
HYCOM	Hybrid Coordinate Ocean Model
lidar	light detection and ranging
NGDC	National Geophysical Data Center
NOAA	National Oceanic and Atmospheric Administration
R^2	coefficient of determination
RMSE	root mean square error
SLR	sea level rise
U	through-channel velocity
V	cross-channel velocity

Effects of Proposed Navigation Channel Improvements on Sediment Transport in Mobile Harbor, Alabama

By Davina L. Passeri, Joseph W. Long, Robert L. Jenkins and David M. Thompson

Abstract

A Delft3D model was developed to evaluate the potential effects of proposed navigation channel deepening and widening in Mobile Harbor, Alabama. The model performance was assessed through comparisons of modeled and observed data of water levels, velocities, and bed level changes; the model captured hydrodynamic and sediment transport patterns in the study area with skill. The validated model was used to simulate changes in sediment transport for existing conditions and with the proposed modifications to the navigational channel (with-project), with and without accounting for 0.5 meter (m) of sea level rise (SLR). Each scenario was simulated for 1 year with a wave climatology representative of the year 2010 as well as for 10 years with a longer-term wave climatology spanning from 1988 to 2016. Bed level differences for the existing and with-project 2010 simulations were minimal, ranging from −0.11 to 0.11 m offshore of Pelican Island and −0.81 to 0.22 m offshore of the Fort Morgan Peninsula. For the simulations accounting for 0.5 m of SLR, differences in bed levels from −0.20 to 0.32 m near Pelican Island and −0.38 to 0.34 m offshore of the Fort Morgan Peninsula. The proposed modifications reduced the channel shoaling volume by 4.77 and 8.09 percent for the 2010 simulations without and with 0.5 m of SLR, respectively. For the 10-year simulations, bed level differences for the existing and with-project simulations ranged from −3.17 to 3.94 m for the simulation without SLR and −1.92 to 1.47 m for the simulation with 0.5 m of SLR. The with-project condition reduced the entrance channel shoaling volume by 5.54 percent for the simulation without SLR and 14.98 percent for the simulation with 0.5 m of SLR.

Introduction

Mobile Harbor is in southwest Alabama in the northern Gulf of Mexico (fig. 1). The U.S. Army Corps of Engineers (USACE) proposed to deepen and widen the existing navigation channel in Mobile Harbor as part of an economic analysis to determine the feasibility of channel improvements. To evaluate the potential effects of channel deepening and widening on the morphology of the ebb tidal shoal and adjacent areas, the USACE Mobile District requested the support of the U.S. Geological Survey in numerical modeling of waves, currents, and sediment transport for the Mobile Harbor General Reevaluation Report. A numerical modeling approach was implemented to quantify relative changes in sediment pathways and the morphological response on the ebb tidal shoal because of the increased channel dimensions. A Delft3D model was developed to simulate changes in sediment transport under existing conditions and accounting for 0.5 m of sea level rise, with and without modifications to the navigation channel. Each scenario was simulated for a 1- and 10-year period; the 1-year simulation used a climatology

representative of the year 2010, and the 10-year simulation used a long-term wave climatology for the region. Model output was used to infer potential effects to sediment delivery at the inlet ebb tidal shoal and towards Dauphin Island, Alabama.

Modeling Approach

A Delft3D model was developed and used to quantify relative changes in sediment transport and the morphologic response on the ebb tidal shoal under existing conditions and with

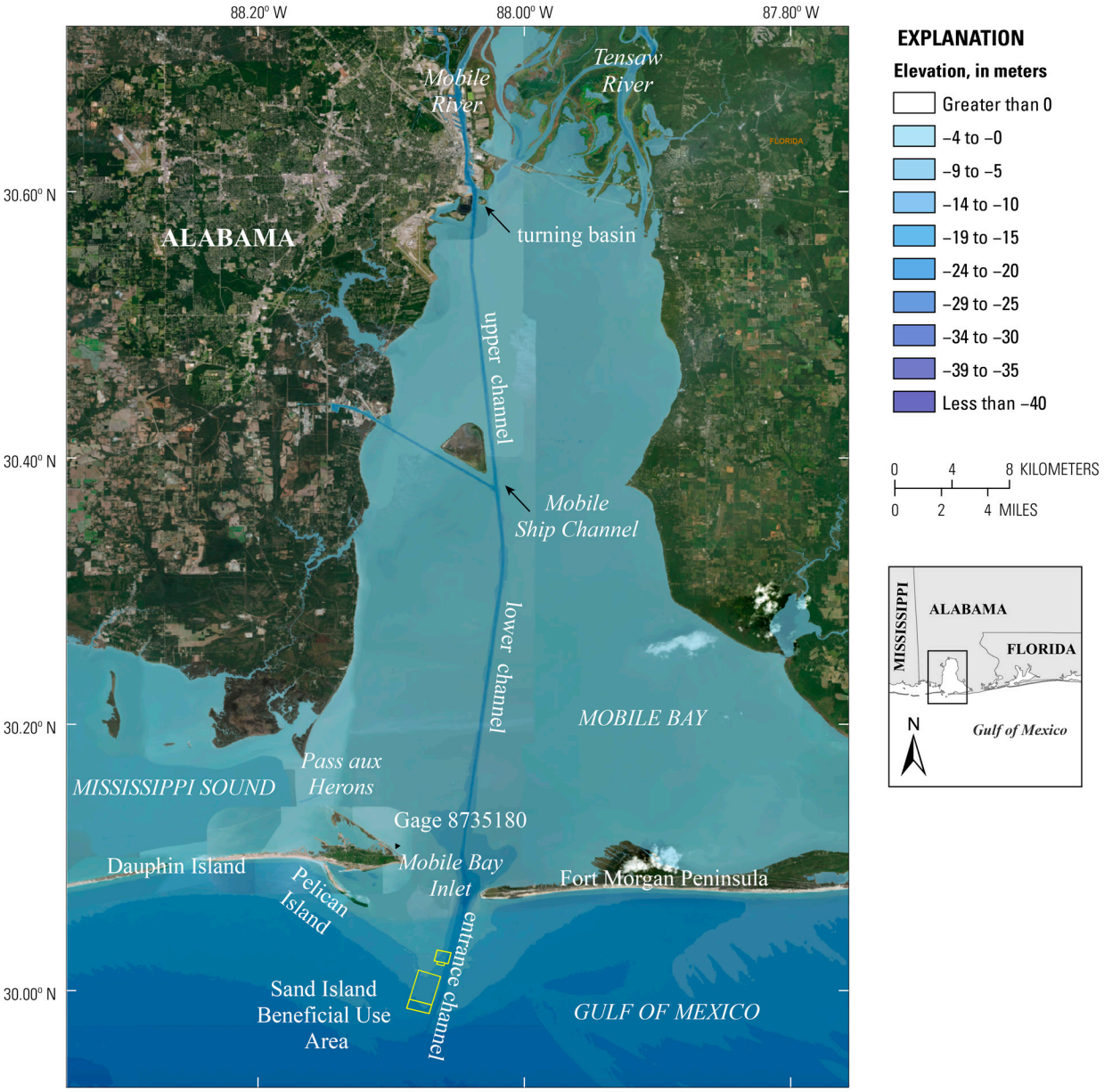

Service Layer Credits: Source: Esri,DigitalGlobe, GeoEye, EarthstarGeographics, CNES/Airbus DS, USDA, USGS, AEX, Getmapping, Aerogrid, IGN,IGP, swisstopo, and the GIS UserCommunity

Figure 1. The Mobile Harbor study area, Alabama, including Mobile Bay and the navigational channel, which consists of the upper bay channel, the lower bay channel, and the entrance channel.

the proposed channel modification. Details on the development of the model grid, initial model elevations, and boundary conditions are provided herein. The model grid and initial elevations are provided in Passeri and others (2018).

Proposed Navigation Channel Modifications

Mobile Harbor includes Mobile Bay, which connects to the Gulf of Mexico through the Mobile Bay inlet bounded by the Fort Morgan Peninsula and Dauphin Island (fig. 1). North of Dauphin Island, Mobile Bay connects to the Mississippi Sound through Pass aux Herons (fig. 1.). The Mobile Harbor navigation channel spans the length of Mobile Bay and includes the entrance channel, which extends from the mouth of Mobile Bay southward into the Gulf of Mexico, and the lower and upper bay channels, which extend from the mouth of the bay northward (fig. 1). The existing depth at the entrance channel is 14.33 meters (m, North American Vertical Datum of 1988) with an additional 0.61 m for advanced maintenance (that is, additional dredging depth to avoid re-dredging) and 0.61 m for allowable overdepth dredging (total of 15.54 m). The existing depth in the lower and upper channels is 13.72 m with an additional 0.61 m for advanced maintenance and 0.61 m for allowable overdepth dredging (total of 14.94 m). The proposed project depths would deepen the entrance channel to 15.85 m with an additional 0.61 m for advanced maintenance and 0.61 m for allowable overdepth dredging (total of 17.07 m), and the lower and upper channels to 15.24 m with an additional 0.61 m for advanced maintenance and 0.61 m for allowable overdepth dredging (total of 16.46 m). The turning basin (fig. 1), at the northernmost part of the upper bay channel would be widened 76.2 m southward. The channel from the mouth of the bay northward for 8.04 kilometers would be widened from 121.92 to 152.4 m to include a passing lane.

Model Description

Delft3D (developed by Deltares; see Lesser and others, 2004) is an integrated process-based model consisting of multiple modules used to simulate wave propagation, wave and tidal currents, sediment transport, and morphologic change. The FLOW module (Deltares, 2018a) solves the nonlinear shallow water equations for incompressible free surface flows in two (depth-integrated) or three dimensions. The WAVE module (Deltares, 2018b) solves the spectral action density equation and computes wave radiation stresses and gradients that drive nearshore circulation. When coupled with the FLOW module, the WAVE module accounts for the effects of water level variations and wave-current interaction processes such as frequency shifting. The sediment transport module solves for suspended and bed load sediment transport. To calculate suspended load, the three-dimensional advection-diffusion equation is solved, accounting for sediment concentration, flow velocities, eddy diffusivity, and sediment settling velocity. For bed load transport of non-cohesive sediments, the transport equation is solved accounting for bed slope, bed composition, spatially variable bed friction coefficients, and concentration of available sediment. Breaking-induced shear stresses, mass flux, and bed shear stress are included in the transport of suspended sediments and fluxes from bed load sediments. The transport module evolves bed morphology on the basis of mass fluxes between suspended and bed load sediments. More detailed information on the Delft3D model is provided in Lesser and others (2004).

Delft3D was operated using the mormerge approach (Roelvink, 2006), which is a configuration of the model in which multiple simulations run simultaneously with identical initial

bed conditions but with unique wave forcing. Each simulation is assigned a weight according to the percent occurrence of the wave conditions from a wave climatological assessment. At each half model time step, the current bathymetry from each of the simulation bins is combined using a weighted-average to form a new shared bathymetry that is passed back to each simulation and applied as the bathymetry for all the concurrent simulations for the next time step. The cumulative effect is a computationally efficient way to perform long-term morphological predictions.

Model Setup

For this study, three computational grids were used (see grid extents in fig. 2). The FLOW module uses a curvilinear grid consisting of 1,368 x 657 grid points. Cross-shore grid resolution ranges from less than 5 m over Dauphin Island and in the surf zone to greater than 300 m in the northernmost reaches of Mobile Bay. The alongshore grid resolution ranges from 40 m at Dauphin Island and across the Mobile Bay inlet to 100 m grid spacing at points in the southeastern quarter of the grid. The WAVE module uses two grids: a coarse outer grid and a nested fine grid. The coarse outer grid covers the study area with 245 x 449 grid points. It has variable alongshore resolution ranging from 250 to 325 m and variable cross-shore resolution ranging from 15 to 300 m. The spatial extent of the nested fine grid is limited in latitude to the mouth of Mobile Bay where substantial wave-current interactions are expected and higher resolution is required. The fine grid consists of 1,367 x 458 grid points with a variable cross-shore resolution less than 5 m

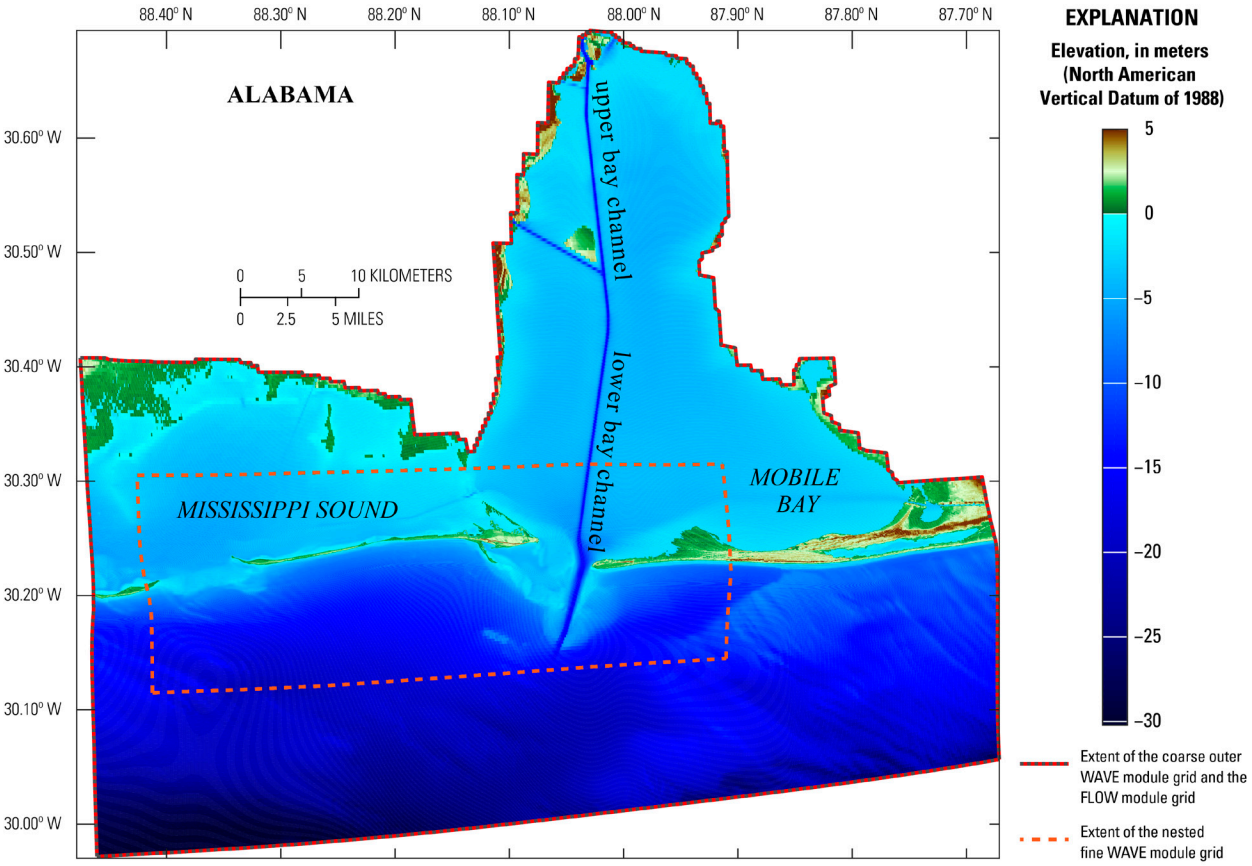

Figure 2. Delft3D model domains (computational grid extents) and initial elevations (existing condition), Mobile Harbor, Alabama.

at the mouth of the bay to more than 250 m offshore and to the north. The alongshore resolution of the fine grid is 100 m along Dauphin Island and becomes coarser east of the Mobile Bay inlet.

Two digital elevation models (DEMs) were created for this study and used to initialize the model to represent (1) the existing bathymetry of Mobile Harbor and the navigation channel and (2) the proposed channel modifications. The base DEM was derived by combining the Coastal National Elevation Database (CoNED) topobathymetric DEM for Mobile Bay (Danielson and others, 2013) and the National Geophysical Data Center (NGDC) coastal DEM (National Geophysical Data Center and others, 2009). The NGDC coastal DEM covers the full extent of the modeling domain and was used primarily for offshore regions that were not included in the CoNED DEM, which contains more recent elevations in the coastal areas. A 2015 bathymetric survey at Dauphin Island (DeWitt and others, 2017) and a 2015 airborne light detection and ranging (lidar) survey of Dauphin Island (U.S. Geological Survey, 2016), also were merged into the DEM using the controlled interpolation methods of Plant and others (2002). For updated coverage, the USACE Mobile District provided elevations within Mobile Bay, including the navigation channel, based on a composite of recent bathymetric surveys (taken by the district) for the existing condition in addition to the altered bathymetry for the proposed with-project condition. These data were incorporated within Mobile Bay east of Pass aux Herons and within the entrance channel limited to the south by the 16-m contour. For depths greater than 5 m, a region was defined using a contour of the minimum difference between the USACE depth and the underlying merged product of NGDC, CoNED, and the 2015 bathymetric and lidar surveys to ensure a continuous bathymetry. The USACE depth was then interpolated onto the FLOW grid and applied only to this defined region.

Boundary Conditions

Wave Climatology

The wave climatology was developed using output from the European Centre for Medium-Range Weather Forecast (ECMWF) ERA-Interim reanalysis model (Dee and others, 2011). For the 10-year simulations, significant wave height (*Hs*), peak wave period (*Tp*) and mean wave direction (*Dm*) from January 1, 1998, to January 1, 2016, at a model grid point at longitude −88.125 W and latitude 30.000 N were used to define the regional wave climatology. Periods with waves not directed towards shore between 110° and 250° (nautical convention) were assumed to minimally affect the study site and therefore were removed from the time series. To validate the model wave height, data from National Data Buoy Center buoy 42040 (National Data Buoy Center, 2018) and from an ECMWF model (Dee and others, 2011) grid point about 6 kilometers away from the buoy were compared for times of overlapping data. A linear regression analysis revealed that using a correction factor of 1.22 improved the modeled wave height; the coefficient of determination (R^2) was 0.86 and the root mean square error (RMSE) was 0.26 m. The Energy Flux Method of Benedet and others (2016) was then used to derive a binned (grouped) wave climatology where wave direction and height bin boundaries were defined such that all bins contained an equal amount of wave energy flux. The wave climate was divided into nine wave classes (three directions and three heights). For each defined bin, wave period is the mean period of the bin, wave direction is mean direction of the bin, and wave height is calculated from the mean wave energy flux in the bin assuming linear wave theory (table 1). For the 2010 simulations, the wave climate was derived similarly using ECMWF ERA-Interim data for 2010 (table 1).

Table 1. Characteristics and percent occurrence of wave conditions for each wave bin for 10-year climatology and 2010 climatology, Mobile Harbor, Alabama.

Row	Significant Wave height (*Hs*), in meters	Peak wave period (*Tp*), in seconds	Mean wave direction (*Dm*), in degrees	Occurrence, in percent
10-year climatology				
Bin 1	0.59	6.24	129.2	26.2
Bin 2	0.59	6.43	154.01	25.4
Bin 3	0.58	5.75	199.77	28.9
Bin 4	1.21	7.3	128.1	5.3
Bin 5	1.18	7.49	154.48	5.4
Bin 6	1.23	7.22	195.49	5.2
Bin 7	2.65	9.09	126.94	0.9
Bin 8	2.17	8.6	155.06	1.4
Bin 9	2.26	8.68	198.13	1.3
2010 climatology				
Bin 1	0.61	6.36	130.13	24.55
Bin 2	0.61	6.52	155.87	23.43
Bin 3	0.61	5.55	201.33	27.69
Bin 4	1.03	7.02	129.71	7.85
Bin 5	1.17	7.75	157.27	5.16
Bin 6	1.39	7.41	197.34	3.92
Bin 7	1.63	8.02	133.33	2.69
Bin 8	1.67	8.13	158.77	2.8
Bin 9	2.01	8.37	201.29	1.91

Morphological Tide

In addition to the wave forcing, a tidal time series or "morphological tide" was applied at the model boundaries to capture current velocities and morphological change associated with the neap-spring tide cycle. The morphological tide was calculated following the method of Lesser (2009), which is applicable in locations where the lunar diurnal K1 and O1 tidal constituents substantially contribute to the tidal signal, as is the case in the study domain. Tidal constituent amplitudes and phases were obtained from the National Oceanic and Atmospheric Administration (NOAA) tide gage (8735180) at the eastern end of Dauphin Island (fig. 1) and used to generate the amplitude and phases of the morphological tide. These were applied at the boundaries of each Delft3D simulation. For model stability, a consistent and progressive phase shift also was added to the morphological tide constituents of each successive wave bin.

Simulations

To assess the model performance, two deterministic simulations were conducted to compare modeled current velocities and water levels with collected data. Acoustic Doppler current profiler (ADCP) measurements were collected at the Mobile Bay inlet from August 27

through 29, 2015 (representing the flood tide), and December 19 through 11, 2015 (representing the ebb tide). For each deterministic simulation, the existing Mobile Harbor DEM was used as the initial depth input with boundary conditions of modeled wind, wave, and water levels from the NOAA Hybrid Coordinate Ocean Model (HYCOM) (Bleck 2002) and the NOAA Wavewatch3 model (Tolman 1989). In comparing the modeled HYCOM water levels to the observed water levels at the Dauphin Island tide gage (station 8735180), the HYCOM water levels on average were 0.21 m lower than the observed; therefore, an offset of 0.21 m was added to the HYCOM water levels. Each simulation was spun-up for 12 hours before the first observation. In addition, a 6-month deterministic simulation from June 19 through November 20, 2005, was done to compare modeled water levels with observations at the Dauphin Island tide gage (Center for Operational Oceanographic Products and Services, 2018).

For the 2010 and 10-year simulations, four scenarios were examined: existing conditions (that is, existing bathymetric conditions of the coastal nearshore areas with no channel modifications), with-project conditions (that is, with the proposed channel modifications), existing conditions with a moderate sea level rise (SLR) of 0.50 m, and with-project conditions with a moderate SLR of 0.50 m. For the 10-year simulations, the channel depths were reset to the initial depths at the start of each year, assuming annual dredging would take place. Additionally, a volume of 503,606.21 cubic meters (m^3) of sand was added to the DEM in the southern section of the Sand Island Beneficial Use Area, on the 10-m contour southeast of Pelican Island (fig. 1), at the end of each year to account for the average annual volume of maintenance dredge material placement during 1999–2015.

Modeling Results

The results of the Delft3D simulations are presented herein. To evaluate the model performance, output in the form of water levels, velocities, and bed level from the deterministic simulations were compared with observations. To assess the effects of the proposed channel modifications, the final bed levels were extracted as output from the model at the end of the 2010 and 10-year simulations, with and without 0.50 m of sea level rise (SLR). Model output from each simulation is provided in Passeri and others (2018).

Model Performance

Modeled Versus Observed Water Levels and Velocities

Modeled water velocities were interpolated to the ADCP transect at the Mobile Bay inlet. Modeled and observed water levels were rotated from their respective native coordinates to stream-wise coordinates so that the resulting velocity constituents were a stream-wise U (through-channel) velocity and a V (cross-channel) velocity. The R^2 and RMSE values between the modeled and observed U and V velocities in the Mobile Bay inlet are summarized in table 2. The R^2 values for the modeled and observed U velocities during ebb and flood tide are 0.93 and 0.66, respectively. The R^2 values for the modeled and observed V velocities during ebb and flood tide were 0.79 and 0.30, respectively. An additional comparison of modeled and observed volumetric fluxes calculated across the transect was done for the two ADCP observational periods (table 2). Fluxes were defined as stream-wise, depth-averaged velocities multiplied by water depth and integrated over the observation transect. A linear fit and R^2 value was calculated for the ebb and flood tide fluxes, resulting in values of 0.98 and 0.79, respectively. The high skill during

ebb tides shows the model's ability to accurately capture the ebb-dominant behavior of the inlet, which affects sediment transport out of the bay.

The observed water levels at the Dauphin Island tide gage were compared with modeled water levels extracted from the closest grid point to the tide gage location (table 2). The R^2 value between the observed and modeled water levels was 0.68. Model error is likely due in part to the absence of lower frequency harmonic constituents in the boundary forcing.

Modeled Versus Observed Bed Level Changes

Modeled and observed changes in bed levels were compared to evaluate the model's capability to accurately simulate sediment transport. The USACE Mobile District provided changes in bed levels at various locations in the study area from the periods of 2009–14, 2002–14, and 2002–15 (the range of uncertainty is plus or minus [±] 0.61 m). The changes in bed level were calculated from bathymetric surveys by Byrnes and others (2012), Flocks and others (2017), and the NGDC (National Ocean Service, 2014). Changes in bed levels from 2002 to 2014 and 2002 to 2015 indicate erosion and deposition along the 5-m contour extending from Pelican Island, and deposition along the eastern edge of the navigation channel offshore of the Fort Morgan Peninsula (figs. 3A, 3B). These changes were compared with the modeled change in bed level at the end of the 10-year existing simulation (that is, the year 10 final bed level minus the year 1 initial bed level). The simulation shows similar patterns of erosion and deposition along the 5-m contour and along the navigation channel (fig. 4*A*). It is important to note that the simulation was not initialized with 2002 bathymetry, so the magnitude of differences is not expected to match exactly. Additionally, the magnitude of the sediment placed in the Sand Island beneficial use area is not expected to match exactly because an annual average was applied in the simulation.

Observed bed level changes on the ebb tidal shoal between 2009 and 2014 indicate plus or minus (±) 1 m erosion and deposition in between the 5- and 10-m contours (fig. 3*C*). For comparison, bed levels were extracted after year 5 in the 10-year simulation and used to calculate the change in bed level. Similar to the observation, there are patterns of erosion and deposition between the 5- and 10-m contours, as well as the dredge placement in the Sand Island Beneficial Use Area (fig. 4*B*). The magnitude of the difference is less than the observed data, but again, this

Table 2. Coefficients of determination and root mean square error values for through-channel and cross-channel velocity components during flood and ebb tide at inlet, volume flux during flood and ebb tide at inlet and water levels at the Dauphin Island tide gage, Mobile Harbor, Alabama.

[R^2, coefficient of determination; RMSE, root mean square error; *U*, through channel; m/s, meter per second; *V*, cross channel; m^3/s, cubic meter per second; m, meter]

Constituent	R^2	RMSE
Ebb *U* velocity	0.93	0.11 m/s
Ebb *V* velocity	0.79	0.06 m/s
Flood *U* velocity	0.66	0.12 m/s
Flood *V* velocity	0.30	0.07 m/s
Ebb tide flux	0.98	1.53×10^6 m^3/s
Flood tide flux	0.79	1.85×10^6 m^3/s
Water level	0.68	0.09 m

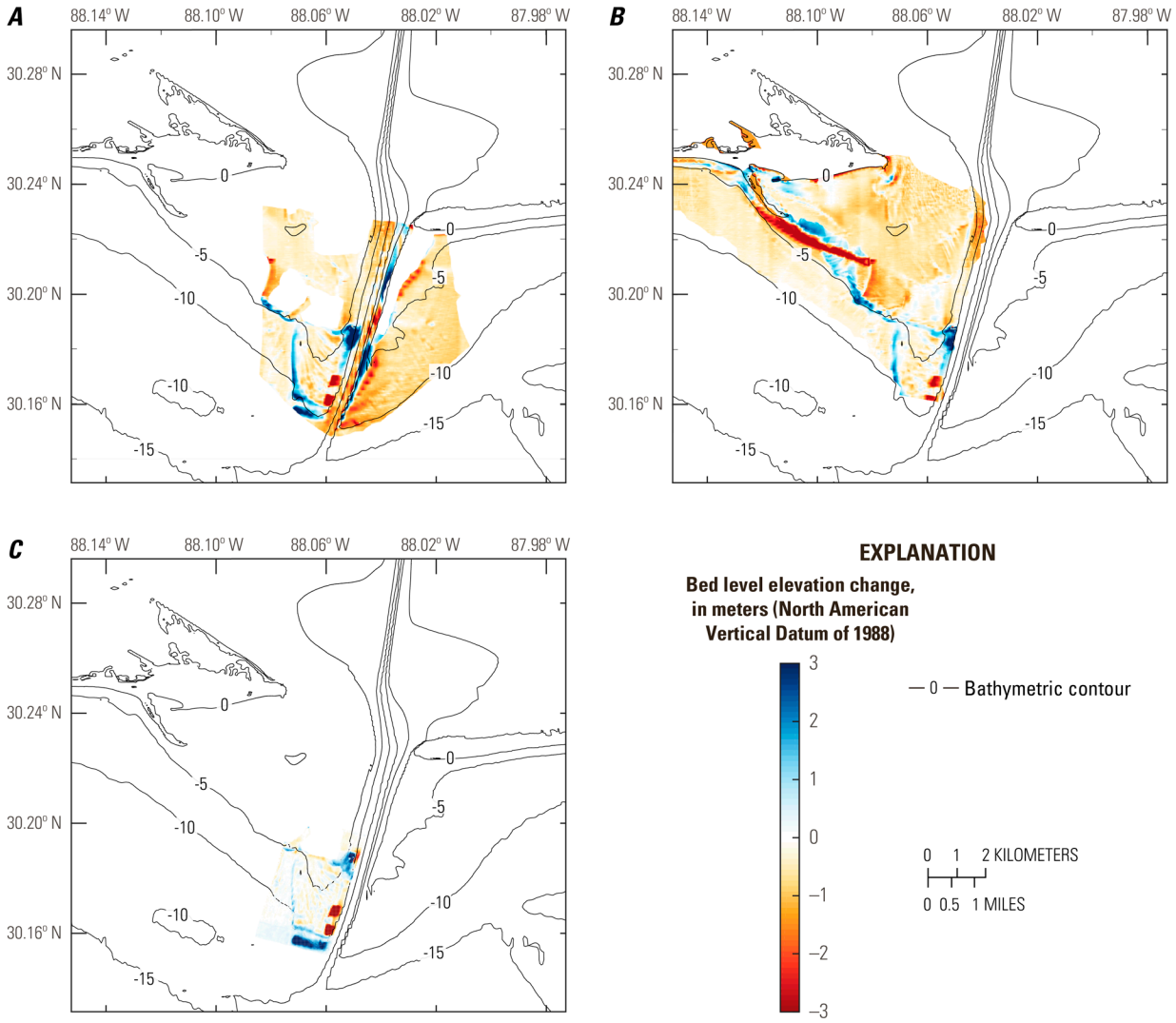

Figure 3. Observed bed level changes in Mobile Harbor, Alabama. *A*, from 2002 to 2014. *B*, from 2002 to 2015. *C*, from 2009 to 2014. Differences greater than 0 indicate deposition, and differences less than 0 indicate erosion.

simulation was not initialized with 2009 bathymetry and does not include tropical storms that would have occurred during this period.

2010 Climatology

The change in bed level at the end of the 2010 simulation for the existing and with-project conditions is illustrated in figures 5A and 5B. Both simulations indicate erosion and deposition along the 5-m contour extending out from Pelican Island, as well as offshore of the Fort Morgan Peninsula. The difference in the final bed levels between the existing and with-project conditions is shown in figure 5*C*. Results indicate that there are minor changes in bed levels near Pelican Island (ranging from −0.11 to 0.11 m) and offshore of the Fort Morgan Peninsula (ranging from −0.81 to 0.22 m) with the proposed channel modification; these changes were confined within the 5-m contour. Similarly, figures 6A and 6B illustrate the change in bed level at the

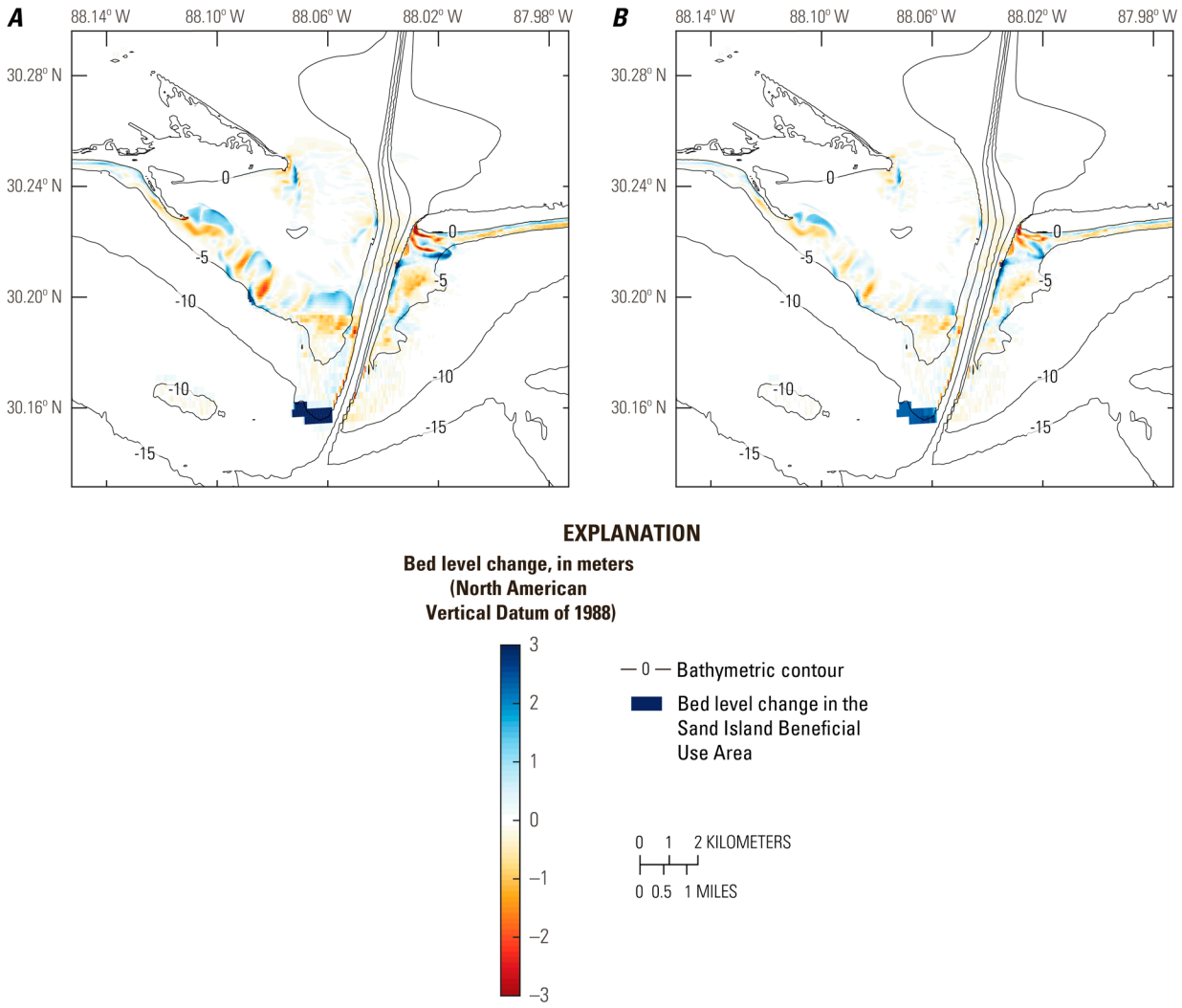

Figure 4. Modeled bed level change in Mobile Harbor, Alabama. *A*, after 10 years in the 10-year existing condition simulation. *B*, after 5 years in the 10-year existing condition simulation. Differences greater than 0 indication deposition, and differences less than 0 indicate erosion.

end of the 2010 simulation for the existing condition with 0.50 m of SLR and the with-project conditions with 0.50 m of SLR. Similar patterns of erosion and deposition can be seen along the 5-m contour offshore of Pelican Island and the Fort Morgan Peninsula. Again, there are minor changes in bed levels for the with-project conditions ranging from −0.20 to 0.32 m near Pelican Island and −0.38 to 0.34 m offshore of the Fort Morgan Peninsula within the 5-m contour (fig. 6*C*).

The volume of sediment eroded and deposited in the entrance channel at the end of the 2010 simulations was calculated by dividing the entrance channel into 15 sections of equal length. The volumes in each section and across the entrance channel are summarized in table 3; the percent change in each section is illustrated in figure 7. The change in volume across the channel for the existing and with-project scenarios is 45,860 and 43,670 m^3 respectively, indicating that the channel is shoaling (sand is being deposited in the channel) for both scenarios. The deeper channel (with-project condition) reduced the overall shoaling volume

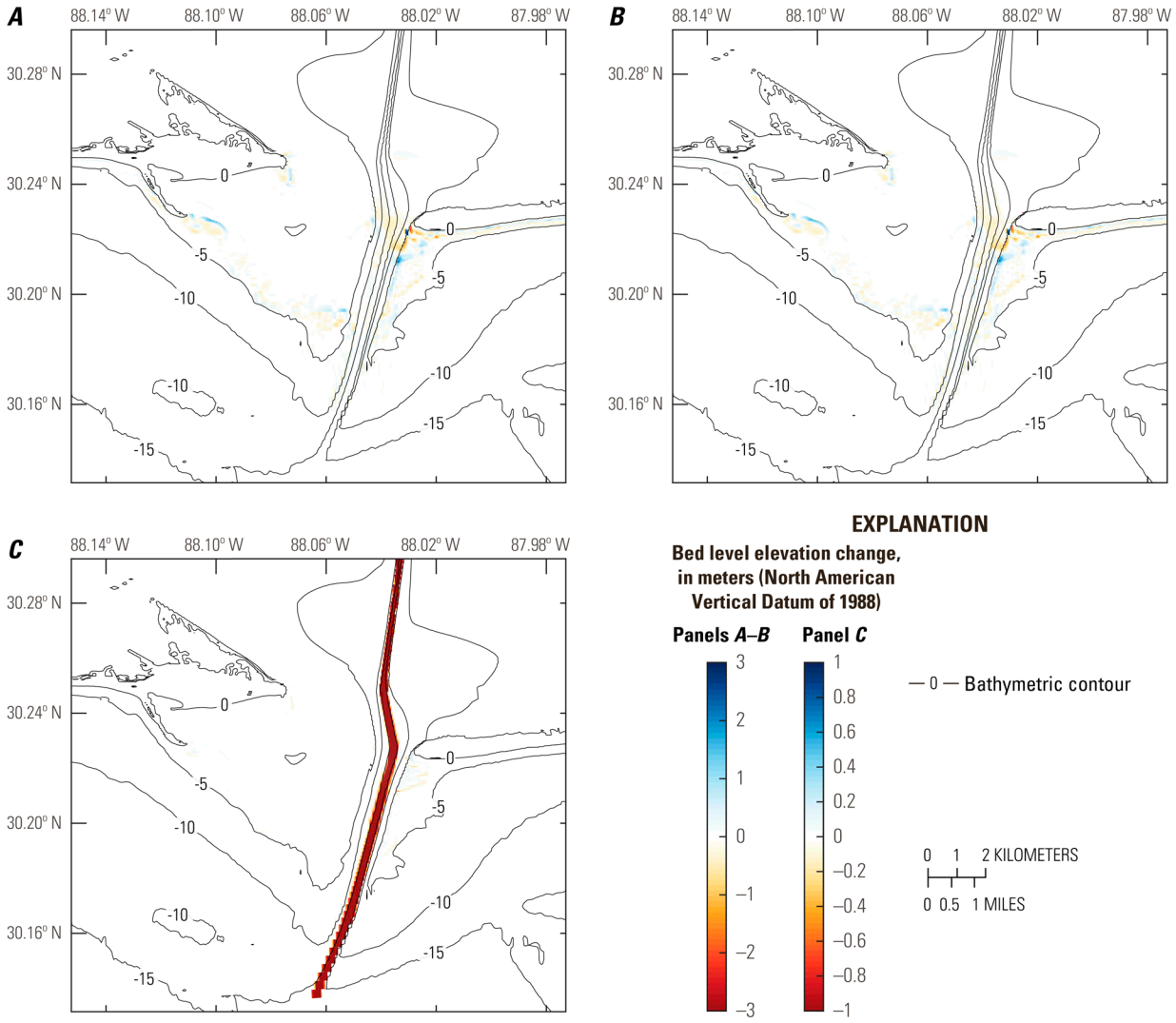

Figure 5. Changes in bed level for the 2010 simulations, Mobile Harbor, Alabama. *A*, existing conditions. *B*, with-project conditions. *C*, difference in final bed level between existing and with-project conditions. For *A* and *B*, differences greater than 0 indicate deposition, differences less than 0 indicate erosion. For *C*, differences greater than 0 indicate the with-project bed level is shallower, and differences less than 0 indicate the with-project bed level is deeper.

by 2,190 m^3 (4.77 percent). Under 0.50 m of SLR, there is less shoaling with channel volumes of 20,662 and 18,991 m^3 for the existing and with-project conditions, respectively. Similarly, the with-project condition reduces the channel shoaling volume by 1,671 m^3 (8.09 percent) from the existing condition. Changes in shoaling volume are negative at most sections of the entrance channel, meaning that less sand is deposited for the with-project condition, as shown in figure 7. However, a few sections in the middle of the entrance channel (6 through 9) and sections 13 and 15 have positive changes, indicating that more sand is deposited in these sections with the deeper (with-project) channel.

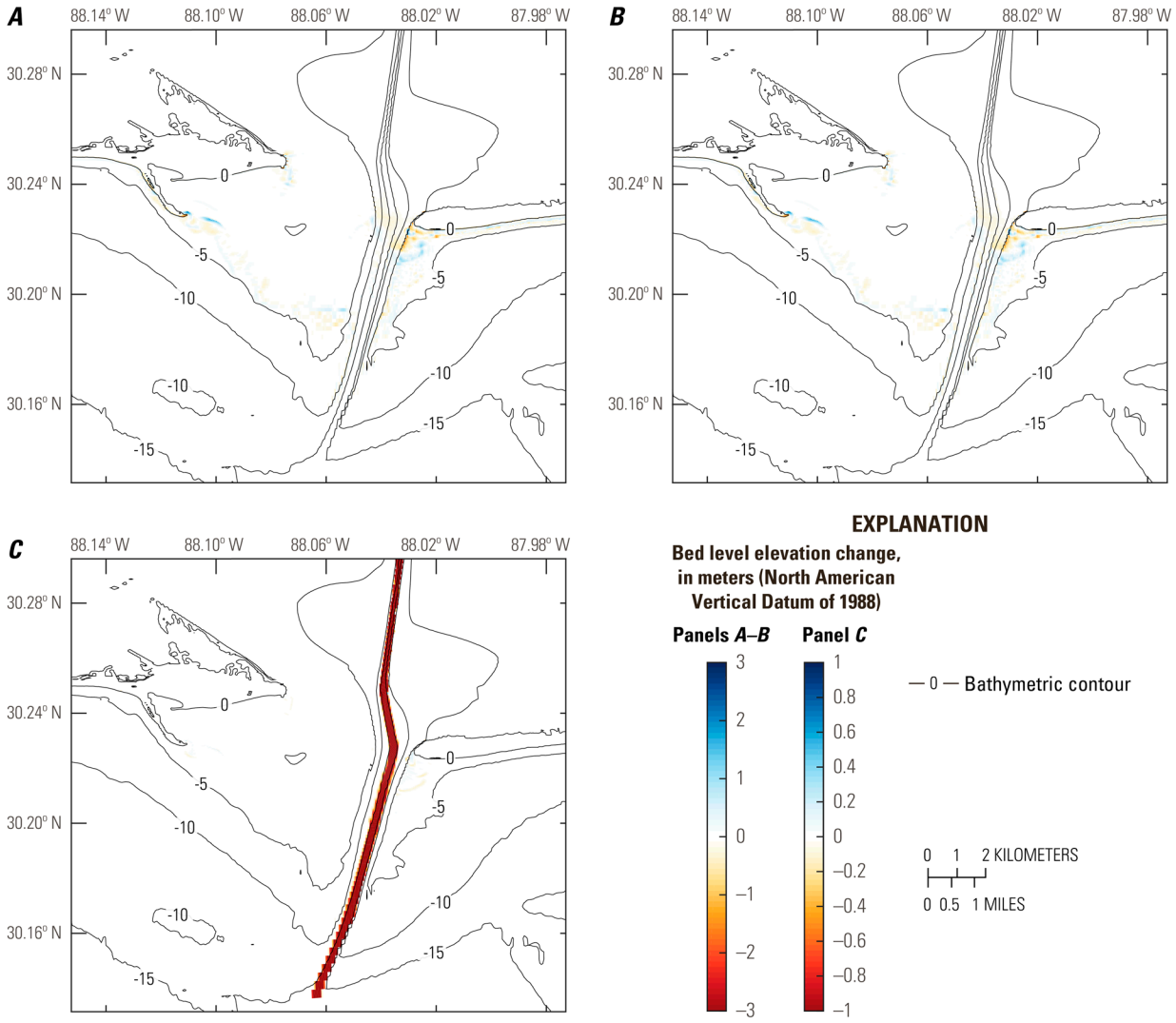

Figure 6. Changes in bed level for the 2010 simulations, Mobile Harbor, Alabama. *A*, existing conditions accounting for 0.5 meter of sea level rise. *B*, with-project conditions accounting for 0.5 meter of sea level rise. *C*, difference in final bed level between existing conditions accounting for 0.5 meter of sea level rise and with-project conditions accounting for 0.5 meter of sea level rise. For *A* and *B*, differences greater than 0 indicate deposition, differences less than 0 indicate erosion. For *C*, differences greater than 0 indicate the bed level for the with-project condition with 0.5 meter of sea level rise is shallower than the bed level for the existing condition with 0.5 meter of sea level rise, and differences less than 0 indicate the bed level for the with-project condition with 0.5 meter of sea level rise is deeper than the bed level for the existing condition with 0.5 meter of sea level rise.

10-Year Climatology

The change in bed level at the end of the 10-year simulation (that is, the difference between the final bed level at the end of year 10 and the initial bed level at the start of the simulation) for the existing and with-project conditions is shown in figures 8A and 8B. Similar to the 2010 simulations, there is erosion and deposition in both simulations along the 5-m contour extending out from Pelican Island, as well as from the Fort Morgan Peninsula. The difference

Table 3. Volume of sediment eroded or deposited in the entrance channel at the end of the 2010 simulations, Mobile Harbor, Alabama.

[Positive numbers indicate sand was deposited in the channel (shoaling); negative numbers indicate sand was eroded from the channel]

Section (figs. 7, 10)	Sediment volume change, in cubic meters			
	Existing conditions	With-project conditions	Existing conditions with 0.50 meter of sea level rise	With-project conditions with 0.50 meter of sea level rise
1	−171	−190	−85	−115
2	−1,144	−1,370	−563	−642
3	−13,012	−15,434	−6,668	−7,878
4	−12,306	−12,704	−6,458	−6,608
5	−21,733	−22,506	−10,157	−10,621
6	−21,858	−20,215	−12,144	−11,446
7	15,200	18,455	5,488	7,621
8	2,433	3,746	−1,569	−668
9	−3,903	−1,735	−6,546	−5,283
10	3,869	3,215	−1,891	−2,117
11	44,910	41,969	20,786	19,041
12	53,606	47,403	34,337	30,728
13	−4,859	−1,833	2,754	3,624
14	3,555	3,358	2,527	2,398
15	1,273	1,511	850	955
All sections	45,860	43,670	20,662	18,991

in the final bed levels between the existing and with-project conditions is shown in figure 8*C*. Results indicate that, with the proposed channel deepening, there are some changes in bed levels along the 5-m contour offshore of Pelican Island, ranging from −2.62 to 2.03 m. Offshore of the Fort Morgan Peninsula, there are larger changes in bed levels ranging from −3.17 to 3.94 m. The change in bed level at the end of the 10-year simulation for the existing and with-project conditions with 0.50 m of SLR is illustrated in figures 9A and 9B. There are similar patterns of erosion and deposition along the 5-m contour and near the Fort Morgan Peninsula for both simulations. With the proposed channel modifications under 0.50 m of SLR, changes in bed levels were smaller than for the 10-year simulations without SLR and range from −0.86 to 1.07 m offshore of Pelican Island and −1.92 to 1.47 m offshore of the Fort Morgan Peninsula (fig. 9*C*).

The volume of sediment in the entrance channel at the end of the year 10 was calculated at each of the 15 sections and across all sections of the channel (table 4); the percent change in each section is illustrated in figure 10. At the end of 10 years, the changes in volume across the entire channel for the existing and with-project scenarios are 40,035 and 37,816 m^3, respectively, indicating that the channel is shoaling (sand was deposited in the channel). The with-project condition reduced the overall channel shoaling volume by 2,219 m^3 (5.54 percent). The change in volume across the entire channel for the existing and with-project scenarios under 0.50 m of SLR is 17,849 and 15,175 m^3, respectively. The with-project condition reduced the overall channel shoaling volume by 2,674 m^3 (14.98 percent). Like the 2010 simulations, the negative changes shown in figure 10 illustrate that less sand is being deposited at most sections of the entrance

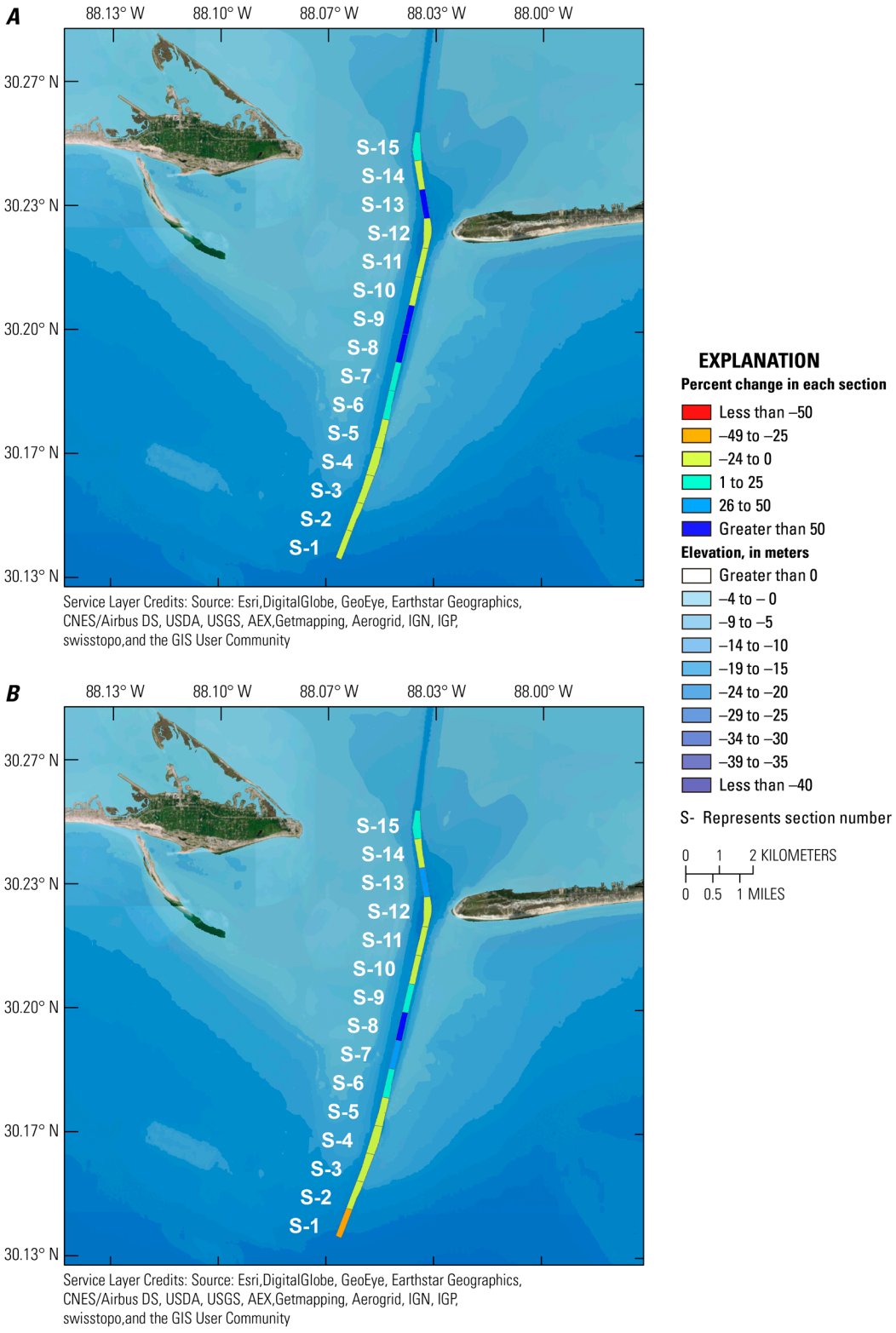

Figure 7. Percent change in the volume of sediment eroded or deposited in the entrance channel, Mobile Harbor, Alabama. *A*, between 2010 existing and 2010 with-project conditions. *B*, between 2010 existing with 0.50 meter of sea level rise and 2010 with-project with 0.50 meter of sea level rise.

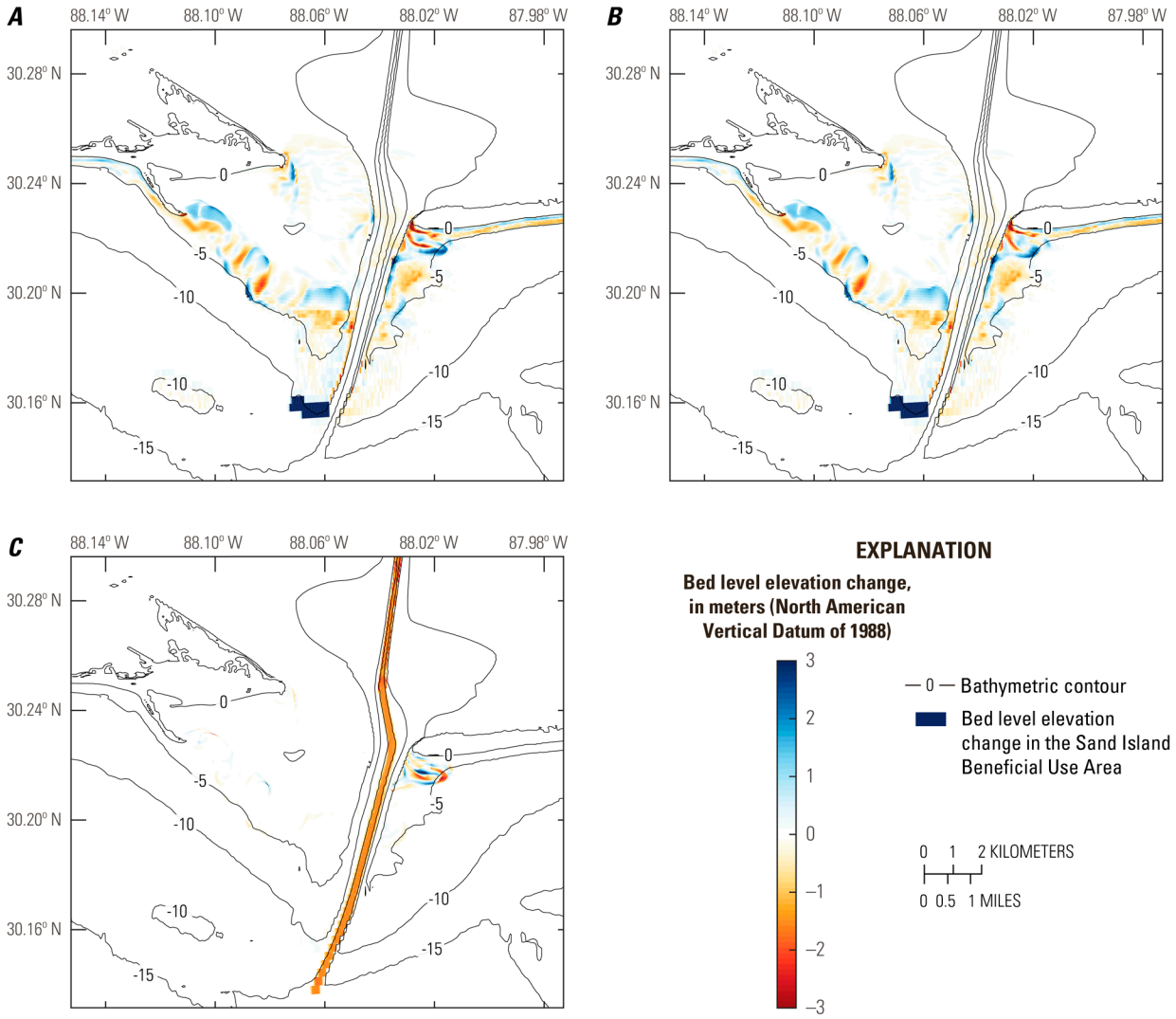

Figure 8. Changes in bed level for the 10-year simulations, Mobile Harbor, Alabama. *A*, existing conditions. *B*, with-project conditions. *C*, difference in final bed level between existing and with-project conditions. For *A* and *B*, differences greater than 0 indicate deposition, differences less than 0 indicate erosion. For *C*, differences greater than 0 indicate the with-project bed level is shallower, and differences less than 0 indicate the with-project bed level is deeper.

channel, especially at the southern end. Again, a few sections in the middle of the entrance channel (6 through 9) and sections 13 and 15 have positive changes, indicating that more sand is deposited in these sections with the deeper (with-project) channel.

The shoaling volume across the entire entrance channel also was calculated at the end of each year in the 10-year simulation (table 5). Although elevations in the channel were reset to the initial depth at the beginning of each year, the shoaling volume at the end of each year was not equal for all simulations; the percent change in the volume varied from a 1.47-percent decrease to a 9.99-percent increase from the previous year. These fluctuations indicate that as sand shifts in offshore areas (especially near the Fort Morgan Peninsula), the resulting sediment transport into the entrance channel changes.

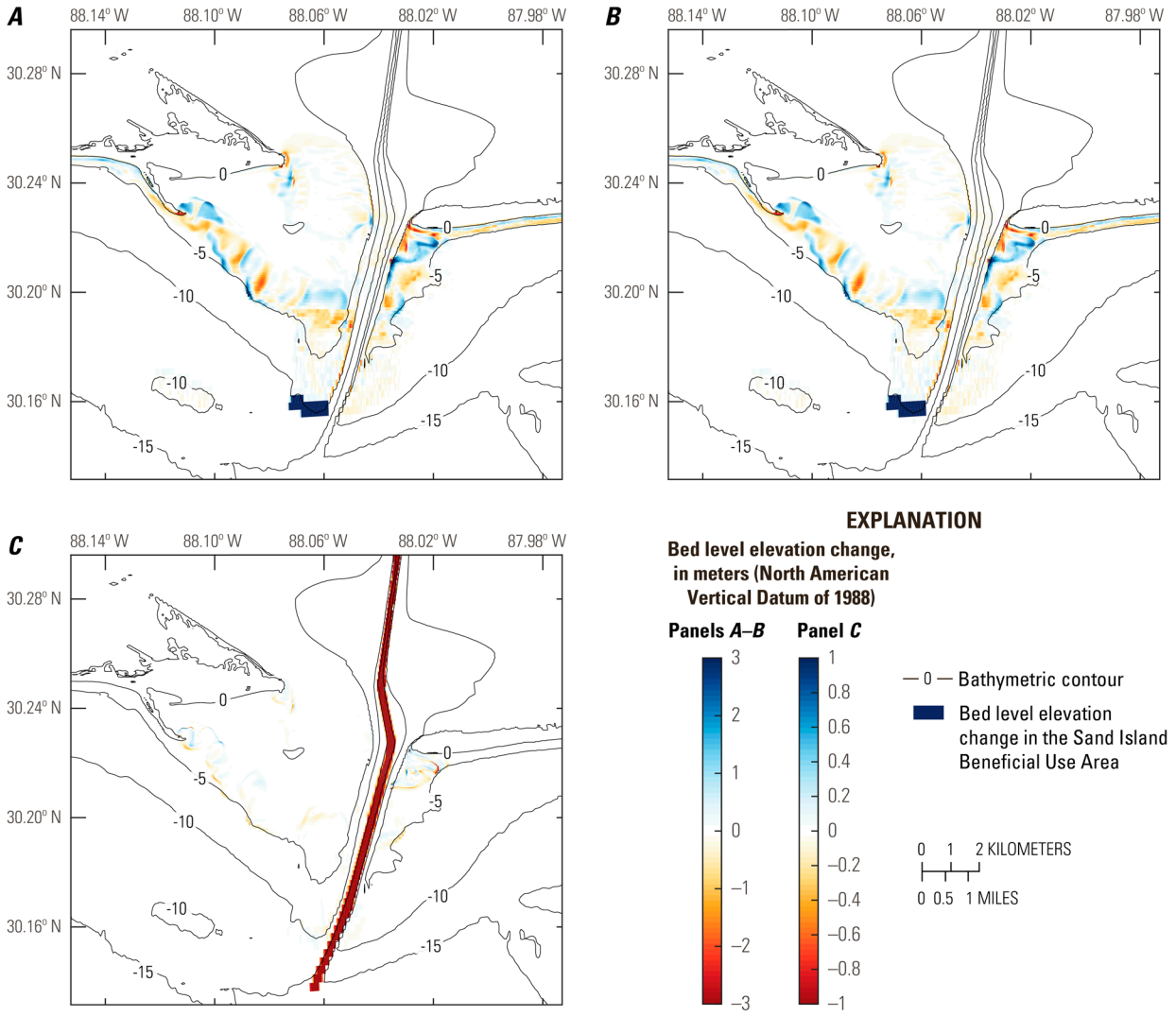

Figure 9. Changes in bed level for the 10-year simulations, Mobile Harbor, Alabama. *A*, existing conditions accounting for 0.5 meter of sea level rise. *B*, with-project conditions accounting for 0.5 meter of sea level rise. *C*, difference in final bed level between existing conditions accounting for 0.5 meter of sea level rise and with-project conditions accounting for 0.5 meter of sea level rise. For *A* and *B*, differences greater than 0 indicate deposition, differences less than 0 indicate erosion. For *C*, differences greater than 0 indicate the bed level for the with-project condition with 0.5 meter of sea level rise is shallower than the existing condition with 0.5 meter of sea level rise, and differences less than 0 indicate the bed level for the with-project condition with 0.5 meter of sea level rise is deeper than the existing condition with 0.5 meter of sea level rise.

Discussion

The results and patterns from the existing and future with-project conditions indicated some changes in the overall dynamics of the system, especially for the 10-year simulations. There were minimal differences in morphologic change in the nearshore areas of Dauphin Island and Pelican Island because of the channel modifications (figs. 8, 9). This suggests that sediment delivery away from the ebb tidal shoal to these areas is similar under these two scenarios and that

Table 4. Volume of sediment eroded or deposited in the entrance channel for the 10-year climatology simulations, Mobile Harbor, Alabama.

[Positive numbers indicate sand was deposited in the channel (shoaling); negative numbers indicate sand was eroded from the channel]

Section (figs. 7, 10)	Sediment volume change, in cubic meters			
	Existing conditions	With-project conditions	Existing conditions with 0.50 meter of sea level rise	With-project conditions with 0.50 meter of sea level rise
1	−1,328	−1,581	−596	−742
2	−534	−1,108	−63	−230
3	−15,532	−18,680	−9,042	−10,819
4	−11,984	−12,367	−5,618	−5,687
5	−24,782	−26,482	−10,693	−11,355
6	−29,023	−28,022	−14,088	−13,393
7	10,243	13,260	5,626	7,250
8	−2,156	1,450	−6,203	−4,547
9	−11,460	−8,587	−16,910	−15,473
10	24,661	21,423	21,054	18,829
11	54,818	54,185	23,400	22,004
12	52,207	44,659	24,076	21,709
13	1,052	4,897	3,727	4,458
14	4,562	4,446	2,402	2,297
15	1,619	1,969	777	876
All sections	52,364	49,462	17,849	15,175

shoreline positions are unlikely to be affected because of the modified channel. Although comparison of the two simulations shows some spatial shifting of sand offshore of the Fort Morgan Peninsula, the patterns of erosion and deposition in the two simulations are quite similar. Based on these results, it also seems unlikely that these changes would alter sediment delivery to the peninsula, and only minor effects to the terminal end of the peninsula closest to the channel could occur.

A limitation in the modeling framework is the exclusion of peak wave and storm surge characteristics associated with tropical storms. Although larger wave heights from storms are included in the full time series of the waves used to define the climatology, the nine bins were defined using mean characteristics of all waves within each bin. Therefore, the model was not forced with wave heights larger than 2.26 m, which is smaller than peak wave heights observed during tropical storms in the Gulf of Mexico (for example, see Bilskie and others, 2016). Additionally, the simulation of each bin contains a tidal time series but does not include storm surge, which is associated with individual storms rather than the wave conditions represented by each bin. River inflow from the Mobile and Tensaw Rivers (fig. 1) also was not considered for this study because it was assumed that riverine effects on hydrodynamics and marine sediment transport would be minor around the ebb tidal shoal and Dauphin Island.

To simulate morphological change over decadal time scales, two-dimensional depth averaged velocities were used in the Delft3D simulations. This neglects the effects of vertically varying velocity profiles and boundary layer processes on morphological change. Studies have

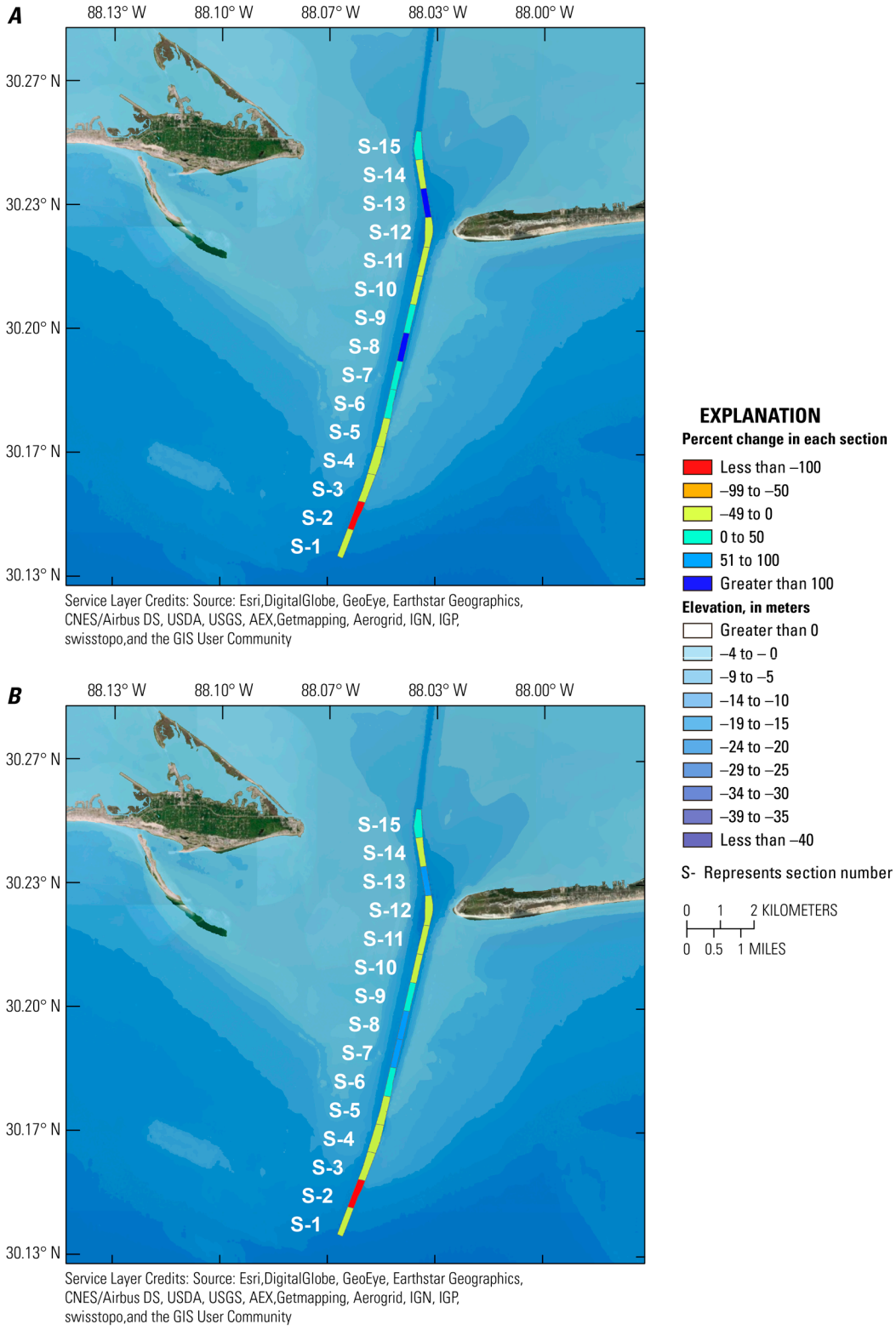

Figure 10. Percent change in the volume of sediment eroded or deposited in the entrance channel, Mobile Harbor, Alabama. *A*, between the 10-year existing and 10-year with-project conditions. *B*, between the 10-year existing condition with 0.50 meter of sea level rise and 10-year with-project condition with 0.50 meter of sea level rise.

Table 5. Shoaling volume in the entrance channel at the end of each year for the 10-year simulations, Mobile Harbor, Alabama.

Period	Shoaling volume, in cubic meters (percent change in volume from the previous year)			
	Existing conditions	With-project conditions	Existing conditions with 0.50 meter of sea level rise	With-project conditions with 0.50 meter of sea level rise
After year 1	38,442	37,482	15,459	12,808
After year 2	42,284 (9.99)	38,474 (2.65)	15,726 (1.73)	13,283 (3.71)
After year 3	41,705 (−1.37)	40,078 (4.17)	15,633 (−0.59)	13,268 (−0.11)
After year 4	41,583 (−0.29)	39,681 (−0.99)	15,879 (1.57)	13,509 (1.82)
After year 5	41,520 (−0.15)	39,677 (−0.01)	16,322 (2.79)	13,836 (2.42)
After year 6	41,470 (−0.12)	39,404 (−0.69)	16,687 (2.24)	14,234 (2.88)
After year 7	41,217 (−0.61)	39,035 (−0.94)	17,041 (2.12)	14,545 (2.19)
After year 8	40,798 (−1.02)	38,473 (−1.44)	17,218 (1.04)	14,651 (0.72)
After year 9	40,305 (−1.21)	37,907 (−1.47)	17,218 (0.00)	14,607 (−0.30)
After year 10	40,035 (−0.67)	37,816 (−0.24)	17,849 (3.66)	15,175 (3.89)

determined that overall sediment transport patterns and morphology change can be accurately simulated using depth-averaged velocities, but the inclusion of three-dimensional processes could change the patterns or magnitudes shown here (Hu and others, 2009; Lapetina and Sheng, 2015). However, the relative difference between simulations with and without project conditions would likely be comparable.

Summary and Conclusions

A Delft3D model was developed to evaluate the potential effects of proposed navigation channel deepening and widening in Mobile Harbor, Alabama. Comparisons of model output from deterministic simulations with observed data of water levels, velocities, and bed level changes indicated that the model was able to capture hydrodynamic and sediment transport patterns in the study area with skill (coefficient of determination [R^2] values were 0.93 and 0.66 for modeled versus observed through-channel (U) velocities during ebb and flood tide, respectively, 0.79 and 0.30 for modeled versus observed cross-channel (V) velocities during ebb and flood tide, respectively, 0.98 and 0.79 for ebb tide flux and flood tide flux, respectively, and 0.68 for modeled versus observed water levels). The model was then used to simulate changes in sediment transport with and without modifications to the navigational channel and accounting for 0.5 meter (m) of sea level rise (SLR). Each scenario was simulated for 1 year with a wave climatology representative of the year 2010 as well as for 10 years with a longer-term wave climatology spanning from 1988 to 2016. Comparisons of model output for the with-project and existing conditions for the 2010 simulations indicated differences in bed levels ranging from −0.11 to 0.11 m offshore of Pelican Island and −0.81 to 0.22 m offshore of the Fort Morgan Peninsula. For the simulations with 0.5 m of SLR, differences in bed levels ranged from −0.20 to 0.32 m near Pelican Island and −0.38 to 0.34 m offshore of the Fort Morgan Peninsula. The with-project condition reduced shoaling in the entrance channel by 4.77 and 8.09 percent for the 2010 simulations without and with 0.5 m of SLR, respectively. For the 10-year simulations, there were larger changes in bed levels with the proposed channel deepening; at the end of 10 years, the largest changes were

offshore of the Fort Morgan Peninsula and ranged from −3.17 to 3.94 m for the simulation without SLR and −1.92 to 1.47 m for the simulation with 0.5 m of SLR. The with-project condition reduced the entrance channel shoaling volume by 5.54 percent for the simulation without SLR and 14.98 percent for the simulation with 0.5 m of SLR. Spatially, most of the entrance channel had less deposition except for the middle of the entrance channel, which had more deposition with the proposed channel modifications. Lastly, the shoaling volume at the end of each year in the 10-year simulations was not equal, indicating that offshore changes in bed levels especially around the Fort Morgan Peninsula affect the quantity of sediment that is transported into the channel.

References Cited

Benedet, L., Dobrochinski, J.P.F., Walstra, D.J.R., Klein, A.H.F., and Ranasinghe, R., 2016, A morphological modeling study to compare different methods of wave climate schematization and evaluate strategies to reduce erosion losses from a beach nourishment project: Coastal Engineering, v. 112, p. 69–86. [Also available at https://doi.org/10.1016/j.coastaleng.2016.02.005.]

Bilskie, M.V., Hagen, S.C., Medeiros, S.C., Cox, A.T., Salisbury, M., and Coggin, D., 2016, Data and numerical analysis of astronomic tides, wind-waves, and hurricane storm surge along the northern Gulf of Mexico: Journal of Geophysical Research. Oceans, v. 121, no. 5, p. 3625–3658. [Also available at https://doi.org/10.1002/2015JC011400.]

Bleck, R., 2002, An oceanic general circulation model framed in hybrid isopycnic-cartesian coordinates: Ocean Modeling, v. 4, p. 55–88. [Also available at https://doi.org/10.1016/S1463-5003(01)00012-9.]

Byrnes, M.R., Rosati, J.D., Griffee, S.F., and Berlinghoff, J.L., 2012, Littoral sediment budget for the Mississippi Sound Barrier Islands: Vicksburg, Miss., U.S. Army Engineer Research and Development Center/Coastal and Hydraulics Laboratory (ERDC/CHL) TR–12–9, 171 p. [Also available at http://www.sam.usace.army.mil/Portals/46/docs/program_management/mscip/docs/Appendix%20B%20-%20Littoral%20Sediment%20Budget%20Report.pdf.]

Center for Operational Oceanographic Products and Services, 2018, National Oceanic and Atmospheric Administration, Dauphin Island, AL – Station ID: 8735180 web page, accessed November 1, 2017 at https://tidesandcurrents.noaa.gov/stationhome.html?id=8735180.

Danielson, J.J., Brock, J.C., Howard, D.M., Gesch, D.B., Bonisteel-Cormier, J.M., and Travers, L.J., 2013, Topobathymetric model of Mobile Bay, Alabama: U.S. Geological Survey Data Series 769, accessed October 1, 2017, at https://pubs.usgs.gov/ds/769/.

Dee, D.P. and others, 2011, The ERA-Interim reanalysis: configuration and performance of the data assimilation system: Quarterly Journal of the Royal Meteorological Society, v. 137, no. 656, p. 553-597. [Also available at https://rmets.onlinelibrary.wiley.com/doi/abs/10.1002/qj.828.]

Deltares, 2018a, Delft3D–FLOW—Simulation of multi-dimensional hydrodynamic flows and transport phenomena, including sediments—User manual (ver. 3.15): The Netherlands, Deltares, accessed June 6, 2018, at https://content.oss.deltares.nl/delft3d/manuals/Delft3D-FLOW_User_Manual.pdf.

Deltares, 2018b, Delft3D–WAVE—Simulation of short-crested waves with SWAN—User manual (ver. 3.05): The Netherlands, Deltares, accessed June 6, 2018, at https://content.oss.deltares.nl/delft3d/manuals/Delft3D-WAVE_User_Manual.pdf.

DeWitt, N.T., Stalk, C.A., Flocks, J.G., Bernier, J.C., Kelso, K.W., Fredericks, J.J., and Tuten, T., 2017, Single-beam bathymetry data collected in 2015 nearshore Dauphin Island, Alabama: U.S. Geological Survey data release, accessed December 15, 2017, at https://doi.org/10.5066/F7BZ648W.

Flocks, J.G., DeWitt, N.T., and Stalk, C.A., 2018, Analysis of seafloor change around Dauphin Island, Alabama, 1987–2015 (ver. 1.1, February 2018): U.S. Geological Survey Open-File Report 2017–1112, 19 p. [Also available at https://doi.org/10.3133/ofr20171112.]

Hu, K., Ding, P., Wang, Z., and Yang, S., 2009, A 2D/3D hydrodynamic and sediment transport model for the Yangtze Estuary, China: Journal of Marine Systems, v. 77, nos. 1–2, p. 114–136. [Also available at https://doi.org/10.1016/j.jmarsys.2008.11.014.]

Lapetina, A., and Sheng, Y.P., 2015, Simulating complex storm surge dynamics—Three-dimensionality, vegetation effect, and onshore sediment transport: Journal of Geophysical Research. Oceans, v. 120, no. 11, p. 7363–7380. [Also available at https://doi.org/10.1002/2015JC010824.]

Lesser, G.R., 2009, An approach to medium-term coastal morphological modelling: Leiden, The Netherlands, CRC Press/Balkema, Delft University of Technology, Doctoral dissertation. [Also available at https://repository.tudelft.nl/islandora/object/uuid%3A27a1ffa0-580e-4eae-907b-ce-6f901e652e.]

Lesser, G.R., Roelvink, J.A., van Kester, J.A.T.M., and Stelling, G.S., 2004, Development and validation of a three-dimensional morphological model: Coastal Engineering, v. 51, nos. 8–9, p. 883–915. [Also available at https://doi.org/10.1016/j.coastaleng.2004.07.014.].

National Data Buoy Center, 2018, Station 42040: National Oceanic and Atmospheric Administration web page, accessed December 1, 2017 at https://www.ndbc.noaa.gov/station_page.php?station=42040.

National Geophysical Data Center, National Environmental Satellite, Data, and Information Service, National Oceanic and Atmospheric Administration, and U.S. Department of Commerce, 2009, Mobile, Alabama 1/3 MHW coastal digital elevation model: National Oceanic and Atmospheric Administration, National Centers for Environmental Information web page, accessed December 1, 2017 at https://www.ngdc.noaa.gov/metaview/page?xml=NOAA/NESDIS/NGDC/MGG/DEM/iso/xml/673.xml&view=getDataView&header=none)/.

National Ocean Service, 2014, Report for H12656: National Oceanic and Atmospheric Administration, National Centers for Environmental Information web page, accessed December 1, 2017 at https://www.ngdc.noaa.gov/nos/H12001-H14000/H12656.html.

Passeri, D.L., Long, J.W., Jenkins, R.L., and Thompson, D.M., 2018, Mobile Harbor navigation channel Delft3D model inputs and results: U.S. Geological Survey data release, https://doi.org/10.5066/P9SS1DJW.

Plant, N.G., Holland, K.T., and Puleo, J.A., 2002, Analysis of the scale of errors in nearshore bathymetric data: Marine Geology, v. 191, nos. 1–2, p. 71–86. [Also available at https://doi.org/10.1016/S0025-3227(02)00497-8.]

Roelvink, J.A., 2006, Coastal morphodynamic evolution techniques: Coastal Engineering, v. 53, nos. 2–3, p. 277–287. [Also available at https://doi.org/10.1016/j.coastaleng.2005.10.015.]

Tolman, H.L., 1989, The numerical model WAVEWATCH: a third generation model for the hindcasting of wind waves on tides in shelf seas: Communications on Hydraulic and Geotechnical Engineering, Delft University of Technology, Report 89-2, 72 p. [Also available at https://repository.tudelft.nl/islandora/object/uuid:5d12fc8b-6fa3-4c09-826c-d6955e1d33ab/datastream/OBJ/download].

U.S. Geological Survey, 2016, USGS Lidar Point Cloud LA SoTerrebonne-GI 2015 15RCU7060 LAS 2016: U.S. Geological Survey, accessed October 1, 2017 at http://nationalmap.gov/viewer.html.

ISSN 2331-1258 (online)
https://doi.org/10.3133/ofr20181123

ATTACHMENT A-3

SHIP SIMULATION REPORT

DEPARTMENT OF THE ARMY
ENGINEER RESEARCH AND DEVELOPMENT CENTER, CORPS OF ENGINEERS
COASTAL AND HYDRAULICS LABORATORY
WATERWAYS EXPERIMENT STATION, 3909 HALLS FERRY ROAD
VICKSBURG, MISSISSIPPI 39180-6199

REPLY TO
ATTENTION OF

CEERD-HNN

2 October 2017

MEMORANDUM FOR Commander, U.S. Army Corps of Engineers, Mobile District (CESAM-EN-HH/Ms. Elizabeth Godsey), P.O. Box 2288, Mobile, AL 36628-0001

SUBJECT: Mobile Bay Deepening and Widening Feasibility Ship Simulation Study Data Report

1. Enclosed is the Mobile Bay Deepening and Widening Feasibility Ship Simulation Study (FLSSP) Data Report.

2. The purpose of the FLSSP was to test varying channel widths for the two-way traffic area in the lower Mobile Bay Channel, to test a bend easing, and to determine the feasibility of only deepening the Little Sand Island turning basin. Enclosed is a synopsis of the testing performed from 23-26 May 2017 as well as trackplots and runsheets (Appendix A) and pilot questionnaires (Appendix B). The results from this FLSSP should be used to drive a more comprehensive ship simulation study performed during the Preconstruction, Engineering, and Design (PED) portion of the project.

3. If you have any questions, please contact Ms. Morgan Johnston at (601) 634-2365 or Mr. Tim Shelton, Chief, Navigation Branch, at (601) 634-2304.

Encl

FOR JOSÉ E. SÁNCHEZ, PE, SES
Director

ERDC/CHL

Engineer Research and Development Center

Coastal and Hydraulics Laboratory

US Army Corps of Engineers®
Engineer Research and Development Center

Data Report *Mobile Bay Deepening and Widening Feasibility Ship Simulation Study*

Morgan Johnston

August 2017

Mobile Bay Deepening and Widening
Feasibility Ship Simulation Study
Data Report

1. Introduction

The U.S. Army Engineer Research and Development Center (ERDC) assisted the U.S. Army Corps of Engineers District, Mobile (CESAM) in screening proposed deepening and widening alternatives in Mobile Bay by completing a Feasibility Level Screening Simulation Program (FLSSP). The two areas of interest for the study included a turning basin near Little Sand Island and an area which included a bend easing connected to a two-way traffic area in the lower part of Mobile Bay. These areas of interest are shown in Figure 1.

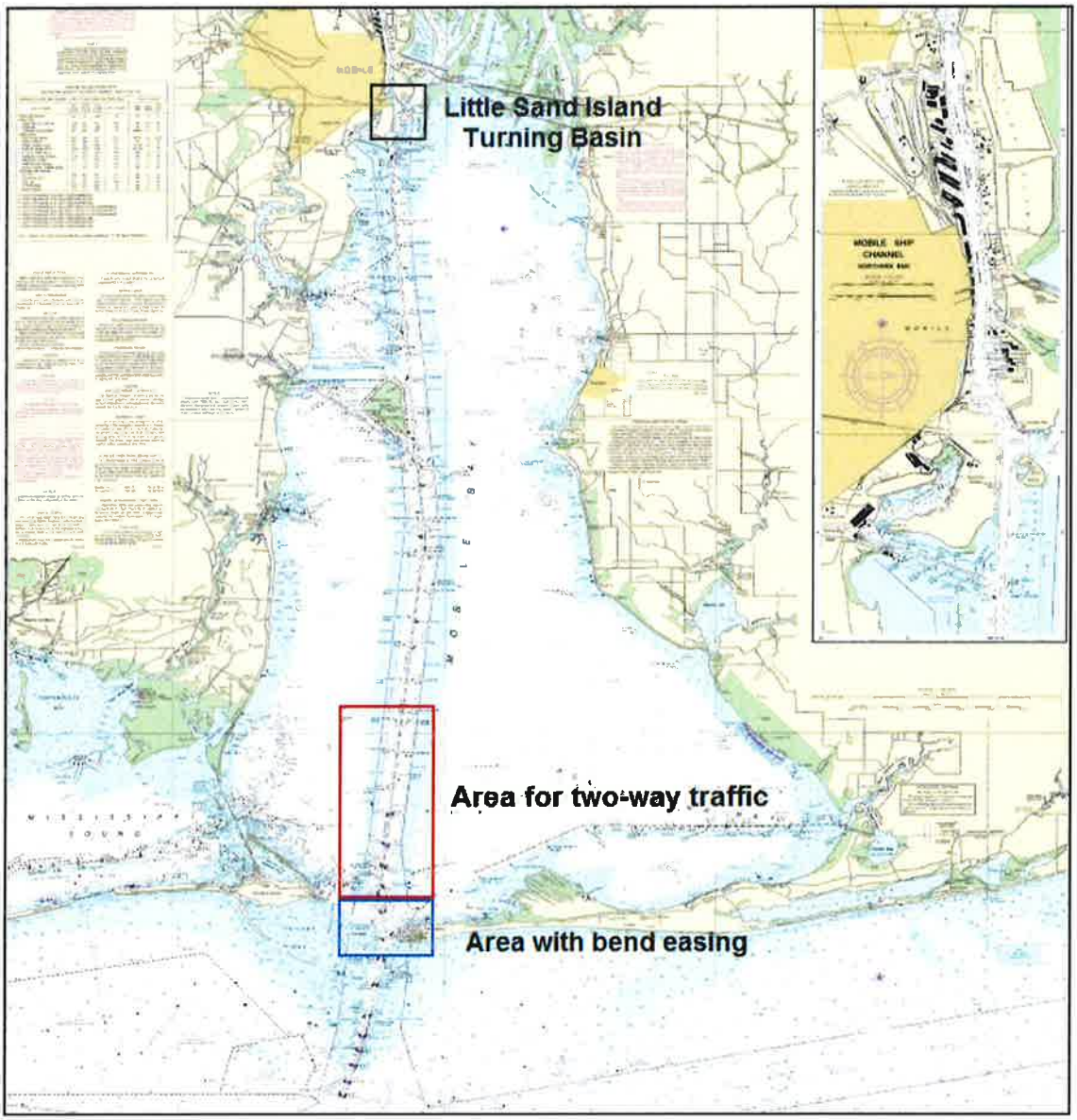

Figure 1. Areas of interest for Mobile Bay FLSSP

2. Proposed Alternatives Tested

For all proposed simulations, the depth was deepened from 45-ft (47-ft at entrance channel) to 51-ft (53-ft at entrance channel). Two different widths were screened for the passing area (500-ft and 550-ft). Each passing lane width spanned approximately 5 miles. All proposed passing lane testing included bend easing on the inside at buoys 18 and 21. The width increases of the bends were approximately 185-ft at buoy 18 and 50-ft at buoy 21. The proposed bend easing is shown in Figure 2. The passing lane begins immediately north of buoy 22 as shown in Figure 2. The Little Sand Island Turning Basin was deepened to 51-ft for proposed testing. The design vessel chosen for the study by the district was a containership (1100-ft x 158-ft x 48-ft). As this ship was not in ERDC's ship library, replacement ships had to be chosen for testing. For passing, the *MSC Daniella 2* (1200-ft x 159-ft x 50-ft) was chosen as a replacement ship to closely match beam, which is vital to passing. There were also a variety of passing scenarios tested that did not include the design vessel, but were of economic interest to the district. For the turning basin, the *Humber Bridge* (1102-ft x 150-ft x 46-ft) was chosen as a replacement ship to match length, which is essential to turning.

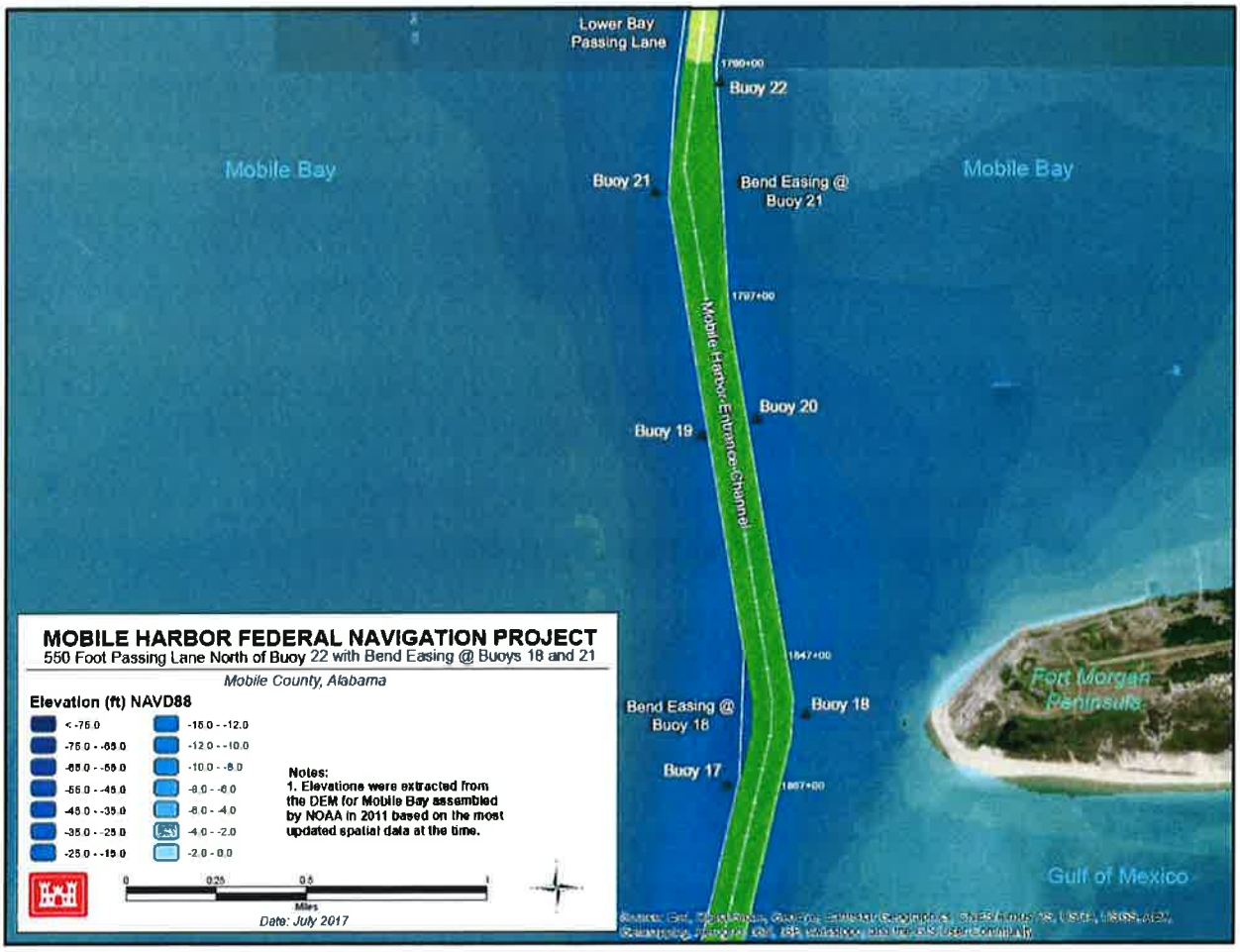

Figure 2. Proposed bend easing

3. Purpose

The purpose of a FLSSP is to screen proposed alternatives using lower resolution databases to limit monetary and time commitments while still providing vital insight of the proposed alternatives moving forward. The lower resolution databases are quicker and less costly to develop and easier to quickly manipulate during the course of testing. This method allows for discussion after the completion of each simulated run, necessary modifications to be implemented, and then the same simulations re-run. By allowing for quick manipulation, the suggested adjustments can be made during the testing week and then tested with the same group of pilots. Conclusions drawn from actual data should be limited due to the use of these lower resolution databases. Data processing is limited to trackplots and run sheets shown in Appendix A. One of the most vital aspects of a FLSSP is providing the means to conduct expert elicitations. The collaboration of all parties occurred throughout the testing week as well as the final group discussion at the conclusion of the testing.

4. Participants

The FLSSP included representatives from ERDC, CESAM, and Mobile Bar Pilots. The individuals listed below were present for the entirety of the testing week, 23-26 May 2017.

ERDC: Morgan Johnston, Keith Martin, Mary Claire Allison, Mario Sanchez, and Dennis Webb, P.E. (former ERDC employee under contract to CHL)

CESAM: Elizabeth Godsey, P.E.

Mobile Bar Pilots: Capt. Chris Brock and Capt. Curtis Wilson

5. Database Development

Due to this study falling under the guidelines of a FLSSP, model development was completed with fairly low resolution.

a. Simulated ships were limited to ships in ERDC's ship library. Ships used during simulations are shown in Table 1 below.

b. Since the development of the exact design ships was not able to be contracted due to time constraints, the ships used from ERDC's ship library had drafts which were unrealistic for the proposed deepening. Tide had to be added to compensate for the extra draft on the *MSC Daniella 2* and *MT Brittania* during testing and when using the *Sovereign Maersk* during validation.

c. Wind conditions were set at run time.

d. Visual scenes were developed using the high level of detail necessary for the more in-depth Preconstruction Engineering and Design (PED) phase of the project. The visual database should be able to be used with minimal adjustments during PED.

e. Currents were developed for the existing channel and the 550-ft proposed channel. During testing of the 500-ft channel, the currents developed for the 550-ft channel were used. This approach was acceptable based off this being a FLSSP and pilots' comments of minimal difference occurring between existing and proposed currents felt during passing. The dominant force felt during passing was ship-to-ship interaction.

f. Ebb currents used for the proposed turning basin included an increased Mobile River flow to create a similar vessel response expected during existing ebb tide.

g. A constant depth of 51-ft was set for the testing of the extended turning basin.

Table 1. Ships used in simulations

Model Name	Vessel Name	LOA (ft)	Beam (ft)	Draft (ft)	Area Tested
CNTNR28L	*Sovereign Maersk*	1138.5	140.4	47.6	Passing, bends, and validation of turning basin
CNTNR40	*MSC Daniella 2*	1201.1	158.8	49.9	Passing, bends, and turning basin
CNTNR20L	*KMSS Dainty*	964.9	105.7	41.0	Validation only, replaced by *Zim Piraeus* for testing of passing
CNTNR44	*Zim Piraeus*	964.9	105.6	43.0	Passing and bends
CNTNR33L	*Humber Bridge*	1102.4	150.3	46.2	Passing, bends, and turning basin
VLCC15L	*MT Brittania*	859.6	137.8	49.2	Passing and bends
TANK10L	*MT Danita II*	750.0	105.8	45.9	Used only as docked vessel near turning basin

6. Validation

Validation for the passing lane occurred on Tuesday, 23 May 2017. Validation started with passing scenarios using the *KMSS Dainty*; however it quickly became clear that the pilots felt that the ship was not experiencing enough response from the banks. The *KMSS Dainty* was replaced with the *Zim Piraeus* which had similar dimensions and has called to port before. This replacement allowed for a much more accurate vessel response from the banks which is vital when testing passing scenarios; however it did come with a slight increase in draft. Once this ship was replaced, pilots felt the appropriate bank effects, including the expected shear off the bank toward the middle of the channel. Pilots expressed that wind, ship-to-ship reaction, ship responses, and currents all felt appropriate for the existing conditions.

Validation of the turning basin occurred during Tuesday, 23 May and Wednesday, 24 May 2017. On Tuesday, it quickly became evident that the currents created for the existing conditions in the turning basin were not sufficient. During turning, these large vessels block most of the channel that conveys the flow of the Mobile River causing the currents and force on the vessel to greatly intensify. An example of this turning vessel which blocks river flow is shown in Figure 3 below. The simulator operates using a pre-

calculated current field. Real-time recalculation of currents to account for ship blockage is beyond the ability of present day ship simulation modeling. The decision was made to improve the effect felt by these turning ships by simply increasing the magnitude of the currents. On Wednesday, a new ebb current was developed which increased the original Mobile River flow used to create the ebb currents by 75%. The pilots found this increased current to be a much more accurate representation of what they experience in existing conditions. The same +75% river flow was then developed for the deepening alternative which was used for the rest of the proposed turning basin testing.

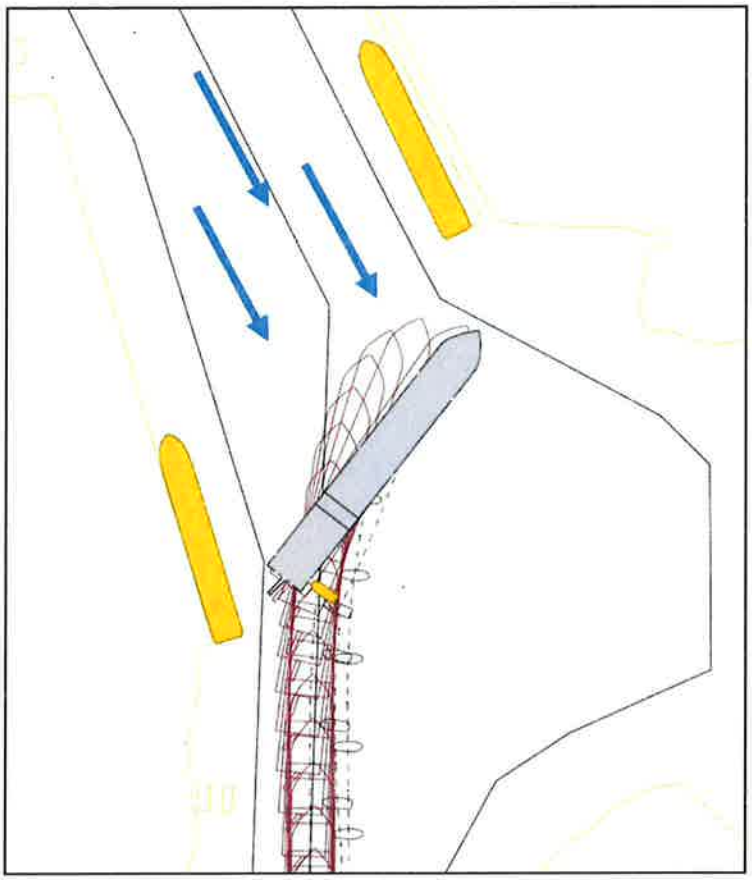

Figure 3. Turning vessel which dams majority of the river flow heading south

7. Passing Lane Testing

Passing lane and bend easing testing began on Wednesday morning. The first run was in the 550-ft channel passing the *MSC Daniella 2* and *Zim Piraeus* using the currents developed for the 550-ft channel. Pilots stated they did not feel much of a difference between the existing currents and the currents developed for the 550-ft channel. This is due to the dominant force of ship-to-ship reaction felt during passing. Due to the minimal difference felt and this being a FLSSP, the currents developed for the 550-ft channel were used for both the 500-ft and 550-ft channels for the remainder of the simulations.

The inbound vessel has a more difficult transit when passing as this ship must navigate through the bends in the lower part of Mobile Bay, and then set up to pass an outbound

vessel. For screening purposes, the more challenging ship typically headed inbound to test the worst case scenario. This more difficult ship was usually selected as the longer ship or the *MT Brittania* as loaded tankers do not steer as easily as containerships. After the first run, the starting positions of the ships were shifted to allow for the inbound ship to completely navigate the bends and then pass the outbound ship.

Table 2 shows the passing lane simulations which were run over the course of the testing week. Twelve passing lane/bend easing runs were simulated with varying passing combinations. It should be noted that drafts were not able to be manipulated to realistically simulate certain passing scenarios. During PED, vessels which have the appropriate loaded and unloaded drafts should be developed. Most runs simulated used flood current with a 20 knot southeasterly wind. Pilots stated this was a critical condition with the ebb current and a 20 knot northern wind being a secondary concern. Run 10 used the existing flood current and a 20 knot eastern wind to test cross-currents felt along the transit. Existing flood currents with an easterly wind were used for this simulation as the proposed channel modification had not been developed with this wind condition.

Table 2. Passing simulations completed

Run #	Passing Lane Width (ft)	Inbound Ship (ft)	Outbound Ship (ft)	Combined Dimensions (ft)	Current	Wind
1	550	*MSC Daniella 2* (1200 x 159)	*Zim Piraeus* (965 x 106)	2165 x 266	Alt Flood	20 SE
3	500	*MSC Daniella 2* (1200 x 159)	*Zim Piraeus* (965 x 106)	2165 x 266	Alt Flood	20 SE
4	500	*MT Brittania* (860 x 138)	*Zim Piraeus* (965 x 106)	1825 x 244	Alt Flood	20 SE
5	500	*MT Brittania* (860 x 138)	*Zim Piraeus* (965 x 106)	1825 x 244	Alt Flood	20 SE
6	500	*Humber Bridge* (1102 x 150)	*Zim Piraeus* (965 x 106)	2067 x 256	Alt Flood	20 SE
7	500	*Humber Bridge* (1102 x 150)	*Zim Piraeus* (965 x 106)	2067 x 256	Alt Ebb	20 N
8	500	*MSC Daniella 2* (1200 x 159)	*MT Brittania* (860 x 138)	2060 x 297	Alt Ebb	20 N
9	500	*Sovereign Maersk* (1140 x 140)	*Sovereign Maersk* (1140 x 140)	2280 x 280	Alt Ebb	20 N
10	500	*MSC Daniella 2* (1200 x 159)	*Sovereign Maersk* (1140 x 140)	2340 x 299	Existing Flood	20 E
23	550	*MT Brittania* (860 x 138)	*MSC Daniella 2* (1200 x 159)	2060 x 297	Alt Flood	20 SE
24	550	*MSC Daniella 2* (1200 x 159)	*Sovereign Maersk* (1140 x 140)	2340 x 299	Alt Flood	20 SE
29	500	*Sovereign Maersk* (1140 x 140)	*Sovereign Maersk* (1140 x 140)	2280 x 280	Alt Flood	20 SE

8. Bend Easing Testing

While simulations that tested only the bend easings were not performed, the entire bend easing was tested during all passing scenario runs after the first run by the inbound vessel. Figure 4 shows the effect the bend easing had on the transit of the inbound vessel. Figure 4 compares the *MT Brittania* trackplots for Run 4 and Run 23. In Run 4, the vessel did not utilize the given bend easing and shows a trackplot that would be similar to a vessel transit in the existing conditions. The bend easing was likely not utilized due to pilots becoming acquainted with the new bend easing and being the initial tanker run. In this simulation, the vessel experienced a much harder turn which pushed it out of the east side of the channel. Run 23 shows better utilization of the bend easing. In this simulation, the same vessel was able to use the bend easing to maintain its course in the center of the channel.

Pilots stated that the bend easing was extremely beneficial in passing scenarios. The extra room at buoy 18 and 21 allowed for the inbound vessel to prepare earlier to pass the outbound vessel which is vital when passing. Pilots suggested that the bend be eased further on the outside of the bend near buoy 21 as to provide extra room for inbound vessels utilizing this segment of the bend.

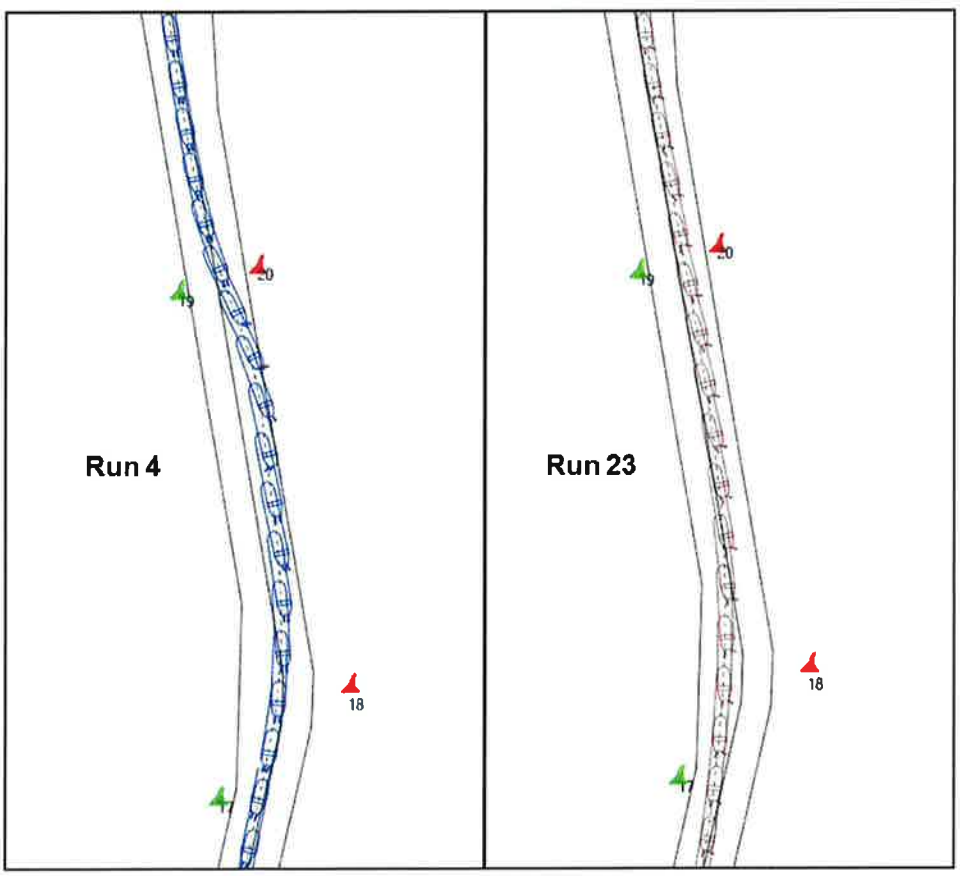

Figure 4. Bend easing impact on inbound vessel transit

9. One-way existing channel with *MSC Daniella 2*

The existing channel with no bend easing or passing lanes added was tested using the *MSC Daniella 2* inbound with flood current and a 20 knot southeasterly wind in Run 26. During this simulation, the vessel clipped the channel near buoy 17 and had to use several hard over rudder commands to traverse the existing channel. However, these navigational difficulties likely occurred due to the lack of bend easing and not the channel width. The pilot who completed this simulation said the width of the existing channel felt adequate. The existing channel width should be sufficient for a vessel with similar dimensions of the *MSC Daniella 2* if the bend easing is implemented.

10. Turning Basin Testing

Turning Basin testing began on Thursday morning as the proposed ebb current had to be updated to include an increase river flow to mimic the vessel response felt during turning with strong ebb currents. The proposed testing utilized the deepened channel, the increased river flow ebb current, and a 20 knot wind from the north. Pilots stated that this was by far the hardest condition typically navigated. They were confident if they were able to turn a vessel with the ebb current and north wind, then they would be able to turn the vessel in other conditions.

For all turning basin simulations, cranes were placed at the southern container terminal berth to act as a visual que for the pilots. For most simulations, a docked tanker (750-ft x 106-ft) was placed at the southern berth of the container terminal and at the Pinto terminal. The placement and size of these ships is typical of docked ships expected to be seen by pilots.

Table 3 shows the different turning basin simulations which were ran over the course of the testing week. Runs 13-16 tested the *Humber Bridge* turning and then going towards the dock and the *Humber Bridge* pulling off the dock and then turning. Two tugs were used for these first simulations as this is what is typically available to the pilots in current conditions. In the simulations that pulled the vessel off the dock (Runs 15 and 16), both pilots went outside of the federal channel and had to rely on the container terminal berthing area to complete the turn. In the simulations testing the vessel docking (Runs 13, 14, and 19), the vessel barely stayed within the federal limits (roughly averaged 21-ft from stern of turning vessel to the federal channel limit near the berthing area) and had about 150-ft of clearance from the docked vessel at the container terminal.

Pilots were very uncomfortable with these turning scenarios. To use the turning basin inbound for existing conditions in ebb tide, pilots position the stern of the turning ship as close to the dock or docked vessel as possible. This maneuver often requires the vessel to go outside of the federal channel and rely on the container terminal berthing area. Once the vessel is perpendicular with the ebb current, tugs are positioned on the stern. These tugs attempt to hold the stern in place while the bow of the vessel falls to the south due to the strong ebb current. Due to the docked vessel at the southern berth of the container terminal, pilots had to go further east into the turning basin which they avoid in existing conditions. The further east the vessel commits into the turning basin,

the greater the risk of the bow of the vessel clipping the southern edge of the turning basin in the vicinity of Little Sand Island. A more easterly approach also forces the pilot to rely on engines working full astern to pull out of the turning basin. This leaves the pilots without a safety factor. With engines pulling full astern and tugs working at full power, there is no room for error or engine failure. Due to this added risk, pilots were uncomfortable with the maneuver necessary to turn this larger vessel with a docked vessel.

For Runs 17 and 18, the *MSC Daniella 2* was tested going to the dock with three tugs by both pilots. Both of these runs were unsuccessful. The 1200-ft length of the *MSC Daniella 2* was not feasible for the deepened only turning basin with a docked vessel at the southern berth. For Runs 19 and 20, the *Humber Bridge* was tested going to the dock with an extra 60 ton tug. The pilots did not find that this extra tug had much of an effect on the turning maneuver; however, pilots stated that if this sized vessel were to come to port, they would complete the turn with three tugs. Therefore, the rest of the simulations were completed using three tugs. Run 20 was completed in the deepened only turning basin, but with an aggressive easterly approach that would not be attempted in existing conditions. This run allowed the team to visualize the maneuver and dimensions necessary for more utilization of the eastern portion of the turning basin. Modifications were made for subsequent simulations to eliminate the concern of the falling bow clipping the southern edge of the turning basin.

For Runs 21-22, 25-28, and 30-32, a flat bottom of constant depth 51-ft was used for the entire database. A flat bottom of constant depth allows for the vessel to leave the channel boundaries without stopping the simulation. This provides insight into what may be necessary as a channel improvement. This assumption is appropriate for a FLSSP and is consistent with assumptions used in previous FLSSP studies. For Runs 21 and 22, a flat bottom was used; however the Electronic Chart Display and Information System (ECDIS) maintained the existing turning basin lines. Pilots expressed interest in adding an extension to the turning basin lines in the ECDIS to better visualize the room available. For Runs 25 and after, a new file was created on the ECDIS with a 100-ft extension on the southern edge of the turning basin. This 100-ft extension of the turning basin can be seen in Figure 5. In Run 31, a *Humber Bridge* was turned with a docked *MSC Daniella 2* in the southern berth of the container terminal to visually represent further expansion of the container terminal.

Of the nine simulations completed with a flat bottom, only one simulation went outside of the federal channel near the container terminal berthing area, Run 28. In Run 28, there was no docked vessel at the southern berth so the turning vessel utilized part of the berthing area to complete the turn. The average distance from the federal channel limit near the southern berth to the turning *Humber Bridge* for all of the flat bottom simulations (Runs 21-22, 25-28, and 30-32) was about 183-ft. The average distance from the federal channel limit near the southern berth to the turning *Humber Bridge* for the deepened only turning basin simulations (Runs 13-16, and 19) was about 11-ft.

Pilots thought overall the extension of the turning basin greatly assisted in the safety of completing the turn with the *Humber Bridge* by allowing for more room for the falling

bow. However, even with the extension, pilots still had to use more of the engine's power than they would typically be comfortable with. While the extension of the turning basin increased the room for error during the turn for this larger vessel, further improvements may be required. Turning basin testing should be revisited during PED as testing was limited, utilized a flat bottom instead of actual bathymetry, operated with a replacement design vessel, and used currents developed for the deepened only turning basin. After the previous simplifications are addressed, PED testing can be completed to further test turning basin modification.

Table 3. Turning basin simulations completed

Run #	Plan	Vessel (ft)	To dock/ Off dock	Docked Vessel (south berth, Pinto terminal)	Tugs (tons)	Pilot
13	P1	*Humber Bridge* (1102 x 150)	To dock	Tank10L, Tank10L	50 and 60	Brock
14	P1	*Humber Bridge* (1102 x 150)	To dock	Tank10L, Tank10L	50 and 60	Wilson
15	P1	*Humber Bridge* (1102 x 150)	Off dock	Tank10L, Tank10L	50 and 60	Brock
16	P1	*Humber Bridge* (1102 x 150)	Off dock	Tank10L, Tank10L	50 and 60	Wilson
17	P1	*MSC Daniella 2* (1200 x 159)	To dock	Tank10L, Tank10L	50, 60, and 60	Brock
18	P1	*MSC Daniella 2* (1200 x 159)	To dock	Tank10L, Tank10L	50, 60, and 60	Wilson
19	P1	*Humber Bridge* (1102 x 150)	To dock	Tank10L, Tank10L	50, 60, and 60	Brock
20	P1	*Humber Bridge* (1102 x 150)	To dock	Tank10L, Tank10L	50, 60, and 60	Wilson
21	P2	*Humber Bridge* (1102 x 150)	To dock	Tank10L, Tank10L	50, 60, and 60	Brock
22	P2	*Humber Bridge* (1102 x 150)	To dock	Tank10L, Tank10L	50, 60, and 60	Wilson
25	P2	*Humber Bridge* (1102 x 150)	To dock	Tank10L, Tank10L	50, 60, and 60	Wilson
26	P2	*Humber Bridge* (1102 x 150)	Off dock	Tank10L, Tank10L	50, 60, and 60	Brock
27	P2	*Humber Bridge* (1102 x 150)	To dock	None, Tank10L	50, 60, and 60	Brock
28	P2	*Humber Bridge* (1102 x 150)	Off dock	None, Tank10L	50, 60, and 60	Wilson
30	P2	*Humber Bridge* (1102 x 150)	To dock	Tank10L, Tank10L	50, 60, and 60	Brock
31	P2	*Humber Bridge* (1102 x 150)	To dock	Tank10L, *MSC Daniella 2*	50, 60, and 60	Wilson
32	P2	*Humber Bridge* (1102 x 150)	Off dock	Tank10L, Tank10L	50, 60, and 60	Wilson

*All runs used the increased river flow ebb current for the deepened alternative and a 20 knot northern wind
**P1 is a deepened only turning basin (51-ft) , P2 is deepened using a flat bottom depth of 51-ft

Figure 5. Turning basin extension

11. TSP Channel

The following aspects of the study were determined based upon the final FLSSP discussion on Friday afternoon, observations throughout the testing week, and the final pilot surveys (shown in Appendix B):

a. The 500-ft channel was deemed acceptable for a variety of passing scenarios:

   (1) *Zim Piraeus* (965-ft x 106-ft) and *Zim Piraeus* (965-ft x 106-ft)

   (2) *Zim Piraeus* (965-ft x 106-ft) and *MT Brittania* (860-ft x 138-ft)*

b. The 550-ft channel was deemed acceptable for a variety of passing scenarios:

   (1) *Zim Piraeus* (965-ft x 106-ft) and *Zim Piraeus* (965-ft x 106-ft)

   (2) *Zim Piraeus* (965-ft x 106-ft) and *MT Brittania* (860-ft x 138-ft)

   (3) *Sovereign Maersk* (1140-ft x 140-ft) and *Sovereign Maersk* (1140-ft x 140-ft)

(4) *Sovereign Maersk* (1140-ft x 140-ft) and *Zim Piraeus* (965-ft x 106-ft)

(5) *MSC Daniella 2* (1200-ft x 159-ft) and *MT Brittania* (860-ft x 138-ft)*

(6) *Sovereign Maersk* (1140-ft x 140-ft) and *MT Brittania* (860-ft x 138-ft)*

*It should be noted that pilots believe draft restrictions in both the 500-ft and 550-ft passing lanes will be enforced for passing scenarios using tankers.

c. The bend easing was found to greatly influence the ease in which passing could be completed. If further modifications to ease the bend even more were possible, the passing lane may be able to be shortened slightly.

The biggest interest for further softening of the bends was near buoy 21 on the west side of the channel.

d. While testing was completed using a 5 mile passing lane, it is likely that the full 5 mile length may not be necessary.

Most likely the passing lane length will fall in-between 3 and 5 miles.

e. The turning basin should be modified for the design vessel to safely and confidently use the turning basin. This will be required when a docked vessel is present at the container terminal. Further testing should be completed for this modification, but it is likely that a minimum of a 100-ft addition will be necessary on the southern edge of the turning basin.

If the turning basin is enlarged, it is possible that only two tugs would be necessary to complete the turn using ships similar in size to the *Humber Bridge* (1102-ft x 150-ft).

During a follow-up call with Capt. Brock on 27 May 2017, the following passing situations were discussed:

a. *Sovereign Maersk* (1140-ft x 140-ft) and *Zim Piraeus* (965-ft x 106-ft) would be feasible with draft restrictions in the 500-ft channel.

b. Humber Bridge (1102-ft x 150-ft) and *Zim Piraeus* (965-ft x 106-ft) in the 500-ft channel would be feasible with environmental and draft restrictions.

c. *MT Brittania* (860-ft x 138-ft) and *MT Brittania* (860-ft x 138-ft) in 550-ft channel

Although not simulated, Capt. Brock believed this scenario would be possible with draft restrictions.

Mobile Bay Feasibility Simulations – Passing Lane / Bend Ease

Run #: 1 Date: 5/24/17

Pilot:
1. Captain Chris Brock — Inbound ✓ Outbound ___ Buoy Start 17 Bridge ~~A~~ B
2. Captain Curtis Wilson — Inbound ___ Outbound ✓ Buoy Start 31 Bridge A

Out 31
In 17

Wind: (20 KNT) E W (SE) Other: ___

Currents: Flood(E wind) Flood(W wind) (Flood(SE wind)) Ebb(E wind) Ebb(W wind) Other: ___

Tide added: None (+0.7m (Daniella 2 or MT Brittania)) Other: ___

Plan: P0 (Existing) P1(500ft) (P2(550ft))

Vessel:

Pilot #	Model Name	Ship Name	LOA (ft)	Beam (ft)	Draft (ft)	LOA (m)	Beam (m)	Draft (m)
	CNTNR28L	Sovereign Maersk (SovMae)	1138.5	140.4	47.6	347.0	42.8	14.5
1	CNTNR40	MSC Daniella 2 (Dan2)	1201.1	158.8	49.9	366.1	48.4	15.2
2	CNTNR44	Zim Piraeus (Zim)	964.9	105.6	43.0	294.1	32.2	13.1
	CNTNR33L	Humber Bridge (HumB)	1102.4	150.3	46.2	336.0	45.8	14.1
	VLCC15L	MT Brittania (MTBrit)	859.6	137.8	49.2	262.0	42.0	15.0
	TANK23	Eagle Kanger (EagleK)	799.9	137.8	40.0	243.8	42.0	12.2

Naming convention - Plan_Area_IShipInbound_OShipoutbound_Currents_Wind_Repetition
(Ex:P0_PassingLane_IZim_ODan2_Flood_20E_1)

Filename: P2-PassingLane-OZim-IDan2-Flood-20SE-1

Comments:

* Alt 1 Flood

- Ships handled Realistic
- More time to recover once ~~was~~ passing was completed

[redacted]
02:09
02:26

Record File 02:02

Appendix A

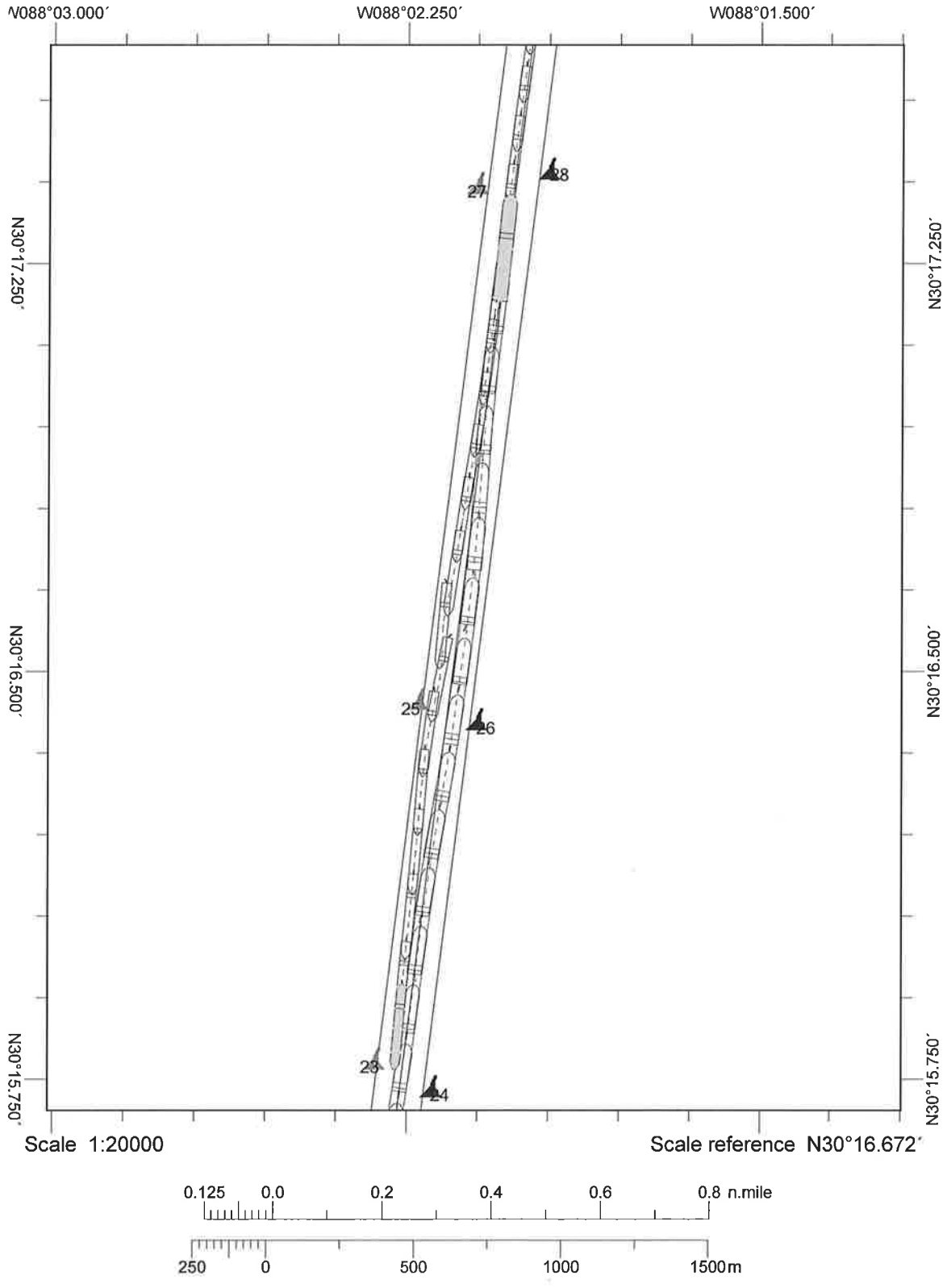

Line sample period (s)	30
Course marker every	00:30
Heading marker period (s)	30
Shape outline every	00:30

Mobile Bay Feasibility Simulations – Passing Lane / Bend Ease

Run #: 2

Date: 5/24/2017

Pilot:

1. Captain Chris Brock — Inbound ✓ Outbound ___ Buoy Start 15 Bridge B
2. Captain Curtis Wilson — Inbound ___ Outbound ✓ Buoy Start 33 Bridge A

Wind: (20 KNT) E W (SE) Other: _____

Currents: Flood(E wind) Flood(W wind) (Flood(SE wind)) Ebb(E wind) Ebb(W wind) Other: _____

Tide added: None (+0.7m (Daniella 2 or MT Brittania)) Other: _____

Plan: P0 (Existing) (P1(500ft)) P2(550ft)

Vessel:

Pilot #	Model Name	Ship Name	LOA (ft)	Beam (ft)	Draft (ft)	LOA (m)	Beam (m)	Draft (m)
	CNTNR28L	Sovereign Maersk (SovMae)	1138.5	140.4	47.6	347.0	42.8	14.5
1	CNTNR40	MSC Daniella 2 (Dan2)	1201.1	158.8	49.9	366.1	48.4	15.2
2	CNTNR44	Zim Piraeus (Zim)	964.9	105.6	43.0	294.1	32.2	13.1
	CNTNR33L	Humber Bridge (HumB)	1102.4	150.3	46.2	336.0	45.8	14.1
	VLCC15L	MT Brittania (MTBrit)	859.6	137.8	49.2	262.0	42.0	15.0
	TANK23	Eagle Kanger (EagleK)	799.9	137.8	40.0	243.8	42.0	12.2

Naming convention - Plan_Area_IShipInbound_OShipoutbound_Currents_Wind_Repetition
(Ex:P0_PassingLane_IZim_ODan2_Flood_20E_1)

Filename: P1_PASSING LANE_0'ZIM_IDAN2_FLOOD_20SE-2

Comments:

* ALT 1 FLOOD

03:04

DAN2 GROUNDED AROUND G-21
DOING ALMOST 16 KT.

RECORD FILE

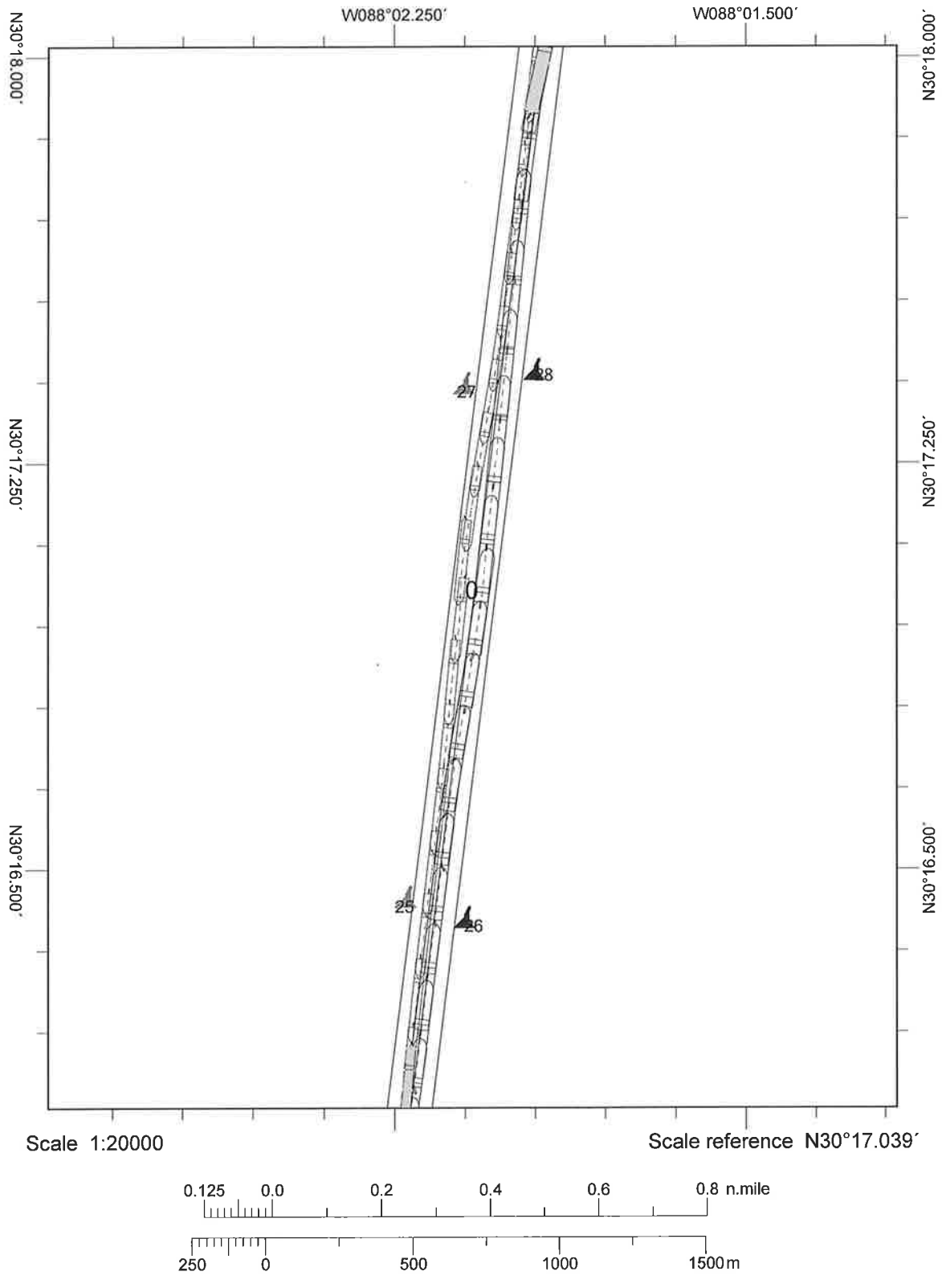

Line sample period (s)	30
Course marker every	00:30
Heading marker period (s)	30
Shape outline every	00:30

Mobile Bay Feasibility Simulations – Passing Lane / Bend Ease

Run #: 4 Date: 5/24/2017

Pilot:

1. Captain Chris Brock	Inbound ✓	Outbound___	Buoy Start 15	Bridge B
2. Captain Curtis Wilson	Inbound___	Outbound ✓	Buoy Start 33	Bridge A

Wind: 20 KNT	E	W	SE		Other:
Currents: Flood(E wind)	Flood(W wind)	Flood(SE wind)	Ebb(E wind)	Ebb(W wind)	Other:
Tide added:	None	+0.7m (Daniella 2 or MT Brittania)	+ 1.2m		Other:
Plan:	P0 (Existing)	P1(500ft)	P2(550ft)		

Vessel:

Pilot #	Model Name	Ship Name	LOA (ft)	Beam (ft)	Draft (ft)	LOA (m)	Beam (m)	Draft (m)
	CNTNR28L	Sovereign Maersk (SovMae)	1138.5	140.4	47.6	347.0	42.8	14.5
	CNTNR40	MSC Daniella 2 (Dan2)	1201.1	158.8	49.9	366.1	48.4	15.2
2	CNTNR44	Zim Piraeus (Zim)	964.9	105.6	43.0	294.1	32.2	13.1
	CNTNR33L	Humber Bridge (HumB)	1102.4	150.3	46.2	336.0	45.8	14.1
1	VLCC15L	MT Brittania (MTBrit)	859.6	137.8	49.2	262.0	42.0	15.0
	TANK23	Eagle Kanger (EagleK)	799.9	137.8	40.0	243.8	42.0	12.2

Naming convention - Plan_Area_IShipInbound_OShipoutbound_Currents_Wind_Repetition
(Ex:P0_PassingLane_IZim_ODan2_Flood_20E_1)

Filename: P1_PassLan - OZim_I MT Brit_Flood-20SE_1

Comments:

* All 1 Foods.

Start - 0412
End - 0440

Meeting @ 23:30

Record File 0346

Pilot observed inbound Tanker handled very sluggish, otherwise the passing was realistic

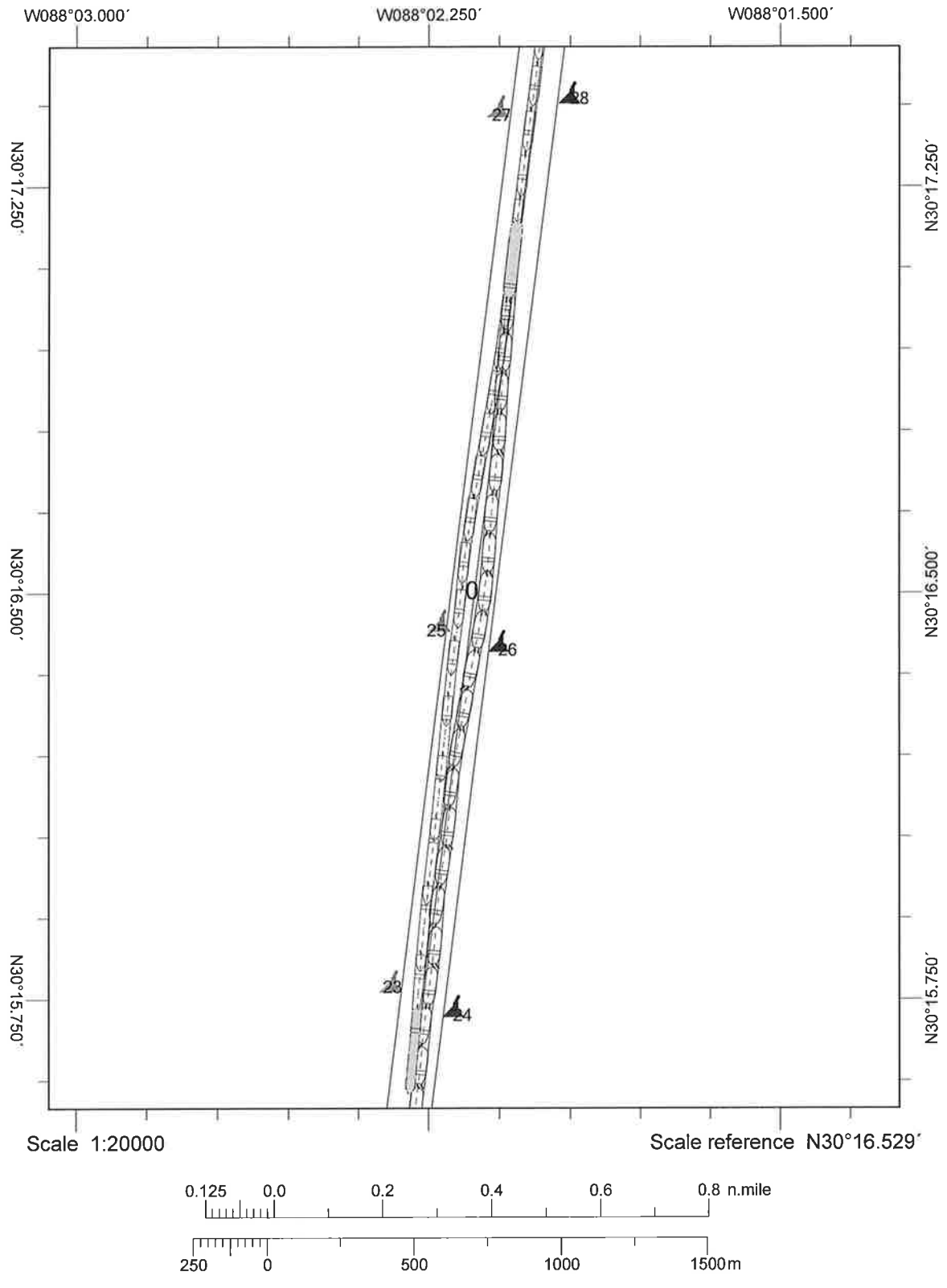

Line sample period (s)	30
Course marker every	00:30
Heading marker period (s)	30
Shape outline every	00:30

Mobile Bay Feasibility Simulations – Passing Lane / Bend Ease

Run #: 5

Date: 5/24/2017

Pilot:

1. Captain Chris Brock — Inbound ___ Outbound ✓ Buoy Start 35 Bridge B
2. Captain Curtis Wilson — Inbound ✓ Outbound ___ Buoy Start 15 Bridge A

Wind: 20 KNT E W SE Other: _____

Currents: Flood(E wind) Flood(W wind) Flood(SE wind) Ebb(E wind) Ebb(W wind) Other: _____

Tide added: None +0.7m (Daniella 2 or MT Brittania) +1.2 m Other: _____

Plan: P0 (Existing) P1(500ft) P2(550ft)

Vessel:

Pilot #	Model Name	Ship Name	LOA (ft)	Beam (ft)	Draft (ft)	LOA (m)	Beam (m)	Draft (m)
	CNTNR28L	Sovereign Maersk (SovMae)	1138.5	140.4	47.6	347.0	42.8	14.5
	CNTNR40	MSC Daniella 2 (Dan2)	1201.1	158.8	49.9	366.1	48.4	15.2
1	CNTNR44	Zim Piraeus (Zim)	964.9	105.6	43.0	294.1	32.2	13.1
	CNTNR33L	Humber Bridge (HumB)	1102.4	150.3	46.2	336.0	45.8	14.1
2	VLCC15L	MT Brittania (MTBrit)	859.6	137.8	49.2	262.0	42.0	15.0
	TANK23	Eagle Kanger (EagleK)	799.9	137.8	40.0	243.8	42.0	12.2

Naming convention - Plan_Area_IShipInbound_OShipoutbound_Currents_Wind_Repetition
(Ex:P0_PassingLane_IZim_ODan2_Flood_20E_1)

Filename: P1_PassLan_OZim_IMTBrit_Flood_20SE_2

Comments:

* Alt 1 Flood

START 05:00
END 05:24

Meeting @ 20:40

Record File 04:41

Bend Easings were very much an improvement, Tanker handled fine, Meeting in channel was good w/ sufficient room.

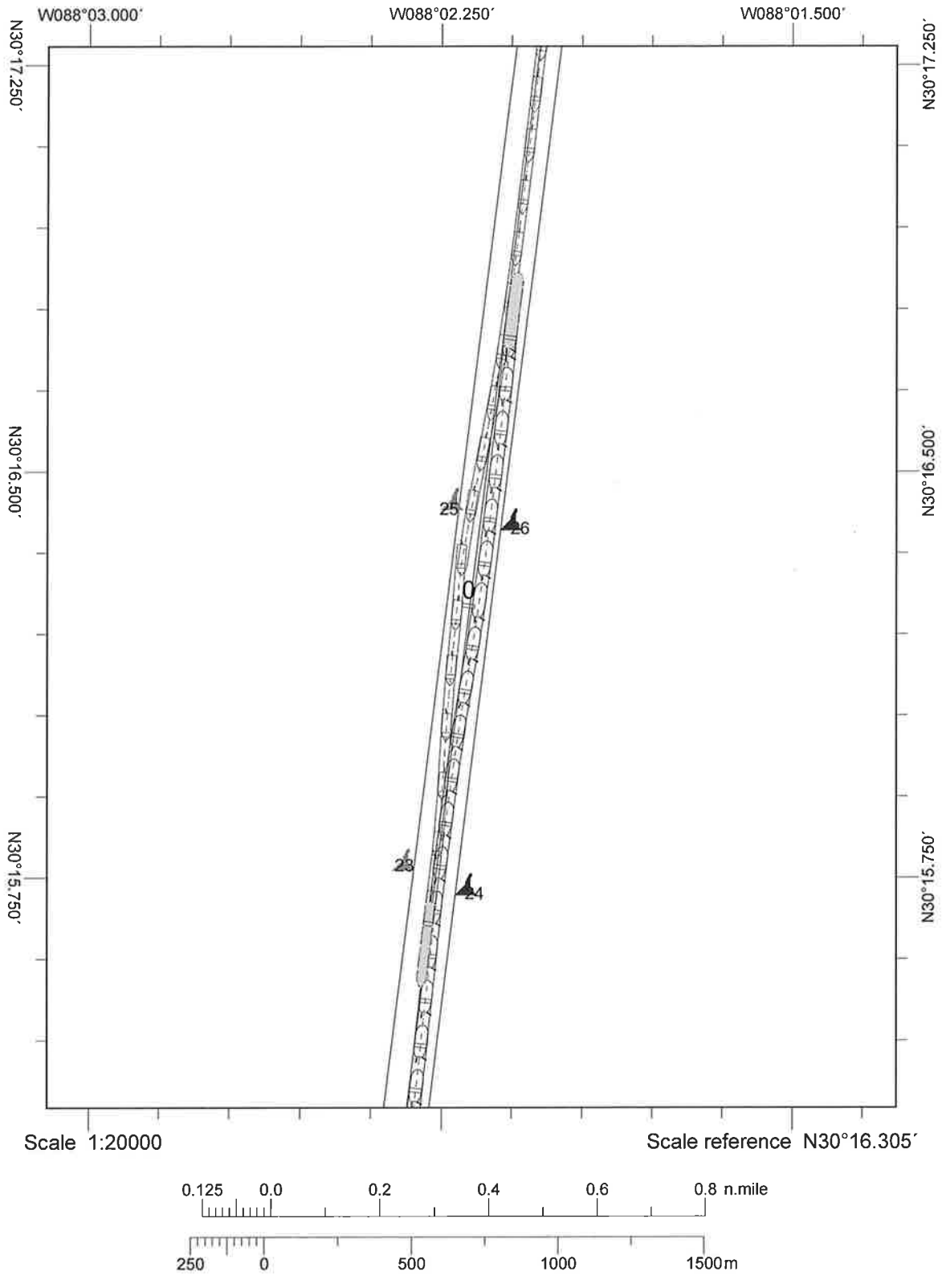

Line sample period (s)	30
Course marker every	00:30
Heading marker period (s)	30
Shape outline every	00:30

Mobile Bay Feasibility Simulations – Passing Lane / Bend Ease

Run #: 6 Date: 5/24/17

Pilot:

1. Captain Chris Brock — Inbound ___ Outbound ✓ Buoy Start 33 Bridge B
2. Captain Curtis Wilson — Inbound ✓ Outbound ___ Buoy Start 15 Bridge A

Bridge
OWN 2 A
OWN 1 B

Wind: 20 KNT E W SE Other: ___

Currents: Flood(E wind) Flood(W wind) Flood(SE wind) Ebb(E wind) Ebb(W wind) Other: ___

Tide added: None +0.7m (Daniella 2 or MT Brittania) +1.2m Other: ___

Plan: P0 (Existing) P1(500ft) P2(550ft)

Vessel:

Pilot #	Model Name	Ship Name	LOA (ft)	Beam (ft)	Draft (ft)	LOA (m)	Beam (m)	Draft (m)
	CNTNR28L	Sovereign Maersk (SovMae)	1138.5	140.4	47.6	347.0	42.8	14.5
	CNTNR40	MSC Daniella 2 (Dan2)	1201.1	158.8	49.9	366.1	48.4	15.2
1	CNTNR44	Zim Piraeus (Zim)	964.9	105.6	43.0	294.1	32.2	13.1
2	CNTNR33L	Humber Bridge (HumB)	1102.4	150.3	46.2	336.0	45.8	14.1
3	VLCC15L	MT Brittania (MTBrit)	859.6	137.8	49.2	262.0	42.0	15.0
	TANK23	Eagle Kanger (EagleK)	799.9	137.8	40.0	243.8	42.0	12.2

Naming convention - Plan_Area_IShipInbound_OShipoutbound_Currents_Wind_Repetition
(Ex:P0_PassingLane_IZim_ODan2_Flood_20E_1)

Filename: P1_Passinglane_ I HumB _ O Zim _ ~~I MT Britt~~ O HumB _ Flood _ 20SE _ 1

Comments:

PASSING WENT WELL, AMPLE ROOM IN 500 Ft Channel

Start - 0644
End -
Meet -

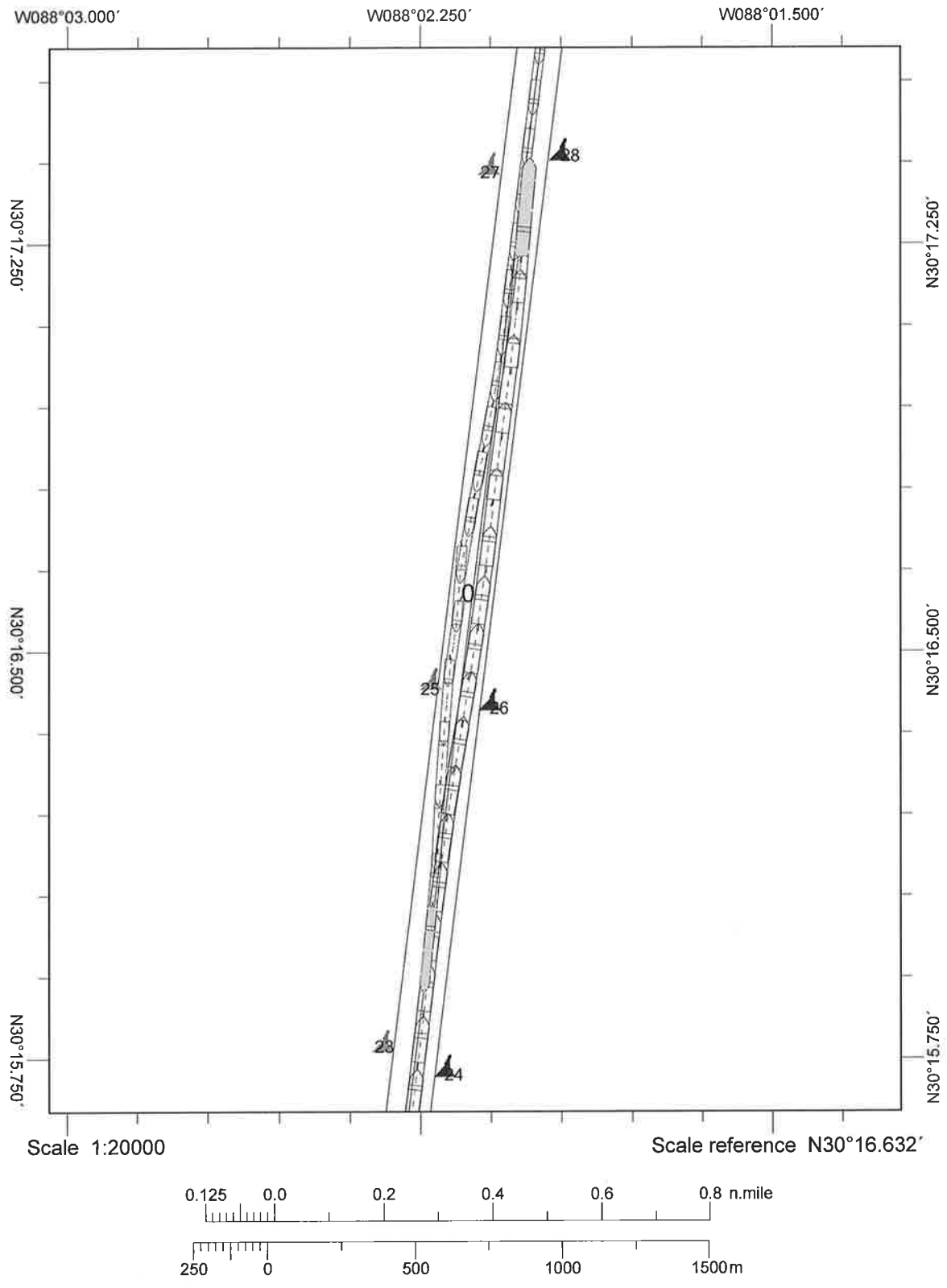

Line sample period (s)	30
Course marker every	00:30
Heading marker period (s)	30
Shape outline every	00:30

Mobile Bay Feasibility Simulations – Passing Lane / Bend Ease

Run #: 7 Date: 5/24/17

Pilot:

1. Captain Chris Brock — Inbound ___ Outbound ✓ Buoy Start 33 (29) Bridge B
2. Captain Curtis Wilson — Inbound ✓ Outbound ___ Buoy Start 15 Bridge A

Wind: (20 KNT) E W SE (N) Other: N

Currents: Flood(E wind) Flood(W wind) Flood(SE wind) Ebb(E wind) Ebb(W wind) Other: ~~Flood~~ Ebb (N wind)

Tide added: None (+0.7m (Daniella 2 or MT Brittania)) Other: ___

Plan: P0 (Existing) (P1(500ft)) P2(550ft)

Vessel:

Pilot #	Model Name	Ship Name	LOA (ft)	Beam (ft)	Draft (ft)	LOA (m)	Beam (m)	Draft (m)
	CNTNR28L	Sovereign Maersk (SovMae)	1138.5	140.4	47.6	347.0	42.8	14.5
	CNTNR40	MSC Daniella 2 (Dan2)	1201.1	158.8	49.9	366.1	48.4	15.2
1	CNTNR44	Zim Piraeus (Zim)	964.9	105.6	43.0	294.1	32.2	13.1
2	CNTNR33L	Humber Bridge (HumB)	1102.4	150.3	46.2	336.0	45.8	14.1
	VLCC15L	MT Brittania (MTBrit)	859.6	137.8	49.2	262.0	42.0	15.0
	TANK23	Eagle Kanger (EagleK)	799.9	137.8	40.0	243.8	42.0	12.2

Naming convention - Plan_Area_IShipInbound_OShipoutbound_Currents_Wind_Repetition
(Ex:P0_PassingLane_IZim_ODan2_Flood_20E_1)

Filename: P1-Passinglane_IHumB_OZim_~~Flood~~ Ebb_20N_1
* File name says Flood, but Ebb was used

Comments:

Ship reaction after passing needs to be improved

Start - 709 (720)
End - 737
Meet -
↑ elapsed time

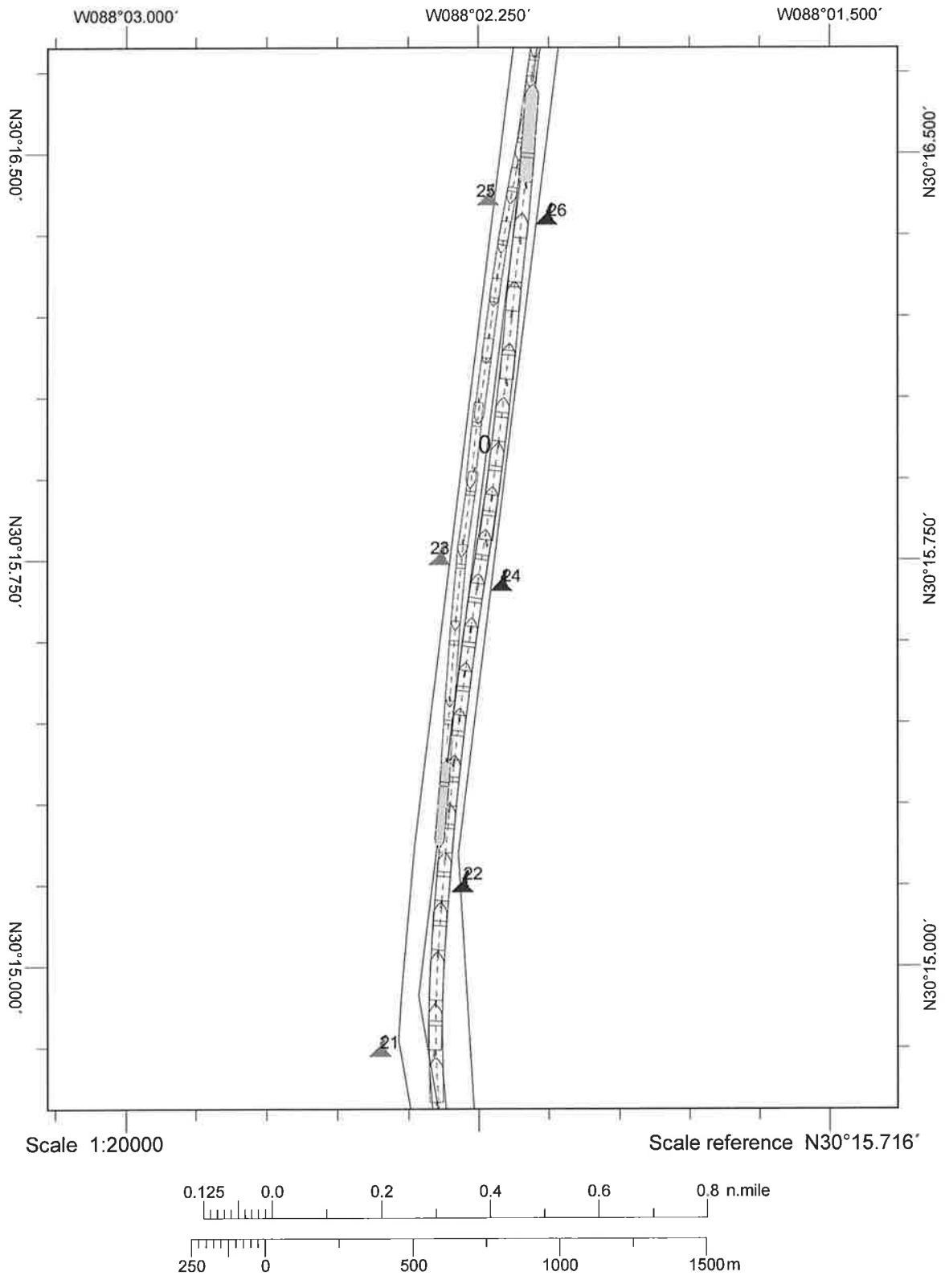

Line sample period (s)	30
Course marker every	00:30
Heading marker period (s)	30
Shape outline every	00:30

Mobile Bay Feasibility Simulations – Passing Lane / Bend Ease

Run #: 8 Date: 24 May 2017

Pilot:
1. Captain Chris Brock — Inbound X — Outbound ___ — Buoy Start 15 — Bridge B
2. Captain Curtis Wilson — Inbound ___ — Outbound X — Buoy Start ~~31~~ 29 — Bridge A

Wind: (20 KNT) E W SE N Other: N

Currents: Flood(E wind) Flood(W wind) Flood(SE wind) Ebb(E wind) Ebb(W wind) Other: Ebb N

Tide added: None ~~+0.7m~~ 1.2 (Daniella 2 or MT Brittania) Other: ___

Plan: P0 (Existing) (P1(500ft)) P2(550ft)

Vessel:

Pilot #	Model Name	Ship Name	LOA (ft)	Beam (ft)	Draft (ft)	LOA (m)	Beam (m)	Draft (m)
	CNTNR28L	Sovereign Maersk (SovMae)	1138.5	140.4	47.6	347.0	42.8	14.5
1 (B)	CNTNR40	MSC Daniella 2 (Dan2)	1201.1	158.8	49.9	366.1	48.4	15.2
	CNTNR44	Zim Piraeus (Zim)	964.9	105.6	43.0	294.1	32.2	13.1
	CNTNR33L	Humber Bridge (HumB)	1102.4	150.3	46.2	336.0	45.8	14.1
2 (A)	VLCC15L	MT Brittania (MTBrit)	859.6	137.8	49.2	262.0	42.0	15.0
	TANK23	Eagle Kanger (EagleK)	799.9	137.8	40.0	243.8	42.0	12.2

Naming convention - Plan_Area_IShipInbound_OShipoutbound_Currents_Wind_Repetition
(Ex:P0_PassingLane_IZim_ODan2_Flood_20E_1)

Filename: P1_PassLan_I Dan2_O MTBrit_Ebb_20N_1

Comments: Passing executed safely, combined beam approaching extreme maximum. Distance between ships very close.

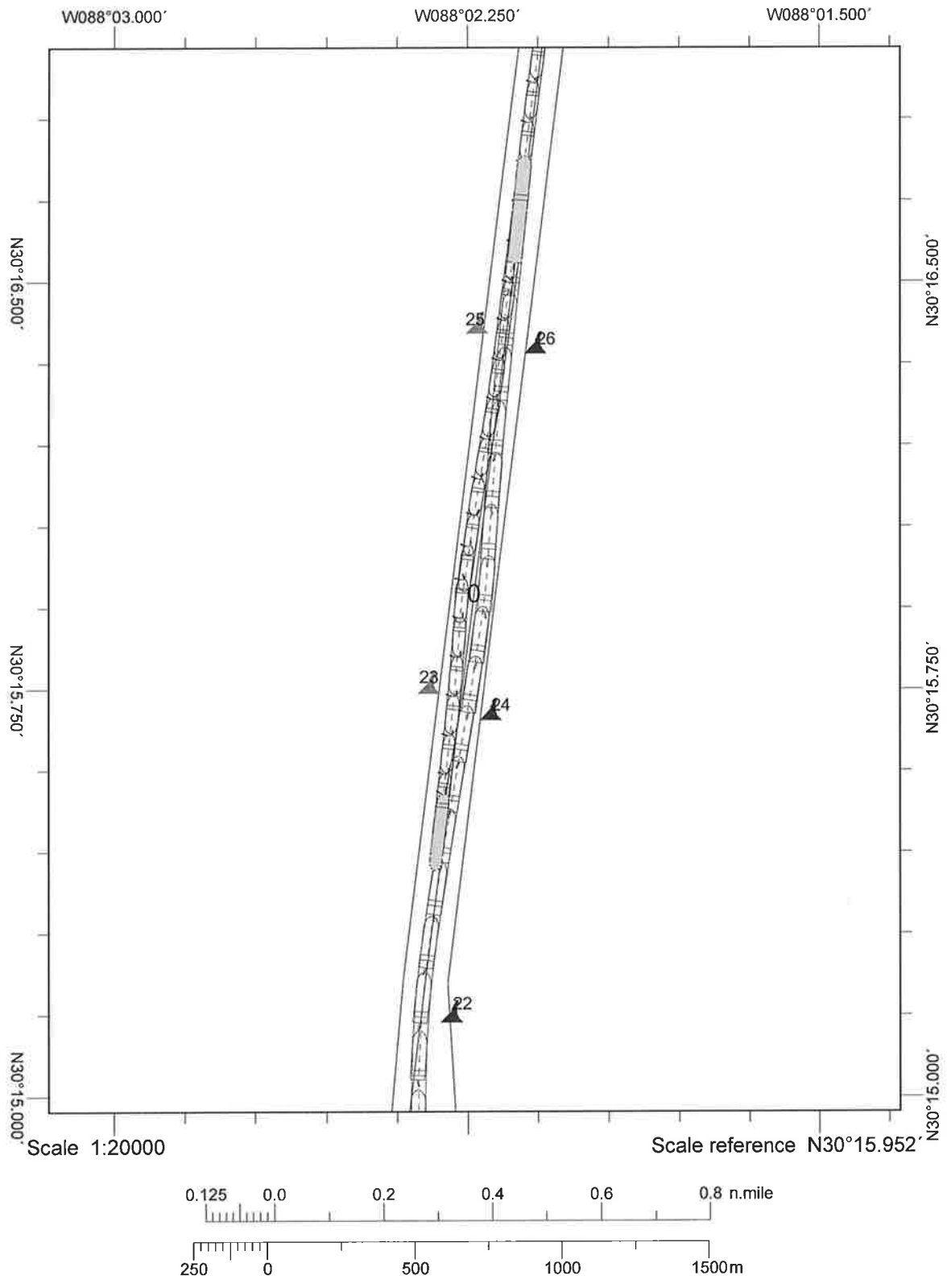

Line sample period (s)	30
Course marker every	00:30
Heading marker period (s)	30
Shape outline every	00:30

Mobile Bay Feasibility Simulations – Passing Lane / Bend Ease

Run #: 9 Date: 5/24/2017

Pilot:

1. Captain Chris Brock — Inbound X — Outbound ___ — Buoy Start 15 — Bridge B
2. Captain Curtis Wilson — Inbound ___ — Outbound X — Buoy Start 29 — Bridge A

Wind: 20 KNT — W — SE — Other: N

Currents: Flood(E wind) — Flood(W wind) — Flood(SE wind) — Ebb(E wind) — Ebb(W wind) — Other: Ebb N

Tide added: None — +~~0.7~~1.2m (Daniella 2 or MT Brittania) — Other: _____

Plan: P0 (Existing) — P1(500ft) — P2(550ft)

Vessel:

Pilot #	Model Name	Ship Name	LOA (ft)	Beam (ft)	Draft (ft)	LOA (m)	Beam (m)	Draft (m)
1, 2	CNTNR28L	Sovereign Maersk (SovMae)	1138.5	140.4	47.6	347.0	42.8	14.5
	CNTNR40	MSC Daniella 2 (Dan2)	1201.1	158.8	49.9	366.1	48.4	15.2
	CNTNR44	Zim Piraeus (Zim)	964.9	105.6	43.0	294.1	32.2	13.1
	CNTNR33L	Humber Bridge (HumB)	1102.4	150.3	46.2	336.0	45.8	14.1
	VLCC15L	MT Brittania (MTBrit)	859.6	137.8	49.2	262.0	42.0	15.0
	TANK23	Eagle Kanger (EagleK)	799.9	137.8	40.0	243.8	42.0	12.2

Naming convention - Plan_Area_IShipInbound_OShipoutbound_Currents_Wind_Repetition
(Ex:P0_PassingLane_IZim_ODan2_Flood_20E_1)

Filename: P1_PassLan_ISovMae_OSovMae_Ebb_20N_1

Comments: Passing went well, 500' channel gave sufficient room to pass safely.

Bow
107 ft

m.s
112 ft

stern
118 ft

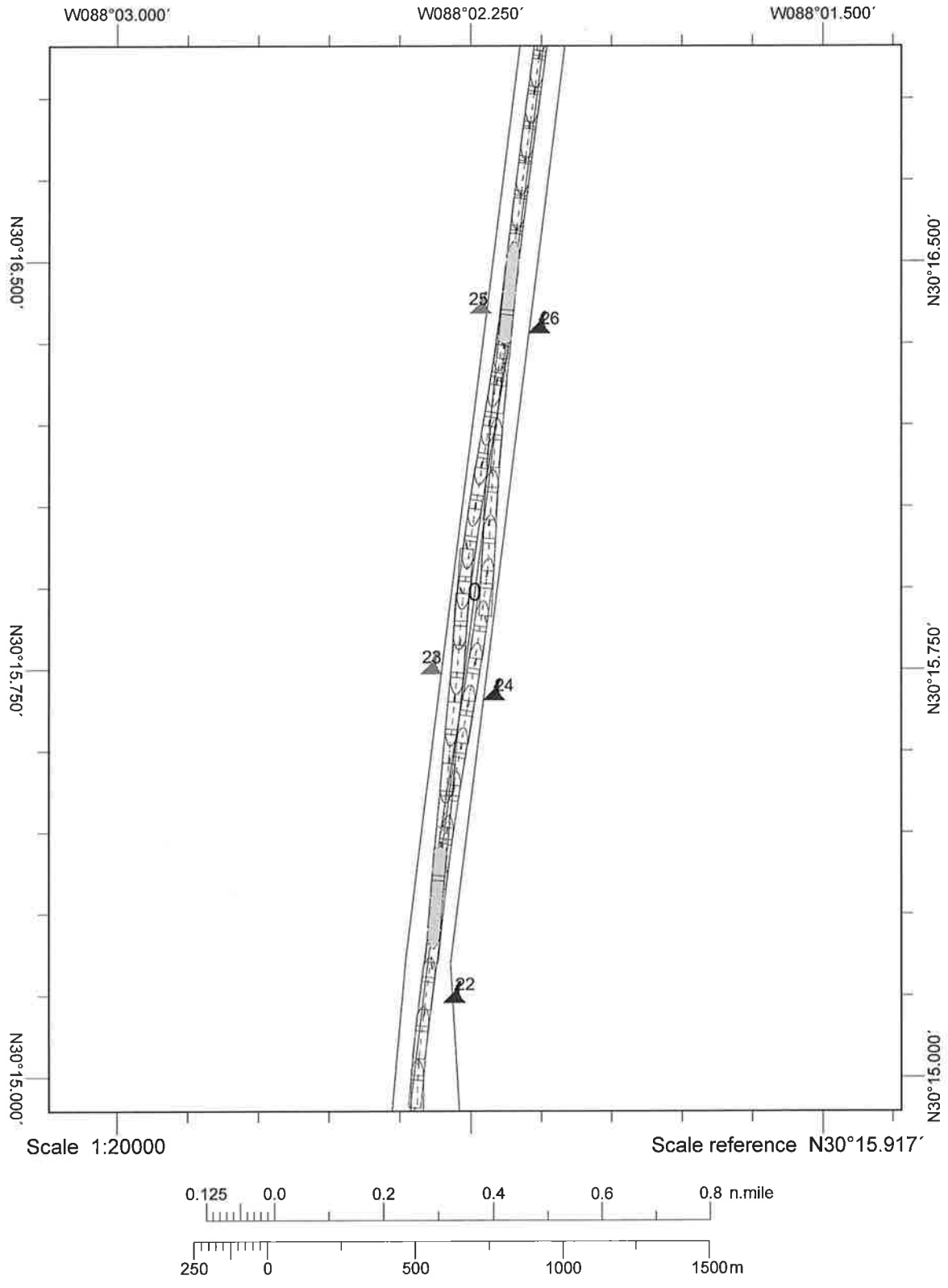

Line sample period (s)	30
Course marker every	00:30
Heading marker period (s)	30
Shape outline every	00:30

Mobile Bay Feasibility Simulations – Passing Lane / Bend Ease

Run #: 10 Date: 5/24/2017

Pilot:

1. Captain Chris Brock	Inbound X	Outbound___	Buoy Start 15	Bridge B
2. Captain Curtis Wilson	Inbound___	Outbound X	Buoy Start 29	Bridge A

Wind: 20 KNT (E)		W	SE		Other: _____
Currents: Flood(E wind)	Flood(W wind)	Flood(SE wind)	Ebb(E wind)	Ebb(W wind)	Other: _____
Tide added:	None	~~+0.7m~~ 1.2 (Daniella 2 or MT Brittania)			Other: _____
Plan:	P0 (Existing)	P1(500ft)	P2(550ft)		

Vessel:

Pilot #	Model Name	Ship Name	LOA (ft)	Beam (ft)	Draft (ft)	LOA (m)	Beam (m)	Draft (m)
2	CNTNR28L	Sovereign Maersk (SovMae)	1138.5	140.4	47.6	347.0	42.8	14.5
1	CNTNR40	MSC Daniella 2 (Dan2)	1201.1	158.8	49.9	366.1	48.4	15.2
	CNTNR44	Zim Piraeus (Zim)	964.9	105.6	43.0	294.1	32.2	13.1
	CNTNR33L	Humber Bridge (HumB)	1102.4	150.3	46.2	336.0	45.8	14.1
	VLCC15L	MT Brittania (MTBrit)	859.6	137.8	49.2	262.0	42.0	15.0
	TANK23	Eagle Kanger (EagleK)	799.9	137.8	40.0	243.8	42.0	12.2

Naming convention - Plan_Area_IShipInbound_OShipoutbound_Currents_Wind_Repetition
(Ex:P0_PassingLane_IZim_ODan2_Flood_20E_1)

Filename: P1-PassLan_I Dan2_O SovMae_Flood_20E_1

Comments: EXTREMELY TIGHT. DOABLE BUT DON'T WANT TO

Bow
140 ft
Mid
114 ft
Stern
105 ft

0924

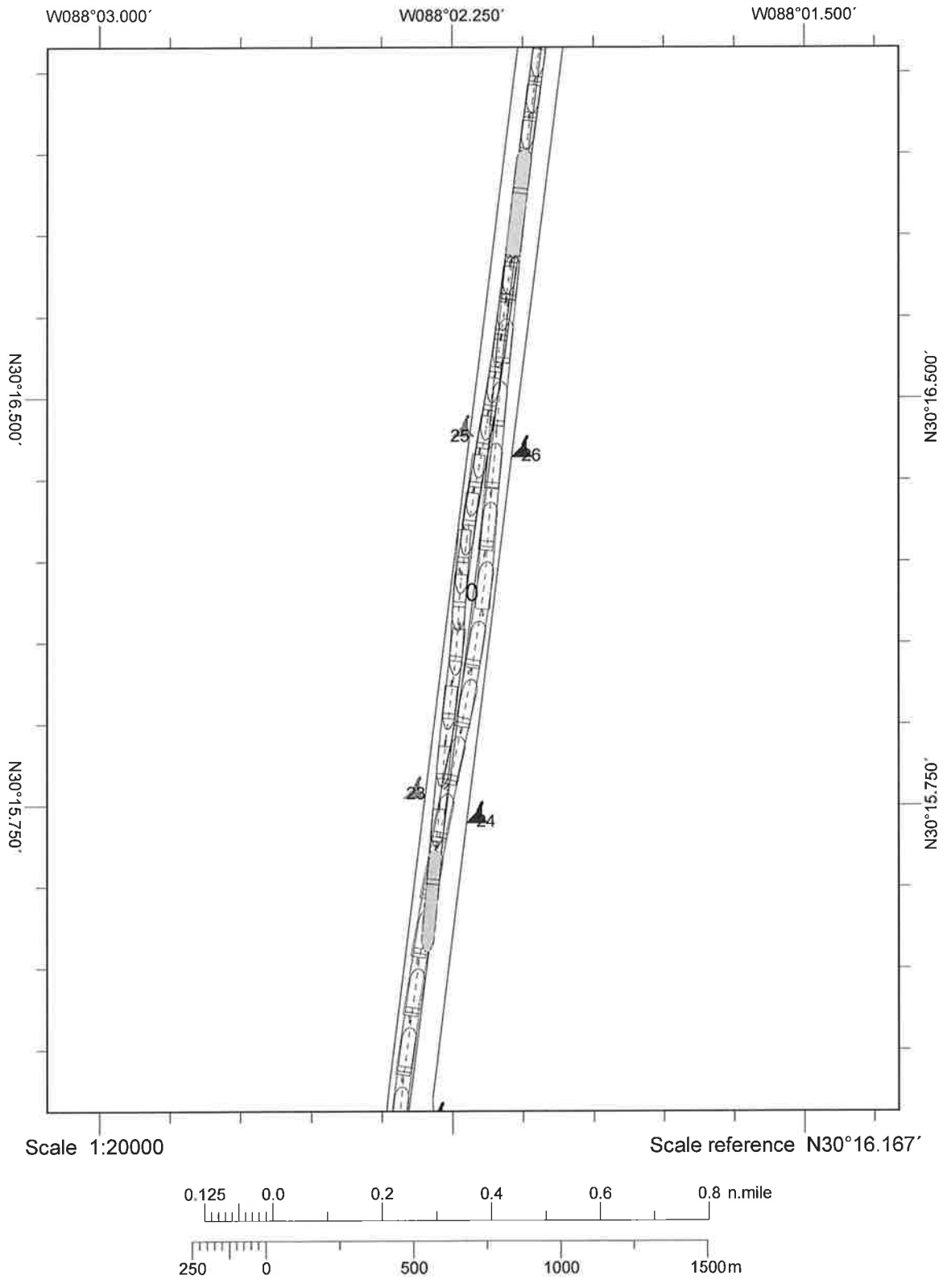

Line sample period (s)	30
Course marker every	00:30
Heading marker period (s)	30
Shape outline every	00:30

Mobile Bay Feasibility Simulations – Turning Basin

Run #: 13 Date: 5/25

Pilot:

1. Captain Chris Brock	Off Dock___	To Dock ✓	Bridge A
2. Captain Curtis Wilson	Off Dock___	To Dock___	Bridge___

Wind: 20 KNT N Other: _____

Currents: Ebb turning basin (north wind) Other: 7520

Tide added: None +0.7m (Daniella 2 or MT Britt) Other: _____

Plan: P0 (Existing) P1 or P2 (Deepened only -51 ft) Other: _____

Vessel:

Pilot #	Model Name	Ship Name	LOA (ft)	Beam (ft)	Draft (ft)	LOA (m)	Beam (m)	Draft (m)
	CNTNR28L	Sovereign Maersk (SovMae)	1138.5	140.4	47.6	347.0	42.8	14.5
	CNTNR40	MSC Daniella 2 (Dan2)	1201.1	158.8	49.9	366.1	48.4	15.2
1	CNTNR33L	Humber Bridge (HumB)	1102.4	150.3	46.2	336.0	45.8	14.1
	VLCC15L	MT Brittania (MTBrit)	859.6	137.8	49.2	262.0	42.0	15.0
	CNTNR20L	KMSS Dainty (Dainty)	964.9	105.7	41.0	294.1	32.2	12.5

Naming convention - Plan_Area_Transit_Shipname_Currents_Wind_PilotName_Repetition
(Ex:P0_TurningBasin_Offdock_SovMae_Ebb_20N_CWilson_1)

Filename: P1_TurningBasin_ToDock_HumB_ebb_20N_BRisk_2

Comments:

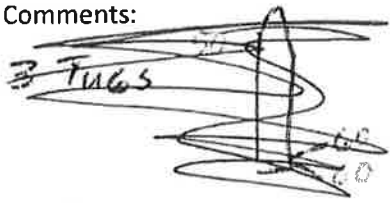

Start 0459
STOP 0513

DOABLE BUT SHIP AT SOUTH BERTH MAKES YOU GO MUCH FURTHER INTO BASIN THAN ACCUSTOMED TO. FALL ROOM WITH STRONG RIVER & WIND IS CONCERN.

RF 0453

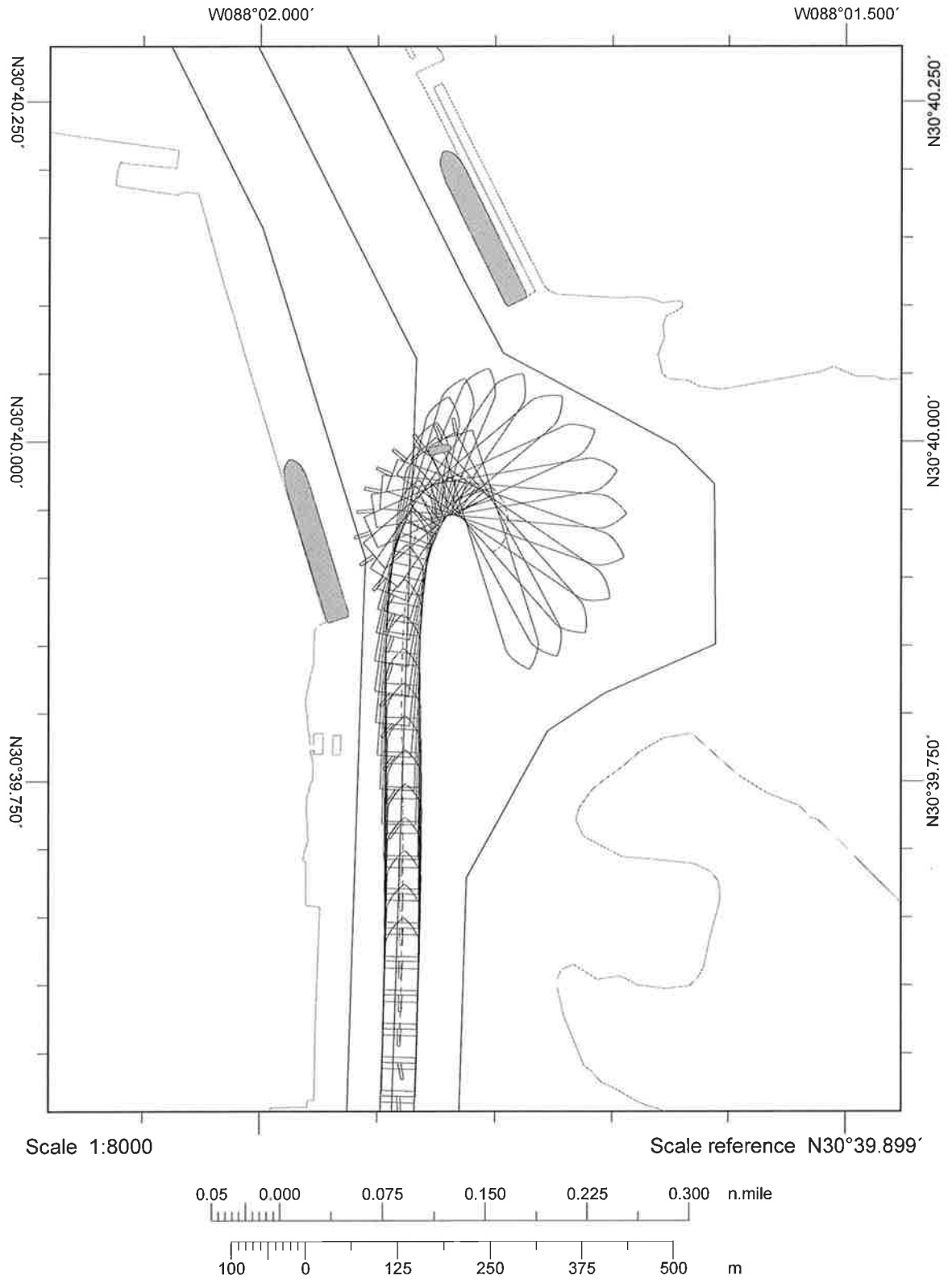

Line sample period (s)	30
Course marker every	00:30
Heading marker period (s)	30
Shape outline every	00:30

Mobile Bay Feasibility Simulations – Turning Basin

Run #: 14 Date: 5/25/2017

Pilot:

1. Captain Chris Brock	Off Dock___	To Dock___	Bridge___
2. Captain Curtis Wilson	Off Dock___	To Dock X	Bridge B

Wind: 20 KNT (N) Other: _____

Currents: Ebb turning basin (north wind) Other: 75%

Tide added: (None) +0.7m (Daniella 2 or MT Britt) Other: _____

Plan: P0 (Existing) (P1 or P2 (Deepened only -51 ft) Other: _____

Vessel:

Pilot #	Model Name	Ship Name	LOA (ft)	Beam (ft)	Draft (ft)	LOA (m)	Beam (m)	Draft (m)
	CNTNR28L	Sovereign Maersk (SovMae)	1138.5	140.4	47.6	347.0	42.8	14.5
	CNTNR40	MSC Daniella 2 (Dan2)	1201.1	158.8	49.9	366.1	48.4	15.2
2	CNTNR33L	Humber Bridge (HumB)	1102.4	150.3	46.2	336.0	45.8	14.1
	VLCC15L	MT Brittania (MTBrit)	859.6	137.8	49.2	262.0	42.0	15.0
	CNTNR20L	KMSS Dainty (Dainty)	964.9	105.7	41.0	294.1	32.2	12.5

Naming convention - Plan_Area_Transit_Shipname_Currents_Wind_PilotName_Repetition
(Ex:P0_TurningBasin_Offdock_SovMae_Ebb_20N_CWilson_1)

Filename: P1-Turning Basin_To Dock_HumB_Ebb_20N_Wilson_2

Comments:

~~[illegible]~~

This size vessel requires a very aggressive maneuver to get in proper position to turn with given environmentals. Turn executed effectively, but in manner + with speed that isn't practical in reality.

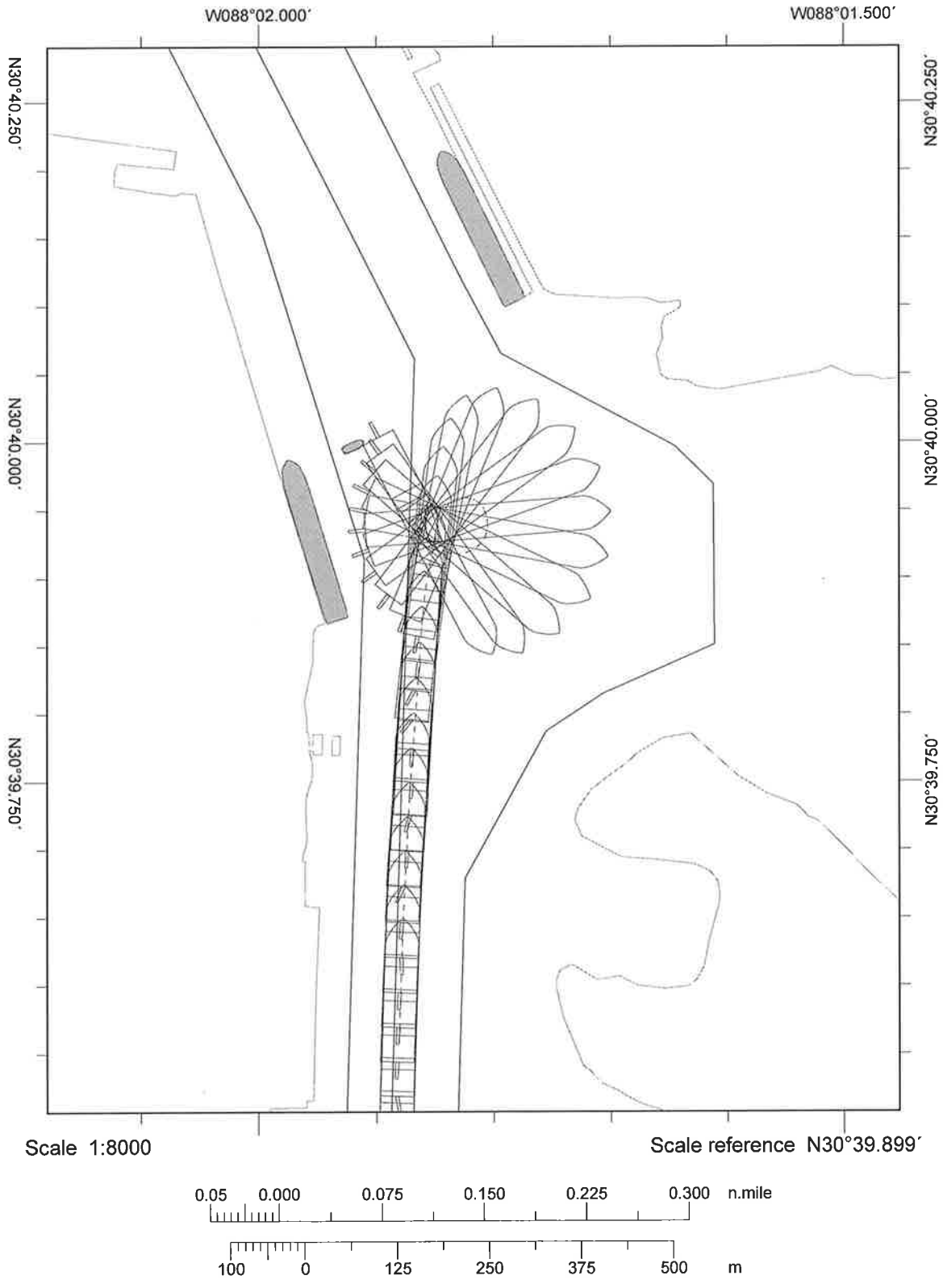

Line sample period (s)	30
Course marker every	00:30
Heading marker period (s)	30
Shape outline every	00:30

Mobile Bay Feasibility Simulations – Turning Basin

Run #: 15 Date: 5/25/17

Pilot:

1. Captain Chris Brock	Off Dock ✓	To Dock___	Bridge A
2. Captain Curtis Wilson	Off Dock___	To Dock___	Bridge___

Wind: (20 KNT N) Other: _____

Currents: (Ebb turning basin (north wind)) Other: 75%

Tide added: ✓ None (+0.7m (Daniella 2 or MT Britt)) Other: [redacted]

Plan: P0 (Existing) (P1 or P2 (Deepened only -51 ft)) Other: _____

Vessel:

Pilot #	Model Name	Ship Name	LOA (ft)	Beam (ft)	Draft (ft)	LOA (m)	Beam (m)	Draft (m)
	CNTNR28L	Sovereign Maersk (SovMae)	1138.5	140.4	47.6	347.0	42.8	14.5
	CNTNR40	MSC Daniella 2 (Dan2)	1201.1	158.8	49.9	366.1	48.4	15.2
1	CNTNR33L	Humber Bridge (HumB)	1102.4	150.3	46.2	336.0	45.8	14.1
	VLCC15L	MT Brittania (MTBrit)	859.6	137.8	49.2	262.0	42.0	15.0
	CNTNR20L	KMSS Dainty (Dainty)	964.9	105.7	41.0	294.1	32.2	12.5

Naming convention - Plan_Area_Transit_Shipname_Currents_Wind_PilotName_Repetition
(Ex:P0_TurningBasin_Offdock_SovMae_Ebb_20N_CWilson_1)

Filename: P1_TurningBasin_Offdock_HumB_Ebb_20N_BrockL1

Comments: STERN TUG WAS ABLE TO HOLD BUT NOT LIFT. FALLING DOWN ON ISLAND IS STILL CONCERN

Record File 0708

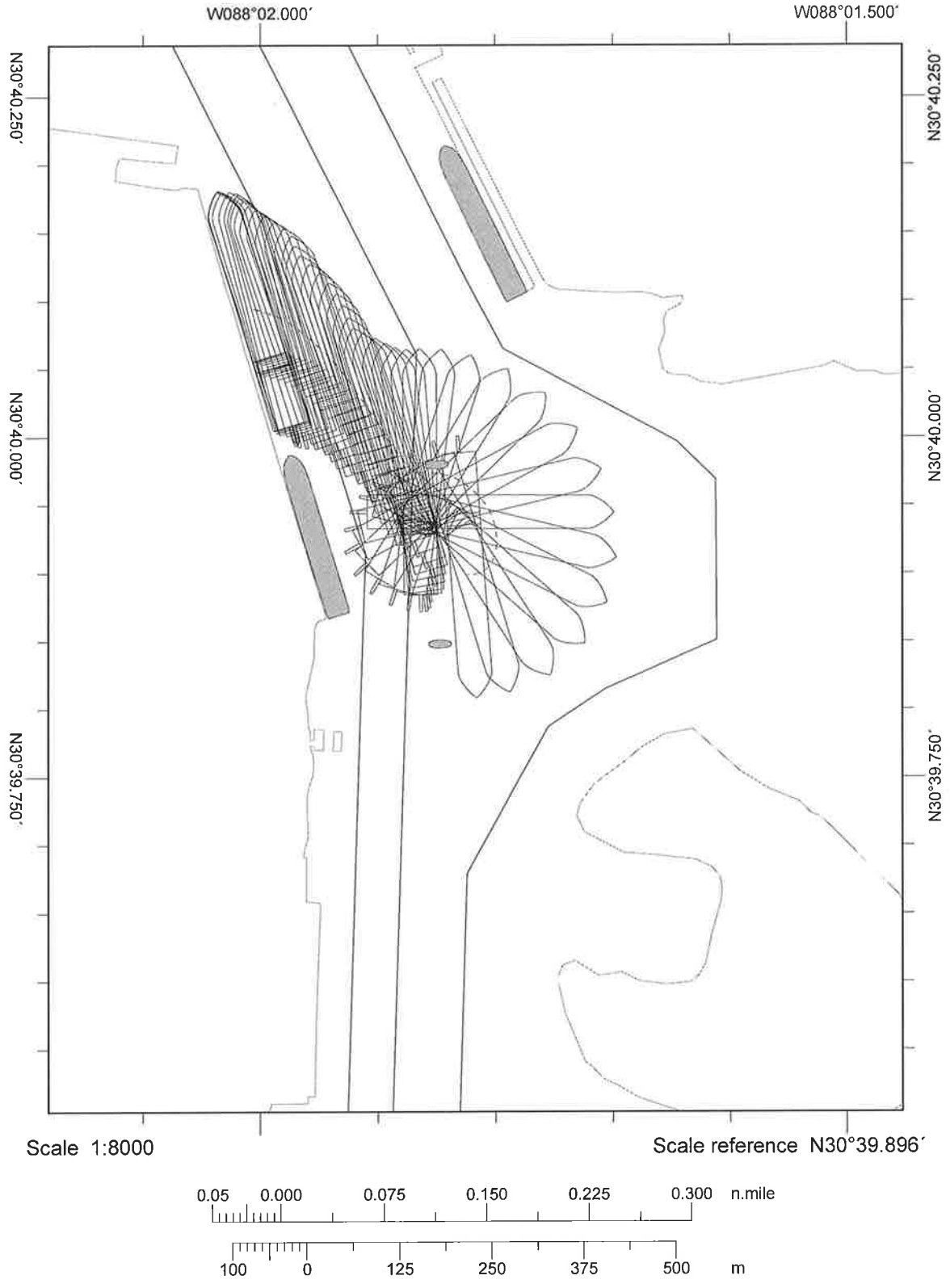

Line sample period (s)	30
Course marker every	00:30
Heading marker period (s)	30
Shape outline every	00:30

Mobile Bay Feasibility Simulations – Turning Basin

Run #: 16 Date: 5/25/17

Pilot:

1. Captain Chris Brock Off Dock___ To Dock___ Bridge___
2. Captain Curtis Wilson Off Dock✓ To Dock___ Bridge B

Wind: 20 KNT N Other: _____

Currents: Ebb turning basin (north wind) Other: 75%

Tide added: ~~None~~ +0.7 since dock +0.7m (Daniella 2 or MT Britt) Other: _____

Plan: P0 (Existing) P1 or P2 (Deepened only -51 ft) Other: _____

Vessel:

Pilot #	Model Name	Ship Name	LOA (ft)	Beam (ft)	Draft (ft)	LOA (m)	Beam (m)	Draft (m)
	CNTNR28L	Sovereign Maersk (SovMae)	1138.5	140.4	47.6	347.0	42.8	14.5
	CNTNR40	MSC Daniella 2 (Dan2)	1201.1	158.8	49.9	366.1	48.4	15.2
2	CNTNR33L	Humber Bridge (HumB)	1102.4	150.3	46.2	336.0	45.8	14.1
	VLCC15L	MT Brittania (MTBrit)	859.6	137.8	49.2	262.0	42.0	15.0
	CNTNR20L	KMSS Dainty (Dainty)	964.9	105.7	41.0	294.1	32.2	12.5

Naming convention - Plan_Area_Transit_Shipname_Currents_Wind_PilotName_Repetition
(Ex:P0_TurningBasin_Offdock_SovMae_Ebb_20N_CWilson_1)

Filename: P1_TurningBasin_Offdock_HumB_Ebb_20N_Wilson_1

Start: 0705

Comments:

Stern outside Channel
~120 ft Stern to docked ship

Ship handled well, current effected ship dramatically, bow Falling onto Little Sand Island greatest concern. No room to Fall South. unless perfect position + speed.

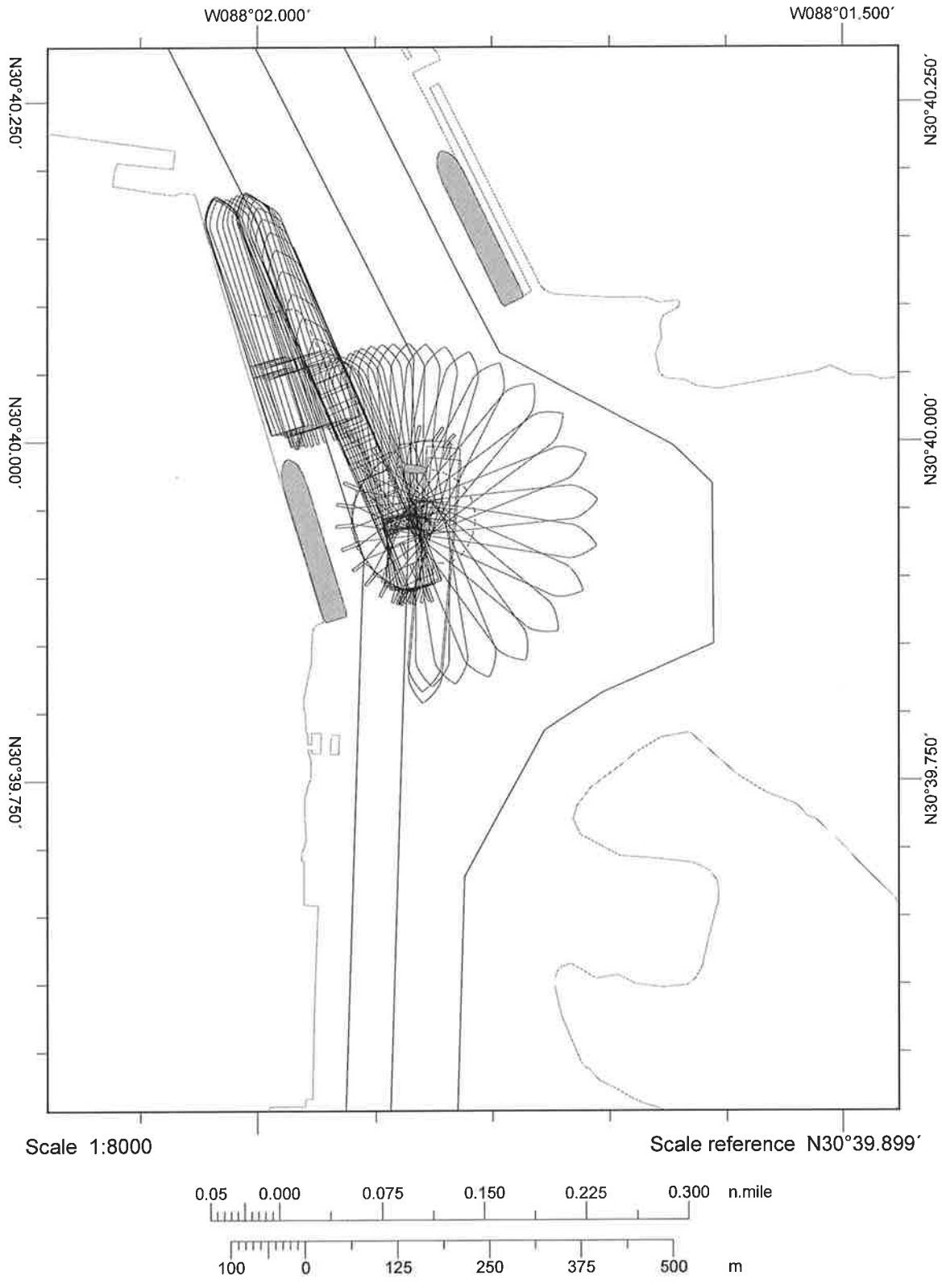

Line sample period (s)	30
Course marker every	00:30
Heading marker period (s)	30
Shape outline every	00:30

Mobile Bay Feasibility Simulations – Turning Basin

Run #: 17 Date: 25 MAY

Pilot:

1. Captain Chris Brock	Off Dock___	To Dock✓	Bridge A
2. Captain Curtis Wilson	Off Dock___	To Dock___	Bridge___

Wind: 20 KNT N Other: _____

Currents: Ebb turning basin (north wind) Other: 75 %

Tide added: None +0.7m (Daniella 2 or MT Britt) Other: _____

Plan: P0 (Existing) P1 or P2 (Deepened only -51 ft) Other: _____

Vessel:

Pilot #	Model Name	Ship Name	LOA (ft)	Beam (ft)	Draft (ft)	LOA (m)	Beam (m)	Draft (m)
	CNTNR28L	Sovereign Maersk (SovMae)	1138.5	140.4	47.6	347.0	42.8	14.5
1	CNTNR40	MSC Daniella 2 (Dan2)	1201.1	158.8	49.9	366.1	48.4	15.2
	CNTNR33L	Humber Bridge (HumB)	1102.4	150.3	46.2	336.0	45.8	14.1
	VLCC15L	MT Brittania (MTBrit)	859.6	137.8	49.2	262.0	42.0	15.0
	CNTNR20L	KMSS Dainty (Dainty)	964.9	105.7	41.0	294.1	32.2	12.5

Naming convention - Plan_Area_Transit_Shipname_Currents_Wind_PilotName_Repetition
(Ex:P0_TurningBasin_Offdock_SovMae_Ebb_20N_CWilson_1)

Filename: P1_TurningBasin_Todock_DAN2_ebb_20N_Brock_1

Comments: 3 Tugs

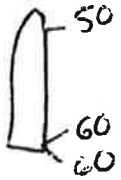

RF 0753

Grounded

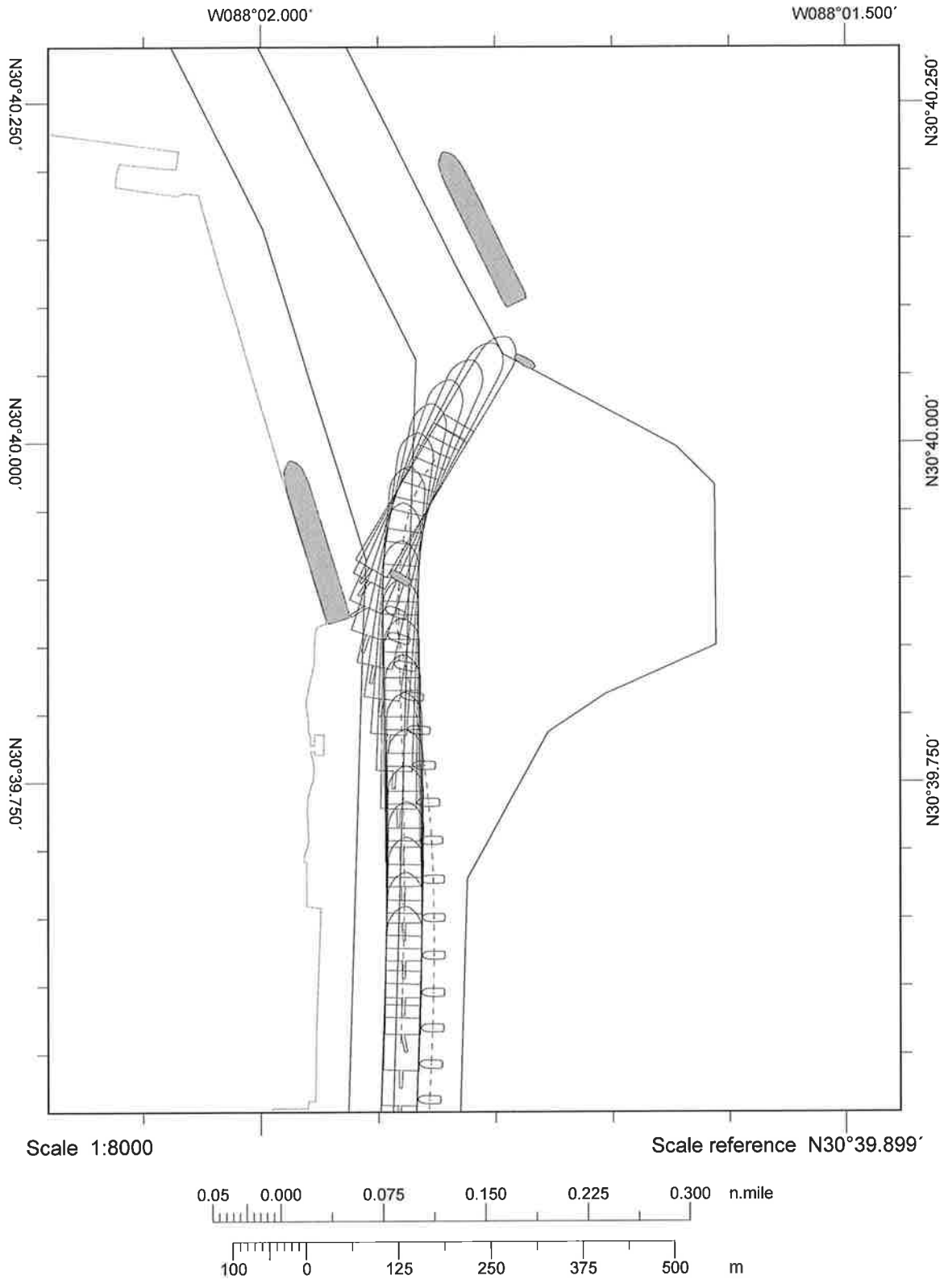

Line sample period (s)	30
Course marker every	00:30
Heading marker period (s)	30
Shape outline every	00:30

Mobile Bay Feasibility Simulations – Turning Basin

Run #: 18 Date: _____

Pilot:

1. Captain Chris Brock	Off Dock___	To Dock___	Bridge___
2. Captain Curtis Wilson	Off Dock___	To Dock ✓	Bridge B

Wind: 20 KNT N Other: _____

Currents: Ebb turning basin (north wind) Other: 75%

Tide added: None +1m +0.7m (Daniella 2 or MT Britt) Other: _____

Plan: P0 (Existing) P1 or P2 (Deepened only -51 ft) Other: _____

Vessel:

Pilot #	Model Name	Ship Name	LOA (ft)	Beam (ft)	Draft (ft)	LOA (m)	Beam (m)	Draft (m)
	CNTNR28L	Sovereign Maersk (SovMae)	1138.5	140.4	47.6	347.0	42.8	14.5
2	CNTNR40	MSC Daniella 2 (Dan2)	1201.1	158.8	49.9	366.1	48.4	15.2
	CNTNR33L	Humber Bridge (HumB)	1102.4	150.3	46.2	336.0	45.8	14.1
	VLCC15L	MT Brittania (MTBrit)	859.6	137.8	49.2	262.0	42.0	15.0
	CNTNR20L	KMSS Dainty (Dainty)	964.9	105.7	41.0	294.1	32.2	12.5

0749

Naming convention - Plan_Area_Transit_Shipname_Currents_Wind_PilotName_Repetition
(Ex:P0_TurningBasin_Offdock_SovMae_Ebb_20N_CWilson_1)

Filename: P1_TurningBasin_Todock_Dan2_Ebb_20N_CWilson_1

Comments: 2
3 tugs, 5t Qtr ~~stern~~ port bow
~100ft ~~Stern~~ to docked vessel, stern outside channel
Grounded on Southern end

Turn is not feasible in these environmental conditions, if two tugs cannot pick up the stern. Ship falls too far bodily to South, No room for bow on island.

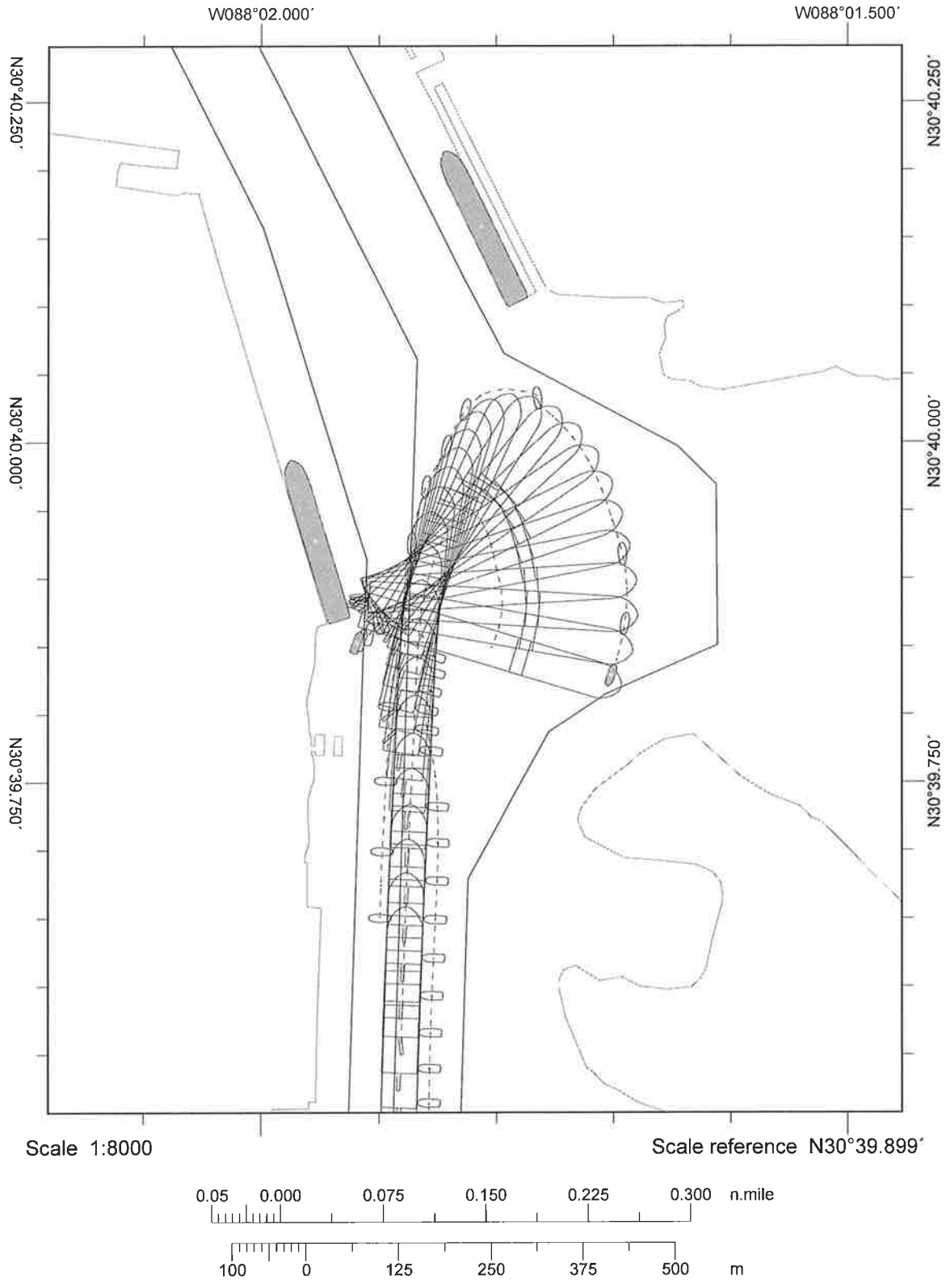

Line sample period (s)	30
Course marker every	00:30
Heading marker period (s)	30
Shape outline every	00:30

Mobile Bay Feasibility Simulations – Turning Basin

Run #: 19 Date: 25 May

Pilot:

1. Captain Chris Brock	Off Dock___	To Dock X	Bridge A
2. Captain Curtis Wilson	Off Dock___	To Dock___	Bridge___

Wind:	20 KNT	N	Other:_____
Currents:	Ebb turning basin (north wind)		Other: 75%
Tide added:	None	+0.7m (Daniella 2 or MT Britt)	Other:_____
Plan:	P0 (Existing)	P1 or P2 (Deepened only -51 ft)	Other:_____

Vessel:

Pilot #	Model Name	Ship Name	LOA (ft)	Beam (ft)	Draft (ft)	LOA (m)	Beam (m)	Draft (m)
	CNTNR28L	Sovereign Maersk (SovMae)	1138.5	140.4	47.6	347.0	42.8	14.5
	CNTNR40	MSC Daniella 2 (Dan2)	1201.1	158.8	49.9	366.1	48.4	15.2
1	CNTNR33L	Humber Bridge (HumB)	1102.4	150.3	46.2	336.0	45.8	14.1
	VLCC15L	MT Brittania (MTBrit)	859.6	137.8	49.2	262.0	42.0	15.0
	CNTNR20L	KMSS Dainty (Dainty)	964.9	105.7	41.0	294.1	32.2	12.5

Naming convention - Plan_Area_Transit_Shipname_Currents_Wind_PilotName_Repetition
(Ex:P0_TurningBasin_Offdock_SovMae_Ebb_20N_CWilson_1)

Filename: P1_TurningBasin_ToDock_HumB_Ebb_20N_Brock_3

Comments:

3 Tugs

RF 0834

Speed of turn with 3 tugs was not much different than with 2. I used furthest most edge of basin to to north to start turn. Putting bow too far in basin to east is worrisome in fact that you may not get ship out of the basin before fetching up on island.

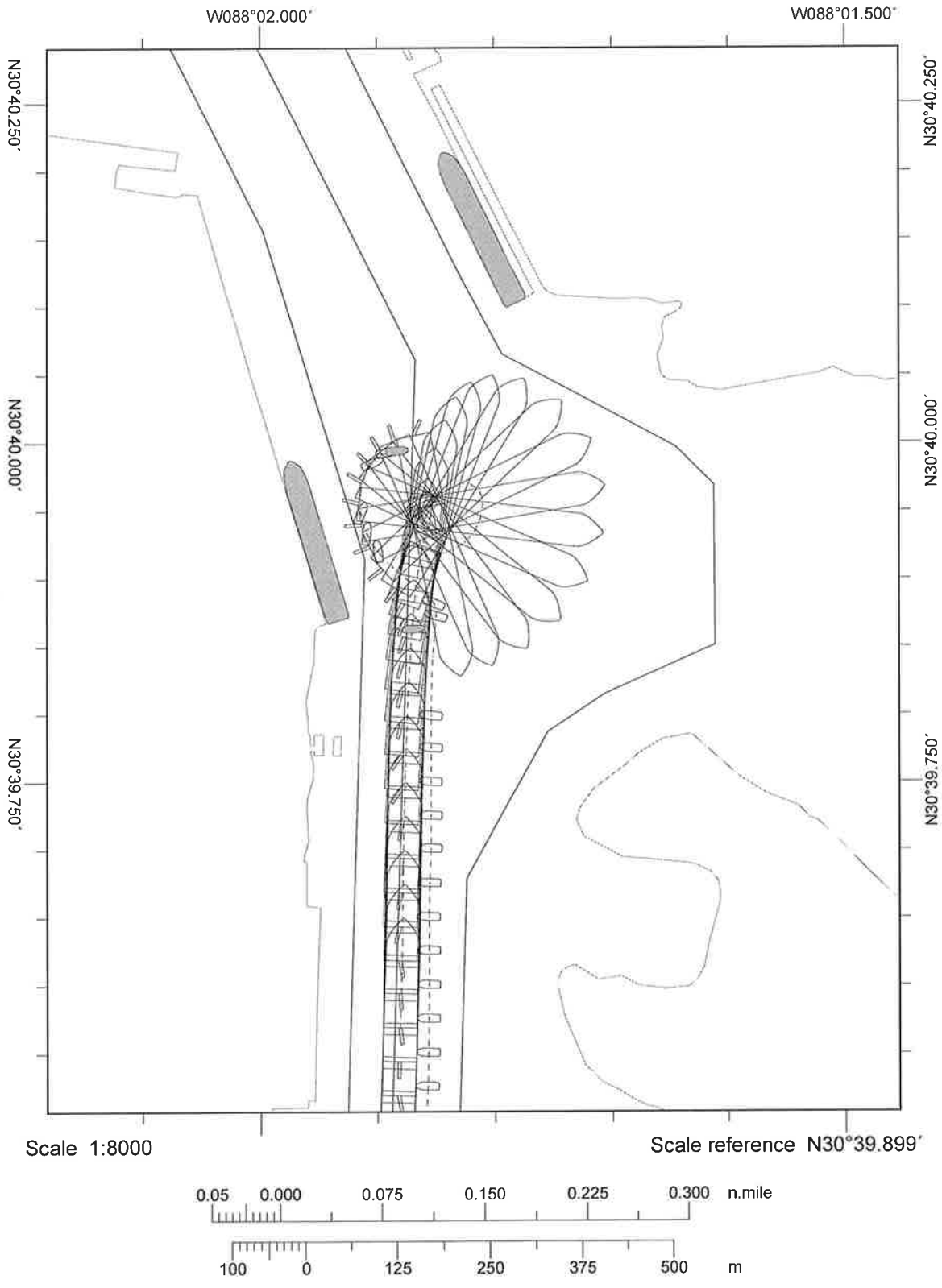

Line sample period (s)	30
Course marker every	00:30
Heading marker period (s)	30
Shape outline every	00:30

Mobile Bay Feasibility Simulations – Turning Basin

Run #: 20 Date: _____

Pilot:

1. Captain Chris Brock	Off Dock___	To Dock___	Bridge___
2. Captain Curtis Wilson	Off Dock___	To Dock ✓	Bridge B

Wind: 20 KNT N Other: _____

Currents: Ebb turning basin (north wind) Other: 75%e

Tide added: None +0.7m (Daniella 2 or MT Britt) Other: _____

Plan: P0 (Existing) P1 or P2 (Deepened only -51 ft) Other: _____

Vessel:

Pilot #	Model Name	Ship Name	LOA (ft)	Beam (ft)	Draft (ft)	LOA (m)	Beam (m)	Draft (m)
	CNTNR28L	Sovereign Maersk (SovMae)	1138.5	140.4	47.6	347.0	42.8	14.5
	CNTNR40	MSC Daniella 2 (Dan2)	1201.1	158.8	49.9	366.1	48.4	15.2
2	CNTNR33L	Humber Bridge (HumB)	1102.4	150.3	46.2	336.0	45.8	14.1
	VLCC15L	MT Brittania (MTBrit)	859.6	137.8	49.2	262.0	42.0	15.0
	CNTNR20L	KMSS Dainty (Dainty)	964.9	105.7	41.0	294.1	32.2	12.5

Naming convention - Plan_Area_Transit_Shipname_Currents_Wind_PilotName_Repetition
(Ex:P0_TurningBasin_Offdock_SovMae_Ebb_20N_CWilson_1)

830

Filename: P1_TurningBasin_Todock_Humb_Ebb_20N_Wilson_3

Comments:

3 tugs, 50 ton Pt Bow, 260 ton St Qtr

Deliberate attempt to commit bow as far east into basin as possible ~~within~~ + back ship out with strong environmental conditions. Executed on simulator with very aggressive operation. Very unrealistic due to excessive speed + reliability on tug / ship's engine perfect operation. Extreme East side of basin unusable in these environmental conditions.

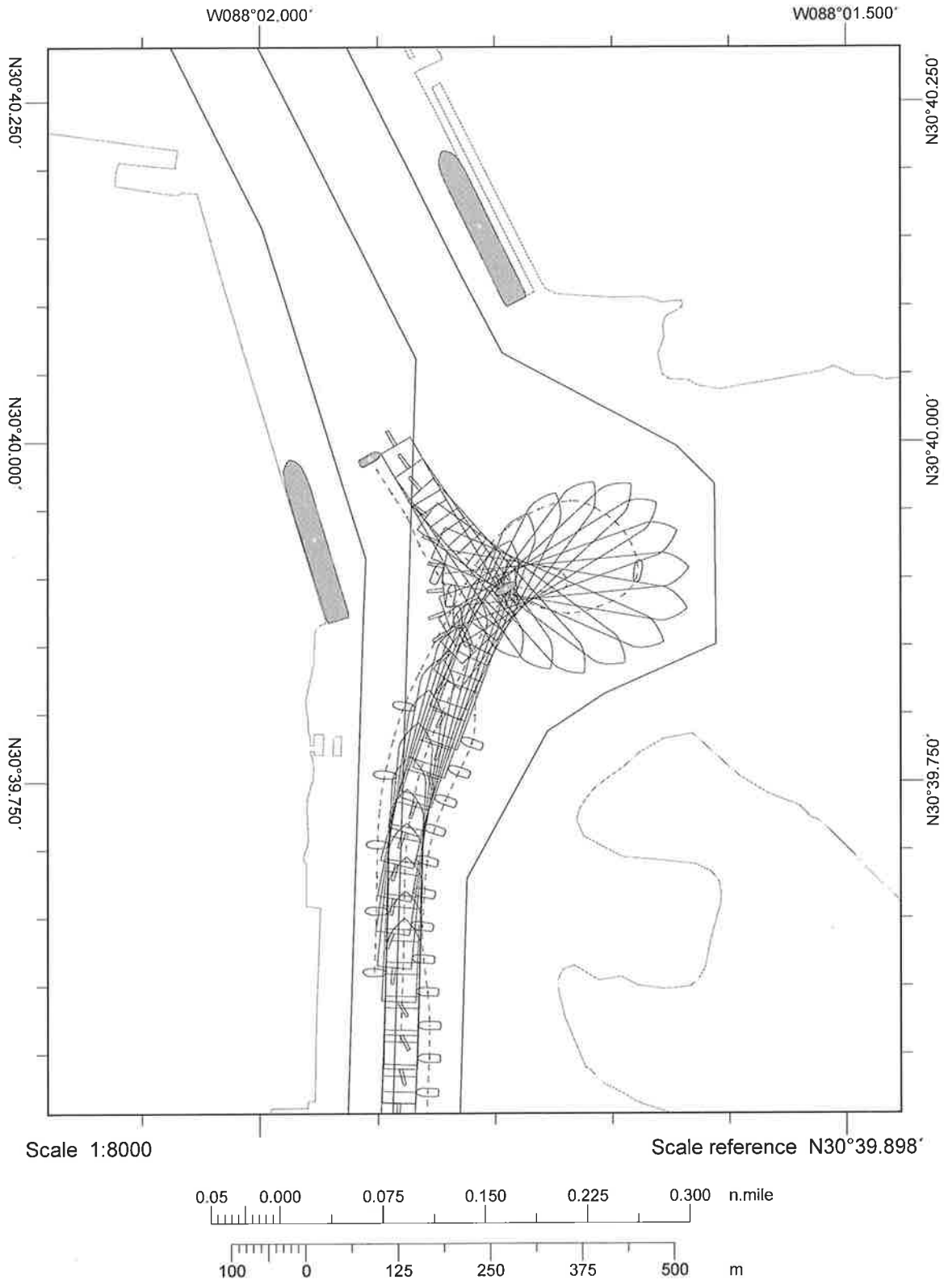

Line sample period (s)	30
Course marker every	00:30
Heading marker period (s)	30
Shape outline every	00:30

Mobile Bay Feasibility Simulations – Turning Basin

Run #: 21 Date: _____

Pilot:

1. Captain Chris Brock	Off Dock___	To Dock ✓	Bridge A
2. Captain Curtis Wilson	Off Dock___	To Dock___	Bridge___

Wind: 20 KNT N Other: _____

Currents: Ebb turning basin (north wind) Other: _____

Tide added: None +0.7m (Daniella 2 or MT Britt) Other: FLAT BOTTOM

Plan: P0 (Existing) P1 or P2 (Deepened only -51 ft) Other: _____

Vessel:

Pilot #	Model Name	Ship Name	LOA (ft)	Beam (ft)	Draft (ft)	LOA (m)	Beam (m)	Draft (m)
	CNTNR28L	Sovereign Maersk (SovMae)	1138.5	140.4	47.6	347.0	42.8	14.5
	CNTNR40	MSC Daniella 2 (Dan2)	1201.1	158.8	49.9	366.1	48.4	15.2
	CNTNR33L	Humber Bridge (HumB)	1102.4	150.3	46.2	336.0	45.8	14.1
	VLCC15L	MT Brittania (MTBrit)	859.6	137.8	49.2	262.0	42.0	15.0
	CNTNR20L	KMSS Dainty (Dainty)	964.9	105.7	41.0	294.1	32.2	12.5

Naming convention - Plan_Area_Transit_Shipname_Currents_Wind_PilotName_Repetition
(Ex:P0_TurningBasin_Offdock_SovMae_Ebb_20N_CWilson_1)

Filename: P1_TurningBasin_Todock_HumB_ebb_20N_Brock_FB

Comments:

3 Tugs

RF 0857

BACKING FULL FOR BOW TO CLEAR ISLAND. GROUNDING IS CONCERN WITH STRONG CURRENT AND WIND CLEARANCE IS UNSAFE IN MY OPINION

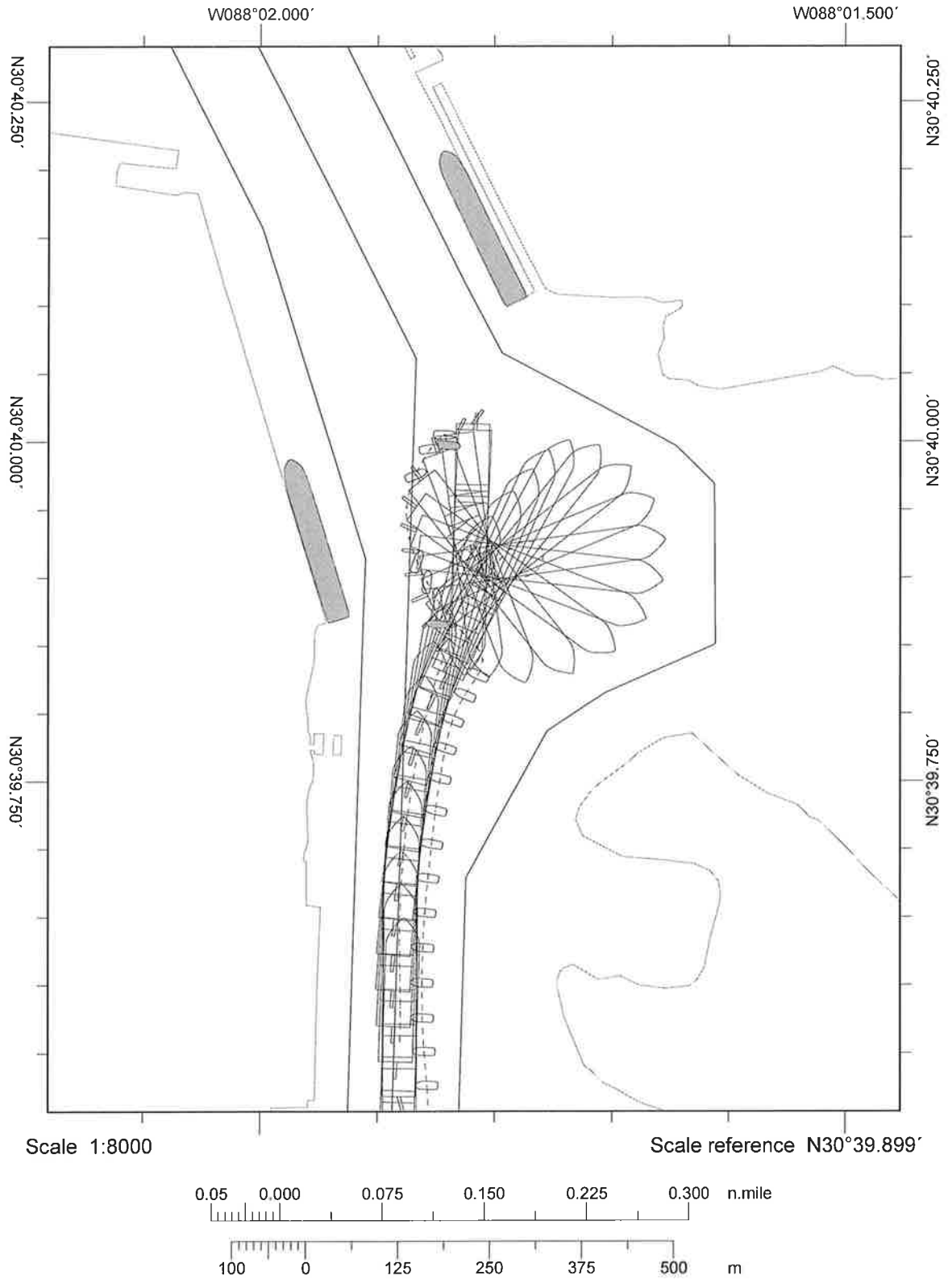

Line sample period (s)	30
Course marker every	00:30
Heading marker period (s)	30
Shape outline every	00:30

Mobile Bay Feasibility Simulations – Turning Basin

Run #: 22 Date: 25 May 2017

Pilot:

1. Captain Chris Brock	Off Dock___	To Dock #	Bridge___
2. Captain Curtis Wilson	Off Dock___	To Dock √	Bridge B

Wind: 20 KNT N Other: _____

Currents: Ebb turning basin (north wind) Other: _____

Tide added: None +0.7m (Daniella 2 or MT Britt) Other: Flat bottom

Plan: P0 (Existing) P1 or P2 (Deepened only -51 ft) Other: _____

Vessel:

Pilot #	Model Name	Ship Name	LOA (ft)	Beam (ft)	Draft (ft)	LOA (m)	Beam (m)	Draft (m)
	CNTNR28L	Sovereign Maersk (SovMae)	1138.5	140.4	47.6	347.0	42.8	14.5
	CNTNR40	MSC Daniella 2 (Dan2)	1201.1	158.8	49.9	366.1	48.4	15.2
2	CNTNR33L	Humber Bridge (HumB)	1102.4	150.3	46.2	336.0	45.8	14.1
	VLCC15L	MT Brittania (MTBrit)	859.6	137.8	49.2	262.0	42.0	15.0
	CNTNR20L	KMSS Dainty (Dainty)	964.9	105.7	41.0	294.1	32.2	12.5

Naming convention - Plan_Area_Transit_Shipname_Currents_Wind_PilotName_Repetition
(Ex:P0_TurningBasin_Offdock_SovMae_Ebb_20N_CWilson_1)

Filename: P1_TurningBasin_Todock_HumB_ebb_20N_Wilson_flat_bottom

Comments: 3 tugs and flat bottom, 51 ft

Executed turn using as much basin area as possible. Maneuver went well, but conclusion is that the execution of this turn is unrealistic due to absolute commitment into the basin with no emergency recourse. Doable on simulator, would never attempt with this ship in reality.

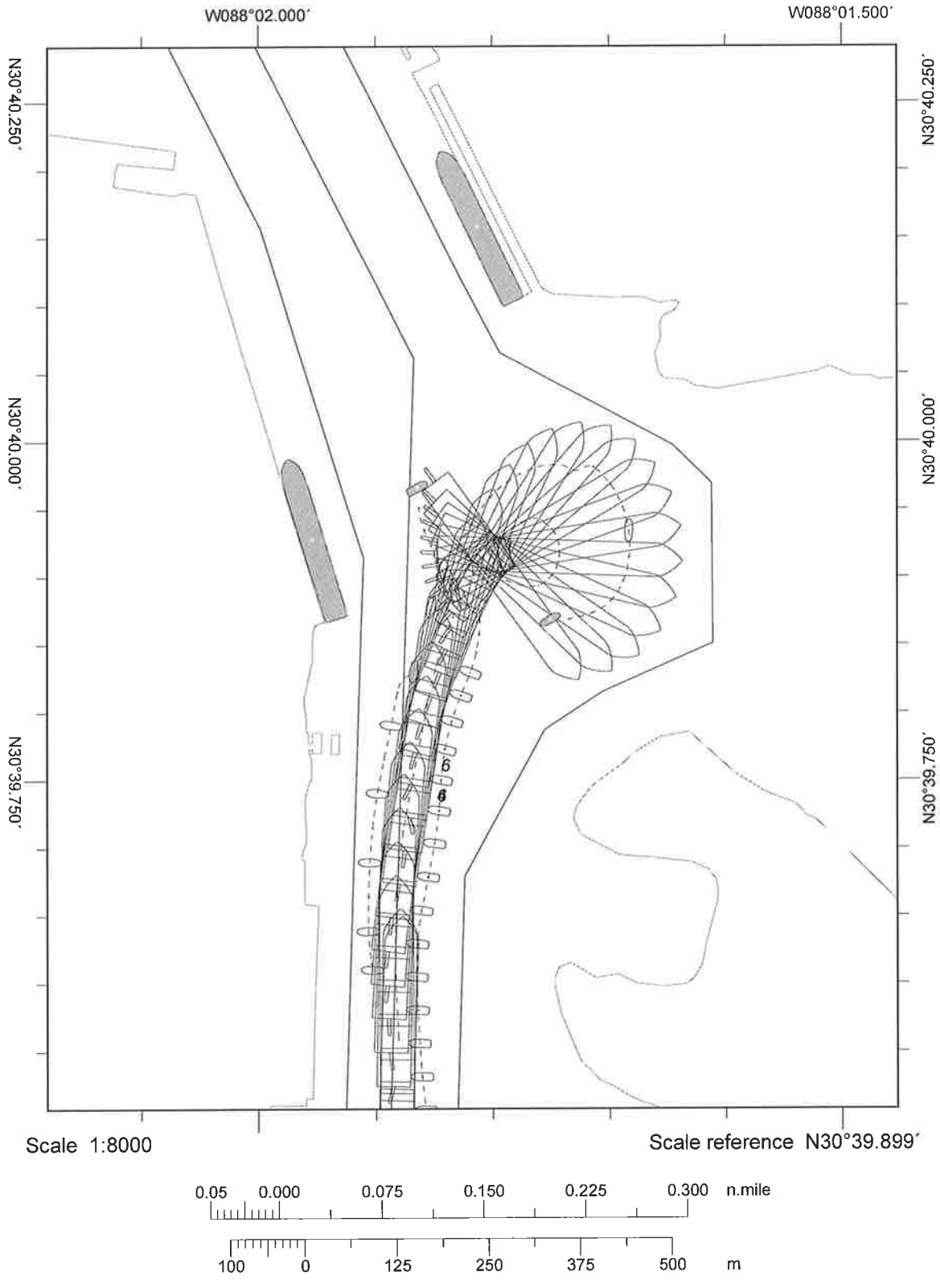

Line sample period (s)	30
Course marker every	00:30
Heading marker period (s)	30
Shape outline every	00:30

Mobile Bay Feasibility Simulations – Passing Lane / Bend Ease

Run #: 23 Date: 25 May

Pilot:
1. Captain Chris Brock — Inbound ___ Outbound O Buoy Start 29 Bridge A
2. Captain Curtis Wilson — Inbound I Outbound ___ Buoy Start ~~27~~ 15 Bridge B

Wind: (20 KNT) E W (SE) Other: ___

Currents: Flood(E wind) Flood(W wind) (Flood(SE wind)) Ebb(E wind) Ebb(W wind) Other: ___

Tide added: None +0.7m (Daniella 2 or MT Brittania) Other: 1.2 m

Plan: P0 (Existing) P1(500ft) (P2(550ft))

Vessel:

Pilot #	Model Name	Ship Name	LOA (ft)	Beam (ft)	Draft (ft)	LOA (m)	Beam (m)	Draft (m)
	CNTNR28L	Sovereign Maersk (SovMae)	1138.5	140.4	47.6	347.0	42.8	14.5
	CNTNR40	MSC Daniella 2 (Dan2) O	1201.1	158.8	49.9	366.1	48.4	15.2
	CNTNR44	Zim Piraeus (Zim)	964.9	105.6	43.0	294.1	32.2	13.1
	CNTNR33L	Humber Bridge (HumB)	1102.4	150.3	46.2	336.0	45.8	14.1
	VLCC15L	MT Brittania (MTBrit) I	859.6	137.8	49.2	262.0	42.0	15.0
	TANK23	Eagle Kanger (EagleK)	799.9	137.8	40.0	243.8	42.0	12.2

Naming convention - Plan_Area_IShipInbound_OShipoutbound_Currents_Wind_Repetition
(Ex:P0_PassingLane_IZim_ODan2_Flood_20E_1)

Filename: P2_PassLan_ODan2_IMTBrit_Flood_20SE_1

Comments: 550' channel was comfortable to pass in. Adequate room b/t vessels while also not feeling too much bank effect.

RF 10:05

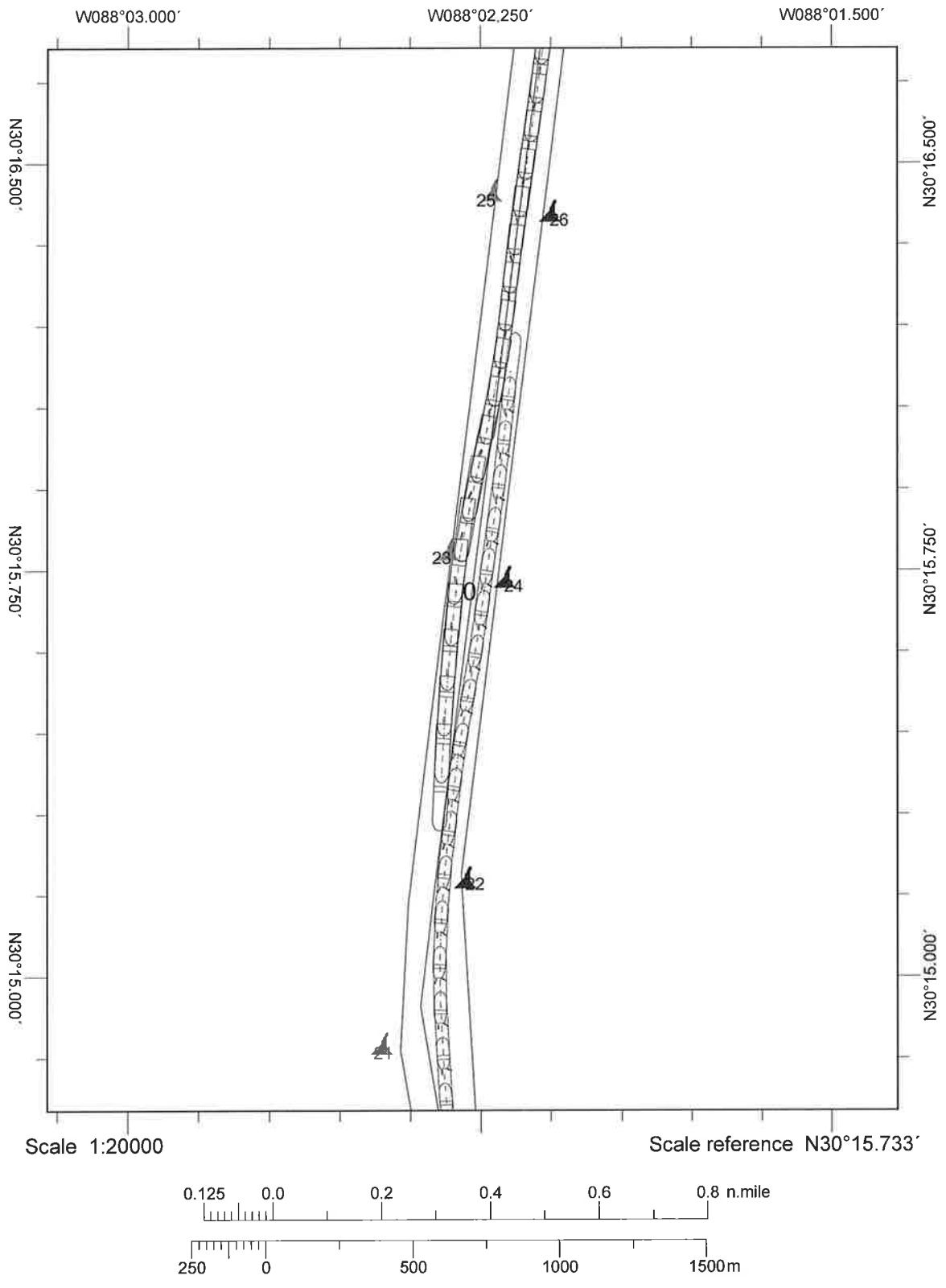

Line sample period (s)	30
Course marker every	00:30
Heading marker period (s)	30
Shape outline every	00:30

Mobile Bay Feasibility Simulations – Passing Lane / Bend Ease

Run #: 24 Date: 25 MAY

Pilot:
1. Captain Chris Brock — Inbound ___ Outbound ✓ Buoy Start 29 Bridge A
2. Captain Curtis Wilson — Inbound ✓ Outbound ___ Buoy Start 15 Bridge B

Wind: (20 KNT) E W (SE) Other: _____

Currents: Flood(E wind) Flood(W wind) (Flood(SE wind)) Ebb(E wind) Ebb(W wind) Other: _____

Tide added: None (1.2 +0.7m (Daniella 2 or MT Brittania)) Other: _____

Plan: P0 (Existing) P1(500ft) (P2(550ft))

Vessel:

Pilot #	Model Name	Ship Name	LOA (ft)	Beam (ft)	Draft (ft)	LOA (m)	Beam (m)	Draft (m)
1	CNTNR28L	Sovereign Maersk (SovMae)	1138.5	140.4	47.6	347.0	42.8	14.5
2	CNTNR40	MSC Daniella 2 (Dan2)	1201.1	158.8	49.9	366.1	48.4	15.2
	CNTNR44	Zim Piraeus (Zim)	964.9	105.6	43.0	294.1	32.2	13.1
	CNTNR33L	Humber Bridge (HumB)	1102.4	150.3	46.2	336.0	45.8	14.1
	VLCC15L	MT Brittania (MTBrit)	859.6	137.8	49.2	262.0	42.0	15.0
	TANK23	Eagle Kanger (EagleK)	799.9	137.8	40.0	243.8	42.0	12.2

Naming convention - Plan_Area_IShipInbound_OShipoutbound_Currents_Wind_Repetition
(Ex:P0_PassingLane_IZim_ODan2_Flood_20E_1)

Filename: P2_PassingLane_OSovMae_IDan2_Flood_20SE_1

Comments: 160' between ships during passing

550' channel was needed, inbound ship very sluggish response, outbound vessel needed extra width to clear safely. 500' channel would have been very tight.

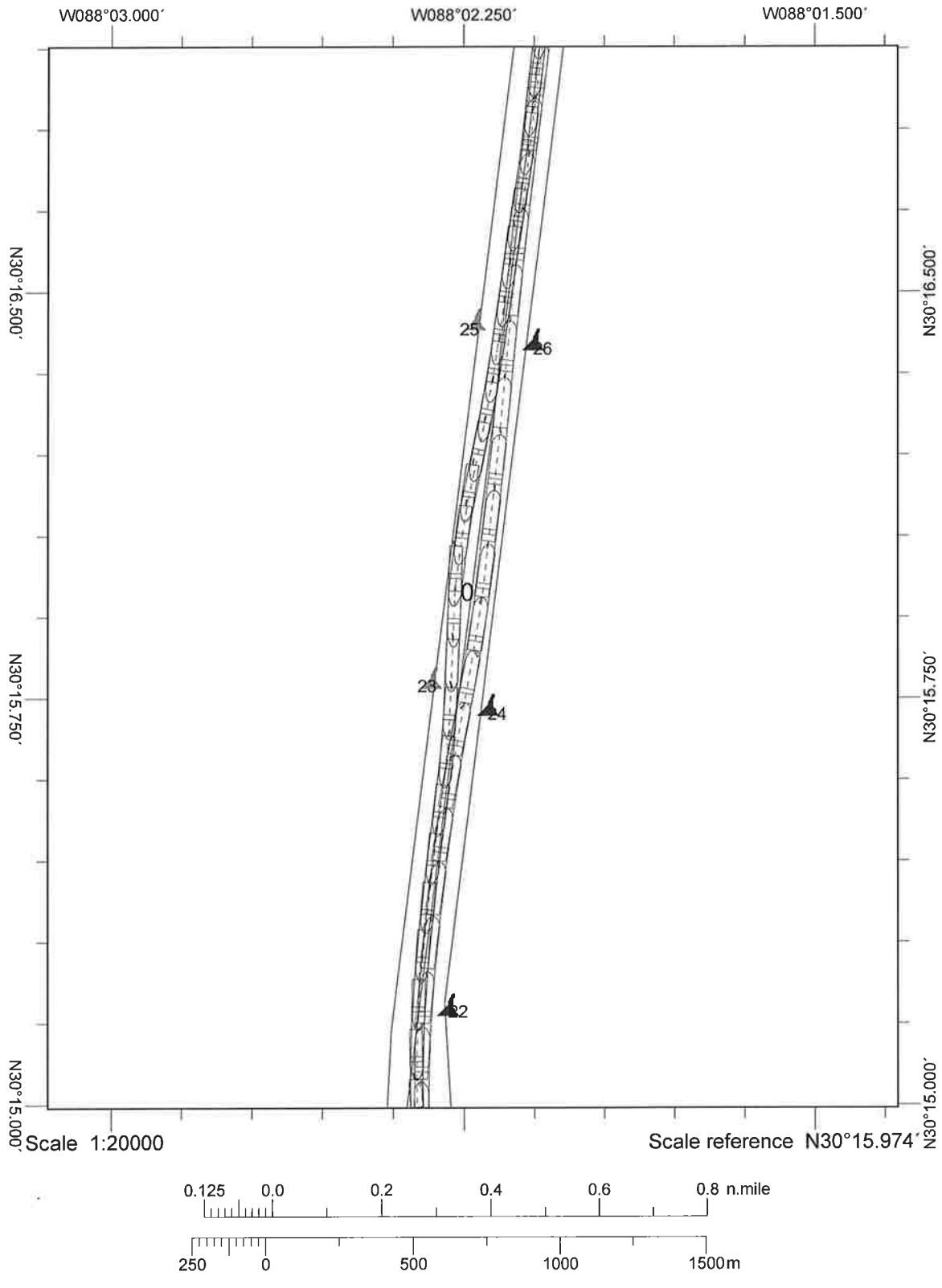

Line sample period (s)	30
Course marker every	00:30
Heading marker period (s)	30
Shape outline every	00:30

Mobile Bay Feasibility Simulations – Turning Basin

Run #: 25 Date: 26 MAY

Pilot:

1. Captain Chris Brock	Off Dock___	To Dock___	Bridge___
2. Captain Curtis Wilson	Off Dock___	To Dock✓	Bridge B

Wind: (20 KNT N) Other: _____

Currents: (Ebb turning basin (north wind)) Other: 75%

Tide added: (None) +0.7m (Daniella 2 or MT Britt) Other: _____

Plan: P0 (Existing) (P1 or P2 (Deepened only -51 ft)) Other: Flat Bottom w/ increased TB dimension

Vessel:

Pilot #	Model Name	Ship Name	LOA (ft)	Beam (ft)	Draft (ft)	LOA (m)	Beam (m)	Draft (m)
	CNTNR28L	Sovereign Maersk (SovMae)	1138.5	140.4	47.6	347.0	42.8	14.5
	CNTNR40	MSC Daniella 2 (Dan2)	1201.1	158.8	49.9	366.1	48.4	15.2
2	CNTNR33L	Humber Bridge (HumB)	1102.4	150.3	46.2	336.0	45.8	14.1
	VLCC15L	MT Brittania (MTBrit)	859.6	137.8	49.2	262.0	42.0	15.0
	CNTNR20L	KMSS Dainty (Dainty)	964.9	105.7	41.0	294.1	32.2	12.5

Naming convention - Plan_Area_Transit_Shipname_Currents_Wind_PilotName_Repetition
(Ex:P0_TurningBasin_Offdock_SovMae_Ebb_20N_CWilson_1)

Filename: P2_TurningBasin_Todock_~~Humber bridge~~ HumB_Ebb_20N_Wilson_1

Comments: Bow

Plot ship deep into turn basin. Approached with bow high to North. Had to use both tug boats on quarter Full ahead + continuously backed ship between slow + half astern. Relying on the ships engine working astern that long greatly increases risk as bow drops south to Little Sand Island.

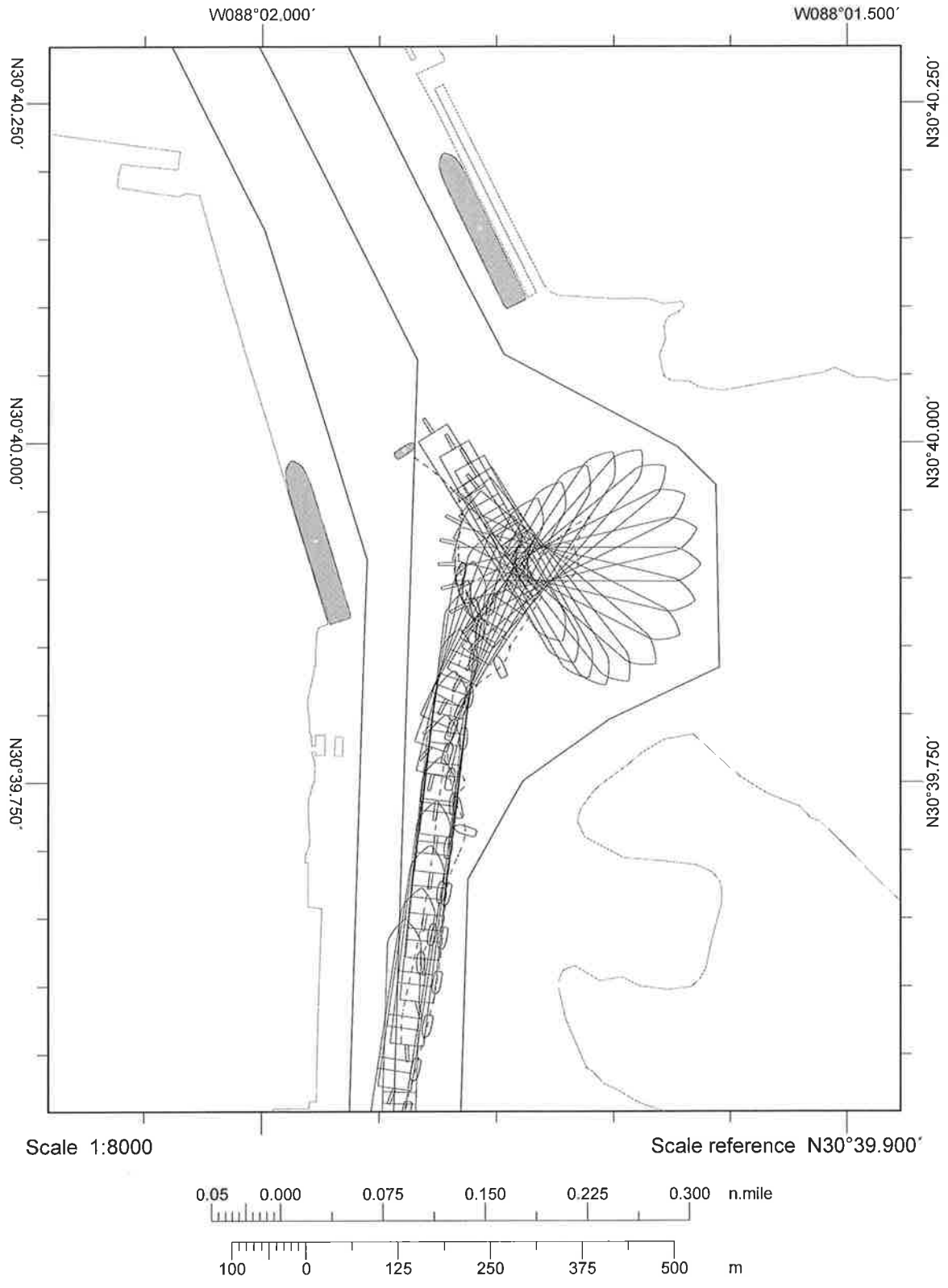

Line sample period (s)	30
Course marker every	00:30
Heading marker period (s)	30
Shape outline every	00:30

Mobile Bay Feasibility Simulations – Passing Lane / Bend Ease

Run #: 26 Date: 26 May 2017

Pilot:

1. Captain Chris Brock	Inbound 2	Outbound___	Buoy Start___	Bridge___	
2. Captain Curtis Wilson	Inbound ✓	Outbound___	Buoy Start___	Bridge 3	

Wind: (20 KNT)	E	W	(SE)		Other:_____
Currents: Flood(E wind)	Flood(W wind)	(Flood(SE wind))	Ebb(E wind)	Ebb(W wind)	Other:_____
Tide added:	None	+0.7m (Daniella 2 or MT Brittania)			Other: 2m
Plan:	(P0 (Existing))	P1(500ft)	P2(550ft)		

Vessel:

Pilot #	Model Name	Ship Name	LOA (ft)	Beam (ft)	Draft (ft)	LOA (m)	Beam (m)	Draft (m)
	CNTNR28L	Sovereign Maersk (SovMae)	1138.5	140.4	47.6	347.0	42.8	14.5
2	CNTNR40	MSC Daniella 2 (Dan2)	1201.1	158.8	49.9	366.1	48.4	15.2
	CNTNR44	Zim Piraeus (Zim)	964.9	105.6	43.0	294.1	32.2	13.1
3	CNTNR33L	Humber Bridge (HumB)	1102.4	150.3	46.2	336.0	45.8	14.1
	VLCC15L	MT Brittania (MTBrit)	859.6	137.8	49.2	262.0	42.0	15.0
	TANK23	Eagle Kanger (EagleK)	799.9	137.8	40.0	243.8	42.0	12.2

Naming convention - Plan_Area_IShipInbound_OShipoutbound_Currents_Wind_Repetition
(Ex:P0_PassingLane_IZim_ODan2_Flood_20E_1)

Filename: P0_OneWay_IDan2_Flood_20SE_CWilson_1

Comments: Very large ship with sluggish steering. Required hard over rudder several times, especially making bend into 400' channel. Pretty narrow.

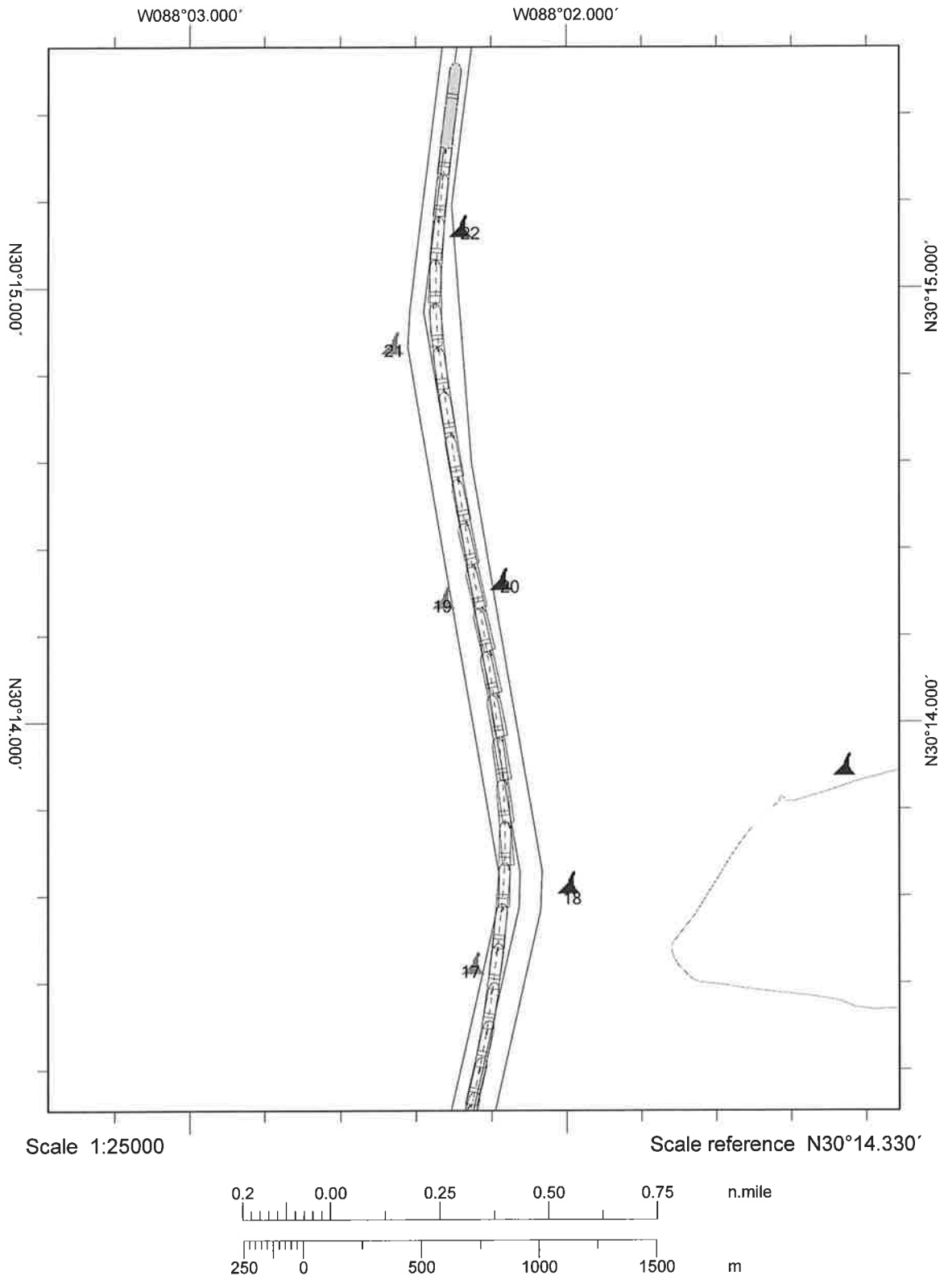

Line sample period (s)	30
Course marker every	00:30
Heading marker period (s)	30
Shape outline every	00:30

Mobile Bay Feasibility Simulations – Turning Basin

Run #: 26 Date: 26 MAY

Pilot:
1. Captain Chris Brock Off Dock ✓ To Dock___ Bridge A
2. Captain Curtis Wilson Off Dock___ To Dock___ Bridge___

Wind: (20 KNT N) Other:___

Currents: (Ebb turning basin (north wind)) Other: 75%

Tide added: (None) +0.7m (Daniella 2 or MT Britt) Other:___

Plan: P0 (Existing) (P1 or P2 (Deepened only -51 ft)) Other: Flatbottom, new turning basin lines

Vessel:

Pilot #	Model Name	Ship Name	LOA (ft)	Beam (ft)	Draft (ft)	LOA (m)	Beam (m)	Draft (m)
	CNTNR28L	Sovereign Maersk (SovMae)	1138.5	140.4	47.6	347.0	42.8	14.5
	CNTNR40	MSC Daniella 2 (Dan2)	1201.1	158.8	49.9	366.1	48.4	15.2
1	CNTNR33L	Humber Bridge (HumB)	1102.4	150.3	46.2	336.0	45.8	14.1
	VLCC15L	MT Brittania (MTBrit)	859.6	137.8	49.2	262.0	42.0	15.0
	CNTNR20L	KMSS Dainty (Dainty)	964.9	105.7	41.0	294.1	32.2	12.5

Naming convention - Plan_Area_Transit_Shipname_Currents_Wind_PilotName_Repetition
(Ex:P0_TurningBasin_Offdock_SovMae_Ebb_20N_CWilson_1)

Filename: P2_TurningBasin_offdock_Humb_Ebb_20N_Brock_1

Comments: WAS ABLE TO GIVE MYSELF SAFE CLEARANCE ON SHIP AT SOUTH BERTH WITH POST PANAMAX (RF 0153) CRANES OUTREACHED. STILL ISSUE OF GETTING DEEP INTO BASIN IS HAVING TO BACK FULL ON THE SHIP TO TRY AND MAINTAIN MIDDLE AND NOT GROUND ON THE ISLAND.

* within 39 ft of new turning basin lines.

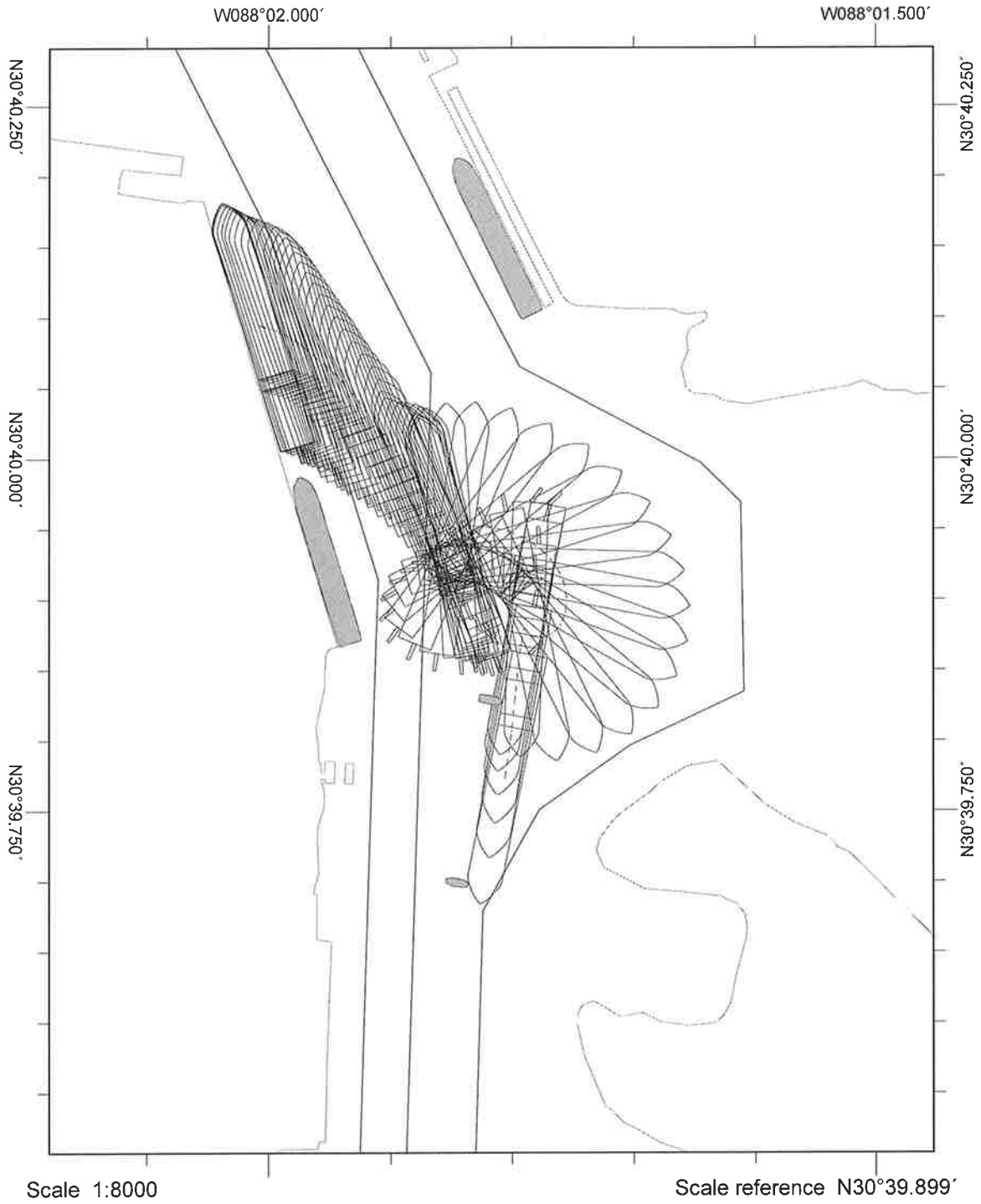

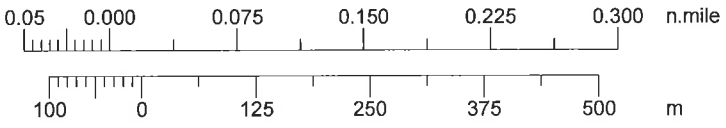

Line sample period (s)	30
Course marker every	00:30
Heading marker period (s)	30
Shape outline every	00:30

Mobile Bay Feasibility Simulations – Turning Basin

Run #: 27

Date: 26 May 2017

Pilot:

1. Captain Chris Brock — Off Dock___ — To Dock X — Bridge A
2. Captain Curtis Wilson — Off Dock___ — To Dock___ — Bridge___

Wind: (20 KNT) (N) — Other:_____

Currents: (Ebb) turning basin (north wind) — Other:_____

Tide added: None — +0.7m (Daniella 2 or MT Britt) — Other: Flat Bottom 15.5m

Plan: P0 (Existing) — P1 or (P2) (Deepened only -51 ft) — Other:_____

Vessel:

Pilot #	Model Name	Ship Name	LOA (ft)	Beam (ft)	Draft (ft)	LOA (m)	Beam (m)	Draft (m)
	CNTNR28L	Sovereign Maersk (SovMae)	1138.5	140.4	47.6	347.0	42.8	14.5
	CNTNR40	MSC Daniella 2 (Dan2)	1201.1	158.8	49.9	366.1	48.4	15.2
	CNTNR33L	Humber Bridge (HumB)	1102.4	150.3	46.2	336.0	45.8	14.1
	VLCC15L	MT Brittania (MTBrit)	859.6	137.8	49.2	262.0	42.0	15.0
	CNTNR20L	KMSS Dainty (Dainty)	964.9	105.7	41.0	294.1	32.2	12.5

Naming convention - Plan_Area_Transit_Shipname_Currents_Wind_PilotName_Repetition
(Ex:P0_TurningBasin_Offdock_SovMae_Ebb_20N_CWilson_1)

Filename: P2_TurningBasin_ToDock_HumB_Ebb_20N_CBrock_2

Comments:

Extended turning basin

WAS ABLE TO GIVE PLENTY OF CLEARANCE OFF CONTAINER TERMINAL. ACTUALLY USED FEDERAL BASIN. WITH THESE CONDITIONS I'M STILL HAVING TO BACK SHIP FULL TO STAY OFF OF SAND ISLAND.

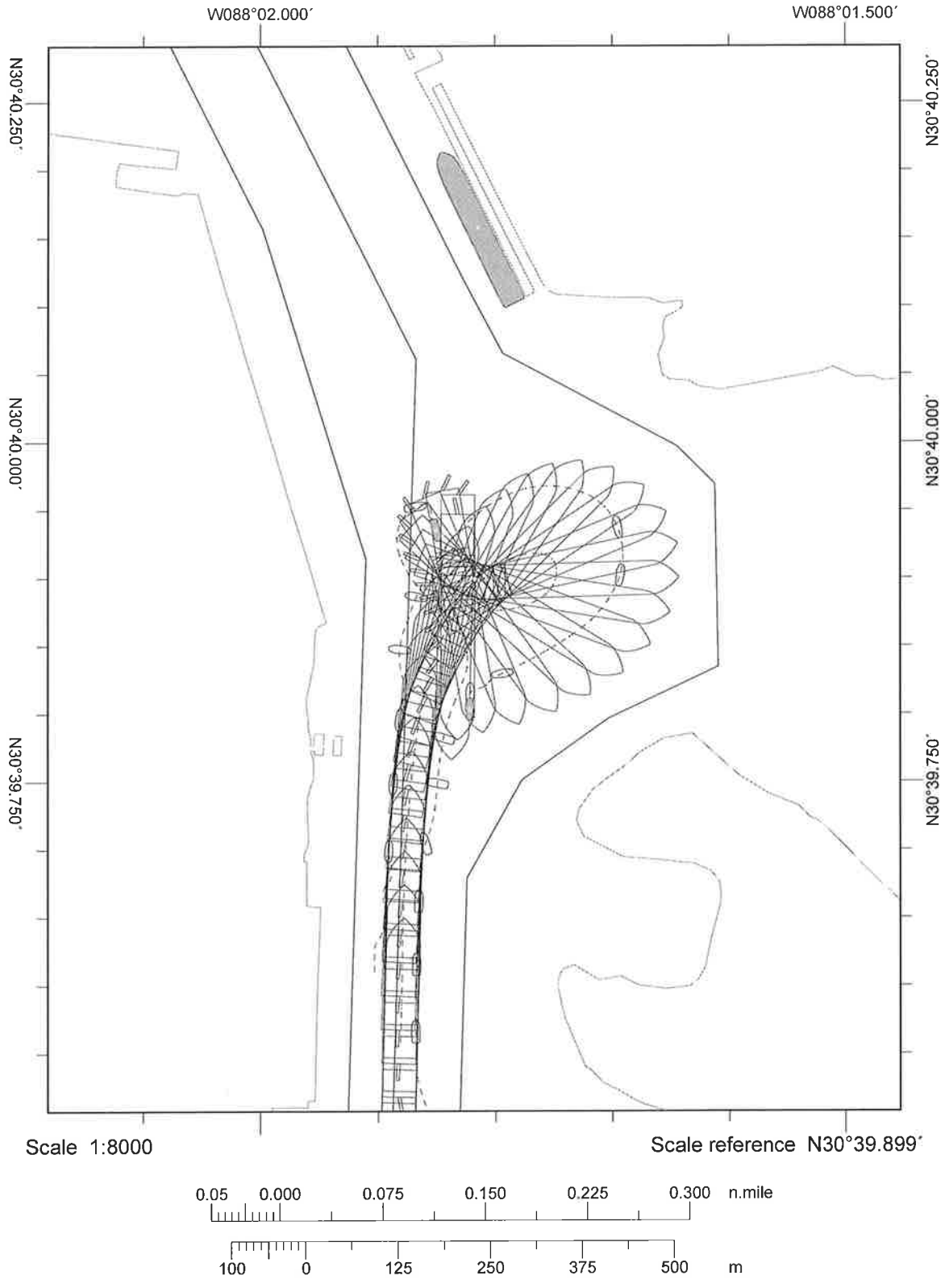

Line sample period (s)	30
Course marker every	00:30
Heading marker period (s)	30
Shape outline every	00:30

Mobile Bay Feasibility Simulations – Turning Basin

Run #: 28

Date: 26 May 2017

Pilot:

1. Captain Chris Brock — Off Dock___ — To Dock___ — Bridge___
2. Captain Curtis Wilson — Off Dock ✓ — To Dock___ — Bridge B

Wind: 20 KNT N — Other: _____

Currents: Ebb turning basin (north wind) — Other: +75%

Tide added: None — +0.7m (Daniella 2 or MT Britt) — Other: flat-bottom

Plan: P0 (Existing) — P1 or P2 (Deepened only -51 ft) — Other: _____

Vessel:

Pilot #	Model Name	Ship Name	LOA (ft)	Beam (ft)	Draft (ft)	LOA (m)	Beam (m)	Draft (m)
	CNTNR28L	Sovereign Maersk (SovMae)	1138.5	140.4	47.6	347.0	42.8	14.5
	CNTNR40	MSC Daniella 2 (Dan2)	1201.1	158.8	49.9	366.1	48.4	15.2
2	CNTNR33L	Humber Bridge (HumB)	1102.4	150.3	46.2	336.0	45.8	14.1
	VLCC15L	MT Brittania (MTBrit)	859.6	137.8	49.2	262.0	42.0	15.0
	CNTNR20L	KMSS Dainty (Dainty)	964.9	105.7	41.0	294.1	32.2	12.5

Naming convention - Plan_Area_Transit_Shipname_Currents_Wind_PilotName_Repetition
(Ex:P0_TurningBasin_Offdock_SovMae_Ebb_20N_CWilson_1)

Filename: P2_TurningBasin_OffDock_HumB_Ebb_20N_CWilson_1

Comments:

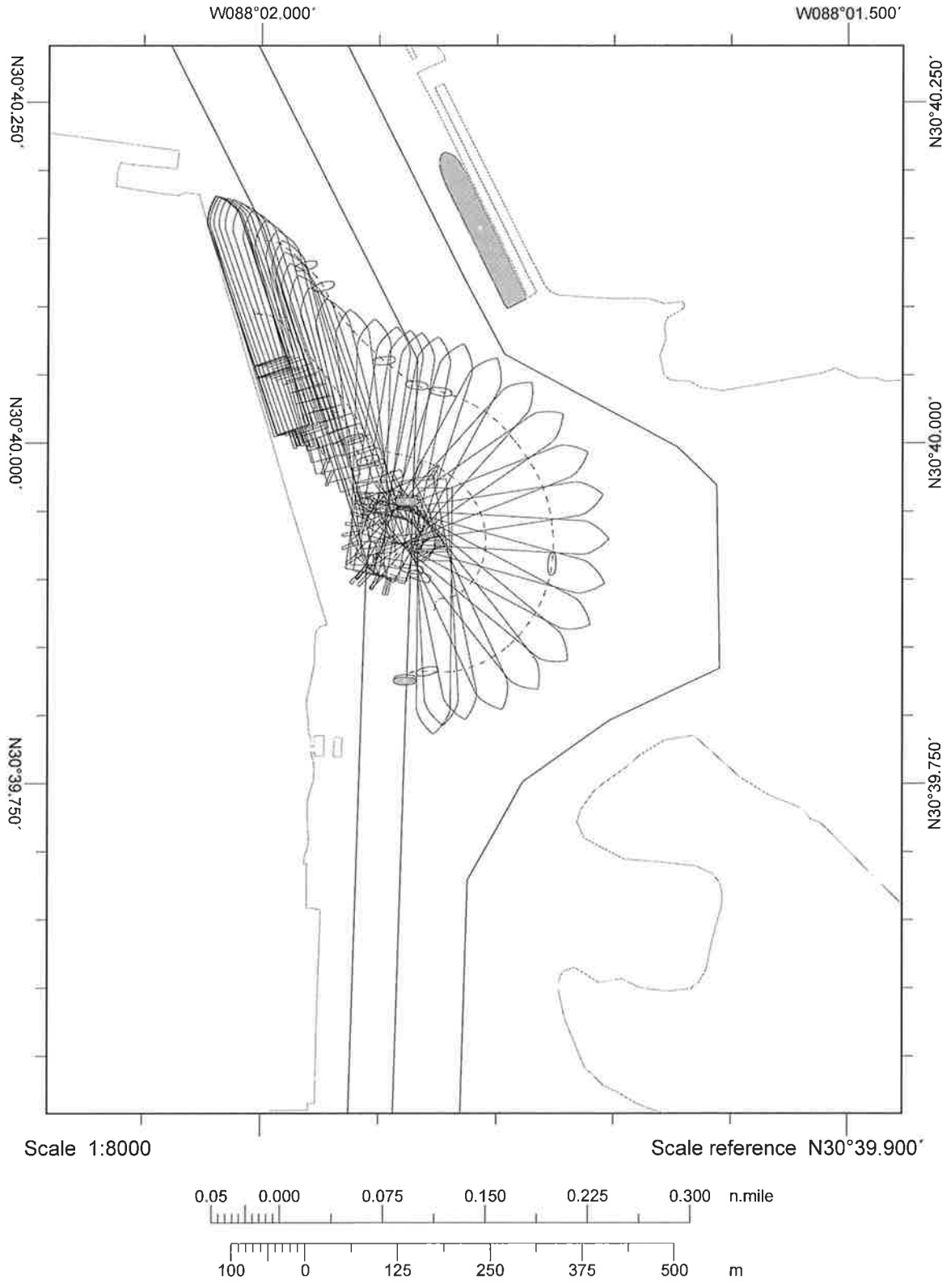

Line sample period (s)	30
Course marker every	00:30
Heading marker period (s)	30
Shape outline every	00:30

Mobile Bay Feasibility Simulations – Passing Lane / Bend Ease

Run #: 29 Date: 26 May 2017

Pilot:
1. Captain Chris Brock — Inbound ~~X~~ Outbound X — Buoy Start 15 — Bridge A
2. Captain Curtis Wilson — Inbound X — Outbound ~~X~~ — Buoy Start 29 — Bridge B

Wind: 20 KNT E W SE Other: _____

Currents: Flood(E wind) Flood(W wind) Flood(SE wind) Ebb(E wind) Ebb(W wind) Other: _____

Tide added: ~~None~~ +0.7m (Daniella 2 or MT Brittania) Other: _____

Plan: P0 (Existing) P1(500ft) P2(550ft)

Vessel:

Pilot #	Model Name	Ship Name	LOA (ft)	Beam (ft)	Draft (ft)	LOA (m)	Beam (m)	Draft (m)
1, 2	CNTNR28L	Sovereign Maersk (SovMae)	1138.5	140.4	47.6	347.0	42.8	14.5
	CNTNR40	MSC Daniella 2 (Dan2)	1201.1	158.8	49.9	366.1	48.4	15.2
	CNTNR44	Zim Piraeus (Zim)	964.9	105.6	43.0	294.1	32.2	13.1
	CNTNR33L	Humber Bridge (HumB)	1102.4	150.3	46.2	336.0	45.8	14.1
	VLCC15L	MT Brittania (MTBrit)	859.6	137.8	49.2	262.0	42.0	15.0
	TANK23	Eagle Kanger (EagleK)	799.9	137.8	40.0	243.8	42.0	12.2

Naming convention - Plan_Area_IShipInbound_OShipoutbound_Currents_Wind_Repetition
(Ex:P0_PassingLane_IZim_ODan2_Flood_20E_1)

Filename: P1_PassLan_I SovMae_O SovMae_Flood_20SE_1

Bow 140

Comments: Passing distance in this channel w/ 2 ships this size is Fairly tight. Even at low speeds ~~[illegible]~~ there is substantial bank effect felt due to the proximity.

Mid 130

Stern 120

TOO CLOSE PASSING. LOW SPEED PASSING AND SHIP STILL GOT CRAZY WHEN WE PASSED WAS CONCERNED WITH TOUCHING BANK WHEN TRYING TO GET BACK IN MIDDLE AFTER PASSING

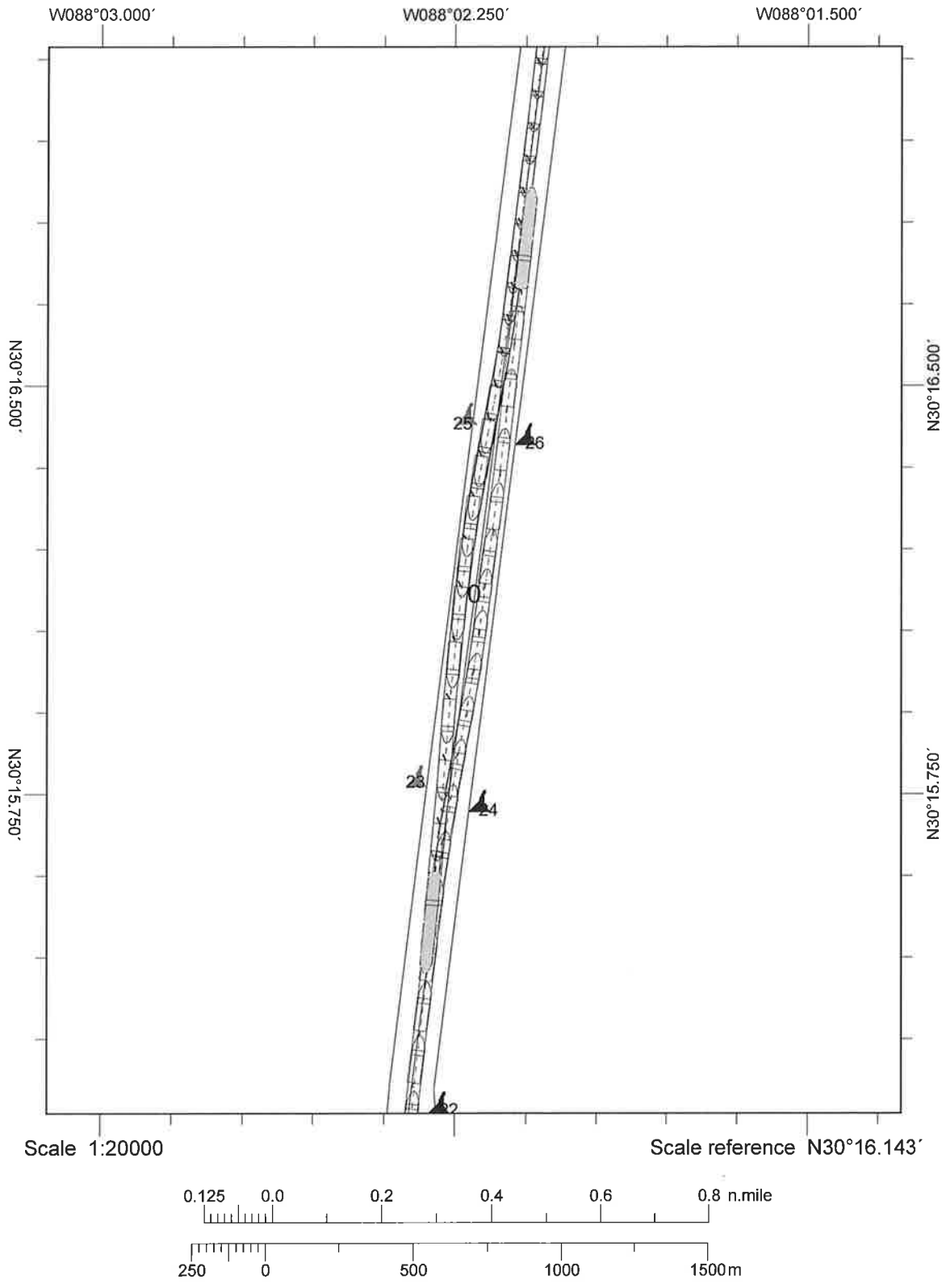

Line sample period (s)	30
Course marker every	00:30
Heading marker period (s)	30
Shape outline every	00:30

Mobile Bay Feasibility Simulations – Turning Basin

Run #: 30

Date: 26 May 2017

Pilot:

1. Captain Chris Brock	Off Dock___	To Dock X	Bridge A
2. Captain Curtis Wilson	Off Dock___	To Dock___	Bridge___

Wind: 20 KNT (N) Other: _____

Currents: Ebb turning basin (north wind) Other: _____

Tide added: None (0.7m) (Daniella 2 or MT Britt) Other: _____

Plan: P0 (Existing) P1 or (P2) (Deepened only -51 ft) Other: _____

Vessel:

Pilot #	Model Name	Ship Name	LOA (ft)	Beam (ft)	Draft (ft)	LOA (m)	Beam (m)	Draft (m)
	CNTNR28L	Sovereign Maersk (SovMae)	1138.5	140.4	47.6	347.0	42.8	14.5
	CNTNR40	MSC Daniella 2 (Dan2)	1201.1	158.8	49.9	366.1	48.4	15.2
1	CNTNR33L	Humber Bridge (HumB)	1102.4	150.3	46.2	336.0	45.8	14.1
	VLCC15L	MT Brittania (MTBrit)	859.6	137.8	49.2	262.0	42.0	15.0
	CNTNR20L	KMSS Dainty (Dainty)	964.9	105.7	41.0	294.1	32.2	12.5

Naming convention - Plan_Area_Transit_Shipname_Currents_Wind_PilotName_Repetition
(Ex:P0_TurningBasin_Offdock_SovMae_Ebb_20N_CWilson_1)

Filename: P2_TurningBasin_ToDock_HumB_Ebb_20N_CBrock_3

North Boundary
143

Southe
125

Comments:

Tank 10L berthed at Southern Tip
Extended Basin

SAFE ROOM ALL AROUND, STILL TAKING A LOT TO GET SHIP OUT OF BASIN ONCE YOU COMMITT

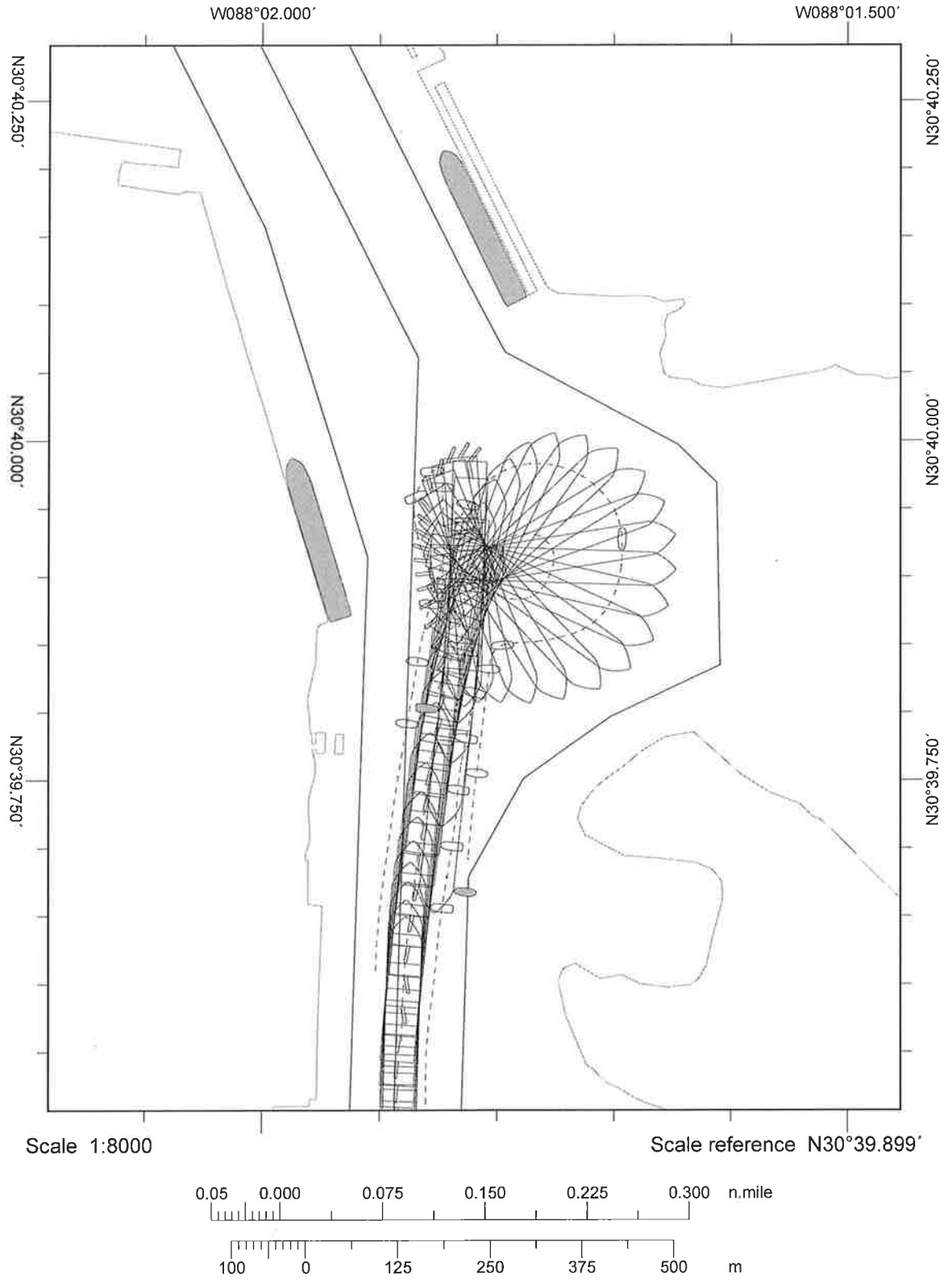

Line sample period (s)	30
Course marker every	00:30
Heading marker period (s)	30
Shape outline every	00:30

Mobile Bay Feasibility Simulations – Turning Basin

Run #: 31

Date: 26 May 2017

Pilot:

1. Captain Chris Brock — Off Dock___ — To Dock___ — Bridge___
2. Captain Curtis Wilson — Off Dock___ — To Dock ✓ — Bridge B

Wind: 20 KNT N — Other: _____

Currents: Ebb turning basin (north wind) — Other: +75%

Tide added: None — +0.7m (Daniella 2 or MT Britt) — Other: flat-bottom

Plan: P0 (Existing) — P1 or P2 (Deepened only -51 ft) — Other: _____

Vessel:

Pilot #	Model Name	Ship Name	LOA (ft)	Beam (ft)	Draft (ft)	LOA (m)	Beam (m)	Draft (m)
	CNTNR28L	Sovereign Maersk (SovMae)	1138.5	140.4	47.6	347.0	42.8	14.5
	CNTNR40	MSC Daniella 2 (Dan2)	1201.1	158.8	49.9	366.1	48.4	15.2
2	CNTNR33L	Humber Bridge (HumB)	1102.4	150.3	46.2	336.0	45.8	14.1
	VLCC15L	MT Brittania (MTBrit)	859.6	137.8	49.2	262.0	42.0	15.0
	CNTNR20L	KMSS Dainty (Dainty)	964.9	105.7	41.0	294.1	32.2	12.5

Naming convention - Plan_Area_Transit_Shipname_Currents_Wind_PilotName_Repetition
(Ex:P0_TurningBasin_Offdock_SovMae_Ebb_20N_CWilson_1)

Filename: P2_TurningBasin_ToDock_HumB_Ebb_20N_CWilson_2

Comments: Changed berthed ship at proposed container terminal ↑ to Daniella 2 expansion

Got bow to extreme North edge of basin. Had to use both tugs Full ahead on stern to execute turn + not fall too far south. Being that far north helped bow from getting too close to L.S.I. but Far From realistic

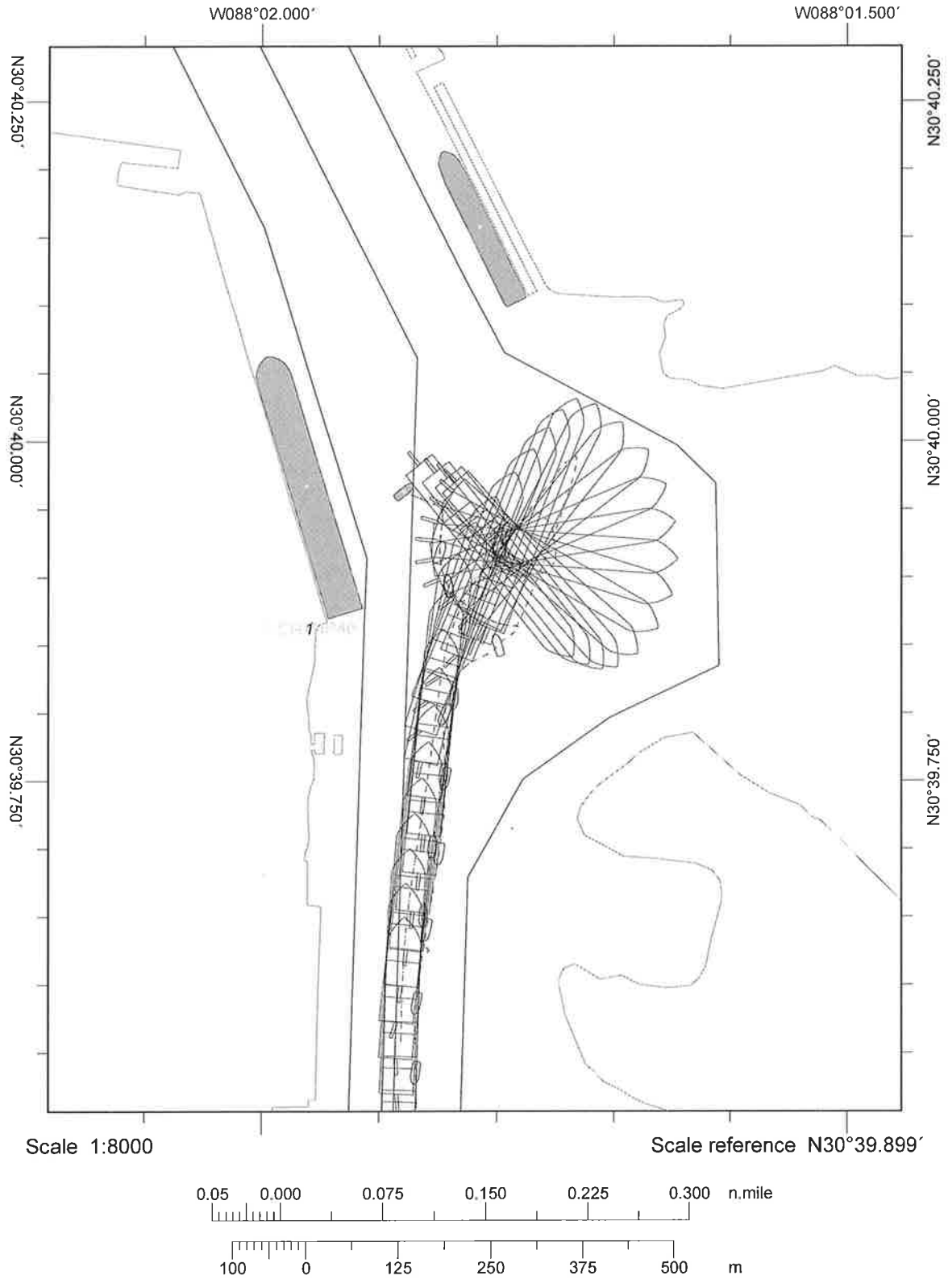

Line sample period (s)	30
Course marker every	00:30
Heading marker period (s)	30
Shape outline every	00:30

Mobile Bay Feasibility Simulations – Turning Basin

Run #: 32 Date: 26 May 2017

Pilot:

1. Captain Chris Brock	Off Dock___	To Dock___	Bridge___
2. Captain Curtis Wilson	Off Dock✓	To Dock___	Bridge B

Wind: 20 KNT N Other: _____

Currents: Ebb turning basin (north wind) Other: _____

Tide added: None +0.7m (Daniella 2 or MT Britt) Other: flat bottom

Plan: P0 (Existing) P1 or P2 (Deepened only -51 ft) Other: _____

Vessel:

Pilot #	Model Name	Ship Name	LOA (ft)	Beam (ft)	Draft (ft)	LOA (m)	Beam (m)	Draft (m)
	CNTNR28L	Sovereign Maersk (SovMae)	1138.5	140.4	47.6	347.0	42.8	14.5
	CNTNR40	MSC Daniella 2 (Dan2)	1201.1	158.8	49.9	366.1	48.4	15.2
2	CNTNR33L	Humber Bridge (HumB)	1102.4	150.3	46.2	336.0	45.8	14.1
	VLCC15L	MT Brittania (MTBrit)	859.6	137.8	49.2	262.0	42.0	15.0
	CNTNR20L	KMSS Dainty (Dainty)	964.9	105.7	41.0	294.1	32.2	12.5

Naming convention - Plan_Area_Transit_Shipname_Currents_Wind_PilotName_Repetition
(Ex:P0_TurningBasin_Offdock_SovMae_Ebb_20N_CWilson_1)

Filename: P2_TurningBasin_OffDock_HumB_Ebb_20N_CWilson_3

Comments: Turning with ship @ south dock requires movement to the EAST. While turning, ship engine working at least half astern to check headway.

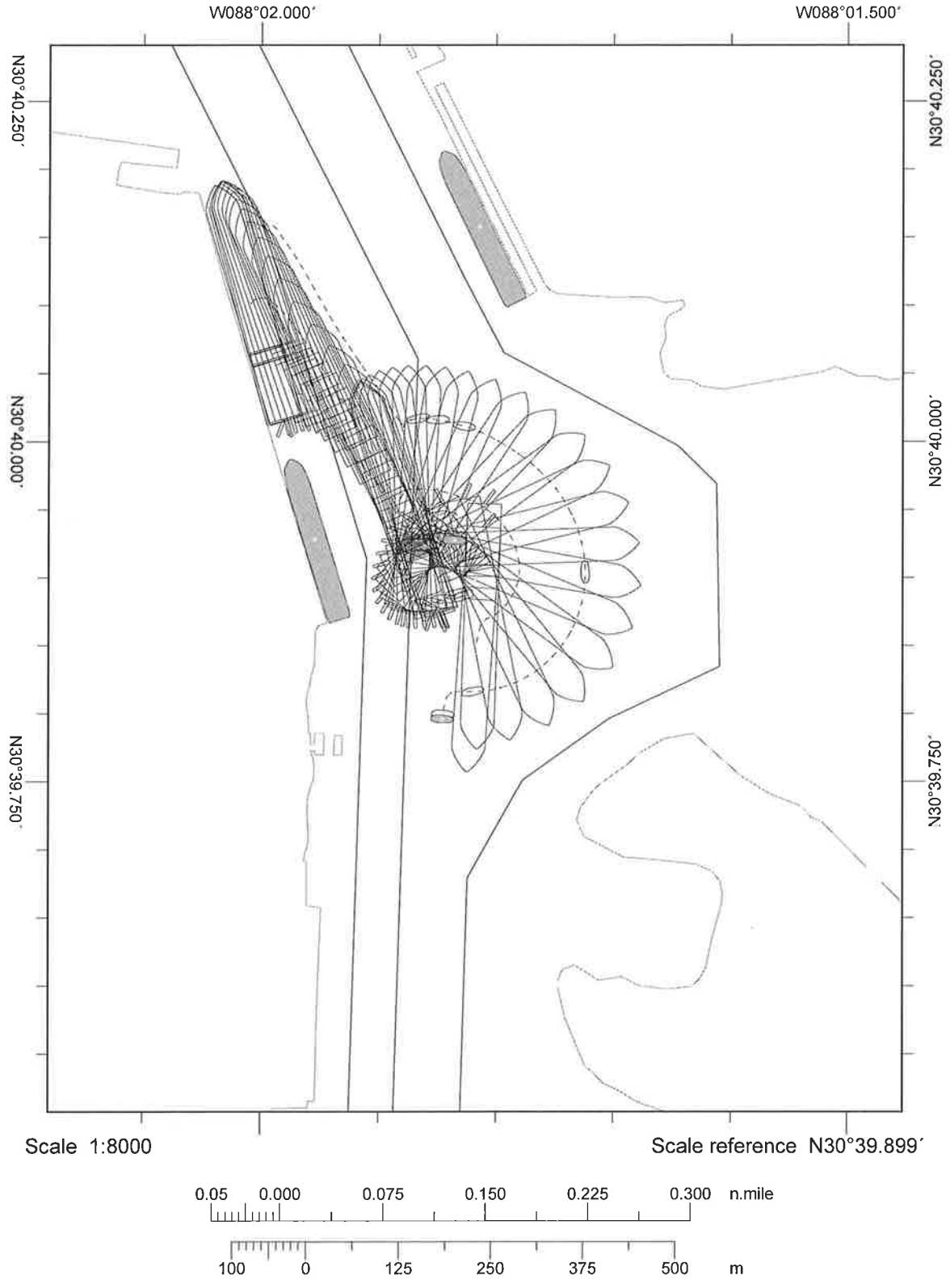

Line sample period (s)	30
Course marker every	00:30
Heading marker period (s)	30
Shape outline every	00:30

Mobile Bay Feasibility Level Simulation Study – Final Questionnaire

Name: Chris Brock

Screening of the proposed deepening and widening for a passing area and the proposed deepening of the turning basin in Mobile Bay was conducted at ERDC's Ship/Tow Simulator (STS) 23-26 May 2017. The purpose was to provide a preliminary evaluation of proposed deepening and widening in lower Bay passing area (550ft x 53/51ft or 500ft by 53/51ft) and deepening of the turning basin near Little Sand Island (51ft). The channel extents agreed upon at the end of this week will be used for the remainder of the Feasibility Study. Additional and final simulation will be conducted during the PED portion of the study to address any additional concerns raised between Feasibility and PED.

1. As a Feasibility Level simulation, several assumptions were made to reduce the overall time and cost of the project compared to a full ship simulation study.
   a. Were the environment conditions (wind and current combinations) reasonable?

YES. PRETTY REALISTIC

   b. Screening for the project only lasted about a week. This is about one third of the simulation testing typically done for final channel design. Do you think the number of pilots participating and time spent testing was adequate for a Feasibility Level study?

FOR FINAL DESIGN I WOULD WANT MORE PILOTS ATTENDING. PRELIMINARY TESTING TWO WAS SUFFICIENT

   c. The Corps of Engineers were represented by ERDC and Mobile District. Pilots were represented by the Mobile Bar Pilots. Do you think additional parties should've been represented during this testing effort? ~~THE~~ STATE PORT AUTHORITY

Note: Captain Brock contacted ERDC after testing that he wished to add the Mobile Container Terminal as a party that should be represented as well.

Appendix B

d. Please comment on the response of the vessels models, both ships and tugs.

MOST SEEMED TRUE TO LIFE

e. How were the other aspects of the simulation?

GOOD

2. Did you consider the 5 mile, 500ft , 53/51ft channel adequate for passing in the following situations:
   a. Zim Piraeus (964.9 x 105.6 x 43.0) and MSC Daniella 2 (1200.1 x 158.8 x 49.9)
   b. Zim Piraeus (964.9 x 105.6 x 43.0) and the MT Brittania (859.6 x 137.8 x 49.2)
   c. Zim Piraeus (964.9 x 105.6 x 43.0) and the Humber Bridge (1102 x 150 x 46.2)
   d. Sovereign Maersk (1138.5 x 140.4 x 47.6) and the Sovereign Maersk (1138.5 x 140.4 x 47.6)

   Why or why not?

a) DOABLE BUT DON'T ADVISE. DEPENDS ON ENVIRONMENTALS AND combined DRAFTS

b) YES

c) DOABLE BUT DON'T ADVISE. RECOVERY ROOM MINIMAL

d) NO. NOT ENOUGH TIME TO RECOVER ONCE PASSED FOR FEAR OF TOUCHING BANK

3. Did you consider the 5 mile, 550ft , 53/51ft channel adequate for passing in the following situations:
   a. MSC Daniella 2 (1200.1 x 158.8 x 49.9) and the Sovereign Maersk (1138.5 x 140.4 x 47.6)
   b. Sovereign Maersk (1138.5 x 140.4 x 47.6) and the Sovereign Maersk (1138.5 x 140.4 x 47.6)*
   c. MSC Daniella 2 (1200.1 x 158.8 x 49.9) and the MT Brittania (859.6 x 137.8 x 49.2)

   Why or why not?

   *Note: The Sovereign Maersk passing the Sovereign Maersk was not tested in the 550ft channel. Based on passing in the 500ft channel, do you believe the 550ft channel would be adequate?

a) DOABLE BUT DON'T ADVISE. TIGHT RECOVERY TIME

b) YES

c) YES WITH DRAFT RESTRICTIONS

4. Based upon the simulator runs, what possible limits or restrictions MIGHT be considered by the Mobile Bar Pilots for two way traffic in the passing zone?

For the 500 ft wide channel:

- COMBINED length
- COMBINED DRAFT

For the 550 ft wide channel:

- Combined length
- Combined draft

5. Please comment on the proposed 3 mile length for the passing lanes.

- TIMING IS CRITICAL
- BEND BASING @ 22 WOULD HELP INBOUND LINE UP TO MEET the outbound
- transition ZONE isn't beneficial as ~~far as~~ timing for passing goes
- 5 miles GIVES both vessels time to slow DOWN AND position themselves for ~~passing~~

6. Did the bend easings improve the setup for meeting of the large vessels in the passing lane?

BEND EASING AT 21/22 ESPECIALLY IF IT CAN BE DONE ON GREEN SIDE (WEST) WOULD BE BENEFICIAL

7. Was the deepened turning basin (51ft) adequate (please include comments concerning docked ships) for turning the following vessels:
   a. MSC Daniella 2 (1200.1 x 158.8 x 49.9)
   b. Humber Bridge (1102 x 150 x 46.2)

   Why or why not?

a) DEPTH DIDN'T HELP SPEED OF TURN / NO

b) DEPTH DIDN'T HELP SPEED OF TURN / NO

8. Did the expansion of turning basin tested improve the turning maneuver for the Humber Bridge? Why or why not?

YES. IT GAVE ME ADEQUATE ROOM TO SWING OFF VESSEL BERTHED AT SOUTH END OF CONTAINER TERMINAL AND STILL ENOUGH ROOM TO FALL AND RECOVER

Note: Captain Brock contacted ERDC after testing that he wanted to clarify that he believed a minimum 100-ft addition would be needed on the southern edge of the turning basin.

9. Do you consider the existing channel adequate for the MSC Daniella 2 (1200.1 x 158.8 x 49.9) in one way traffic?

CHANNEL YES

TURNING BASIN WOULD BE EXTREMELY TIGHT

10. Were simulations representative of real life piloting operations?

YES. VERY GOOD

11. Are there any aspects of the project that were not adequately addressed by USACE and should be updated going forward?

NO

11. Any additional comments?

VERY THOROUGH

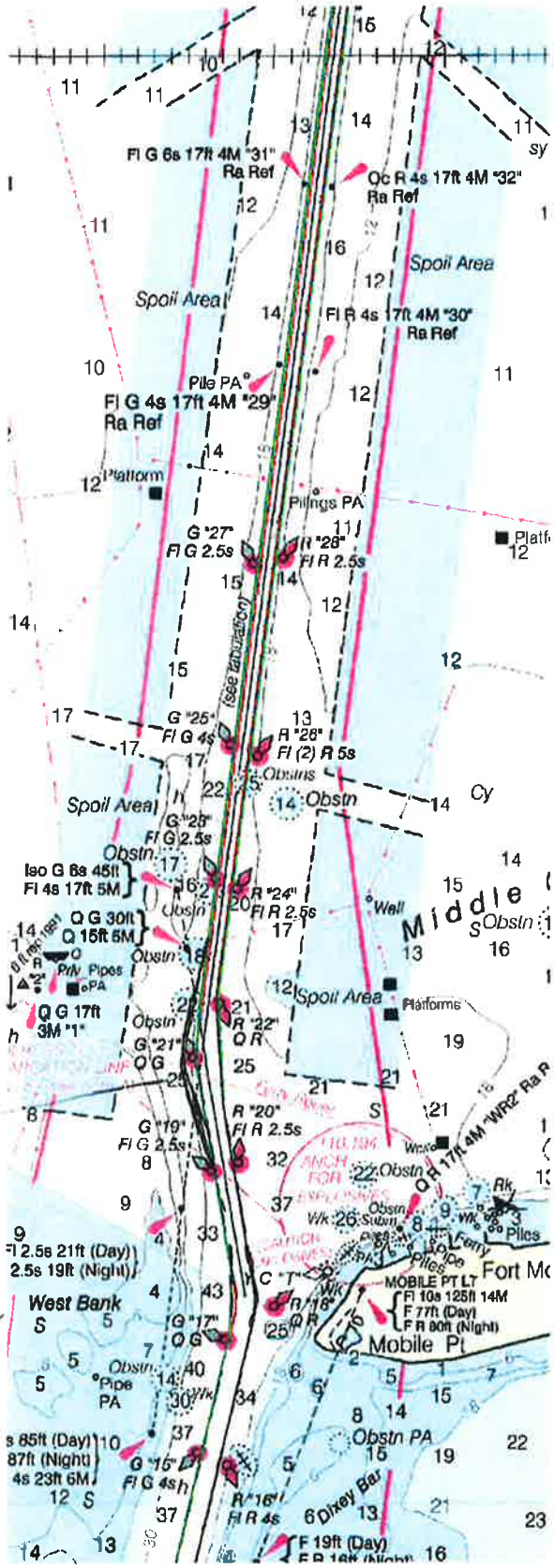

WOULD HELP COME OUT OF TURN & LINE UP QUICKER

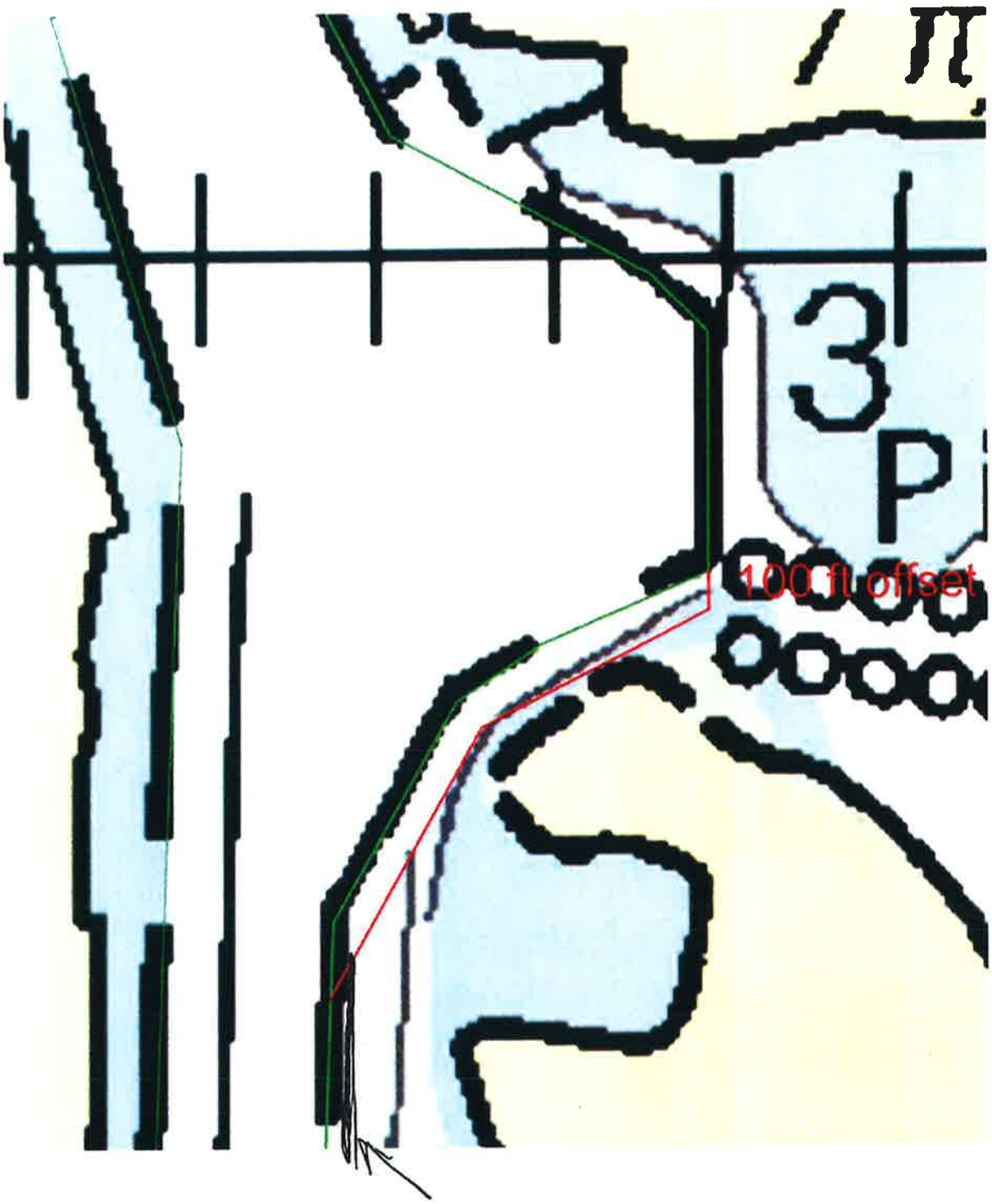

STILL WOULD ENTERTAIN WIDENER OFF MCDUFFIE. SHIP SIZE HAS INCREASED SINCE last WIDENER WAS DONE. EVEN AT EXTREMELY SLOW SPEEDS PULLING SHIPS OFF DOCK IS HUGE CONCERN. ESPECIALLY WITH NEWER CLASS CONTAINER VESSELS

Mobile Bay Feasibility Level Simulation Study – Final Questionnaire

Name: Curtis Wilson

Screening of the proposed deepening and widening for a passing area and the proposed deepening of the turning basin in Mobile Bay was conducted at ERDC's Ship/Tow Simulator (STS) 23-26 May 2017. The purpose was to provide a preliminary evaluation of proposed deepening and widening in lower Bay passing area (550ft x 53/51ft or 500ft by 53/51ft) and deepening of the turning basin near Little Sand Island (51ft). The channel extents agreed upon at the end of this week will be used for the remainder of the Feasibility Study. Additional and final simulation will be conducted during the PED portion of the study to address any additional concerns raised between Feasibility and PED.

1. As a Feasibility Level simulation, several assumptions were made to reduce the overall time and cost of the project compared to a full ship simulation study.
   a. Were the environment conditions (wind and current combinations) reasonable?

      Yes, both in turning basin & South end of bay.

   b. Screening for the project only lasted about a week. This is about one third of the simulation testing typically done for final channel design. Do you think the number of pilots participating and time spent testing was adequate for a Feasibility Level study?

      Two pilots were adequate, more participating pilots would have been optimal.

   c. The Corps of Engineers were represented by ERDC and Mobile District. Pilots were represented by the Mobile Bar Pilots. Do you think additional parties should've been represented during this testing effort?

      Port of Mobile representation to answer questions about possible Future operations would have been helpful

d. Please comment on the response of the vessels models, both ships and tugs.

Ship + tug simulation was certainly adequate.

e. How were the other aspects of the simulation?

Landmarks, Aids to navigation, + environmentals were realistic.

2. Did you consider the 5 mile, 500ft , 53/51ft channel adequate for passing in the following situations:
   a. Zim Piraeus (964.9 x 105.6 x 43.0) and MSC Daniella 2 (1200.1 x 158.8 x 49.9)
   b. Zim Piraeus (964.9 x 105.6 x 43.0) and the MT Brittania (859.6 x 137.8 x 49.2)
   c. Zim Piraeus (964.9 x 105.6 x 43.0) and the Humber Bridge (1102 x 150 x 46.2)
   d. Sovereign Maersk (1138.5 x 140.4 x 47.6) and the Sovereign Maersk (1138.5 x 140.4 x 47.6)

   Why or why not?

a) No, Daniella did not handle adequately to provide enough room for other ship.

b) yes, contingent on drafts. Room felt adequate.

c) [redacted] was Doable, severe bank effect makes it hard to advise.

d) No, too much bank effect.

3. Did you consider the 5 mile, 550ft , 53/51ft channel adequate for passing in the following situations:
   a. MSC Daniella 2 (1200.1 x 158.8 x 49.9) and the Sovereign Maersk (1138.5 x 140.4 x 47.6)
   b. Sovereign Maersk (1138.5 x 140.4 x 47.6) and the Sovereign Maersk (1138.5 x 140.4 x 47.6)*
   c. MSC Daniella 2 (1200.1 x 158.8 x 49.9) and the MT Brittania (859.6 x 137.8 x 49.2)

   Why or why not?

   *Note: The Sovereign Maersk passing the Sovereign Maersk was not tested in the 550ft channel. Based on passing in the 500ft channel, do you believe the 550ft channel would be adequate?

a) No, Daniella responds too poorly to meet other ship.

b) yes, ample room between ships

c) yes, but with lighter draft on tanker.

4. Based upon the simulator runs, what possible limits or restrictions MIGHT be considered by the Mobile Bar Pilots for two way traffic in the passing zone?

For the 500 ft wide channel:

Current rules dictating combined length/draft restrictions.

For the 550 ft wide channel:

See above.

5. Please comment on the proposed 3 mile length for the passing lanes.

3 miles would potentially not be adequate for a passing lane length. Ships of this size & speed (maneuverable) would need more flexibility & distance to guarantee an effective passing arrangement.

5 miles more practical.

6. Did the bend easings improve the setup for meeting of the large vessels in the passing lane?

yes, substantially.

7. Was the deepened turning basin (51ft) adequate (please include comments concerning docked ships) for turning the following vessels:
   a. MSC Daniella 2 (1200.1 x 158.8 x 49.9)
   b. Humber Bridge (1102 x 150 x 46.2)

   Why or why not?

a) No, depth not a factor. That size ship in extreme environmentals needs bigger basin.

b) yes, 1,102' turned ok okay.

8. Did the expansion of turning basin tested improve the turning maneuver for the Humber Bridge? Why or why not?

yes, especially with a ship docked at South End of Container terminal. A ship this length requires the bow to be in East side of basin, but MUST have room to fall. Expansion of basin helped

9. Do you consider the existing channel adequate for the MSC Daniella 2 (1200.1 x 158.8 x 49.9) in one way traffic? Yes. Turning basin possibly an issue.

10. Were simulations representative of real life piloting operations?

Yes.

11. Are there any aspects of the project that were not adequately addressed by USACE and should be updated going forward? No.

11. Any additional comments?

Good operation of equipment from staff. Good Exercise.

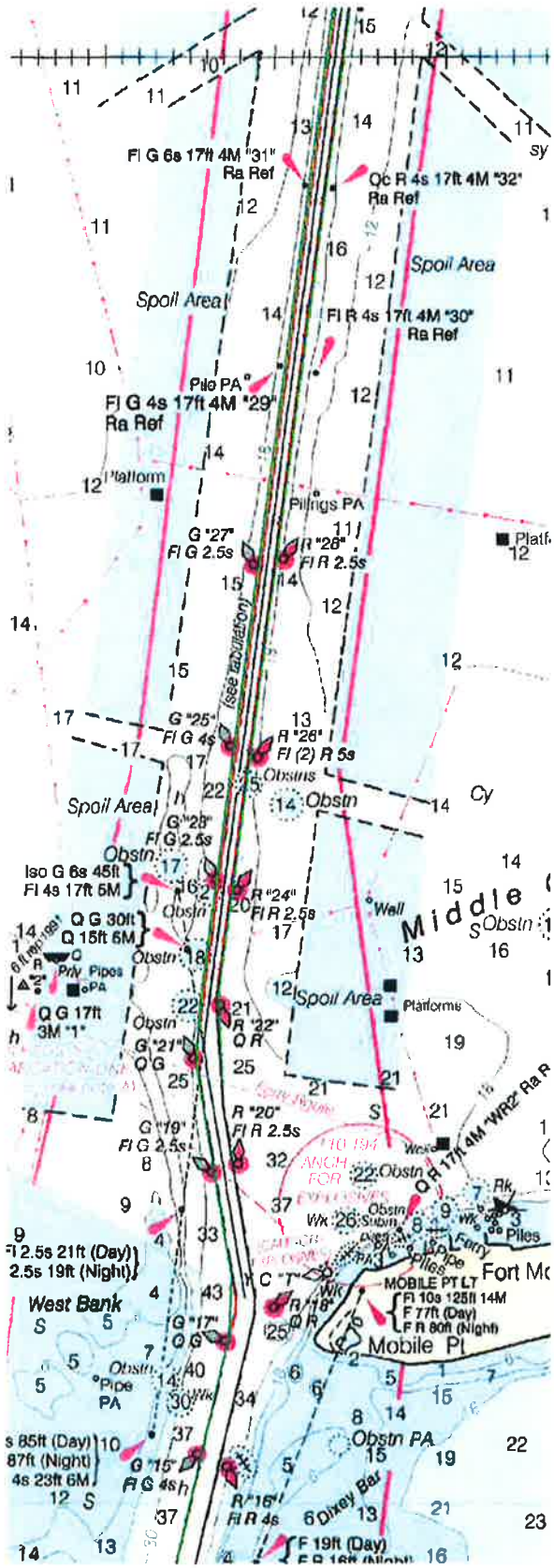

Bend Easings are a substantial improvement.

Any Additional room on West side of channel near #21 would be a great improvement.

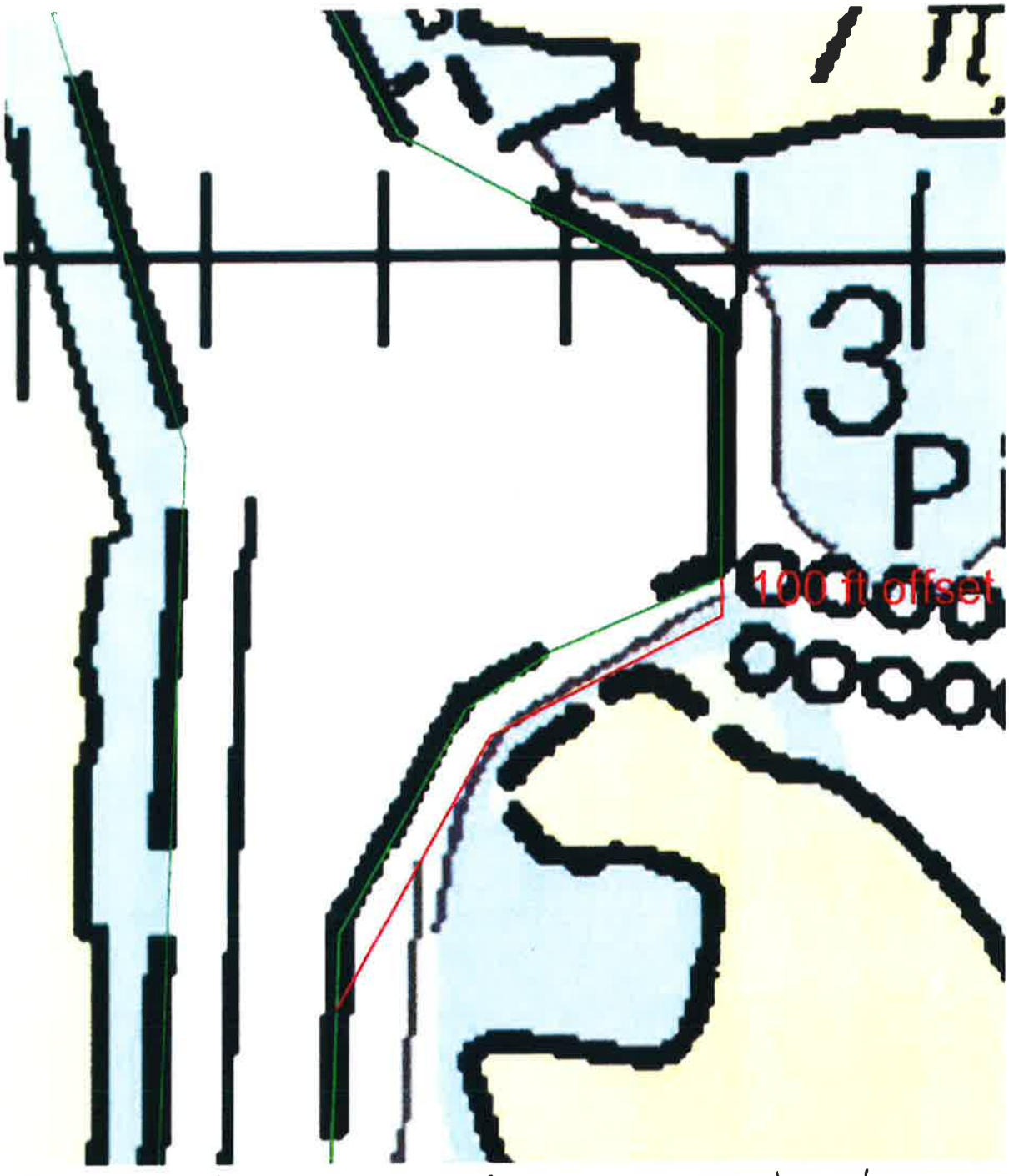

The ships tested on simulator demand an aggressive approach into basin + execution of turn. (in standard Environmentals). Committing to the East side of basin requires extremely close proximity to North + South boundaries. It is not feasible to turn an 1,100' ship that deep in basin without more room for bow to fall South, if another ship docked @ South end of Container Terminal.

ATTACHMENT A – 4
VESSEL GENERATED
WAVE ENERGY REPORT

Vessel Generated Wave Energy: Field Data Collection, Prediction, and Impacts Assessment

Mobile Bay, Alabama

Richard J. Allen

U.S. Army Corps of Engineers, Mobile District
109 Saint Joseph Street
Mobile, AL 36602

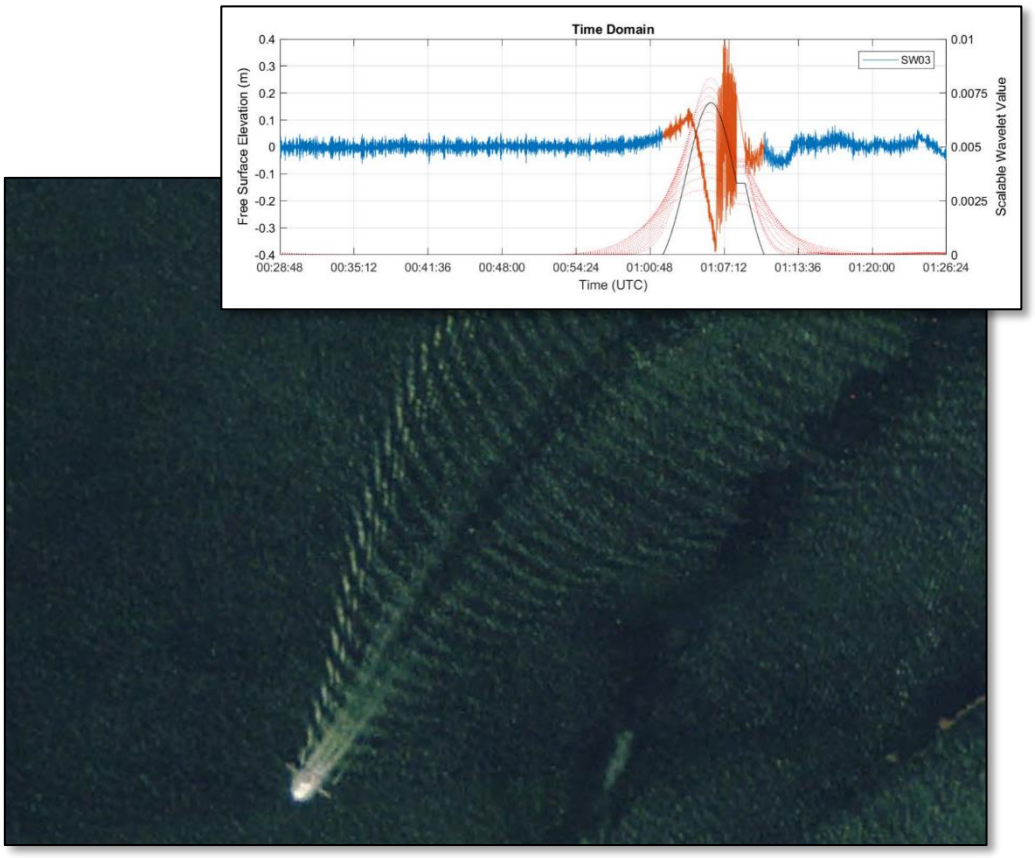

Draft Report
(03 MAR 2019)

US Army Corps of Engineers
Mobile District

April 2018

Abstract

The U.S. Army Corps of Engineers, Mobile District, is completing a General Re-Evaluation Report (GRR) for the Mobile Harbor Federal Navigation Channel. The GRR will determine if it is justifiable to deepen and widen the channel. As part of the analysis, potential for environmental impacts must be assessed. Vessel generated wave energy (VGWE) is a source of potential environmental impacts. A vessel generated wave energy (VGWE) assessment was conducted to quantify the relative changes in wave energy due to future vessels calling the port. The investigation included field data collection using a suite of 5 pressure sensors located north of Gaillard Island. A unique and efficient method of data processing was employed using a continuous wavelet transformation (CWT) to extract the vessel generated disturbances from a continuous time series by utilizing frequency modulation or "chirp" signal produced and shown to be valid within the context of large data sets where random errors can be averaged. VGWE was computed on the extracted time series using a fast Fourier transformation which is widely accepted and used for describing energy of a time series. The method proved successful for this study with the exception of cases with higher background energy or weak VGWE signals. VGWE computed using field data compared well with expected results based on theoretical values and dependencies. Overall, the field data collection collected for this study proved to be valid when used for general trending. VGWE was also estimated using the model described by Schoellhamer (1996) and compared to the collected data described in previous paragraph. The results were found to underestimate at all measured stations for Froude numbers greater than 0.5. For Froude numbers less than 0.5 the model tends to overestimate at the far field stations and underestimate for near measurement stations. The original field data and model were validated using a similar methodology to collect data between December 2018 and February 2019 in the southern bay. The southern bay validation indicated agreement with the Schoellhamer model but with less accuracy. As a result of this analysis, it is recommend the Schoellhamer (1996) should only be applied to Mobile Bay for low precision prediction of far field VGWE at Froude numbers greater than 0.5 with the understanding values could be slightly underestimated. Potential impacts of VGWE were evaluated at two locations in the Bay (i.e., the area where data was collected and another area in the southern part of the Bay where validation data was collected) by comparing the relative difference of with and without project conditions using forecasted vessel calls for years 2025 and 2035. Vessel speed was obtained from a statistical summary of 2016 Automatic Identification System (AIS) data categorized by vessel length. Cumulative VGWE was computed using the model published by Schoellhamer (1996). No increase in VGWE was determined as a result of the proposed project. The confidence of this finding was tested with respect to the assumption of vessel speed which determined for realistic potential increases in vessel speed as a result of the project the relative difference in VGWE does not become impactful. A cumulative impacts analysis of vessel generated wave energy (VGWE) effects on Mobile Bay shorelines was completed at three representative locations along the

western shore. One of these locations indicated a possible correlation between shoreline change rates and vessel calls from 1957 till approximately 1997, and no correlation at all sites between 1997 and present. Because there was no correlation found at any of the sites since 1997 and VGWE associated with the recommended plan is expected to be reduced, the present and foreseeable cumulative impacts of VGWE on Mobile Bay shorelines are considered not significant.

Contents

1 Introduction

Purpose
Study Area
Climatology
Theoretical Background

2 Field Investigation

Field Stations
AIS Data
Measured VGWE Processing Methodology
Results
Discussion and Data Quality
Summary

3 Computing Vessel Generated Wave Energy

Predictive Models
Discussion
Validation
South Bay Validation
Summary

4 Impact Assessment

Vessel Traffic Frequency
Vessel Speed
Spatial Representation
Computed Impact
Sensitivity Analysis
Summary

5 Cumulative Impacts Assessment

Vessel Callings
Shoreline Inventory
Federal Navigation Channel Dimensions
Shoreline Characterization and Change Analysis
Comparison of Shoreline Change and Vessel Calls
Summary

6 References

Appendix A – Vessel Generated Wave Energy Data by Transit

Appendix B – Detailed Inventory of Forecasted Fleet

Figures and Tables

Figures

Figure 1: Map of Mobile Bay, Alabama along with bathymetric contours obtained from NOAA (2010).

Figure 2: Wind Rose applicable to Mobile Bay obtained from WIS station 73154.

Figure 3: Percent occurrence of wind speed and direction at WIS station 73154.

Figure 4: Spatial distribution of significant wave heights in Mobile Bay as a result of southern wind field (reproduced from Chen et al, 2005).

Figure 5: Definition sketch of vessel disturbance in plan-form described by Havelock (1908).

Figure 6: Map of Station Locations

Figure 7: Typical Pressure Sensor Setup

Figure 8: Sensor Mounting System and Installation

Figure 9: RBR pressure sensor deployment parameters

Figure 10: Automatic Information System (AIS) System Schematic. (IMO, 2015)

Figure 11: Time-Frequency plane representing scenerios for time variance and frequency variance of the Heisenberg box used in the CWT computation. (Mallet, 2009)

Figure 12: Ideal case of CWT used for automatic identification of a vessel generated disturbance at Station SW04, Event ID: 259 for an inbound traveling vessel with dimensions of L = 229 m, B = 32 m, D = 13.7 m. The orange highlighted area is the signal assumed to be generated by the vessel.

Figure 13: Comparison of measured background energy density measured at each station with the recorded wind speeds at NOAA station 8736897. The horizontal axis is indexed by vessel transit event ID.

Figure 14: Examples of possible inaccuracies using CWT method for extracting vessel disturbances from station time series; (upper) Event ID: 8, SW05, outbound, L = 176m, B = 35m, D = 5.8m; (lower) Event ID: 24, SW02, inbound, L = 228m, B = 42m, D = 12.2m.

Figure 15: Multiple vessel transits with small time intervals between events.

Figure 16: Vessel Generated Wave Energy (VGWE) partial identification error using the continuous wavelet transformation (CWT) method. Event ID: 203, SW01, outbound, L = 228m, B = 32m, D = 8.1m.

Figure 17: Vessel generated wave energy (VGWE) identification using a continuous wavelet transformation (CWT) (bottom) and frequency distribution using a fast Fourier transformation (FFT) for an ideal vessel transit event.

Figure 18: Vessel generated wave energy (VGWE) identification using a continuous wavelet transformation (CWT) (bottom) and frequency distribution using a fast Fourier transformation (FFT) for a case of high background wave energy with respect to VGWE.

Figure 19: Example of vessel generated disturbance transformation of the free surface elevation as a function of distance from the sailing line

Figure 20: Measured vessel generated wave energy (VGWE) verses distance from the sailing line with respect to individual events.

Figure 21: Observed breaking of vessel generated wake. Photos taken looking west from an outbound tanker on 09 November 2017. Vessel dimension: L = 244 m, B = 42m. Vessel draft on the date of picture was 8.5m. Left picture was 7 km and right picture 4km north of instrumentation stations.

Figure 22: Observed wave breaking of an inbound containership approximately 2 km north of Gaillard Island from aerial imagery collected 06 November 2013. Detailed vessel description is unavailable.

Figure 23: Vessel generated significant wave height computed using a wave train analysis verses distance from the sailing line with respect to individual events.

Figure 24: Measured vessel generated wave energy verses the depth based Froude number for all stations.

Figure 25: Measure vessel generated wave energy (VGWE) verse vessel draft (top) and vessel length (bottom).

Figure 26: One-to-One correlation plot of measured vessel generated wave energy (VGWE) and the equation from Schoellhamer (1996) for stations SW01 through SW04.

Figure 27: One-to-One correlation plot of measured vessel generated wave energy (VGWE) categorized by Froude number and the equation from Schoellhamer (1996) for stations SW01 through SW04. The regression line follows Froude numbers greater than 0.5.

Figure 28: One-to-One correlation plot of measured vessel generated wave energy (VGWE) and the equation from Schoellhamer (1996) for stations SW01 through SW04 categorized by direction of vessel transit. The regression line is color coded to match the respective transit direction.

Figure 29: Southern Bay Station Locations

Figure 30: One-to-One correlation plot of measured vessel generated wave energy (VGWE) at the south bay validation sites and the equation from Schoellhamer (1996) for stations SWS01 through SWS03 and SW05.

Figure 31: One-to-One correlation plot of measured vessel generated wave energy (VGWE) at the south bay validation sites categorized by Froude number and the equation from Schoellhamer (1996) for stations SWS01 through SWS03 and SW05. The regression line follows Froude numbers greater than 0.5.

Figure 32: One-to-One correlation plot of measured vessel generated wave energy (VGWE) at the south bay validation sites and the equation from Schoellhamer (1996) for stations SWS01 through SWS03 and SW05 categorized by direction of vessel transit. The regression line is color coded to match the respective

Figure 33: Location of sites used for spatial representation of Vessel Generated Wave Energy (VGWE) impact analysis within Mobile Bay, Alabama

Figure 34: Summary statistics of vessel speed using Shipborne Automated Identification System (AIS) data obtain for the 2016 calendar year for Mobile Bay, Alabama deep draft channel delineated by vessel length.

Figure 35: Variation of vessel speed for all classes and categories in Mobile Bay, Alabama with respect to three locations of interest.

Figure 36: Graphical sketch defining cross-sectional variables used in VGWE and vessel speed computations.

Figure 37: Summary of class 1 and 2 vessel calls obtained from WCUS annual reports (1956-2017) aggregated by draft plotted as a function of year.

Figure 38: All class 1 and 2 vessel calls obtained from WCUS annual reports (1956-2017) by year for all drafts greater than or equal to 19 feet.

Figure 39: Selected sites used to evaluate shoreline change.

Figure 40: Linear regression rate of shoreline change for SL1 for 1849/1850 through 2010/2011.

Figure 41: Linear regression rate of shoreline change for SL3 for 1849/1850 through 2010/2011.

Figure 42: Linear regression rate of shoreline change for SL6 for 1849/1850 through 2010/2011.

Figure 43: Temporal plot of channel modifications between 1913 and 1989. Channel dimensions are represented as a cross-sectional area in square feet of the navigable portion

Figure 44: Spatial and Temporal Distribution of shoreline armoring between 1955 and 1997 extracted from Douglass and Pickel (1999).

Figure 45: Temporal distribution of shoreline change rates at SL1 between 1917/18 and 2010/11 with linearly interpolated rate of rate of change.

Figure 46: Temporal distribution of shoreline change rates at SL3 between 1917/18 and 2010/11 with linearly interpolated rate of rate of change.

Figure 47: Temporal distribution of shoreline change rates at SL3 between 1917/18 and 2010/11 with linearly interpolated rate of rate of change.

Figure 48: Plot of vessel count for Mobile Harbor between 1956 and 2017 of all vessels having a draft greater than 19 feet compared to combined average shoreline change rates for sites SL1, SL3, and SL6. Channel dimension changes are identified using the plot background.

Figure 49: Plot of vessel count for Mobile Harbor between 1956 and 2017 of all vessels having a draft greater than 19 feet compared to average shoreline change rates computed for each site. Channel dimension changes are identified using the plot background color.

Tables

Table 1: Station Details

Table 2: AIS Dataset Summary Statistics

Table 3: Average H_{mo} (VGWE) at each station categorized by vessel length

Table 4: Average H_{mo} (VGWE) at each station categorized by vessel draft

Table 5: Average H_{mo} (VGWE) at each station categorized by transit direction

Table 6: Average H_{mo} (VGWE) at each station categorized by speed

Table 7: Average H_{mo} (VGWE) at each station categorized by wind speed recorded at NOAA station 8736897

Table 8: Dependent variables used to evaluate Vessel Generated Wave Energy (VGWE) with respect to locations of interest.

Table 9: Forecast summary for the base year 2025 vessel calls delineated by vessel classes for with and without project conditions.

Table 10: Forecast summary for year 2035 vessel calls delineated by vessel classes for with and without project conditions.

Table 11: Computed Vessel Generated Wave Energy (VGWE) of with and without project scenarios using the forecasted base year 2025 at the upper bay site.

Table 12: Computed Vessel Generated Wave Energy (VGWE) of with and without project scenarios using the forecasted base year 2025 at the lower bay site.

Table 13: Computed Vessel Generated Wave Energy (VGWE) of with and without project scenarios using the forecasted year 2035 at the upper bay site.

Table 14: Computed Vessel Generated Wave Energy (VGWE) of with and without project scenarios using the forecasted year 2035 at the lower bay site.

Table 15: Results of three unique vessel speed sensitivity tests for the 2025 forecasted arrivals at the upper bay site.

Table 16: Inventory of shoreline position data, applicable locations, source, and selected data quality parameters.

Table 17: Summary of Channel Modifications between 1913 and 1989.

1 Introduction

Purpose

The U.S. Army Corps of Engineers, Mobile District, is completing a General Re-Evaluation Report (GRR) for the Mobile Harbor Federal Navigation Channel. The GRR will determine if it is justifiable to deepen and widen the channel. As part of the analysis, potential for environmental impacts must be assessed. Vessel generated wave energy (VGWE) is a source of potential environmental impacts. This report describes the data collection of VGWE in Mobile Bay, Alabama and provides an assessment of relative change in VGWE as a result of deepening the Federal channel from 45 feet to 49 feet using a forecasted vessel fleet for the years 2025 and 2035 that may be used for assessment of impacts to various shoreline types and other environmental features identified by public comment, other government agencies, and local stakeholders.

Study Area

Mobile Bay, Alabama can be described as a micro-tidal, drowned river valley located along the north central coastline of the Gulf of Mexico (Figure 1). Mobile Bay is approximately 50 km from the U.S. Highway 90 causeway in the north to Fort Morgan peninsula in the south. The width averages 17 km and is widest in the south (36 km). The Mobile Bay watershed is the sixth largest river basin in the United States and the fourth largest in terms of streamflow. It drains water from three-fourths of Alabama as well as portions of Georgia, Tennessee and Mississippi into Mobile Bay. Mobile bay has an average water depth of 3 meters and is transected by a 13 to 15 meter deep channel.

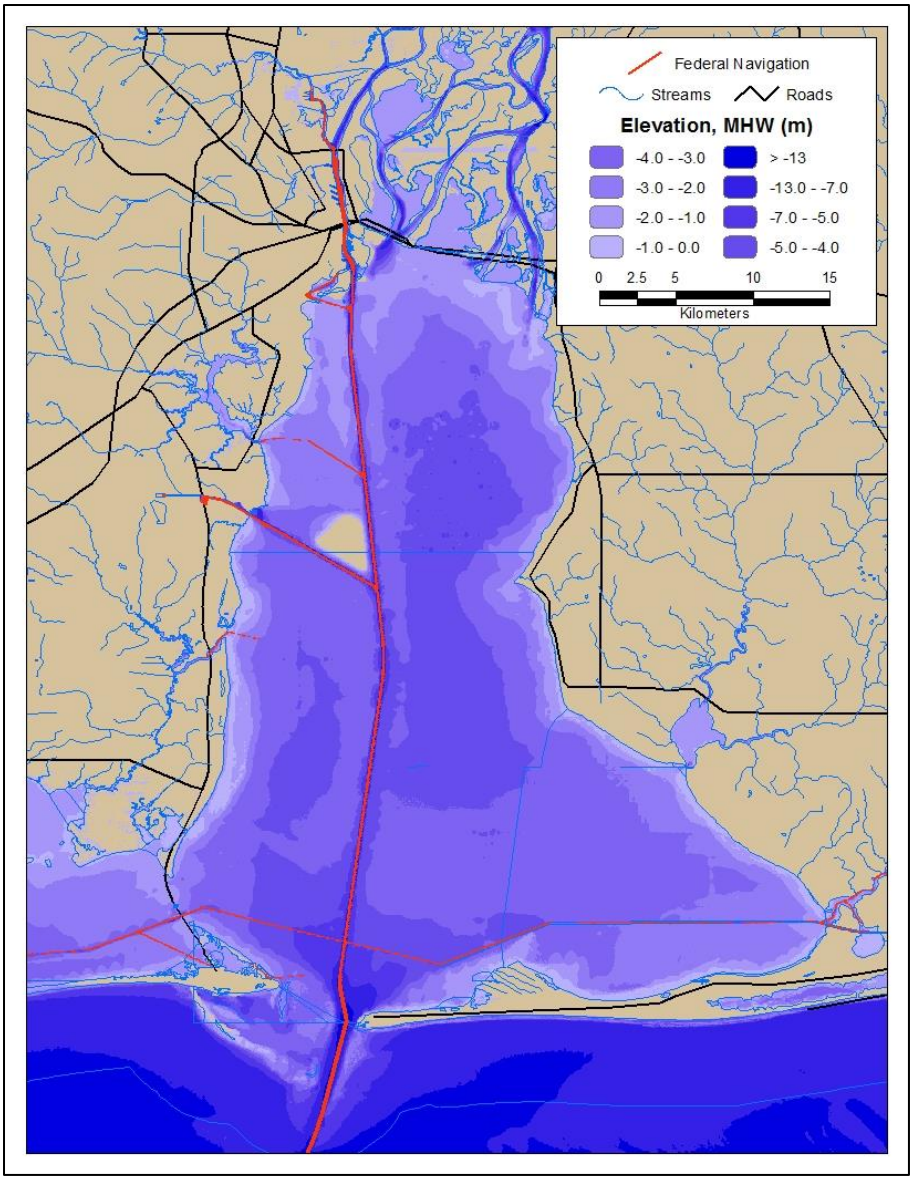

Figure 1: Map of Mobile Bay, Alabama along with bathymetric contours obtained from NOAA (2010).

Climatology

Mobile Bay is located in a temperate climate with average temperatures of 30º C in the summer and 10º C in the winter. The wind climate is generally mild except for episodic events associated with tropical systems. A wind rose in Figure 2 and tabulated percent occurrence of wind speed and direction in Figure 3 obtained from WIS Station 73154 shows the dominate wind directions being between 90º and 135º. Seasonally, winds are northerly in the winter months, south easterly in the spring and early summer, then southwesterly in late summer to early fall.

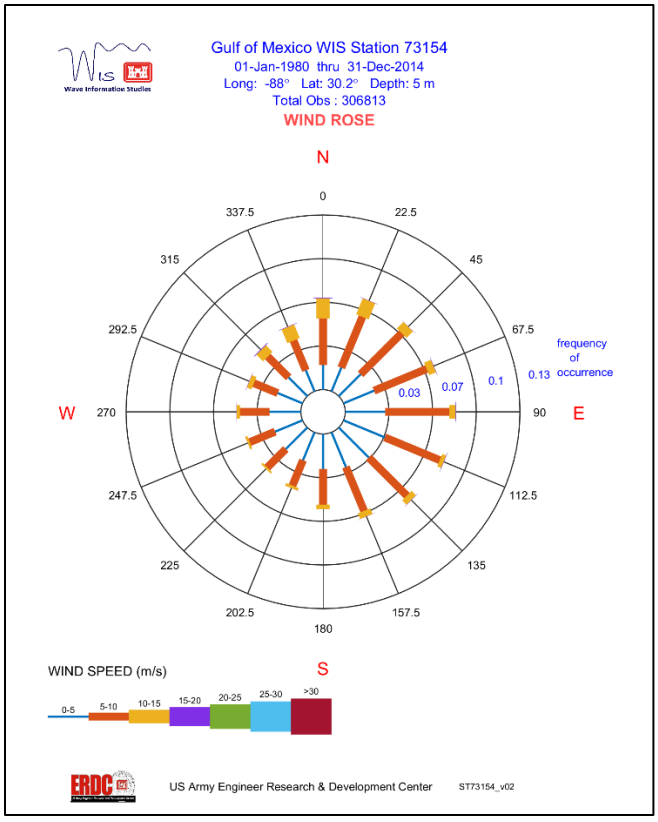

Figure 2: Wind Rose applicable to Mobile Bay obtained from WIS station 73154.

GULF OF MEXICO HINDCAST WAM4.5.1C : ST73154_v02
ALL MONTHS FOR YEARS PROCESSED : 1980 - 2014
STATION LOCATION : (-88.00 W / 30.20 N)
DEPTH : 5.0 m

PERCENT OCCURRENCE (X1000) OF WIND SPEED AND DIRECTION
CENTRAL LOCAL ANGLE BANDS OF (+/- 11.25 DEG)

NO. CASES : 306812

WND DIR	WIND SPEED (M/S)										
DEG	<2.5	2.5-4.9	5.0-7.4	7.5-9.9	10.0-12.4	12.5-14.9	15.0-17.4	17.5-19.9	20.0-24.9	25.0-GREATER	TOTAL
0.0	43	1756	1715	1843	1190	404	57	2	0	0	7010
22.5	48	1829	2129	2071	1080	301	23	0	0	0	7481
45.0	42	2204	2638	1851	671	86	10	0	0	0	7502
67.5	40	2375	2736	1667	501	91	24	6	1	0	7441
90.0	54	2856	3299	1682	419	85	30	7	5	3	8440
112.5	60	3197	3318	1338	285	50	21	6	4	1	8280
135.0	66	3013	2959	1275	393	99	18	2	0	2	7827
157.5	58	2691	2516	1189	362	117	14	0	0	1	6948
180.0	67	2504	1933	861	278	70	6	0	4	1	5724
202.5	81	2131	1642	522	191	38	4	0	1	0	4610
225.0	71	2154	1633	438	136	27	1	1	0	0	4461
247.5	69	2097	1731	442	148	34	4	0	0	0	4525
270.0	73	2235	1801	517	191	75	14	0	2	0	4908
292.5	68	1887	1501	537	276	106	22	3	0	0	4400
315.0	61	1885	1471	817	527	210	50	4	2	0	5027
337.5	43	1620	1317	1157	876	287	38	0	0	0	5338
TOTAL	944	36434	34339	18207	7524	2080	336	31	19	8	

MEAN WS(M/S) = 6.2 MAX WS(M/S) = 35.9 MEAN WIND DIR(DEG) = 211.0 FINITE

Figure 3: Percent occurrence of wind speed and direction at WIS station 73154.

Mobile Bay is a semi-enclosed estuary such that wave energy is mostly locally driven by the wind climate. Pendygraft and Gefenbaum (1994) collected wind and wave data at a site near Gaillard Island over a 2.5 year period. Data were segregated by seasons as well as wind directions in the report and found north winds generated a maximum significant wave height of 0.97 m, east winds generated a significant wave height of 1.00 m, and south winds generated a maximum measured significant wave height of 1.55 m. These finding tend to suggest a fetch limited wave condition in the northern part of the bay. Chen et al. (2005) used the data collected by Pendygraft and Gefenbaum (1994) to validate a numerical model for Mobile Bay confirming the fetch limited wind directions of north, east, and west. Comparatively, Chen et al. (2005) found a nearly fully developed wave field in the central part of the bay as shown in Figure 4 produced by south-southeast wind direction. The wave height decays in the northern part of the bay; this is likely a result of depth induced shoaling and wave breaking. Reduced wave heights are also observed north (leeward) of Gaillard Island and from this figure there appears to be no amplification or focusing of the wave height in the far leeward area north of the island.

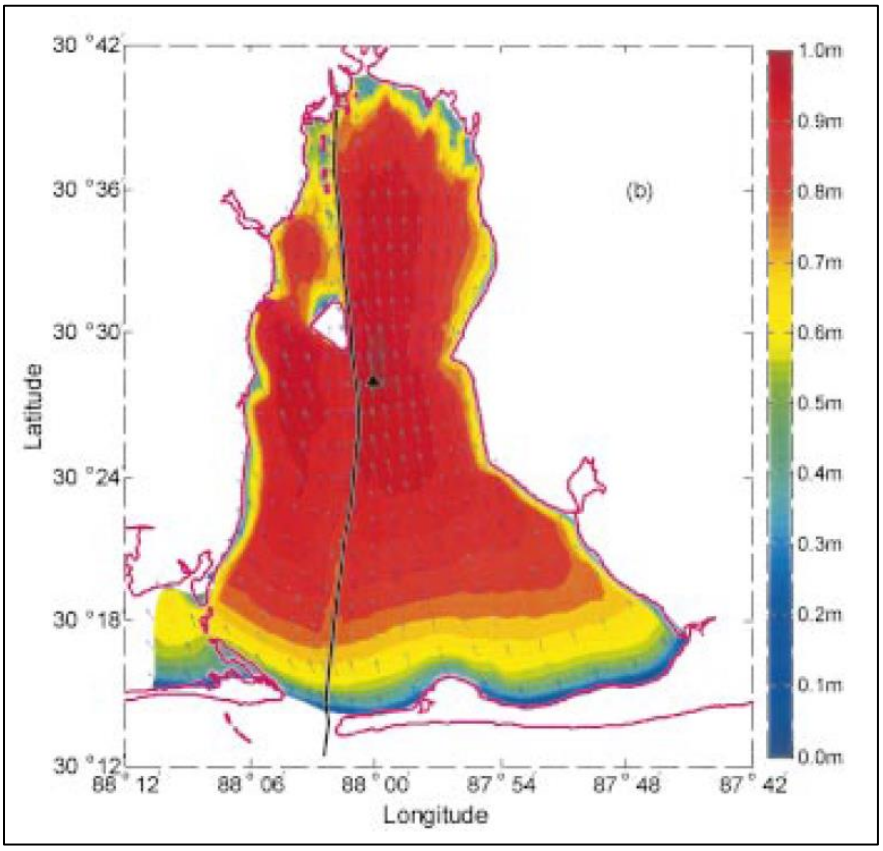

Figure 4: Spatial distribution of significant wave heights in Mobile Bay as a result of southern wind field (reproduced from Chen et al, 2005).

Theoretical Background

Quantification or at least an understanding of vessel generated wave characteristics is of high importance to the practice of coastal engineering when designing in close proximity to frequently trafficked areas by small and large vessels or within quiescent coastal settings that include large deep-draft navigation channels, as is the case for nearly all major estuarine environments in the United States. Over the past century researchers and practitioners have produced a comprehensive collection of theories and methodologies for describing aspects of vessels wakes for a large range of applications. References identified for this report pertain to the theoretical components (Havelock, 1908), laboratory experiment derived models (Sorensen and Weggel, 1984; Weggel and Sorensen, 1986), field study derived models (Schoellhamer, 1996; Kriebel and Seelig, 2005; Maynord, 2011), and interaction with complex bathymetry and/or channel geometry (Rapaglia et al. 2011; de Jong et al 2013; Rodin et al 2015; Javanmardi et al. (2017). A summation of these references and a general understanding of vessel disturbances along with dependencies is described in the follow paragraphs.

Water surface disturbances generated by a moving vessel create pressure gradients. As a vessel with forward motion displaces water a pressure gradient is formed at three locations, the bow, midship, and the stern. These pressure gradients are a function of relative change in water velocity induced by the vessel. The bow of the vessel causes water to abruptly change direction and speed creating a pressure gradient and will always be a function of vessel speed and hull geometry. A second gradient along the side of the vessel, also a function of vessel speed, is of lesser magnitude than the bow gradient but can be further exacerbated as a function of bathymetry or channel cross-section. As water passes the stern of the vessel a second positive pressure gradient is formed as the water changes direction and speed once more to return the free surface to equilibrium. These gradients cause the free surface elevation to rise at the bow and to a lesser magnitude at the stern while creating a negative free surface elevation at midship. As a result, the change in free surface elevation creates two patterns of surface oscillations (diverging and transverse waves) which propagate out from the sailing line. (Havelock, 1908)

Magnitude of VGWE can be assimilated to the formation of pressure gradients such that it is proportional to relative vessel speed, inversely proportional to channel cross-section area, and a complex function of hull geometry typically described using vessel dimensions, displacement, and the blocking coefficient. The root of these dependents are shown in Equation 1. Other less significant contributions usually described through coefficients in regression equations or “noise” in field studies could be derived from vessel asymmetry in a confined channel, vessel heading vs. course over ground (yaw), direction of propeller rotation, and vessel asymmetry with respect to free surface elevation. For this study only the variables described in Equation 1 will be considered in addition to those as dictated by published methodologies used in this study.

$$VGWE = f(V, L, B, D, C_b, d_c, x) \quad (1)$$

Where:

V = Vessel Speed, L = Vessel Length, B = Vessel Beam, D = Vessel Draft, C_b = Blocking Coefficient, d_c = Channel Depth, x = perpendicular distance from sailing line

Wave energy generated at the sailing line propagates laterally based on the Kelvin wave theory (Thompson 1887), shown in Figure 5. Notably and relevant, Havelock (1908) showed the magnitude of the diverging wave cusp line intercept points are inversely proportional to the cube root of distance from the bow, and the transverse wave magnitude is inversely proportional to the square root of the perpendicular distance from the sailing line. This decay, however, is only applicable for deep-water waves and does not include energy losses as a result of shoaling, breaking, and channel cross-section.

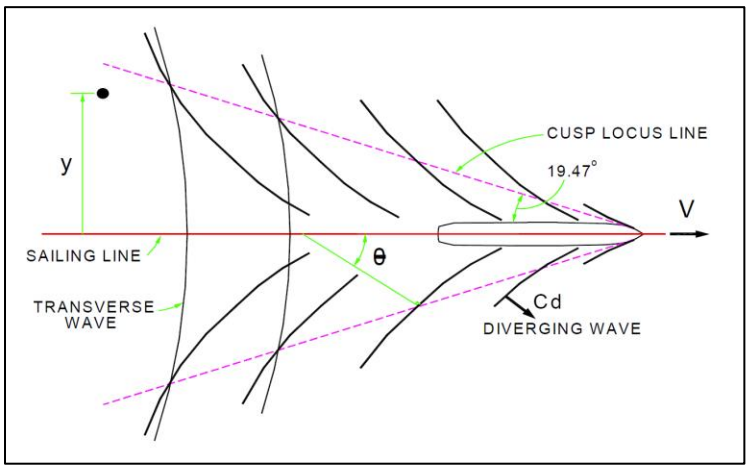

Figure 5: Definition sketch of vessel disturbance in plan-form described by Havelock (1908).

Using the depth-based Froude number, F_d, defined by Equation 2 effects on diverging waves would be evident at values greater than 0.56 and significantly affected for values greater than 0.70 (Sorensen, 1973). Transverse waves have a longer wave period and therefore will begin feeling the bottom sooner. As a result, the wave crest angle of the diverging wave will approach 90 degrees to the sailing line as the Froude number approaches unity due to the increased wave celerity using linear wave theory.

$$F_d = \frac{V}{\sqrt{g d_c}} \quad (2)$$

In general, wave energy generated by a vessel in a semi-confined channel, observed through measurement of the free surface, can be described as a large asymmetrical trough with little to no amplification above the still water surface or undulating pattern; as the disturbance propagates away from the sailing line, up the channel side slopes and into shallow water the free surface begins to respond. The small crest preceding the trough is traveling at a higher celerity and tends to decay as a function of distance from the sailing line. The trailing end of the larger trough begins to steepen as smaller, high frequency, oscillations moving at a higher celerity attempt to overtake the larger trough. Further from the channel the magnitude of the trough decays as the trailing oscillations slightly grow in magnitude and duration then begin to decay in magnitude but further increasing duration. The non-linear characteristics (asymmetric trough) of the initial vessel generated disturbance are of particular interest.

Linear wave theory is historically used for describing vessel generated disturbances (Havelock, 1908; Sorensen, 1973; Kriebel and Seelig, 2005). However, more recent investigations show the traditional kelvin wedge is often inadequate to describe vessel disturbances in detail for complex bathymetry, as the case for Mobile Bay. Several weak to fully non-linear approaches typically referred to as surge, rouge, and tsunami have been investigated such as the Boussinesq-type solutions (Bernoulli wake) (Jiang et al. 2002; David et al. 2017), modified Kadomtsev-Petviashvili (KP) equations for multi solitonic waves (Soomere, 2006), Riemann (simple) waves of depression (Rodin et al. 2015), and Korteweg-de Vries equations (Pelinvovsky et al, 2001). Each method or theory involves some form of application based on the Froude number relationship. Most define an inflection point between 0.5 and 0.7 for transcritical speeds. Where events having a Froude number less than 0.5, in certain instances, can weakly be associated with linear wave theory for initial generation and propagation from the sailing line. However, linear wave theory becomes less valid for Froude numbers in the transcritical speed regime ($F > 0.5$).

An important note in the application of non-linear wave theories is rate of decay a lateral distance from the sailing line can be far less than assumed using linear wave theory (Soomere, 2006). Observations of vessel generated disturbances at large distances can be seen in Mobile Bay and have been documented in other sheltered estuaries and harbors with deep draft navigation such as Venice Lagoon, Italy (Parnell et al. 2015). A full understanding of the non-linear propagation is not considered in this study but could be considered in future work.

2 Field Investigation

Field Stations

Data were collected at 5 stations between 18 November 2017 and 19 January 2018 (62 days). VGWE was measured identically at all stations using a pressure sensor. Stations, shown in Figure 6, were located in the upper reach of the bay at a latitude around 30.55º. Four stations were located north of Gaillard Island and west of the federal navigation channel and one east of the channel. Station locations were based on availability of existing infrastructure to affix instrumentation. Station details are provided in Table 1.

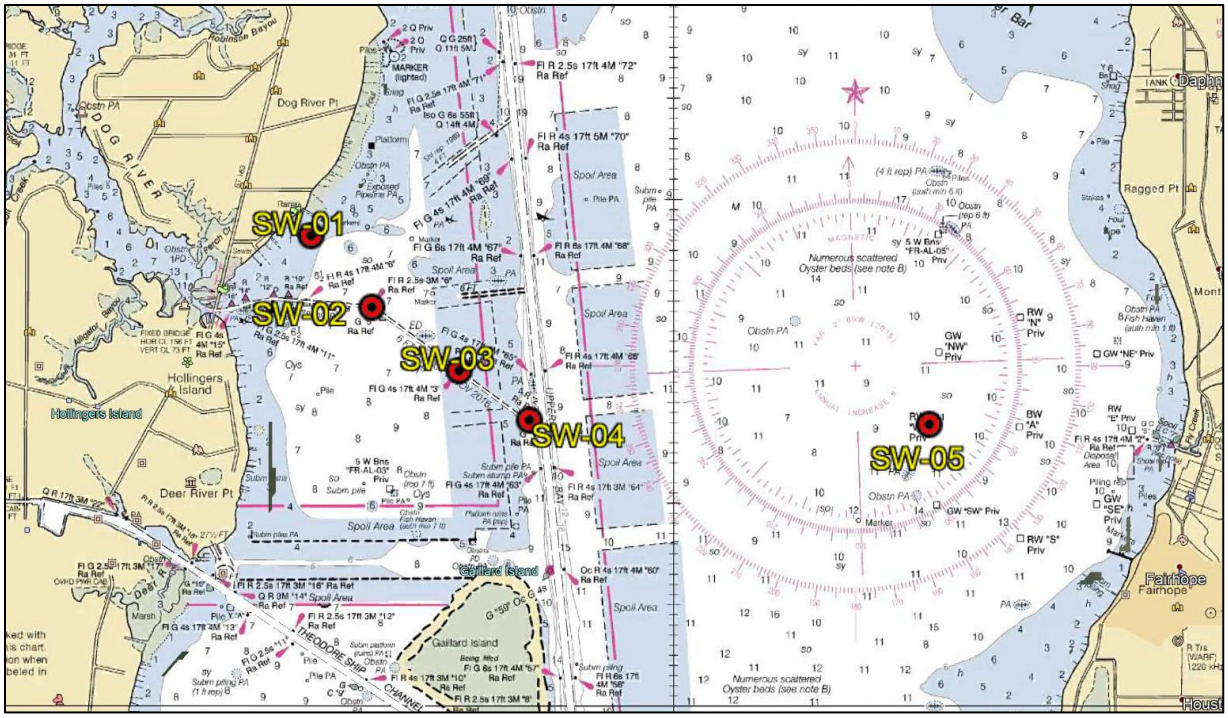

Figure 6: Map of Station Locations

Pressure sensors are manufactured by RBR Limited with a published pressure range of 20 meters, accuracy of +/- 0.05% full scale, and resolution of <0.001% (full scale) (RBR Limited, 2012). Sampling rate was set at 8 Hz and collected in bursts of 32,768 samples or 4,096 seconds followed by a rest period of 104 seconds to process and store data then repeated for the duration of the sampling campaign. A screen shot from the sensor software of the typical setup is shown in Figure 7. The sampling scheme produced a near continuous record for identifying the transient non-ergodic nature of VGWE. Raw data are stored as absolute pressure. Conversion to water surface elevation is completed internally based on pressure attenuation in the water column.

Table 1: Station Details

Station ID	Latitude	Longitude	Mean Water Depth, h (m)	Distance From Channel, x (m)	Sensor Serial Number
SW01	30.57770	-88.06896	2.13	3890	041460
SW02	30.56592	-88.05732	2.68	2890	041458
SW03	30.55550	-88.04062	2.6	1420	041456
SW04	30.54739	-88.02719	4.67	230	041459
SW05	30.54665	-87.97071	3.84	7080	041461

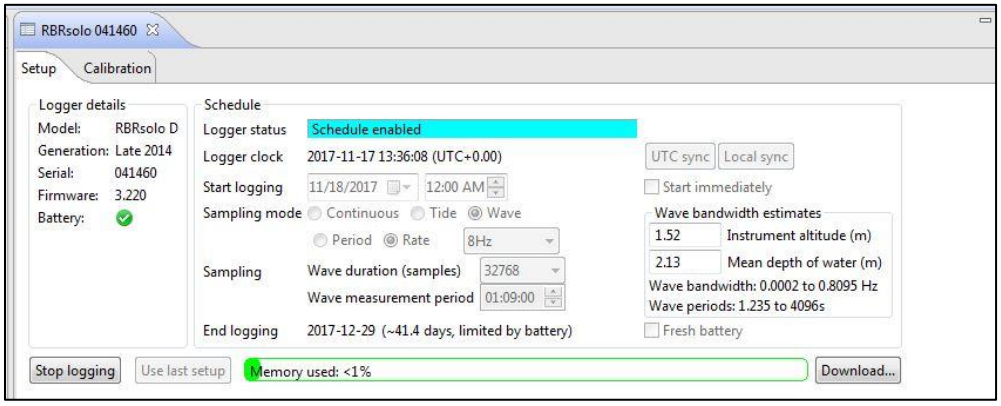

Figure 7: Typical Pressure Sensor Setup

Sensors were affixed to existing infrastructure (wooden piles) using a mount composed of rigid electrical conduit allowing the sensor to be mounted from above water and stand off the pile approximately 150 mm, see Figure 8. This mounting system provided rapid access for servicing and data downloads without requiring a diver, while maintaining a near static position.

Figure 8: Sensor Mounting System and Installation

Valid measurement frequency ranges of a pressure sensor are highly reliant on the vertical positioning in the water column. The goal is to mount the sensor as close to the surface without being exposed during extreme low tides or in this case large drawdown from a passing vessel. This phenomenon is based on the attenuation of orbital velocities and hence pressure with depth. High frequency waves, typically wind waves, attenuate more quickly than low frequency waves and can be unaccounted for in the time series if care is not taken to optimize the deployment. The sensor corrects for depth attenuation by way of the manufacture software based on the vertical location with respect to the seafloor, called altitude, and the mean depth of water. These parameters are shown graphically in Figure 9. The exact methods for attenuation used by the software are beyond the scope of this report but can be found in Gibbons et al. (2015).

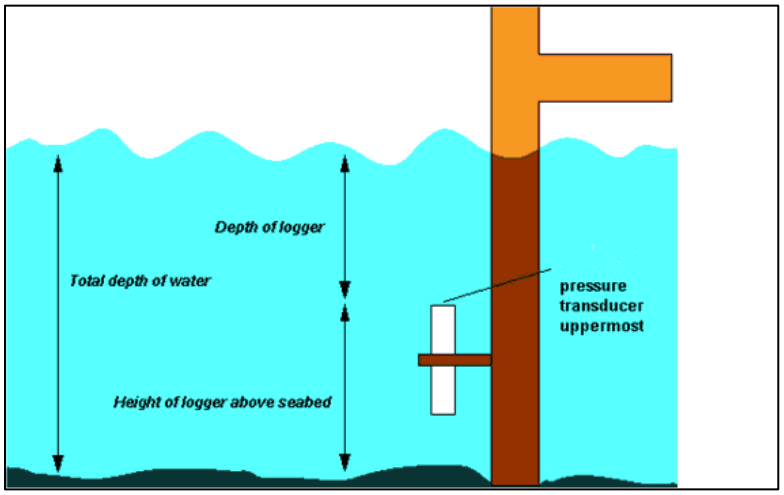

Figure 9: RBR pressure sensor deployment parameters

AIS Data

Starting in 2002 the International Maritime Organization (IMO) began a phased implementation for certain merchant vessels to be fitted with shipborne Automatic Identification Systems (AIS) to enhance safety and efficiency in the maritime environment. The AIS system utilizes Very High Frequency (VHF) signals to transmit and receive vessel data via ship-to-ship and ship-to-shore. A network of shore-based stations are maintained by the U. S. Coast Guard (USCG). These stations receive and store AIS data which can be used in the future. A schematic of the AIS network is shown in Figure 10. Data transmission rates are dynamically based on speed over ground (SOG) and change in course over ground (COG). Average transmission rates for Class A vessels is 3 minutes but can be as fast as 2 seconds. AIS transmissions include three types of data (1) static information, (2) dynamic Information, and (3) voyage related information. (IMO, 2015)

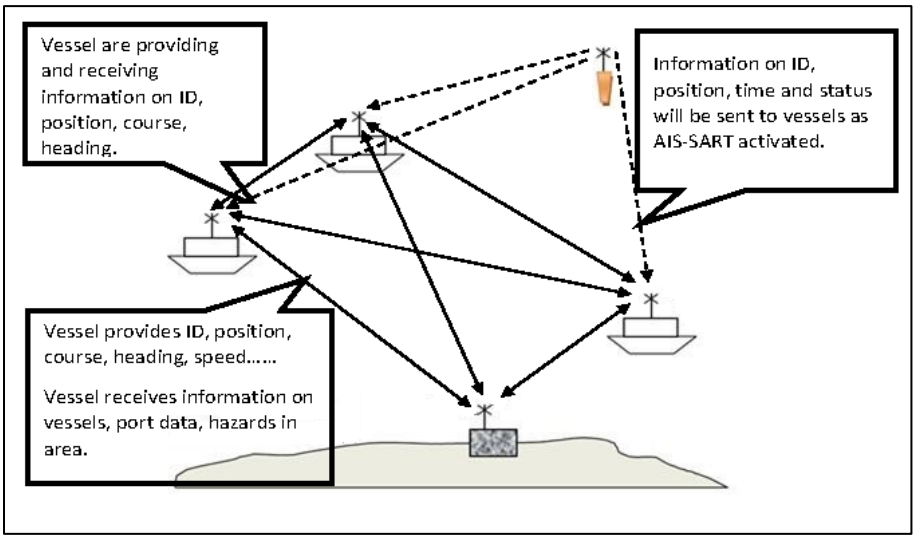

Figure 10: Automatic Information System (AIS) System Schematic. (IMO, 2015)

AIS data were used in this study to identify vessels transiting the channel in the vicinity of the field stations. For the duration of sensor deployment (18 November 2017 – 19 January 2018), AIS data were queried from the USCG via a USACE web portal which down-sampled the data to a constant rate of 5 minutes. Data were exported as vessel reports which includes some static and all dynamic data. Additionally, a single voyage record for each vessel was queried containing the remaining static and voyage data.

The static, dynamic, and voyage data records were coupled using a computer program based on the MMSI number. Continuing in the same program a data structure was created and the vessel length overall (LOA) and width (Beam) was computed based on the static location of the EPFS antenna information. The compiled AIS data were then parsed based on the needs of this study by position, length, and direction with a dependence of time. Transmissions with a position contained

in a bounding box having an upper left coordinate of 30.55919º, -88.02872º and a lower right coordinate of 30.53440º, -88.01940º were extracted. This box was defined based on the vicinity of the field stations and large enough to capture at least one record per transit for a given ship assuming an average speed of 10 knots and a sample rate of 5 minutes. Since AIS data transmission can come from all types and sizes of vessels it was found that a minimum vessel length would be needed to avoid tugs, tows, and non-commercial vessels. A minimum length of 120 m was chosen based on a review of the records and known vessel types to be avoided. Furthermore, vessels less than 120 m are not likely to generate a large enough wave energy signal to be impactful. The last filtering procedure queried within the parsed data to find records with all the same MMSI, direction, and date. If multiple records were found to have the same parameters all but one was parsed. An assumption was made that any one vessel would not transit the channel twice in the same day. This assumption proved accurate except for the Carnival Fantasy where records were manually corrected.

Vessel draft was identified at the beginning of this study to likely have a high dependence w.r.t. the VGWE. The AIS data query used unfortunately did not include the voyage file specific to the transit. Even if the voyage records were correctly attributed to a transit the data is manually entered and reliant on the crew of the vessel. Due to the reliance on vessel draft, this study requested vessel draft recorded by the Mobile Harbor Pilots for the duration of sampling which were compared and attributed to the transits.

The final AIS transit dataset for this study includes 327 records. Data quality checks were completed by randomly sampling and searching publically available data for the vessel record to verify the dimensions and class. All checks returned accurate vessel dimensions however the vessel class (type of ship) was incorrectly reported numerous times. Most incorrect entries were container ships being classified as cargo. In lieu of checking each record a length of 225 m was chosen as a break point between cargo and container vessel, where any vessel classed as cargo greater than 225 m was changed to container. The impact of this assumption could be inaccurately assigning hull geometry in the VGWE computations; however, the risk is warranted in the essence of time efficiency. Impacts to the analysis are assumed to be negligible since VGWE computations are not dependent on vessel class. Table 2 is a summary of the dataset as well as selected statistical values.

Table 2: AIS Dataset Summary Statistics

Vessel Type	Num. Transits	% Fleet	Average Speed (kts)	Average Length (m)	Average Width (m)	Average Draft (m)
Overall	**327**	**100**	**10.57**	**220.1**	**32.34**	**8.96**
Cargo	115	35.17	10.81	173.7	27.62	7.63
Container	117	35.78	10.44	264.4	34.85	10.57
Tanker	61	18.65	9.85	208.9	37.13	8.96
Passenger	28	8.56	11.96	260.9	32.71	8.16
Other	6	1.83	9.50	167.67	23.33	6.63

Measured VGWE Processing Methodology

Continuous pressure data collected at a rate of 8 Hz from the 5 stations over an approximately 2 month duration equated to nearly 200 million data points. The data were imported as a water surface elevation time-series from the instrumentation software interface. From this dataset transient disturbances of short duration associated with vessel transits identified from the AIS record and thus vessel characteristics must be identified. A time dependent window is identified using the AIS data and an approximate celerity of the disturbance. The window size was chosen as 1 hour, which is much larger than the actual disturbance but served two purposes; ensure the complete vessel disturbance is captured and provide a long enough time series to estimate the measured background noise for filtering later in the data processing steps.

The standard, well established, understood, and simplistic method for completing this task is a manual delineation of the time series based on idealized water surface profiles and visual identification of maximum wave height. However this technique is subjective and not replicable for identifying the complete wave packet produced by the vessel; such that a more automated method based on a frequency spectrum would provide a more efficient and systematic approach. Spectrum analysis using a discrete Fourier transform results in a frequency domain while useful for ergodic (time-invariant) signals it is not applicable for identifying vessel generated disturbances (non-ergodic) within a larger time domain. To apply spectral analysis to a transient signal the Fourier transform can be computed in a time-frequency domain (i.e. compute Fourier transformation incrementally over the time domain). Alternatively, wavelet base transformations are similar to a Fourier base transform but defines transient and singularities using piecewise sparse representation of regular signals where coefficients are a function of the beginning and end points in small domains as well as sharp irregularities. Wavelet transformations are used widely in one-Dimensional signal processing for harmonics like audio and vibration data sets as well as two-Dimensional image processing but examples in literature for application to water waves is limited or non-existent (Chuang et al, 2013; Didenkulova et al, 2013; Sheremet, 2013).

Wavelet computations use various methodologies where a secondary but equal time dependent function, *f(t)*, is transformed over the time domain integral using dilation, time shift, or windowing; then summed over the time domain compared to the original *f(t)* in a time dependent integral over the frequency domain which creates larger coefficients across the time domain as a function of frequency modulation or a sparse representation. Wavelets for signal processing are described in more detail by Mallet (2009). A continuous wavelet transformation (CWT) variant (dilation) of the wavelet theory will be used in this study and is typically referenced in equations as $\psi_{u,s}$, where *u* is the time variable and *s* is the frequency variable. A CWT is well suited to 1 Dimensional, non-ergodic, datasets with sharp changes in frequency that occur in a relatively short time duration. The process can be described as a Fourier transform dilated by *1/s* in the nonzero positive frequency interval centered about a variable η creating a Heisenberg rectangle in the time-frequency plane with a range of (u, η/s) with time and frequency widths, respectively, proportional to *s* and *1/s* such that a variation of *s* will vary the cell size but not the area of the rectangle. This process is shown numerically in Equation 3 and graphically in Figure 11.

$$W f(u,s) = \langle f, \varphi_{u,s} \rangle = \int_{-\infty}^{+\infty} f(t) \frac{1}{\sqrt{s}} \varphi^* \left(\frac{t-u}{s} \right) dt \tag{3}$$

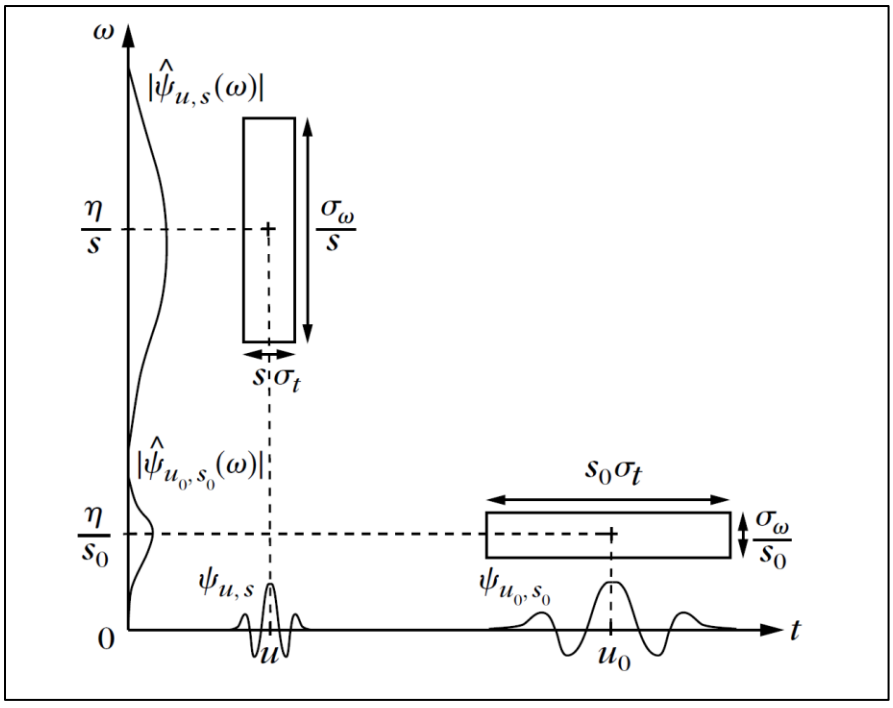

Figure 11: Time-Frequency plane representing scenerios for time variance and frequency variance of the Heisenberg box used in the CWT computation. (Mallet, 2009)

The CWT resultant is a time dependent frequency modulation (time-frequency amplitude) "spike", related to the magnitude of frequency dissimilarity as a function of time, which is used as an identifier to parse the larger amplitude vessel disturbances from the complete time series at each station. Unfortunately, a numerical relationship between the vessel disturbance and the CWT magnitudes is not well understood or easily obtainable and was not used for directly extracting magnitudes of the vessel disturbance. The process for identification of the start and ending points begins by summing the magnitude of all frequency bins (resolution) with respect to the time domain and the resulting plot is demeaned to center about the x-axis of the time series. Demeaning the data is assumed to move lesser peaks of the resultant corresponding to noise below the x-axis. The process then identifies the maximum value and the corresponding location to either side of that maxima where it crosses the x-axis. The corresponding time of this crossing is used as the bounds and the inner data is assumed to contain the entire vessel generated disturbance. An ideal example of this process is shown in Figure 12.

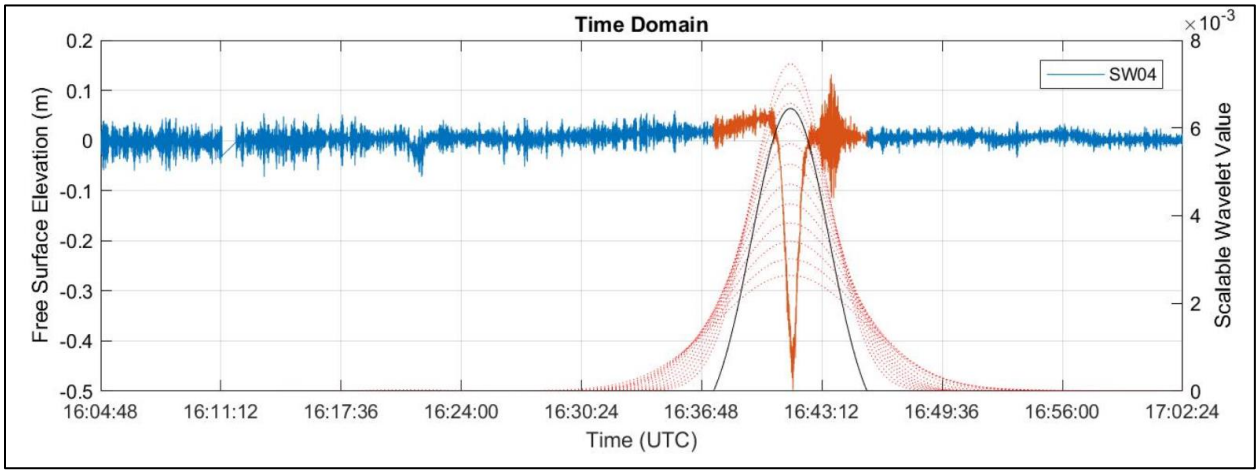

Figure 12: Ideal case of CWT used for automatic identification of a vessel generated disturbance at Station SW04, Event ID: 259 for an inbound traveling vessel with dimensions of L = 229 m, B = 32 m, D = 13.7 m. The orange highlighted area is the signal assumed to be generated by the vessel.

Total energy density is rarely used to describe vessel disturbances. A majority of models compute the maximum vessel generated wave height, which is a good identifier and easily obtainable from a time series wave record, and some use a proxy for wave energy, *E*, based on the peak wave computed using Equation 4 which is based on linear wave theory and the resultant is a measure of Energy per unit crest width.

$$E = \frac{\gamma_w H^2 L}{8} \tag{4}$$

This study requires a quantifiable method to evaluate the total energy density imparted by the vessel to the water column and subsequent propagation from the sailing line to potentially impacted sites (i.e. shorelines) for adequately determining the totality of impacts investigated. The challenge for describing vessel disturbances as energy density as defined in linear wave theory is defining the length of record for an event in a repetitive method. It has been suggested to base the energy of each event on a percent of the waves within the record (Sorensen 1997) which is a good method if the record is processed using the simplistic wave train method. However, a more inclusive approach would use spectral analysis to describe the energy density in a repeatable manner.

Frequency spectrums for each event at each station were determined using a fast Fourier transform computed on the extracted time series obtained from the CWT analysis. This spectral analysis allows the energy density or in other words the spectrally significant wave height H_{mo}, to be computed by summing the area under the spectral energy curve. This method is widely used and accepted in the coastal engineering community and recommend by the Coastal Engineering Manual (2006) (CEM). H_{mo} is known as the equivalent deep water wave height. A transformation of this value to a shallow water wave height was found to create unnecessary error in the results due to multiple dependencies on origin, non-linearity, and environmental forcings. All other values describing the water surface profile in the study use the spectrally significant wave height as well which eliminates the bias within the dataset.

A summary of the data processing methodology is provided in the following logical steps.

I. Automated Vessel Identification (AIS)

1. Query and download data from USCG for the period of data collection (18Nov2017 - 19 Jan18).
2. Filter reports using an AOI box over the channel in close proximity to the instrumentation stations.
3. Parse filtered reported based on direction, date, and vessel so only one report will be kept for each unique vessel transit.
4. Associate vessel characteristics with the reports based on the MMSI number
5. Verify and correct drafts for each report using observed drafts obtained from the harbor pilots.
6. Filter events for vessels to return only those greater than 120 meter in length
7. Complete a quality check of data and format.

II. Vessel Generated Wave Energy (VGWE)

1. Download continuous attenuation corrected WSE time series from instrumentation and format.
2. Define a 1 hour time window for each AIS event.
3. Identify the vessel disturbance using the CWT method.
4. Compute the frequency spectrum using a fast Fourier transformation.
5. Compute the statistically significant wave height, H_{mo}, for each event at each station by summing the area under the frequency spectrum curve.

Results

Vessel generated wave energy (VGWE) was computed for 327 transits of vessels greater than 120 meters in length at 5 stations in Mobile Bay north of Gaillard Island. Average VGWE represented as the statistically significant wave height, H_{mo}, is provided in the following tables grouped by station and length (Table 3), draft (Table 4), transit direction (Table 5), and vessel speed (Table 6). These tables may be used to compare relative differences between measurement sites and are discussed later in this study for evaluating the relationship, holistically, with respect to vessel and transit characteristics. VGWE tabulated for each transit as well as selected AIS vessel attributes is provided in Appendix A. It should be noted, background energy density has not been filtered from any of the measured data reported unless otherwise specified.

Table 3: Average H_{mo} (VGWE) at each station categorized by vessel length

Station ID	All Vessels	Length, L (m)			
		L < 175 m	175 < L < 225	225 < L < 275	L > 275 m
SW01	0.0050	0.0026	0.0037	0.0063	0.0069
SW02	0.0084	0.0036	0.0058	0.0105	0.0132
SW03	0.0252	0.0102	0.0170	0.0276	0.0504
SW04	0.0442	0.0165	0.0278	0.0503	0.0887
SW05	0.0069	0.0055	0.0067	0.0078	0.0067

Table 4: Average H_{mo} (VGWE) at each station categorized by vessel draft

Station ID	All Vessels	Draft, D (m)			
		D < 5	5 < D < 8	8 < D < 11	D > 11
SW01	0.0050	0.0009	0.0056	0.0067	0.0041
SW02	0.0084	0.0011	0.0100	0.0117	0.0072
SW03	0.0252	0.0091	0.0316	0.0317	0.0299
SW04	0.0442	0.0106	0.0566	0.0529	0.0611
SW05	0.0069	0.0032	0.0073	0.0075	0.0071

Table 5: Average H_{mo} (VGWE) at each station categorized by transit direction

Station ID	All Vessels	Inbound	Outbound
SW01	0.0050	0.0064	0.0036
SW02	0.0084	0.0111	0.0058
SW03	0.0252	0.0269	0.0234
SW04	0.0442	0.0456	0.0428
SW05	0.0069	0.0077	0.0060

Table 6: Average H_{mo} (VGWE) at each station categorized by speed

Station ID	All Vessels	Speed, V (kts)			
		V < 8	8 < V < 10	10 < V < 12	V > 12
SW01	0.0050	0.0014	0.0027	0.0048	0.0099
SW02	0.0084	0.0017	0.0031	0.0086	0.0175
SW03	0.0252	0.0051	0.0135	0.0316	0.0277
SW04	0.0442	0.0173	0.0298	0.0546	0.0447
SW05	0.0069	0.0050	0.0073	0.0071	0.0069

Background wave energy was computed using a 1 hour time series bracketing the identified VGWE and associated with wind speed and direction data obtained from NOAA station 8736897 located approximately 10 km north of the field stations at U.S. Coast Guard Sector, Mobile, Alabama. A comparison of the measured background energy at each station with the wind speeds obtained from NOAA Station 8736897 is provided in Figure 13 where the horizontal axis is indexed by vessel transit event ID. Figure 7 is the average VGWE measured at each station categorized by recorded wind speed at NOAA station 8736897.

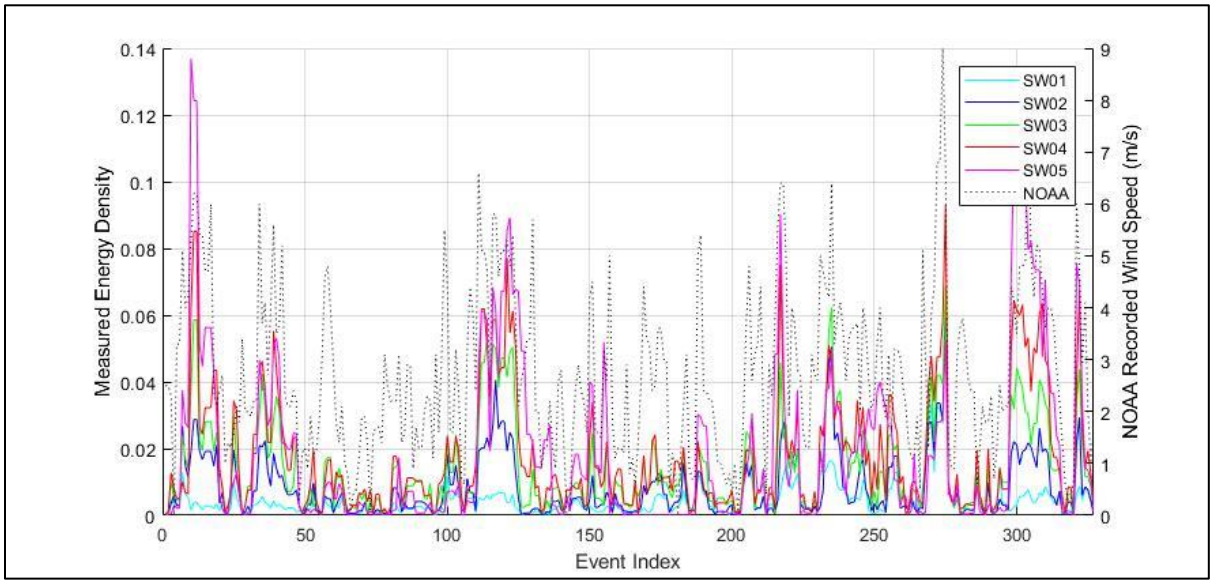

Figure 13: Comparison of measured background energy density measured at each station with the recorded wind speeds at NOAA station 8736897. The horizontal axis is indexed by vessel transit event ID.

Table 7: Average H_{mo} (VGWE) at each station categorized by wind speed recorded at NOAA station 8736897

Station ID	All Vessels	NOAA Recorded Wind Speed, V_w (m/s)			
		$V_w < 1$	$1 < V_w < 3$	$3 < V_w < 5$	$V_w > 5$
SW01	0.0050	0.0047	0.0045	0.0052	0.0070
SW02	0.0084	0.0071	0.0082	0.0085	0.0108
SW03	0.0252	0.0220	0.0267	0.0215	0.0304
SW04	0.0442	0.0378	0.0446	0.0386	0.0618
SW05	0.0069	0.0017	0.0034	0.0102	0.0188

Discussion and Data Quality

This study obtained measured VGWE for 327 vessel transits at 5 stations in Mobile Bay, Alabama based on standard, accepted, field data collection methods as well as a unique and novel post processing approach using a CWT method for VGWE demarcation. Field data are a valuable resource when properly used within bounds of the methods used to collect the data. As with any field data collection and processing, the quality and applicability should be examined. Field data are especially susceptible to poor quality and use in excess of the data collection methods. A thorough evaluation of data using expected theoretical results and comparison with any existing available data is good practice. The following paragraphs will discuss applicability of the methods,

examine data quality, and compare the field data collected in this study with expected results based on literature and theory.

The CWT method for automated identification of the vessel disturbance was efficient for this study since it involved a large number of vessel transits over long time series datasets. However, no quantitative analysis of the accuracy was completed, but observations tend to show the accuracy decreasing further from the channel. As vessel disturbances propagated SW03 and SW04 appeared more accurate than SW01 and SW02, while SW05 appears to contain the most inaccuracy. Sources of this error are a result of the numerical computation of the CWT as a function of the magnitude of background frequencies, the magnitude of the vessel disturbance, demarcation of the VGWE methods, and the width of the time window used to identify the vessel disturbance. The CWT method used in this study assumed the background frequencies and the vessel disturbance frequencies are dissimilar. If this assumption is violated the ability to identify the vessel disturbance decreases. Two examples of potential inaccurate identification are shown in Figure 14: Examples of possible inaccuracies using CWT method for extracting vessel disturbances from station time series; (upper) Event ID: 8, SW05, outbound, L = 176m, B = 35m, D = 5.8m; (lower) Event ID: 24, SW02, inbound, L = 228m, B = 42m, D = 12.2m

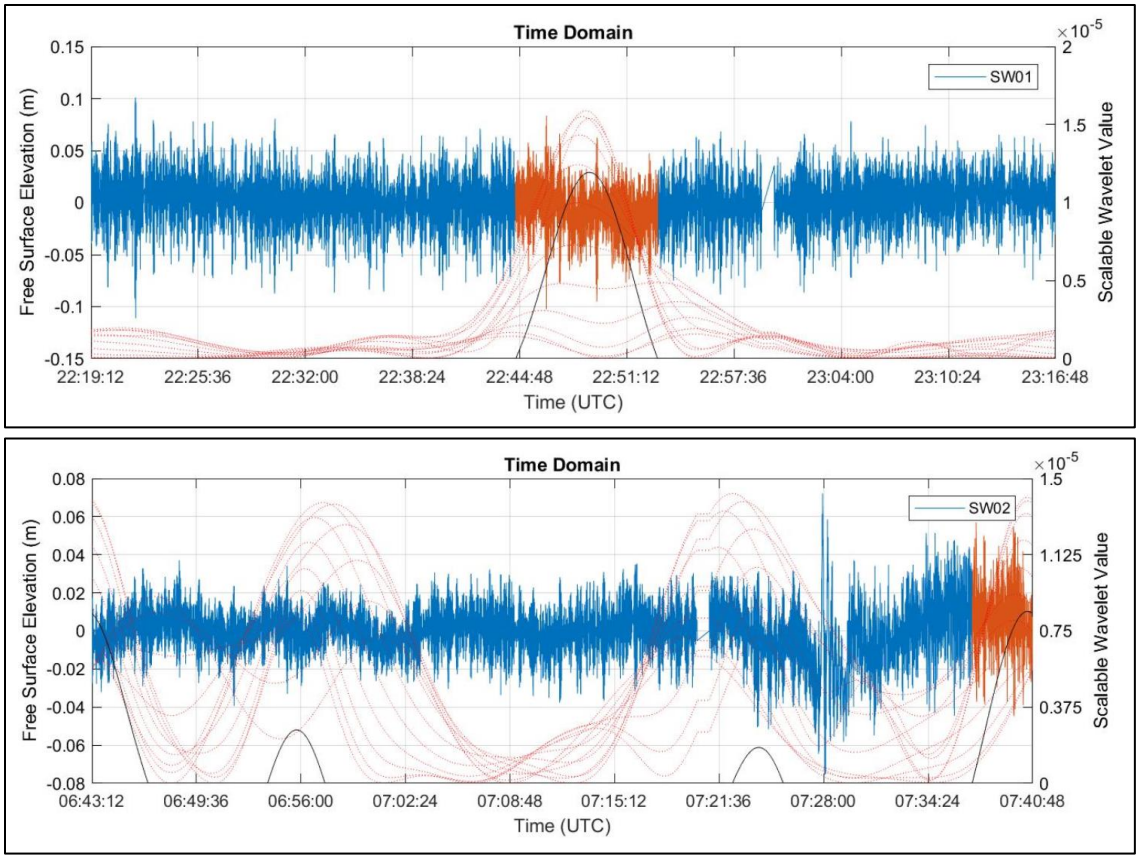

Figure 14: Examples of possible inaccuracies using CWT method for extracting vessel disturbances from station time series; (upper) Event ID: 8, SW05, outbound, L = 176m, B = 35m, D = 5.8m; (lower) Event ID: 24, SW02, inbound, L = 228m, B = 42m, D = 12.2m.

Multiple vessels transiting the channel in intervals less than 1 hour creates a second problem, when applying the CWT methods of identification. Pilots in Mobile Harbor are known to schedule multiple vessels traveling inbound or outbound within close proximity (Figure 15). And using the larger window can capture more than one vessel disturbance. The logical sequence in the automated CWT identification program does not account for this phenomenon. Since the program is only looking for the highest magnitudes of the frequency modulation (dotted red lines and black line in Figures 14-18), it can associate larger vessel disturbances with smaller vessels. While this is an inaccuracy the implications are conservative, therefore a solution is not considered for this study but could be addressed in future work.

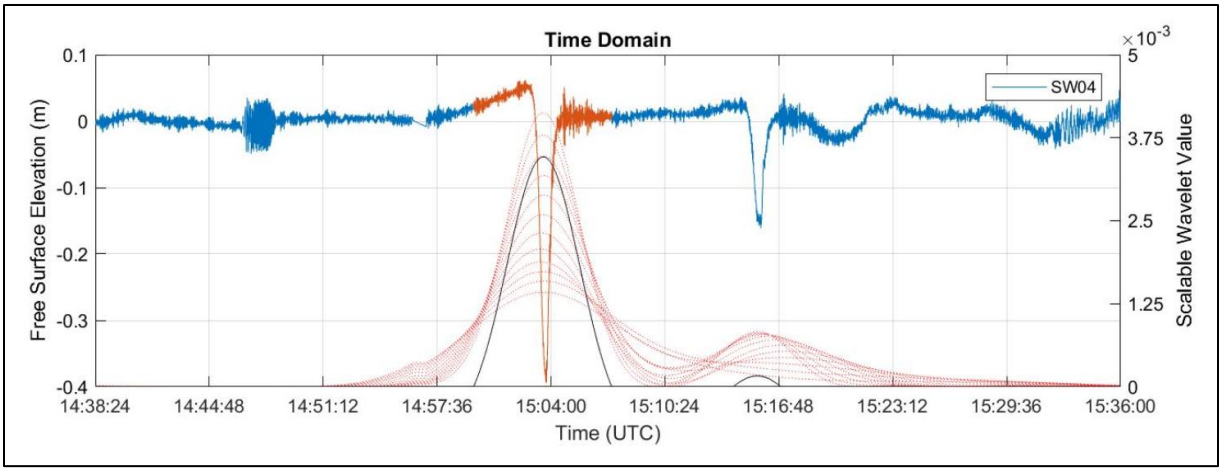

Figure 15: Multiple vessel transits with small time intervals between events.

A final observation to be noted from the CWT identification methodology is the potential for not capturing the entire VGWE signature. Again, no quantified investigation of this error was completed in the study but the error is observed more often for stations SW01, SW02, and SW05 which are farther from the sailing line. An example of this error is shown in Figure 16.

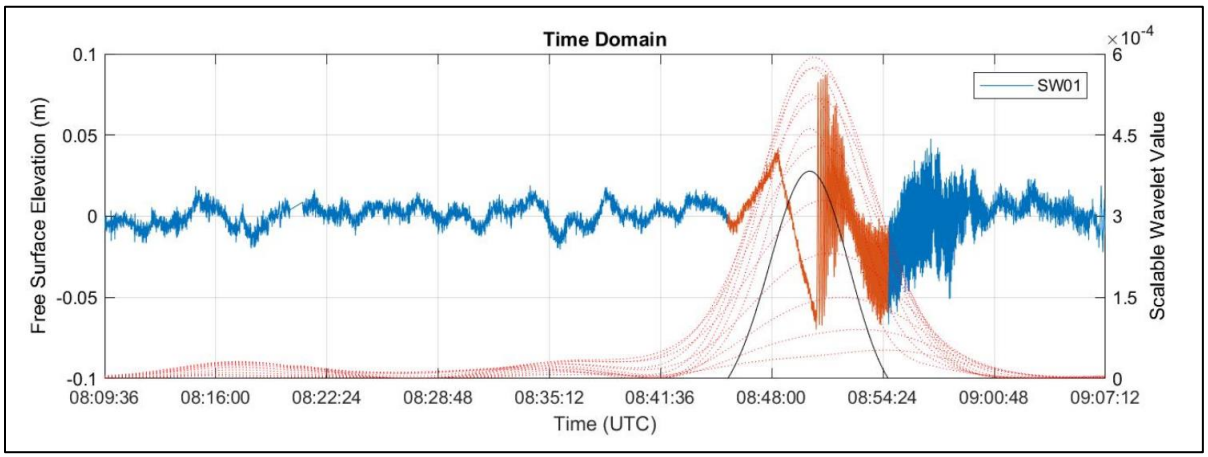

Figure 16: Vessel Generated Wave Energy (VGWE) partial identification error using the continuous wavelet transformation (CWT) method. Event ID: 203, SW01, outbound, L = 228m, B = 32m, D = 8.1m.

Quantifying the VGWE for each event at each station was completed using a fast Fourier transformation (FFT) which computed the frequency distribution, or sum of the sine waves, over the time series identified with the CWT method. The FFT provided a way to characterize the vessel disturbance by the energy density which enabled a similar and repeatable method for describing the total VGWE instead of subjective observations of the maximum wave height. Figure 17 is an example of the CWT identification method and resulting FFT for computing the frequency distribution.

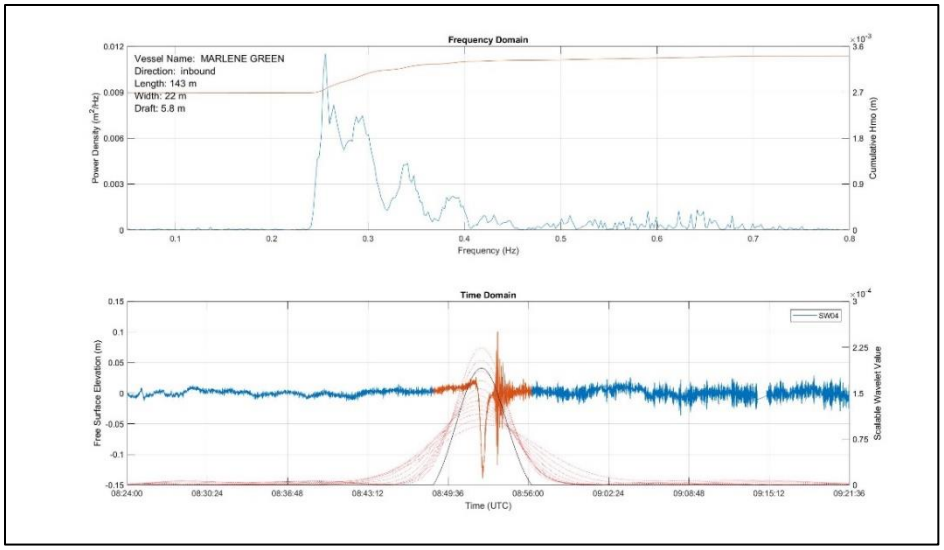

Figure 17: Vessel generated wave energy (VGWE) identification using a continuous wavelet transformation (CWT) (bottom) and frequency distribution using a fast Fourier transformation (FFT) for an ideal vessel transit event.

Figure 17 shows the distribution of frequencies in the range expected for a vessel disturbance with the peak frequencies greater than 0.05 but less than 0.4 Hz or wave periods of 2.5 to 20 seconds. The remaining higher frequencies are likely a result of the background wind-wave energy in the system or remnant disturbance of the vessel transit. However, Figure 17 is an ideal case of the CWT methodology and little background noise.

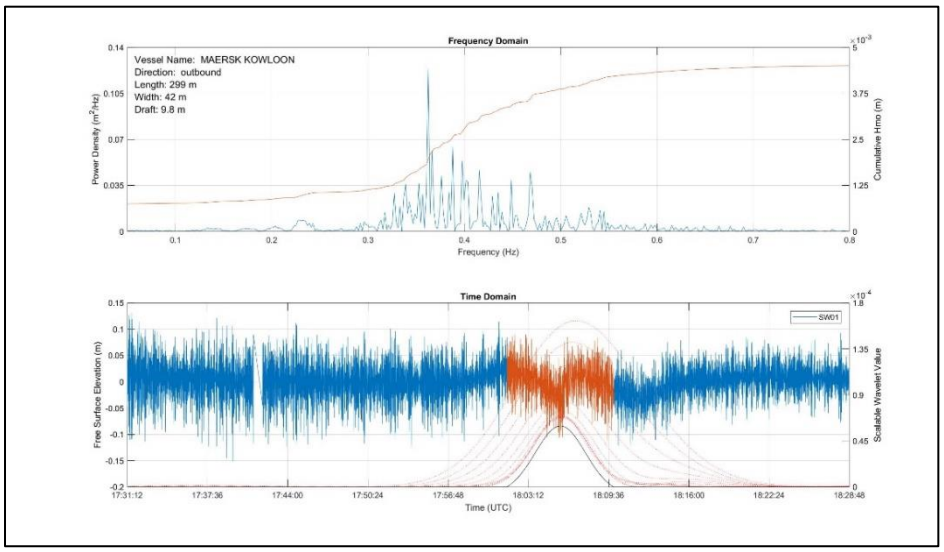

Figure 18: Vessel generated wave energy (VGWE) identification using a continuous wavelet transformation (CWT) (bottom) and frequency distribution using a fast Fourier transformation (FFT) for a case of high background wave energy with respect to VGWE.

Figure 18 represents a case of high background noise relative to the VGWE. While the CWT was able to accurately identify the VGWE signature the FFT does not appear to easily delineate the frequency distribution. The peak of distribution is located within the range of VGWE as well as a large percentage of the distribution being less than 0.4 Hz but without further investigation it would be difficult to definitively quantify the VGWE from the background energy. Due to the uncertainty caution should be used when utilizing VGWE values when the difference in magnitude of the background energy is relatively small.

VGWE propagating from the channel undergoes a transformation as a result of the interaction with bathymetry, background wind-wave energy magnitude and direction, and instabilities (non-linearity) of the signal. A detailed description of vessel generated wave transformation from a semi-confined channel is provided in the introductory theoretical background. Figure 19 is an example of that transformation across all sites.

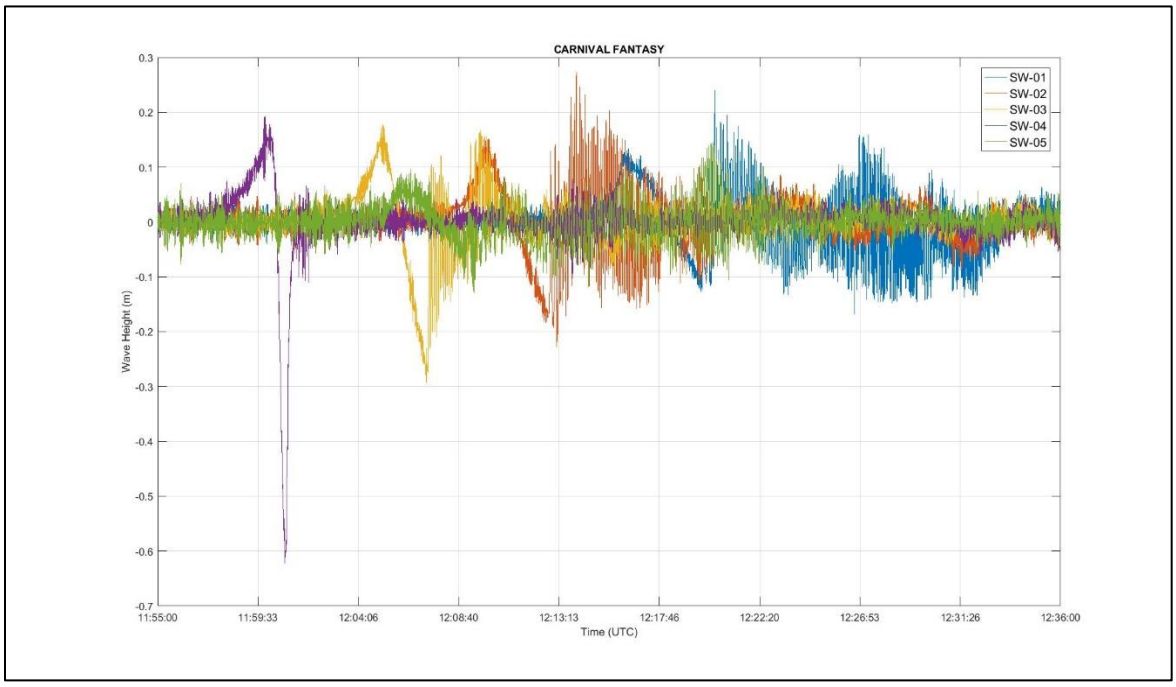

Figure 19: Example of vessel generated disturbance transformation of the free surface elevation as a function of distance from the sailing line

Several interesting, unique, and expected results are observed in Figure 19. At the station closest to the sailing line, SW04, a large asymmetric trough is observed with the leading positive surge, as the wave travels in time and spatially from the sailing line the magnitude of the trough decreases and a series of shorter period waves begin to trail the larger trough. At SW02 and further to SW01 the trough is further reduced and the trailing short period waves increase duration; however, the magnitude of trailing short period waves in SW01 is less than SW02. The leading trough in SW05 (furthest from the sailing line and opposite side of the channel) follows the same trending decay

and similarly the elongated duration of the trailing short period waves. Interestingly, the magnitude of the leading positive surge wave does not decay at the same rate as the primary trough. Surprisingly, the transformation shown in Figure 19 follows the expected theoretical decay of vessel generated disturbances. This finding confirms that regardless of the potential shortfalls in the data processing using the CWT and FFT method the time series data quality is sufficient and could be used independently for future analysis utilizing other data processing methods.

Individually, the data processing steps contain errors and in no way should those errors be discounted but as a whole the resulting VGWE should be evaluated by comparison with expected theoretical trends and dependencies. As previously mentioned this study is not intended to gain a complete and full understanding of the generation and propagation of VGWE, whereas this study intends to use data density as a way to minimize the effects of data error for the analysis. A means to determine if sufficient data density has been achieved the cumulative data measured will be compared with expected trends and more specifically the propagation of VGWE from the sailing line.

Already shown in Figure 19 the decay of VGWE as a function of distance from the sailing line is shown. However, this is a single idealized event and not necessarily representative of all transits. To better understand the cumulative data Figure 20 shows a relationship of VGWE measured over the four stations located to the west of the sailing line and the trend within each event by connecting the respective VGWE value at each station for a vessel transit.

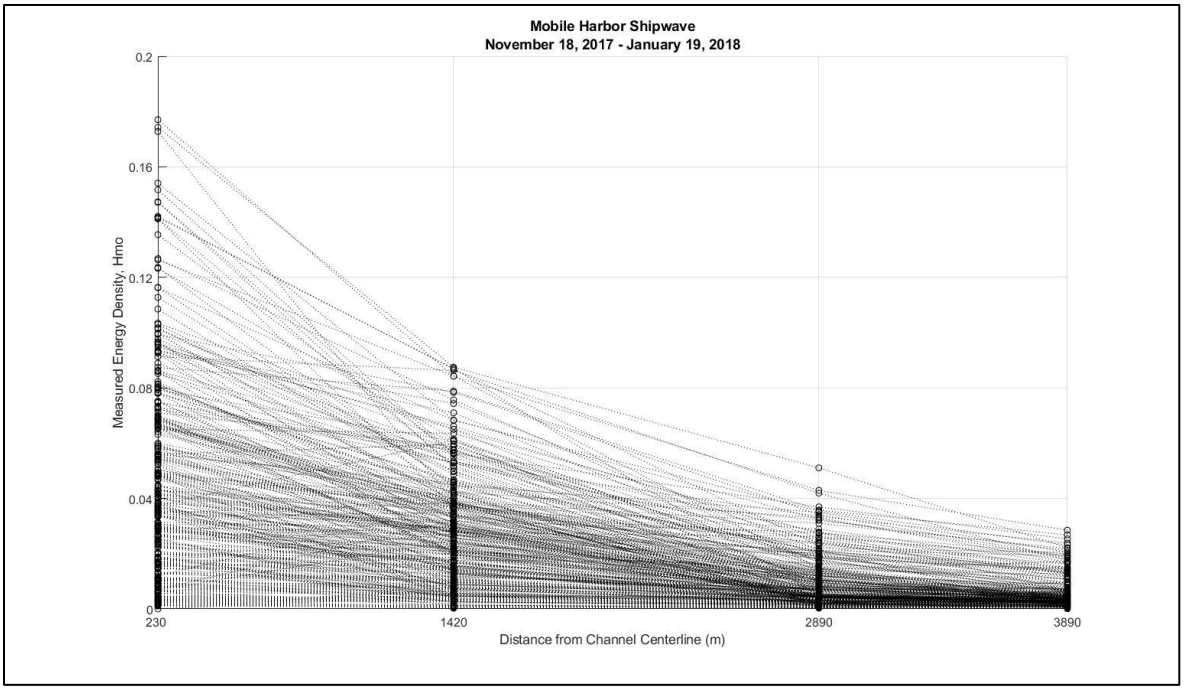

Figure 20: Measured vessel generated wave energy (VGWE) verses distance from the sailing line with respect to individual events.

The theoretical decay of VGWE as a function of distance from the sailing line in deep water is said to be, $x^{-0.333}$, where x is the distance from the sailing line (Havelock, 1908). However, Havelock (1908) did specify a separate exponent of -0.5 for transverse waves and Kriebel and Seelig (2005) measured ranges between -0.25 and -1.5 using field and laboratory data. Observation of Figure 20 appears to indicate the data measured in this study follow a similar trend of exponential decay with an exponent of -0.5 between stations but considerably more variation at SW01and SW02. The variation could be a result of increased shoaling and potentially wave breaking due to water depths decreasing farther from the channel leading to a higher influence of bathymetry; all of which are not considered in the exponential decay model for VGWE.

Figure 21: Observed breaking of vessel generated wake. Photos taken looking west from an outbound tanker on 09 November 2017. Vessel dimension: L = 244 m, B = 42m. Vessel draft on the date of picture was 8.5m. Left picture was 7 km and right picture 4km north of instrumentation stations.

Figure 22: Observed wave breaking of an inbound containership approximately 2 km north of Gaillard Island from aerial imagery collected 06 November 2013. Detailed vessel description is unavailable.

Wave breaking has been observed during operations on transiting vessels and instrumentation servicing. Both pictures in Figure 21 are taken from a large outbound tanker on 09 November 2017 looking west-northwest. During this trip the observed wave breaking diminished and the breaking line moved farther from the vessel as it traveled south to a point where the breaking line was no longer visible just north of Gaillard Island. Figure 22 is aerial imagery captured on 06 November 2013 appearing to show sporadic breaking of the vessel wake produced by a large containership. Details of the vessel are not available. Figure 22 also confirms observations made while servicing instrumentation for this study and unrelated work in the vicinity north of Gaillard Island but south of the instrumentation stations. Observed wave breaking is not immediately discernable in Figure 20 for VGWE decay across the stations; however, measured data from this study were processed using a wave train analysis where vessel generated significant wave heights, H_s, (Figure 23) show a general increase in magnitude for a majority events at station SW03. This is indicative of wave

breaking and should be considered when describing VGWE propagation from the sailing line. Capturing the potential wave breaking phenomenon in the significant wave height is interesting. It also supports the use of the data processing methods described in this report in lieu of the more standard wave train approach. While future work may investigate the implication of wave breaking on VGWE to a further detail, for the study it is noted but not warranted.

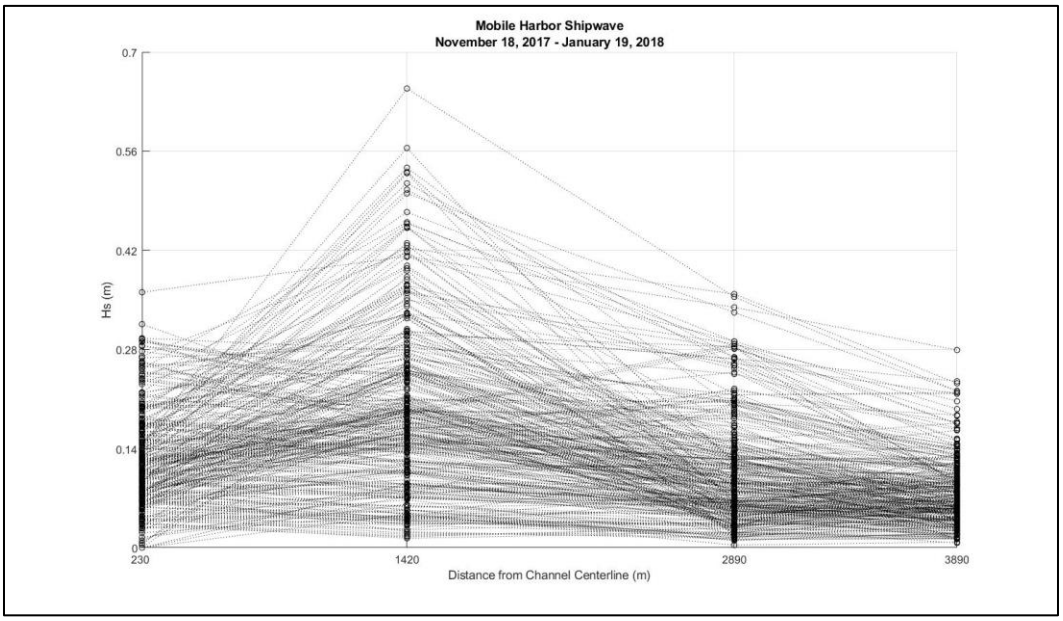

Figure 23: Vessel generated significant wave height computed using a wave train analysis verses distance from the sailing line with respect to individual events.

A secondary cause of increase of significant wave height from station SW04 to SW03 in Figure 23 is the data collection method and the manner in which the VGWE propagates over the initial distance from the sailing line. Observation while servicing instrumentation suggest the VGWE does not manifest as an undulating free surface prior to reaching SW04. This phenomenon is likely caused by the semi-confined geometry of the channel and the surge effect described in the theoretical background. The wave train method is based on a zero-crossing routine where a wave height is measured based on crossings of the horizontal axis. If undulations or crossings of the horizontal axis are not present it is impossible to quantify the energy within the vessel disturbance.

Most literature cites dependencies on vessel dimensions and speed, as described in Equation 1. Data collected in this study should follow similar dependency trends to be considered valid. VGWE relationship to vessel speed, V, is often the strongest dependency but varies significantly in literature with exponents from 0.587 (Bhowmik, 1975) to around 5.0 (Kriebel and Seelig, 2005) but most are near 2 (Gates and Herbich, 1977; U.S. Army Corps of Engineers, 1980; Blaauw et al. 1985). Vessel speed is typically non-dimensionalized and represented as the Froude Number, F_d, as presented in Equation 2. A relationship of measured VGWE and the Froude number is plotted in Figure 24 and shows a similar dependence as provided in literature. Of interest and importance

to be discussed later is the inflection, or peak, VGWE at a Froude number between 0.45 and 0.50 which is strikingly similar to a nodal point observed by Schoellhamer (1996). Sorensen and Weggel (1984) also identified a point within the Froude number range where the functional relationship changes but slightly higher. The relevance of this nodal point is the transition from subcritical to transcritical speed. It should be noted that vessel speed is reported as whole numbers. With the high dependency on vessel speed it would be advantageous to compute vessel speed from the AIS reports data to further resolve the inflection point observed in Figure 24 during future work with this data.

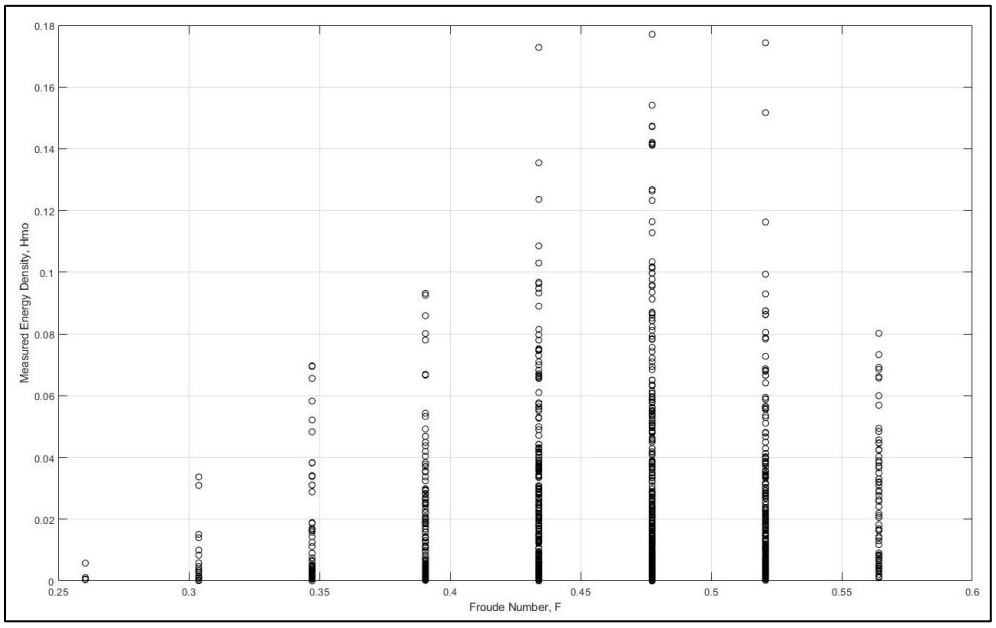

Figure 24: Measured vessel generated wave energy verses the depth based Froude number for all stations.

Vessel length is commonly referenced in published models as being a function of the VGWE to varying degrees (Sorensen, 1997). Most models in literature imbed the vessel dimension within a secondary parameter or function such as the blocking coefficient, S_c, (defined later in this study) or some other non-dimensional parameter. For simplicity the vessel length, *L*, and draft, *D*, were compared to the measured VGWE independently (Figure 25); vessel width is not shown as there was no distinctly observed relationship. While this simplistic method is difficult to compare directly with existing literature it will provide a relative understanding of the relationships to draw conclusions during the second part of this study.

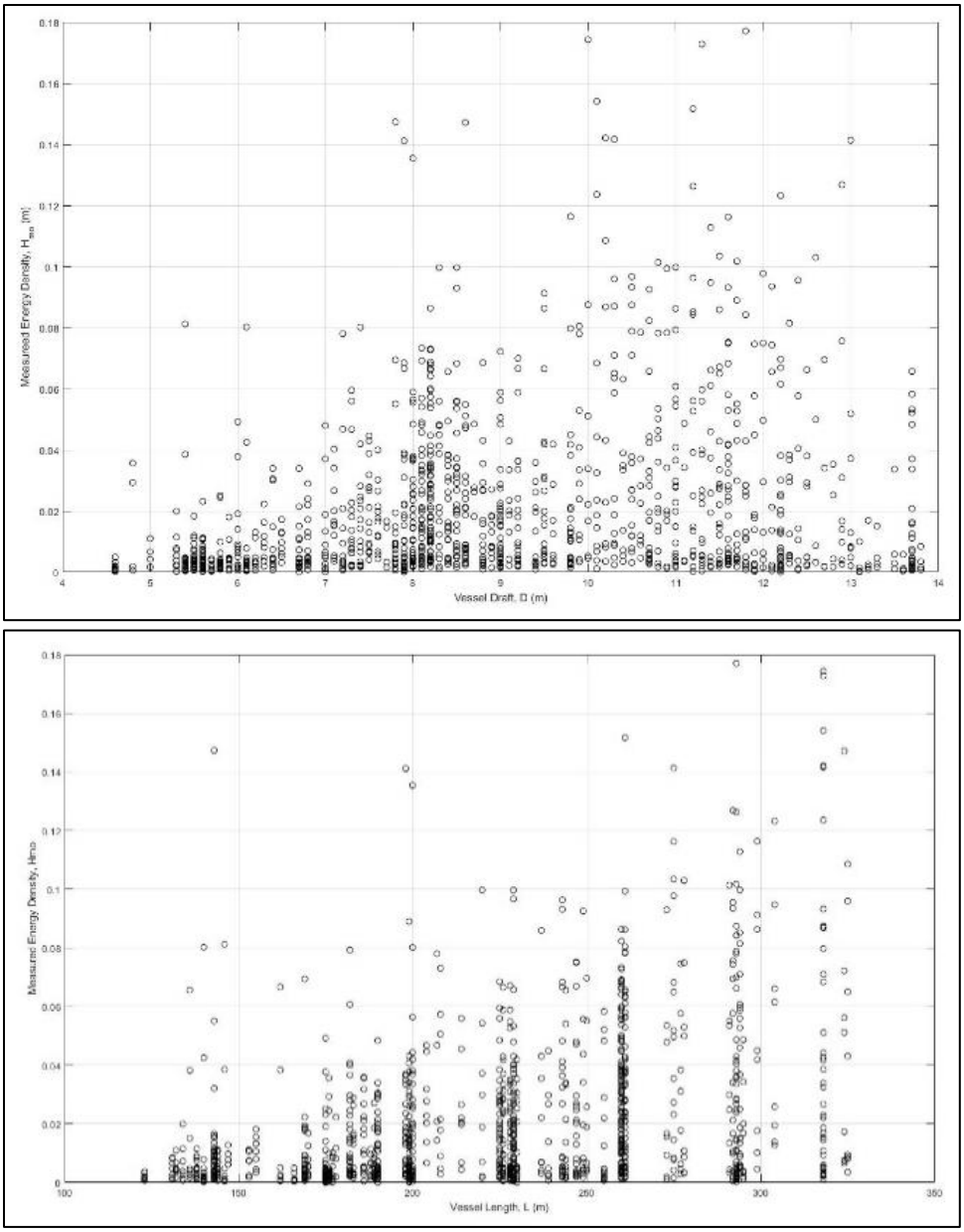

Figure 25: Measure vessel generated wave energy (VGWE) verse vessel draft (top) and vessel length (bottom).

Background energy density was computed using the same methods as for the VGWE except the window size of the data was chosen to be 1 hour. It is assumed all of the background energy computed is attributed to wind-wave energy and Figure 13 shows the measured background energy follows a similar trend as the recorded wind speed at NOAA station 8736897 supporting this assumption. A few exceptions to the trend are noted and appear to be lapses in either measured or NOAA data. The relationship between background wave energy and measured VGWE was investigated and found not to be related. It is well known wind-wave interaction and wave-wave interaction are realized; however, data quality errors are likely larger than influence of background

energy such that background energy cannot be extracted from the VGWE without potentially further inducing data errors in the VGWE.

Summary

This field data study investigated vessel generated wave energy (VGWE) in Mobile Bay, Alabama using a suite of 5 pressure sensors located north of Gaillard Island. Data were collected continuously at a rate of 8 Hz between 18 November 2017 and 19 January 2018 (62 days). A unique and efficient method of data processing was employed using a continuous wavelet transformation (CWT) to extract the vessel generated disturbances from a continuous time series by utilizing frequency modulation or "chirp" signal produced. The CWT method is shown to be valid within the context of large data sets where random errors can be averaged. The VGWE was computed on the extracted time series using a fast Fourier transformation which is widely accepted and used for describing energy of a time series and the method proved successful for this study with the exception of cases with higher background energy or weak VGWE signals, specifically SW01, SW02, and SW05. VGWE at station SW05 was extremely weak and difficult to identify within the background energy, therefore it is recommended data from SW05 not be used for any further analysis. VGWE computed using field data in this study compared well with expected results based on theoretical values and dependencies. Overall, the field data collected in this study has proved to be valid when used for general trending. However, any subsampling of the dataset should be used with caution as random errors are realized.

Vessel characteristics were attributed to the computed VGWE using data from the Shipborne Automatic Identification System (AIS). AIS data was shown to be accurate for vessel dimensions but several errors in actual vessel draft were identified. Vessel speed is reported by the AIS data as whole numbers. While this is a practical definition for speed in the maritime industry, better understanding of the strong dependence between vessel speed and VGWE could be improved with higher precision computed using distance and time between AIS reports.

3 Computing Vessel Generated Wave Energy

Computing VGWE for semi-constricted channels is a complex task due to dependence on site specific variables. A large number of predictive models, using regression analysis, are published and careful consideration should be given to selecting an approach applicable to Mobile Bay. Mobile Bay is considered a semi-constricted channel and this study is focused on the VGWE a distance from the channel which implies channel geometry and distance from the sailing line should be included in the selected model in addition to variables identified previously for vessel characteristics such as speed and dimensions. A review of well-established and other recent and less known methods resulted in three models being identified for further evaluation along with several supporting references to better refine determinants. This chapter describes the three models identified as most applicable to the study area and validation using the measured data.

Predictive Models

Sorensen and Weggel (1984):

Sorensen and Weggel (1984) and Weggel and Sorenson (1986) is an often cited method for computing vessel generated maximum wave heights. Sorensen and Weggel (1984) is an interim report describing the initial model development and applicability based on an accumulation of data available in literature for laboratory and field studies. The initial regression analysis was based on field data provided in Sorensen (1966) which included vessels having a displacement between 0.00136 tonnes (3 tons) and 8.528 tonnes (18,800 tons), lengths from 7 m (23 ft) to 154 m (504 ft), and drafts of 0.52 m (1.7 feet) to 8.53 m (28 feet). The authors focused on the relationship of displacement, *W*, and through dimensional analysis developed the variables provided in the following equations for wave height, distance from sailing line, and depth as well as the Froude number, F_d, defined in Equation 2.

$$\frac{H}{W^{1/3}} = H^* \qquad dimensionless\ wave\ height$$

$$\frac{x}{W^{1/3}} = x^* \qquad dimensionless\ distance\ from\ sailing\ line$$

$$\frac{d}{W^{1/3}} = d^* \qquad dimensionless\ depth$$

Explicit non-dimensional terms for vessel length, beam, and draft having a similar relationship to vessel displacement were considered as well but not included in the resulting regression analysis model publish. Since the vessel dimensions can be considered dependent variables of the

displacement it is logical these relationships were omitted since the dimensions would be captured in the vessel displacement. Using the non-dimensional variables described above Sorensen and Weggel (1984) presented the following empirical equation to predict maximum wave height generated by a passing vessel.

$$H^* = \alpha\, x^{*^n} \tag{5}$$

The equation is based on the exponential relationship of distance from sailing line Havelock (1908) suggested and where Weggel and Sorensen (1984) showed the exponent, n, to be a function of the Froude number by the following relationship.

$$n = \beta d^{*^\delta} \tag{6}$$

Both β and δ are functions of the Froude number and defined by explicit ranges shown below

$$\beta = -0.225\, F_d{}^{-0.699} \quad \text{for} \quad 0.2 \le F_d \le 0.55$$
$$\beta = -0.342 \quad \text{for} \quad 0.55 \le F_d \le 0.88$$

and,

$$\delta = -0.118\, F_d{}^{-0.356} \quad \text{for} \quad 0.2 \le F_d \le 0.55$$
$$\delta = -0.146 \quad \text{for} \quad 0.55 \le F_d \le 0.88$$

The variable α is also a function of the Froude number as well as the non-dimensional depth, *d**, as shown in the logarithmic second degree polynomial expression.

$$\log_{10}\alpha = a + b\log_{10}(d^*) + c\log^2{}_{10}(d^*) \tag{7}$$

where,

$$a = \frac{-0.6}{F_d} \qquad b = 0.75F_d{}^{-1.125} \qquad c = 2.653F_d - 1.95$$

The equations presented above by Sorensen and Weggel (1984) provide a method to compute vessel generated maximum wave heights within the bounds of data provided in Sorensen (1966). Weggel and Sorensen (1986) went on to provide a validation of the method using data from 11 data sources for 12 classes of vessels resulting in a modified version of Equation 5 using two additional coefficients *A'* and *B'* which are vessel class specific. The coefficients better define the vessel geometry, are vessel class specific, and range from 0.0 to 3.52.

$$H^* = A' H^* \left(\alpha x^{*^n} \right) - B' \quad (8)$$

The modified method provided by Weggel and Sorensen (1986) in Equation 8 increased the applicability to additional vessel classes. However, it is noted by the authors the data were not consistent and sometimes not well defined leading to uncertainty. It is recommended the model only be used to compute the maximum vessel generated wave height, H_m, for low vessel draft to water depth rations and limited ranges of the Froude number as defined in Weggel and Sorensen (1986).

Kriebel and Seelig (2005):

An empirical model for computing vessel generated wave heights was investigated by Kriebel and Seelig (2005). The model was based on 1,200 unique tests of laboratory data available in literature. The empirical relationship was then validated using field trials in a controlled setting within Chesapeake Bay, Maryland conducted by the authors using a small naval training vessel. The vessel was 31.1 m in length, 6.5 m beam, draft of 1.83 m, 154.7 m^3 displacement, block coefficient, C_b, of 0.41 and a *Le/L* ratio of 0.4. Tests were varied by vessel speed and ranged from 3.6 to 5.1 m/sec and data were collected at intervals of distance from the sailing line between 15 and 122 m.

Model development sought to more explicitly define the velocity head, $V^2/2g$, by normalizing in the form of gH/V^2. A second, and more significant, improvement over prior models was simplifying and normalizing model dependencies for wave attenuation as a ratio of distance from sailing line, *x*, to length of vessel, *L* given in Equation 9.

$$\left(\frac{x}{L} \right)^{-1/3} \quad (9)$$

The exponential decay of this relationship with respect to wave height was tested independently using all 1,200 unique tests which found the theoretical exponent given by Havelock (1908) of -0.3333 gave the best fit to the majority of data points and was used in the final model. However, it is noted the best fit for each set of test data ranged from -0.2 to -1.5 but no conclusive trend was apparent. The authors stated an exponent of -0.333 was most appropriate for higher speed tests but did not quantify the speed range or trend to side.

From the velocity head and distance attenuation dependencies the model was developed and incorporated sufficient function using a modified Froude number F* given in Equation 10 which incorporated length and depth based Froude number relationships to function over deep and shallow water applications.

$$F^* = \frac{V}{\sqrt{gL}} exp(\alpha\, D/d) \quad (10)$$

The modified Froude number was included in the empirical relationship and along with the velocity head and distance attenuation relationships, Equation 11 was produced for computing maximum vessel generated wave heights.

$$\frac{gH}{V^2} = \beta(F^* - 0.1)^2 \left(\frac{x}{L}\right)^{-1/3} \quad (11)$$

where,

$$\alpha = 2.35(1 - C_b) \qquad \beta = 1 + 8\tanh^3\left(0.45\left(\frac{L}{L_e} - 2\right)\right)$$

$$C_b = \frac{W}{L*B*D}$$

The entrance length, *Le*, is typically a measured value representative of the bow geometry but can be estimated using Equation 12 provided in Gates and Herbich (1977) based on 16 tanker and bulk cargo ships.

$$\frac{L_e}{L} = 0.417 - 0.00235L \quad (12)$$

The model presented in Kriebel and Seelig (2005) was validated over a range of vessel speeds and distances but it is noted a range of 0.1 to 0.5 for the modified Froude number, *F**, computed using Equation 10 should be observed for applicability, and further limited to when the velocity head, gH/V_2, does not exceed 0.4.

Schoellhamer (1996):

A regression analysis using data collected for a site specific field study developed a relationship between amplitude of vessel generated long wave (normalized by water depth at measurement location), the depth-based Froude number, F_d, and the blocking coefficient, S_c. The blocking coefficient is a ratio of the vessel cross-section and the channel cross-section as defined in Equation 13.

$$S_c = \frac{B*D}{b*d} \quad (13)$$

The field study was completed in Hillsborough Bay, FL which has an average depth of 3.2 m and is transected by a semi-confined deep draft navigation channel approximately 11-13 m deep and 150 m wide with depths of 5 m immediately adjacent, according to current nautical charts. Three field sites were established, two within 1 km of the channel in water depths of approximately 5 meters and a third approximately 3 km from the channel with a water depth of approximately 1 meter. Instrumentation included near bottom velocity probes and a pressure transducer sampling at a rate of 2 Hz. Instrument deployment was sporadic and varied between sites but for the vessel long wave analysis 4 continuous days of sampling were used. During these 4 days a total of 28 large vessels (> 100 m) transiting the channel were identified. Using data from these vessels a regression analysis provided a simple model defined by Equation 14.

$$\frac{H}{h} = {F_d}^{2.4} {S_c}^{1.6} \tag{14}$$

The vessels used in this analysis were characterized by the Froude number ranging from 0.29 – 0.84 and the blocking coefficient ranging from 0.033 – 0.22. It is stated that only 57% of the vessels generated a long wave at the near channel sites and 29% of vessel transits observed long waves at the far site which the author correlated to ranges of Froude numbers such that long waves were not observed when the Froude number was less than 0.48 and always observed for Froude numbers greater than 0.54.

Discussion

The first two models, Sorensen and Weggel (1984) and Kriebel and Seelig (2005) are well known and commonly cited for predicting vessel generated maximum wave heights. Both of these models have parts that may be applicable and provides a base of theory and approach when evaluating vessel wakes by emphasizing the criticality of dependence on the Froude number and vessel dimensions. However, neither model take into account channel geometry. It is known channel geometry will affect the vessel disturbance and as such each of these models as a whole should be discarded for use in Mobile Bay, less the knowledge gleaned from the magnitude of dependencies of those variables presented. Kriebel and Seelig (2005) went beyond the original Sorensen and Weggel (1984) work by better and more simplistically defining and validating the theoretical relationship of distance from the sailing line. A novel approach to normalize the inverse cube root distance function, described in the theoretical background, as a ratio to vessel length will be considered for applicability in the computation of VGWE for this study in Mobile Bay, Alabama as well as the variation of exponential decay as a function of vessel speed.

Schoellhamer (1996) is lesser known for contributions to the computation of vessel generated disturbances but was identified for this study based on the stark similarities between Mobile Bay and the field study site used in his analysis. The vessel ranges and speeds used are also surprisingly similar and will be helpful for comparison in this study. Finally, the simplistic and inclusive nature

of the predictive equation published by Schoellhamer (1996) is appealing. However, the field data collection chapter showed vessel length and distance from sailing line have some relationship with VGWE and neither are considered in the Schoellhamer (1996) model implying VGWE does not decay as a function of distance from the sailing line such that at a constant depth VGWE would continue infinitely. If assuming a Kelvin wake theory this assumption would be illogical but more recent work by Soomere (2006) using non-linear wave theories suggests VGWE does not decay at an exponential rate, potentially persists for long distances from the sailing line, and consistent with properties of non-linear wave theory discussed by others in Chapter 1.

Schoellhamer (1996) did not provide any discussion to omitting distance from the sailing line but considering the farthest station in his work was not validated in the model suggests a potential shortfall when applied to far lateral distances. In Equation 14, water depth at the point of measurement is used to non-dimensionalize the left hand side of the equation. However, depth at the measurement station cannot be directly related to VGWE theories for either linear or non-linear waves. Inclusion of depth at the measurement station is most likely to compensate or at least provide a proxy for distance from the sailing line such that the decay in Equation 14 is entirely dependent on shallow water dispersion relationships.

Predictive models for computed maximum vessel generated wave heights presented in Sorensen and Weggel (1984), Kriebel and Seelig (2005), and Schoellhamer (1996) were reviewed in the previous section and critically discussed above. The methodology and resulting equations were presented in detail as well as the stated applicability per the respective author. Each model was shown to have some constructive qualities and this study will attempt to leverage each of these model's strengths to produce a model that may be more applicable to Mobile Bay, Alabama.

Validation

Vessel Generated Wave Energy (VGWE) was best estimated at stations SW01 through SW04 (SW05 omitted due to data quality) using the model from Schoellhamer (1996) as described in Equation 14. The computed values were compared using a one-to-one plot with the measured VGWE. Figure 26 shows all data points and a best fit linear regression curve (red line). The black line represents a perfect one-to-one relationship.

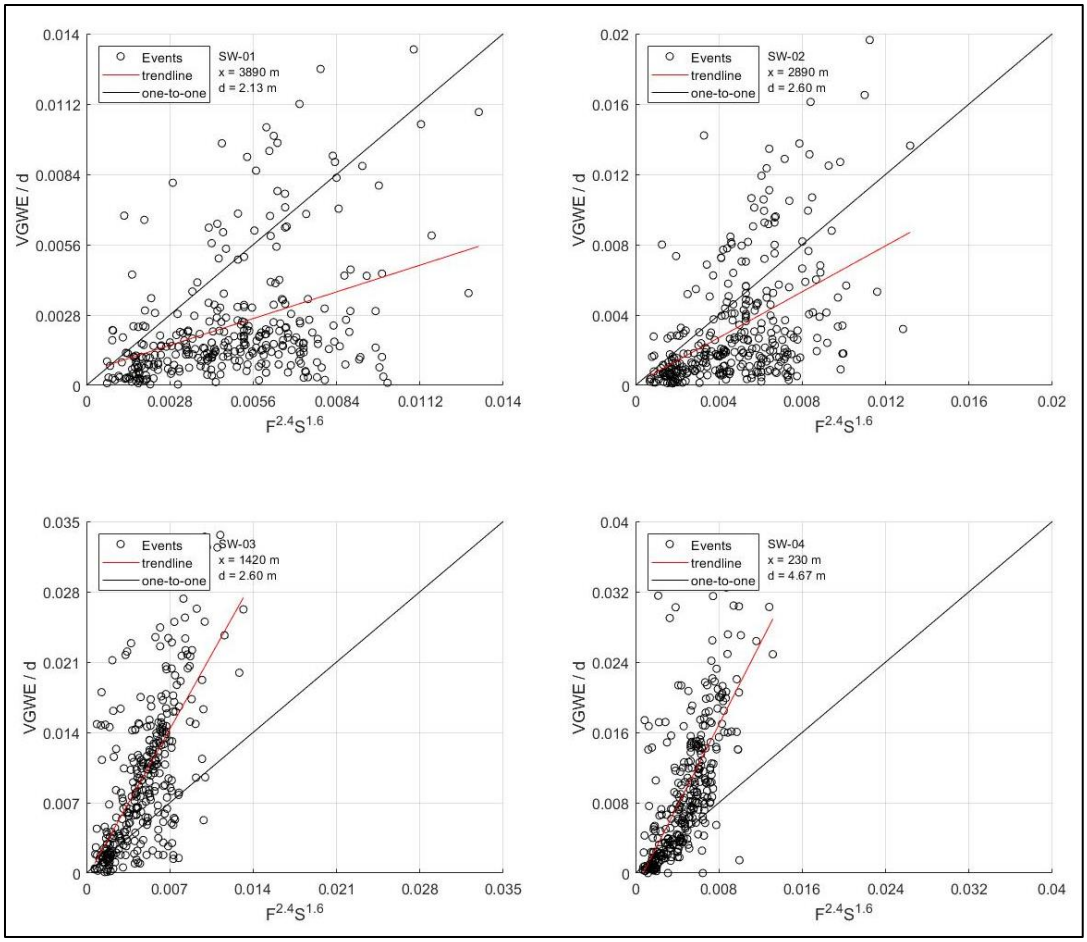

Figure 26: One-to-One correlation plot of measured vessel generated wave energy (VGWE) and the equation from Schoellhamer (1996) for stations SW01 through SW04.

It is evident from Figure 26, Equation 14 underestimates the VGWE at Stations SW03 and SW04 but appear to follow a related trend and are collapsed on the regression curve. SW01 and SW02 are over predicted for all but the higher values of measured VGWE which do not appear consistent with the majority grouping below the one-to-one line. Filtered points for the higher measured energy density for SW01 and SW02 have a strong correlation to the Froude number within a range of $F > 0.5$. This secondary correlation (Figure 27) shows the relationship for Froude numbers greater than 0.5 with the regression line following those values of the Froude number.

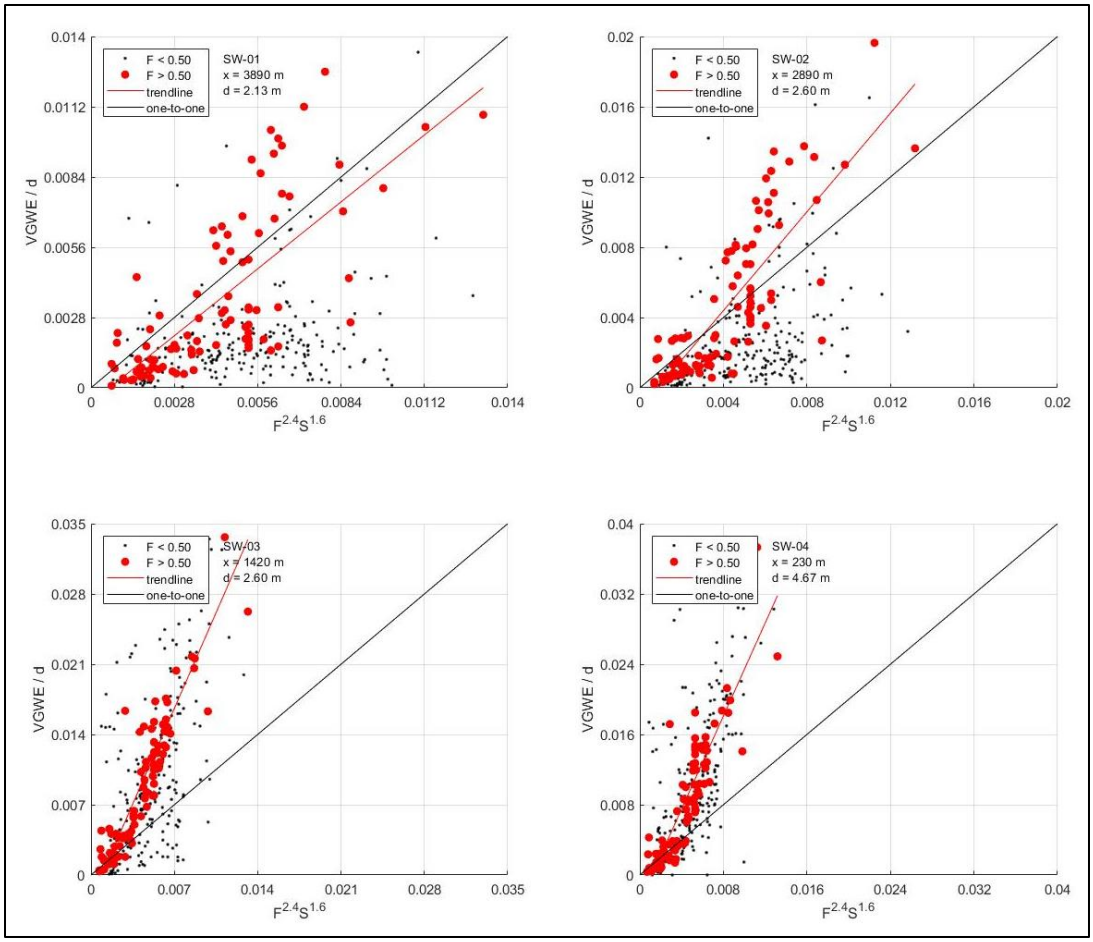

Figure 27: One-to-One correlation plot of measured vessel generated wave energy (VGWE) categorized by Froude number and the equation from Schoellhamer (1996) for stations SW01 through SW04. The regression line follows Froude numbers greater than 0.5.

Data points corresponding to F > 0.5 collapse about the linear regression curve (red line) at all sites and to a higher degree for SW01 and SW02 but now data points corresponding to F > 0.5 for SW01 and SW02 are above the one-to-one line leading to the Schoellhamer (1996) model now over predicting these stations as well. With the information presented in the theoretical background and field data collection chapter as it relates to the inflection point of the Froude number, it is interesting to note the Schoellhamer (1996) equation collapses data points more for larger Froude numbers in the transcritical range as opposed to the subcritical values which are better described using linear wave theory methods. Other data point filters based on known dependent relationships were tested and none produced as strong a relationship as the Froude number. However, one interesting find is the relationship to transit direction. Figure 28 is the same one-to-one plot relationship but the data are categorized by transit direction.

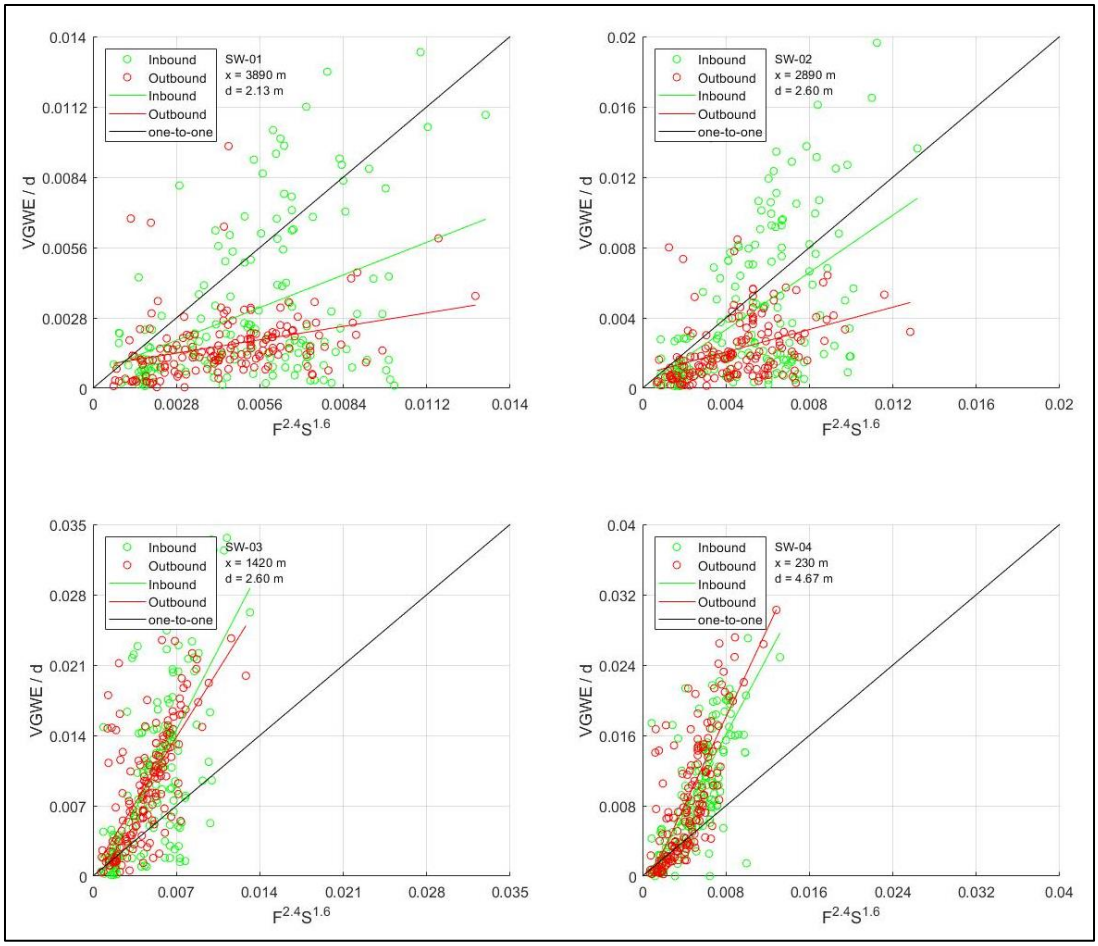

Figure 28: One-to-One correlation plot of measured vessel generated wave energy (VGWE) and the equation from Schoellhamer (1996) for stations SW01 through SW04 categorized by direction of vessel transit. The regression line is color coded to match the respective transit direction.

From Figure 28, SW01 and SW02 appear to show a relationship with transit direction. SW03 and SW04 do not show this same variance nor any other distinguishable characteristics between the transit directions. From the field data collection chapter wave breaking was observed to a higher degree on outbound transits. Wave breaking is, by definition, a loss of energy where by the outbound transits should be measured lower than computed using Equation 15. As a result it can be assumed wave breaking is likely contributing to the scatter observed at SW01 and SW02. Since wave breaking is not a function within Equation 14 these values should not be considered when evaluating the applicability within the correlation plots. However, without further evaluation and better spatial resolution the wave breaking relationship could be a coincidence and not realized in the data.

South Bay Validation

Following the initial study and upon external and internal peer review it was suggested the lower bay may not be in agreement with results from the field study and regression analysis completed in the northern bay. In response, this study initiated additional field data collection efforts in southern Mobile Bay at the sites shown in Figure 29. Instrumentation was deployed over a period between December 21, 2018 and February 5, 2019. The sampling plan followed the same methodology and processing as the original northern bay deployment described in Chapter 3.

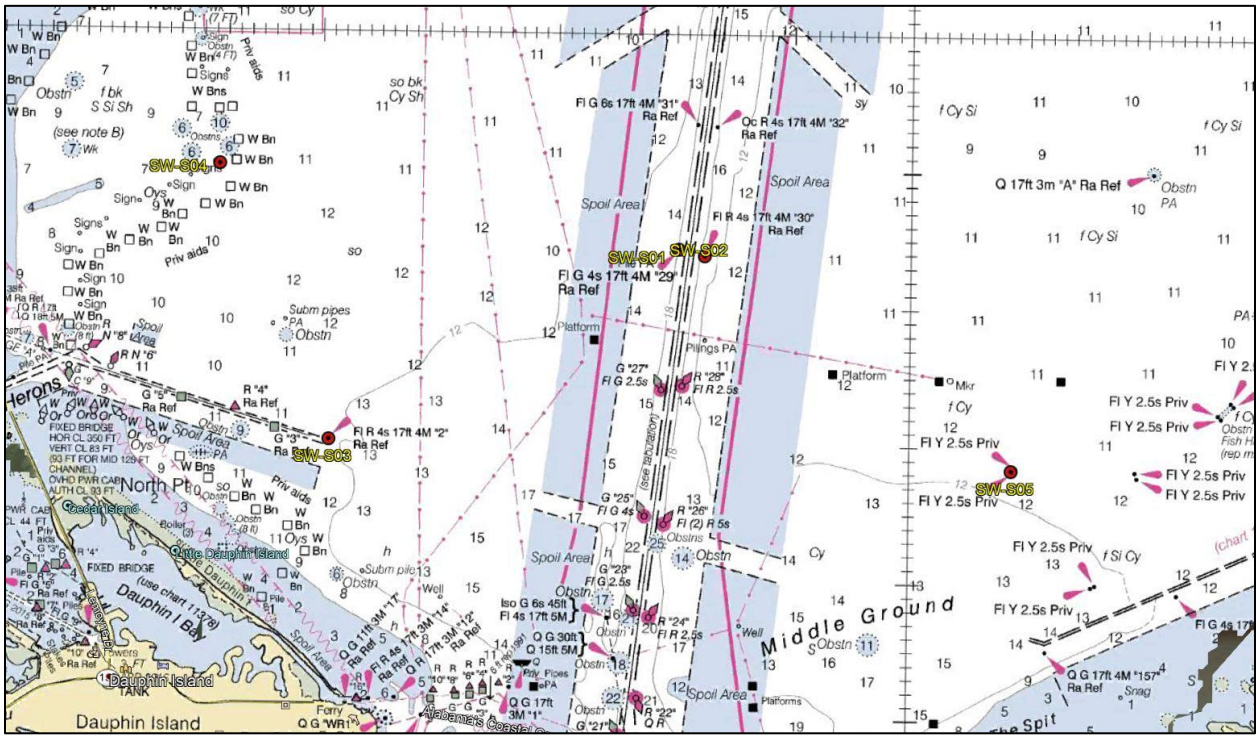

Figure 29: Southern Bay Station Locations

Over the period of deployment 214 vessel transits were obtained from the AIS data for vessel greater than 122 meters. These transits were made up of a similar distribution of vessel dimensions and classes. Meteorological conditions during this period were similar but not identical such that precipitation over the watershed was greater resulting in higher river flows. This difference is insignificant based on the lack of dependence proven during the original deployment. An obvious and relevant difference between the deployments is the distance of sites to the channel. The relationship of site location to channel is noted but accounted for in the processing and does not bias the validation findings. Validation of the Schoellhamer (1996) model based on one-to-one plots is shown in the follow figures.

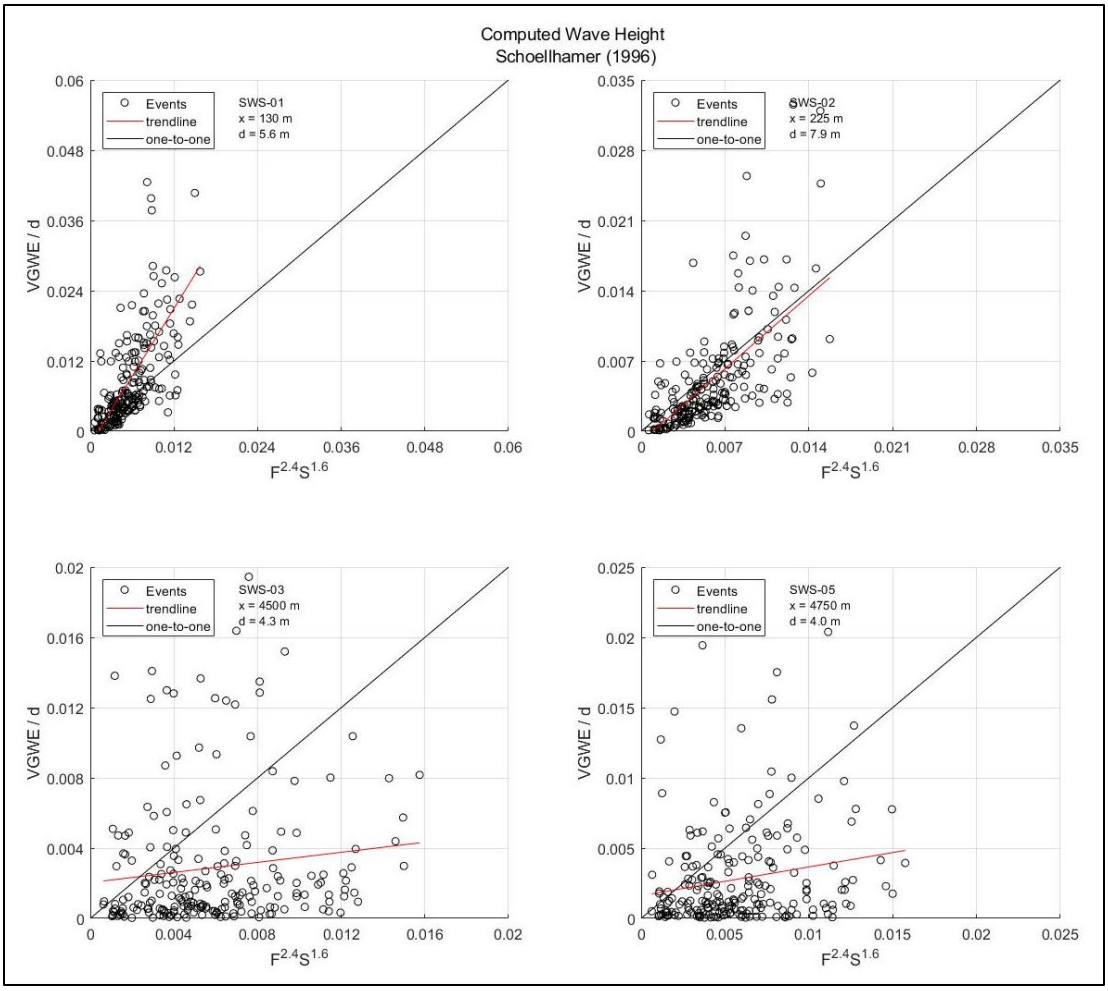

Figure 30: One-to-One correlation plot of measured vessel generated wave energy (VGWE) at the south bay validation sites and the equation from Schoellhamer (1996) for stations SWS01 through SWS03 and SW05.

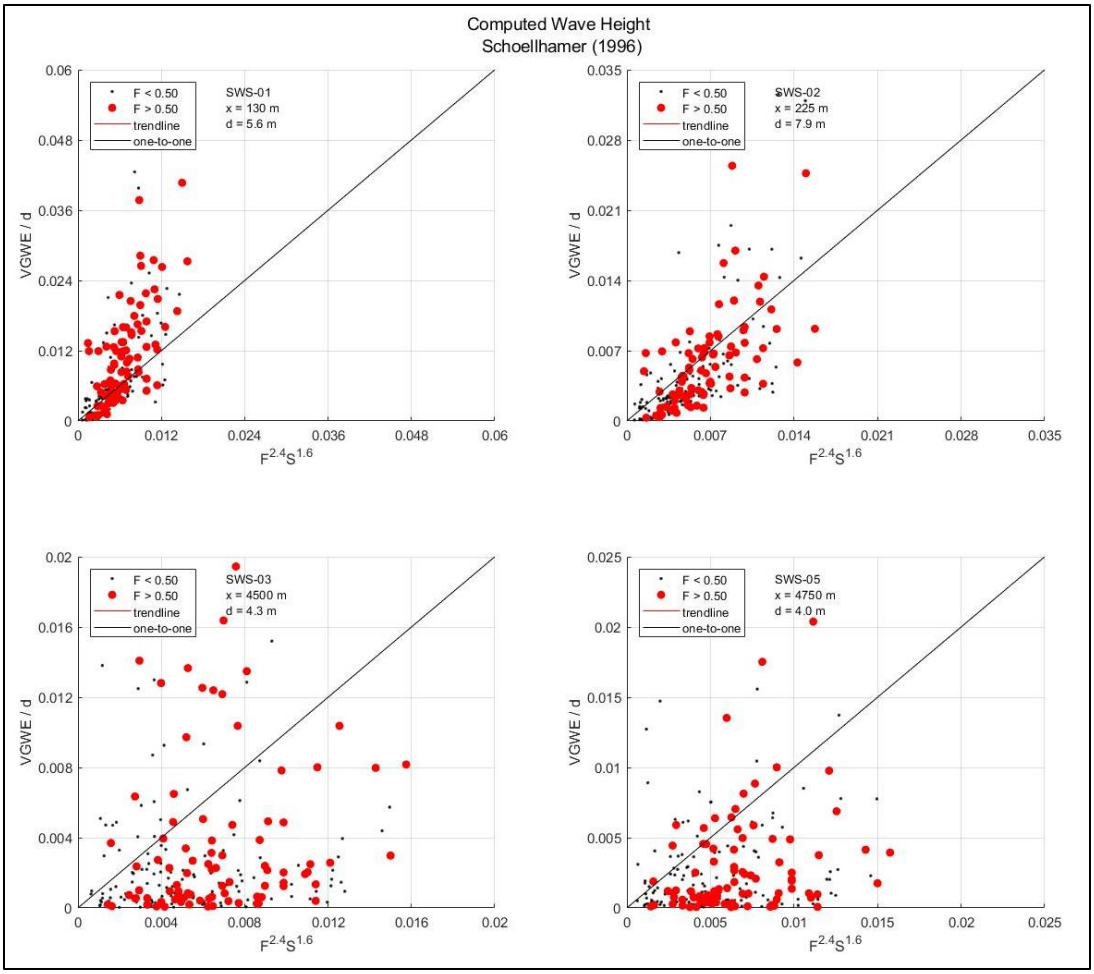

Figure 31: One-to-One correlation plot of measured vessel generated wave energy (VGWE) at the south bay validation sites categorized by Froude number and the equation from Schoellhamer (1996) for stations SWS01 through SWS03 and SW05. The regression line follows Froude numbers greater than 0.5.

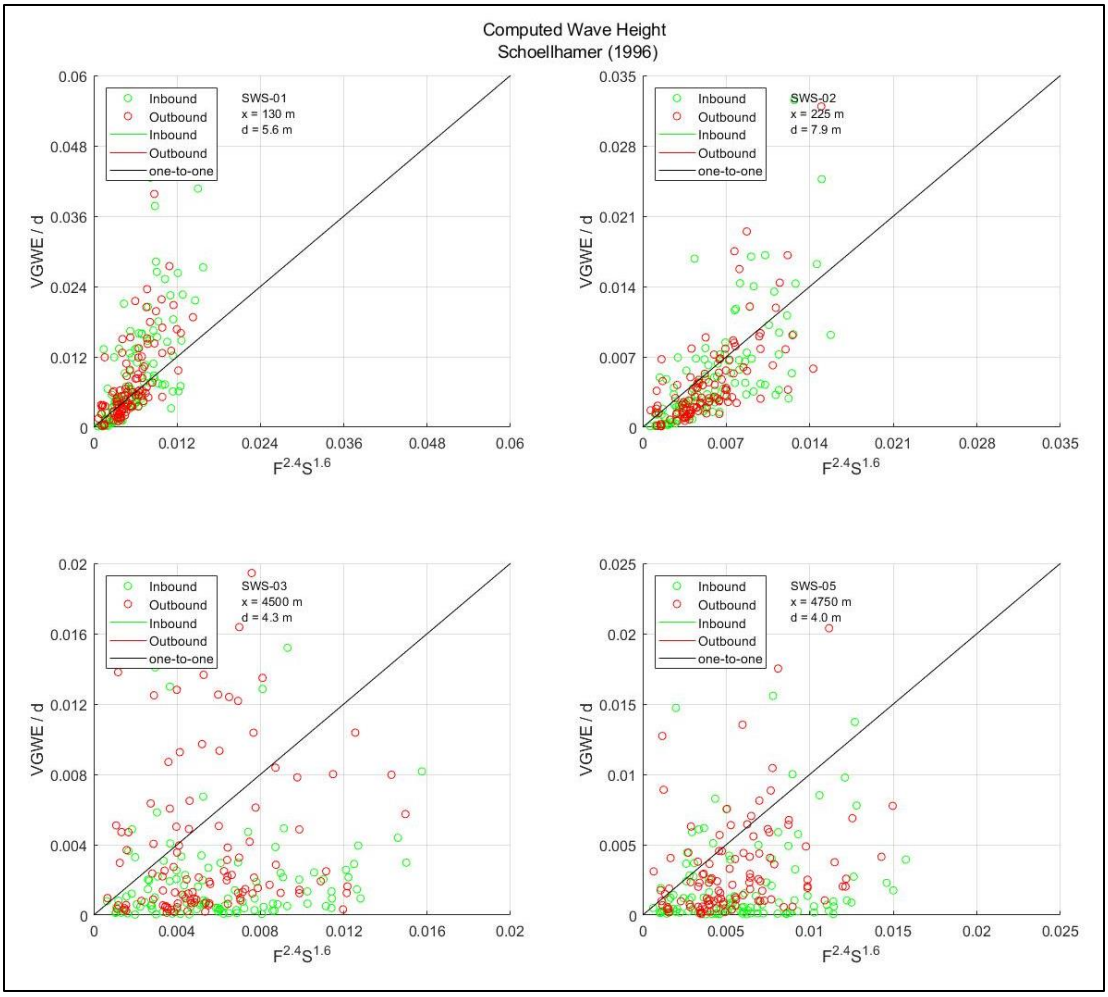

Figure 32: One-to-One correlation plot of measured vessel generated wave energy (VGWE) at the south bay validation sites and the equation from Schoellhamer (1996) for stations SWS01 through SWS03 and SW05 categorized by direction of vessel transit. The regression line is color coded to match the respective

The south bay validation set appears to follow the Schoellhamer (1996) model for SWS01 and SWS02 then largely scattered at the far field sites. Notable there does not appear to be a discernable trend or differentiation for the Froude number or transit direction as was the case at the northern deployment leading to the conclusion that vessel transiting this reach of the channel are not changing in speed as a function of direction. Lack of dependence on the Froude number could indicate VGWE may follow more of a linear wave theory relationship. However, application of the Schoellhamer (1996) model to the south bay is within the range of predictive accuracy.

Summary

VGWE in Mobile Bay, Alabama was estimated using the model described by Schoellhamer (1996) in Equation 14 and found to underestimate at all measured stations for Froude numbers greater

than 0.5. For Froude numbers less than 0.5 the model tends to overestimate at the far field stations (SW01 and SW02) and underestimate for near measurement stations (SW03 and SW04). The model shows a trend for near field stations implying the model's relationship to VGWE for these stations could be improved to provide a more accurate computation. The increasing spread of data at stations SW01 and SW02 are likely a result of additional dependencies such as wave breaking and dispersion. Absence of vessel length and distance from the sailing line in the model could contribute to the under prediction at the near field stations (vessel length) and lack of precision at the far field stations (distance from sailing line). Validation of the initial study results using data collected in a similar manner between December 21, 2018 and February 5, 2019 is shown to agree with the Schoellhamer (1996) model but with less accuracy. As a result of this analysis, it is recommend the Schoellhamer (1996) should only be applied to Mobile Bay for low precision prediction of far field VGWE at Froude numbers greater than 0.5 with the understanding values could be slightly underestimated.

4 Impact Assessment

Describing potential impacts of VGWE as a result of the Mobile Harbor Federal Navigation channel proposed deepening project, for this study, is defined as a relative difference between with and without project channel geometry and forecasted vessel class distribution and frequency. This impact analysis relies on finding from Chapters 2 and 3 for prediction of VGWE in Mobile Bay using the model published by Schoellhamer (1996), defined in Equation 14. Fortunately, the proposed changes will not alter the alignment such that the model's lack of dependence on distance from the sailing line, *x*, will not vary and therefore the relative difference is zero and negligible. Two locations of interest along the length of the channel, shown in Figure 33, are considered which represent distinctly different geometries along the federal channel reach. Depth, *h*, at these locations is extracted from available bathymetric data obtained on February 2018 by the USACE Operations Hydrographic Survey Team at the inflection point of the channel side slope and the native bay elevation. This depth is chosen as it is within the range of applicability of the predictive model validation provided in Chapter 3 and outside the area of influence of channel dredging activities. Dependent variables with respect to these locations are provided in Table 8.

Table 8: Dependent variables used to evaluate Vessel Generated Wave Energy (VGWE) with respect to locations of interest.

Site ID	w/o Project		w/ Project		Adjacent Water Depth, h (m)
	Channel Depth, dc (m)	Channel Width, b (m)	Channel Depth, dc (m)	Channel Width, b (m)	
Upper Bay	14.9	234.9	16.2	247.9	3.6
Lower Bay	14.9	219.9	16.2	263.4	5.1

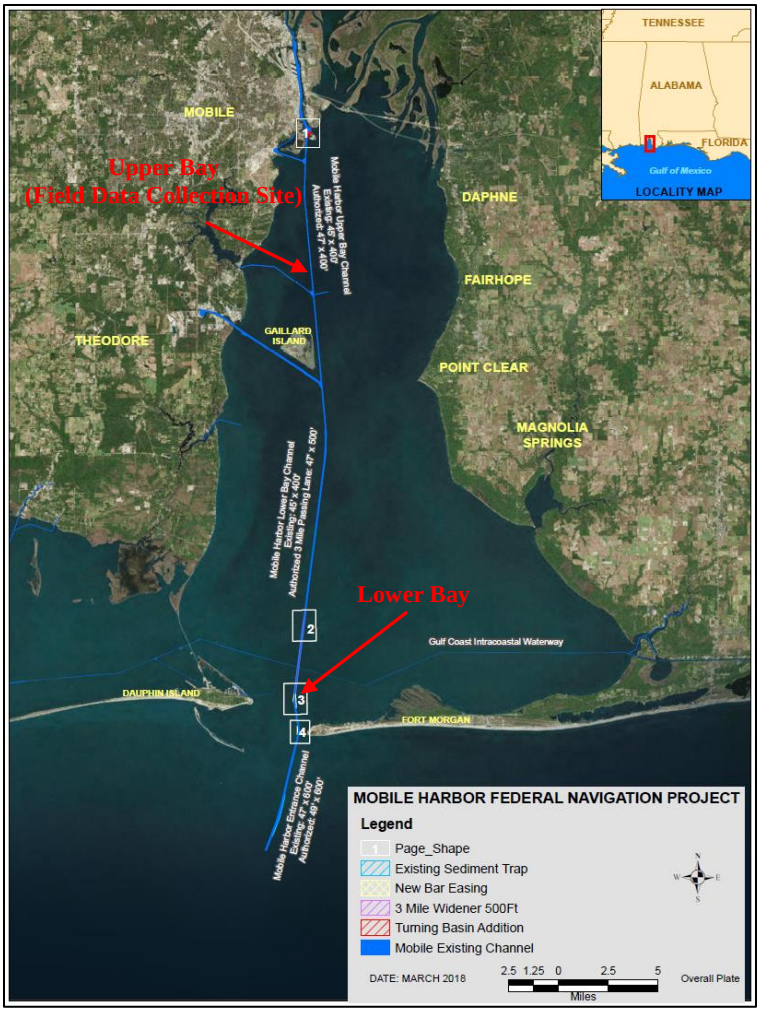

Figure 33: Location of sites used for spatial representation of Vessel Generated Wave Energy (VGWE) impact analysis within Mobile Bay, Alabama

Vessel Traffic Frequency

Size and frequency of vessels calling the Mobile Harbor was determined through an economic analysis using the base year of 2025 and a future condition year of 2035. Frequency analysis, summarized in Table 9 for 2025 and Table 10 for 2035, categorized vessels by class with associated max vessel dimensions, number of calls, and percent of the total calls for with and without project. This forecasting was completed as part of the Mobile Harbor General Re-evaluation study and details of methods used can be found in documentation associated with that study. The forecasted fleet detailed with respect to distribution of vessel draft within each class and used for the impact analysis, is provided in Appendix B.

Table 9: Forecast summary for the base year 2025 vessel calls delineated by vessel classes for with and without project conditions.

Vessel Class	Max Length (m)	Max Beam (m)	w/o Project	% Fleet	With Project	% Fleet
Bulk Carrier 2	194	32	7	0%		0%
Bulk Carrier 3	228	32	398	13%	386	13%
Bulk Carrier 4	238	32	449	15%	450	15%
Bulk Carrier 5	247	42	77	3%	74	3%
Bulk Carrier 6	258	44	2	0%	2	0%
Bulk Carrier 7	274	44	12	0%	12	0%
Chemical Tanker	182	40	156	5%	156	5%
SubPX	206	30	20	1%	20	1%
Panamax	292	32	461	15%	415	14%
PPXGn1	302	40	236	8%	236	8%
PPXGn2	325	43	188	6%	186	6%
PPXGn3						
Cruise	261	36	182	6%	182	6%
General Cargo 1	183	32	399	13%	399	14%
General Cargo 2	258	36	293	10%	293	10%
Tanker Panamax	241	32	61	2%	101	3%
Aframax Tanker	271	49	72	2%	32	1%
Total			**3013**		**2944**	

Table 10: Forecast summary for year 2035 vessel calls delineated by vessel classes for with and without project conditions.

Vessel Class	Max Length (m)	Max Beam (m)	w/o Project	% Fleet	With Project	% Fleet
Bulk Carrier 2	194	32	5	0%		0%
Bulk Carrier 3	228	32	333	10%	403	12%
Bulk Carrier 4	238	32	418	12%	434	13%
Bulk Carrier 5	247	42	82	2%	77	2%
Bulk Carrier 6	258	44	2	0%	2	0%
Bulk Carrier 7	274	44	14	0%	14	0%
Chemical Tanker	182	40	238	7%	238	7%
SubPX	206	30	31	1%	29	1%
Panamax	292	32	260	8%	131	4%
PPXGn1	302	40	295	9%	269	8%
PPXGn2	325	43	187	6%	173	5%
PPXGn3	325	48	268	8%	248	8%
Cruise	261	36	172	5%	172	5%
General Cargo 1	183	32	453	14%	453	14%
General Cargo 2	258	36	347	10%	347	11%
Tanker Panamax	241	32	131	4%	131	4%
Aframax Tanker	271	49	111	3%	111	3%
Total			**3347**		**3232**	

Each class of vessels represent a range of vessel lengths and beams. VGWE computed using Equation 14 is proportional to the vessel beam such that the max beam within each vessel class will produce the largest value of VGWE vis-a-vis the largest potential impact. The vessel length is not a variable in Equation 14 but is presented here for awareness and clarity.

The total number and distribution of forecasted vessel calls to the Port of Mobile are generally equal. This is largely due to the methods used for predicting vessel calls and the nature of the proposed project. Northern extents of the proposed deepening project terminate at the Interstate 10 tunnel crossing. The majority of port facilities are north of the tunnel and hence are unchanged as a result of the project. The noticeable difference in number and distribution of calls relates to the containership vessel types between the 2025 and 2035 forecasted fleet. This is a result of the anticipated addition of Post Panamax Generation 3 (PPXGn3) vessels being introduced to the fleet. However, the PPXGn3 vessels will not result in a large net increase in vessel calls but a redistribution of all containership classes where tonnage once carried by several smaller vessel classes will now be transported on fewer larger vessels. Furthermore, the without project distribution also realizes the addition of the PPXGn3 vessel class where the relative difference in with and without project remain similar.

Vessel Speed

VGWE is known to be highly dependent on vessel speed. Equation 14 shows vessel speed is raised to a power of 2.4 where a small change in speed will equate to a large change in VGWE. The forecasted fleet described in the previous section does not provided vessel speed. As a result, vessel speed used in this study is determined based on the current AIS data calling to Mobile Harbor. An annualized summary of vessel speed was extracted from the 2016 calendar year AIS database and delineated by vessel length. Figure 34 is the distribution of vessel speeds with respect to vessel length categories.

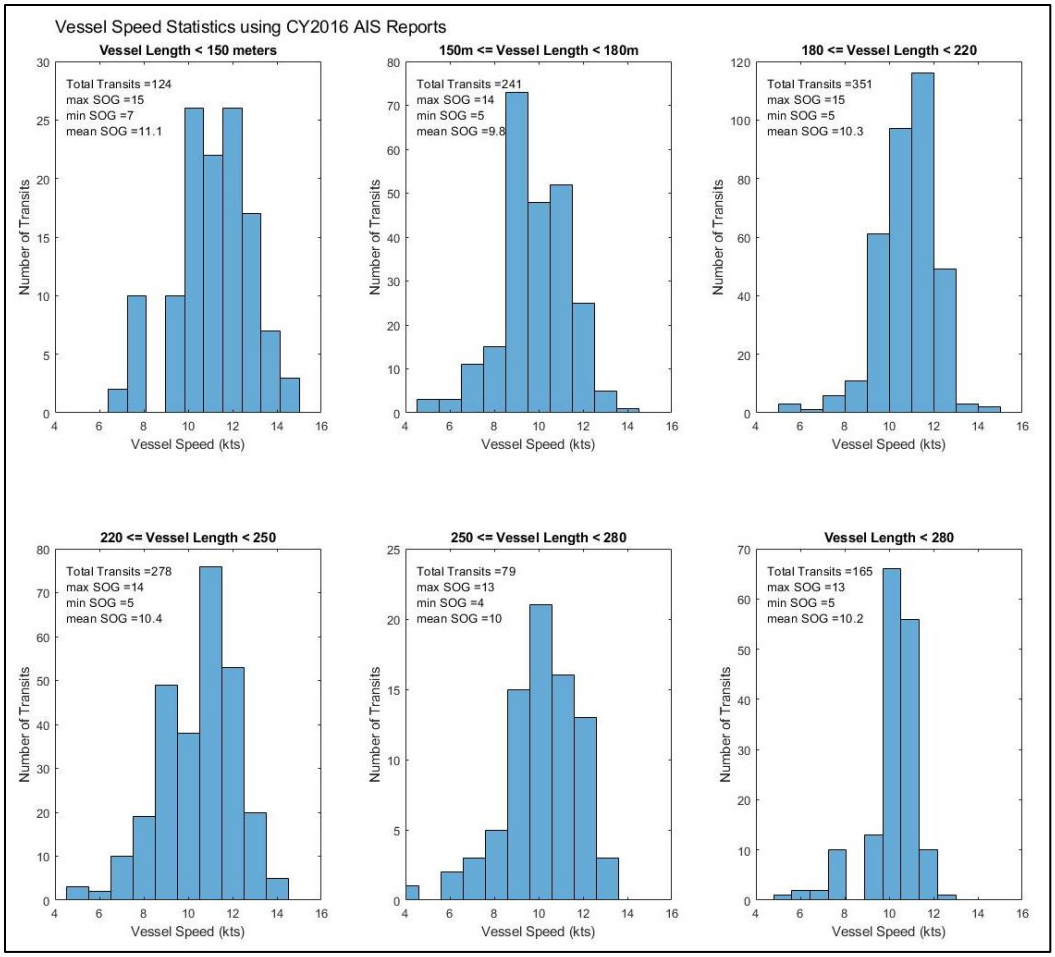

Figure 34: Summary statistics of vessel speed using Shipborne Automated Identification System (AIS) data obtain for the 2016 calendar year for Mobile Bay, Alabama deep draft channel delineated by vessel length.

The majority of vessels transiting Mobile Bay have a speed of around 10 knots, as shown in Figure 34, which is consistent with the vessel speeds recorded during the field investigation. Intuitively, smaller vessels are traveling faster than larger vessels and discussions with the Mobile Harbor Pilots Association confirmed this finding. However, Figure 34 shows maximum vessel speeds up to 15 knots for small vessels and 13 knots for the largest vessels.

Evaluation of vessel speed with respect to two locations along the bay channel sections shown in Figure 35 describes vessel speed variation between these points. To account for this variance and in lieu of a quantified assessment, vessel speed provided in the 2016 AIS summary statistics will be varied as a percentage such that the upper bay is 10% greater and the lower bay is 20% greater than the mean value provided in Figure 34. These values are believed to be conservative and within practical limits but a sensitivity analysis presented later in this study will test these assumptions and maximum values within practical limits.

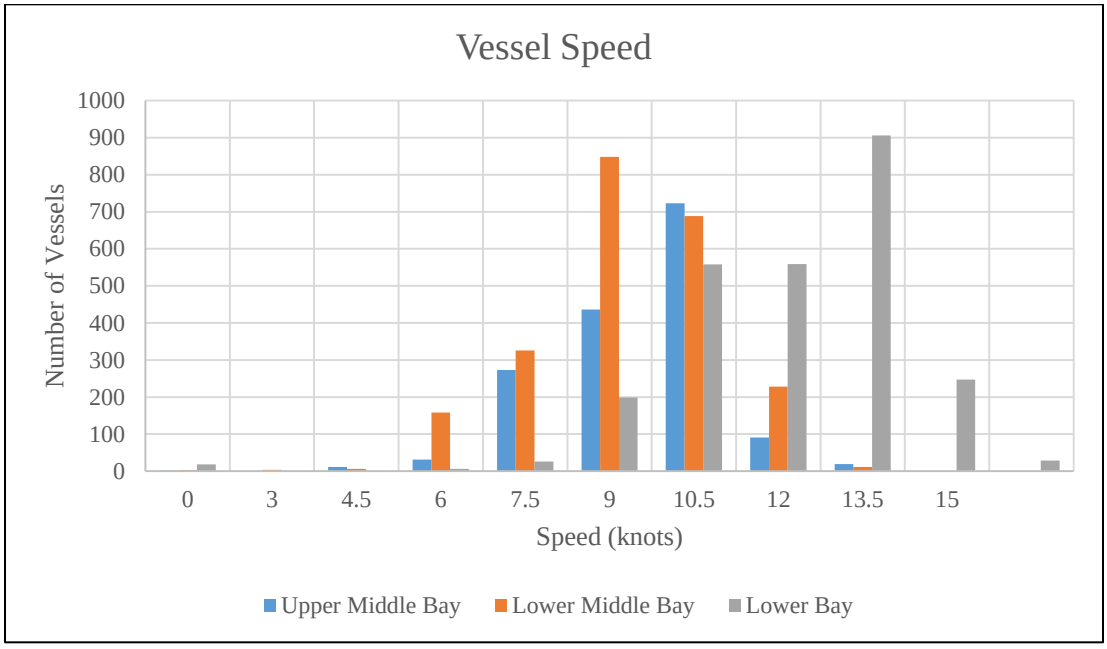

Figure 35: Variation of vessel speed for all classes and categories in Mobile Bay, Alabama with respect to three locations of interest.

This study has shown VGWE is highly dependent on vessel speed and this section has described the magnitude and variation of vessel speed at three discrete points. It is important to note limits and restrictions on vessel speed as it relates to theoretical maximums for confined and semi-confined channels such as Mobile Harbor. Several considerations for theoretical maximums are discussed in literature and relate to the Froude number and ratio of channel cross-section to vessel cross-section. PIANC (1987) found in constricted channels vessel speed cannot exceed $F_d > 1$ and usually limited by 0.9F due to the method of propulsion creating a critical velocity at the midsection of the vessel. Therefore vessel speed is limited since the propeller cannot move more water than allowed to flow past the vessel. EM 1110-2-1613, *Hydraulic Design of Deep-Draft Navigation Projects*, provides further restrictions to vessel speed for practical applications in terms of the depth based Froude number, F_d, such that in restricted channels F_d will not exceed 0.6. Schijf and Jansen (1953) investigated limits of vessel speed as a function of the depth based Froude number and the ratio of the channel and vessel cross-section, for constricted channels, and found a relationship known as Schijf's equation shown below (derivation as provided in EM 1110-2-1613) which is based on Bernoulli's Equation for conservation of energy.

$$F_{hL} = \frac{V_L}{\sqrt{gh}} = \sqrt{8\cos^3\left(\frac{\pi}{3} + \frac{\arccos}{3}\left(1 - \frac{1}{B_R}\right)\right)} \quad (15)$$

Where B_R is equal to S_c and V_L is the limiting velocity. Channel width for the purposes of this analysis is considered to be the width at the inflection of the overbank area graphically shown in

Figure 36 for trench type channels. Schijf's equation has been verified by many researchers with good results but found to only be valid for ships transiting the centerline of a channel and if not the eccentricity should be substituted for the value of A_c according to PIANC (1985). The eccentricity relationship is noted but for this study all vessels are assumed to be transiting the channel centerline.

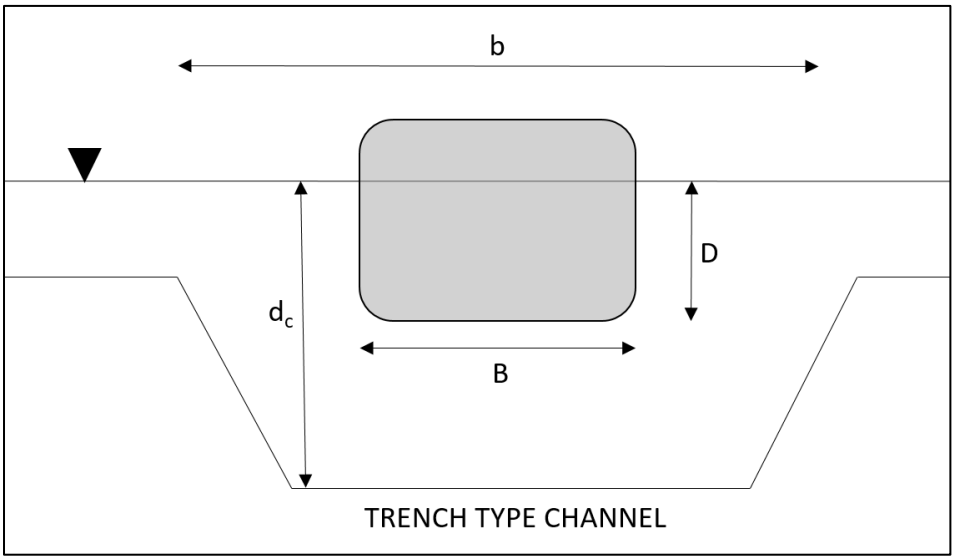

Figure 36: Graphical sketch defining cross-sectional variables used in VGWE and vessel speed computations.

Schijf's equation is used as provided in Equation 15 to valid the practical limits of vessel speed in Mobile Bay for all impact and sensitivity analyses. A comparison of vessel speeds measured using AIS and results using Equation 15 applied to the detailed forecasted fleet as provided in Appendix B show measured vessel speeds are much less than the theoretical maximum. However, this method does not consider squat, bank effects, currents, and other operational factors which are likely more limiting.

Spatial Representation

Interpolating VGWE over the domain of Mobile Bay requires gross assumptions and presents several challenges. The first and foremost challenge is spatial extrapolation of the recommended model for predicting VGWE validated using data obtained from north of Gaillard Island and west of the federal navigation channel. Depths in this region are slightly less than other regions and features a shallow draft navigation channel (Dog River) which could influence VGWE and applicability to other regions. Furthermore, the northern reach, where model validation was completed, is shown to have a dependence on transit direction.

Influence of the Dog River channel is assumed to be negligible due to the small difference between channel depths and surrounding bathymetry in addition to a relatively narrow channel width. The field data collection chapter noted the influence of transit direction and it was present in the model validation. Examination of vessel speeds (known dependent of VGWE) shows inbound and outbound vessels differ. The combination of vessel speed variance and the observed wave breaking patterns in the field data chapter suggests other regions would not realize a similar dependence on transit direction where inbound and outbound vessels are assumed to exhibit similar magnitudes of VGWE outside of this region as long as consideration for speed and bathymetric features are observed.

For this study two locations of interest, inclusive of the field data collection site, are identified in Figure 33. Site selection was based on the known locations where variables in Equation 14 may change spatially and relative to with and without project. The recommended model provided in Equation 14 computes VGWE as a function of Vessel speed, *V*, Beam, *B*, and draft, *D*, channel depth, d_c, and width, *b*, as well as depth at the point of interest, *h*. Channel geometry is the only variable meeting the site selection criteria. The lower bay site is representative of a change in channel width and depth from existing conditions and different than the change defined at the field data collection site. Site specific values for with and without project as well as other dependent variables are provided in Table 8.

Computed Impacts

The objective of this study is to evaluate the relative difference in VGWE for the current fleet and forecasted fleet as a result of deepening the channel. The methods to compute VGWE were presented in Chapter 3 and the dependent variables for each scenario were described previously in this chapter. Results using these values are provided in the following tables.

Table 11: Computed Vessel Generated Wave Energy (VGWE) of with and without project scenarios using the forecasted base year 2025 at the upper bay site.

Vessel Class	2025 Arrival				2025 Departure			
	# of Vessels		VGWE		# of Vessels		VGWE	
	w/o Project	w/ Project	w/o Project	w/ Project	w/o Project	w/ Project	w/o Project	w/ Project
Bulk Carrier 1								
Bulk Carrier 2	4		0.025		3		0.055	
Bulk Carrier 3	229	223	1.702	1.208	169	163	2.551	1.768
Bulk Carrier 4	250	250	1.747	1.268	199	200	2.516	1.924
Bulk Carrier 5	38	36	1.057	0.738	39	38	1.320	1.014
Bulk Carrier 6	1	1	0.010	0.007	1	1	0.033	0.024
Bulk Carrier 7	6	6	0.057	0.042	6	6	0.210	0.171
Chemical Tanker	78	78	0.427	0.310	78	78	0.659	0.479
SubPX	10	10	0.113	0.082	10	10	0.102	0.074
Panamax	232	208	3.260	2.120	229	207	3.308	2.148
PPXGn1	117	118	2.688	2.211	119	118	2.765	2.347
PPXGn2	94	94	2.430	1.979	94	92	2.531	2.031
PPXGn3								
Cruise	91	91	0.931	0.676	91	91	0.901	0.654
General Cargo 1	199	199	1.037	0.752	200	200	1.103	0.801
General Cargo 2	146	146	0.837	0.607	147	147	1.080	0.784
Tanker Panamax	32	72	0.359	0.685	29	29	0.202	0.147
Aframax Tanker	72	32	1.698	0.468				
	1599	**1564**	**18.376**	**13.153**	**1414**	**1380**	**19.337**	**14.366**

Table 12: Computed Vessel Generated Wave Energy (VGWE) of with and without project scenarios using the forecasted base year 2025 at the lower bay site.

Vessel Class	2025 Arrival				2025 Departure			
	# of Vessels		VGWE		# of Vessels		VGWE	
	w/o Project	w/ Project	w/o Project	w/ Project	w/o Project	w/ Project	w/o Project	w/ Project
Bulk Carrier 1								
Bulk Carrier 2	4		0.048		3		0.106	
Bulk Carrier 3	229	223	3.303	1.914	169	163	4.949	2.800
Bulk Carrier 4	250	250	3.389	2.009	199	200	4.882	3.048
Bulk Carrier 5	38	36	2.051	1.168	39	38	2.562	1.607
Bulk Carrier 6	1	1	0.019	0.011	1	1	0.063	0.039
Bulk Carrier 7	6	6	0.111	0.066	6	6	0.407	0.270
Chemical Tanker	78	78	0.829	0.491	78	78	1.279	0.758
SubPX	10	10	0.220	0.130	10	10	0.199	0.118
Panamax	232	208	6.324	3.358	229	207	6.417	3.403
PPXGn1	117	118	5.214	3.503	119	118	5.363	3.718
PPXGn2	94	94	4.714	3.135	94	92	4.910	3.217
PPXGn3								
Cruise	91	91	1.806	1.071	91	91	1.748	1.036
General Cargo 1	199	199	2.011	1.192	200	200	2.141	1.269
General Cargo 2	146	146	1.623	0.962	147	147	2.096	1.242
Tanker Panamax	32	72	0.696	1.085	29	29	0.392	0.233
Aframax Tanker	72	32	3.294	0.742				
	1599	**1564**	**35.650**	**20.838**	**1414**	**1380**	**37.514**	**22.759**

Table 13: Computed Vessel Generated Wave Energy (VGWE) of with and without project scenarios using the forecasted year 2035 at the upper bay site.

Vessel Class	2035 Arrival				2035 Departure			
	# of Vessels		VGWE		# of Vessels		VGWE	
	w/o Project	w/ Project	w/o Project	w/ Project	w/o Project	w/ Project	w/o Project	w/ Project
Bulk Carrier 1								
Bulk Carrier 2	3		0.018		2		0.037	
Bulk Carrier 3	199	199	1.689	1.226	134	204	2.105	1.890
Bulk Carrier 4	199	218	1.371	1.082	219	216	2.616	1.921
Bulk Carrier 5	40	38	1.035	0.725	42	39	1.437	1.058
Bulk Carrier 6	1	1	0.010	0.007	1	1	0.033	0.024
Bulk Carrier 7	7	7	0.067	0.049	7	7	0.245	0.201
Chemical Tanker	120	120	0.671	0.487	118	118	1.003	0.728
SubPX	16	15	0.178	0.122	15	14	0.151	0.103
Panamax	130	66	1.822	0.672	130	65	1.897	0.704
PPXGn1	147	134	3.366	2.508	148	135	3.568	2.629
PPXGn2	93	86	2.377	1.777	94	87	2.513	1.891
PPXGn3	135	124	4.150	3.107	133	124	4.250	3.244
Cruise	86	86	0.880	0.639	86	86	0.852	0.618
General Cargo 1	226	226	1.190	0.864	227	227	1.217	0.884
General Cargo 2	173	173	0.993	0.721	174	174	1.276	0.926
Tanker Panamax	65	65	0.688	0.499	66	66	0.435	0.316
Aframax Tanker	55	55	1.295	0.940	56	56	1.216	0.882
	1695	**1613**	**21.799**	**15.425**	**1652**	**1619**	**24.850**	**18.019**

Table 14: Computed Vessel Generated Wave Energy (VGWE) of with and without project scenarios using the forecasted year 2035 at the lower bay site.

Vessel Class	2035 Arrival				2035 Departure			
	# of Vessels		VGWE		# of Vessels		VGWE	
	w/o Project	w/ Project	w/o Project	w/ Project	w/o Project	w/ Project	w/o Project	w/ Project
Bulk Carrier 1								
Bulk Carrier 2	3		0.036		2		0.059	
Bulk Carrier 3	199	199	3.276	1.942	134	204	3.314	2.430
Bulk Carrier 4	199	218	2.659	1.714	219	216	4.118	2.470
Bulk Carrier 5	40	38	2.007	1.148	42	39	2.263	1.360
Bulk Carrier 6	1	1	0.019	0.011	1	1	0.051	0.031
Bulk Carrier 7	7	7	0.130	0.077	7	7	0.385	0.258
Chemical Tanker	120	120	1.302	0.772	118	118	1.579	0.936
SubPX	16	15	0.346	0.193	15	14	0.238	0.132
Panamax	130	66	3.535	1.065	130	65	2.986	0.905
PPXGn1	147	134	6.530	3.974	148	135	5.618	3.380
PPXGn2	93	86	4.612	2.815	94	87	3.957	2.432
PPXGn3	135	124	8.051	4.923	133	124	6.691	4.171
Cruise	86	86	1.707	1.012	86	86	1.341	0.795
General Cargo 1	226	226	2.309	1.368	227	227	1.917	1.136
General Cargo 2	173	173	1.927	1.142	174	174	2.009	1.191
Tanker Panamax	65	65	1.335	0.791	66	66	0.685	0.406
Aframax Tanker	55	55	2.513	1.490	56	56	1.914	1.134
	1695	**1613**	**42.292**	**24.436**	**1652**	**1619**	**39.124**	**23.167**

Computed VGWE in the tables above is representative of the deep water statistically significant wave height, H_{mo}. The equivalent deep water wave height, H_{mo}, is not generally used to describe VGWE in this manner but this study chose not to compute the wave power (energy/unit length) to give the reader a direct comparison and relationship to VGWE measured and provided in Chapter 3 without bias or needed conversions. Forgoing the conversion to wave power does not induce bias in the comparison as dependent variables in the conversion are indifference between with and without project scenarios.

Comparison of with and without project for any case or combination thereof shows no increase in VGWE as a result of the proposed project. The comparison proves further within all vessel classes the without project condition VGWE is less than with project and can be contributed to the decrease in vessel transits as a result of project construction. Comparing Table 11 and Table 12 or Table 13 and Figure 14 shows a diverging relationship between the lower bay site and upper bay site proving a larger channel cross-section will result in less VGWE. These findings are not unexpected and make clear the impact/relationship of channel geometry in confined channels. In Chapter 1, the theoretical background of VGWE suggested vessels transiting confined channels tend to create a larger disturbance in the water surface elevation and is proportional to the VGWE. The results of this study agree with this theoretical relationships and strengthens the finding of no increase in VGWE for the proposed project.

Sensitivity Analysis

Methods used in this study to compute VGWE relied on assumptions of vessel speed being invariable between with and without project conditions. Other degrees of freedom for channel geometry and vessel dimensions were incorporated in the computed VGWE from previous sections of this chapter and found to be insignificant. Vessel speed is discussed numerous times in this chapter and previous chapters as being a significant and proportional function of VGWE. For this study vessel speed was assumed equivalent to the mean speed derived from AIS data obtained for the 2016 calendar year, categorized by vessel length, and associated with vessel types. However, Figure 34 showed maximum vessel speed may far exceed the mean values, and further, speed could be related to the channel depth to vessel draft ratio or more explicitly the Froude number, F_d, such that vessel speed increases as the under keel clearance increases. This sensitivity is tested in the most simplistic manner using the results of Table 11 (2025, upper bay) for departures since the computed VGWE difference between with and without project is smallest (4.971). Three test conditions, described below, are used evaluate vessel speed sensitivity.

- Constant multiplier of 1.25 (+25%) applied to all vessel types for with and without project conditions.
- Constant multiplier of 1.25 (+25%) applied only to with project condition.

- Froude number, F_d, held constant for computed VGWE, with respect to each vessel class and respective draft, for with and without project conditions.

Table 15: Results of three unique vessel speed sensitivity tests for the 2025 forecasted arrivals at the upper bay site.

Sensitivity Test Case	VGWE w/o Project	VGWE w/ Project	Difference
2025 Forecasted (Table 11)	19.337	14.366	4.971
Equivalent 1.25 Speed Multiplier	26.28	19.524	6.756
1.25 Multiplier for w/Project	19.337	19.524	-0.187
2025 Forecasted Equivalent Froude Number	19.337	15.883	3.454

Sensitivity test results in Table 15 show variation in vessel speed for with and without project conditions create a case where impacts may be realized as a result of the proposed project. However, the case of vessel speed arbitrarily increased for the with project condition and no change to vessel speed for the without project is likely impractical. Previously in this chapter, maximum vessel speed of large vessels transiting the semi-confined channel in Mobile Bay was shown to be limited by channel geometry, vessel squat, and most importantly safety and as a matter of economic efficiency it is reasonable to assume vessels are transiting the channel at the maximum speed possible within these constraints. Ignoring safety as a limiting factor and only considering the quantifiable constraints as a relationship between vessel dimensions and channel geometry, the last sensitivity case where the Froude number is considered equivalent between with and without project conditions is the most probable case to evaluate the highest likelihood of potential impacts from VGWE. In this practical case, it is shown total VGWE for with project condition does not exceed the without project total VGWE, whereby it is proven for practical variances in vessel speed between with and without project conditions there will be no impact as a result of the proposed project.

Summary

Potential impacts of VGWE were evaluated by comparing the relative difference of with and without project conditions using forecasted vessel calls for years 2025 and 2035. Vessel speed was obtained from a statistical summary of 2016 AIS data categorized by vessel length. VGWE was computed using the model published by Schoellhamer (1996), defined in Equation 14. No increase in VGWE was determined as a result of the proposed project. The confidence of this finding was tested with respect to the assumption of vessel speed which determined for practical potential increases in vessel speed as a result of the project the relative difference in VGWE does not become negative.

5 Cumulative Impacts Assessment

Cumulative impacts related to the Mobile Harbor Federal Navigation Channel is investigated using the rate of shoreline change along the western shore of Mobile Bay as a proxy for determining cumulative impacts, associated with vessel generated wave energy, with respect to modification of the federal navigation channel as a function of vessel callings to the port of Mobile. It is hypothesized the number of vessels transiting the federal navigation channel is inversely related to the rate of shoreline change represented as length per year. This hypothesis relies on a firm understanding of all forces acting on the shoreline. However, this is generally not fully understood and instead will be inferred and qualitatively assessed by way of documented channel modifications and shoreline characterization.

Potential for error is high due to the uncertainties and will be minimized to the greatest extent possible. Possible sources of error are shoreline delineation, vessel counts, and density of temporal shoreline data points. The absence of temporal data for shoreline change over the period examined is one of the largest uncertainties. An assumption of linear rate of change between points will be used.

Vessel Callings

Number of vessel callings is obtained from the Waterborne Commerce of the United States (WCUS). The WCUS compiles an annual report of vessel traffic and associated commodities for all U.S. navigable waterways. Publication of these reports was authorized by the River and Harbor Act of September 22, 1922. The methodology used to obtain the data can be found in these reports and will not be detailed here. The resulting data available and used in this report for vessel calling is delineated by vessel class, draft, inbound/outbound, and origin (foreign/domestic). The cumulative impacts analysis in this report obtained reports for all calendar years between 1956 and 2017. These data were filtered for vessel classes 1 and 2 for all directions and origins then aggregated by 1 foot increments of draft greater than or equal to 19 feet. A summary plot of all vessel calls as a function of vessel draft and year is shown in Figure 37 and aggregated by year in Figure 38.

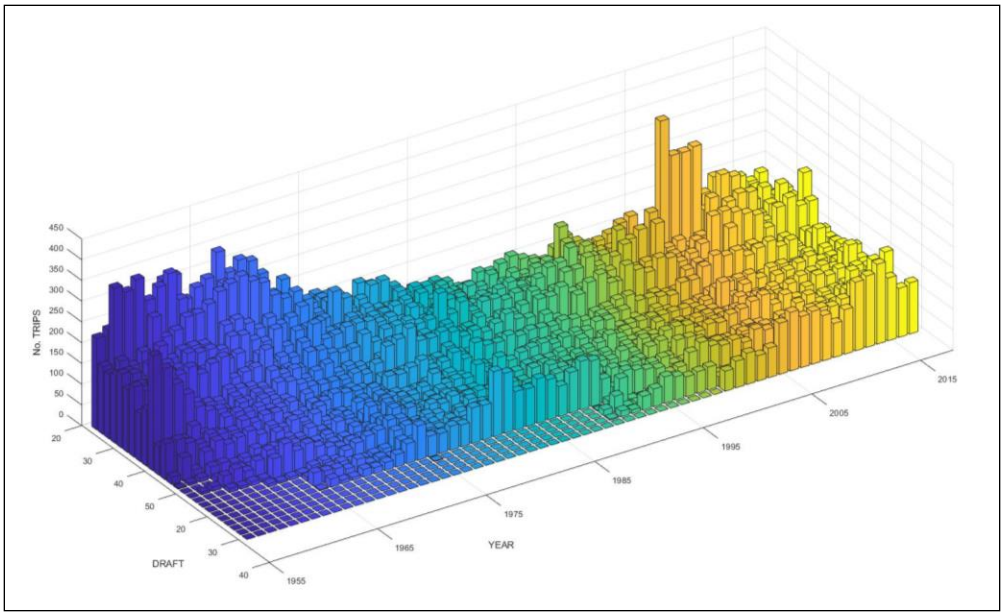

Figure 37: Summary of class 1 and 2 vessel calls obtained from WCUS annual reports (1956-2017) aggregated by draft plotted as a function of year.

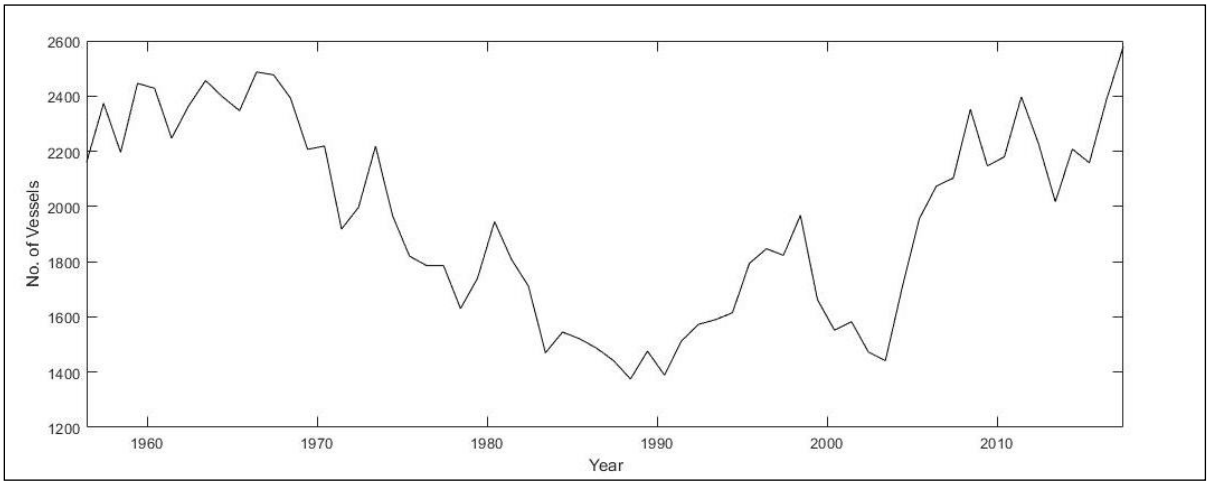

Figure 38: All class 1 and 2 vessel calls obtained from WCUS annual reports (1956-2017) by year for all drafts greater than or equal to 19 feet.

Shoreline Inventory

Shoreline position data were compiled at 7 selected locations along the western shoreline of Mobile Bay from Brookley Aeroplex (approx. latitude 30.6060º) to Alabama Port (approx. latitude 30.3400º) defined by tributaries, orientation, recognized unincorporated communities and qualitative visual observation of shoreline classification, see Figure 39. These sites were screened for locations having greater than 10 points of shoreline position data between 1840 and 2011. Three locations (SL1, SL3, and SL6) met the screening criteria and carried forward in the analysis.

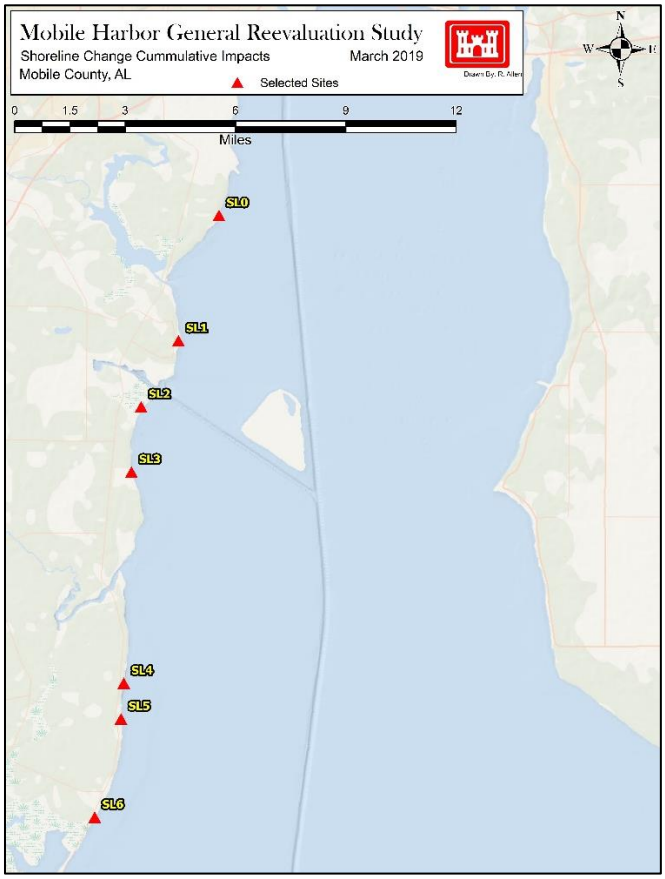

Figure 39: Selected sites used to evaluate shoreline change.

Shoreline position data were extracted from the National Oceanic and Atmospheric Administration (NOAA) Shoreline Database (NOAA, 2019) and augmented using historical aerial imagery obtained from the University of Alabama (University of Alabama, 2019). Aerial imagery obtained from the University of Alabama was processed using manual shoreline delineation methods (Li et al., 2001; Morton et al., 2004; Boak and Turner, 2005; Zarillo et al., 2008; Byrnes et al., 2013; Eulie et al., 2013). The methodology consisted of geo-rectifying the imagery using a minimum of 6 consistent control points at each site which were identifiable through the temporal range of analysis. The rectified image must have less than 1 meter of error in the rectification process. The high water line was used to delineate the shoreline based on a hierarchy of visual criteria developed by Byrnes et al., (2008) and consistent with other methods used for developing NOS T-sheet shorelines (Shalowitz, 1964). A list of applicable shorelines with, source, estimated error, and site applicability is provided in Table 16. The estimated random error related to these shorelines is based on the uncertainty described by Byrnes et al., 2008. While the error generally exceeds the computed changes, this study assumes it to be negligible but acknowledges this will likely result in a large distribution of values. The distribution will be minimized to the greatest extent through finer sampling resolution within each site and averaging of the error along with professional

judgment used for omission of sample transects indicating extreme error in the delineation technique.

Table 16: Inventory of shoreline position data, applicable locations, source, and selected data quality parameters.

Date	Source	Type	Scale	Estimated Error (ft)	SL1	SL3	SL6
1849-06-01	Applied Coastal	T-Sheet, Surveyed	1:20,000	+/- 36 ft		1	1
1850-06-01	Applied Coastal	T-Sheet, Surveyed	1:20,000	+/- 36 ft	1		
1918-04-01	Applied Coastal	T-Sheet, Surveyed	1:40,000	+/- 36 ft	1	1	1
1934-07-16	NOAA	T-Sheet from interpreted Imagery	1:20,000	+/- 33 ft	1	1	1
1940-06-01	UA Maps	Rectified Aerial Imagery	1:3,500	+/- 60 ft		1	1
1950-06-01	UA Maps	Rectified Aerial Imagery	1:3,500	+/- 60 ft			1
1952-06-01	UA Maps	Rectified Aerial Imagery	1:3,500	+/- 60 ft	1		
1957-11-01	NOAA	T-Sheet from interpreted Imagery	1:10,000	+/- 20 ft	1	1	
1957-11-19	NOAA	T-Sheet from interpreted Imagery	1:10,000	+/- 20 ft			1
1960-06-01	UA Maps	Rectified Aerial Imagery	1:2,500	+/- 12 ft	1		1
1974-06-01	UA Maps	Rectified Aerial Imagery	1:2,500	+/- 12 ft	1	1	1
1982-03-01	NOAA	T-Sheet from interpreted Imagery	1:20,000	+/- 13 ft	1	1	1
1992-06-01	UA Maps	Rectified Aerial Imagery	1:2,500	+/- 12 ft			1
1993-06-01	UA Maps	Rectified Aerial Imagery	1:2,500	+/- 12 ft	1	1	
1997-06-01	UA Maps	Rectified Aerial Imagery	1:2,500	+/- 12 ft	1	1	1
2009-06-01	UA Maps	Rectified Aerial Imagery	1:2,500	+/- 8 ft	1	1	1
2010-10-09	Applied Coastal	Orthorectified Imagery	1:2,000	+/- 6 ft	1	1	
2011-05-07	Applied Coastal	Orthorectified Imagery	1:2,000	+/- 6 ft			1
		Total:			**12**	**11**	**13**

Shoreline positions for all time periods were imported to a desktop mapping program at the three locations aforementioned. Shore perpendicular transects were generated at 20 meter (65.6 feet) intervals connected to an onshore baseline. The USGS program Digital Shoreline Analysis System (DSAS) the distance from baseline was computed for the shorelines along each transect. The incremental linear distance between temporal shoreline positions was computed along with the respective rate of change (feet/year), where negative values represent erosion. A linear regression fit rate of change between the 1849/1850 and 2010/2011 shoreline positions was also computed to evaluate the overall trend spanning the dataset. Figure 40, Figure 41, and Figure 42 are the results of the linear regression, where the transect lines are colored by rate of shoreline change. The linear regression rate of change is clearly net erosion for all locations with the exception of a few outlying transects for the temporal range of 1849/50 to 2010/11. The result is largely due to the shoreline position between 1849/50 and 1917/18. Detailed shoreline change analysis is shown later in the report.

Figure 40: Linear regression rate of shoreline change for SL1 for 1849/1850 through 2010/2011.

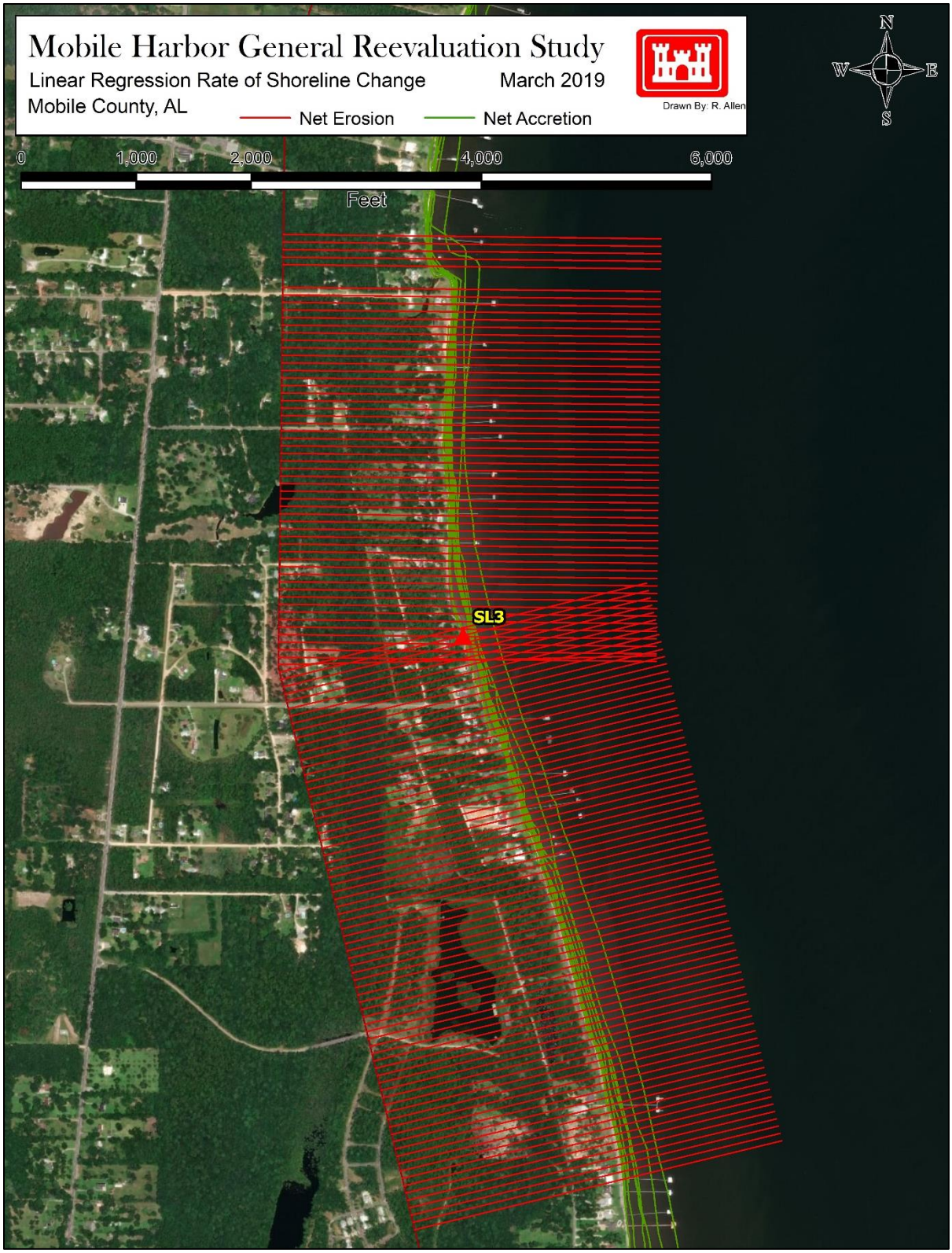

Figure 41: Linear regression rate of shoreline change for SL3 for 1849/1850 through 2010/2011.

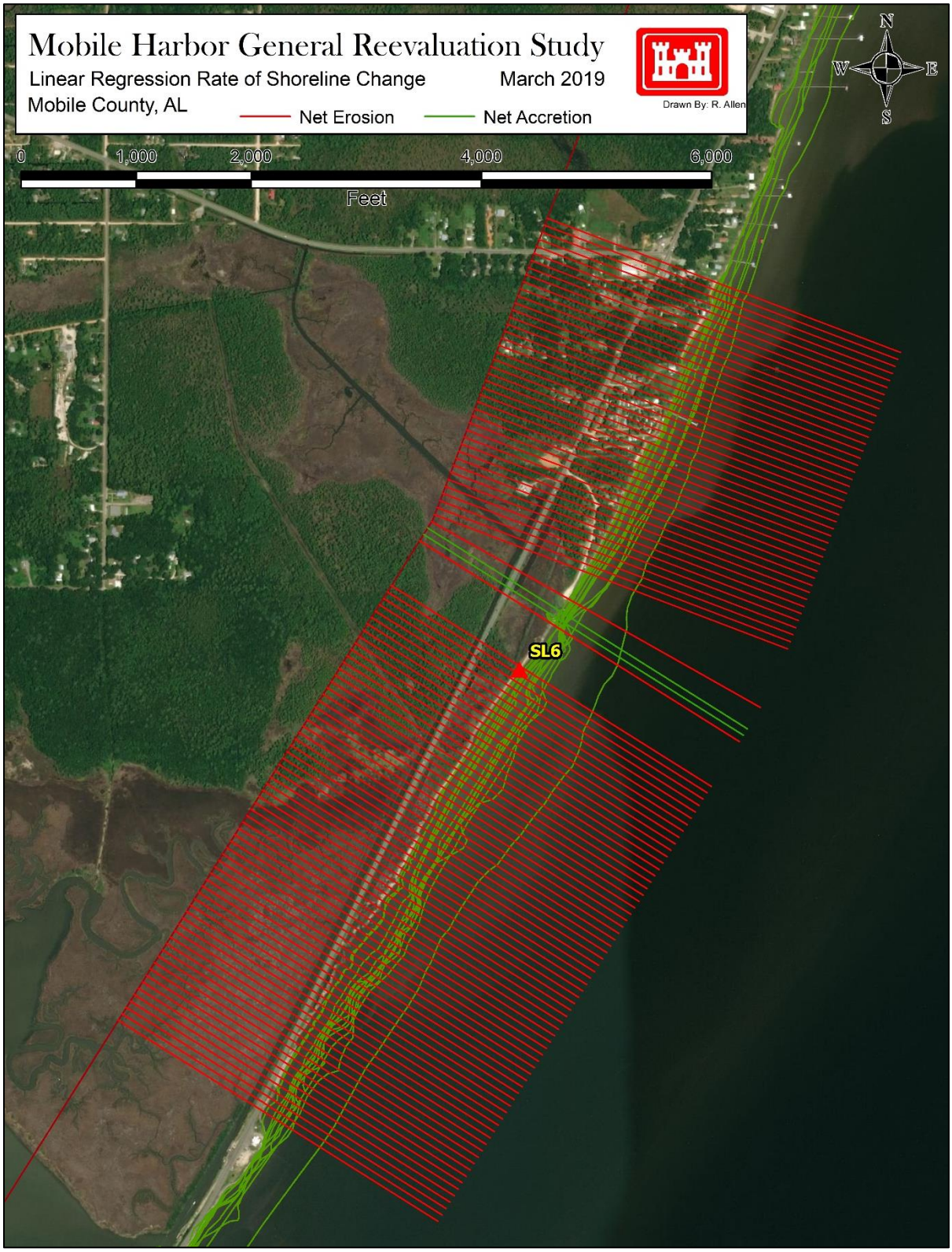

Figure 42: Linear regression rate of shoreline change for SL6 for 1849/1850 through 2010/2011.

Mobile Bay Ship Channel Dimensions

The Mobile Bay Federal Navigation Channel has undergone multiple improvement through the years. The first recorded authorization for the channel occurred in the early 1800's with dredging at various sections along the present alignment. It was not until the River and Harbor Act of June 25, 1910 authorized a continuous channel 27 feet deep by 200 feet wide channel, completed in 1913, from Dauphin Island to the Mobile River along the present day alignment. Following this the channel was deepened and widened four additional times between 1913 and 1989 to the current maintained dimensions of 45 ft x 400 ft. The dates and dimensions for these channel modifications are provided in Table 17 plotted as total cross-sectional area of the navigable portion of the channel (i.e. depth x bottom width) in Figure 43.

Table 17: Summary of Channel Modifications between 1913 and 1989.

Date Completed	Channel Dimensions (ft)
August 15, 1913	27 x 200
July 25, 1926	30 x 300
July 19, 1933	32 x 300
November 10, 1964	40 x 400
July 3, 1989	45 x 400

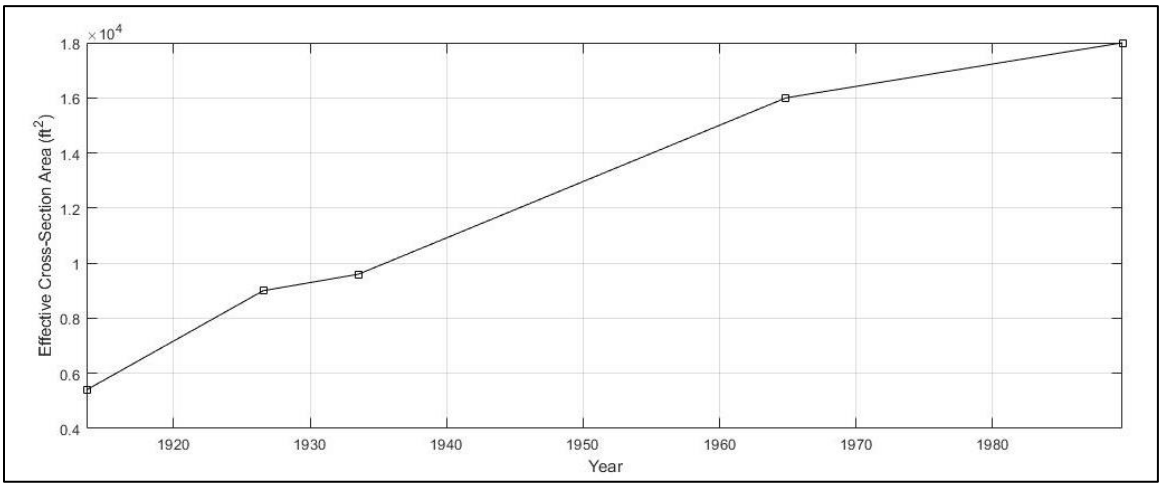

Figure 43: Temporal plot of channel modifications between 1913 and 1989. Channel dimensions are represented as a cross-sectional area in square feet of the navigable portion

Shoreline Characterization and Change Analysis

Shoreline composition along the western shore of Mobile Bay is generally classified as, sloped sandy beach, vegetated marsh, or structured. Byrnes et al., (2013) completed a comprehensive spatial and temporal dependent classification of shorelines delineated by zones for Mobile Bay.

Byrnes et al., (2013) found a mostly erosive environment for the western shore over the analysis period and between points. The general shoreline classifications from Byrnes et al., (2013) will be used in this analysis for describing shoreline type to the extent applicable.

Douglass and Pickel (1999) investigated shoreline development/armoring along the shorelines of Mobile Bay between 1955 and 1997 using aerial photography and determined the rate of armoring to be increasing and generally follows the population growth for Mobile and Baldwin Counties during the study period. Spatial and temporal distribution of shoreline armoring concluded by Douglass and Pickel (1999) is shown in Figure 44 and an annual rate of change between 0.3 and 1.1 percent armored per year.

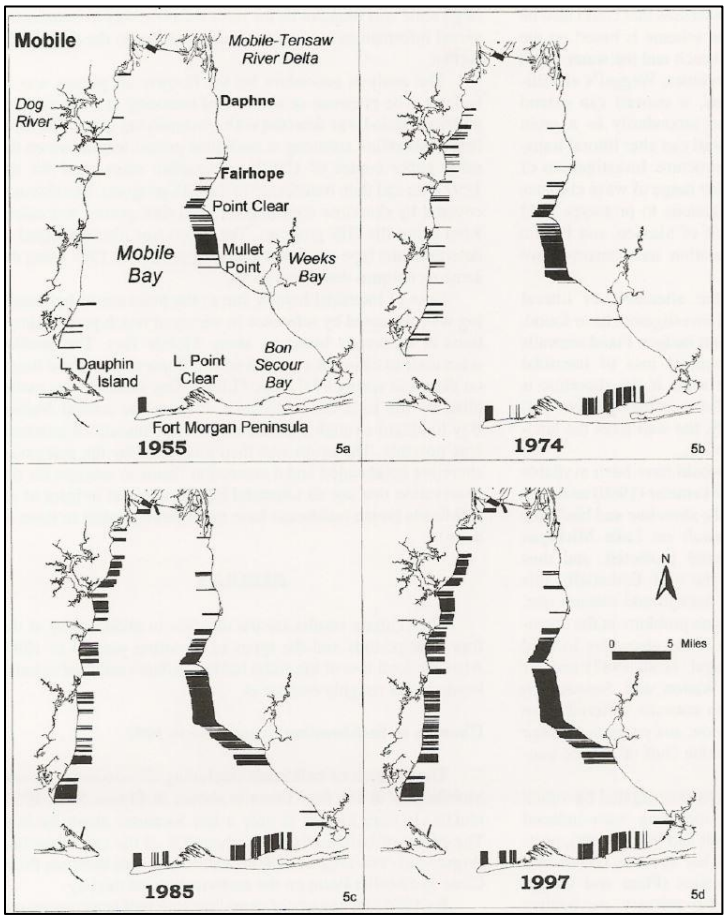

Figure 44: Spatial and Temporal Distribution of shoreline armoring between 1955 and 1997 extracted from Douglass and Pickel (1999).

SL1 Site Characterization and Shoreline Change Results

SL1 includes approximately 1800 meters (5906 feet) of linear shoreline located south of Dog River and north of the Theodore Ship Channel along a shoreline generally known as Hollinger's Island.

The shore normal incident angles range between 82º and 105º. The offshore bathymetry is gently sloping. In 1943 discrete placements of dredge material related to excavation of Hollinger's Channel occurred along the shoreline and dominate the SL1 reach. These sites are distinguish by un-natural undulations in the shoreline. The Theodore Ship Channel and Gaillard Island, constructed between 1979 and 1981, are located to the southeast and could influence the temporal trend of change. Examination of aerial imagery from 1952 to 2011 indicates a high rate of development and armoring beginning in 1993.

Shoreline change computations found the average linear regression rate of change from 1917/18 to 2010/11 for all transects was -0.28 m/yr (0.9 ft/yr). The temporal trend of shoreline change rates computed at each available shoreline position are shown graphically below.

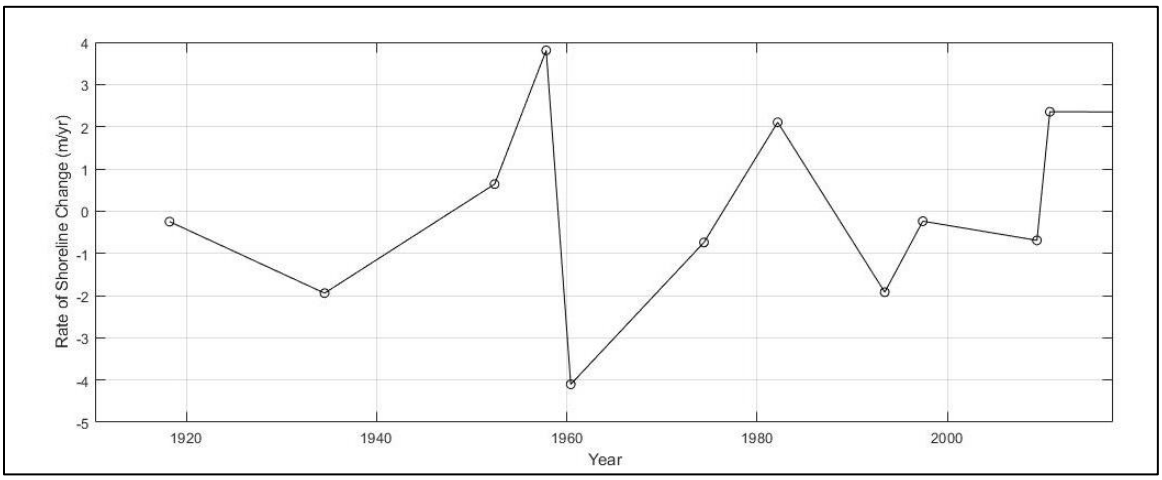

Figure 45: Temporal distribution of shoreline change rates at SL1 between 1917/18 and 2010/11 with linearly interpolated rate of rate of change.

Shoreline change rate magnitude changes over time are consistent with the results of Byrnes et al., (2013) and indicative of the evolutional changes to the shoreline characteristics. The highest rate of change of erosion rate between 1957 and 1960 shoreline position is a result of the termination of dredge material placement with a reducing trend of erosion rates between 1960 and 1982 as the constructed marsh areas equilibrated. From 1982 and 1993 the erosion rates increased and could be attributed to extensive shoreline development, observed in aerial photography, related to Theodore Ship Channel operations. A second decreasing trend between 1993 and present is likely related to shoreline armoring and perhaps a "shadowing" effect of Gaillard Island from dominate southeast winds.

SL3 Site Characterization and Shoreline Change Results

SL3 includes approximately 2500 meters (8203 feet) of linear shoreline located South of Theodore Ship Channel and North of Fowl River. The shore normal incident angles range between 76º and

91º with a gently sloping, unobstructed, offshore bathymetry. Theodore Ship Channel and Gaillard Island, constructed between 1979 and 1981, are located to the northeast and could influence the temporal trend of change. Aerial photography in 1940 indicates most of the shoreline is undeveloped with a sandy shoreline backed by forested areas with no clear visually identified armoring until 1997. In 2009 the conversion of sandy beach to armored shorelines is more prevalent; however, sandy shorelines are still the majority. Adjacent shorelines are similar is characteristics and trends and should pose little differing influence.

Shoreline change computations found the average linear regression rate of change from 1917/18 to 2010/11 for all transects was -0.47 m/yr (1.5 ft/yr). The temporal trend of shoreline change rates computed at each available shoreline position are shown graphically below.

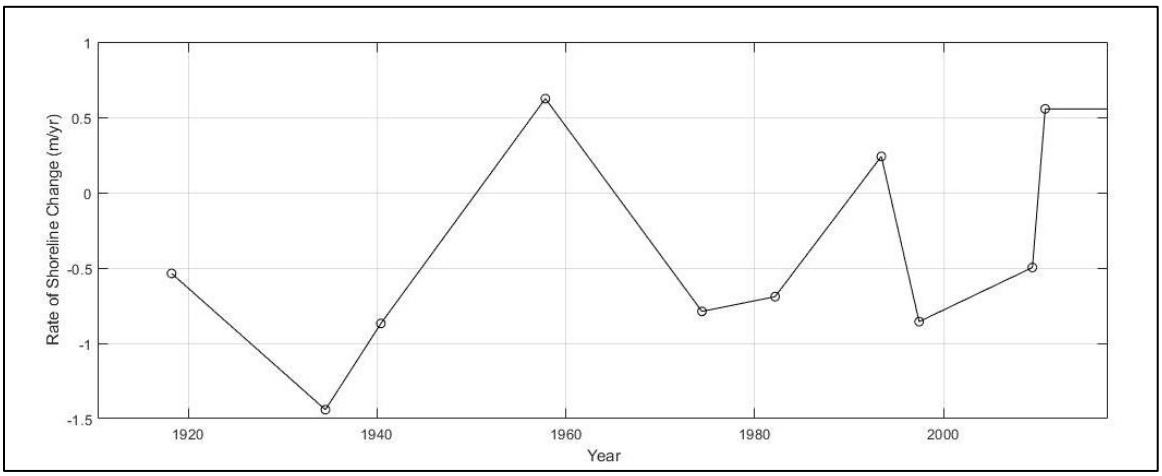

Figure 46: Temporal distribution of shoreline change rates at SL3 between 1917/18 and 2010/11 with linearly interpolated rate of rate of change.

Shoreline change rate magnitude changes over time are consistent with the results of Byrnes et al., (2013) and indicative of the evolutional changes to the shoreline characteristics. The transition of erosional to accretion between 1934 and 1957 Byrnes et al., (2013) related this to construction of Hollinger's Ship Channel; however, this site is situated south of the channel where sediment transport and dominate wave directions would not be influenced and unrelated. The accretional trend dictated by the 1957 point then returning to erosional in 1974 is more than likely a product of error in the shoreline interpretation method and likely should be omitted. Comparison of aerial imagery from 1940 and 1974 shows minor development but no clear indications of shoreline armoring further supporting the erroneous shoreline position in 1957. Reviewing the trend shown in Figure 46, ignoring the 1957 point, closely follows an undeveloped shoreline with a possible influence of sea level rise and minimal development influence. The rate of shoreline change rate has a slight positive slope until visible vertical armoring is seen around 1997 and continued to increase (decreasing erosional rate) in subsequent years.

SL6 Site Characterization and Shoreline Change Results

SL6 includes approximately 2500 meters (8203 feet) of linear shoreline located south of Fowl River, just north of Cedar Point, and generally referred to as Alabama Port. The shore normal incident angles range between 111º and 122º with a gently sloping unobstructed offshore bathymetry. SL6 is within close proximity to Cedar Point which is a known focal point with high rates of erosion prior to construction of U. S. Highway 193 bridge abutment, effectively fixing the point and altering astronomical tide exchange between Heron and Mobile Bay. This modification appears to have also influenced regional sediment transport pathways based on the large morphological change of the ebb and flood shoals associated with Pass aux Herons, determined using a visual comparison of aerial photography in 1940 and 1974.

Shoreline change computations found the average linear regression rate of change from 1917/18 to 2010/11 for all transects was -0.82 m/yr (2.7 ft/yr). The temporal trend of shoreline change rates computed at each available shoreline position are shown graphically below.

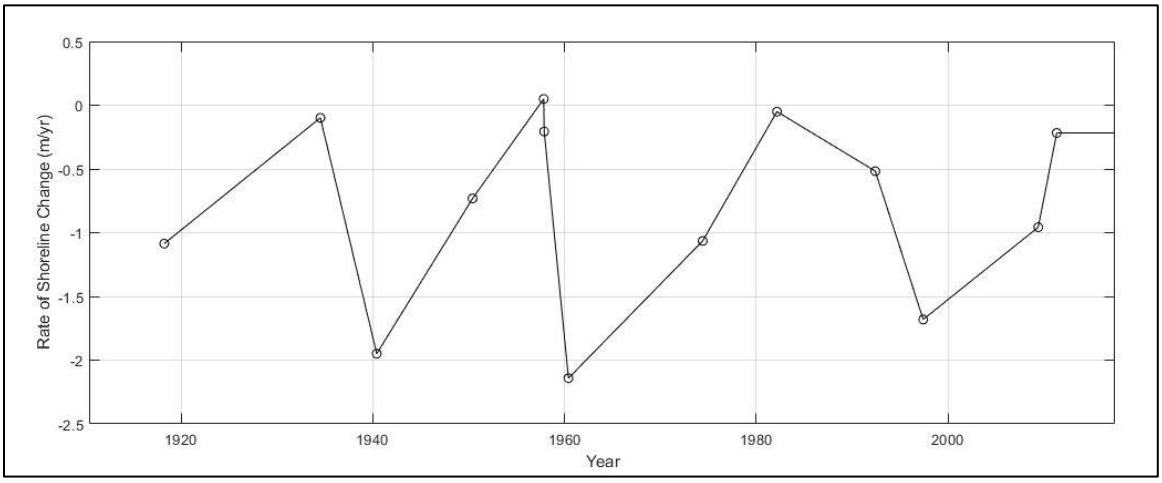

Figure 47: Temporal distribution of shoreline change rates at SL3 between 1917/18 and 2010/11 with linearly interpolated rate of rate of change.

Temporal trends of shoreline change rates at SL6 in Figure 47 do not show an immediate discernable pattern. The fluctuation could be associated with error or some function of extreme events as suggested by Byrnes et al., (2013). Overall, there does not appear to be a positive or negative net change in shoreline change rates.

Comparison of Shoreline Change and Vessel Calls

The previous section described shoreline change rates and the trend thereof without consideration of influence by the Mobile Ship Channel. This section will attempt to make correlations of trends

in shoreline change rates to annual vessel call counts. As stated the hypothesis of this analysis is the number of vessels transiting the federal navigation channel is inversely related to the rate of shoreline change represented as length per year. The analysis will first look holistically at the vessel counts and the combined trend of shoreline change from all three sites (Figure 48) followed by subsets and samples of vessel counts and shoreline lengths.

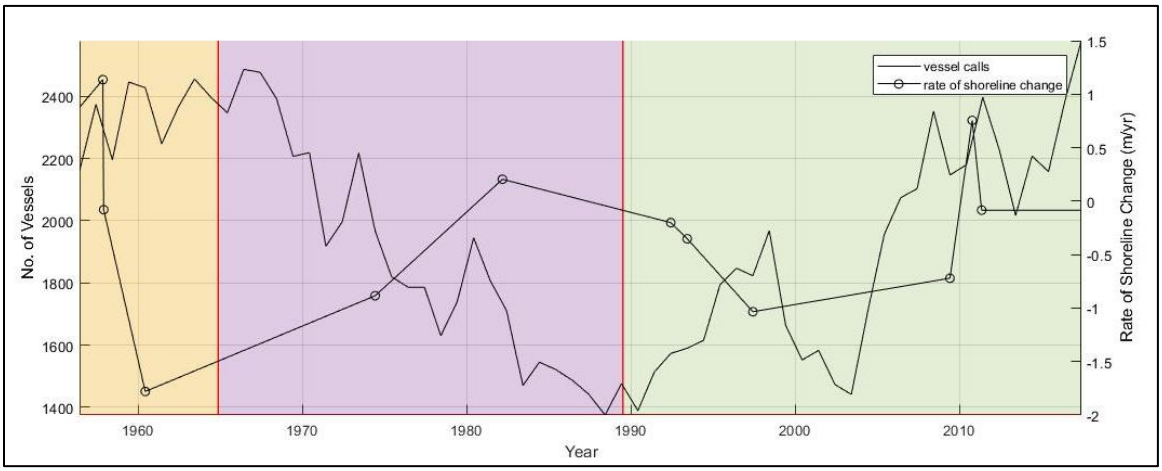

Figure 48: Plot of vessel count for Mobile Harbor between 1956 and 2017 of all vessels having a draft greater than 19 feet compared to combined average shoreline change rates for sites SL1, SL3, and SL6. Channel dimension changes are identified using the plot background.

Figure 48 appears to show an inverse correlation between shoreline change and vessel calls between 1957 and around 2000 indicating the more vessels calling to port results in an increase in shoreline erosion rates. The lack of correlation after 2000 is expected as shoreline armoring becomes much more prevalent after this time (Douglass and Pickel, 1999)

While the holistic approach does indicate an inverse correlation of temporal shoreline change rates as a function of vessel callings, a detailed assessment, on a site-by-site basis, is warranted to confirm it is not a coincidence or explained by other means such as locality, extreme events, and wave climate. The first step, site dependency, is plotted in Figure 49 followed by discussion of other forcings relationships and trends at each site.

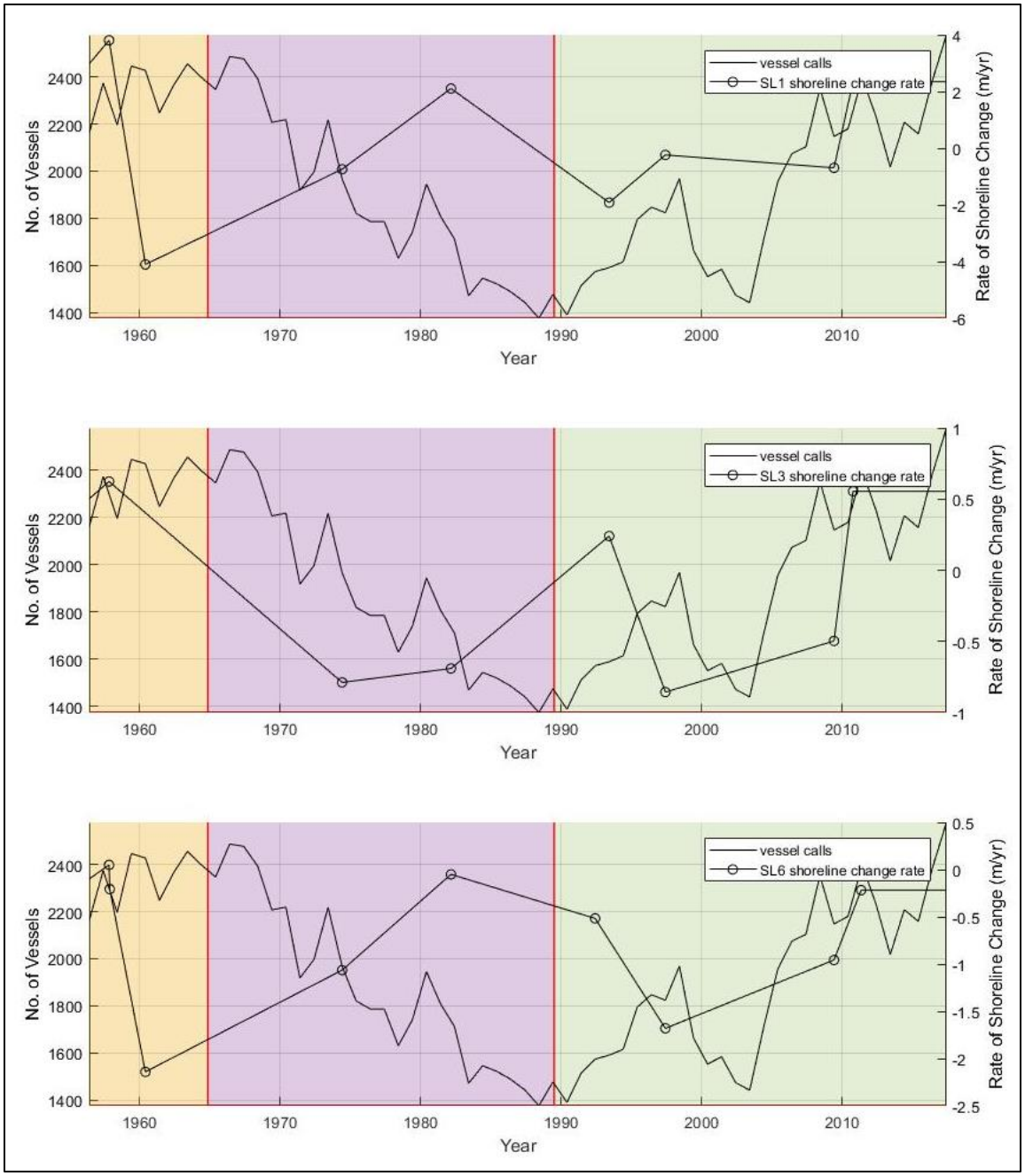

Figure 49: Plot of vessel count for Mobile Harbor between 1956 and 2017 of all vessels having a draft greater than 19 feet compared to average shoreline change rates computed for each site. Channel dimension changes are identified using the plot background color.

Correlations of vessel calls to temporal trends in the shoreline rate of change for each site generally agree (varying magnitude) from 1997 to present with a positive trend (less erosion) which is, again, expected based on the increased percentage of shoreline armoring. However, the trend between 1960 and 1993 for SL3 appears to be starkly different than SL1 and SL6 and does not follow the inverse correlation with vessel calls. Reasons for this dissimilarity are unknown. Of the two sites

that follow the inverse relationship with vessel calls, SL1 represents a much larger magnitude than SL6. The range of shoreline change rates for SL1 is between -4.1 and 3.8 meters/year while SL6 ranges between -2.1 and 0.05 meters/year. While the range is greater for SL1 it is generally centered about the zero axis whereas SL6 is more consistently erosional. The higher range at SL1 is most likely correlated to the placement of dredge material during construction of Hollinger's Island Ship Channel, construction of Gaillard Island, and in bay dredge material placement practices north of Gaillard Island and along the Mobile Ship Channel. The drastic fluctuations between erosional and accretional appear to be more similarly related to placement (accretion) and equilibration (erosion) as a result of these activities. Influence of other activities in the vicinity of SL1 does question the correlation of vessel calls to the visual trends shown in Figure 49 and where the trend of shoreline change rates and the influence of the Mobile Ship Channel is not able to be quantifiably correlated using the available data. SL6 is much further than SL1 from other anthropogenic changes and does appear to have an inversely correlated trend to vessel calls. However, the range of shoreline change rates is small and error associated with delineation of shoreline positions in inherently large (Byrnes et al., 2013) such that additional work would not lead to a more precise result. Furthermore, the unavailability of additional shoreline data points induces large interpolated ranges masking additional temporal trends.

Summary

An investigation of cumulative impacts resulting from construction and proposed deepening of the Mobile Harbor Federal navigation channel was completed. The assessment sought to correlate temporal trends in shoreline change rates at three representative locations along the western shore of Mobile Bay to annualized vessel transits. Shoreline position data at 10 points between 1917/18 and 2010/11 was obtained or generated as part of the study. Vessels calling to the Port of Mobile for 1956 to 2017 were obtained from the Water Borne Commerce of the United States (WCUS) annual summary reports. These data were plotted along a temporal scale and indicate a possible inverse correlation where an increase in vessel calls results in increased erosion. In detail only one site (SL6) cannot be explained elsewise but to have a weak correlation; however, the range of shoreline change rates falls within the error band and likely a product of random error in the shoreline position delineation. As for long term effect arising from constructing the recommended plan, it is clear the vast majority of shoreline is armored an all sites agree that from 1997 to present there is no relationship between the number of vessel calls and shoreline change rates. Therefore, present and foreseeable cumulative impacts of VGWE on Mobile Bay shorelines are considered not significant.

6 References

Bhowmik, N. G. (1975). Boat-Generated Waves in Lakes. Technical Note, Journal of the Hydraulics Division. American Society of Civil Engineers. pp. 1465-1468.

Blaauw, H.G., de Groot, M.T., Knaap, F. C. M., Pilarczyk, K.W. (1985). Design of Bank Protection of Inland Navigation Fairways. Proceedings of the Conference on Flexible Armoured Revetments Incorporating Geotextiles, Thomas Telford, London, England, pp. 39-66.

Capilier, C., Rousseaux, G., Calluaud, D., David. L. (2015). An Experimental Study of the Effects of Finite Water Depth and Lateral Confinement of Ship Wake and Drag. Congres SHF: Hydrodynamics and Simulation Applied to Inland Waterway and Port Approaches. Meudon.

Chen, Q., Zhao, H,. Hu, K,. Douglass, S. L. (2005). Prediction of Wind Waves in a Shallow Estuary. Journal of Waterway, Port, Coastal, and Ocean Engineering. American Society of Civil Engineers. 131(4), pp. 137-148.

Chuang, L. Z., Wu, L., Wang, J. (2013). Continuous Wavelet Transform Analysis of Acceleration Signals Measured from a Buoy. Sensors 2013(13). MDPI, Basel, Switzerland. pp. 10909-10930.

David, C. G., Roeber, V., Goseberg, N., Schlurmann, T. (2017). Generation and Propagation of Ship-Borne Waves – Solutions from a Boussinesq-Type Model. Journal of Coastal Engineering, 127(2017), pp. 170-187.

de John, M. P. C., Roelvink, D., Reijmerink, S.P., Breederveld, C. (2013). Numerical Modelling of Passing-Ship Effects in Complex Geometries and on Shallow Water. Smart Rivers 2013, PIANC, Maastricht, The Netherlands.

Didenkulova, I., Sheremet, A. Torsvik, T., Soomere, T. (2013). Characteristic Properties of Different Vessel Wake Signals. Proceedings 12th International Coastal Symposium (Plymouth, England), Journal of Coastal Research, Special Issue No. 65, pp. 213-218.

Gates, E. T. and Herbich, J. B. (1977). Mathematical Model to Predict the Behavior of Deep-Draft Vessels in Restricted Waterways. Report TAMU-SG-77-206. Texas A&M University, College Station, Texas.

Gibbons, D. T., Jones, G., Siegel, E., Hay, A., Johnson, F. (2015). Performance of a New Submersible Tide-Wave Recorder. RBR Limited. Ottawa, Ontario, Canada.

Havelock, T.H. (1908). The Propagation of Groups of Waves in Dispersive Media, with Application to Waves on Water Produced by a Travelling Disturbance. Proceedings of the Royal Society of London. 81(549), pp. 398-430.

International Maritime Organization (IMO) (2015). Revised Guidelines for the Onboard Operational Use of Shipborne Automatic Identification Systems (AIS). 29th Session, Agenda Item 10. Resolution A.1106(29). International Maritime Organization, London, England.

Javanmardi, M., Binns, J., Renilson, M., Thomas, G. (2017). Influence of Channel Shape on Wave-Generated Parameters by a Pressure Source in Shallow Water. Journal of Waterway, Port, Coastal, Ocean Engineering. American Society of Civil Engineers. 143(5), pgs. 9.

Jiang, T., Henn, R., Sharma, S. D. (2002). Wash Waves Generated by Ships Moving on Fairways of Varying Topography. 24th Symposium on Naval Hydrodynamics, Fukuoka, Japan, pgs. 15.

Kriebel, D.L. and Seelig, W. N. (2005). An Empirical Model for Ship-Generated Waves. 7th International Conference on Mathematical and Numerical Aspects of Waves (Waves 05), Madrid, Spain.

Mallet, S. (2009). A Wavelet Tour of Signal Processing – The Sparse Way. Academic Press as an Imprint of Elsevier. Burlington, Massachusetts.

Maynord, S. (2007). Ship Forces on the Shoreline of the Savannah Harbor Project. Technical Report ERDC/CHL TR-06-19, U.S. Army Corps of Engineers, Engineering Research and Development Center, Vicksburg, Mississippi.

Maynord, S. (2011). Reanalysis of Ship Forces at the Shoreline using Updated Draft Information, Savannah Harbor, Savannah, Georgia. Draft Report, U.S. Army Corps of Engineers, Engineering Research and Development Center, Vicksburg, Mississippi.

National Oceanic and Atmospheric Administration (NOAA) (2018). Coast Guard Sector Mobile, Alabama – Station ID: 8736897. Center for Operational Oceanographic Products and Services (CO-OPS), Silver Spring, Maryland.

Parnell, K. E., Soomere, T., Zaggia, L., Rodin, A., Lorenzetti, G., Rapaglia, J., Scarpa, G. M. (2015). Ship-Induced Solitary Riemann Waves of Depression in Venice Lagoon. Physical Letters A(2015), http://dx.doi.org/10.1016/j.physleta.2014.12.004.

Pelinovsky, E., Talipova, T., Kurkin, A., Kharif, C. (2001). Nonlinear Mechanism of Tsunami Wave Generation by Atmospheric Disturbances. Natural Hazards and Earth System Sciences, European Geophysical Society, pp. 243-250.

Pendygraft, S. L. and Gelfenbaum, G. R (1994) Wave Data in Mobile Bay, Alabama from March 1991 to May 1992. OF 94-0017, U.S. Geological Survey, St. Petersburg, Florida.

Permanent International Association of Navigation Congresses (PIANC) (1987). Guidelines for the Design and Construction of Flexible Revetments Incorporating Geotextiles for Inland Waterways. Working Group 4 of the Permanent Technical Committee, Brussels.

Permanent International Association of Navigation Congresses (PIANC) (1985). Underkeel Clearance for Large Ships in Maritime Fairways with Hard Bottom. Supplement to Bulletin No. 51, Brussels, Belgium.

Rapaglia, J., Zaggia, L., Ricklefs, K., Gelinas, M., Bokuniewicz, H., (2011). Characteristics of Ships' Depression Waves and Associated Sediment Resuspension in Venice Lagoon, Italy. Journal of Marine Systems. 85(2011), pp. 45-56.

RBR Limited (2012). RBRsolo User Guide. Document RBR0000215, RBR Ltd, Ottawa, Ontario, Canada.

Rodin, A., Soomere, T., Parnell, K. E., Zaggia, L. (2015). Numerical Simulation of the Propagation of Ship-Induced Riemann Waves of Depression into the Venice Lagoon. Proceedings of the Estonian Academy of Sciences. 64(1), pp. 22-35.

Schijf, J.B. and Jansen, P.P. (1953). Eighteenth International Navigation Conference, Section I, Communications 1, Rome, Italy.

Schoellhamer, D. H. (1996). Anthropogenic Sediment Resuspension Mechanisms in a Shallow Microtidal Estuary. Estuarine, Coastal, and Shelf Science. Academic Press Limited. 43:533-548.

Sheremet, A., Gravois, U., Tian, M. (2013). Boat-Wake Statistics at Jensen Beach, Florida. Journal of Waterway, Port, Coastal, and Ocean Engineering. American Society of Civil Engineers. 139, pp. 286-294.

Soomere, T. (2006). Nonlinear Ship Wake Waves as a Model of Rouge Waves and a Source of Danger to the Coastal Environment: A Review. Oceanologia, Institute of Oceanology, 48(S), pp. 185-202.

Sorensen, R. (1966). Ship Waves. Technical Report HEL-12-2. University of California, Berkeley, California.

Sorensen, R. M. (1973). Ship-Generated Waves. Advances in Hydroscience, Academic Press, New York, Illinois. pp. 49-83.

Sorensen, R. M. and Weggel, J. R. (1984). Development of Ship Wave Design Information. Proceedings of the 19th Conference on Coastal Engineering, Houston, Texas. American Society of Civil Engineers. New York, Illinois. pp. 3227-3243.

Sorensen, R. M. (1997), Prediction of Vessel-Generated Waves with Reference to Vessels Common to the Upper Mississippi River System. ENV Report 4. Lehigh University, Bethlehem, Pennsylvania.

Thompson, W. (Lord Kelvin) (1887). On Ship Waves. Proceedings of the Institute of Mechanical Engineering, London, England. 38(1), pp. 409-433.

U.S. Army Corps of Engineers, (2006), Coastal Engineering Manual (CEM), U.S. Army Corps of Engineers, Washington, D.C. (6 volumes). EM 1110-2-1100.

U. S. Army Corps of Engineers. (2006). Hydraulic Design of Deep Draft Navigation Projects. U.S. Army Corps of Engineers, Washington, D.C. EM 1110-2-1613.

U. S. Army Corps of Engineers (2010). Wave Information Studies (WIS), Station 73154. U.S. Army Corps of Engineers, Engineering Research and Development Center, Vicksburg, Mississippi.

U.S. Army Corps of Engineers, Huntington District. (1980). Gallipolis Locks and Dam Replacement, Ohio River, Phase I – Advanced Engineering and Design Study. General Design Memorandum, Huntington, West Virginia.

Weggel J. and Sorensen, R. (1986). Ship Wave Prediction for Port and Channel Design. Proceedings of the Ports ’86 Conference, Oakland, California. American Society of Civil Engineers, New York. pp 797-814.

Appendix A

Vessel Generated Wave Energy Data by Transit

ID	MMSI	Class	Length (m)	Width (m)	Draft (m)	SOG	Direction	SW01_Hmo	SW02_Hmo	SW03_Hmo	SW04_Hmo	SW05_Hmo
1	636017004	2	134	16	7.2	12	'outbound'	0.0007	0.0013	0.0028	0.0038	0.0003
2	249944000	3	229	37	13.8	7	'outbound'	0.0008	0.0016	0.0034	0.0084	0.0004
3	477178300	3	292	32	12.9	11	'outbound'	0.0098	0.0167	0.0757	0.1268	0.0061
4	353486000	4	260	32	8.2	13	'inbound'	0.0206	0.0350	0.0447	0.0661	0.0054
5	249550000	1	244	42	8.2	10	'outbound'	0.0042	0.0018	0.0215	0.0339	0.0026
6	538003413	2	190	32	6.7	10	'outbound'	0.0042	0.0018	0.0215	0.0339	0.0026
7	305367000	2	132	16	5.4	12	'inbound'	0.0047	0.0044	0.0047	0.0037	0.0081
8	563635000	2	176	35	5.8	8	'outbound'	0.0028	0.0030	0.0042	0.0032	0.0070
9	353486000	4	260	32	8.2	11	'outbound'	0.0068	0.0104	0.0246	0.0180	0.0096
10	538006092	1	239	42	11.9	9	'inbound'	0.0007	0.0021	0.0139	0.0449	0.0170
11	309587000	2	190	31	9	11	'outbound'	0.0028	0.0071	0.0287	0.0484	0.0409
12	248092000	2	169	27	7.8	11	'outbound'	0.0043	0.0059	0.0194	0.0694	0.0533
13	370261000	2	178	29	6.3	11	'outbound'	0.0019	0.0081	0.0117	0.0223	0.0202
14	309689000	2	131	20	7	11	'inbound'	0.0010	0.0027	0.0047	0.0065	0.0164
15	305057000	2	138	21	6	13	'inbound'	0.0050	0.0074	0.0074	0.0090	0.0216
16	305057000	3	138	21	6	13	'inbound'	0.0050	0.0074	0.0074	0.0090	0.0216
17	636091328	3	275	40	11.6	12	'inbound'	0.0232	0.0354	0.0682	0.1162	0.0174
18	311053600	3	229	32	13.7	10	'inbound'	0.0039	0.0068	0.0208	0.0657	0.0094
19	305367000	2	132	16	5	12	'outbound'	0.0017	0.0042	0.0067	0.0110	0.0080
20	338302000	1	182	36	11.3	10	'inbound'	0.0030	0.0042	0.0245	0.0400	0.0011
21	311923000	1	186	32	8.2	12	'inbound'	0.0109	0.0183	0.0318	0.0356	0.0032
22	305057000	2	138	21	5.6	13	'outbound'	0.0010	0.0043	0.0049	0.0084	0.0010
23	538006092	1	239	42	8.1	10	'outbound'	0.0028	0.0048	0.0267	0.0298	0.0022
24	352179000	1	228	42	12.2	9	'inbound'	0.0007	0.0014	0.0039	0.0255	0.0014
25	477077800	3	261	32	10.9	12	'inbound'	0.0189	0.0342	0.0784	0.0994	0.0021
26	636091328	3	275	40	13	11	'outbound'	0.0078	0.0083	0.0518	0.1414	0.0088
27	235070707	2	198	33	10.4	11	'inbound'	0.0072	0.0137	0.0349	0.0335	0.0016
28	338302000	1	182	36	8.1	10	'outbound'	0.0027	0.0024	0.0083	0.0085	0.0011
29	210516000	3	226	30	9.8	11	'inbound'	0.0031	0.0049	0.0144	0.0131	0.0005
30	538004997	2	200	32	12.2	10	'inbound'	0.0026	0.0040	0.0079	0.0381	0.0005
31	477077800	3	261	32	11.4	10	'outbound'	0.0016	0.0020	0.0610	0.0374	0.0018
32	371208000	3	293	32	11.6	10	'inbound'	0.0026	0.0043	0.0282	0.0416	0.0028
33	210516000	3	226	30	9.6	10	'outbound'	0.0026	0.0044	0.0287	0.0419	0.0027
34	564939000	1	237	42	11.5	9	'inbound'	0.0041	0.0067	0.0221	0.0859	0.0184
35	255805596	3	318	42	10.2	11	'inbound'	0.0093	0.0229	0.0868	0.1421	0.0142
36	371208000	3	293	32	11.7	11	'outbound'	0.0045	0.0071	0.0487	0.1018	0.0121
37	235070707	2	198	33	9.8	11	'outbound'	0.0043	0.0029	0.0175	0.0206	0.0067
38	352179000	1	228	42	8.5	10	'outbound'	0.0027	0.0016	0.0309	0.0344	0.0076
39	563936000	1	247	42	11.6	10	'inbound'	0.0024	0.0063	0.0247	0.0752	0.0152
40	563775000	1	175	36	5.6	9	'inbound'	0.0011	0.0025	0.0063	0.0110	0.0153
41	353486000	4	260	32	8	13	'inbound'	0.0144	0.0258	0.0372	0.0484	0.0166
42	311923000	1	186	32	9.4	10	'outbound'	0.0026	0.0050	0.0211	0.0359	0.0089
43	353486000	4	260	32	8.2	12	'outbound'	0.0040	0.0146	0.0287	0.0727	0.0089
44	255805596	3	318	42	10	8	'outbound'	0.0046	0.0053	0.0167	0.0338	0.0056
45	257881000	2	199	32	7.1	11	'outbound'	0.0045	0.0053	0.0156	0.0341	0.0056
46	538004997	2	200	32	9.2	10	'outbound'	0.0024	0.0054	0.0203	0.0336	0.0052
47	219219000	3	292	32	12.1	11	'inbound'	0.0005	0.0213	0.0743	0.0935	0.0059
48	305859000	2	155	23	8.9	12	'inbound'	0.0080	0.0131	0.0155	0.0181	0.0017
49	563775000	1	175	36	5.9	9	'outbound'	0.0023	0.0006	0.0038	0.0026	0.0006
50	563936000	1	247	42	8.8	9	'outbound'	0.0024	0.0033	0.0159	0.0270	0.0016
51	311053600	3	229	32	7.6	12	'outbound'	0.0057	0.0120	0.0215	0.0400	0.0042
52	219219000	3	292	32	12.4	11	'outbound'	0.0037	0.0105	0.0577	0.0955	0.0032
53	538006564	3	293	40	11.8	11	'inbound'	0.0285	0.0429	0.0843	0.1771	0.0039
54	564939000	1	237	42	8.8	10	'outbound'	0.0030	0.0069	0.0355	0.0431	0.0039
55	305859000	2	155	23	8.4	12	'outbound'	0.0044	0.0034	0.0106	0.0133	0.0013
56	311071300	2	143	22	5.8	12	'inbound'	0.0009	0.0017	0.0033	0.0034	0.0004

ID	MMSI	Class	Length (m)	Width (m)	Draft (m)	SOG	Direction	SW01_Hmo	SW02_Hmo	SW03_Hmo	SW04_Hmo	SW05_Hmo
57	477464400	3	261	32	10.5	11	'inbound'	0.0118	0.0238	0.0378	0.0119	0.0013
58	305598000	2	146	18	5.4	11	'inbound'	0.0047	0.0021	0.0385	0.0812	0.0021
59	538006564	3	293	40	9.2	10	'outbound'	0.0045	0.0019	0.0362	0.0700	0.0022
60	305598000	2	146	18	5.4	11	'outbound'	0.0006	0.0004	0.0011	0.0012	0.0008
61	477464400	3	261	32	10.4	11	'outbound'	0.0054	0.0035	0.0390	0.0632	0.0044
62	636016708	2	199	32	8.4	11	'inbound'	0.0046	0.0132	0.0298	0.0262	0.0021
63	353486000	4	260	32	7.9	13	'inbound'	0.0219	0.0310	0.0390	0.0685	0.0013
64	353486000	4	260	32	8.1	12	'outbound'	0.0042	0.0112	0.0256	0.0481	0.0032
65	311071300	2	143	22	7.8	12	'outbound'	0.0033	0.0034	0.0095	0.0091	0.0014
66	636016708	2	199	32	8.1	11	'outbound'	0.0023	0.0028	0.0150	0.0145	0.0005
67	311000236	2	200	32	9.4	11	'inbound'	0.0035	0.0009	0.0197	0.0262	0.0005
68	257314000	2	198	30	8.8	11	'inbound'	0.0030	0.0049	0.0170	0.0267	0.0004
69	248092000	2	169	27	5.5	11	'inbound'	0.0006	0.0016	0.0040	0.0044	0.0004
70	563635000	2	176	35	5.6	9	'inbound'	0.0004	0.0004	0.0010	0.0032	0.0005
71	636091916	3	225	28	8.6	12	'inbound'	0.0078	0.0209	0.0293	0.0314	0.0044
72	353445000	3	226	32	13.7	9	'inbound'	0.0011	0.0006	0.0047	0.0371	0.0003
73	636091916	3	225	28	8.8	13	'outbound'	0.0041	0.0118	0.0293	0.0685	0.0028
74	563635000	2	176	35	6.1	9	'outbound'	0.0005	0.0009	0.0035	0.0029	0.0003
75	354891000	3	295	32	11.1	11	'inbound'	0.0038	0.0035	0.0343	0.0487	0.0007
76	374459000	3	293	45	9	8	'inbound'	0.0015	0.0017	0.0050	0.0111	0.0008
77	367416750	NaN	166	22	5.4	10	'inbound'	0.0005	0.0004	0.0006	0.0011	0.0004
78	257314000	2	198	30	7.8	11	'outbound'	0.0026	0.0044	0.0128	0.0149	0.0014
79	248092000	2	169	27	7.8	10	'outbound'	0.0013	0.0006	0.0028	0.0094	0.0002
80	354891000	3	295	32	10.9	9	'outbound'	0.0013	0.0019	0.0168	0.0200	0.0000
81	257532000	2	198	31	7.9	11	'inbound'	0.0021	0.0046	0.0370	0.1412	0.0061
82	636017642	3	318	43	10.3	11	'inbound'	0.0024	0.0047	0.0870	0.1417	0.0019
83	367416750	NaN	166	22	4.6	10	'outbound'	0.0007	0.0010	0.0049	0.0032	0.0026
84	309689000	2	131	20	8.9	13	'outbound'	0.0015	0.0015	0.0082	0.0085	0.0010
85	353486000	4	260	32	8	12	'inbound'	0.0107	0.0207	0.0379	0.0589	0.0065
86	636017642	3	318	43	9.8	10	'outbound'	0.0032	0.0026	0.0418	0.0798	0.0039
87	311000236	2	200	32	7.4	9	'outbound'	0.0034	0.0019	0.0420	0.0801	0.0022
88	305463000	2	140	26	6.1	13	'inbound'	0.0033	0.0021	0.0425	0.0802	0.0022
89	636017006	3	294	32	10.3	11	'inbound'	0.0088	0.0187	0.0587	0.0710	0.0009
90	338302000	1	182	36	11	11	'inbound'	0.0051	0.0199	0.0607	0.0793	0.0012
91	308045000	4	273	42	8.3	11	'inbound'	0.0011	0.0018	0.0166	0.0479	0.0011
92	353486000	4	260	32	8.1	13	'outbound'	0.0068	0.0130	0.0403	0.0569	0.0043
93	353445000	3	226	32	7.4	12	'outbound'	0.0066	0.0021	0.0247	0.0282	0.0037
94	636092722	3	260	43	8.1	10	'inbound'	0.0012	0.0068	0.0381	0.0490	0.0008
95	563775000	1	175	36	5.6	9	'inbound'	0.0002	0.0003	0.0003	0.0014	0.0002
96	305463000	2	140	26	6.1	13	'outbound'	0.0012	0.0032	0.0047	0.0078	0.0011
97	308045000	4	273	42	8.5	12	'outbound'	0.0093	0.0156	0.0536	0.0930	0.0058
98	636017006	3	294	32	11	11	'outbound'	0.0061	0.0149	0.0608	0.0998	0.0020
99	636014410	3	293	40	11.2	11	'inbound'	0.0002	0.0148	0.0843	0.1263	0.0015
100	338302000	1	182	36	9.5	11	'outbound'	0.0073	0.0068	0.0153	0.0199	0.0019
101	538004241	3	229	32	7	12	'inbound'	0.0134	0.0188	0.0371	0.0479	0.0043
102	563775000	1	175	36	6	9	'outbound'	0.0140	0.0191	0.0378	0.0492	0.0044
103	477004700	3	261	32	10.3	11	'inbound'	0.0127	0.0241	0.0636	0.0651	0.0016
104	374459000	3	293	45	13.5	7	'outbound'	0.0029	0.0011	0.0058	0.0337	0.0010
105	636014410	3	293	40	12.4	9	'outbound'	0.0012	0.0008	0.0143	0.0405	0.0001
106	311071300	2	143	22	5.5	12	'inbound'	0.0014	0.0017	0.0028	0.0037	0.0002
107	477004700	3	261	32	10.1	10	'outbound'	0.0038	0.0068	0.0085	0.0236	0.0020
108	304968000	2	143	23	9	12	'inbound'	0.0059	0.0078	0.0166	0.0153	0.0008
109	257532000	2	198	31	7.9	10	'outbound'	0.0061	0.0078	0.0186	0.0153	0.0016
110	636091685	1	244	42	12.1	10	'inbound'	0.0015	0.0024	0.0137	0.0656	0.0007
111	636016824	2	190	32	12.3	9	'inbound'	0.0055	0.0052	0.0125	0.0295	0.0122
112	371245000	3	324	43	9	11	'inbound'	0.0065	0.0173	0.0562	0.0722	0.0168

ID	MMSI	Class	Length (m)	Width (m)	Draft (m)	SOG	Direction	SW01_Hmo	SW02_Hmo	SW03_Hmo	SW04_Hmo	SW05_Hmo
113	257457000	2	208	32	8.2	10	'inbound'	0.0046	0.0179	0.0573	0.0731	0.0169
114	353486000	4	260	32	8.1	13	'inbound'	0.0212	0.0321	0.0457	0.0692	0.0198
115	636091685	1	244	42	8.1	11	'outbound'	0.0052	0.0078	0.0334	0.0541	0.0049
116	538004241	3	229	32	10.5	10	'outbound'	0.0067	0.0078	0.0269	0.0967	0.0249
117	311000508	2	220	30	8.5	11	'inbound'	0.0070	0.0189	0.0372	0.0997	0.0286
118	353486000	4	260	32	8.2	12	'outbound'	0.0068	0.0136	0.0396	0.0666	0.0174
119	371245000	3	324	43	8.6	11	'outbound'	0.0073	0.0075	0.0512	0.1471	0.0234
120	311071300	2	143	22	7.8	11	'outbound'	0.0074	0.0085	0.0551	0.1473	0.0201
121	352652000	3	255	43	13.7	8	'inbound'	0.0028	0.0046	0.0125	0.0583	0.0301
122	477177100	3	260	32	10.8	11	'inbound'	0.0069	0.0195	0.0360	0.0502	0.0301
123	357405000	3	294	31	11.2	11	'inbound'	0.0135	0.0250	0.0527	0.0852	0.0247
124	563635000	2	176	35	5.8	9	'inbound'	0.0016	0.0033	0.0099	0.0244	0.0403
125	477177100	3	260	32	10.7	11	'outbound'	0.0034	0.0063	0.0308	0.0823	0.0213
126	563635000	2	176	35	5.9	9	'outbound'	0.0006	0.0006	0.0042	0.0046	0.0105
127	305560000	2	144	18	6.4	12	'inbound'	0.0007	0.0018	0.0027	0.0043	0.0096
128	246580000	1	136	23	6.7	12	'inbound'	0.0016	0.0028	0.0047	0.0151	0.0041
129	636092722	3	260	43	13.3	7	'outbound'	0.0016	0.0028	0.0047	0.0151	0.0041
130	357405000	3	294	31	12.3	10	'outbound'	0.0028	0.0056	0.0368	0.0815	0.0064
131	477001700	3	261	32	10.6	11	'inbound'	0.0089	0.0120	0.0225	0.0283	0.0033
132	636016080	1	247	42	12	10	'inbound'	0.0063	0.0130	0.0295	0.0750	0.0032
133	248092000	2	169	27	5.4	12	'inbound'	0.0018	0.0023	0.0047	0.0041	0.0027
134	304968000	2	143	23	8.8	11	'outbound'	0.0010	0.0021	0.0090	0.0158	0.0043
135	311000508	2	220	30	11	9	'outbound'	0.0016	0.0022	0.0299	0.0543	0.0040
136	636016824	2	190	32	5.9	12	'outbound'	0.0012	0.0044	0.0107	0.0180	0.0051
137	374900000	2	199	33	13.2	8	'inbound'	0.0009	0.0017	0.0025	0.0169	0.0007
138	477001700	3	261	32	11.5	10	'outbound'	0.0019	0.0030	0.0280	0.0428	0.0002
139	563722000	3	277	40	11.9	10	'inbound'	0.0063	0.0177	0.0577	0.0746	0.0040
140	257457000	2	208	32	9	11	'outbound'	0.0029	0.0090	0.0216	0.0506	0.0022
141	305560000	2	144	18	6.2	12	'outbound'	0.0006	0.0018	0.0035	0.0047	0.0005
142	353486000	4	260	32	8.2	13	'inbound'	0.0165	0.0289	0.0384	0.0600	0.0057
143	311000221	1	243	42	9.2	10	'inbound'	0.0087	0.0021	0.0364	0.0666	0.0006
144	636016080	1	247	42	8.6	10	'outbound'	0.0032	0.0080	0.0259	0.0472	0.0056
145	246580000	1	136	23	8.4	8	'outbound'	0.0041	0.0026	0.0382	0.0656	0.0036
146	563722000	3	277	40	12.3	8	'outbound'	0.0046	0.0028	0.0311	0.0383	0.0088
147	353486000	4	260	32	8.1	13	'outbound'	0.0035	0.0140	0.0331	0.0733	0.0041
148	248092000	2	169	27	7.3	11	'outbound'	0.0021	0.0024	0.0062	0.0080	0.0028
149	370235000	3	229	32	13.6	6	'outbound'	0.0006	0.0004	0.0011	0.0058	0.0024
150	210516000	3	226	30	9.1	12	'inbound'	0.0131	0.0235	0.0335	0.0429	0.0138
151	311000221	1	243	42	8.5	10	'outbound'	0.0027	0.0054	0.0268	0.0683	0.0125
152	215724000	3	294	32	11.3	11	'inbound'	0.0053	0.0096	0.0597	0.0559	0.0050
153	239746000	3	225	33	7.3	11	'inbound'	0.0023	0.0098	0.0595	0.0560	0.0050
154	210516000	3	226	30	9.5	12	'outbound'	0.0032	0.0092	0.0313	0.0666	0.0042
155	477620700	2	199	32	9.9	11	'inbound'	0.0042	0.0121	0.0290	0.0408	0.0098
156	215724000	3	294	32	11.4	11	'outbound'	0.0035	0.0050	0.0459	0.1128	0.0135
157	218582000	3	325	43	10.3	11	'inbound'	0.0095	0.0088	0.0650	0.0959	0.0007
158	352652000	3	255	43	6.8	10	'outbound'	0.0021	0.0045	0.0220	0.0290	0.0009
159	370273000	3	275	32	11.5	11	'inbound'	0.0145	0.0273	0.0650	0.1034	0.0028
160	218582000	3	325	43	10.2	10	'outbound'	0.0035	0.0081	0.0431	0.1085	0.0034
161	374900000	2	199	33	6.8	11	'outbound'	0.0035	0.0049	0.0070	0.0130	0.0021
162	565671000	2	186	28	11.3	11	'inbound'	0.0004	0.0055	0.0224	0.0268	0.0000
163	636015526	1	228	42	12.2	10	'inbound'	0.0007	0.0047	0.0248	0.0068	0.0005
164	305614000	2	123	18	5.5	12	'inbound'	0.0007	0.0009	0.0014	0.0019	0.0003
165	477620700	2	199	32	9	11	'outbound'	0.0021	0.0042	0.0185	0.0225	0.0019
166	370273000	3	275	32	12	11	'outbound'	0.0015	0.0041	0.0497	0.0977	0.0000
167	311000222	1	243	42	11.2	10	'inbound'	0.0018	0.0051	0.0392	0.0963	0.0000
168	255805674	3	278	40	11.6	10	'inbound'	0.0033	0.0108	0.0530	0.0749	0.0000

ID	MMSI	Class	Length (m)	Width (m)	Draft (m)	SOG	Direction	SW01_Hmo	SW02_Hmo	SW03_Hmo	SW04_Hmo	SW05_Hmo
169	311071300	2	143	22	5.6	12	'inbound'	0.0024	0.0034	0.0057	0.0069	0.0000
170	305614000	2	123	18	5.4	12	'outbound'	0.0008	0.0016	0.0037	0.0032	0.0000
171	308268000	2	188	29	11.8	9	'inbound'	0.0009	0.0018	0.0025	0.0114	0.0000
172	239746000	3	225	33	12.5	9	'outbound'	0.0025	0.0048	0.0280	0.0293	0.0000
173	636015526	1	228	42	8.6	11	'outbound'	0.0054	0.0054	0.0240	0.0548	0.0000
174	563775000	1	175	36	5.8	9	'inbound'	0.0024	0.0014	0.0012	0.0063	0.0000
175	353486000	4	260	32	8	8	'inbound'	0.0034	0.0019	0.0020	0.0064	0.0000
176	477752400	3	261	32	10.8	11	'inbound'	0.0151	0.0208	0.0463	0.0783	0.0000
177	366235000	2	207	23	7.2	9	'outbound'	0.0144	0.0208	0.0468	0.0780	0.0000
178	255805674	3	278	40	12.6	10	'outbound'	0.0032	0.0087	0.0500	0.1030	0.0000
179	353486000	4	260	32	8.2	12	'outbound'	0.0034	0.0106	0.0344	0.0641	0.0000
180	477752400	3	261	32	11.2	12	'outbound'	0.0056	0.0070	0.0561	0.1517	0.0000
181	311000222	1	243	42	8.3	11	'outbound'	0.0044	0.0083	0.0413	0.0482	0.0000
182	311071300	2	143	22	7.9	12	'outbound'	0.0014	0.0031	0.0102	0.0104	0.0000
183	565671000	2	186	28	6.3	12	'outbound'	0.0036	0.0048	0.0097	0.0163	0.0000
184	563775000	1	175	36	5.8	8	'outbound'	0.0027	0.0014	0.0040	0.0035	0.0000
185	538003248	2	190	32	6.7	11	'inbound'	0.0014	0.0026	0.0072	0.0000	0.0000
186	308976000	3	230	32	12.2	10	'inbound'	0.0018	0.0023	0.0047	0.0000	0.0000
187	367006560	NaN	175	24	7.9	8	'inbound'	0.0019	0.0017	0.0047	0.0000	0.0019
188	636091916	3	225	28	8.4	12	'inbound'	0.0108	0.0150	0.0385	0.0348	0.0072
189	563635000	2	176	35	5.6	9	'inbound'	0.0025	0.0017	0.0041	0.0036	0.0093
190	248092000	2	169	27	5.5	12	'inbound'	0.0023	0.0032	0.0052	0.0184	0.0064
191	352468000	3	229	32	13	10	'inbound'	0.0021	0.0048	0.0129	0.0372	0.0053
192	235103314	2	177	28	7.4	11	'inbound'	0.0017	0.0024	0.0083	0.0101	0.0026
193	636012630	1	228	32	11.7	10	'inbound'	0.0018	0.0041	0.0090	0.0527	0.0028
194	367006560	NaN	175	24	6.1	10	'outbound'	0.0006	0.0005	0.0028	0.0022	0.0014
195	308976000	3	230	32	9.5	10	'outbound'	0.0028	0.0051	0.0305	0.0419	0.0011
196	538003248	2	190	32	6.4	10	'outbound'	0.0026	0.0047	0.0301	0.0305	0.0012
197	563635000	2	176	35	5.6	9	'outbound'	0.0020	0.0019	0.0040	0.0016	0.0006
198	636091916	3	225	28	8.5	12	'outbound'	0.0054	0.0069	0.0199	0.0292	0.0026
199	353486000	4	260	32	8.4	13	'inbound'	0.0162	0.0241	0.0366	0.0494	0.0016
200	353486000	4	260	32	8.2	12	'outbound'	0.0036	0.0095	0.0273	0.0595	0.0030
201	367115000	NaN	162	24	7.9	10	'inbound'	0.0005	0.0008	0.0005	0.0026	0.0008
202	235103314	2	177	28	7	10	'outbound'	0.0001	0.0012	0.0089	0.0054	0.0000
203	636012630	1	228	32	8.1	11	'outbound'	0.0036	0.0052	0.0198	0.0173	0.0022
204	636018018	3	299	42	9.5	11	'inbound'	0.0176	0.0419	0.0863	0.0913	0.0069
205	308268000	2	188	29	7.5	9	'outbound'	0.0063	0.0041	0.0094	0.0068	0.0024
206	248092000	2	169	27	7.9	9	'outbound'	0.0051	0.0033	0.0178	0.0223	0.0033
207	636018018	3	299	42	9.8	11	'outbound'	0.0045	0.0101	0.0450	0.1164	0.0111
208	305394000	2	140	16	4.6	12	'inbound'	0.0020	0.0006	0.0012	0.0018	0.0069
209	219217000	3	293	32	11.8	9	'inbound'	0.0032	0.0107	0.0284	0.0249	0.0028
210	368589000	1	183	32	11.5	8	'inbound'	0.0026	0.0028	0.0158	0.0288	0.0021
211	477832300	3	261	32	11	12	'inbound'	0.0150	0.0278	0.0566	0.0862	0.0027
212	305394000	2	140	16	4.6	12	'outbound'	0.0002	0.0009	0.0010	0.0017	0.0003
213	219217000	3	293	32	12.5	10	'outbound'	0.0049	0.0020	0.0380	0.0662	0.0044
214	367115000	NaN	162	24	7.9	9	'outbound'	0.0050	0.0020	0.0384	0.0667	0.0046
215	477832300	3	261	32	11.6	11	'outbound'	0.0056	0.0046	0.0418	0.0581	0.0086
216	368589000	1	183	32	7.7	10	'outbound'	0.0033	0.0016	0.0167	0.0146	0.0109
217	636014069	1	250	40	12.2	8	'inbound'	0.0047	0.0066	0.0189	0.0697	0.0407
218	477334100	2	170	27	9.6	10	'inbound'	0.0030	0.0056	0.0125	0.0169	0.0117
219	538007510	2	200	32	10.7	10	'inbound'	0.0054	0.0079	0.0283	0.0443	0.0025
220	338302000	1	182	36	11	10	'inbound'	0.0038	0.0051	0.0228	0.0366	0.0012
221	538007655	2	199	33	10.7	9	'inbound'	0.0027	0.0029	0.0058	0.0169	0.0018
222	563775000	1	175	36	5.8	9	'inbound'	0.0016	0.0021	0.0032	0.0251	0.0053
223	353486000	4	260	32	8	10	'inbound'	0.0038	0.0045	0.0046	0.0162	0.0109
224	311071300	2	143	22	5.7	12	'inbound'	0.0016	0.0022	0.0038	0.0043	0.0003

ID	MMSI	Class	Length (m)	Width (m)	Draft (m)	SOG	Direction	SW01_Hmo	SW02_Hmo	SW03_Hmo	SW04_Hmo	SW05_Hmo
225	636014069	1	250	40	8.2	11	'outbound'	0.0046	0.0039	0.0258	0.0552	0.0030
226	372197000	1	144	23	5.6	12	'inbound'	0.0017	0.0073	0.0107	0.0112	0.0006
227	305663000	2	153	22	6.7	12	'inbound'	0.0017	0.0073	0.0107	0.0112	0.0006
228	636092187	2	144	23	8.6	12	'inbound'	0.0032	0.0045	0.0088	0.0065	0.0002
229	353486000	4	260	32	8.2	12	'outbound'	0.0047	0.0120	0.0313	0.0687	0.0024
230	563775000	1	175	36	6	8	'outbound'	0.0006	0.0013	0.0064	0.0023	0.0019
231	247275300	1	249	44	10.7	9	'inbound'	0.0041	0.0042	0.0196	0.0926	0.0033
232	352652000	3	255	43	13.7	8	'inbound'	0.0036	0.0013	0.0037	0.0483	0.0018
233	338302000	1	182	36	9.2	10	'outbound'	0.0042	0.0072	0.0144	0.0180	0.0110
234	352468000	3	229	32	8.3	11	'outbound'	0.0058	0.0123	0.0388	0.0997	0.0075
235	311968000	3	225	32	7.4	10	'inbound'	0.0172	0.0142	0.0208	0.0234	0.0170
236	249249000	1	147	24	6.5	12	'inbound'	0.0061	0.0077	0.0097	0.0127	0.0069
237	247275300	1	249	44	8.5	10	'outbound'	0.0048	0.0083	0.0341	0.0557	0.0100
238	311000222	1	243	42	11.6	9	'inbound'	0.0036	0.0039	0.0324	0.0932	0.0076
239	477334100	2	170	27	5.3	12	'outbound'	0.0024	0.0019	0.0053	0.0078	0.0024
240	255805597	3	318	43	10.5	10	'inbound'	0.0031	0.0153	0.0710	0.0933	0.0011
241	311968000	3	225	32	13.7	8	'outbound'	0.0016	0.0020	0.0075	0.0163	0.0021
242	311071300	2	143	22	8	11	'outbound'	0.0018	0.0022	0.0074	0.0107	0.0041
243	305663000	2	153	22	7.3	12	'outbound'	0.0018	0.0024	0.0075	0.0106	0.0031
244	255805597	3	318	43	11.3	10	'outbound'	0.0022	0.0108	0.0386	0.1728	0.0068
245	210516000	3	226	30	9.2	11	'outbound'	0.0036	0.0096	0.0241	0.0588	0.0090
246	538005562	2	204	32	7.5	13	'inbound'	0.0066	0.0277	0.0319	0.0446	0.0046
247	255805595	3	318	42	10.1	11	'inbound'	0.0186	0.0325	0.0684	0.1541	0.0109
248	215209000	2	190	32	9.1	10	'inbound'	0.0022	0.0043	0.0187	0.0200	0.0108
249	314277000	2	138	21	6.7	12	'inbound'	0.0015	0.0021	0.0029	0.0032	0.0079
250	255805595	3	318	42	10.1	10	'outbound'	0.0011	0.0145	0.0442	0.1236	0.0098
251	351160000	2	190	33	6.8	11	'outbound'	0.0026	0.0039	0.0172	0.0239	0.0128
252	353486000	4	260	32	8.2	12	'inbound'	0.0054	0.0127	0.0236	0.0334	0.0147
253	353486000	4	260	32	8.2	11	'outbound'	0.0031	0.0114	0.0257	0.0538	0.0134
254	563775000	1	175	36	5.7	9	'inbound'	0.0004	0.0003	0.0008	0.0025	0.0068
255	370633000	2	190	32	12.2	10	'inbound'	0.0018	0.0052	0.0132	0.0301	0.0066
256	257424000	2	198	31	8	11	'outbound'	0.0032	0.0043	0.0235	0.0365	0.0057
257	636017757	3	229	32	7.1	12	'inbound'	0.0121	0.0201	0.0267	0.0403	0.0030
258	538005562	2	204	32	7.3	12	'outbound'	0.0137	0.0203	0.0227	0.0467	0.0027
259	353594000	3	229	32	13.7	9	'inbound'	0.0011	0.0012	0.0158	0.0533	0.0005
260	477195100	3	291	32	10.8	11	'inbound'	0.0134	0.0248	0.0535	0.1014	0.0038
261	563775000	3	175	36	5.7	9	'outbound'	0.0006	0.0006	0.0038	0.0022	0.0003
262	314277000	2	138	21	6.8	12	'outbound'	0.0008	0.0032	0.0046	0.0115	0.0006
263	477464500	3	261	32	9.9	12	'inbound'	0.0239	0.0335	0.0529	0.0805	0.0061
264	477195100	3	291	32	11.7	10	'outbound'	0.0043	0.0033	0.0299	0.0551	0.0054
265	431501000	3	292	46	12.7	8	'outbound'	0.0019	0.0017	0.0341	0.0695	0.0002
266	477464500	3	261	32	9.8	11	'outbound'	0.0038	0.0111	0.0212	0.0382	0.0055
267	215209000	2	190	32	6.2	12	'outbound'	0.0028	0.0033	0.0113	0.0131	0.0020
268	308371000	1	214	32	7.6	11	'inbound'	0.0044	0.0067	0.0198	0.0266	0.0007
269	311071300	2	143	22	5.5	12	'inbound'	0.0094	0.0069	0.0120	0.0112	0.0027
270	636014357	3	304	40	11.4	10	'inbound'	0.0195	0.0258	0.0661	0.0948	0.0039
271	353884000	2	199	36	11.6	10	'inbound'	0.0026	0.0042	0.0078	0.0378	0.0016
272	353486000	4	260	32	8.3	12	'inbound'	0.0194	0.0212	0.0450	0.0559	0.0039
273	308371000	1	214	32	8.5	11	'outbound'	0.0205	0.0220	0.0456	0.0560	0.0037
274	636014357	3	304	40	12.2	11	'outbound'	0.0127	0.0138	0.0615	0.1232	0.0118
275	538006041	2	200	32	8	10	'inbound'	0.0253	0.0370	0.0564	0.1354	0.0155
276	353486000	4	260	32	8.2	12	'outbound'	0.0066	0.0103	0.0283	0.0413	0.0032
277	353594000	3	229	32	7.3	12	'outbound'	0.0063	0.0021	0.0227	0.0181	0.0038
278	636017757	3	229	32	13.7	9	'outbound'	0.0034	0.0020	0.0112	0.0337	0.0033
279	636091916	3	225	28	8.7	13	'inbound'	0.0182	0.0263	0.0277	0.0485	0.0054
280	370633000	2	190	32	6.5	12	'outbound'	0.0031	0.0050	0.0131	0.0173	0.0021

ID	MMSI	Class	Length (m)	Width (m)	Draft (m)	SOG	Direction	SW01_Hmo	SW02_Hmo	SW03_Hmo	SW04_Hmo	SW05_Hmo
281	311044500	2	200	30	11.9	9	'inbound'	0.0003	0.0009	0.0027	0.0188	0.0005
282	308976000	3	230	32	8	11	'inbound'	0.0054	0.0103	0.0207	0.0280	0.0006
283	311071300	2	143	22	8.5	11	'outbound'	0.0026	0.0135	0.0321	0.0070	0.0006
284	636091916	3	225	28	8.9	10	'outbound'	0.0045	0.0062	0.0271	0.0185	0.0031
285	538003048	2	189	32	11.6	9	'inbound'	0.0045	0.0062	0.0271	0.0185	0.0031
286	257496000	3	228	32	9	12	'inbound'	0.0199	0.0275	0.0336	0.0588	0.0054
287	215679000	3	229	32	7.6	12	'inbound'	0.0116	0.0166	0.0177	0.0302	0.0031
288	538006041	2	200	32	7.1	12	'outbound'	0.0036	0.0046	0.0152	0.0165	0.0019
289	563635000	2	176	35	5.3	9	'inbound'	0.0003	0.0003	0.0003	0.0024	0.0000
290	255805596	3	318	42	10	12	'inbound'	0.0221	0.0511	0.0875	0.1743	0.0040
291	248092000	2	169	27	5.5	11	'inbound'	0.0015	0.0024	0.0076	0.0045	0.0008
292	311044500	2	200	30	9.8	10	'outbound'	0.0024	0.0015	0.0104	0.0127	0.0008
293	257496000	3	228	32	9	10	'outbound'	0.0031	0.0044	0.0150	0.0206	0.0016
294	636091452	3	293	32	10.5	12	'inbound'	0.0268	0.0358	0.0788	0.0874	0.0070
295	255805596	3	318	42	9.5	10	'outbound'	0.0049	0.0059	0.0426	0.0266	0.0027
296	308976000	3	230	32	12.8	9	'outbound'	0.0018	0.0044	0.0253	0.0353	0.0026
297	563635000	2	176	35	4.8	9	'outbound'	0.0006	0.0018	0.0293	0.0356	0.0029
298	636016080	1	247	42	12.2	9	'inbound'	0.0020	0.0038	0.0202	0.0669	0.0344
299	538006145	2	199	32	6.4	12	'inbound'	0.0040	0.0074	0.0149	0.0340	0.0495
300	338302000	1	182	36	11	10	'inbound'	0.0033	0.0095	0.0281	0.0408	0.0343
301	353486000	4	260	32	8.1	12	'inbound'	0.0052	0.0068	0.0206	0.0382	0.0490
302	636012630	1	228	32	11.5	10	'inbound'	0.0030	0.0122	0.0335	0.0671	0.0782
303	636091452	3	293	32	9.9	10	'outbound'	0.0034	0.0106	0.0239	0.0780	0.0539
304	353884000	2	199	36	8.4	8	'outbound'	0.0034	0.0047	0.0144	0.0310	0.0381
305	248092000	2	169	27	8.6	8	'outbound'	0.0023	0.0046	0.0090	0.0187	0.0395
306	353486000	4	260	32	8.2	12	'outbound'	0.0036	0.0147	0.0344	0.0864	0.0319
307	215679000	3	229	32	12.9	7	'outbound'	0.0026	0.0039	0.0140	0.0310	0.0220
308	353594000	3	229	32	7.5	12	'inbound'	0.0130	0.0212	0.0278	0.0388	0.0239
309	636016080	1	247	42	8.6	11	'outbound'	0.0028	0.0080	0.0212	0.0480	0.0165
310	563775000	1	175	36	5.6	9	'inbound'	0.0050	0.0037	0.0075	0.0232	0.0357
311	636017004	2	134	16	5.3	12	'inbound'	0.0038	0.0072	0.0115	0.0200	0.0163
312	338302000	1	182	36	9.4	10	'outbound'	0.0021	0.0031	0.0134	0.0297	0.0117
313	538003048	2	189	32	6	9	'outbound'	0.0024	0.0015	0.0063	0.0083	0.0125
314	636012630	1	228	32	8.1	11	'outbound'	0.0024	0.0046	0.0171	0.0350	0.0089
315	477765800	3	261	32	10.7	13	'inbound'	0.0169	0.0330	0.0424	0.0657	0.0081
316	352652000	3	255	43	13.7	8	'inbound'	0.0007	0.0015	0.0046	0.0522	0.0003
317	563775000	1	175	36	6.1	9	'outbound'	0.0004	0.0004	0.0039	0.0011	0.0003
318	477765800	3	261	32	10.6	11	'outbound'	0.0046	0.0103	0.0371	0.0785	0.0041
319	311681000	2	199	30	11.7	10	'inbound'	0.0050	0.0125	0.0431	0.0890	0.0024
320	538006145	2	199	32	13.1	7	'outbound'	0.0001	0.0004	0.0015	0.0100	0.0001
321	368589000	1	183	32	11.8	9	'inbound'	0.0024	0.0049	0.0131	0.0263	0.0263
322	538004242	3	229	32	7.5	11	'inbound'	0.0087	0.0163	0.0267	0.0430	0.0282
323	353486000	4	260	32	8	12	'inbound'	0.0146	0.0183	0.0303	0.0555	0.0102
324	538002319	2	189	30	7.2	10	'inbound'	0.0033	0.0020	0.0053	0.0094	0.0027
325	353486000	4	260	32	8.2	12	'outbound'	0.0041	0.0100	0.0206	0.0679	0.0045
326	311071300	2	143	22	5.5	13	'inbound'	0.0035	0.0040	0.0054	0.0069	0.0027
327	636013275	1	249	44	10.8	9	'inbound'	0.0017	0.0028	0.0069	0.0438	0.0004

Appendix B

Detailed Forecasted Vessel Frequency

Table B-1: Detailed forecast of **arriving** vessel calls for 2025 **without** Project

Draft (m)	Bulk Carrier 2	Bulk Carrier 3	Bulk Carrier 4	Bulk Carrier 5	Bulk Carrier 6	Bulk Carrier 7	Chemical Tanker	SubPX	Panamax	PPXGn1	PPXGn2	PPXGn3	Cruise	General Cargo 1	General Cargo 2	Tanker Panamax	Aframax Tanker
2.1																	
2.4							2										
2.7							5										
3.0							5										
3.4							6								1		
3.7							6								3		
4.0			3				8								10		
4.3		1	5				10								20		
4.6			12				9							12	22		
4.9			10				7							48	17		
5.2			6				4							38	10		
5.5			5				3							12	10		
5.8			5				4							17	8	1	
6.1	4	156	141	8	1	6	3							72	9	1	
6.4		2	4				2								11	3	
6.7		3	4				2								6	3	
7.0		4	3												7	2	
7.3		4	6												7	3	
7.6		11	5				1						44		2	1	
7.9		13	6										47		3	2	
8.2		12	7				1									1	
8.5		8	7														2
8.8		6	6													1	4
9.1		5	3					6	8							1	11
9.4		2	3						1								18
9.8		1	2					1	86	10	6					2	17
10.1		1	3					2	25	5	8					2	13
10.4			1					1	21	10	7					2	5
10.7			2						31	9	9					2	2
11.0			1						28	17	11					1	
11.3				1					13	17	11					2	
11.6				2					11	13	12					1	
11.9				2					5	15	10					1	
12.2				3					1	10	11						
12.5				2					1	5	3						
12.8				3					1	6	6						
13.1				3													
13.4				2													
13.7				12													
14.0																	
14.3																	
14.6																	
14.9																	
Total	4	229	250	38	1	6	78	10	232	117	94	0	91	199	146	32	72

Table B-2: Detailed forecast of **departing** vessel calls for 2025 **without** Project

Draft (m)	Bulk Carrier 2	Bulk Carrier 3	Bulk Carrier 4	Bulk Carrier 5	Bulk Carrier 6	Bulk Carrier 7	Chemical Tanker	SubPX	Panamax	PPXGn1	PPXGn2	PPXGn3	Cruise	General Cargo 1	General Cargo 2	Tanker Panamax	Aframax Tanker
2.1																	
2.4																	
2.7																	
3.0																	
3.4																	
3.7																	
4.0																	
4.3																	
4.6																	
4.9														33			
5.2														41			
5.5														18			
5.8							69							23		15	
6.1		33	94				2							72	111	4	
6.4			4				2								7		
6.7		1	2				1							6	10	3	
7.0		2	3											4	7	3	
7.3		3	3				1							3	6		
7.6		5	5										91		3	1	
7.9		7	4				2								2	1	
8.2		6	1				1								1	1	
8.5		7						5									
8.8		5						1									
9.1		3	1					1	1								
9.4		2						2	29								
9.8			1					1	10	10							
10.1			2						58	4	8						
10.4		1	2						34	9	8						
10.7		2	2						22	10	6					1	
11.0		5	1						23	12	8						
11.3		1	1						22	18	10						
11.6	1	5	3	2					11	14	11						
11.9	1	5	1	1					11	14	12						
12.2		5	7	1					4	10	9						
12.5	1	5	5	2					2	18	11						
12.8		9	5	3					2		11						
13.1		57	7	5	1												
13.4			5	5													
13.7			40	20		6											
14.0																	
14.3																	
14.6																	
14.9																	
Total	3	169	199	39	1	6	78	10	229	119	94	0	91	200	147	29	0

Table B-3: Detailed forecast of **arriving** vessel calls for 2025 **with** Project

Draft (m)	Bulk Carrier 2	Bulk Carrier 3	Bulk Carrier 4	Bulk Carrier 5	Bulk Carrier 6	Bulk Carrier 7	Chemical Tanker	SubPX	Panamax	PPXGn1	PPXGn2	PPXGn3	Cruise	General Cargo 1	General Cargo 2	Tanker Panamax	Aframax Tanker
2.1																	
2.4							2										
2.7							5										
3.0							5										
3.4							6								1		
3.7							6								3		
4.0			3				8								10		
4.3		1	5				10								20		
4.6			12				9							12	22		
4.9			10				7							48	17		
5.2			6				4							38	10		
5.5			5				3							12	10		
5.8			5				4							17	8		1
6.1		150	141	10	1	6	3							72	9		1
6.4		2	4				2								11		3
6.7		3	4				2								6		3
7.0		4	3												7		2
7.3		4	6												7		3
7.6		11	5				1						44		2		1
7.9		13	6										47		3		2
8.2		12	7				1										1
8.5		8	7													2	
8.8		6	6													4	1
9.1		5	3					6	8							11	1
9.4		2	3						1							18	
9.8		1	2					1	77	1	1					17	2
10.1		1	3					2	22	1						13	2
10.4			1					1	18	3	1					5	2
10.7			2						28	6	5					2	2
11.0			1						26	4	8						1
11.3				1					12	11	7						2
11.6				1					10	10	10						1
11.9				1					4	18	10						1
12.2				1						18	14						
12.5				2						13	10						
12.8				1					1	15	12						
13.1				3					1	8	7						
13.4				3						4	5						
13.7				1						5	4						
14.0				1						1							
14.3				3													
14.6				2													
14.9				6													
Total	0	223	250	36	1	6	78	10	208	118	94	0	91	199	146	72	32

Table B-4: Detailed forecast of **departing** vessel calls for 2025 **with** Project

Draft (m)	Bulk Carrier 2	Bulk Carrier 3	Bulk Carrier 4	Bulk Carrier 5	Bulk Carrier 6	Bulk Carrier 7	Chemical Tanker	SubPX	Panamax	PPXGn1	PPXGn2	PPXGn3	Cruise	General Cargo 1	General Cargo 2	Tanker Panamax	Aframax Tanker
2.1																	
2.4																	
2.7																	
3.0																	
3.4																	
3.7																	
4.0																	
4.3																	
4.6																	
4.9														33			
5.2														41			
5.5														18			
5.8							69							23		15	
6.1		33	94				2							72	111	4	
6.4			4				2								7		
6.7		1	2				1							6	10	3	
7.0		2	3											4	7	3	
7.3		3	3				1							3	6		
7.6		5	5										91		3	1	
7.9		7	4				2								2	1	
8.2		6	1				1								1	1	
8.5		7						5									
8.8		5						1									
9.1		3	1					1	1								
9.4		2						2	37								
9.8			1					1	13								
10.1			2						41	1	1						
10.4			1						31		1						
10.7		1	1						22	3	1					1	
11.0		6	1						22	5	5						
11.3		1	1						17	3	7						
11.6		4	4	1					7	9	6						
11.9		6	1	1					9	10	8						
12.2		4	4	1					2	14	10						
12.5		4	8	1					3	18	12						
12.8		8	3	1						14	11						
13.1		55	8	2					1	14	9						
13.4			4	4	1				1	10	11						
13.7			4	4						9	3						
14.0			2	5		1				8	7						
14.3			3	4													
14.6			35	5		1											
14.9				9		4											
Total	0	163	200	38	1	6	78	10	207	118	92	0	91	200	147	29	0

Table B-5: Detailed forecast of **arriving** vessel calls for 2035 **without** Project

Draft (m)	Bulk Carrier 2	Bulk Carrier 3	Bulk Carrier 4	Bulk Carrier 5	Bulk Carrier 6	Bulk Carrier 7	Chemical Tanker	SubPX	Panamax	PPXGn1	PPXGn2	PPXGn3	Cruise	General Cargo 1	General Cargo 2	Tanker Panamax	Aframax Tanker
2.1							1										
2.4							3										
2.7							7										
3.0							7										
3.4							11										
3.7							10								5		
4.0			3				12								13		
4.3			9				19							1	20		
4.6			15				14							15	26		
4.9			15				6							39	22		
5.2		1	5				6							46	14		
5.5			7				3							19	10	1	
5.8			8				3							21	9	3	
6.1	3	76	72	12	1	7	4							85	12	3	
6.4		2	5				6								12	3	
6.7		3	8				1								9	5	
7.0		7	6												7	5	
7.3		11	4				2								6	5	
7.6		19	7				1						42		5	4	
7.9		22	7				1						44		3	5	
8.2		20	5				1									3	
8.5		14	7				1									3	1
8.8		14	4													2	4
9.1		6	3					11	7							3	10
9.4		3	2						2							2	13
9.8		1	1				1	2	42	10	8	10				2	10
10.1			2					2	14	11	5	9				3	11
10.4			1					1	14	10	10	11				3	5
10.7			2						21	18	7	12				3	1
11.0			1						15	20	11	15				3	
11.3				1					5	15	13	21				3	
11.6				2					5	19	14	14				1	
11.9				2					3	17	10	18					
12.2				2						13	10	13					
12.5				2					1	8	2	6					
12.8				2					1	6	3	6					
13.1				3													
13.4				2													
13.7				12													
14.0																	
14.3																	
14.6																	
14.9																	
Total	3	199	199	40	1	7	120	16	130	147	93	135	86	226	173	65	55

Table B-6: Detailed forecast of **departing** vessel calls for 2035 **without** Project

Draft (m)	Bulk Carrier 2	Bulk Carrier 3	Bulk Carrier 4	Bulk Carrier 5	Bulk Carrier 6	Bulk Carrier 7	Chemical Tanker	SubPX	Panamax	PPXGn1	PPXGn2	PPXGn3	Cruise	General Cargo 1	General Cargo 2	Tanker Panamax	Aframax Tanker
2.1																	
2.4																	
2.7																	
3.0																	
3.4																	
3.7																	
4.0																	
4.3																	
4.6																	
4.9														44			
5.2														51			
5.5														21			
5.8							105							25		51	
6.1		46	105				4							83	131	2	
6.4		0	6												11	2	
6.7		0	7				1							1	11	4	
7.0		0	6				1							1	7	2	
7.3		0	4				1							1	6		
7.6		0	5				1						86		6	1	
7.9		0	2				3								1		
8.2		0	2				1								1	1	
8.5		0						10									
8.8		0					1		1								
9.1		0						1	1								56
9.4		0	2					3	14								
9.8		0	4					1	9			1					
10.1		1	5						28	10	9	11					
10.4		0	1						16	10	5	8					
10.7		1	1						11	10	9	11				1	
11.0		2	1						14	16	7	10				1	
11.3		2	1						14	18	11	17				1	
11.6		4	2	1					10	16	12	19					
11.9	1	3	2	1					6	17	14	15					
12.2		3	4	1					3	14	9	14					
12.5	1	3	2	2					2	18	11	15					
12.8		5	4	3					1	19	7	12					
13.1		64	4	5	1												
13.4			5	4													
13.7			44	25		7											
14.0																	
14.3																	
14.6																	
14.9																	
Total	2	134	219	42	1	7	118	15	130	148	94	133	86	227	174	66	56

Table B-7: Detailed forecast of **arriving** vessel calls for 2035 **with** Project

Draft (m)	Bulk Carrier 2	Bulk Carrier 3	Bulk Carrier 4	Bulk Carrier 5	Bulk Carrier 6	Bulk Carrier 7	Chemical Tanker	SubPX	Panamax	PPXGn1	PPXGn2	PPXGn3	Cruise	General Cargo 1	General Cargo 2	Tanker Panamax	Aframax Tanker
2.1																	
2.4																	
2.7																	
3.0																	
3.4																	
3.7																	
4.0																	
4.3																	
4.6																	
4.9														44			
5.2														51			
5.5														21			
5.8							105							25		51	
6.1		74	105				4							83	131	2	
6.4		1	6												11	2	
6.7		2	7				1							1	11	4	
7.0		2	6				1							1	7	2	
7.3		4	4				1							1	6		
7.6		8	5				1						86		6	1	
7.9		8	2				3								1		
8.2		9	2				1								1	1	
8.5		7						9									
8.8		4					1		2								
9.1		2						1									56
9.4		3	2					3	3								
9.8		1	4					1	7	1							
10.1			5						10	1	1	2					
10.4			1						8	2	1						
10.7		2	1						6	3	2	3				1	
11.0		2	1						6	7	6	7				1	
11.3		2	1						7	10	4	7				1	
11.6		4	3						8	10	9	10					
11.9		2	1	1					4	11	6	10					
12.2		2	2	1					1	19	11	16					
12.5		3	4	1					1	14	11	17					
12.8		4	3	2					1	15	14	13					
13.1		58	3	2					1	15	7	15					
13.4			3	4	1					13	10	13					
13.7			4	3						6	2	5					
14.0			4	2						8	3	6					
14.3			3	5		1											
14.6			34	5		1											
14.9				13		5											
Total	0	204	216	39	1	7	118	14	65	135	87	124	86	227	174	66	56

Table B-8: Detailed forecast of **departing** vessel calls for 2035 **with** Project

Draft (m)	Bulk Carrier 2	Bulk Carrier 3	Bulk Carrier 4	Bulk Carrier 5	Bulk Carrier 6	Bulk Carrier 7	Chemical Tanker	SubPX	Panamax	PPXGn1	PPXGn2	PPXGn3	Cruise	General Cargo 1	General Cargo 2	Tanker Panamax	Aframax Tanker
2.1																	
2.4																	
2.7																	
3.0																	
3.4																	
3.7																	
4.0																	
4.3																	
4.6																	
4.9														44			
5.2														51			
5.5														21			
5.8							105							25		51	
6.1		74	105				4							83	131	2	
6.4		1	6												11	2	
6.7		2	7				1							1	11	4	
7.0		2	6				1							1	7	2	
7.3		4	4				1							1	6		
7.6		8	5				1						86		6	1	
7.9		8	2				3								1		
8.2		9	2				1								1	1	
8.5		7						9									
8.8		4					1		2								
9.1		2						1									56
9.4		3	2					3	3								
9.8		1	4					1	7	1							
10.1			5						10	1	1	2					
10.4			2						8	2	1						
10.7		2	3						6	3	2	3				1	
11.0		2	1						6	7	6	7				1	
11.3		2	1						7	10	4	7				1	
11.6		4	3						8	10	9	10					
11.9		2	1	1					4	11	6	10					
12.2		2	2	1					1	19	11	16					
12.5		3	4	1					1	14	11	17					
12.8		4	3	2					1	15	14	13					
13.1		54	3	2					1	15	7	15					
13.4			3	4	1					13	10	13					
13.7			4	3						6	2	5					
14.0			4	2						8	3	6					
14.3			3	5		1											
14.6			34	5		1											
14.9				13		5											
Total	0	200	219	39	1	7	118	14	65	135	87	124	86	227	174	66	56

ATTACHMENT A – 5
DATA COLLECTION REPORTS

Hydrodynamic and Water Quality Field Data Collection in the Mobile-Tensaw Delta, Alabama

Mobile and Baldwin Counties, Alabama

Richard J. Allen
U.S. Army Corps of Engineers, Mobile District
109 Saint Joseph Street
Mobile, AL 36602

Draft Report

US Army Corps of Engineers
Mobile District

May 2018

Contents

1 Introduction

Purpose
Study Area
Background

2 USACE Discrete Data Collection

Overview
Site Selection
Methodology
Data Inventory

3 References

Appendix A – Acoustic Doppler Current Profile (ADCP) Measurement Summary

Appendix B – Vertical Profile Measurement Summary

Figures and Tables

Figures

Figure 1: Overview of hydrologic connectivity of the stream network in the Mobile-Tensaw Delta, Alabama. 3
Figure 2: Overview Map of Discrete Sampling locations in the Mobile-Tensaw Delta. 5
Figure 3: Sontek M9 Acoustic Doppler Current Profiler Field Deployment Configuration. 6
Figure 4: Example Acoustic Doppler Current Profiler (ADCP) transect orientation at Site CO-01 7

Tables

Table 1: Summary Statistics of the 2010 calendar year for the Alabama River at Claiborne Lock and Dam (USGS ID: 02428400) and the Tombigbee River at Coffeeville Lock and Dam (USGS ID: 02469761). 2
Table 2: Discrete sampling site characteristics. 4
Table 3: Summary of available vertical profile and Acoustic Doppler Current Profile (ADCP) measurements by site. 9

1 Introduction

Purpose

The U.S. Army Corps of Engineers, Mobile District, is completing a General Re-Evaluation Report (GRR) for the Mobile Harbor Federal Navigation Channel. The GRR will determine if it is justifiable to deepen and widen the channel up to the authorized dimensions. An extensive field data collection and archival data discovery effort is employed as part of this effort. Field data is vital to accurately characterize the delta and useful for calibration of hydrodynamic and environmental models to evaluate existing conditions and predict changes as a result of the proposed federal channel modifications. Field data measurements obtained by the Mobile District as a part of the GRR are detailed in this report.

Study Area

Mobile Bay, Alabama can be described as a micro-tidal, drowned river valley located along the north central coastline of the Gulf of Mexico. The Mobile-Tensaw Delta watershed is the sixth largest river basin in the United States and the fourth largest in terms of streamflow (Isphording and Flowers, 1987). It drains water from three-fourths of Alabama as well as portions of Georgia, Tennessee and Mississippi into Mobile Bay. The Mobile-Tensaw River Delta is the second largest in the Contiguous U.S. and generally defined as being 45 miles long and 6 to 16 miles wide, encompassing more than 280 square miles. The northern extent is the confluence of the Alabama and Tombigbee Rivers and the southern limit defined as the U.S. Hwy 90/98 causeway. The delta was further subdivided by the U.S. Department of Commerce (1979) into 20,000 acres of open water, 10,000 acres of marshland, 69,000 acres of swamp, and 85,000 acres of mixed bottomland forest. The delta is also recognized as a National Natural Landmark in May 1974 and has been referred to as the "Amazon of the South" due to the diversity of habitat and wildlife.

The hydrologic stream network in the Mobile-Tensaw Delta is classified as braided. Primary stream channels within the delta originate in the north through confluence of the Alabama and Tombigbee Rivers forming the Mobile River then, after a short distance (3 miles), the Tensaw River branches off the left bank. Continuing south the Mobile River experiences relatively little bifurcations prior to reaching the Port of Mobile (southern limit of deltaic features) where discharge measured at USGS streamgage at Barry Steam Plant is near equal to discharge at the Alabama State Docks, based on measurements obtained in this report. Conversely, the Tensaw River develops into a near independent braided network of major and minor channels over the southerly course and leading to divisions of the Blakely and Apalachee Rivers. Figure 1 is a general overview of the primary stream network and hydrologic connectivity in the Mobile-Tensaw Delta.

Freshwater discharge through the Mobile-Tensaw Delta is dominated by the Alabama and Tombigbee Rivers which account for 95% of the total flow (Schroeder, 1978). Marr 2013 computed long-term daily maximum, mean, and minimum cumulative discharge using U.S. Geological Survey (USGS) discharge records for the Alabama River at Claiborne Lock and Dam (USGS ID: 02428400) and the Tombigbee River at Coffeeville Lock and Dam (USGS ID: 02469761) using the respective length of record at each resulting in 238,000 $ft^3\ s^{-1}$, 60,500 $ft^3\ s^{-1}$, and 8,700 $ft^3\ s^{-1}$. In a similar methodology, freshwater discharge from the Mobile River watershed was delineated by seasonal trends using a 35-yr record (1976-2011) resulting a mean daily discharge of 93,800 $ft^3\ s^{-1}$ in late winter to early spring and 28,800 $ft^3\ s^{-1}$ during late summer to early fall (Dzwonkowski et al., 2014). Alternatively, but equally important, describing of freshwater discharge based on the 10 and 90 percent occurrence probability relationships indicate low flow conditions are defined as less than 17,600 $ft^3\ s^{-1}$ and flood conditions when in excess of 247,200 $ft^3\ s^{-1}$ (Schroeder, 1978; Schroeder and Lysinger, 1979). Notably, comparison shows the statistical exceedance for flood conditions is larger than the measured discharge found by Marr 2013 which is likely a result of data availability and processing methods. For the Mobile Harbor General Re-evaluation study these values are of importance when describing the long-term characteristics of the study area, however; numerical analyses were completed based on the 2010 calendar year and attention should be given to this period. Data for the 2010 calendar year were obtained from the USGS at stations 02428400 and 02469761 and provided as summary statistics and cumulative values in Table 1 representing a large range of flow conditions.

Table 1: Summary Statistics of the 2010 calendar year for the Alabama River at Claiborne Lock and Dam (USGS ID: 02428400) and the Tombigbee River at Coffeeville Lock and Dam (USGS ID: 02469761).

2010 Calendar Year	Alabama River at Claiborne Lock and Dam (USGS ID: 02428400)	Tombigbee River at Coffeeville Lock and Dam (USGS ID: 02469761)	Cumulative
Annual Total (ft^3)	10,120,300	8,818,910	18,939,210
Annual Mean ($ft^3\ s^{-1}$)	27,730	24,160	51,890
Highest Daily Mean ($ft^3\ s^{-1}$)	145,000 (16 Mar)	136,000 (10 Feb)	
Lowest Daily Mean ($ft^3\ s^{-1}$)	2,410 (05 Oct)	1,340 (16 Sep)	
10 percent Exceedance ($ft^3\ s^{-1}$)	76,900	75,400	152,300
50 percent Exceedance ($ft^3\ s^{-1}$)	11,400	9,690	21,090
90 percent Exceedance ($ft^3\ s^{-1}$)	4,560	1,960	6,520

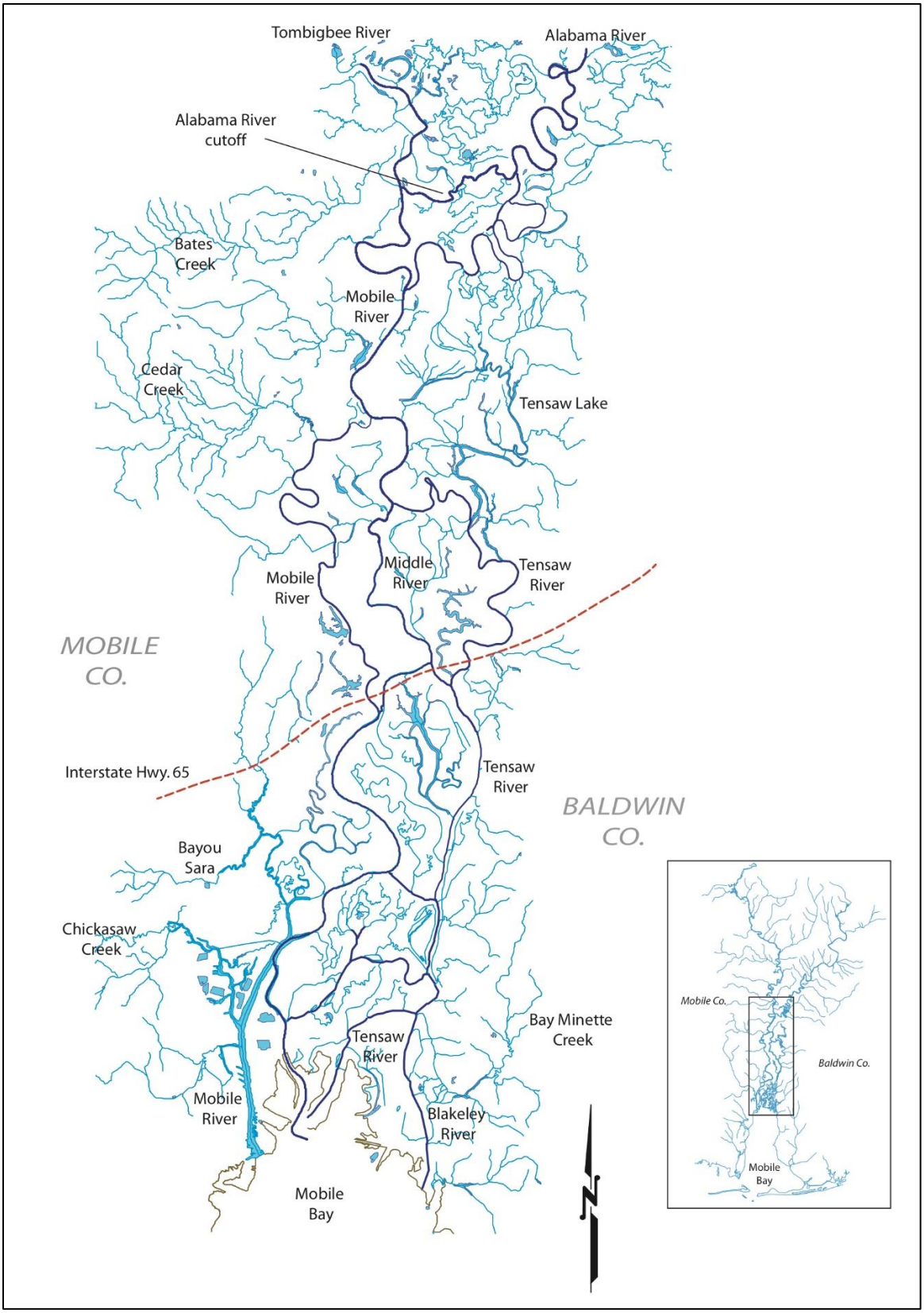

Figure 1: Overview of hydrologic connectivity of the stream network in the Mobile-Tensaw Delta, Alabama.

2 USACE Discrete Data Collection

Overview

Discrete hydrodynamic and water quality data were collected by the Mobile District's Hydrologic Data Collection Team. Multiple locations and times between June 2016 and June 2017 throughout the Mobile-Tensaw Delta were sampled. Datasets include Acoustic Doppler Current Profile (ADCP) transect discharge measurements and vertical profiles of water quality. Three time periods were sampled for reconnaissance of gage deployment (May 2016) initial characterization of flow distribution (June 2016) and tidal influence on water quality constituents (September 2016-Jun 2017).

Site Selection

Discrete sampling locations shown in Figure 2, and listed in Table 2 were identified from aerial imagery and digital terrain models (DEMs) based on bifurcation of the primary channel network in the Mobile-Tensaw Delta. However, it is noted some sites in Figure 2 may not have associated data and some sites were added later based on initial data sampling, field observations, and time efficiencies.

Table 2: Discrete sampling site characteristics.

Site	Latitude	Longitude	Average Channel Width (ft)	Average Cross-Section Area (ft^2)
AR@CW	30.6725	-87.9541	1,300	18,782
BR@CW	30.6675	-87.9267	1,163	24,968
BR-01	30.7144	-87.9416	1,007	26,454
CO-01	30.8186	-87.9478	334	3,823
CO-02	30.8076	-87.9313	369	4,451
MR-01	30.8393	-87.9456	918	15,585
MR-02	30.8206	-87.9546	732	14,954
MR-03	30.8083	-87.9925	1,224	20,493
MR-04	30.7929	-87.9908	498	5,957
MR-06	30.7801	-88.0169	1,078	23,391
MR-08	30.7313	-88.0424	1,034	38,173
MR-09	30.6718	-88.0333	1,040	36,794
SR-02	30.7199	-88.0142	927	15,564
SR-03	30.7619	-87.9313	753	6,094
TR@CW	30.6836	-88.0092	1,311	32,375
TR-01	30.8729	-87.8946	1,242	31,597
TR-02	30.8201	-87.9173	1,126	36,391
TR-03	30.7525	-87.9192	830	43,067
TR-04	30.7464	-87.9458	825	44,134
TR-05	30.7340	-87.9720	604	9,875
TR-06	30.7032	-87.9853	1,001	12,069

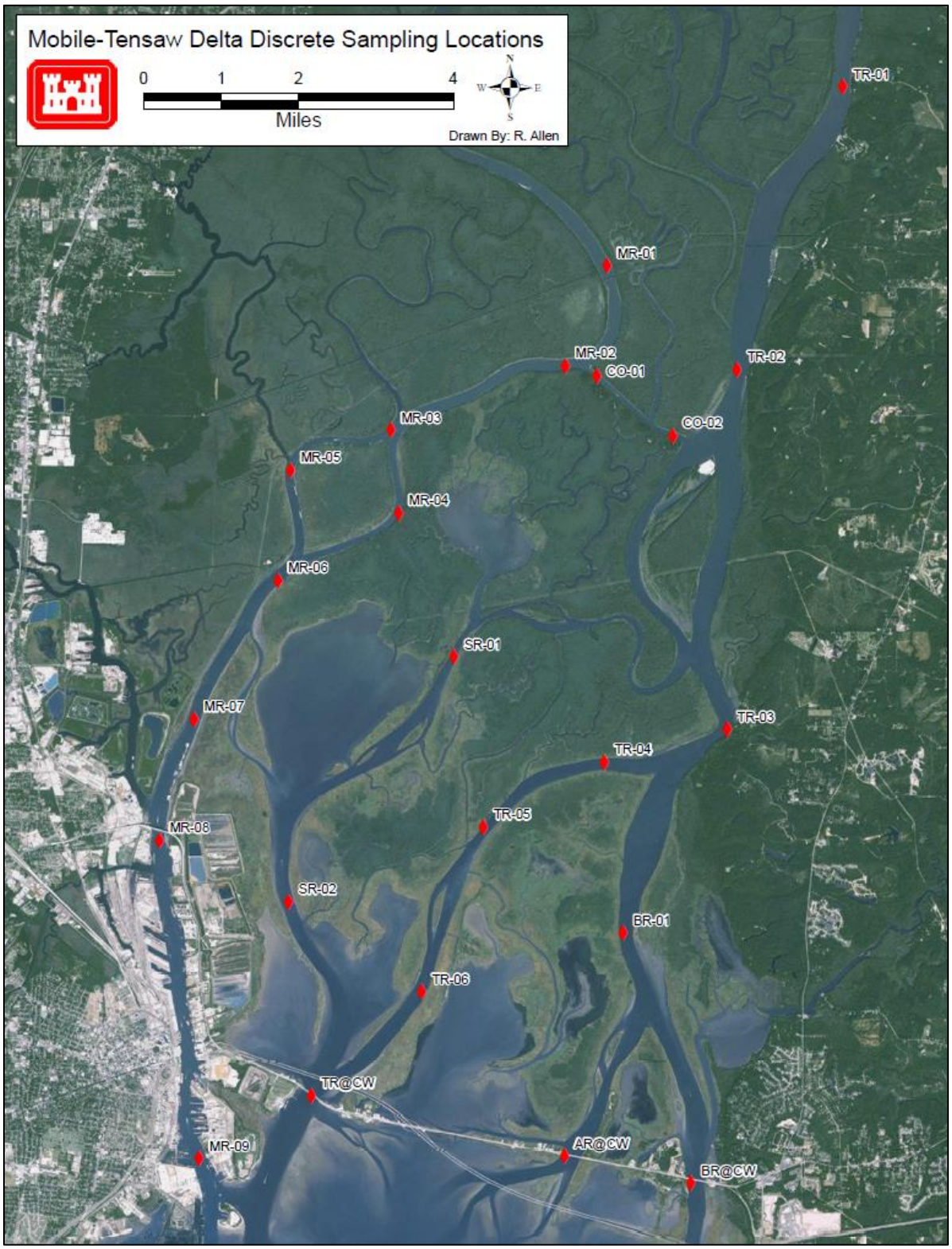

Figure 2: Overview Map of Discrete Sampling locations in the Mobile-Tensaw Delta.

Methodology

Acoustic Doppler Current Profiler

ADCP discharge measurements were collected using a Sontek M9 River Surveyor coupled with a DGPS antenna, mounted to a hydroboard, and tethered to the side of the vessel in accordance with U.S. Geological Survey standard methods (Figure 3). A discharge transect line was predetermined to optimize data quality by orienting the line such that is as near perpendicular to the flow direction as possible and located at a straight segment of the channel alignment with symmetrical and gradual changes in the channel cross-section geometry. An example transect layout is shown in Figure 4 at station CO-01. At least two discharge measurements were obtained at each site and temporal record for quality control. The sign convention for flow direction is positive in the southerly direction. Average total discharge and direction are reported as well as a cross-sectional profile of the water speed.

Figure 3: Sontek M9 Acoustic Doppler Current Profiler Field Deployment Configuration.

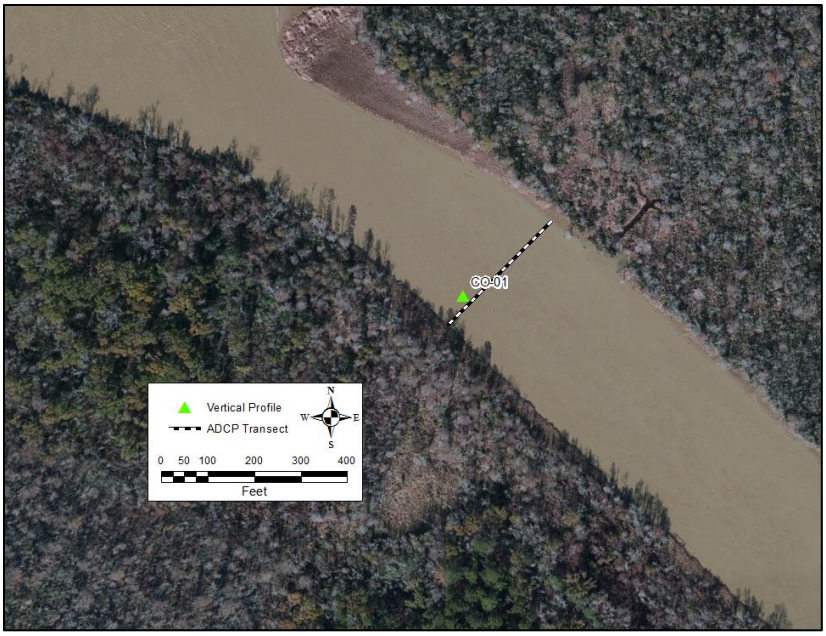

Figure 4: Example Acoustic Doppler Current Profiler (ADCP) transect orientation at Site CO-01.

Post-processing and quality assurance of each ACDP measurement is achieved using the manufacture's software suite, RiverSurveyor Live, and employing methods prescribed by the U.S. Geological Society (USGS, 2013). Reciprocal measurements are compared based on summary variables (total discharge, width, velocity, and cross-section area). In general, if variables exceed 5 percent variance in total discharge additional measurements are obtained while in the field. However, the variance may be valid in certain instances due to astronomical tidal forcing. Influence of tidal forcing between reciprocal measurements was observed but is a seldom occurrence since the time lapsed measurements is relatively small. The most prominent source of invalid measurements is attributed to negligible velocities where validity cannot be ascertained. Data not meeting quality assurance as provided in this paragraph are noted, but not omitted, in the record and caution should be used when applying this data to any analyses.

Water Quality

Vertical profiles of water quality data were obtained using three types of multi-parameter sondes, each having some variation in constituents, maximum depth and post-processing methodologies. Instrument usage per site/measurement is identified in the Data Inventory section. Generally, each instrument type measured depth, temperature, conductivity. The Sontek Castaway measured only the general parameters at a rate of 5 Hz and had a maximum tether length of 50 feet, the Hydrolab MS5 sonde included turbidity with a maximum depth range of 10 meters, and the YSI ProDSS included turbidity, pH, and dissolved oxygen with a maximum depth range of 10 meters and sampled at 2 Hz. All instruments computed salinity based on the Practical Salinity Scale (1978). Field deployment methodology remained consistent and is carried out by identifying the

thalweg of the channel along the ADCP transect, manually lowering the sonde through the water column at an approximate rate of 1 foot (0.305 m) per second until the depth or tether limit is reached, then retrieved at an equal rate.

Post-processing procedures and quality assurance for the Sontek Castaway instrumentation was completed using the manufacture software and an algorithm to combine the downward and upward measured profiles in a bin averaged routine with approximately 1 foot bin intervals. The Hydrolab and YSI instruments were processed in a numerical computing environment using a similar approach but bin intervals were 1.64 feet (0.5 m). It is noted some profiles have missing bin values which is likely due to the instrument moving through the water column too quickly. Quality assurance is achieved on each data set both in the field and after post-processing by observational verification of the profile. The most common source of poor data quality occurred when the instrument made contact with the bottom, seen by a large spike in constituents. These values are not removed from the processed data.

Data Inventory

The data collection campaign between May 2016 and September 2016 resulted in 411 ADCP transects and 203 vertical profiles of water quality. Measurements vary by day, time, and site; a summary of available data by site is provided in **Error! Reference source not found.**. Processed nd/or raw datasets are stored locally in multiple formats described herein. Bin averaged vertical profile measurements are provided in ASCII format for profiles measured with the YSI ProDSS, profiles measured with the Castaway are provided in the exported format (.csv) from the manufacture software, and the Hydrolab MS5 data are provided as raw data exported from the instrument in ASCII format. ADCP transect data are provided in binary format readable with the manufacture's software (RiverSurveyor). File names along with summary data are provided in Appendix A and B sorted by sampling location site name then date/time.

Table 3: Summary of available vertical profile and Acoustic Doppler Current Profile (ADCP) measurements by site.

Site	# of Vertical Profiles	# of ADCP Transects
AR@CW	18	36
BR@CW	16	33
TR@CW	24	50
MR-01	15	45
MR-02	10	20
MR-03	1	2
MR-04	1	2
MR-05	0	0
MR-06	1	5
MR-08	4	20
MR-09	3	2
TR-01	1	3
TR-02	21	56
TR-03	18	46
TR-04	6	2
TR-05	1	2
TR-06	10	10
SR-02	10	11
SR-03	5	10
CO-01	14	25
CO-02	19	28
BR-01	2	2
Other	3	1
Total	**203**	**411**

3 References

Dzwonkowski, B., Park, K., Lee, J., Webb, B.M., Valle-Levinson, A. (2014). Spatial Variability of Flow over a River-Influenced Inner Shelf in Coastal Alabama during Spring. Journal of Continental Shelf Research. Elsevier Ltd. (74)25-34.

Isphording, W.C. and Flowers, G.C. (1987). Mobile Bay: The Right Estuary in the Wrong Place. Symposium on the Natural Resources of Mobile Bay Estuary. Alabama Sea Grant Extension Service. MASGP-87-007. 165-174

Marr, C.D. (2013). Hydrodynamic Modeling of Residence, Exposure, and Flushing Time Response to Riverine Discharge in Mobile Bay, Alabama. A Thesis. College of Engineering, University of South Alabama, Mobile, Alabama.

Schroeder, W.W. (1978). Riverine influence on estuaries: a case study. Estuarine Interactions, M.S. Wiley, ed., Academic Press, New York, New York, 347-364.

Schroeder, W.W., and Lysinger, W.R. (1979). Hydrography and circulation of Mobile Bay. Symposium on the Natural Resources of the Mobile Bay Estuary, H.A. Loyacano and J.P. Smith, eds., U.S. Army Corps of Engineers, Mobile District, Mobile, Alabama, 75-94.

U.S. Geological Survey, (2012a). Water-resources data for the United States, Water Year 2011: U.S. Geological Survey Water-Data Report WDR-US-2011, site 02428400, Alabama River at Claiborne Lock and Dam Near Monroeville, Alabama. Reston, VA.

U.S. Geological Survey, (2012b). Water-resources data for the United States, Water Year 2011: U.S. Geological Survey Water-Data Report WDR-US-2011, site 02469761, Tombigbee River at Coffeeville Lock and Dam Near Coffeeville, Alabama. Reston, VA.

Appendix A

Acoustic Doppler Current Profile (ADCP) Measurement Summary

Site	File name	Start Edge	Date/Time (CST)	Duration	Width (ft)	Area (ft2)	Mean Speed (ft/s)	Total Q (cfs)
AR@CW	20160621082236.riv	Left Bank	06/21/2016 08:25	0:07:33	1,341	19,877	-0.35	-6,849
AR@CW	20160621083018.riv	Right Bank	06/21/2016 08:33	0:06:15	1,354	18,749	-0.38	-7,030
AR@CW	20160907084611.riv	Right Bank	09/07/2016 08:46	0:06:12	1,328	18,641	0.86	15,995
AR@CW	20160907085242.riv	Left Bank	09/07/2016 08:52	0:06:10	1,346	19,107	0.85	16,259
AR@CW	20160907115452.riv	Right Bank	09/07/2016 11:54	0:06:48	1,352	18,336	0.60	11,018
AR@CW	20160907120206.riv	Left Bank	09/07/2016 12:02	0:06:20	1,349	17,318	0.63	10,903
AR@CW	20160907140822.riv	Right Bank	09/07/2016 14:08	0:06:42	1,312	19,218	0.24	4,517
AR@CW	20160907141522.riv	Left Bank	09/07/2016 14:15	0:07:27	1,347	18,921	0.23	4,391
AR@CW	20160907151551.riv	Right Bank	09/07/2016 15:15	0:06:55	1,310	18,994	0.05	974
AR@CW	20160907152306.riv	Left Bank	09/07/2016 15:23	0:07:57	1,311	19,749	0.03	540
AR@CW	20160907153121.riv	Right Bank	09/07/2016 15:31	0:10:13	1,324	20,242	-0.06	-1,152
AR@CW	20160907154311.riv	Left Bank	09/07/2016 15:43	0:07:23	1,334	20,198	-0.13	-2,555
AR@CW	20160907165152.riv	Right Bank	09/07/2016 16:51	0:06:55	1,329	20,055	-0.36	-7,309
AR@CW	20160907165914.riv	Left Bank	09/07/2016 16:59	0:07:14	1,341	22,130	-0.36	-7,891
AR@CW	20160908115427.riv	Right Bank	09/08/2016 11:54	0:05:58	1,335	19,624	0.65	12,658
AR@CW	20160908120042.riv	Left Bank	09/08/2016 12:00	0:06:54	1,350	18,216	0.72	13,039
AR@CW	20160922141802.riv	Right Bank	09/22/2016 14:18	0:05:39	1,339	17,522	0.51	8,976
AR@CW	20160922142358.riv	Left Bank	09/22/2016 14:24	0:05:24	1,345	16,430	0.54	8,825
BR@CW	20160621090037.riv	Right Bank	06/21/2016 09:03	0:07:03	1,178	25,752	-0.46	-11,814
BR@CW	20160621090813.riv	Left Bank	06/21/2016 09:11	0:05:45	1,180	25,805	-0.45	-11,612
BR@CW	20160907092159.riv	Left Bank	09/07/2016 09:22	0:05:33	1,144	25,186	1.12	28,137
BR@CW	20160907092805.riv	Right Bank	09/07/2016 09:28	0:05:49	1,150	25,152	1.16	29,069
BR@CW	20160907122701.riv	Right Bank	09/07/2016 12:27	0:05:57	1,153	25,122	0.73	18,266
BR@CW	20160907123317.riv	Left Bank	09/07/2016 12:33	0:05:59	1,171	25,668	0.77	19,734
BR@CW	20160907144111.riv	Right Bank	09/07/2016 14:41	0:05:55	1,164	25,013	0.35	8,736
BR@CW	20160907144730.riv	Left Bank	09/07/2016 14:47	0:06:59	1,149	24,785	0.36	8,885
BR@CW	20160907160834.riv	Right Bank	09/07/2016 16:08	0:07:06	1,180	25,377	-0.01	-156
BR@CW	20160907161604.riv	Left Bank	09/07/2016 16:16	0:07:47	1,198	25,144	-0.06	-1,574

BR@CW	20160907162413.riv	Right Bank	09/07/2016 16:24	0:06:55	1,161	24,937	-0.06	-1,451
BR@CW	20160908122451.riv	Right Bank	09/08/2016 12:24	0:07:32	1,164	25,057	0.92	23,071
BR@CW	20160908123242.riv	Left Bank	09/08/2016 12:32	0:05:46	1,164	25,597	0.92	23,581
BR@CW	20160922144546.riv	Right Bank	09/22/2016 14:45	0:05:23	1,163	24,197	0.74	17,983
BR@CW	20160922145126.riv	Left Bank	09/22/2016 14:51	0:04:46	1,164	24,411	0.68	16,496
BR-01	20160621093210.riv	Right Bank	06/21/2016 09:35	0:05:53	1,007	26,428	-0.37	-9,737
BR-01	20160621093822.riv	Left Bank	06/21/2016 09:41	0:04:48	1,007	26,480	-0.36	-9,492
CO-01	20160621122755.riv	Left Bank	06/21/2016 12:30	0:03:19	339	3,755	-1.29	-4,854
CO-01	20160621123122.riv	Right Bank	06/21/2016 12:34	0:02:40	345	3,832	-1.23	-4,713
CO-01	20160913081451.riv	Left Bank	09/13/2016 08:14	0:02:04	338	3,802	0.72	2,732
CO-01	20160913081713.riv	Right Bank	09/13/2016 08:17	0:01:59	332	3,789	0.71	2,676
CO-01	20160913090721.riv	Left Bank	09/13/2016 09:07	0:02:08	332	3,894	0.69	2,692
CO-01	20160913090941.riv	Right Bank	09/13/2016 09:09	0:01:50	335	3,928	0.68	2,659
CO-01	20160913102313.riv	Left Bank	09/13/2016 10:23	0:02:07	336	3,840	0.56	2,154
CO-01	20160913102539.riv	Right Bank	09/13/2016 10:25	0:01:49	325	3,945	0.49	1,938
CO-01	20160913112551.riv	Left Bank	09/13/2016 11:25	0:01:58	309	3,694	0.45	1,650
CO-01	20160913112806.riv	Right Bank	09/13/2016 11:28	0:01:54	323	3,752	0.41	1,521
CO-01	20160913123642.riv	Left Bank	09/13/2016 12:36	0:01:55	336	3,925	0.32	1,270
CO-01	20160913123854.riv	Right Bank	09/13/2016 12:38	0:02:14	325	3,933	0.29	1,155
CO-01	20160913133847.riv	Left Bank	09/13/2016 13:38	0:01:46	311	3,832	0.26	985
CO-01	20160913134053.riv	Right Bank	09/13/2016 13:40	0:01:58	318	3,861	0.22	865
CO-01	20160913150800.riv	Left Bank	09/13/2016 15:08	0:02:02	327	3,806	0.12	471
CO-01	20160913151019.riv	Right Bank	09/13/2016 15:10	0:02:11	334	3,958	0.10	379
CO-01	20160913160931.riv	Left Bank	09/13/2016 16:09	0:02:20	335	3,522	-0.25	-892
CO-01	20160913161237.riv	Right Bank	09/13/2016 16:12	0:02:21	338	3,986	-0.26	-1,033
CO-01	20160913161556.riv	Left Bank	09/13/2016 16:16	0:01:56	334	3,695	-0.30	-1,113
CO-01	20160914091157.riv	Left Bank	09/14/2016 09:11	0:02:51	345	3,768	0.65	2,441
CO-01	20160914091505.riv	Right Bank	09/14/2016 09:15	0:02:30	341	3,748	0.71	2,676
CO-01	20160914111246.riv	Left Bank	09/14/2016 11:12	0:02:47	349	3,877	0.72	2,804
CO-01	20160914111550.riv	Right Bank	09/14/2016 11:15	0:02:34	352	3,736	0.70	2,614

CO-01	20160914130508.riv	Left Bank	09/14/2016 13:05	0:02:36	343	3,854	0.54	2,095
CO-01	20160914130801.riv	Right Bank	09/14/2016 13:08	0:02:10	336	3,836	0.57	2,192
CO-02	20160621121336.riv	Right Bank	06/21/2016 12:16	0:02:27	367	4,510	-0.61	-2,733
CO-02	20160621121618.riv	Left Bank	06/21/2016 12:19	0:02:14	368	4,387	-0.68	-2,968
CO-02	20160913075910.riv	Right Bank	09/13/2016 07:59	0:02:07	372	4,594	-0.31	-1,404
CO-02	20160913080136.riv	Left Bank	09/13/2016 08:01	0:02:51	362	4,605	-0.33	-1,510
CO-02	20160913092028.riv	Left Bank	09/13/2016 09:20	0:02:04	348	4,495	0.29	1,321
CO-02	20160913092247.riv	Right Bank	09/13/2016 09:22	0:02:20	365	4,522	0.32	1,446
CO-02	20160913100949.riv	Left Bank	09/13/2016 10:09	0:02:15	373	4,540	0.43	1,931
CO-02	20160913101225.riv	Right Bank	09/13/2016 10:12	0:02:17	361	4,418	0.43	1,884
CO-02	20160913113808.riv	Left Bank	09/13/2016 11:38	0:02:52	395	4,670	0.27	1,240
CO-02	20160913114116.riv	Right Bank	09/13/2016 11:41	0:02:06	374	4,392	0.32	1,398
CO-02	20160913114356.riv	Left Bank	09/13/2016 11:44	0:02:08	370	4,581	0.31	1,428
CO-02	20160913122414.riv	Left Bank	09/13/2016 12:24	0:02:02	369	4,550	0.24	1,095
CO-02	20160913122632.riv	Right Bank	09/13/2016 12:26	0:02:20	355	4,290	0.27	1,176
CO-02	20160913135208.riv	Left Bank	09/13/2016 13:52	0:02:23	371	4,557	0.29	1,315
CO-02	20160913135452.riv	Right Bank	09/13/2016 13:55	0:02:33	380	4,621	0.27	1,226
CO-02	20160913145452.riv	Left Bank	09/13/2016 14:54	0:02:18	367	4,501	0.54	2,444
CO-02	20160913145740.riv	Right Bank	09/13/2016 14:57	0:02:15	374	4,485	0.56	2,502
CO-02	20160913162757.riv	Left Bank	09/13/2016 16:27	0:03:06	346	4,237	0.51	2,149
CO-02	20160913163120.riv	Right Bank	09/13/2016 16:31	0:02:20	363	4,239	0.43	1,805
CO-02	20160913163412.riv	Left Bank	09/13/2016 16:34	0:02:44	359	4,305	0.42	1,823
CO-02	20160914085238.riv	Left Bank	09/14/2016 08:52	0:03:19	377	4,529	0.33	1,476
CO-02	20160914085619.riv	Right Bank	09/14/2016 08:56	0:03:07	376	4,275	0.34	1,447
CO-02	20160914105642.riv	Left Bank	09/14/2016 10:56	0:02:45	381	4,607	0.34	1,547
CO-02	20160914105946.riv	Right Bank	09/14/2016 10:59	0:02:36	376	4,343	0.31	1,363
CO-02	20160914125036.riv	Left Bank	09/14/2016 12:50	0:02:40	372	4,524	0.66	2,995
CO-02	20160914125334.riv	Right Bank	09/14/2016 12:53	0:02:46	374	4,452	0.64	2,851
CO-02	20160923095925.riv	Left Bank	09/23/2016 09:59	0:03:31	354	4,184	0.68	2,851
CO-02	20160923100320.riv	Right Bank	09/23/2016 10:03	0:02:44	368	4,225	0.66	2,773

MR-01	20160506140024.riv	Left Bank	05/06/2016 13:57	0:08:32	985	16,124	1.33	21,457
MR-01	20160621125809.riv	Right Bank	06/21/2016 13:01	0:06:56	967	16,138	-0.05	-754
MR-01	20160621130523.riv	Left Bank	06/21/2016 13:08	0:07:21	966	15,218	-0.20	-2,970
MR-01	20160621131257.riv	Right Bank	06/21/2016 13:15	0:05:06	968	15,203	-0.09	-1,435
MR-01	20160913083036.riv	Left Bank	09/13/2016 08:30	0:03:58	976	15,428	-0.44	-6,743
MR-01	20160913083501.riv	Right Bank	09/13/2016 08:35	0:04:57	946	15,436	-0.45	-6,900
MR-01	20160913104549.riv	Left Bank	09/13/2016 10:45	0:04:17	953	14,953	-0.26	-3,929
MR-01	20160913105021.riv	Right Bank	09/13/2016 10:50	0:04:12	968	15,586	-0.26	-3,981
MR-01	20160913125234.riv	Left Bank	09/13/2016 12:52	0:03:58	966	15,530	-0.14	-2,152
MR-01	20160913125657.riv	Right Bank	09/13/2016 12:56	0:04:55	957	15,800	-0.16	-2,544
MR-01	20160913130214.riv	Left Bank	09/13/2016 13:02	0:03:57	970	15,498	-0.17	-2,682
MR-01	20160913152557.riv	Left Bank	09/13/2016 15:25	0:04:00	961	15,262	0.43	6,608
MR-01	20160913153014.riv	Right Bank	09/13/2016 15:30	0:04:44	968	15,198	0.48	7,304
MR-01	20160913164946.riv	Right Bank	09/13/2016 16:49	0:00:23	36	27	0.00	0
MR-01	20160913165029.riv	Left Bank	09/13/2016 16:50	0:04:27	981	15,330	0.86	13,152
MR-01	20160913165537.riv	Right Bank	09/13/2016 16:55	0:04:41	981	15,463	0.90	13,887
MR-01	20160914093222.riv	Left Bank	09/14/2016 09:32	0:05:05	971	15,728	-0.23	-3,607
MR-01	20160914093745.riv	Right Bank	09/14/2016 09:37	0:05:32	970	14,840	-0.28	-4,162
MR-01	20160914094352.riv	Left Bank	09/14/2016 09:43	0:05:35	978	15,763	-0.25	-3,978
MR-01	20160914112932.riv	Left Bank	09/14/2016 11:29	0:05:25	974	15,610	-0.27	-4,138
MR-01	20160914113512.riv	Right Bank	09/14/2016 11:35	0:05:26	976	15,306	-0.26	-4,048
MR-01	20160914132202.riv	Left Bank	09/14/2016 13:22	0:05:30	977	16,081	0.00	-27
MR-01	20160914132748.riv	Right Bank	09/14/2016 13:27	0:05:51	971	15,900	0.01	188
MR-02	20160621132830.riv	Right Bank	06/21/2016 13:31	0:04:20	738	15,407	-0.33	-5,002
MR-02	20160621133319.riv	Left Bank	06/21/2016 13:36	0:04:02	744	15,135	-0.34	-5,209
MR-02	20160913085201.riv	Right Bank	09/13/2016 08:52	0:04:22	750	15,264	-0.64	-9,803
MR-02	20160913085643.riv	Left Bank	09/13/2016 08:56	0:03:51	746	15,371	-0.63	-9,652
MR-02	20160913110747.riv	Right Bank	09/13/2016 11:07	0:03:55	679	14,459	-0.42	-6,039
MR-02	20160913111201.riv	Left Bank	09/13/2016 11:12	0:03:08	755	15,397	-0.35	-5,409
MR-02	20160913111549.riv	Right Bank	09/13/2016 11:15	0:03:07	753	15,487	-0.37	-5,697

MR-02	20160913131906.riv	Right Bank	09/13/2016 13:19	0:03:57	706	14,620	-0.35	-5,138
MR-02	20160913132321.riv	Left Bank	09/13/2016 13:23	0:03:52	743	15,377	-0.28	-4,346
MR-02	20160913132729.riv	Right Bank	09/13/2016 13:27	0:03:41	710	14,671	-0.29	-4,203
MR-02	20160913154554.riv	Right Bank	09/13/2016 15:45	0:04:21	684	13,891	0.75	10,350
MR-02	20160913155034.riv	Left Bank	09/13/2016 15:50	0:03:34	755	15,014	0.73	10,916
MR-02	20160913171442.riv	Right Bank	09/13/2016 17:14	0:04:15	645	12,862	1.52	19,593
MR-02	20160913171921.riv	Left Bank	09/13/2016 17:19	0:04:08	756	14,853	1.29	19,135
MR-02	20160914100301.riv	Right Bank	09/14/2016 10:03	0:04:55	739	15,306	-0.57	-8,791
MR-02	20160914100812.riv	Left Bank	09/14/2016 10:08	0:04:48	743	15,004	-0.57	-8,484
MR-02	20160914115557.riv	Right Bank	09/14/2016 11:55	0:04:22	748	15,492	-0.42	-6,514
MR-02	20160914120038.riv	Left Bank	09/14/2016 12:00	0:04:52	754	15,358	-0.40	-6,131
MR-02	20160914134611.riv	Right Bank	09/14/2016 13:46	0:04:23	743	15,142	-0.08	-1,175
MR-02	20160914135049.riv	Left Bank	09/14/2016 13:50	0:04:43	751	14,959	-0.04	-625
MR-03	20160621135932.riv	Right Bank	06/21/2016 14:02	0:06:44	1,217	19,842	-0.33	-6,484
MR-03	20160621140633.riv	Left Bank	06/21/2016 14:09	0:06:04	1,231	21,145	-0.34	-7,233
MR-04	20160621142503.riv	Left Bank	06/21/2016 14:27	0:03:17	496	5,940	-0.04	-211
MR-04	20160621142832.riv	Right Bank	06/21/2016 14:31	0:02:57	499	5,975	0.08	463
MR-06	20160506130259.riv	Right Bank	05/06/2016 13:00	0:08:28	1,069	24,102	0.64	15,319
MR-06	20160506131603.riv	Left Bank	05/06/2016 13:13	0:06:20	1,040	21,099	0.70	14,683
MR-06	20160621144532.riv	Left Bank	06/21/2016 14:48	0:05:38	1,118	24,814	-0.13	-3,285
MR-06	20160621145123.riv	Right Bank	06/21/2016 14:54	0:05:43	1,105	22,887	-0.05	-1,155
MR-06	20160621150437.riv	Left Bank	06/21/2016 15:07	0:04:54	1,058	24,056	0.00	23
MR-09	20160908103305.riv	Left Bank	09/08/2016 10:33	0:04:38	1,060	40,066	0.74	29,737
MR-09	20160908103754.riv	Right Bank	09/08/2016 10:37	0:04:28	1,021	33,522	0.90	30,139
Pipeline	20160913170315.riv	Left Bank	09/13/2016 17:03	0:02:02	94	743	0.71	530
SR-02	20160907104300.riv	Right Bank	09/07/2016 10:43	0:05:07	867	15,308	1.05	16,067
SR-02	20160907104839.riv	Left Bank	09/07/2016 10:48	0:05:02	900	15,480	1.03	15,888
SR-02	20160908081956.riv	Right Bank	09/08/2016 08:19	0:06:30	930	15,903	1.05	16,727
SR-02	20160908082646.riv	Left Bank	09/08/2016 08:26	0:04:39	938	15,736	1.08	17,034
SR-02	20160908093856.riv	Left Bank	09/08/2016 09:38	0:04:57	927	15,604	1.11	17,386

SR-02	20160908094413.riv	Right Bank	09/08/2016 09:44	0:04:56	922	15,470	1.14	17,578
SR-02	20160908145017.riv	Right Bank	09/08/2016 14:50	0:05:21	939	15,582	0.28	4,331
SR-02	20160908145609.riv	Left Bank	09/08/2016 14:56	0:05:25	932	15,402	0.21	3,182
SR-02	20160908150258.riv	Right Bank	09/08/2016 15:03	0:04:05	942	15,515	0.21	3,197
SR-02	20160908172129.riv	Left Bank	09/08/2016 17:21	0:03:42	959	15,215	-0.56	-8,498
SR-02	20160908172535.riv	Right Bank	09/08/2016 17:25	0:04:28	937	15,989	-0.55	-8,843
SR-03	20160922081111.riv	Right Bank	09/22/2016 08:11	0:04:40	727	6,311	0.35	2,184
SR-03	20160922081609.riv	Left Bank	09/22/2016 08:16	0:04:27	754	6,299	0.38	2,369
SR-03	20160922102330.riv	Left Bank	09/22/2016 10:23	0:04:32	748	6,049	0.62	3,723
SR-03	20160922102821.riv	Right Bank	09/22/2016 10:28	0:04:47	746	5,974	0.58	3,482
SR-03	20160922121608.riv	Left Bank	09/22/2016 12:16	0:04:42	756	5,661	0.60	3,418
SR-03	20160922122106.riv	Right Bank	09/22/2016 12:21	0:04:59	751	5,747	0.56	3,215
SR-03	20160923090809.riv	Left Bank	09/23/2016 09:08	0:04:40	775	6,516	0.17	1,091
SR-03	20160923091306.riv	Right Bank	09/23/2016 09:13	0:04:11	755	6,544	0.20	1,334
SR-03	20160923113921.riv	Left Bank	09/23/2016 11:39	0:03:40	761	5,810	0.56	3,240
SR-03	20160923114319.riv	Right Bank	09/23/2016 11:43	0:04:39	758	6,034	0.53	3,167
TR@CW	20160621065156.riv	Right Bank	06/21/2016 06:49	0:08:01	1,307	32,860	-0.68	-22,429
TR@CW	20160621070212.riv	Left Bank	06/21/2016 06:59	0:06:27	1,303	33,224	-0.67	-22,145
TR@CW	20160907074848.riv	Left Bank	09/07/2016 07:48	0:10:04	1,301	34,265	0.89	30,374
TR@CW	20160907075917.riv	Right Bank	09/07/2016 07:59	0:07:11	1,330	33,888	0.92	31,047
TR@CW	20160907111244.riv	Right Bank	09/07/2016 11:12	0:08:28	1,336	33,593	0.73	24,473
TR@CW	20160907112142.riv	Left Bank	09/07/2016 11:21	0:06:40	1,329	33,767	0.70	23,682
TR@CW	20160907172750.riv	Right Bank	09/07/2016 17:27	0:08:09	1,358	34,683	-0.73	-25,240
TR@CW	20160907173617.riv	Left Bank	09/07/2016 17:36	0:06:24	1,355	32,827	-0.82	-26,951
TR@CW	20160908072434.riv	Right Bank	09/08/2016 07:24	0:07:13	1,318	33,802	0.76	25,618
TR@CW	20160908073205.riv	Left Bank	09/08/2016 07:32	0:06:35	1,309	32,449	0.80	25,846
TR@CW	20160908084524.riv	Right Bank	09/08/2016 08:45	0:06:24	1,312	33,104	1.02	33,817
TR@CW	20160908085203.riv	Left Bank	09/08/2016 08:52	0:06:21	1,316	34,028	1.02	34,802
TR@CW	20160908100420.riv	Right Bank	09/08/2016 10:04	0:06:37	1,306	33,336	1.05	34,854
TR@CW	20160908101115.riv	Left Bank	09/08/2016 10:11	0:06:15	1,313	33,835	0.99	33,408

TR@CW	20160908112148.riv	Right Bank	09/08/2016 11:21	0:06:17	1,307	31,804	0.77	24,341
TR@CW	20160908112820.riv	Left Bank	09/08/2016 11:28	0:07:16	1,311	33,630	0.73	24,429
TR@CW	20160908135747.riv	Right Bank	09/08/2016 13:57	0:07:43	1,310	32,473	0.40	13,008
TR@CW	20160908140546.riv	Left Bank	09/08/2016 14:05	0:07:05	1,326	33,581	0.34	11,513
TR@CW	20160908153027.riv	Left Bank	09/08/2016 15:30	0:06:02	1,324	31,425	-0.10	-3,086
TR@CW	20160908153909.riv	Right Bank	09/08/2016 15:39	0:07:39	1,281	29,710	-0.25	-7,373
TR@CW	20160908154720.riv	Left Bank	09/08/2016 15:47	0:07:51	1,312	29,928	-0.33	-9,915
TR@CW	20160908155548.riv	Right Bank	09/08/2016 15:55	0:08:30	1,286	29,634	-0.41	-12,046
TR@CW	20160908160447.riv	Left Bank	09/08/2016 16:04	0:07:39	1,300	29,756	-0.43	-12,895
TR@CW	20160908162946.riv	Left Bank	09/08/2016 16:29	0:06:20	1,298	28,500	-0.60	-17,216
TR@CW	20160908163628.riv	Right Bank	09/08/2016 16:36	0:08:19	1,279	30,781	-0.58	-17,888
TR@CW	20160908174535.riv	Right Bank	09/08/2016 17:45	0:07:34	1,258	30,404	-0.70	-21,180
TR@CW	20160908175332.riv	Left Bank	09/08/2016 17:53	0:07:20	1,277	29,664	-0.68	-20,158
TR-01	20160621113145.riv	Right Bank	06/21/2016 11:34	0:06:30	1,238	31,644	-0.16	-4,967
TR-01	20160621113850.riv	Left Bank	06/21/2016 11:41	0:06:12	1,247	31,395	-0.20	-6,346
TR-01	20160621114537.riv	Right Bank	06/21/2016 11:48	0:05:43	1,243	31,751	-0.19	-6,019
TR-02	20160506143054.riv	Left Bank	05/06/2016 14:28	0:05:59	1,142	36,092	0.94	33,810
TR-02	20160621105044.riv	Left Bank	06/21/2016 10:53	0:05:48	1,119	35,776	-0.29	-10,308
TR-02	20160621105642.riv	Right Bank	06/21/2016 10:59	0:06:01	1,088	36,355	-0.30	-10,956
TR-02	20160913072620.riv	Left Bank	09/13/2016 07:26	0:04:52	1,113	34,069	-0.49	-16,552
TR-02	20160913073126.riv	Right Bank	09/13/2016 07:31	0:05:44	1,087	35,912	-0.48	-17,215
TR-02	20160913093525.riv	Left Bank	09/13/2016 09:35	0:04:47	1,111	36,183	-0.25	-8,927
TR-02	20160913094024.riv	Right Bank	09/13/2016 09:40	0:04:12	1,064	36,004	-0.22	-7,879
TR-02	20160913094527.riv	Left Bank	09/13/2016 09:45	0:04:20	1,118	35,402	-0.22	-7,760
TR-02	20160913095031.riv	Right Bank	09/13/2016 09:50	0:04:46	1,045	35,559	-0.20	-7,220
TR-02	20160913115950.riv	Left Bank	09/13/2016 11:59	0:04:51	1,125	36,945	0.01	224
TR-02	20160913120459.riv	Right Bank	09/13/2016 12:05	0:05:23	1,076	36,270	0.00	-22
TR-02	20160913141327.riv	Left Bank	09/13/2016 14:13	0:05:45	1,128	37,184	0.11	4,219
TR-02	20160913141925.riv	Right Bank	09/13/2016 14:19	0:06:03	1,097	36,478	0.16	5,991
TR-02	20160913143215.riv	Left Bank	09/13/2016 14:32	0:04:51	1,128	36,950	0.27	9,963

TR-02	20160913143719.riv	Right Bank	09/13/2016 14:37	0:04:31	1,087	36,198	0.27	9,907
TR-02	20160913173701.riv	Left Bank	09/13/2016 17:37	0:05:50	1,131	36,389	1.13	40,956
TR-02	20160913174304.riv	Right Bank	09/13/2016 17:43	0:06:16	1,106	35,501	1.15	40,695
TR-02	20160914080120.riv	Left Bank	09/14/2016 08:01	0:05:59	1,112	35,147	-0.13	-4,574
TR-02	20160914080734.riv	Right Bank	09/14/2016 08:07	0:06:04	1,124	35,709	-0.14	-5,133
TR-02	20160914081413.riv	Left Bank	09/14/2016 08:14	0:06:06	1,118	35,639	-0.17	-6,119
TR-02	20160914082059.riv	Right Bank	09/14/2016 08:21	0:05:46	1,115	36,336	-0.18	-6,676
TR-02	20160914082729.riv	Left Bank	09/14/2016 08:27	0:06:38	1,125	35,602	-0.22	-7,716
TR-02	20160914103054.riv	Left Bank	09/14/2016 10:30	0:06:28	1,117	36,041	-0.28	-9,957
TR-02	20160914103733.riv	Right Bank	09/14/2016 10:37	0:06:19	1,111	36,360	-0.26	-9,397
TR-02	20160914122419.riv	Left Bank	09/14/2016 12:24	0:06:06	1,108	35,966	-0.01	-327
TR-02	20160914123105.riv	Right Bank	09/14/2016 12:31	0:06:24	1,132	37,493	0.00	84
TR-02	20160914141335.riv	Left Bank	09/14/2016 14:13	0:06:16	1,117	37,018	0.45	16,732
TR-02	20160914142045.riv	Right Bank	09/14/2016 14:20	0:06:51	1,127	37,002	0.48	17,851
TR-02	20160922072844.riv	Left Bank	09/22/2016 07:28	0:12:04	2,288	45,479	0.70	31,899
TR-02	20160922074115.riv	Right Bank	09/22/2016 07:41	0:11:34	2,271	45,204	0.79	35,892
TR-02	20160923093632.riv	Left Bank	09/23/2016 09:36	0:00:49	66	214	0.10	21
TR-02	20160923093751.riv	Left Bank	09/23/2016 09:37	0:05:24	1,103	35,861	0.93	33,214
TR-02	20160923094324.riv	Right Bank	09/23/2016 09:43	0:05:25	1,097	36,141	0.96	34,654
TR-02a	20160922093815.riv	Right Bank	09/22/2016 09:38	0:07:17	1,173	29,230	1.23	35,978
TR-02a	20160922094551.riv	Left Bank	09/22/2016 09:45	0:07:38	1,196	29,787	1.20	35,850
TR-02a	20160922113602.riv	Right Bank	09/22/2016 11:36	0:06:17	1,180	28,786	1.20	34,549
TR-02a	20160922114231.riv	Left Bank	09/22/2016 11:42	0:05:26	1,188	29,308	1.18	34,480
TR-02a	20160923082705.riv	Right Bank	09/23/2016 08:27	0:07:08	1,216	29,327	0.79	23,163
TR-02a	20160923083446.riv	Left Bank	09/23/2016 08:34	0:07:02	1,223	30,411	0.83	25,160
TR-02a	20160923111805.riv	Right Bank	09/23/2016 11:18	0:07:11	1,195	29,133	1.14	33,214
TR-02a	20160923112539.riv	Left Bank	09/23/2016 11:25	0:05:31	1,201	29,588	1.07	31,499
TR-02b	20160922100438.riv	Left Bank	09/22/2016 10:04	0:05:13	779	13,593	0.87	11,760
TR-02b	20160922101010.riv	Right Bank	09/22/2016 10:10	0:04:05	761	13,384	0.89	11,909
TR-02b	20160922115726.riv	Left Bank	09/22/2016 11:57	0:05:12	761	12,378	0.81	9,993

TR-02b	20160922120254.riv	Right Bank	09/22/2016 12:02	0:04:48	755	12,432	0.76	9,461
TR-02b	20160923085029.riv	Left Bank	09/23/2016 08:50	0:04:57	768	13,940	0.89	12,425
TR-02b	20160923085546.riv	Right Bank	09/23/2016 08:55	0:04:22	769	13,799	0.89	12,212
TR-02b	20160923110116.riv	Left Bank	09/23/2016 11:01	0:04:52	734	13,463	0.85	11,475
TR-02b	20160923110711.riv	Right Bank	09/23/2016 11:07	0:03:58	751	13,389	0.88	11,790
TR-03	20160621101857.riv	Left Bank	06/21/2016 10:21	0:04:45	829	42,077	-0.19	-8,041
TR-03	20160621102409.riv	Right Bank	06/21/2016 10:27	0:04:36	831	44,058	-0.21	-9,136
TR-03a	20160922083408.riv	Left Bank	09/22/2016 08:34	0:07:55	1,818	30,184	1.23	37,099
TR-03a	20160922084227.riv	Right Bank	09/22/2016 08:42	0:11:42	1,805	30,978	1.19	36,735
TR-03a	20160922104508.riv	Left Bank	09/22/2016 10:45	0:07:51	1,876	30,708	1.21	37,068
TR-03a	20160922105317.riv	Right Bank	09/22/2016 10:53	0:10:21	1,798	30,431	1.24	37,720
TR-03a	20160922123832.riv	Left Bank	09/22/2016 12:38	0:06:50	1,773	28,042	1.01	28,377
TR-03a	20160922124539.riv	Right Bank	09/22/2016 12:45	0:08:37	1,764	28,799	1.06	30,469
TR-03a	20160922151525.riv	Left Bank	09/22/2016 15:15	0:06:45	1,799	27,934	0.73	20,427
TR-03a	20160922152225.riv	Right Bank	09/22/2016 15:22	0:08:11	1,781	29,692	0.70	20,793
TR-03a	20160923065640.riv	Left Bank	09/23/2016 06:56	0:08:39	1,814	28,972	0.35	10,163
TR-03a	20160923070537.riv	Right Bank	09/23/2016 07:05	0:09:42	1,823	31,495	0.40	12,730
TR-03a	20160923071545.riv	Left Bank	09/23/2016 07:15	0:08:30	1,815	29,679	0.46	13,658
TR-03a	20160923072437.riv	Right Bank	09/23/2016 07:24	0:09:42	1,819	31,832	0.50	15,825
TR-03a	20160923073508.riv	Left Bank	09/23/2016 07:35	0:08:24	1,810	29,425	0.58	17,131
TR-03a	20160923074350.riv	Right Bank	09/23/2016 07:43	0:09:49	1,816	32,165	0.65	21,039
TR-03a	20160923115842.riv	Left Bank	09/23/2016 11:58	0:08:19	1,802	29,001	1.13	32,809
TR-03a	20160923120717.riv	Right Bank	09/23/2016 12:07	0:08:59	1,799	29,837	1.10	32,801
TR-03b	20160922090525.riv	Right Bank	09/22/2016 09:05	0:05:59	1,189	10,778	0.67	7,266
TR-03b	20160922091144.riv	Left Bank	09/22/2016 09:11	0:06:16	1,209	10,629	0.71	7,505
TR-03b	20160922111150.riv	Right Bank	09/22/2016 11:11	0:06:26	1,198	10,354	0.67	6,958
TR-03b	20160922111833.riv	Left Bank	09/22/2016 11:18	0:05:16	1,203	9,983	0.71	7,065
TR-03b	20160922130200.riv	Right Bank	09/22/2016 13:02	0:05:37	1,198	9,959	0.64	6,336
TR-03b	20160922130755.riv	Left Bank	09/22/2016 13:07	0:04:46	1,187	9,886	0.67	6,596
TR-03b	20160922153808.riv	Right Bank	09/22/2016 15:38	0:06:18	1,185	9,642	0.29	2,839

TR-03b	20160922154445.riv	Left Bank	09/22/2016 15:44	0:05:06	1,178	9,687	0.31	3,046
TR-03b	20160923080224.riv	Right Bank	09/23/2016 08:02	0:06:40	1,231	11,604	0.32	3,708
TR-03b	20160923080921.riv	Left Bank	09/23/2016 08:09	0:06:01	1,224	11,084	0.35	3,917
TR-03b	20160923122459.riv	Right Bank	09/23/2016 12:25	0:05:07	1,172	10,189	0.53	5,444
TR-03b	20160923123022.riv	Left Bank	09/23/2016 12:30	0:05:20	1,181	9,807	0.57	5,610
TR-04	20160621100441.riv	Left Bank	06/21/2016 10:07	0:04:45	821	43,791	-0.22	-9,416
TR-04	20160621100955.riv	Right Bank	06/21/2016 10:12	0:04:27	829	44,477	-0.18	-8,085
TR-05	20160621074904.riv	Right Bank	06/21/2016 07:52	0:04:14	605	9,767	-0.25	-2,393
TR-05	20160621075343.riv	Left Bank	06/21/2016 07:57	0:03:31	603	9,983	-0.23	-2,278
TR-06	20160907101317.riv	Right Bank	09/07/2016 10:13	0:07:01	978	12,208	0.60	7,338
TR-06	20160907102041.riv	Left Bank	09/07/2016 10:20	0:04:58	992	12,024	0.59	7,043
TR-06	20160908075232.riv	Right Bank	09/08/2016 07:52	0:05:31	1,000	12,542	0.37	4,583
TR-06	20160908075829.riv	Left Bank	09/08/2016 07:58	0:05:17	1,003	12,290	0.42	5,202
TR-06	20160908090933.riv	Right Bank	09/08/2016 09:09	0:05:11	1,001	12,375	0.54	6,711
TR-06	20160908091505.riv	Left Bank	09/08/2016 09:15	0:04:05	1,003	10,216	0.69	7,006
TR-06	20160908142346.riv	Right Bank	09/08/2016 14:23	0:05:41	1,009	12,113	0.24	2,940
TR-06	20160908142943.riv	Left Bank	09/08/2016 14:29	0:05:42	1,017	12,130	0.21	2,550
TR-06	20160908165402.riv	Right Bank	09/08/2016 16:54	0:05:56	993	12,296	-0.23	-2,868
TR-06	20160908170014.riv	Left Bank	09/08/2016 17:00	0:05:46	1,014	12,491	-0.24	-3,004
TR	20170103130114.riv	Left Bank	01/03/2017 13:01	0:05:53	1,052	35,744	1.48	52,777
NMR	20170103135619.riv	Left Bank	01/03/2017 13:56	0:04:44	913	15,448	2.09	32,355
NMR	20170103140125.riv	Right Bank	01/03/2017 14:01	0:04:28	904	15,464	2.11	32,565
BR@CW	20170104091405.riv	Right Bank	01/04/2017 09:14	0:05:50	1,178	26,070	1.49	38,911
BR@CW	20170104092007.riv	Left Bank	01/04/2017 09:20	0:06:36	1,173	26,327	1.54	40,408
AR@CW	20170104094133.riv	Right Bank	01/04/2017 09:41	0:06:29	1,288	17,512	1.43	25,085
AR@CW	20170104094815.riv	Left Bank	01/04/2017 09:48	0:06:05	1,290	16,875	1.53	25,818
TR	20170104125018.riv	Left Bank	01/04/2017 12:50	0:06:04	976	32,144	1.78	57,227
TR@CW	20170104141837.riv	Left Bank	01/04/2017 14:18	0:05:50	1,310	31,260	0.29	9,145
TR@CW	20170104142519.riv	Right Bank	01/04/2017 14:24	0:06:28	1,292	30,676	0.32	9,915
SD	20170112074733.riv	Left Bank	01/12/2017 07:47	0:04:17	1,070	36,912	1.73	63,839

SD	20170112075307.riv	Right Bank	01/12/2017 07:53	0:04:05	1,075	39,097	1.72	67,370
TR@CW	20170112081427.riv	Right Bank	01/12/2017 08:14	0:05:44	1,294	32,774	1.54	50,608
TR@CW	20170112082020.riv	Left Bank	01/12/2017 08:20	0:05:35	1,284	32,877	1.41	46,269
TR@CW	20170112082644.riv	Right Bank	01/12/2017 08:26	0:05:19	1,287	32,553	1.45	47,136
BR@CW	20170118080516.riv	Right Bank	01/18/2017 08:05	0:06:24	1,171	25,260	0.79	20,010
BR@CW	20170118081150.riv	Left Bank	01/18/2017 08:11	0:06:10	1,165	25,412	0.83	21,151
AR@CW	20170118085800.riv	Right Bank	01/18/2017 08:57	0:07:28	1,298	16,169	0.75	12,166
AR@CW	20170118090538.riv	Left Bank	01/18/2017 09:05	0:07:03	1,299	16,467	0.72	11,901
TR@CW	20170118100021.riv	Right Bank	01/18/2017 10:00	0:06:25	1,333	32,988	0.47	15,503
TR@CW	20170118100655.riv	Left Bank	01/18/2017 10:06	0:06:03	1,328	32,835	0.49	16,051
SD	20170118122723.riv	Right Bank	01/18/2017 12:26	0:05:50	1,106	38,871	0.25	9,820
SD	20170118124016.riv	Right Bank	01/18/2017 12:39	0:05:55	1,064	38,560	0.24	9,261
NMR	20170118135442.riv	Left Bank	01/18/2017 13:54	0:05:31	924	14,723	0.63	9,312
NMR	20170118140022.riv	Right Bank	01/18/2017 14:00	0:05:17	924	14,564	0.64	9,291
NMR	20170118140558.riv	Left Bank	01/18/2017 14:05	0:05:19	922	14,940	0.61	9,161
NMR	20170118141146.riv	Right Bank	01/18/2017 14:11	0:05:03	917	14,668	0.58	8,514
TR	20170118143134.riv	Left Bank	01/18/2017 14:31	0:06:10	1,067	34,899	-0.01	-385
TR	20170118144413.riv	Left Bank	01/18/2017 14:43	0:06:40	1,022	34,611	-0.02	-630
TR	20170118145121.riv	Right Bank	01/18/2017 14:50	0:05:26	1,036	34,813	-0.08	-2,898
TR@CW	20170201065826.riv	Left Bank	02/01/2017 06:58	0:07:34	1,332	33,666	1.34	44,979
TR@CW	20170201070610.riv	Right Bank	02/01/2017 07:06	0:07:30	1,331	32,999	1.37	45,072
SD	20170201090106.riv	Right Bank	02/01/2017 09:01	0:06:29	1,063	38,141	1.51	57,437
SD	20170201090743.riv	Left Bank	02/01/2017 09:07	0:05:28	1,060	37,946	1.52	57,577
NMR	20170201095517.riv	Left Bank	02/01/2017 09:55	0:05:19	906	15,936	2.54	40,525
NMR	20170201100043.riv	Right Bank	02/01/2017 10:00	0:04:47	906	15,646	2.49	38,951
TR	20170201114843.riv	Left Bank	02/01/2017 11:48	0:06:35	1,056	36,484	2.15	78,540
TR	20170201115528.riv	Right Bank	02/01/2017 11:55	0:05:59	1,076	36,037	2.18	78,377
BR@CW	20170201130829.riv	Right Bank	02/01/2017 13:08	0:06:06	1,171	24,970	1.14	28,342
BR@CW	20170201131455.riv	Left Bank	02/01/2017 13:14	0:06:18	1,141	24,849	1.15	28,647
AR@CW	20170201135245.riv	Right Bank	02/01/2017 13:52	0:07:02	1,333	18,089	0.65	11,757

AR@CW	20170201140009.riv	Left Bank	02/01/2017 13:59	0:06:39	1,300	17,577	0.68	12,022
TR@CW	20170214071342.riv	Right Bank	02/14/2017 07:13	0:07:42	1,347	32,407	0.92	29,960
TR@CW	20170214072131.riv	Left Bank	02/14/2017 07:21	0:08:40	1,338	32,755	0.93	30,562
SD	20170214074726.riv	Right Bank	02/14/2017 07:47	0:07:04	993	38,444	0.86	33,038
SD	20170214075439.riv	Left Bank	02/14/2017 07:54	0:06:07	969	38,422	0.88	33,728
NMR	20170214093702.riv	Left Bank	02/14/2017 09:36	0:05:44	898	14,921	1.84	27,449
NMR	20170214094252.riv	Right Bank	02/14/2017 09:42	0:05:53	908	14,677	1.84	26,973
TR	20170214100153.riv	Left Bank	02/14/2017 10:01	0:06:04	1,026	34,526	1.22	42,247
TR	20170214100807.riv	Right Bank	02/14/2017 10:07	0:05:41	1,053	34,812	1.20	41,585
BR@CW	20170214110803.riv	Right Bank	02/14/2017 11:07	0:06:00	1,127	25,007	0.44	11,060
BR@CW	20170214111412.riv	Left Bank	02/14/2017 11:13	0:05:56	1,170	25,877	0.39	10,099
AR@CW	20170214125550.riv	Right Bank	02/14/2017 12:55	0:06:31	1,268	19,498	-0.02	-303
AR@CW	20170214130231.riv	Left Bank	02/14/2017 13:01	0:06:39	1,281	19,202	-0.06	-1,221
TR@CW	20170227071827.riv	Right Bank	02/27/2017 07:18	0:07:20	1,253	30,132	1.17	35,304
TR@CW	20170227072555.riv	Left Bank	02/27/2017 07:25	0:07:02	1,273	30,155	1.05	31,700
SD	20170227075220.riv	Right Bank	02/27/2017 07:52	0:06:26	1,006	38,601	0.80	31,013
SD	20170227075902.riv	Left Bank	02/27/2017 07:58	0:06:05	992	38,165	0.77	29,389
NMR	20170227084745.riv	Left Bank	02/27/2017 08:47	0:05:09	896	15,199	1.23	18,761
NMR	20170227085305.riv	Right Bank	02/27/2017 08:53	0:04:51	894	15,027	1.26	18,855
TR	20170227094405.riv	Left Bank	02/27/2017 09:43	0:06:35	1,061	35,616	0.77	27,520
TR	20170227095050.riv	Right Bank	02/27/2017 09:50	0:06:21	1,047	35,517	0.74	26,378
BR@CW	20170306082336.riv	Right Bank	03/06/2017 08:23	0:06:46	1,271	18,839	-0.30	-5,618
BR@CW	20170306083109.riv	Left Bank	03/06/2017 08:31	0:05:47	1,234	18,032	-0.38	-6,788
AR@CW	20170306085532.riv	Right Bank	03/06/2017 08:55	0:05:43	1,092	24,471	-0.14	-3,497
AR@CW	20170306090127.riv	Left Bank	03/06/2017 09:01	0:04:36	1,098	24,651	-0.13	-3,271
TR@CW	20170316062132.riv	Right Bank	03/16/2017 06:21	0:08:30	1,270	30,358	0.37	11,066
TR@CW	20170316063018.riv	Left Bank	03/16/2017 06:30	0:08:00	1,278	31,477	0.32	10,026
SD	20170316084034.riv	Right Bank	03/16/2017 08:40	0:04:37	1,032	40,170	0.61	24,655
SD	20170316084520.riv	Left Bank	03/16/2017 08:45	0:04:26	1,011	40,855	0.64	26,115
NMR	20170316101933.riv	Left Bank	03/16/2017 10:19	0:04:30	900	15,369	1.95	30,003

NMR	20170316102412.riv	Right Bank	03/16/2017 10:23	0:04:42	909	15,284	2.01	30,644
TR	20170316111543.riv	Right Bank	03/16/2017 11:15	0:04:21	1,006	34,718	1.17	40,741
TR	20170316112009.riv	Left Bank	03/16/2017 11:19	0:04:37	1,025	35,054	1.14	39,990
BR@CW	20170316123646.riv	Left Bank	03/16/2017 12:36	0:04:32	1,133	25,326	0.66	16,688
BR@CW	20170316124125.riv	Right Bank	03/16/2017 12:41	0:04:08	1,136	25,601	0.67	17,096
AR@CW	20170316134920.riv	Right Bank	03/16/2017 13:49	0:04:33	1,276	16,274	0.63	10,170
AR@CW	20170316135403.riv	Left Bank	03/16/2017 13:53	0:04:35	1,288	16,773	0.61	10,153
TR@CW	20170329061254.riv	Left Bank	03/29/2017 06:13	0:05:42	1,312	31,252	1.14	35,469
TR@CW	20170329061856.riv	Right Bank	03/29/2017 06:18	0:04:56	1,309	33,924	0.89	30,094
SD	20170329085516.riv	Right Bank	03/29/2017 08:55	0:05:00	1,073	38,534	0.53	20,296
SD	20170329090025.riv	Left Bank	03/29/2017 09:00	0:05:13	1,045	41,645	0.47	19,549
NMR	20170329094319.riv	Left Bank	03/29/2017 09:43	0:04:24	908	15,588	1.31	20,459
NMR	20170329094754.riv	Right Bank	03/29/2017 09:47	0:04:44	911	15,547	1.35	20,962
TR	20170329105153.riv	Left Bank	03/29/2017 10:51	0:05:24	1,039	36,223	0.36	12,867
TR	20170329105731.riv	Right Bank	03/29/2017 10:57	0:04:39	1,051	36,710	0.29	10,653
BR@CW	20170329122951.riv	Right Bank	03/29/2017 12:29	0:05:06	1,134	27,243	0.20	5,458
BR@CW	20170329123506.riv	Left Bank	03/29/2017 12:34	0:05:16	1,125	26,343	0.22	5,822
AR@CW	20170329131926.riv	Right Bank	03/29/2017 13:18	0:05:59	1,263	18,963	0.15	2,831
AR@CW	20170329132543.riv	Left Bank	03/29/2017 13:24	0:04:58	1,257	19,098	0.16	3,015
TR@CW	20170410060933.riv	Right Bank	04/10/2017 06:09	0:06:48	1,316	33,249	1.36	45,305
TR@CW	20170410061632.riv	Left Bank	04/10/2017 06:16	0:07:45	1,336	33,241	1.34	44,572
SD	20170410064422.riv	Right Bank	04/10/2017 06:44	0:07:42	995	34,411	1.71	58,824
SD	20170410065231.riv	Left Bank	04/10/2017 06:52	0:05:31	993	35,018	1.82	63,591
NMR	20170410074800.riv	Left Bank	04/10/2017 07:47	0:06:16	877	15,844	2.74	43,452
NMR	20170410075425.riv	Right Bank	04/10/2017 07:54	0:05:52	886	16,013	2.73	43,666
TR	20170410083736.riv	Left Bank	04/10/2017 08:37	0:07:19	975	34,378	2.43	83,575
TR	20170410084503.riv	Right Bank	04/10/2017 08:44	0:06:58	987	33,915	2.47	83,790
BR@CW	20170410095127.riv	Right Bank	04/10/2017 09:50	0:06:50	1,143	25,531	1.21	30,858
BR@CW	20170410095826.riv	Left Bank	04/10/2017 09:57	0:07:08	1,159	25,883	1.17	30,203
AR@CW	20170410104214.riv	Right Bank	04/10/2017 10:41	0:07:05	1,261	17,886	0.60	10,797

AR@CW	20170410104931.riv	Left Bank	04/10/2017 10:48	0:07:00	1,277	18,264	0.59	10,699
TR@CW	20170425061537.riv	Right Bank	04/25/2017 06:15	0:08:02	1,356	33,654	0.64	21,437
TR@CW	20170425062349.riv	Left Bank	04/25/2017 06:23	0:06:33	1,347	33,605	0.63	21,113
SD	20170425093802.riv	Right Bank	04/25/2017 09:37	0:05:48	1,017	38,354	-0.17	-6,575
SD	20170425094407.riv	Left Bank	04/25/2017 09:43	0:04:44	994	34,571	-0.20	-6,803
NMR	20170425103758.riv	Left Bank	04/25/2017 10:37	0:04:43	911	16,130	0.31	4,983
NMR	20170425104254.riv	Right Bank	04/25/2017 10:42	0:04:57	915	16,074	0.32	5,118
TR	20170425113907.riv	Left Bank	04/25/2017 11:38	0:05:51	1,082	36,026	-0.34	-12,349
TR	20170425114506.riv	Right Bank	04/25/2017 11:44	0:05:45	1,077	36,026	-0.32	-11,595
TR@CW	20170630072316.riv	Right Bank	06/30/2017 07:23	0:08:01	1,346	34,535	1.82	62,867
TR@CW	20170630073140.riv	Left Bank	06/30/2017 07:31	0:08:29	1,337	34,434	1.80	61,810
SD	20170630080500.riv	Right Bank	06/30/2017 08:04	0:05:43	1,071	40,177	1.69	67,800
SD	20170630081058.riv	Left Bank	06/30/2017 08:10	0:06:12	1,056	36,562	1.90	69,274
NMR	20170630085522.riv	Left Bank	06/30/2017 08:54	0:06:09	905	18,644	2.92	54,514
NMR	20170630090144.riv	Right Bank	06/30/2017 09:01	0:06:08	919	18,654	2.96	55,150
TR	20170630095211.riv	Left Bank	06/30/2017 09:51	0:06:41	1,111	40,061	4.36	174,494
TR	20170630095912.riv	Right Bank	06/30/2017 09:58	0:07:59	1,096	39,818	4.26	169,690
TR	20170630101401.riv	Left Bank	06/30/2017 10:12	0:07:59	1,087	39,721	4.33	171,890
TR	20170630102219.riv	Right Bank	06/30/2017 10:20	0:07:13	1,084	39,385	4.28	168,696
BR@CW	20170630110642.riv	Right Bank	06/30/2017 11:05	0:08:08	1,132	25,210	2.60	65,613
BR@CW	20170630111502.riv	Left Bank	06/30/2017 11:13	0:07:16	1,144	24,971	2.67	66,636
AR@CW	20170630113948.riv	Left Bank	06/30/2017 11:37	0:08:48	1,294	17,661	2.36	41,676
AR@CW	20170630114850.riv	Right Bank	06/30/2017 11:46	0:05:30	1,280	17,392	2.37	41,278

Appendix B

Vertical Profile
Measurement Summary

Site	Instrument	Filename	Start Time (CST)	Latitude	Longitude	Min Temp (°F)	Min DO (%)	Max SAL (ppt)	Mean pH	Max Turbidity (NTU)
AR@CW	HydroLab MS5	AR@CW062116.csv	06/21/2016 08:45:38	30.67247	-87.95408	80.4	NoData	0.62	NoData	3.2
AR@CW	YSI ProDSS	160907-090112.csv	09/07/2016 09:01:12	30.67231	-87.95378	84.0	58.2	5.96	7.16	22.5
AR@CW	YSI ProDSS	160907-090530.csv	09/07/2016 09:05:30	30.67211	-87.95217	86.2	66.3	6.06	7.13	7.3
AR@CW	YSI ProDSS	160907-121007.csv	09/07/2016 12:10:07	30.67225	-87.95403	85.5	58.7	5.55	7.16	54.1
AR@CW	YSI ProDSS	160907-121307.csv	09/07/2016 12:13:07	30.67214	-87.95208	87.1	60.5	5.10	7.15	4.4
AR@CW	YSI ProDSS	160907-142234.csv	09/07/2016 14:22:34	30.67233	-87.95419	84.7	69.4	5.72	7.44	8.1
AR@CW	YSI ProDSS	160907-142524.csv	09/07/2016 14:25:24	30.67203	-87.95200	87.4	61.4	5.06	7.17	4.3
AR@CW	YSI ProDSS	160907-155041.csv	09/07/2016 15:50:41	30.67247	-87.95408	84.7	67.9	5.76	7.45	13.2
AR@CW	YSI ProDSS	160907-155311.csv	09/07/2016 15:53:11	30.67206	-87.95211	87.6	63.3	4.97	7.25	4.1
AR@CW	YSI ProDSS	160907-170607.csv	09/07/2016 17:06:07	30.67244	-87.95417	84.7	59.2	5.68	7.23	10.1
AR@CW	YSI ProDSS	160907-170834.csv	09/07/2016 17:08:34	30.67214	-87.95192	88.2	76.2	4.81	7.33	5.1
AR@CW	YSI ProDSS	160908-120854.csv	09/08/2016 12:08:54	30.67233	-87.95422	85.3	60.0	5.57	7.22	8.0
AR@CW	YSI ProDSS	160908-121106.csv	09/08/2016 12:11:06	30.67203	-87.95189	87.3	55.9	5.23	7.16	5.2
AR@CW	YSI ProDSS	160922-143028.csv	09/22/2016 14:30:28	30.67236	-87.95414	87.1	56.7	6.73	7.29	9.6
AR@CW	Castaway CTD	20170316_195639.csv	03/16/2017 13:56:00	30.67250	-87.95410	60.1	NoData	0.09	NoData	NoData
AR@CW	Castaway CTD	20170329_193339.csv	03/29/2017 13:33:00	30.67240	-87.95440	67.7	NoData	0.11	NoData	NoData
AR@CW	Castaway CTD	20170410_165645.csv	04/10/2017 10:56:00	30.67230	-87.95400	67.2	NoData	0.07	NoData	NoData
AR@CW	Castaway CTD	20170425_200835.csv	04/25/2017 14:08:00	30.67220	-87.95410	72.4	NoData	3.99	NoData	NoData
BR@CW	HydroLab MS5	BR@CW062116.csv	06/21/2016 09:21:31	30.66756	-87.92506	83.3	NoData	0.40	NoData	2.4
BR@CW	YSI ProDSS	160907-093618.csv	09/07/2016 09:36:19	30.66758	-87.92656	85.8	26.9	10.76	7.06	23.1
BR@CW	YSI ProDSS	160907-093940.csv	09/07/2016 09:39:40	30.66747	-87.92481	85.5	23.8	8.42	7.01	9.9
BR@CW	YSI ProDSS	160907-124057.csv	09/07/2016 12:40:57	30.66753	-87.92672	86.2	19.8	10.31	7.04	13.4
BR@CW	YSI ProDSS	160907-124406.csv	09/07/2016 12:44:06	30.66744	-87.92486	86.9	30.6	6.67	7.07	7.6
BR@CW	YSI ProDSS	160907-145418.csv	09/07/2016 14:54:18	30.66761	-87.92667	86.2	16.4	9.55	6.98	9.0
BR@CW	YSI ProDSS	160907-145645.csv	09/07/2016 14:56:45	30.66756	-87.92506	86.7	23.0	7.05	7.03	9.2
BR@CW	YSI ProDSS	160907-163227.csv	09/07/2016 16:32:27	30.66756	-87.92486	86.5	23.6	7.77	7.09	7.3
BR@CW	YSI ProDSS	160907-163440.csv	09/07/2016 16:34:40	30.66747	-87.92653	86.0	20.9	9.50	7.03	9.1

BR@CW	YSI ProDSS	160908-124004.csv	09/08/2016 12:40:04	30.66744	-87.92661	86.9	44.9	5.94	7.14	8.8
BR@CW	YSI ProDSS	160908-124213.csv	09/08/2016 12:42:13	30.66744	-87.92467	87.1	38.4	6.56	7.11	9.6
BR@CW	YSI ProDSS	160922-145717.csv	09/22/2016 14:57:17	30.66775	-87.92664	86.9	45.9	6.23	7.27	21.9
BR@CW	Castaway CTD	20170316_184422.csv	03/16/2017 12:44:00	30.66750	-87.92670	59.9	NoData	0.09	NoData	NoData
BR@CW	Castaway CTD	20170329_184253.csv	03/29/2017 12:42:00	30.66790	-87.92680	67.4	NoData	0.09	NoData	NoData
BR@CW	Castaway CTD	20170410_160530.csv	04/10/2017 10:05:00	30.66760	-87.92670	67.0	NoData	0.07	NoData	NoData
BR@CW	Castaway CTD	20170425_195255.csv	04/25/2017 13:52:00	30.66740	-87.92650	73.4	NoData	0.11	NoData	NoData
BR-01	HydroLab MS5	BR1062116.csv	06/21/2016 09:50:54	30.71280	-87.94080	85.3	NoData	0.37	NoData	3.1
BR-01	Castaway CTD	20170425_190136.csv	04/25/2017 13:01:00	30.71280	-87.94080	73.2	NoData	0.23	NoData	NoData
CO-01	HydroLab MS5	CO1062116.csv	06/21/2016 12:42:51	30.81856	-87.94739	84.4	NoData	11.17	NoData	1429.0
CO-01	HydroLab MS5	CO1062116b.csv	06/21/2016 12:49:21	30.81856	-87.94739	84.4	NoData	11.27	NoData	2.9
CO-01	YSI ProDSS	160909-092203.csv	09/09/2016 09:22:03	30.81856	-87.94739	87.1	10.9	20.80	7.32	5.0
CO-01	YSI ProDSS	160913-082127.csv	09/13/2016 08:21:27	30.81861	-87.94778	86.0	3.9	20.33	7.24	5.2
CO-01	YSI ProDSS	160913-091319.csv	09/13/2016 09:13:19	30.81844	-87.94772	86.0	4.9	20.22	7.34	4.4
CO-01	YSI ProDSS	160913-102929.csv	09/13/2016 10:29:29	30.81850	-87.94778	86.0	4.0	20.54	7.35	6.3
CO-01	YSI ProDSS	160913-113211.csv	09/13/2016 11:32:11	30.81867	-87.94781	85.8	4.5	20.51	7.36	11.0
CO-01	YSI ProDSS	160913-124304.csv	09/13/2016 12:43:04	30.81858	-87.94753	85.8	5.9	20.75	7.48	4.4
CO-01	YSI ProDSS	160913-134537.csv	09/13/2016 13:45:37	30.81856	-87.94767	85.6	5.6	20.87	7.52	5.2
CO-01	YSI ProDSS	160913-151442.csv	09/13/2016 15:14:42	30.81864	-87.94775	85.6	7.7	20.98	7.45	49.6
CO-01	YSI ProDSS	160913-161953.csv	09/13/2016 16:19:53	30.81875	-87.94789	85.6	6.1	20.78	7.50	8.8
CO-01	YSI ProDSS	160914-091904.csv	09/14/2016 09:19:04	30.81861	-87.94781	85.6	4.3	19.89	7.22	4.6
CO-01	YSI ProDSS	160914-112006.csv	09/14/2016 11:20:06	30.81853	-87.94769	85.5	6.3	20.03	7.28	4.5
CO-01	YSI ProDSS	160914-131149.csv	09/14/2016 13:11:49	30.81853	-87.94772	85.5	10.8	20.13	7.37	4.3
CO-02	HydroLab MS5	CO2062116.csv	06/21/2016 12:26:12	30.80756	-87.93117	86.2	NoData	1.89	NoData	50.7
CO-02	YSI ProDSS	160909-092845.csv	09/09/2016 09:28:45	30.80756	-87.93117	87.1	10.0	19.09	7.32	6.2
CO-02	YSI ProDSS	160913-080707.csv	09/13/2016 08:07:07	30.80769	-87.93194	85.5	12.5	16.59	7.24	131.0
CO-02	YSI ProDSS	160913-092640.csv	09/13/2016 09:26:40	30.80772	-87.93189	86.4	9.7	16.60	7.33	12.1
CO-02	YSI ProDSS	160913-101643.csv	09/13/2016 10:16:44	30.80775	-87.93197	86.4	12.6	16.88	7.33	5.5
CO-02	YSI ProDSS	160913-114912.csv	09/13/2016 11:49:12	30.80767	-87.93206	86.5	16.0	17.92	7.40	6.1
CO-02	YSI ProDSS	160913-123042.csv	09/13/2016 12:30:42	30.80767	-87.93189	86.2	9.3	18.88	7.34	7.1

CO-02	YSI ProDSS	160913-135954.csv	09/13/2016 13:59:54	30.80767	-87.93186	86.2	9.8	18.96	7.41	8.0
CO-02	YSI ProDSS	160913-150201.csv	09/13/2016 15:02:02	30.80761	-87.93192	86.0	10.6	19.16	7.33	10.9
CO-02	YSI ProDSS	160913-163822.csv	09/13/2016 16:38:22	30.80769	-87.93186	86.0	10.9	19.34	7.39	8.5
CO-02	YSI ProDSS	160914-090118.csv	09/14/2016 09:01:18	30.80764	-87.93178	86.4	13.1	16.34	7.17	4.7
CO-02	YSI ProDSS	160914-110518.csv	09/14/2016 11:05:18	30.80769	-87.93194	86.2	11.0	17.16	7.25	9.2
CO-02	YSI ProDSS	160914-125807.csv	09/14/2016 12:58:07	30.80775	-87.93186	86.0	13.1	17.46	7.36	11.7
CO-02	YSI ProDSS	160923-100655.csv	09/23/2016 10:06:56	30.80764	-87.93183	86.5	36.3	10.55	7.32	10.0
CO-02	YSI ProDSS	160923-101238.csv	09/23/2016 10:12:38	30.80706	-87.92925	85.3	1.6	18.64	7.30	7.7
CO-02	YSI ProDSS	160923-103606.csv	09/23/2016 10:36:06	30.80181	-87.92756	86.9	68.6	2.18	7.48	6.1
CO-02	YSI ProDSS	160923-104012.csv	09/23/2016 10:40:12	30.80358	-87.92961	87.1	56.6	5.32	7.40	9.4
CO-02	YSI ProDSS	160923-104341.csv	09/23/2016 10:43:41	30.80381	-87.93006	85.8	11.9	16.53	7.37	8.5
CO-02	YSI ProDSS	160923-104948.csv	09/23/2016 10:49:48	30.79822	-87.93372	86.0	7.1	14.55	7.28	11.2
MR-01	HydroLab MS5	MR1062116.csv	06/21/2016 13:26:15	30.83903	-87.94589	87.1	NoData	0.20	NoData	2.8
MR-01	YSI ProDSS	160909-081826.csv	09/09/2016 08:18:26	30.83903	-87.94558	86.9	8.6	19.55	7.29	4.5
MR-01	YSI ProDSS	160913-084303.csv	09/13/2016 08:43:03	30.83933	-87.94567	86.4	8.6	18.21	7.36	4.4
MR-01	YSI ProDSS	160913-105816.csv	09/13/2016 10:58:17	30.83914	-87.94589	86.2	8.5	18.61	7.34	4.5
MR-01	YSI ProDSS	160913-131024.csv	09/13/2016 13:10:24	30.83933	-87.94575	86.2	6.2	18.91	7.37	6.9
MR-01	YSI ProDSS	160913-153745.csv	09/13/2016 15:37:45	30.83933	-87.94578	86.2	6.7	18.90	7.37	7.9
MR-01	YSI ProDSS	160913-170757.csv	09/13/2016 17:07:57	30.83914	-87.94553	86.5	16.5	18.07	7.41	5.4
MR-01	YSI ProDSS	160914-095252.csv	09/14/2016 09:52:52	30.83936	-87.94564	86.0	7.6	18.32	7.20	5.1
MR-01	YSI ProDSS	160914-114322.csv	09/14/2016 11:43:22	30.83925	-87.94567	85.8	7.7	18.58	7.30	15.7
MR-01	YSI ProDSS	160914-133549.csv	09/14/2016 13:35:50	30.83933	-87.94561	85.8	10.5	18.81	7.34	4.4
MR-01	Castaway CTD	20170316_162726.csv	03/16/2017 10:27:00	30.83940	-87.94560	59.3	NoData	0.09	NoData	NoData
MR-01	Castaway CTD	20170329_163051.csv	03/29/2017 10:30:00	30.83920	-87.94540	66.5	NoData	0.08	NoData	NoData
MR-01	Castaway CTD	20170410_140132.csv	04/10/2017 08:01:00	30.83900	-87.94550	66.9	NoData	0.07	NoData	NoData
MR-01	Castaway CTD	20170410_140240.csv	04/10/2017 08:02:00	30.83850	-87.94540	66.9	NoData	0.07	NoData	NoData
MR-01	Castaway CTD	20170425_165012.csv	04/25/2017 10:50:00	30.83920	-87.94570	74.0	NoData	0.09	NoData	NoData
MR-02	HydroLab MS5	MR2062116.csv	06/21/2016 13:44:53	30.82047	-87.95464	83.1	NoData	15.61	NoData	61.0
MR-02	YSI ProDSS	160909-091441.csv	09/09/2016 09:14:41	30.82078	-87.95514	86.7	9.3	21.41	7.30	5.4
MR-02	YSI ProDSS	160913-090218.csv	09/13/2016 09:02:18	30.82039	-87.95453	85.8	3.8	20.83	7.35	40.0

MR-02	YSI ProDSS	160913-112057.csv	09/13/2016 11:20:57	30.82067	-87.95453	85.6	4.4	20.91	7.39	114.9
MR-02	YSI ProDSS	160913-133316.csv	09/13/2016 13:33:17	30.82067	-87.95453	85.6	4.6	21.23	7.37	382.5
MR-02	YSI ProDSS	160913-155643.csv	09/13/2016 15:56:43	30.82042	-87.95475	85.3	3.8	21.20	7.38	450.1
MR-02	YSI ProDSS	160913-172518.csv	09/13/2016 17:25:18	30.82047	-87.95461	85.6	4.0	20.92	7.34	7.5
MR-02	YSI ProDSS	160914-101521.csv	09/14/2016 10:15:21	30.82053	-87.95489	85.5	8.8	20.34	7.31	4.6
MR-02	YSI ProDSS	160914-120726.csv	09/14/2016 12:07:26	30.82053	-87.95464	85.3	11.8	20.44	7.38	4.4
MR-02	YSI ProDSS	160914-135835.csv	09/14/2016 13:58:35	30.82047	-87.95461	85.3	14.3	20.50	7.42	5.6
MR-03	HydroLab MS5	MR3062116.csv	06/21/2016 14:21:09	30.80830	-87.99250	80.6	NoData	22.96	NoData	2.0
MR-04	HydroLab MS5	MR4062116.csv	06/21/2016 14:38:31	30.79290	-87.99080	86.0	NoData	5.19	NoData	3.0
MR-06	HydroLab MS5	MR6062116.csv	06/21/2016 15:17:12	30.78010	-88.01690	78.4	NoData	28.02	NoData	2.1
MR-08	Castaway CTD	20170316_151514.csv	03/16/2017 09:15:00	30.72160	-88.04240	59.6	NoData	31.22	NoData	NoData
MR-08	Castaway CTD	20170329_151145.csv	03/29/2017 09:11:00	30.72130	-88.04080	67.5	NoData	27.88	NoData	NoData
MR-08	Castaway CTD	20170410_125928.csv	04/10/2017 06:59:00	30.72190	-88.04160	67.0	NoData	28.51	NoData	NoData
MR-08	Castaway CTD	20170425_155132.csv	04/25/2017 09:51:00	30.72220	-88.04210	74.2	NoData	27.08	NoData	NoData
MR-09	YSI ProDSS	160908-104558.csv	09/08/2016 10:45:58	30.67211	-88.03242	85.8	21.0	25.49	7.57	6.3
MR-09	YSI ProDSS	160908-104833.csv	09/08/2016 10:48:33	30.67172	-88.03422	85.6	20.8	26.06	7.61	23.1
MR-09	YSI ProDSS	160908-110547.csv	09/08/2016 11:05:47	30.69311	-88.03744	86.0	21.8	24.74	7.49	10.4
Other	YSI ProDSS	160909-083349.csv	09/09/2016 08:33:49	30.87117	-87.98661	88.3	18.9	11.86	7.22	11.0
Other	YSI ProDSS	160909-105503.csv	09/09/2016 10:55:03	30.74258	-87.98647	85.1	65.2	7.25	7.22	144.3
Other	Castaway CTD	20170425_210646.csv	04/25/2017 15:06:00	30.67980	-87.98090	75.5	NoData	1.70	NoData	NoData
SR-02	YSI ProDSS	160907-105545.csv	09/07/2016 10:55:46	30.71714	-88.01411	84.2	2.2	19.18	7.25	19.8
SR-02	YSI ProDSS	160907-105850.csv	09/07/2016 10:58:50	30.71769	-88.01289	84.7	51.5	10.22	7.43	78.1
SR-02	YSI ProDSS	160908-083248.csv	09/08/2016 08:32:48	30.71783	-88.01436	84.2	2.6	19.03	7.22	20.9
SR-02	YSI ProDSS	160908-083538.csv	09/08/2016 08:35:38	30.71831	-88.01281	84.2	45.6	13.28	7.51	28.2
SR-02	YSI ProDSS	160908-095114.csv	09/08/2016 09:51:14	30.71756	-88.01414	84.0	4.0	18.90	7.23	11.2
SR-02	YSI ProDSS	160908-095401.csv	09/08/2016 09:54:01	30.71844	-88.01294	84.4	67.3	10.36	7.53	8.3
SR-02	YSI ProDSS	160908-150904.csv	09/08/2016 15:09:04	30.71811	-88.01267	85.1	75.3	7.66	7.59	6.8
SR-02	YSI ProDSS	160908-151135.csv	09/08/2016 15:11:35	30.71736	-88.01414	85.3	4.4	18.61	7.30	11.4
SR-02	YSI ProDSS	160908-173130.csv	09/08/2016 17:31:30	30.71756	-88.01419	85.3	4.3	18.43	7.28	12.8
SR-02	YSI ProDSS	160908-173426.csv	09/08/2016 17:34:26	30.71833	-88.01292	85.6	48.0	11.00	7.56	6.9

SR-03	YSI ProDSS	160922-082341.csv	09/22/2016 08:23:41	30.76192	-87.92983	85.5	4.0	9.82	7.08	22.4
SR-03	YSI ProDSS	160922-103348.csv	09/22/2016 10:33:48	30.76183	-87.92997	85.6	4.7	9.53	7.22	16.0
SR-03	YSI ProDSS	160922-122705.csv	09/22/2016 12:27:05	30.76197	-87.92994	87.1	82.7	2.67	7.51	12.0
SR-03	YSI ProDSS	160923-091804.csv	09/23/2016 09:18:04	30.76192	-87.92994	86.0	16.4	8.43	7.23	11.0
SR-03	YSI ProDSS	160923-114933.csv	09/23/2016 11:49:33	30.76203	-87.92967	86.2	16.9	7.91	7.30	12.7
TR@CW	HydroLab MS5	TR@CW062116.csv	06/21/2016 07:25:28	30.68303	-88.00861	76.1	NoData	10.81	NoData	53.0
TR@CW	YSI ProDSS	160907-081140.csv	09/07/2016 08:11:40	30.68322	-88.00847	84.4	9.3	20.20	7.28	9.7
TR@CW	YSI ProDSS	160907-081659.csv	09/07/2016 08:16:59	30.68425	-88.01006	83.7	6.5	20.18	7.33	15.7
TR@CW	YSI ProDSS	160907-112947.csv	09/07/2016 11:29:47	30.68431	-88.01014	84.4	3.2	18.29	7.21	69.1
TR@CW	YSI ProDSS	160907-113423.csv	09/07/2016 11:34:23	30.68308	-88.00844	85.5	6.3	18.40	7.29	355.1
TR@CW	YSI ProDSS	160907-174616.csv	09/07/2016 17:46:16	30.68422	-88.01017	86.2	27.0	20.47	7.47	132.6
TR@CW	YSI ProDSS	160907-174920.csv	09/07/2016 17:49:20	30.68311	-88.00853	85.8	27.3	20.30	7.51	73.3
TR@CW	YSI ProDSS	160908-074039.csv	09/08/2016 07:40:39	30.68422	-88.01028	84.7	14.4	21.13	7.37	45.1
TR@CW	YSI ProDSS	160908-074409.csv	09/08/2016 07:44:09	30.68303	-88.00842	84.7	17.1	20.63	7.48	8.9
TR@CW	YSI ProDSS	160908-090007.csv	09/08/2016 09:00:07	30.68419	-88.01014	84.2	18.4	19.47	7.37	13.4
TR@CW	YSI ProDSS	160908-090241.csv	09/08/2016 09:02:41	30.68286	-88.00833	85.5	24.9	19.16	7.51	7.9
TR@CW	YSI ProDSS	160908-101915.csv	09/08/2016 10:19:15	30.68428	-88.01033	85.1	20.4	17.21	7.42	10.2
TR@CW	YSI ProDSS	160908-102202.csv	09/08/2016 10:22:02	30.68300	-88.00850	85.5	18.6	18.06	7.41	9.0
TR@CW	YSI ProDSS	160908-113709.csv	09/08/2016 11:37:09	30.68428	-88.01022	85.3	13.6	17.79	7.37	5.5
TR@CW	YSI ProDSS	160908-113932.csv	09/08/2016 11:39:32	30.68308	-88.00861	85.8	14.1	18.12	7.39	5.5
TR@CW	YSI ProDSS	160908-141421.csv	09/08/2016 14:14:21	30.68414	-88.01017	86.2	15.8	21.49	7.42	118.1
TR@CW	YSI ProDSS	160908-141641.csv	09/08/2016 14:16:41	30.68292	-88.00839	86.2	14.5	20.93	7.38	6.2
TR@CW	YSI ProDSS	160908-161403.csv	09/08/2016 16:14:03	30.68464	-88.00992	86.2	18.1	21.53	7.44	9.4
TR@CW	YSI ProDSS	160908-161841.csv	09/08/2016 16:18:41	30.68328	-88.00778	86.4	26.3	15.75	7.53	7.4
TR@CW	YSI ProDSS	160908-180300.csv	09/08/2016 18:03:00	30.68464	-88.00983	86.0	28.6	21.01	7.52	7.1
TR@CW	YSI ProDSS	160908-180717.csv	09/08/2016 18:07:17	30.68322	-88.00775	86.2	36.6	16.20	7.60	8.2
TR@CW	Castaway CTD	20170329_122953.csv	03/29/2017 06:29:00	30.68380	-88.01020	70.0	NoData	2.93	NoData	NoData
TR@CW	Castaway CTD	20170410_122546.csv	04/10/2017 06:25:00	30.68360	-88.00940	67.6	NoData	0.10	NoData	NoData
TR@CW	Castaway CTD	20170425_123334.csv	04/25/2017 06:33:00	30.68330	-88.00950	72.1	NoData	23.12	NoData	NoData
TR-01	HydroLab MS5	TR1062116.csv	06/21/2016 11:59:11	30.87290	-87.89460	85.8	NoData	0.08	NoData	4.1

TR-02	HydroLab MS5	TR2062116.csv	06/21/2016 11:21:02	30.82008	-87.91742	85.6	NoData	0.29	NoData	5.5
TR-02	YSI ProDSS	160909-094139.csv	09/09/2016 09:41:39	30.82000	-87.91742	87.1	32.5	5.65	7.22	4.3
TR-02	YSI ProDSS	160913-074718.csv	09/13/2016 07:47:19	30.81989	-87.91611	85.8	39.5	3.44	7.21	7.6
TR-02	YSI ProDSS	160913-075006.csv	09/13/2016 07:50:06	30.82011	-87.91739	85.6	40.2	3.50	7.21	6.7
TR-02	YSI ProDSS	160913-095758.csv	09/13/2016 09:57:58	30.81994	-87.91633	85.8	44.1	3.60	7.30	8.6
TR-02	YSI ProDSS	160913-100132.csv	09/13/2016 10:01:32	30.82008	-87.91742	86.0	44.0	3.51	7.20	6.2
TR-02	YSI ProDSS	160913-121345.csv	09/13/2016 12:13:45	30.82000	-87.91628	86.2	43.3	3.68	7.31	7.6
TR-02	YSI ProDSS	160913-121635.csv	09/13/2016 12:16:35	30.82008	-87.91739	86.0	49.1	3.47	7.24	5.6
TR-02	YSI ProDSS	160913-144408.csv	09/13/2016 14:44:08	30.82000	-87.91622	86.4	42.4	3.81	7.29	6.4
TR-02	YSI ProDSS	160913-144656.csv	09/13/2016 14:46:56	30.82006	-87.91742	86.4	42.3	3.82	7.27	6.4
TR-02	YSI ProDSS	160913-175154.csv	09/13/2016 17:51:54	30.81986	-87.91647	87.1	55.9	2.96	7.46	7.5
TR-02	YSI ProDSS	160913-175505.csv	09/13/2016 17:55:05	30.82006	-87.91767	87.3	54.9	2.60	7.41	6.1
TR-02	YSI ProDSS	160914-083705.csv	09/14/2016 08:37:05	30.82003	-87.91700	86.0	44.1	3.35	7.14	6.8
TR-02	YSI ProDSS	160914-104702.csv	09/14/2016 10:47:02	30.82008	-87.91747	86.4	39.2	3.51	7.18	7.7
TR-02	YSI ProDSS	160914-124014.csv	09/14/2016 12:40:14	30.82008	-87.91731	86.5	33.9	4.34	7.22	7.6
TR-02	YSI ProDSS	160914-143116.csv	09/14/2016 14:31:16	30.82006	-87.91753	86.5	32.1	4.69	7.28	9.4
TR-02	YSI ProDSS	160923-094959.csv	09/23/2016 09:49:59	30.82008	-87.91744	86.4	42.3	2.98	7.35	7.6
TR-02	Castaway CTD	20170316_172454.csv	03/16/2017 11:24:00	30.82000	-87.91740	59.2	NoData	0.08	NoData	NoData
TR-02	Castaway CTD	20170329_170613.csv	03/29/2017 11:06:00	30.82010	-87.91730	66.9	NoData	0.08	NoData	NoData
TR-02	Castaway CTD	20170410_145511.csv	04/10/2017 08:55:00	30.82000	-87.91730	66.7	NoData	0.07	NoData	NoData
TR-02	Castaway CTD	20170425_175442.csv	04/25/2017 11:54:00	30.82030	-87.91730	73.2	NoData	0.55	NoData	NoData
TR-03	HydroLab MS5	TR3062116.csv	06/21/2016 10:36:40	30.75153	-87.92028	85.8	NoData	0.32	NoData	2.8
TR-03	YSI ProDSS	160909-100833.csv	09/09/2016 10:08:33	30.75153	-87.92028	86.7	37.4	6.39	7.19	4.8
TR-03	YSI ProDSS	160922-075640.csv	09/22/2016 07:56:40	30.76864	-87.92456	85.8	19.7	6.56	7.00	8.5
TR-03	YSI ProDSS	160922-080139.csv	09/22/2016 08:01:39	30.76847	-87.92753	85.6	9.5	11.99	7.14	47.1
TR-03	YSI ProDSS	160922-085624.csv	09/22/2016 08:56:24	30.74244	-87.93122	86.0	25.6	9.35	7.07	24.6
TR-03	YSI ProDSS	160922-095503.csv	09/22/2016 09:55:04	30.76958	-87.92489	86.2	23.3	5.66	7.19	19.3
TR-03	YSI ProDSS	160922-101539.csv	09/22/2016 10:15:39	30.76961	-87.92825	86.2	14.2	11.35	7.21	32.9
TR-03	YSI ProDSS	160922-110500.csv	09/22/2016 11:05:01	30.74250	-87.93178	86.5	28.3	7.10	7.19	8.8
TR-03	YSI ProDSS	160922-115020.csv	09/22/2016 11:50:20	30.76953	-87.92489	86.7	25.2	5.13	7.21	12.7

TR-03	YSI ProDSS	160922-120851.csv	09/22/2016 12:08:51	30.76981	-87.92853	86.7	20.1	10.51	7.30	30.6
TR-03	YSI ProDSS	160922-125535.csv	09/22/2016 12:55:35	30.74250	-87.93181	86.5	31.6	6.31	7.20	9.6
TR-03	YSI ProDSS	160922-153125.csv	09/22/2016 15:31:26	30.74256	-87.93083	86.7	35.2	5.20	7.23	6.9
TR-03	YSI ProDSS	160923-075534.csv	09/23/2016 07:55:35	30.74231	-87.93103	86.2	22.4	9.04	7.13	11.1
TR-03	YSI ProDSS	160923-084423.csv	09/23/2016 08:44:23	30.76936	-87.92486	85.5	26.0	5.66	7.22	9.0
TR-03	YSI ProDSS	160923-090117.csv	09/23/2016 09:01:18	30.76978	-87.92850	85.6	15.1	11.16	7.23	53.1
TR-03	YSI ProDSS	160923-111209.csv	09/23/2016 11:12:09	30.76978	-87.92847	86.7	12.2	11.03	7.27	48.0
TR-03	YSI ProDSS	160923-113159.csv	09/23/2016 11:31:59	30.76956	-87.92486	86.4	31.0	4.88	7.27	10.2
TR-03	YSI ProDSS	160923-121721.csv	09/23/2016 12:17:21	30.74244	-87.93106	86.7	24.8	6.98	7.17	9.1
TR-04	YSI ProDSS	160922-091958.csv	09/22/2016 09:19:58	30.74628	-87.93747	85.5	10.0	12.95	7.18	91.4
TR-04	YSI ProDSS	160922-112458.csv	09/22/2016 11:24:58	30.74647	-87.93753	85.6	10.9	13.01	7.24	22.7
TR-04	YSI ProDSS	160922-131343.csv	09/22/2016 13:13:43	30.74631	-87.93742	85.5	8.8	13.03	7.27	37.1
TR-04	YSI ProDSS	160922-155116.csv	09/22/2016 15:51:17	30.74633	-87.93708	85.6	12.3	13.02	7.27	26.7
TR-04	YSI ProDSS	160923-081623.csv	09/23/2016 08:16:23	30.74636	-87.93742	85.3	8.4	12.69	7.22	19.8
TR-04	YSI ProDSS	160923-123619.csv	09/23/2016 12:36:19	30.74636	-87.93719	86.0	11.3	12.59	7.19	168.3
TR-05	HydroLab MS5	TR5062116.csv	06/21/2016 07:47:47	30.73400	-87.97200	75.2	NoData	1.00	NoData	46.5
TR-06	YSI ProDSS	160907-102721.csv	09/07/2016 10:27:21	30.69864	-87.99089	85.5	33.2	13.16	7.33	6.7
TR-06	YSI ProDSS	160907-102956.csv	09/07/2016 10:29:56	30.69756	-87.98950	85.8	8.3	16.70	7.42	4.7
TR-06	YSI ProDSS	160908-080549.csv	09/08/2016 08:05:49	30.69833	-87.99128	85.8	43.9	13.40	7.46	7.2
TR-06	YSI ProDSS	160908-080802.csv	09/08/2016 08:08:02	30.69739	-87.98972	84.2	11.6	17.06	7.38	5.1
TR-06	YSI ProDSS	160908-092045.csv	09/08/2016 09:20:45	30.69836	-87.99108	85.6	37.1	13.19	7.37	7.9
TR-06	YSI ProDSS	160908-092245.csv	09/08/2016 09:22:45	30.69764	-87.98950	84.6	11.5	17.15	7.42	4.9
TR-06	YSI ProDSS	160908-143702.csv	09/08/2016 14:37:02	30.69833	-87.99114	86.9	60.8	11.23	7.50	6.5
TR-06	YSI ProDSS	160908-143852.csv	09/08/2016 14:38:52	30.69767	-87.98989	86.5	54.7	12.33	7.49	40.5
TR-06	YSI ProDSS	160908-170735.csv	09/08/2016 17:07:35	30.69839	-87.99136	86.7	69.5	10.81	7.60	39.8
TR-06	YSI ProDSS	160908-170942.csv	09/08/2016 17:09:42	30.69769	-87.98981	86.9	47.5	12.21	7.57	5.7

ERDC/CHL

Coastal and Hydraulics Laboratory

US Army Corps of Engineers®
Engineer Research and Development Center

Mobile Harbor Study Quantifying Sediment Characteristics and Discharges into Mobile Bay

Michael Ramirez, Matthew B. Taylor, Naveen Ganesh, Richard J. Allen, and Thad C. Pratt

US Army Corps of Engineers

Engineer Research and Development Center

Coastal and Hydraulics Laboratory

April 2018

Contents

Contents 2
Introduction 1
Site Information 1
Data Processing Methodology 4
Water Samples 4
Water Quality 4
HADCP 5
ADV 5
Boat-Based ADCP 5
Water Discharge Calibration 5
Suspended Sediment Concentration 6
Boat-Based Suspended Sediment 6
Results by Site 6
North Mobile River (NMR) 6
Location 6
Site Instrumentation and Specifications 7
Site Timeline 8
Discharge Time Series 10
Suspended Sediment Cross-Section Calibration 11
Suspended Sediment Time Series 12
Full Time Series 15
Tensaw River (TR) 16
Location 16
Site Instrumentation and Specifications 17
Site Timeline 18
Discharge Time Series 20
Suspended Sediment Cross-Section Calibration 21
Suspended Sediment Time Series 22
Full Time Series 25
South Mobile River 26
Location 26
Site Instrumentation and Specifications 27
Site Timeline 27
Discharge Time Series 28
Suspended Sediment Time Series 29
Full Time Series 32
Shipwave1 (SW1) 33
Location 33
Site Instrumentation and Specifications 34
Site Timeline 35
Shipwave2 (SW2) 35

Location 35
Site Instrumentation and Specifications 35
Site Timeline 36
Suspended Sediment Time Series 38
Tensaw River at Causeway (TCW) 40
Location 40
Site Instrumentation and Specifications 41
Site Timeline 42
Discharge Time Series 44
Suspended Sediment Cross-Section Calibration ..... **Error! Bookmark not defined.**
Suspended Sediment Time Series 45
Full Time Series 48
Apalachee River (AR) 49
Location 49
Site Instrumentation and Specifications 50
Site Timeline 51
Discharge Time Series 52
Suspended Sediment Cross-Section Calibration 53
Suspended Sediment Time Series 54
Full Time Series 57
Blakely River (AR) 58
Location 58
Site Instrumentation and Specifications 59
Site Timeline 60
Discharge Time Series 61
Suspended Sediment Cross-Section Calibration 63
Suspended Sediment Time Series 64
Full Time Series 67
State Docks (SD) 68
Location 68
Site Instrumentation and Specifications 69
Site Timeline 70
Discharge Time Series 71
Suspended Sediment Cross-Section Calibration 72
Suspended Sediment Time Series 73
Full Time Series 76
Middle Bay (MB) 77
Fairhope Yacht Club (FYC) 79
Range Marker (RM) 80
Conclusions 81
References 82

Figures

Figure 1. Overview map of the 7 river stations, 2 shipwave stations, and 3 AWAC stations in Mobile Bay. 2

Figure 2. Timeline of data collection periods for each of the study sites. Black points represent service dates for each site. 4

Figure 3. North Mobile River site detail. The location of the site instrumentation is shown with a blue circle, the location of the boat-based ADCP transect is shown with a white line, and the extent of the horizontally averaged HADCP beam is shown in red. 7

Figure 4. North Mobile River (NMR) Measured Discharge vs. H-ADCP Velocities..... 10

Figure 5. Time series of HADCP-calculated discharge at North Mobile River (NMR) site. 10

Figure 6. North Mobile River (NMR) Boat Mounted ADCP vs. SSC Calibration. 11

Figure 7. North Mobile River (NMR) Turbidity vs. ISCO SSC Calibration. 12

Figure 8. North Mobile River (NMR) H-ADCP vs. ISCO SSC Calibration. 13

Figure 9. Time series of calibrated CTD turbidity, HADCP backscatter, and ISCO suspended sediment concentration at North Mobile River site. 14

Figure 10. Full Time Series of Discharge and Suspended Sediment Concentrations for the North Mobile River Site 15

Figure 11. Relationships between water discharge and suspended sediment concentrations calculated from turbidity and ADCP backscatter 16

Figure 12. Tensaw River (TR) site detail. The location of the site instrumentation is shown with a blue circle, the location of the boat-based ADCP transect is shown with a white line, and the extent of the horizontally averaged HADCP beam is shown in red. 17

Figure 13. Tensaw River (TR) Measured Discharge vs. H-ADCP Velocities 20

Figure 14. Time series of HADCP-calculated discharge at Tensaw River (TR) site. 20

Figure 15. Tensaw River (TR) Boat Mounted ADCP vs. SSC Calibration. 21

Figure 16. Tensaw River (TR) Turbidity vs. ISCO SSC Calibration..... 22

Figure 17. Tensaw River (TR) Percentile-Based CTD Turbidity and HADCP vs. ISCO SSC Calibration. 23

Figure 18. Time series of calibrated CTD turbidity, HADCP backscatter, and ISCO suspended sediment concentration at Tensaw River site. 24

Figure 19. Full Time Series of Discharge and Suspended Sediment Concentrations for the Tensaw River Site. 25

Figure 20. Relationships between water discharge and suspended sediment concentrations calculated from turbidity and ADCP backscatter. 26

Figure 21. South Mobile River (SMR) site detail. The location of the site instrumentation is shown with a blue circle, the location of the boat-based ADCP transect is shown with a white line, and the extent of the horizontally-averaged HADCP beam is shown in red. 27

Figure 22. South Mobile River (SMR) Measured Discharge vs. H-ADCP Velocities 28

Figure 23. Time series of HADCP-calculated discharge at South Mobile River (SMR) site..... 29

Figure 24. South Mobile River (SMR) CTD turbidity and HADCP vs. ISCO SSC Calibration. 30

Figure 25. Time series of calibrated CTD turbidity, HADCP backscatter, and ISCO suspended sediment concentration at South Mobile River site. 31

Figure 26. Full Time Series of Discharge and Suspended Sediment Concentrations for the South Mobile River Site. 32

Figure 27. Relationships between water discharge and suspended sediment concentrations calculated from turbidity and ADCP backscatter. 33

Figure 28. Shipwave Sites in detail. The locations of the two sites (SW1 and SW2) are shown with blue circles. 34
Figure 29. Shipwave Turbidity vs. ISCO SSC Calibration. 38
Figure 30. Shipwave Percentile-Based CTD Turbidity and ADV vs. ISCO SSC Calibration. 39
Figure 31. Time series of calibrated CTD turbidity, ADV backscatter, and ISCO suspended sediment concentration at Shipwave site. 40
Figure 32. Tensaw River at Causeway (TCW) site detail. The location of the site instrumentation is shown with a blue circle, the location of the boat-based ADCP transect is shown with a white line (just south of bridge), and the extent of the horizontally averaged HADCP beam is shown in red... 41
Figure 33. Tensaw River at Causeway (TCW) Measured Discharge vs. H-ADCP Velocities 44
Figure 34. Time series of HADCP-calculated discharge at Tensaw River at Causeway (TCW) site. ..44
Figure 35. Tensaw River at Causeway (TR) Turbidity vs. ISCO SSC Calibration. 45
Figure 36. Tensaw River at Causeway (TCW) Percentile-Based CTD Turbidity and HADCP vs. ISCO SSC Calibration. 46
Figure 37. Time series of calibrated CTD turbidity, HADCP backscatter, and ISCO suspended sediment concentration at Tensaw River at Causeway site. 47
Figure 38. Full Time Series of Discharge and Suspended Sediment Concentrations for the Tensaw River at Causeway Site. 48
Figure 39. Relationships between water discharge and suspended sediment concentrations calculated from turbidity and ADCP backscatter. 49
Figure 40. Apalachee River (AR) site detail. The location of the site instrumentation is shown with a blue circle, the location of the boat-based ADCP transect is shown with a while line, and the extent of the horizontally averaged HADCP beam is shown in red. 50
Figure 41. Apalachee River (AR) Measured Discharge vs. H-ADCP Velocities 52
Figure 42. Time series of HADCP-calculated discharge at Apalachee River (AR) site. 53
Figure 43. Apalachee River (AR) Turbidity vs. ISCO SSC Calibration. 54
Figure 44. Apalachee River (AR) Percentile-Based CTD Turbidity and HADCP vs. ISCO SSC Calibration. 55
Figure 45. Time series of calibrated CTD turbidity, HADCP backscatter, and ISCO suspended sediment concentration at Apalachee River site. 56
Figure 46. Full Time Series of Discharge and Suspended Sediment Concentrations for the Apalachee River Site. 57
Figure 47. Relationships between water discharge and suspended sediment concentrations calculated from turbidity and ADCP backscatter. 58
Figure 48. Blakely River (BR) site detail. The location of the site instrumentation is shown with a blue circle, the location of the boat-based ADCP transect is shown with a white line, and the extent of the horizontally average HADCP beam is shown in red. 59
Figure 49. Blakely River (BR) Measured Discharge vs. H-ADCP Velocities 61
Figure 50. Time series of HADCP-calculated discharge at Blakely River (BR) site. 62
Figure 51. Blakely River (BR) Boat Mounted ADCP vs. SSC Calibration. 63
Figure 52. Blakely River (BR) Turbidity vs. ISCO SSC Calibration. 64
Figure 53. Blakely River (AR) Percentile-Based CTD Turbidity and HADCP vs. ISCO SSC Calibration. 65
Figure 54. Time series of calibrated CTD turbidity, HADCP backscatter, and ISCO suspended sediment concentration at Blakely River site. 66

Figure 55. Full Time Series of Discharge and Suspended Sediment Concentrations for the Blakely River Site. 67
Figure 56. Relationships between water discharge and suspended sediment concentrations calculated from turbidity and ADCP backscatter. 68
Figure 57. State Docks (SD) site detail. The location of the primary site instrumentation as well as the location of the water-level gage are shown with blue circles, the location of the boat-based ADCP transects is shown with a white line, and the extent of the horizontally averaged HADCP beam is shown in red. 69
Figure 58. State Docks (SD Measured Discharge vs. H-ADCP Velocities 71
Figure 59. Time series of HADCP-calculated discharge at State Docks (SD) site. 71
Figure 60. State Docks (SD) Boat Mounted ADCP vs. SSC Calibration. 72
Figure 61. State Docks (SD) Turbidity vs. ISCO SSC Calibration. 73
Figure 62. State Docks (SD) Percentile-Based CTD Turbidity and HADCP vs. ISCO SSC Calibration. 74
Figure 63. Time series of calibrated CTD turbidity, HADCP backscatter, and ISCO suspended sediment concentration at State Docks site. 75
Figure 64. Full Time Series of Discharge and Suspended Sediment Concentrations for the State Docks Site. 76
Figure 65. Relationship between water discharge and suspended sediment concentrations calculated from turbidity. 77
Figure 66. AWAC Sites Detail. The location of the AWAC deployments at Middle Bay (MB), Fairhope Yacht Club (FYC), and Range Marker (RM) are shown with blue circles. 78

Tables

Table 1. List of monitoring stations in the Mobile Bay area, including location, instrumentation, and dates of service. RTU refers to the real-time data monitoring units, ISCO refers to the Teledyne Isco 6712 Portable Water Sampler, CTD refers to conductivity temperature and depth sensors which were also equipped with optical turbidity sensors (manufacturer specified for each station), HADCP refers to Teledyne RDI Workhorse horizontal acoustic Doppler profilers (frequency specified for each station), ADV refers to acoustic Doppler velocimeter, Wavestaff refers to an Ocean Sensor Systems capacitance wavestaff, Anemometer refers an ultrasonic wind speed and direction sensor (manufacturer specified for each station), and AWAC refers to Aquadopp Wave and Current sensors. Additional information servicing dates are given in the results section for each station. 2
Table 2. Servicing dates and notes from NMR Site. 8
Table 3. Servicing dates and notes from the TR site. 18
Table 4. Servicing dates and notes from the SMR site 28
Table 5. Servicing dates and notes for the SW2 site. 36
Table 6. Servicing dates and notes from the TCW site 42
Table 7. Servicing dates and notes from the AR site 51
Table 8. Servicing dates and notes from the BR site. 60
Table 9. Servicing dates and notes from the SD site 70

Introduction

The U.S. Army Corps of Engineers, Mobile District, is completing a General Re-Evaluation Report (GRR) for the Mobile Harbor Federal Navigation Channel. The GRR will determine if it is justifiable to deepen and widen the channel up to the authorized dimensions. An extensive field data collection and archival data discovery effort is employed as part of this effort. Field data is vital to accurately characterize the influence area and more particularly useful for calibration of hydrodynamic and environmental models to evaluate existing conditions and predict changes as a result of the proposed federal channel modifications. This report summarizes h data obtained from continuously operating, near real-time, hydrodynamic and water quality stations installed and serviced in a collaborative effort between ERDC and the Mobile District over a period from May 2016 to July 2017.

Remote monitoring stations were used to quantify sediment fluxes into the bay from riverine sources, measure the discharge of these rivers, monitor salinity, and measure waves in Mobile Bay. These stations were equipped with physical samplers, conductivity, temperature, turbidity, and depth sensors, and acoustic instruments for measure water velocity and acoustic backscatter. The long-term datasets were augmented with local, boat-based measurements of the same quantities to calibrate the remote records. The combined datasets were used to derive calibrated, continuous time series of water discharge and suspended sediment concentrations at each of the remote sites. Additional instruments were placed on the seabed in the open water of Mobile Bay to measure wave statistics.

Site Information

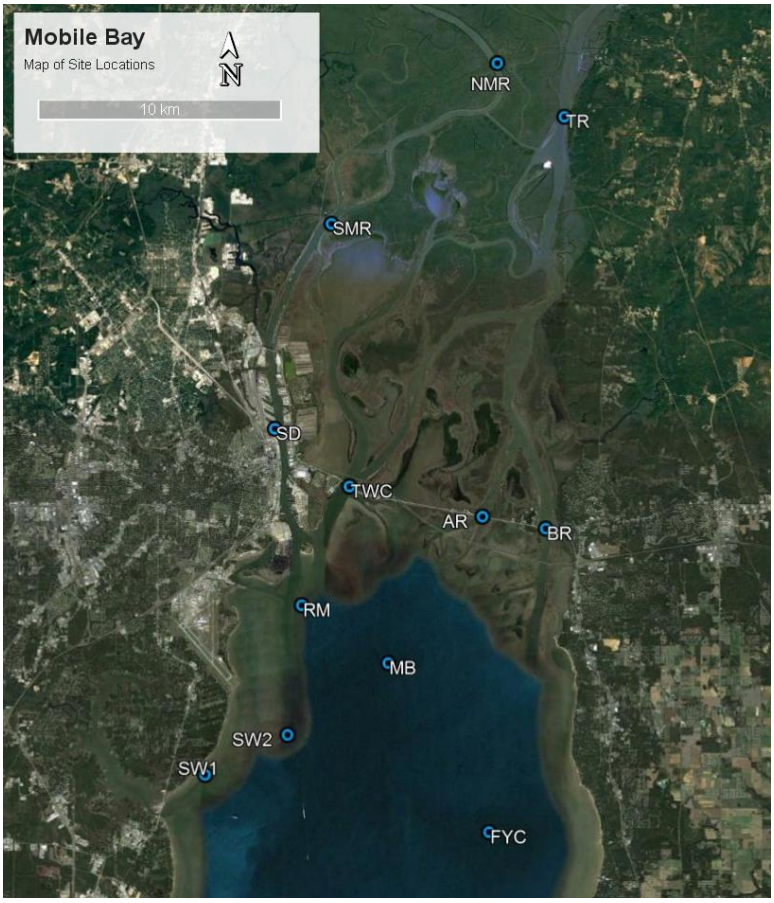

Figure 1. Overview map of the 7 river stations, 2 shipwave stations, and 3 AWAC stations in Mobile Bay.

Table 1. List of monitoring stations in the Mobile Bay area, including location, instrumentation, and dates of service. RTU refers to the real-time data monitoring units, ISCO refers to the Teledyne Isco 6712 Portable Water Sampler, CTD refers to conductivity temperature and depth sensors which were also equipped with optical turbidity sensors (manufacturer specified for each station), HADCP refers to Teledyne RDI Workhorse horizontal acoustic Doppler profilers (frequency specified for each station), ADV refers to acoustic Doppler velocimeter, Wavestaff refers to an Ocean Sensor Systems capacitance wavestaff, Anemometer refers an ultrasonic wind speed and direction sensor (manufacturer specified for each station), and AWAC refers to Aquadopp Wave and Current sensors. Additional information servicing dates are given in the results section for each station.

Site Name	Longitude, Latitude	Instruments	Data Begin Date	Data End Date
North Mobile River (NMR)	-87.9446, 30.8395	RTU, ISCO, CTD (Hydrolab MS5), HADCP (600 kHz)	5/13/2016	7/31/2017
Tensaw River (TR)	-87.9159, 30.8195	RTU, ISCO, CTD (Hydrolab MS5), HADCP (300 kHz)	6/1/2016	7/31/2017

South Mobile River (SMR)	-88.0158, 30.7798	RTU, ISCO, CTD (Hydrolab MS5), HACDP (300 kHz)	5/15/2016	11/23/2016
Shipwave1	-88.0684, 30.5795	RTU, ISCO, CTD (Hydrolab MS5), ADV, Wavestaff, Anemometer (RM Young)	5/12/2016	12/4/2016
Shipwave2 (SW)	-88.0338, 30.5938	RTU, ISCO, CTD (Hydrolab MS5), ADV, Wavestaff, Anemometer (Vaisala)	12/8/2016	7/4/2017
Tensaw River at Causeway (TCW)	-88.0080, 30.6835	RTU, ISCO, CTD (Hydrolab MS5), HADCP (300 kHz)	12/18/2016	8/1/2017
Apalachee River (AR)	-87.9516, 30.6726	RTU, ISCO, CTD (YSI), HADCP (600 kHz), Pressure	1/12/2017	8/1/2017
Blakely River (BR)	-87.9248, 30.6682	RTU, ISCO, CTD (YSI), HADCP (600 kHz), Pressure	1/11/2017	8/1/2017
State Docks (SD)	-88.0397, 30.7045	RTU, HADCP 250 kHz), ISCO, CTD (YSI)	12/16/2016	6/13/2017
Middle Bay (MB)	-87.9915, 30.61965	AWAC	5/12/2016	7/18/2016
Fairhope Yacht Club (FYC)	-87.9492, 30.5591	AWAC	7/1/2016	7/28/2016
Range Marker (RM)	-88.0280, 30.6404	AWAC	7/29/2016	8/1/2017

Data were collected at nine remote monitoring stations in the Mobile Bay area (Figure 1): North Mobile River (NMR), Tensaw River (TR), South Mobile River (SMR), Shipwave1 (SW1), Shipwave2 (SW2), Tensaw River at Causeway (TCW), Apalachee River (AR), Blakely

River (BR), and State Docks (SD). Additionally, self-recording Aquadopp Wave and Current (AWAC) instruments were deployed at three locations in Mobile Bay (these were serial deployments, not parallel): Middle Bay (MB), Fairhope Yacht Club (FYC), and Range Marker (RM). Information about each site's location, instrumentation, and dates of service are included in Table 1. A timeline of data collection and service dates for each station is shown in Figure 2

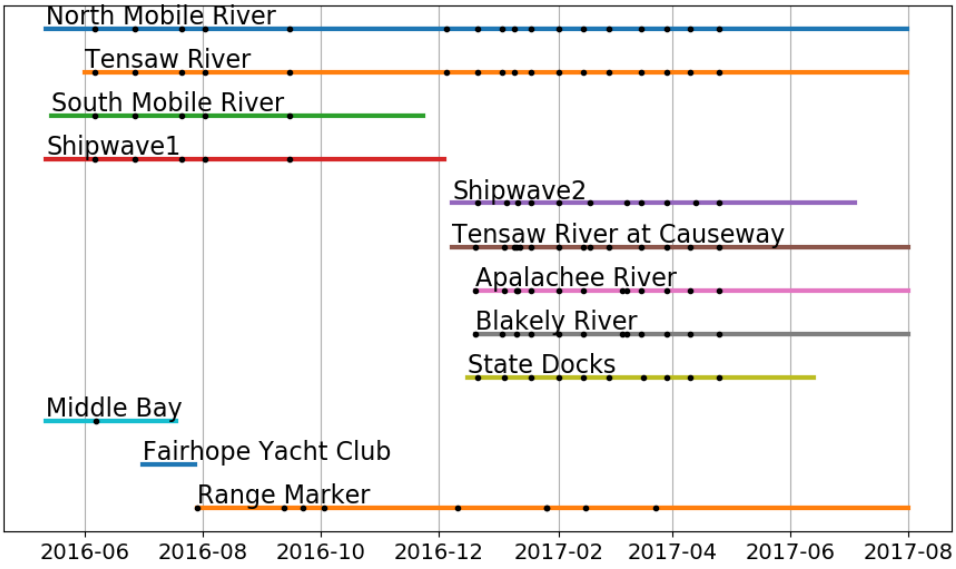

Figure 2. Timeline of data collection periods for each of the study sites. Black points represent service dates for each site.

Data Processing Methodology

Water Samples

Pumped water samples were collected daily at each station using the ISCO water sampler, which has internal storage for 24 1 liter samples. These samples were periodically retrieved from the sites for laboratory processing and replacement with empty bottles. Sediment concentration analysis was performed according to ASTM D3977, Method B – filtration. Samples were filtered by vacuum filtration through 90-mm diameter glass fiber filters with retention rating of 0.7 μm. The filtered samples were rinsed with lab-grade clean water at the end of filtration to clear the filter of dissolved solids. Samples from 2016 were analyzed at the ERDC-CHL Sediment Transport Laboratory, while samples from 2017 were analyzed at TestAmerica Laboratories using the same methodology.

Water Quality

CTD data, including date/time, water temperature, water depth (above the sensor), conductivity, and turbidity were collected at regular intervals throughout the study period. The daily-recorded CTD files for each site were concatenated to generate times series of available data for each site. The CTD instruments were prone to biofouling throughout the study, particularly at intervals prior to servicing trips (at which time the instruments were cleaned of algae, barnacles, etc.). These intervals could be identified in the turbidity record as biofouling

produces anomalously large turbidity values due to material blocking the optical path of the turbidity sensor. For this reason, all turbidity data with values greater than 200 NTU were removed from the record as turbidity values this high were found to result in poor calibration with the ISCO suspended sediment concentrations. The final turbidity time series were smoothed with a rolling average window of 2 hours to attenuate any remaining noise in the signal.

HADCP

Horizontal ADCP data were collected at each station using either a 300 kHz or a 600 kHz Teledyne/RDI Channelmaster instrument. These instruments collected velocity and acoustic backscatter data ensembles at regular intervals throughout the study period, with each ensemble being an average of 10-200 pings. HADCP data at the State Docks site was obtained from NOAA PORTS station mb0301 as an average velocity measured at a 6-minute interval. The velocities along each profile were converted from East-North-Up coordinates to stream-oriented coordinates using a rotation algorithm, and then the mean streamwise velocity was calculated for each ensemble to generate a time series of water velocities in the channel. In generating a time series of acoustic backscatter data for calibration to the ISCO data, only the 5 measurement bins closest to the instrument (~10 m) were used to remove any cross-stream variability that would not be present in the ISCO record. The acoustic backscatter values for these five bins were averaged, and—like the turbidity data—were filtered using a threshold (150 counts) and a rolling window average of 2 hours to attenuate any remaining noise in the signal. Acoustic backscatter data were not available for the site at State Docks.

ADV

The acoustic Doppler velocimeter operates on the same principles as an ADCP, but measures velocity and acoustic backscatter at a single point, rather than along a profile. The ADV instrument was used at the Shipwave1 and Shipwave2 sites. ADV data were collected at a sample rate of 8 Hz for 120 seconds every 20 minutes. Acoustic backscatter data from this instrument were treated similarly to the HADCP backscatter data: these were averaged with a rolling window of 2 hours to attenuate any remaining noise.

Boat-Based ADCP

Cross-sectional measurements of river discharge were collected by ERDC-CHL personnel using a boat-based Teledyne/RDI Workhorse Rio Grande ADCP, and by SAM personnel using a Sontek RiverSurveyor M9 ADCP. In each case the cross section was measured once in each direction and the calculated water discharges between the two cross sections were averaged.

Water Discharge Calibration

For calculating water discharge at each site, the cross-sectional ADCP data were treated as snapshots (i.e. known water discharges measured at discrete points in time), with the horizontal ADCP (HADCP) data used to interpolate the water discharge for times in between the boat-based surveys. The HADCP measures only water velocity along a subsection of the river, so in order to use it for calculating the total water discharge of the channel it was calibrated to the boat-based measurements of the full channel. This was done by comparing the boat-based water discharges with the HADCP-measurements of water velocities within a window of 10 minutes. Average alongstream water velocity for bins 5-70 within that 10 minute window was plotted against water discharge for the cross-sectional measurement, and a least-squares linear

regression was used between these two data sets to derive a calibration curve. This calibration curve was applied to the HADCP data for calculation of a 15 minute interval water discharge time series. These water discharge time series were found to be rather noisy, as HADCP data were affected by transient or local fluctuations in water velocity not representative of the river's total discharge. To remove any remaining noise in the data, a despiking algorithm (Goring & Nikora, 2002; Wahl, 2003) was applied to the final time series.

Suspended Sediment Concentration

For calculating suspended sediment concentration at each site, the ISCO sample concentrations were calibrated to the CTD turbidity records and the HADCP backscatter records. Two approaches were used to these calibrations. First the ISCO sample concentrations were matched with turbidity measurements within one hour of sample collection and the quantities were correlated on a one-to-one basis to generate calibration curves. This approach with the HADCP data was found to result in poor correlations, so it was only applied to the turbidity data.

A percentile-based approach was found to improve calibrations over the one-to-one correlation. With this methodology, the population of sediment concentrations from the ISCO samples were divided into 25 equal-interval percentile bins. These percentile quantities were correlated with the same percentile bins from the CTD turbidity records and the HADCP backscatter records for each station. The calibration curves derived from the one-to-one and percentile-based methodologies were applied to the turbidity and backscatter records to generate 15 minute interval sediment concentration time series for each site.

Boat-Based Suspended Sediment

Water samples from the river at each site were collected using a pump aboard the survey vessel during the same timeframe as the ADCP cross sections. These samples were accompanied by vertical profiles using a CTD to measure turbidity in the water, as well as vertical measurements of acoustic backscatter by ADCP at the same time as the sample collection. A similar approach was used to the percentile method outlined above: equal interval percentiles were calculated for the population of turbidity data and matched with the population of suspended sediment concentrations from the water sample data, and a calibration curve was calculated between the two quantities.

Results by Site

North Mobile River (NMR)

Location

Data were collected along the east bank of the Mobile River 200 m upstream of the railroad bridge at River Mile 14 (NMR Site 30.84N, 87.94W; Figure 3) over the period 12 May 2016 through 31 July 2017. This site was outfitted with CTD (conductivity, temperature, and turbidity), HADCP (water velocity), and ISCO (water samples for suspended sediment concentration) instruments. Periodic boat-based ADCP cross-sectional measurements (Figure 3) were collected for calibrating the fixed HADCP instrument.

Figure 3. North Mobile River site detail. The location of the site instrumentation is shown with a blue circle, the location of the boat-based ADCP transect is shown with a white line, and the extent of the horizontally averaged HADCP beam is shown in red.

Site Instrumentation and Specifications

The NMR Site was equipped with a Hydrolab MS5 for measurement of conductivity, temperature, depth, and turbidity. This instrument recorded these data at 15 minute intervals for the entire study period. A 600 kHz Teledyne/RD Instruments Workhorse horizontal ADCP was also deployed at this site. This HADCP was configured to record one 10 ping ensemble every minute for the period 13 May 2016 – 10 January 2017, and one 60 ping ensemble every five minutes for the period 10 January 2017 – 31 July 2017. HADCP bin size was 2.5 m throughout the study period. This site was also equipped with an ISCO 6712 automatic water sampler configured to sample every 14 hours for a total of 24 samples per program period, resulting in a service timeline of ~14 days.

Figure 4. Platform setup at North Mobile River site.

Site Timeline

This site was installed on 13 May 2016, and serviced on the dates indicated in Table 2. The ISCO water sampler was removed on 25 April 2017 to save money by requiring less frequent servicing of the station. Dates of boat-based ADCP transects and sediment profiles are also indicated in Table 2.

Table 2. Servicing dates and notes from NMR Site.

Service Date	Servicing Notes	Boat-based Measurements
13 May 2016	Installation	ADCP transects (RDI Workhorse 1200 kHz), Sediment Profiles
7 June 2016		ADCP transects (RDI Workhorse 1200 kHz), Sediment Profiles
30 June 2016	No notes available	ADCP transects (RDI Workhorse 1200 kHz)
21 July 2016	No notes available	
2 August 2016	No notes available	
25 August 2016		ADCP transects (RDI Workhorse 1200 kHz), Sediment Profiles
22 September 2016	No notes available	ADCP transects (RDI Workhorse 1200 kHz), Sediment Profiles
5 December 2016	No notes available	
21 December 2016	No notes available	ADCP transects (Sontek RiverSurveyor M9)

3 January 2017	Retrieved ISCO samples, restarted ISCO program	ADCP transects (Sontek RiverSurveyor M9)
9 January 2017	Previous ISCO program did not start, restarted ISCO program, HADCP reconfigured to 5 minute ensembles	ADCP transects (RDI Workhorse 1200 kHz), Sediment Profiles
18 January 2017	Retrieved ISCO samples, restarted ISCO program, cleaned MS5, ISCO intake, and HADCP	ADCP transects (Sontek RiverSurveyor M9)
1 February 2017	Retrieved ISCO samples, restarted ISCO program, cleaned MS5, ISCO intake and HADCP, cleared log jam at station	ADCP transects (Sontek RiverSurveyor M9)
14 February 2017	Retrieved ISCO samples, restarted ISCO program	ADCP transects (Sontek RiverSurveyor M9)
27 February 2017	Retrieved ISCO samples, restarted ISCO program	ADCP transects (Sontek RiverSurveyor M9)
16 March 2017	Retrieved ISCO samples, restarted ISCO program, cleaned MS5, ISCO intake, and HADCP	ADCP transects (Sontek RiverSurveyor M9)
29 March 2017	Retrieved ISCO samples, restarted ISCO program, cleaned MS5, ISCO intake, and HADCP	ADCP transects (Sontek RiverSurveyor M9)
10 April 2017	Retrieved ISCO samples, restarted ISCO program, cleaned MS5, ISCO intake, and HADCP	ADCP transects (Sontek RiverSurveyor M9)
25 April 2017	Retrieved ISCO samples, removed ISCO from station, cleaned MS5	ADCP transects (Sontek RiverSurveyor M9)
1 August 2017	Site removed	

Discharge Time Series

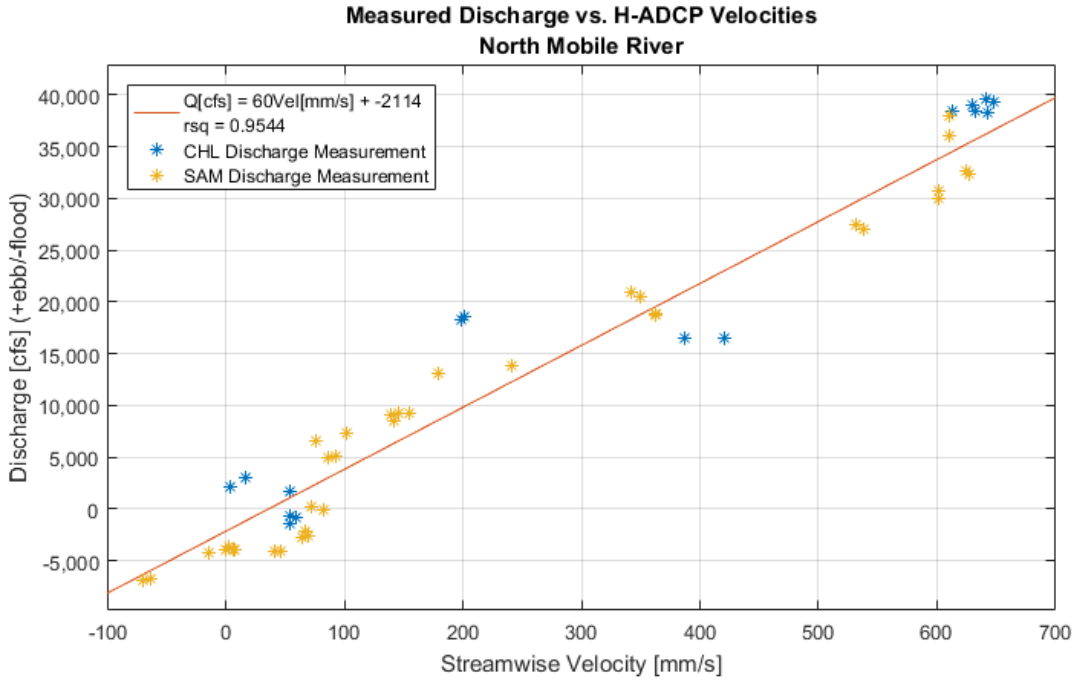

Figure 5. North Mobile River (NMR) Measured Discharge vs. H-ADCP Velocities

The average streamwise water velocities measured by the stationary HADCP were highly correlated ($R^2 = 0.95$) with the periodic discharge measurements collected with boat-based ADCP (Figure 5). Calibration of these cross-sectional ADCP measurements to the observed horizontal water velocities allows the calculation of a continuous synthetic discharge time series.

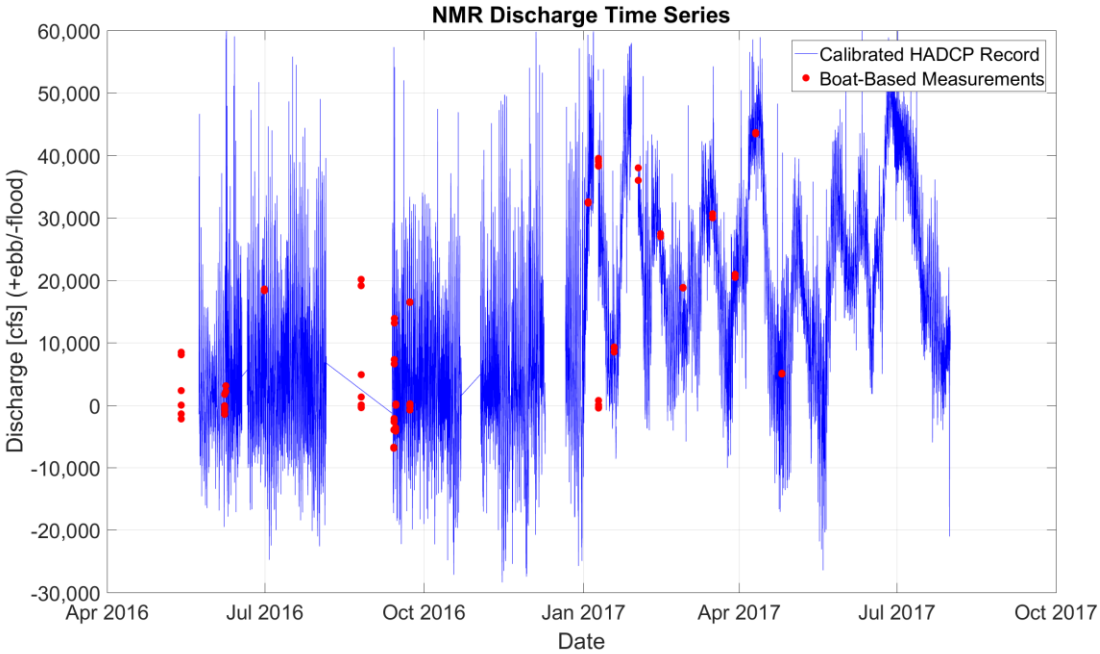

Figure 6. Time series of HADCP-calculated discharge at North Mobile River (NMR) site.

The resulting time series of HADCP data calibrated to water discharge retains some noise, particularly in the first half of the time series, in late summer-autumn 2016. During this time period, the discharge was observed to vary above and below zero, indicating flow reversal with the daily tidal variability. When river discharge increased in the spring-summer of 2017, the signal becomes cleaner as flow becomes more unidirectional.

Suspended Sediment Cross-Section Calibration

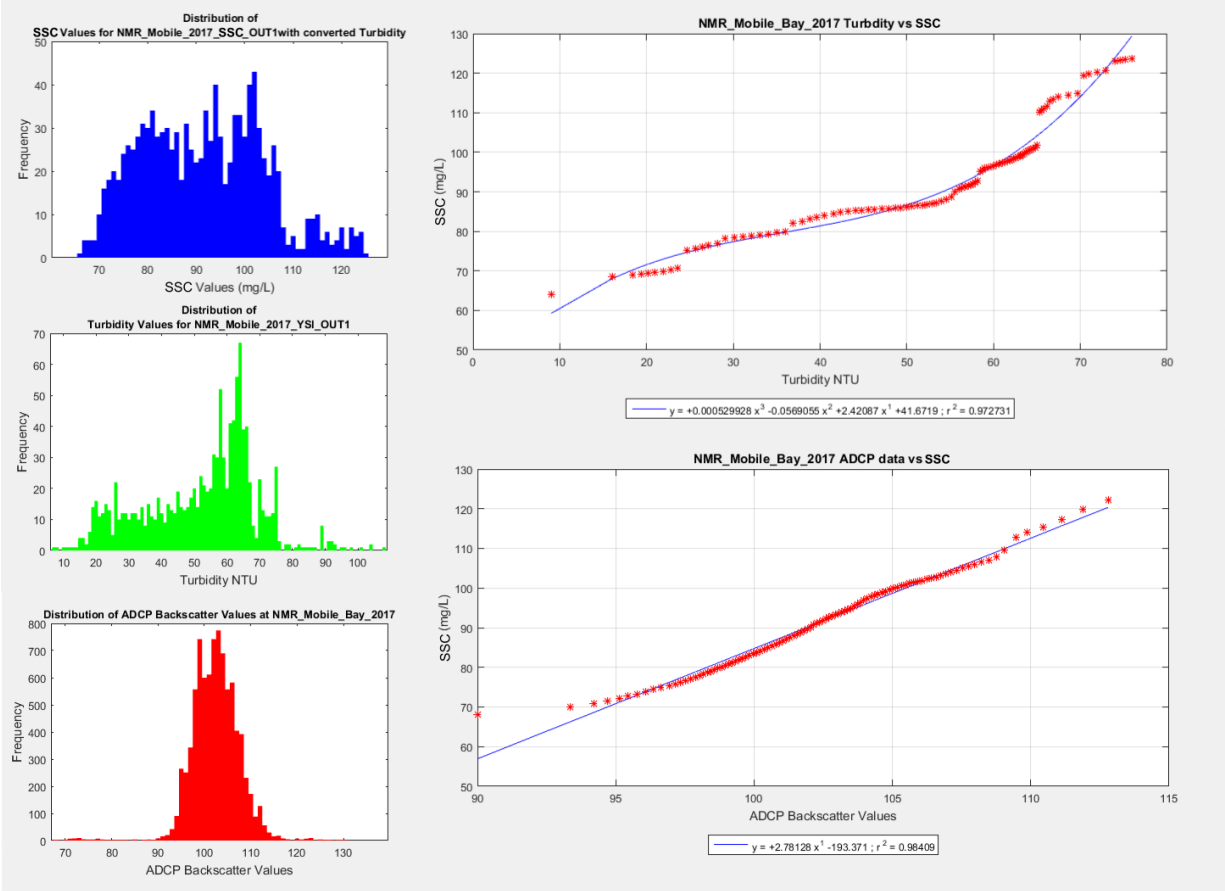

Figure 7. North Mobile River (NMR) Boat Mounted ADCP vs. SSC Calibration.

High correlations were observed between the three boat-based measurements of suspended sediment (Figure 7): suspended sediment concentration (SSC) from the water samples, turbidity from the vertical CTD profiles, and acoustic backscatter from the ADCP cross sections. With these calibrations, snapshots of suspended sediment concentration can be calculated from the ADCP cross-sectional data.

Suspended Sediment Time Series

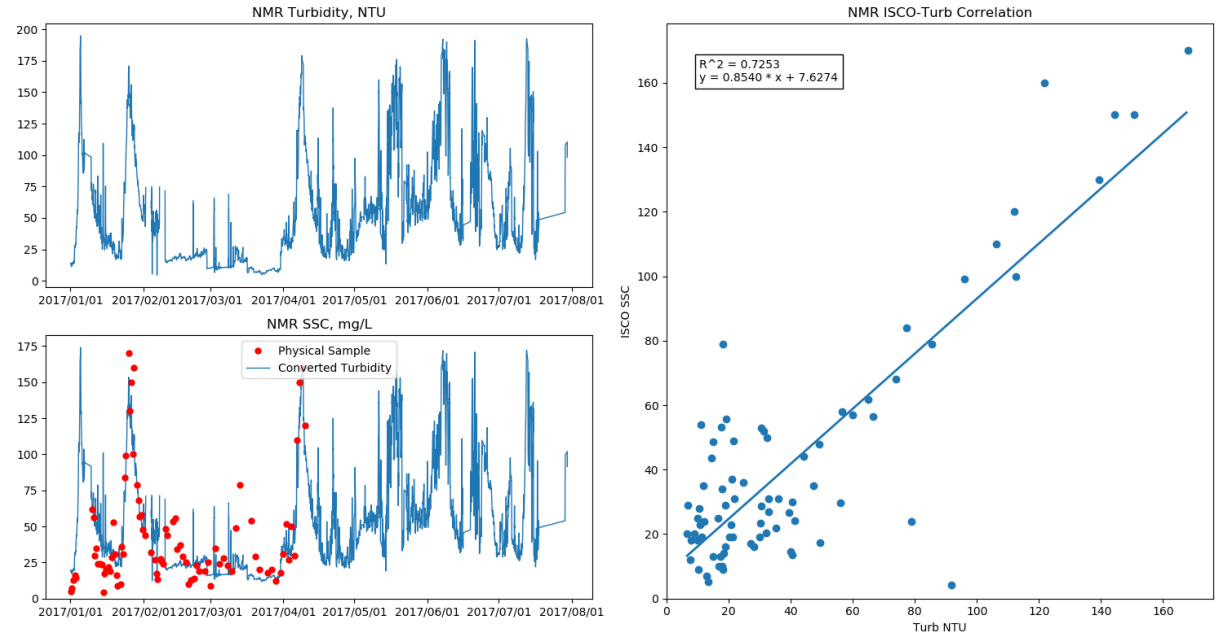

Figure 8. North Mobile River (NMR) Turbidity vs. ISCO SSC Calibration.

One-to-one (time based) calibration of turbidity and ISCO suspended sediment concentration at the North Mobile River were positively correlated ($R^2 = 0.73$), and the resulting time series (Figure 8, bottom left) matched well with the discrete sample data. For this calibration, only the turbidity data from 2017 were used, as the data from late 2016 were too noisy (likely the result of biofouling) to generate an adequate calibration.

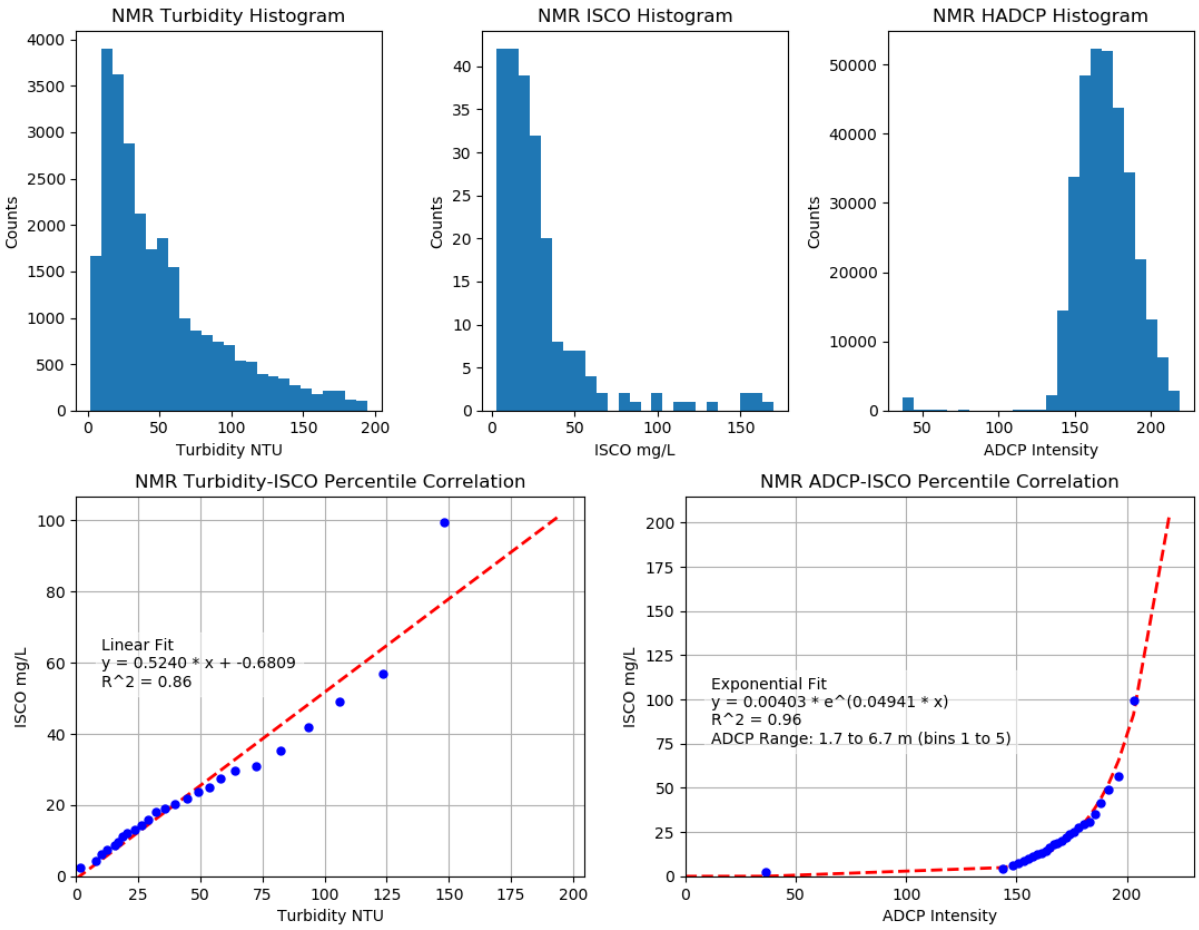

Figure 9. North Mobile River (NMR) H-ADCP vs. ISCO SSC Calibration.

The percentile calibration method resulted in high correlations for the CTD turbidity data (R^2 = 0.86, linear fit) and HADCP backscatter data (R^2 = 0.96, exponential fit). The resulting time series from these calibrations (Figure 10) remains quite noisy, particularly for the 2016 data and all of the HADCP data, suggesting the HADCP backscatter intensities are sensitive to other factors than only the suspended sediment concentration of the river. The turbidity-derived time series from 2017, while containing some noise, matches well with the discrete samples (except at very high sediment concentrations), and may be considered a better record to use for estimating suspended sediment concentration.

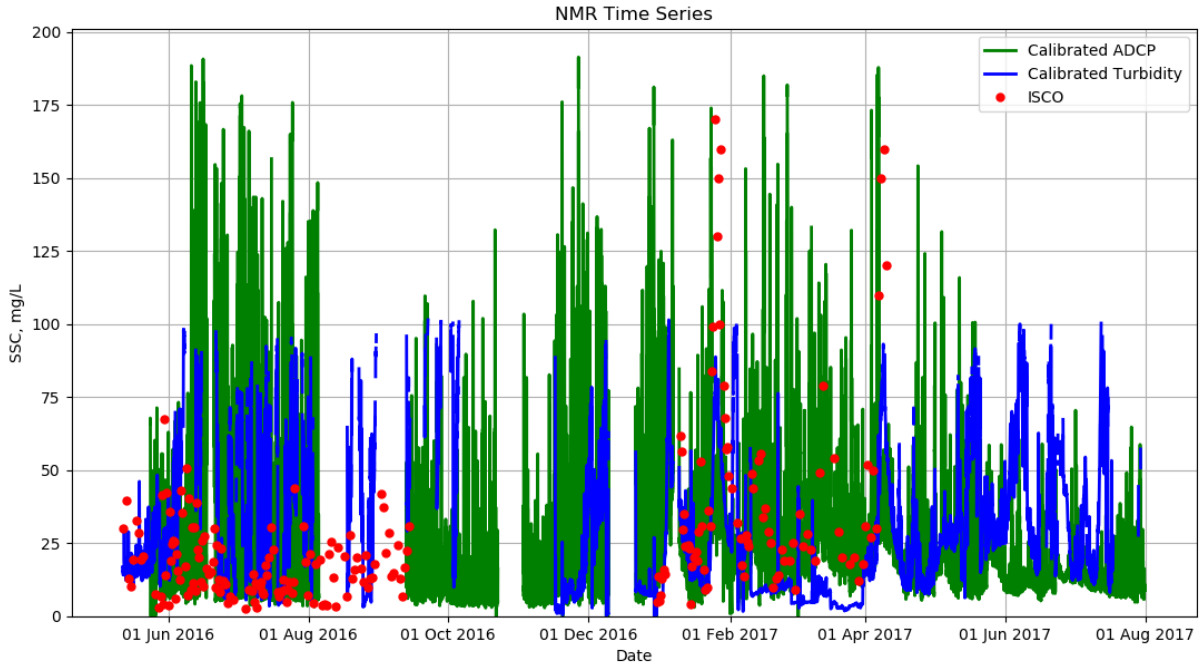

Figure 10. Time series of calibrated CTD turbidity, HADCP backscatter, and ISCO suspended sediment concentration at North Mobile River site.

Full Time Series

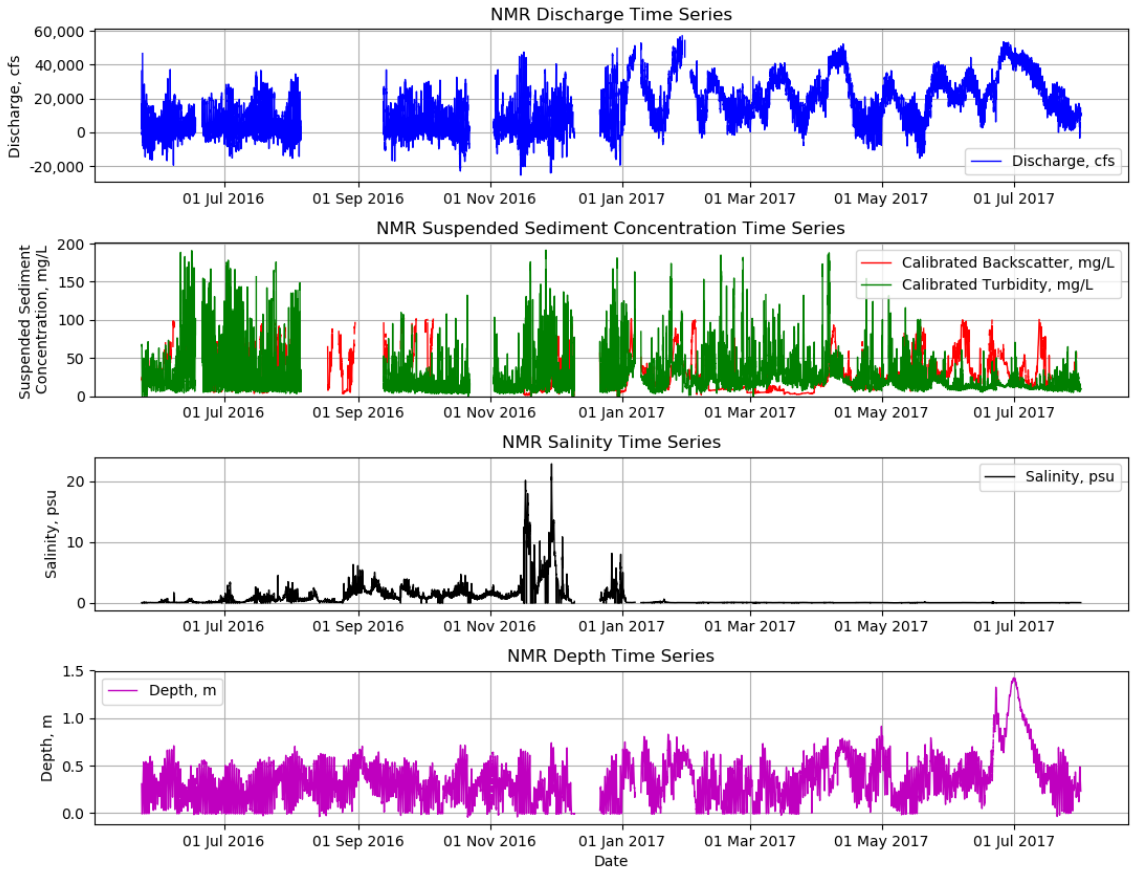

Figure 11. Full Time Series of Discharge, Suspended Sediment Concentration, Salinity, and Water Depth for the North Mobile River Site

The full time series results for the North Mobile River Site (Figure 11) showed that water discharge in the Summer-Autumn of 2016 was dominated largely by tidal variability, while the Spring-Summer of 2017 was dominated by periodic flooding of river discharge. These river floods lasted about 2 weeks each, and each pulse of floodwater is associated with a peak in suspended sediment concentration. These trends can be observed in the salinity record as well, where the Autumn 2016 period shows highly variable salinity as the tide move in and out of the river, while freshwater discharge in the Spring 2017 period was high enough to push the tidal influence further downstream.

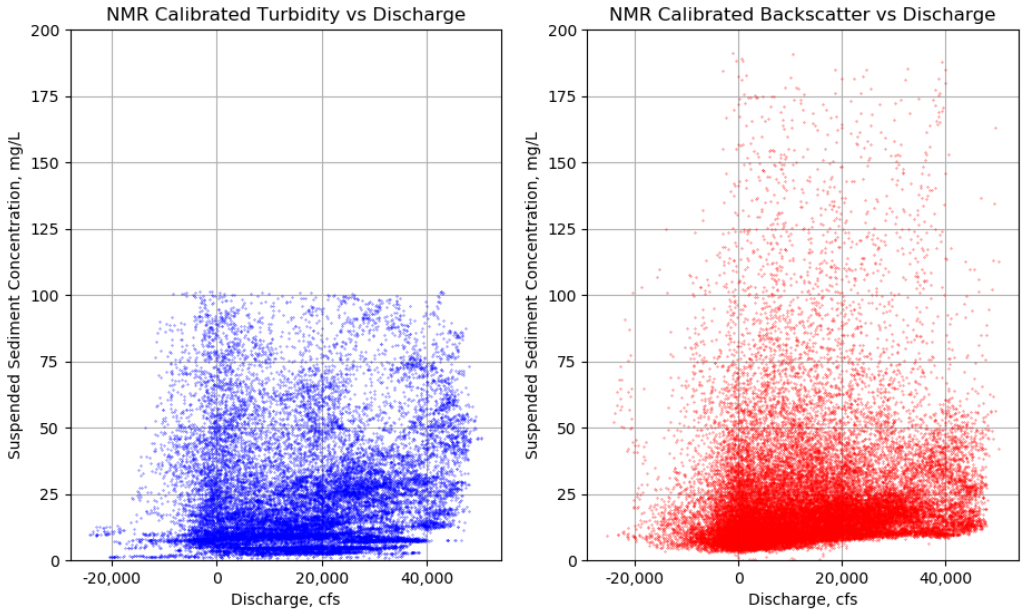

Figure 12. Relationships between water discharge and suspended sediment concentrations calculated from turbidity and ADCP backscatter

Comparing the final 15 minute records of water discharge and suspended sediment concentration shows some positive correlation between the quantities. Water discharges below 0 (indicating upstream flow during flood tide) were generally associated with low sediment concentrations, however positive discharges (ebb-tide and river flood) exhibited the full range of suspended sediment concentrations.

Tensaw River (TR)

Location

Data were collected in the Tensaw River 2.6 km south of the railroad bridge (TR Site 30.82N, 87.92W; Figure 13) over the period 1 June 2016 through 31 July 2017. This site was outfitted with CTD (conductivity, temperature, and turbidity), HADCP (water velocity), and ISCO (water samples for suspended sediment concentration) instruments. Periodic boat-based ADCP cross-sectional measurements were collected for calibrating the fixed HADCP instrument.

Figure 13. Tensaw River (TR) site detail. The location of the site instrumentation is shown with a blue circle, the location of the boat-based ADCP transect is shown with a white line, and the extent of the horizontally averaged HADCP beam is shown in red.

Site Instrumentation and Specifications

The TR site was equipped with a Hydrolab MS5 for measurement of conductivity, temperature, depth, and turbidity. This instrument recorded data at 15 minute intervals from 1 June 2016 – 10 January 2017, and at 1 minute intervals from 11 January 2017 – 31 July 2017. A 300 kHz Teledyne/RD Instruments Workhorse horizontal ADCP was also deployed at this site. This HADCP was configured to record one 200 ping ensemble every 3 minutes throughout the study period. HADCP bin size was 1 m throughout the study period. This site was also equipped with an ISCO 6712 automatic water sample configured to sample every 14 hours for a total of 14 samples per program period, resulting in a service interval of ~1 fortnight.

Figure 14. Platform setup at Tensaw River site.

Site Timeline

This site was installed on 13 May 2016, and serviced on the dates indicated in Table 3. The ISCO water sampler was removed on 25 April 2017 to save money by requiring less frequent servicing of the station. Dates of boat-based ADCP and sediment profiles are also indicated in Table 3.

Table 3. Servicing dates and notes from the TR site.

Service Date	Servicing Notes	Boat-based Measurements
13 May 2016	Installation	ADCP transects (RDI Workhorse 1200 kHz), Sediment Profiles
7 June 2016		ADCP transects (RDI Workhorse 1200 kHz)

8 June 2016		ADCP transects (RDI Workhorse 1200 kHz)
30 June 2016		ADCP transects (RDI Workhorse 1200 kHz)
25 August 2016		ADCP transects (RDI Workhorse 1200 kHz), Sediment Profiles
23 September 2016		ADCP transects (RDI Workhorse 1200 kHz), Sediment Profiles
21 December 2016	Solar panel missing and HADCP mount broken, removed HADCP from site	
3 January 2017	Installed new solar panel, reinstalled HADCP, reprogrammed ISCO	ADCP transects (Sontek RiverSurveyor M9)
9 January 2017	Previous ISCO program did not start, reprogrammed ISCO, reprogrammed MS5 to record every 1 minute	ADCP transects (Sontek RiverSurveyor M9), Sediment Profiles
18 January 2017	Retrieved ISCO samples, reprogrammed ISCO, cleaned MS5, ISCO intake, and HADCP	ADCP transects (Sontek RiverSurveyor M9)
1 February 2017	Retrieved ISCO samples, reprogrammed ISCO, cleaned MS5, ISCO intake, and HADCP	ADCP transects (Sontek RiverSurveyor M9)
14 February 2017	Retrieved ISCO samples, reprogrammed ISCO, cleaned MS5, ISCO intake, and HADCP	ADCP transects (Sontek RiverSurveyor M9)
27 February 2017	Retrieved ISCO samples, reprogrammed ISCO, cleaned MS5, ISCO intake, and HADCP, observed platform to be structurally unsound	ADCP transects (Sontek RiverSurveyor M9)
16 March 2017	Retrieved ISCO samples, reprogrammed ISCO, cleaned MS5, ISCO intake, and HADCP	ADCP transects (Sontek RiverSurveyor M9)
29 March 2017	Retrieved ISCO samples, reprogrammed ISCO, cleaned MS5, ISCO intake, and HADCP	ADCP transects (Sontek RiverSurveyor M9)
10 April 2017	Retrieved ISCO samples, reprogrammed ISCO, cleaned MS5, ISCO intake, and HADCP	ADCP transects (Sontek RiverSurveyor M9)
25 April 2017	Retrieved ISCO samples, removed ISCO from site, cleaned MS5 and HADCP	ADCP transects (Sontek RiverSurveyor

Discharge Time Series

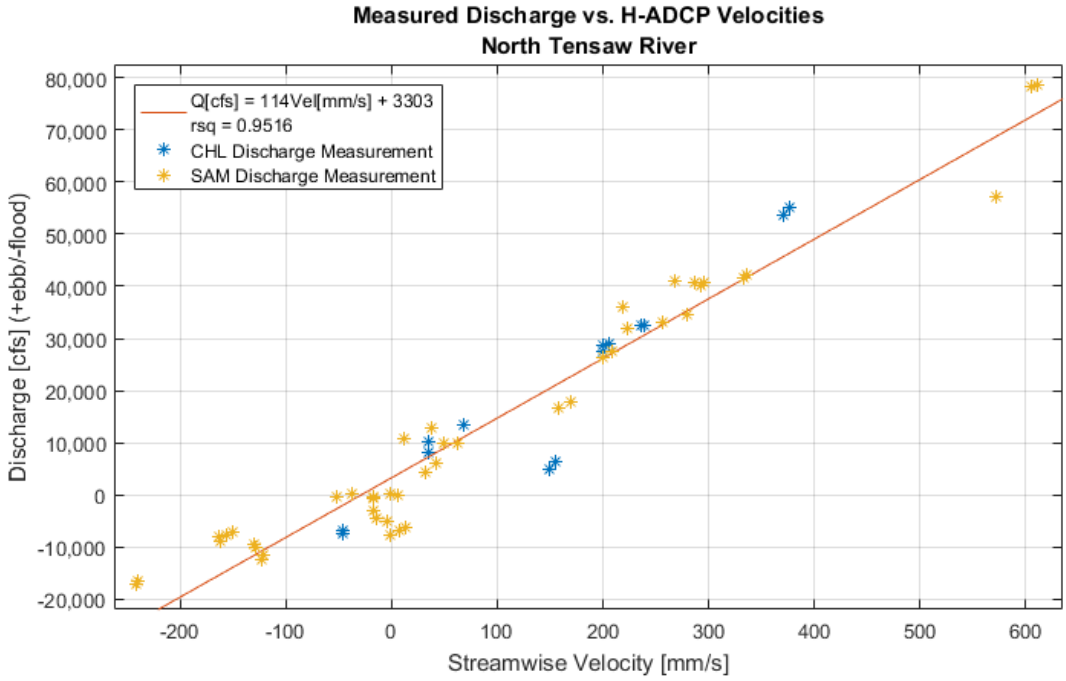

Figure 15. Tensaw River (TR) Measured Discharge vs. H-ADCP Velocities

The average streamwise water velocities measured by the stationary HADCP were highly correlated ($R^2 = 0.95$) with the periodic discharge measurements collected by boat-based ADCP (Figure 15). Calibration of these cross-sectional ADCP measurements to the observed horizontal water velocities allows the calculation of a continuous synthetic discharge time series.

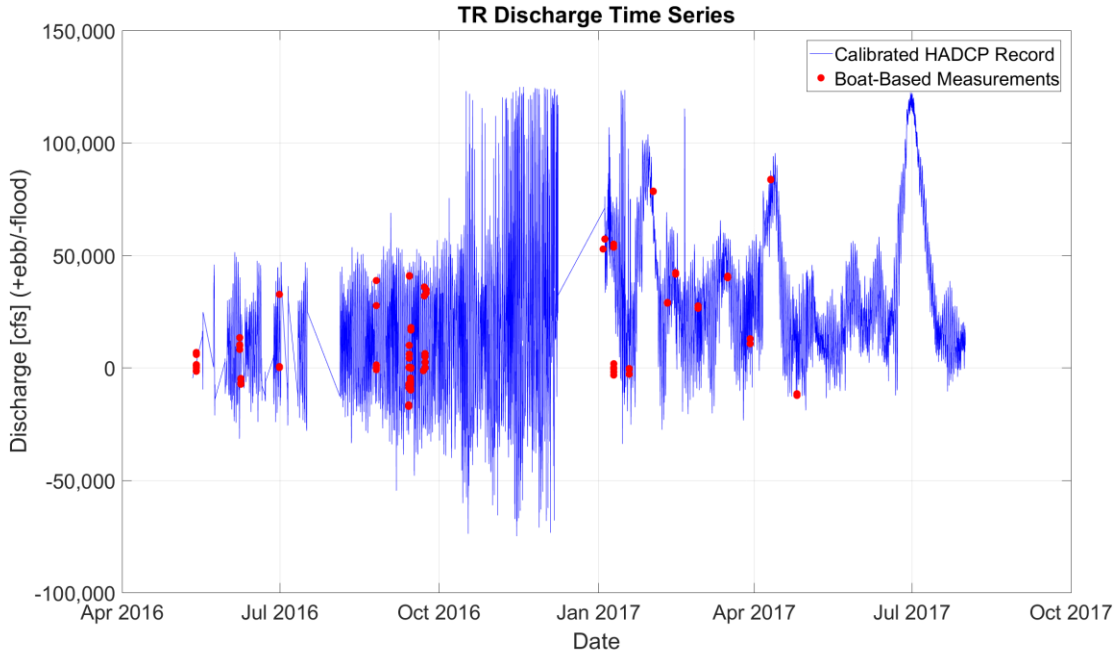

Figure 16. Time series of HADCP-calculated discharge at Tensaw River (TR) site.

Like the time series from the North Mobile River site, the resulting time series of HADCP data calibrated to water discharge retains some noise, particularly in late summer-autumn 2016. The discharge here is more highly variable about zero, indicating the tidal signal is stronger at this location during this period. The spring flood peaks at this location however, resulted in about twofold higher water discharge (80,000-120,000 cfs) than those same floods from the NMR site (40,000-50,000 cfs). These results suggest the Tensaw River is a preferential flow pathway for these spring freshets, as the two distributaries are hydrologically connected ~20 miles upstream.

Suspended Sediment Cross-Section Calibration

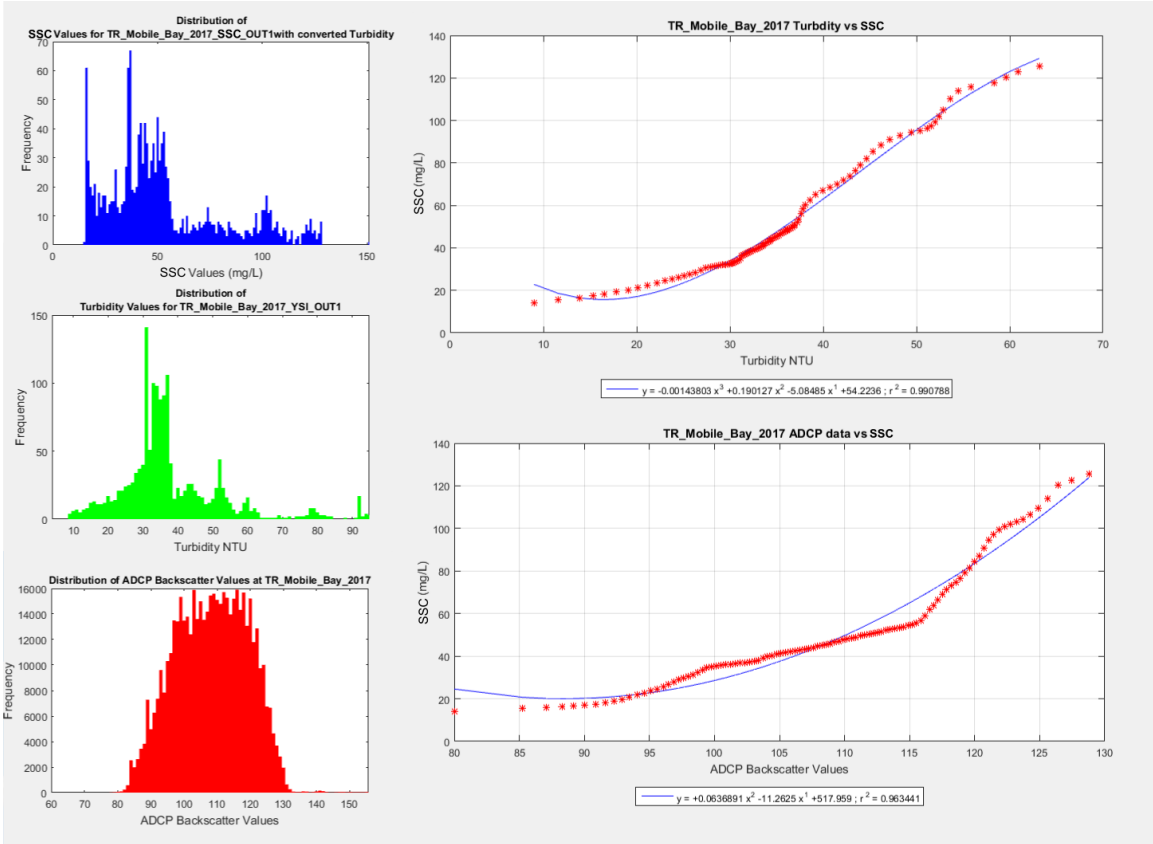

Figure 17. Tensaw River (TR) Boat Mounted ADCP vs. SSC Calibration.

The three boat-based measurements of suspended sediment were highly correlated (Figure 17): suspended sediment concentration (SSC) from the water samples, turbidity from the vertical CTD profiles, and acoustic backscatter from the ADCP cross sections. From these calibrations, snapshots of suspended sediment concentration can be calculated from the ADCP cross-sectional data.

Suspended Sediment Time Series

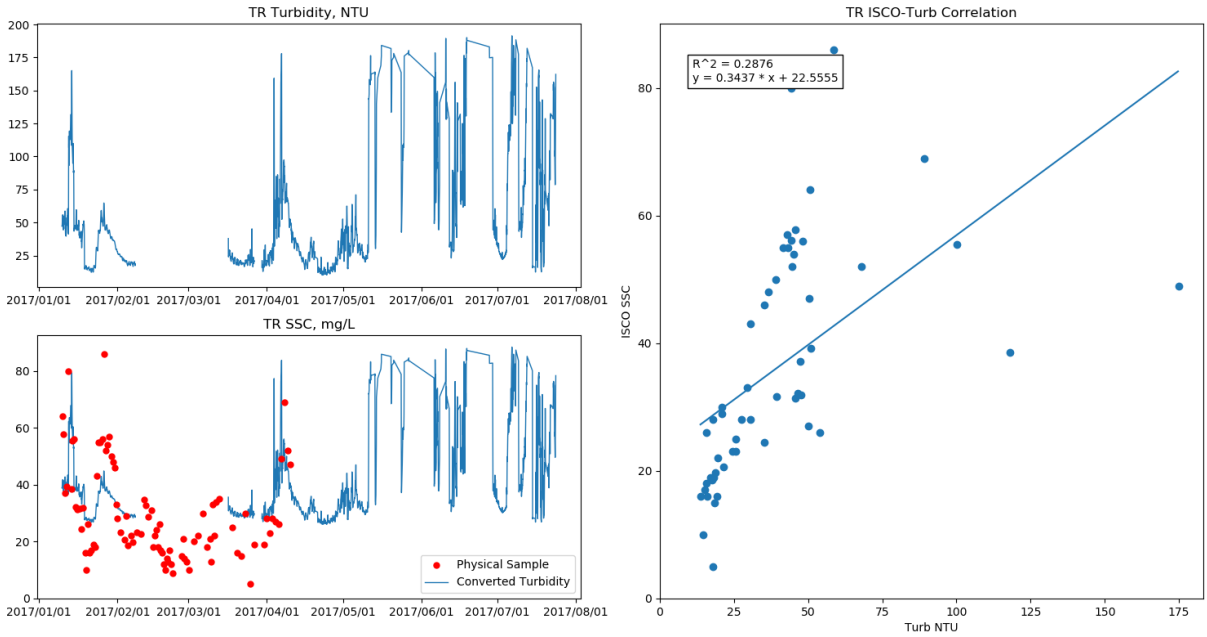

Figure 18. Tensaw River (TR) Turbidity vs. ISCO SSC Calibration.

The one-to-one (time based) calibration of turbidity and ISCO suspended sediment concentration at the Tensaw River site showed a positive, but low (R^2 = 0.29). The resulting time series (Figure 18, bottom left) can be seen to overestimate sediment concentration (compared to the discrete ISCO sample data) at low concentrations, and slightly underestimate high concentrations. For this calibration, only the turbidity data from 2017 were used, as the data from late 2016 were too noisy (likely the result of biofouling) to generate an adequate calibration. This biofouling appears to be present in the Summer 2017 turbidity record as well, but did not affect the calibration, as there were no ISCO samples collected during this period.

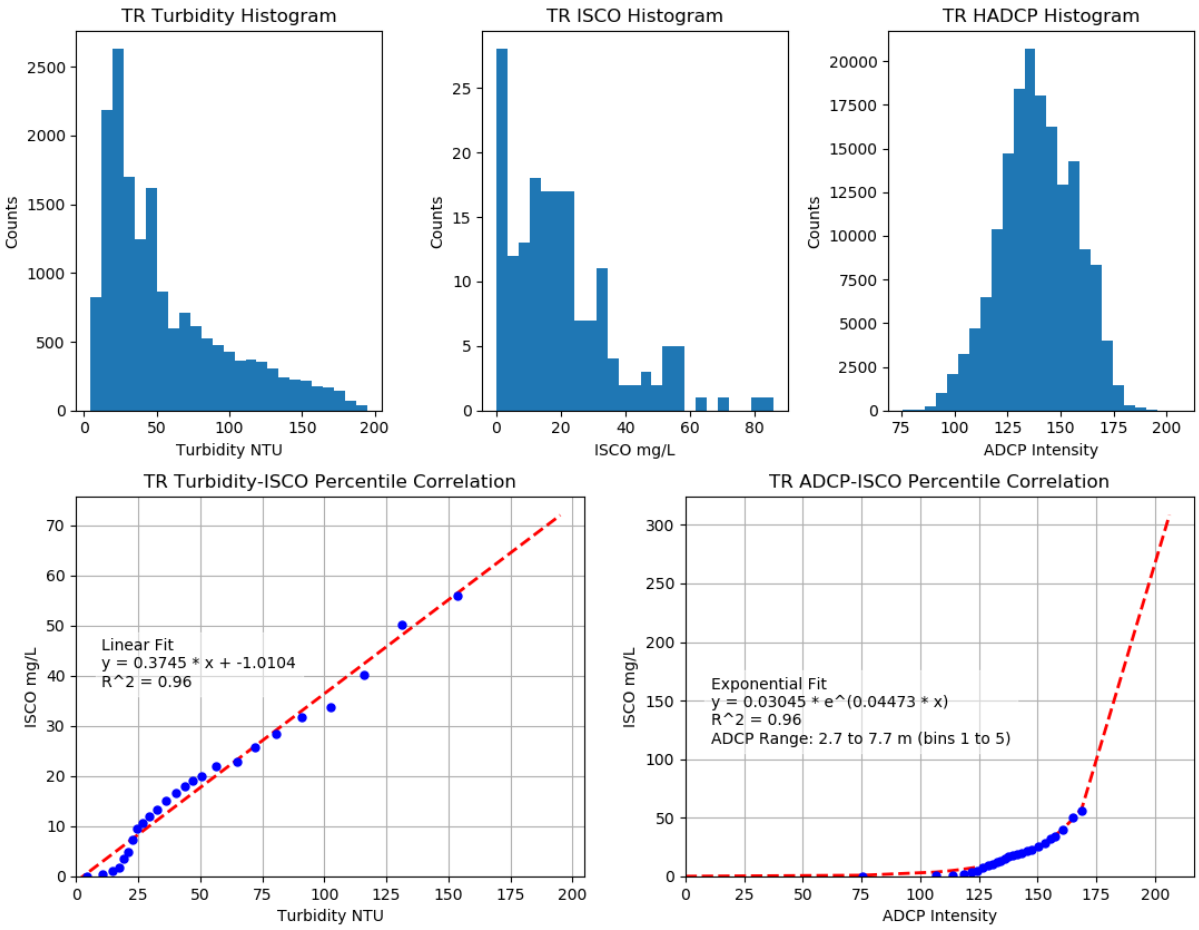

Figure 19. Tensaw River (TR) Percentile-Based CTD Turbidity and HADCP vs. ISCO SSC Calibration.

The percentile calibration method resulted in high correlations for the CTD turbidity data (R^2 = 0.96, linear fit) and HADCP backscatter data (R^2 = 0.96, exponential fit). Like at the North Mobile River site, the resulting time series from these calibrations (Figure 20) was quite variable. The turbidity-derived time series, like the one-to-one calibrated time series, overestimated concentration for low periods, and overestimated concentration for more turbid flows. The HADCP-derived time series contained some very high peaks in sediment concentration, which could not be removed by filtering the data.

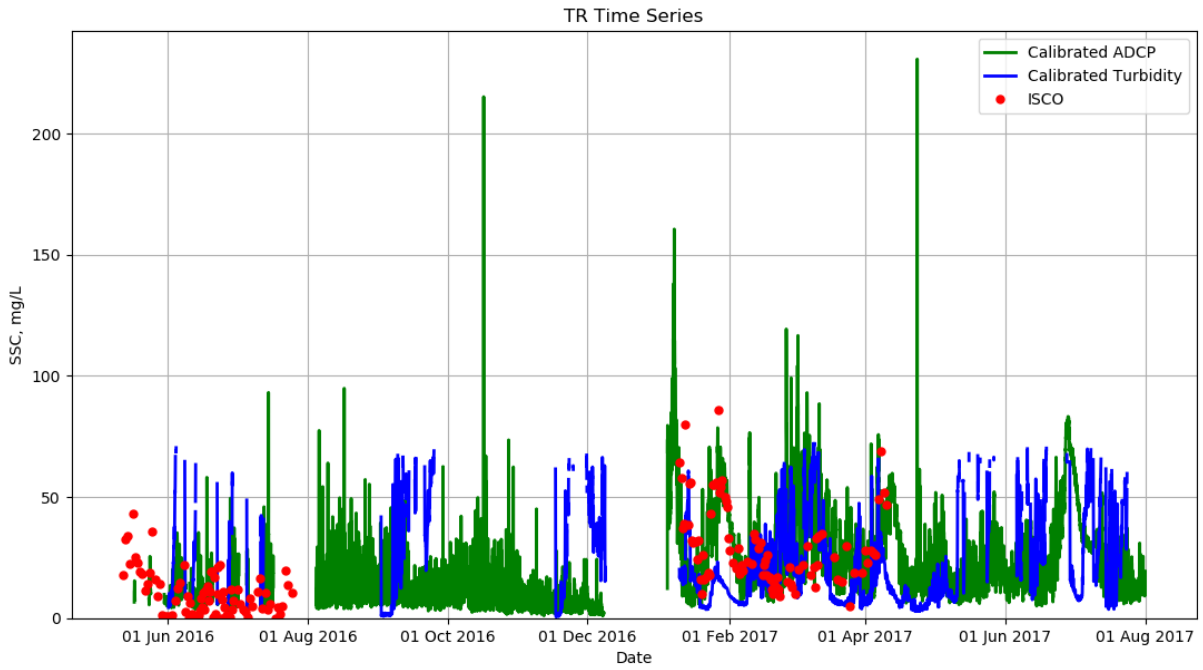

Figure 20. Time series of calibrated CTD turbidity, HADCP backscatter, and ISCO suspended sediment concentration at Tensaw River site.

Full Time Series

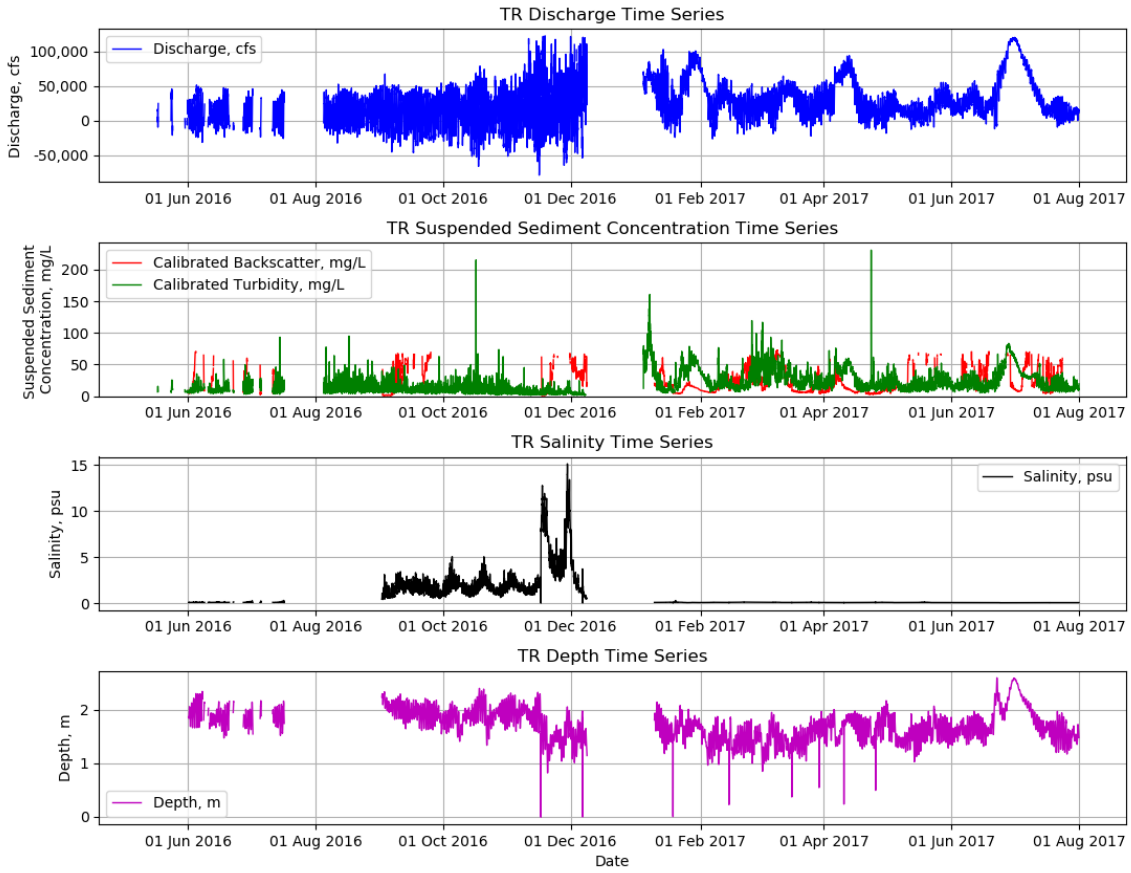

Figure 21. Full Time Series of Discharge, Suspended Sediment Concentration, Salinity, and Water Depth for the Tensaw River Site.

The full time series results for the Tensaw River Site (Figure 21) showed tidally-dominated discharge in the Summer-Autumn of 2016 and a largely flood-dominated discharge history for the Spring-Summer of 2017. These river floods lasted about 2 weeks each, but smaller in magnitude relative to baseline conditions than the North Mobile River Record. The salinity record corroborates this seasonal response, particularly during the October-December 2016 period, while the water level record shows a drawdown during the river-dominated Spring 2017 period.

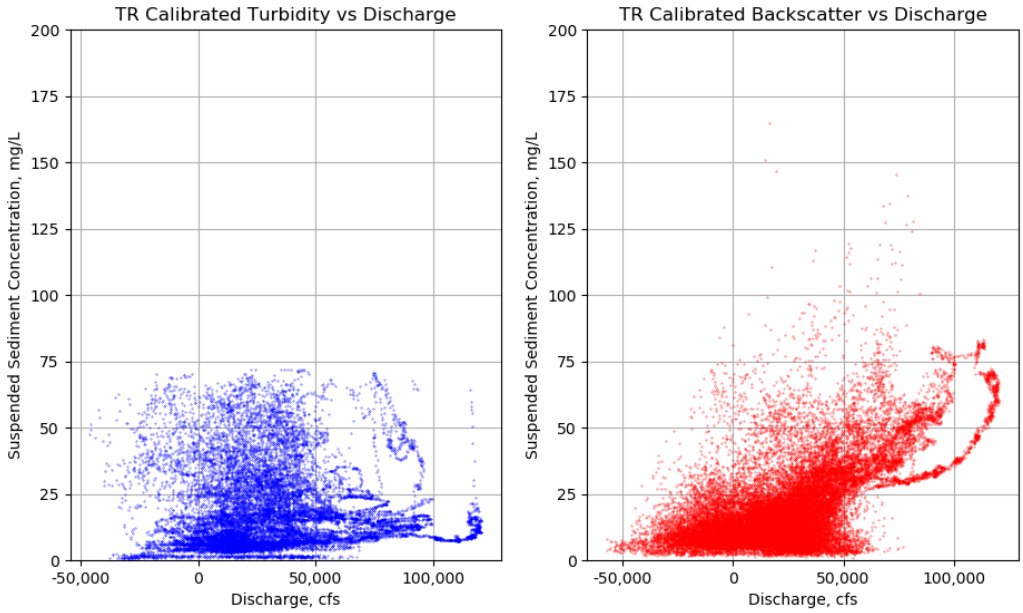

Figure 22. Relationships between water discharge and suspended sediment concentrations calculated from turbidity and ADCP backscatter.

At the Tensaw River site, suspended sediment concentration correlated positively with water discharge, particularly for the suspended sediment concentrations calculated from the HADCP backscatter record. In this record, the river flood of July 2017 can be seen as an arc of high discharge and suspended sediment concentration (Figure 22, right panel).

South Mobile River

Location

Data were collected in the Mobile River 5 km upstream of the Cochrane-Africatown USA Bridge (SMR Site 30.78N, 88.02W; Figure 23) over the period 15 May 2016 through 23 November 2016. This site was outfitted with CTD (conductivity, temperature, and turbidity), HADCP (water velocity), and ISCO (water samples for suspended sediment concentration) instruments. Periodic boat-based ADCP cross-sectional measurements were collected for calibrating the fixed HADCP instrument.

Figure 23. South Mobile River (SMR) site detail. The location of the site instrumentation is shown with a blue circle, the location of the boat-based ADCP transect is shown with a white line, and the extent of the horizontally-averaged HADCP beam is shown in red.

Site Instrumentation and Specifications

The SMR site was equipped with a Hydrolab MS5 for measurement of conductivity, temperature, depth, and turbidity. This instrument recorded these data at 15 minute intervals for the entire study period. A 300 kHz RDI Workhorse horizontal ADCP was also deployed at this site. This HADCP was configured to record one ensemble (average of 200 pings) every 3 minutes throughout the study period. HADCP bin size was 2.5 m throughout the study period. This site was also equipped with an ISCO 6712 automatic water sampler configured to sample every 14 hours for a total of 24 samples per program period, resulting in a service timeline of one fortnight.

Site Timeline

This site was installed on 14 May, and serviced on the dates indicated in Table 4. Dates of boat-based ADCP transects and sediment profiles are also indicated in Table 4.

Table 4. Servicing dates and notes from the SMR site

Service Date	Service Notes	Boat-based Measurements
14 May 2016	Installation	ADCP transects (RDI Workhorse 1200 kHz)
7 June 2016		ADCP transects (RDI Workhorse 1200 kHz)
30 June 2016		ADCP transects (RDI Workhorse 1200 kHz)
25 August 2016		ADCP transects (RDI Workhorse 1200 kHz),
22 September 2016		ADCP transects (RDI Workhorse 1200 kHz),

Discharge Time Series

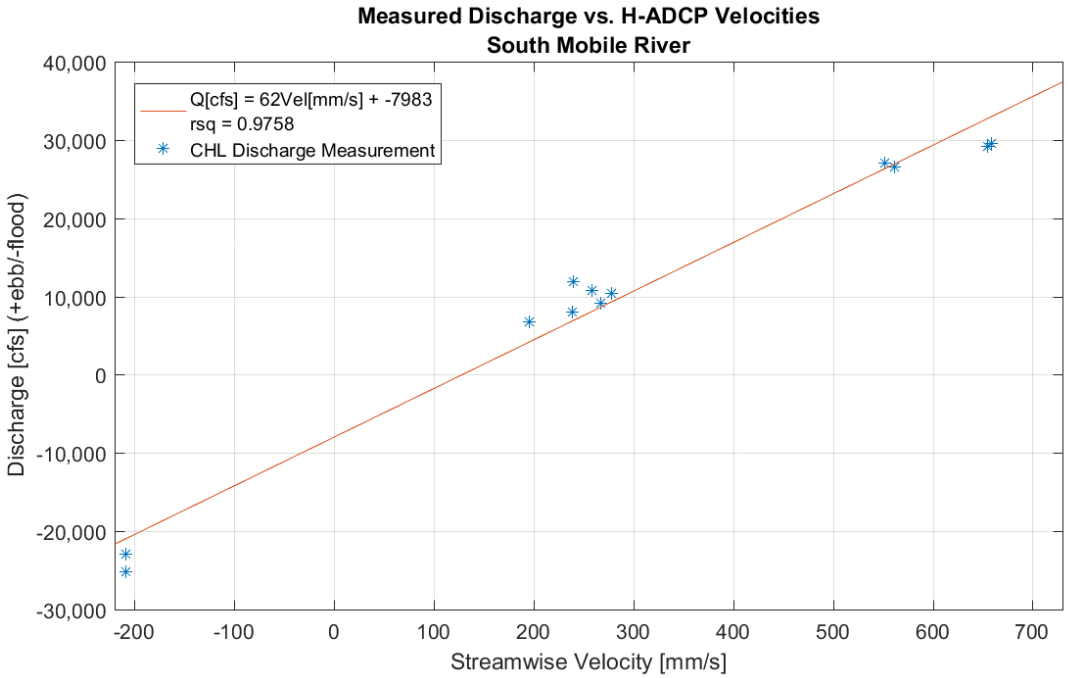

Figure 24. South Mobile River (SMR) Measured Discharge vs. H-ADCP Velocities

The average streamwise water velocities measured by the stationary HADCP were highly correlated ($R^2 = 0.97$) with the periodic discharge measurements collected using boat-based ADCP (Figure 24).

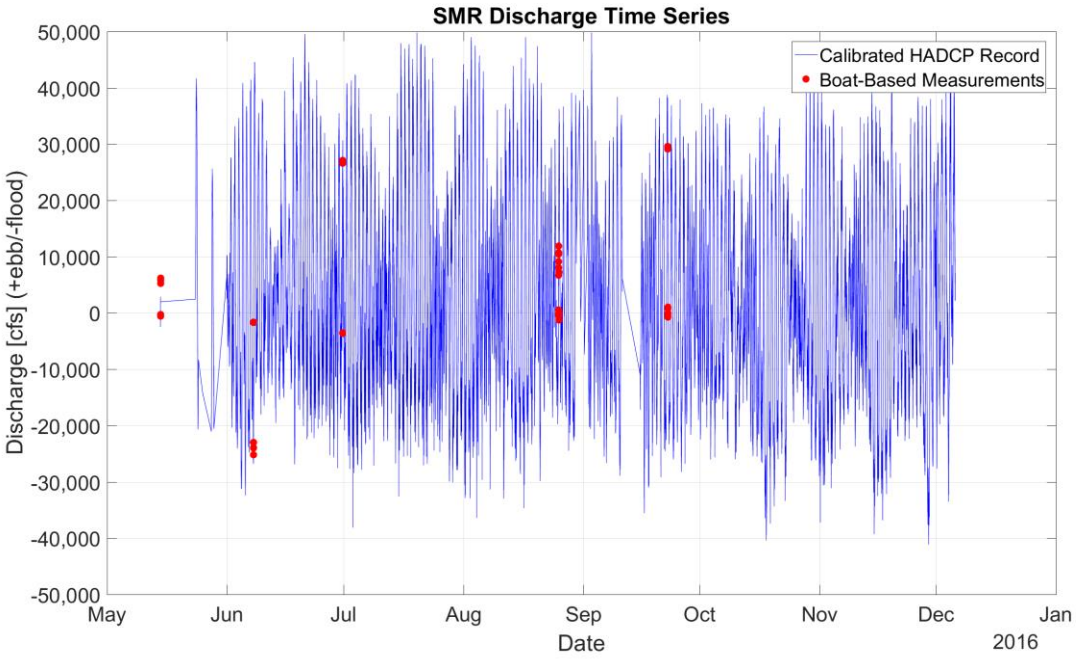

Figure 25. Time series of HADCP-calculated discharge at South Mobile River (SMR) site.

The times series of water discharge calculated from the HADCP at the South Mobile River site shows a very strong tidal influence, particularly as this site was only in place during the low-river-discharge summer-autumn of 2016. The daily and spring-neap tidal cycles can be clearly observed to modulate the flow here both upstream and downstream.

Suspended Sediment Time Series

There was no apparent correlation ($R^2 = 0.02$) between the CTD turbidity values and the suspended sediment concentration of the ISCO samples for the one-to-one calibration method.

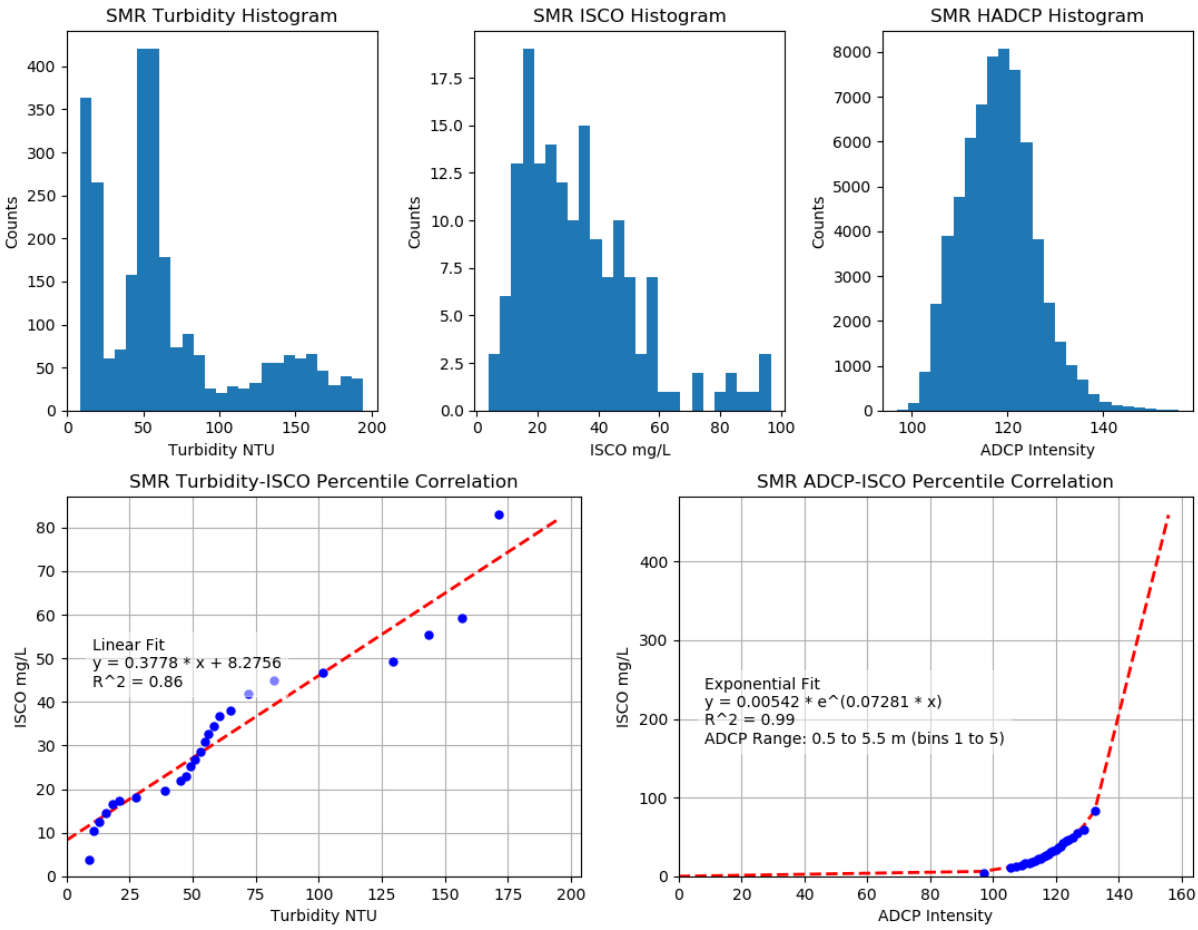

Figure 26. South Mobile River (SMR) CTD turbidity and HADCP vs. ISCO SSC Calibration.

The percentile calibration method resulted in high correlations for the CTD turbidity data (R^2 = 0.86, linear fit) and HADCP backscatter data (R^2 = 0.99, exponential fit). The CTD turbidity histogram (Figure 26, top left) shows a long tail, indicative of the noise prevalent in the signal. The resulting time series for both instruments (Figure 27) show little agreement with the discrete ISCO samples.

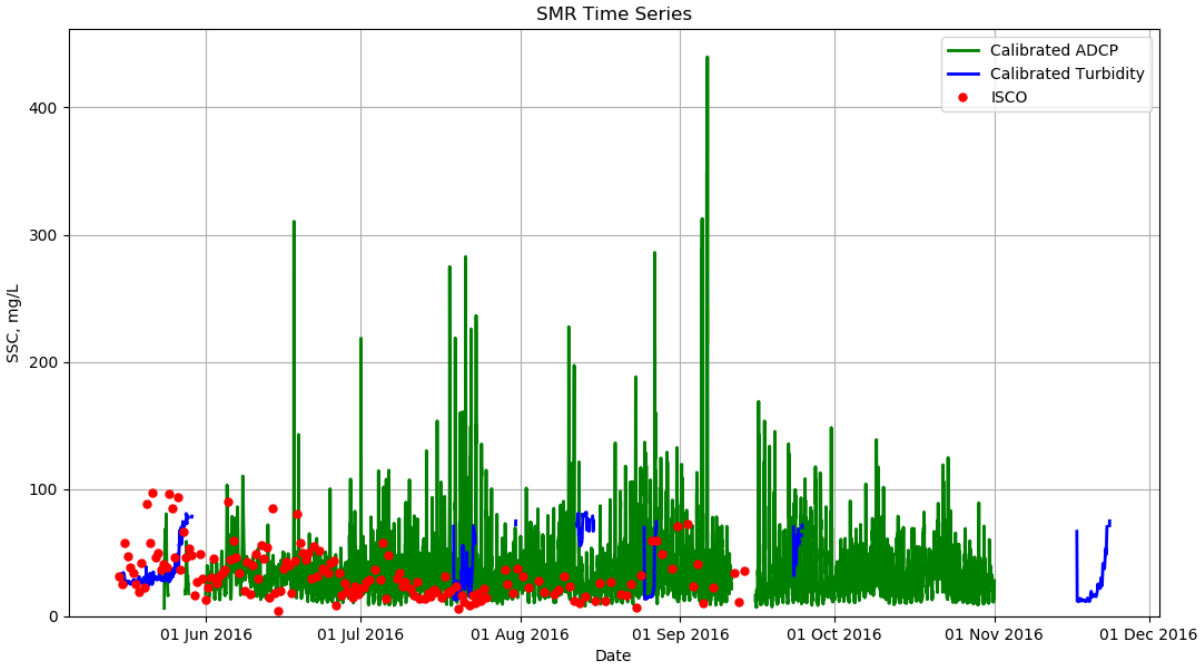

Figure 27. Time series of calibrated CTD turbidity, HADCP backscatter, and ISCO suspended sediment concentration at South Mobile River site.

Full Time Series

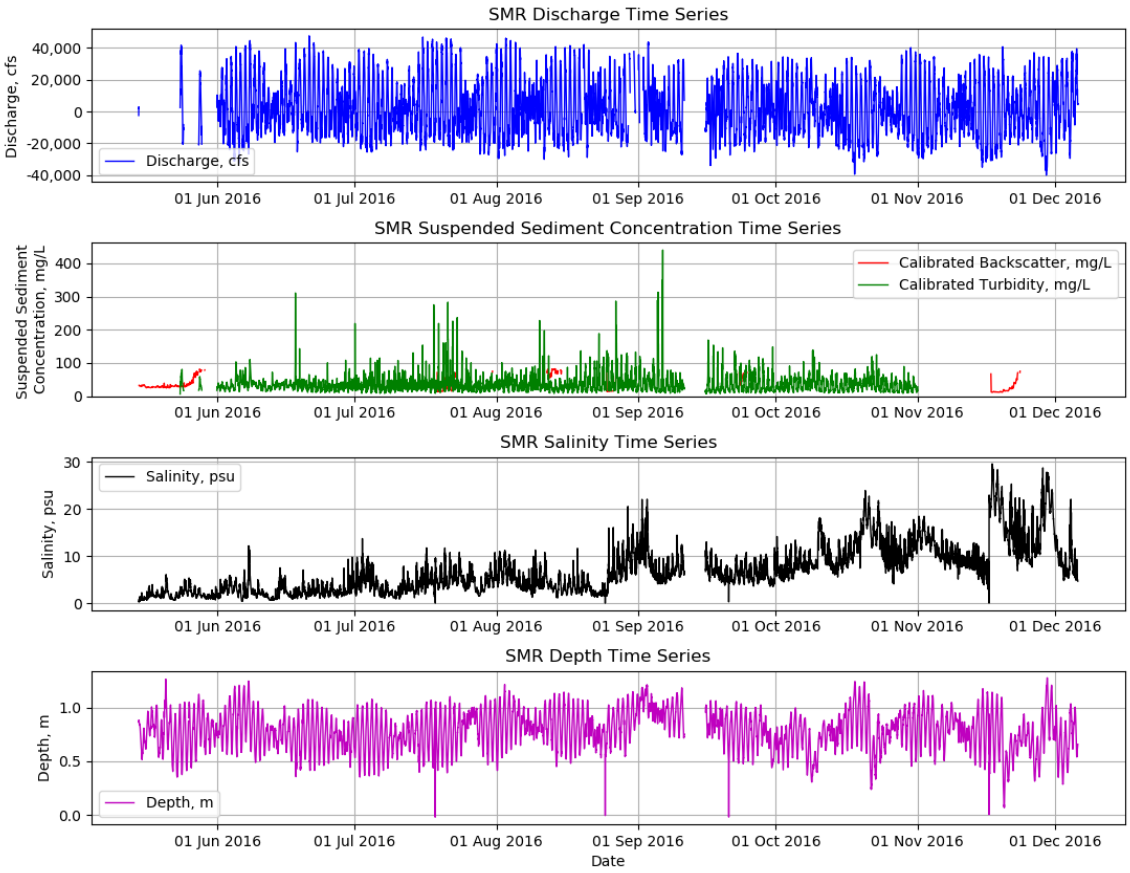

Figure 28. Full Time Series of Discharge, Suspended Sediment Concentration, Salinity, and Water Depth for the South Mobile River Site.

The 15 minute discharge time series for the South Mobile River site showed a hydrograph which was completely dominated by spring-neap and diurnal tidal variation during the Summer-Autumn of 2016. The salinity and water level records show tidal influence throughout, with increasing salinities into the winter months.

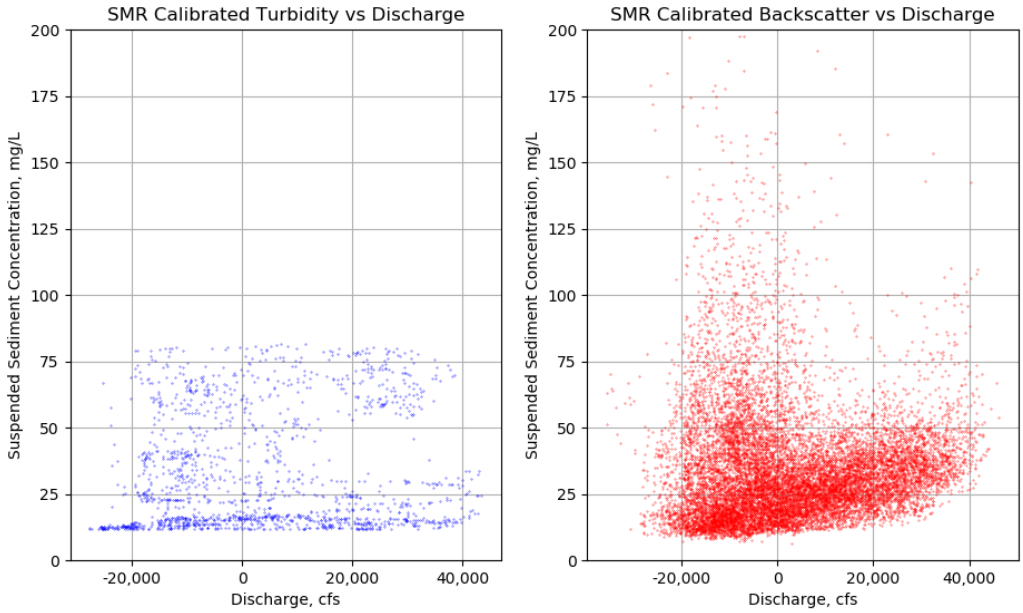

Figure 29. Relationships between water discharge and suspended sediment concentrations calculated from turbidity and ADCP backscatter.

The correlation between suspended sediment concentrations calculated from turbidity showed little correspondence with the water discharge, however suspended sediment concentrations calculated from HADCP backscatter exhibited a bimodal distribution, with high sediment concentrations observed for negative (flood tide) discharges and positive (ebb tide) discharges. These results indicated the sediment transport at this site was largely driven by the ebb and flood of tides, rather than the contribution of upstream river sediments.

Shipwave1 (SW1)

Location

Data were collected in Mobile Bay near Buccaneer Yacht Club (SW1 Site; 30.58N, 88.07W; Figure 30). This site was outfitted with a CTD (conductivity, temperature, depth, and turbidity), ADV (water velocity), ISCO sampler, anemometer (wind speed and direction), and wavestaff (capacitance wave gage) instruments.

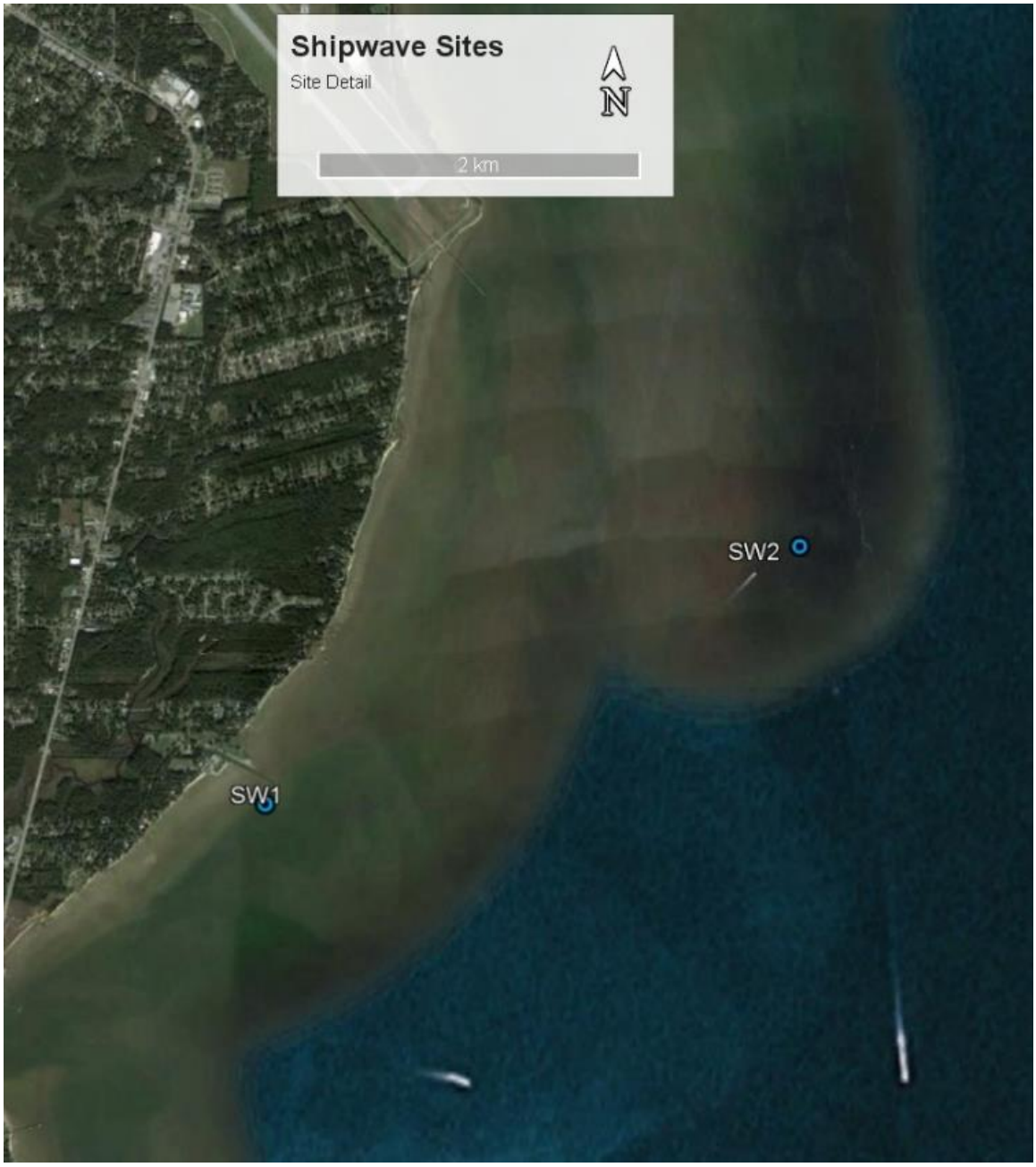

Figure 30. Shipwave Sites in detail. The locations of the two sites (SW1 and SW2) are shown with blue circles.

Site Instrumentation and Specifications

The SW1 site was equipped with a Hydrolab MS5 for measurement of conductivity, temperature, depth, and turbidity. This instrument was programmed to record these data at 15 minute intervals throughout the site deployment. A Nortek Vector ADV was also deployed at this site to measure point water velocity at 5 minute intervals throughout the site deployment. This site was also equipped with an ISCO 6712 automatic water sample configured to sample every 14 hours for a total of 24 samples per program period, resulting in a service timeline of one fortnight. In addition, a motion-sensing camera was installed to capture photographic evidence of ships generating wakes.

Figure 31. Platform setup at Shipwave1 site.

Site Timeline

This site was installed on 12 May 2016, and relocated on 5 December 2016. Each instrument at the site was plagued by problems, and the data from this site will not be analyzed here. The instruments in the water (MS5, ISCO, and ADV) were observed to be biofouled within one week of each servicing, providing little valid data. The capacitance wavestaff deployed at the site displayed confounding evidence of electrical malfunction, and the motion sensing camera captured many more false positives for ship motion than actual images of ships, as it was not programmed correctly.

The site was relocated in December 2016 to be closer to the Mobile Ship Channel.

Shipwave2 (SW2)

Location

Data were collected along the Mobile ship Channel 7 km south of the mouth of the Mobile River (SW2 Site 30.59N, 88.03W; Figure 30) over the period 8 December 2016 through 4 July 2017. This site was outfitted with CTD (conductivity, temperature, depth, and turbidity), ADV (water velocity), ISCO sampler, anemometer (wind speed and direction), and wavestaff (capacitance wave gage) instruments.

Site Instrumentation and Specifications

The SW2 site was equipped with the same instrumentation as SW1. A Hydrolab MS5 was used for measurement of conductivity, temperature, depth, and turbidity. This instrument was programmed to record these data at 15 minute intervals throughout the site deployment. A

Nortek Vector ADV was also deployed at this site to measure point water velocity at 5 minute intervals throughout the site deployment. This site was equipped with an ISCO 6712 automatic water sample configured to sample every 14 hours for a total of 24 samples per program period, resulting in a service timeline of one fortnight. In addition, a motion-sensing camera was installed to capture photographic evidence of ships generating wakes.

Figure 32. Platform setup at Shipwave2 site.

Site Timeline

This site was installed on 7 December 2016, and serviced on the dates indicated in Table 5. The ISCO water sampler was removed on 25 April 2017 to save money by requiring less frequent servicing of the station. This station was plagued by various computer system problems, and spent more time down than up. Data were only available for a total 66 days of the 7 months that the station was installed. The data that do exist for this site are confounded by the same issues as the data from the first Shipwave site.

Table 5. Servicing dates and notes for the SW2 site.

Service Date	Service Notes
21 December 2016	Programmed ISCO
5 January 2017	Previous ISCO program did not start, computer system down
9 January 2017	Replaced computer system battery backup, did not improve
11 January 2017	Replaced anemometer, diagnosed computer system needs new SD card

18 January 2017	Retrieved ISCO samples, restarted ISCO program, cleaned MS5, ISCO intake, and ADV
1 February 2017	Retrieved ISCO samples, restarted ISCO program
17 February 2017	Retrieved ISCO samples, restarted ISCO program, computer system still down
8 March 2017	Retrieved ISCO samples, restarted ISCO program, replaced computer system
16 March 2017	Previous ISCO program did not start, restarted ISCO program, replaced system batteries
20 March 2017	Cleaned MS5, ISCO intake, and ADV, repaired wavestaff wire
29 March 2017	Retrieved ISCO samples, restarted ISCO program, unable to service sensors due to high water
10 April 2017	Unable to service due to high water
13 April 2017	Previous ISCO program did not start, restarted ISCO program, cleaned MS5, ISCO intake, ADV, replaced system batteries, disconnected anemometer
25 April 2017	Retrieved ISCO samples, removed ISCO from station, cleaned MS5 and ADV

Suspended Sediment Time Series

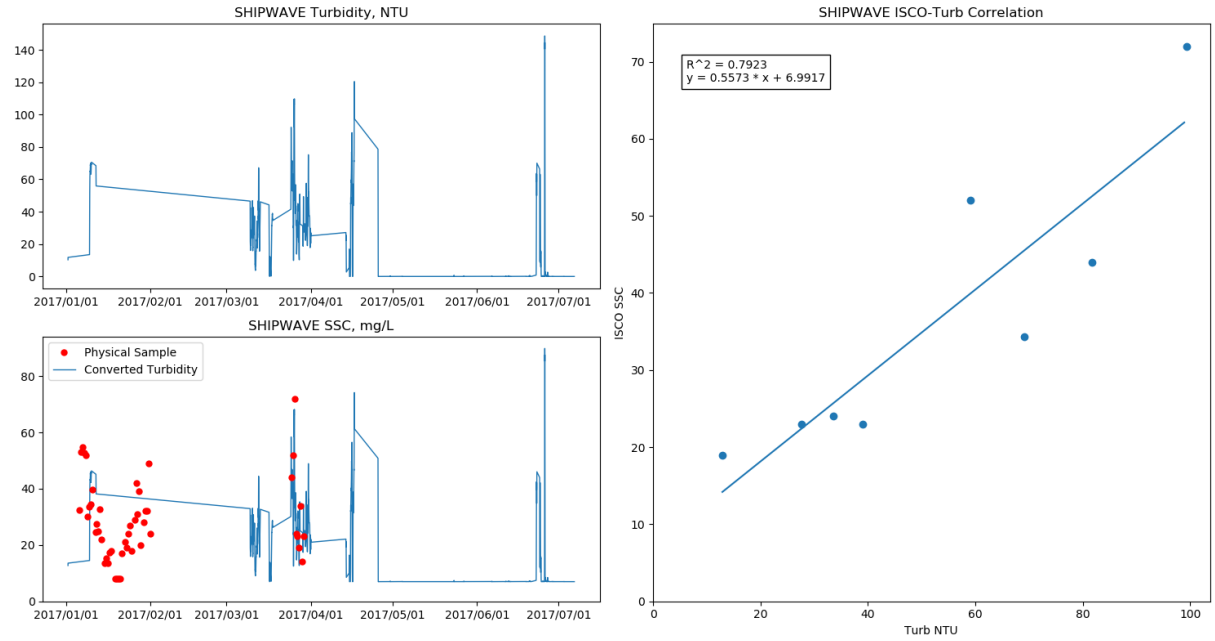

Figure 33. Shipwave Turbidity vs. ISCO SSC Calibration.

Much of the CTD turbidity time series at the Shipwave site was removed due to fouling, but the one-to-one calibration of remaining turbidity data and ISCO suspended sediment concentration showed a positive correlation ($R^2 = 0.79$). The resulting time series (Figure 33, bottom left) is missing large portions of the record, but it successfully tracked the concentrations observed from the ISCO bottles in late March 2017.

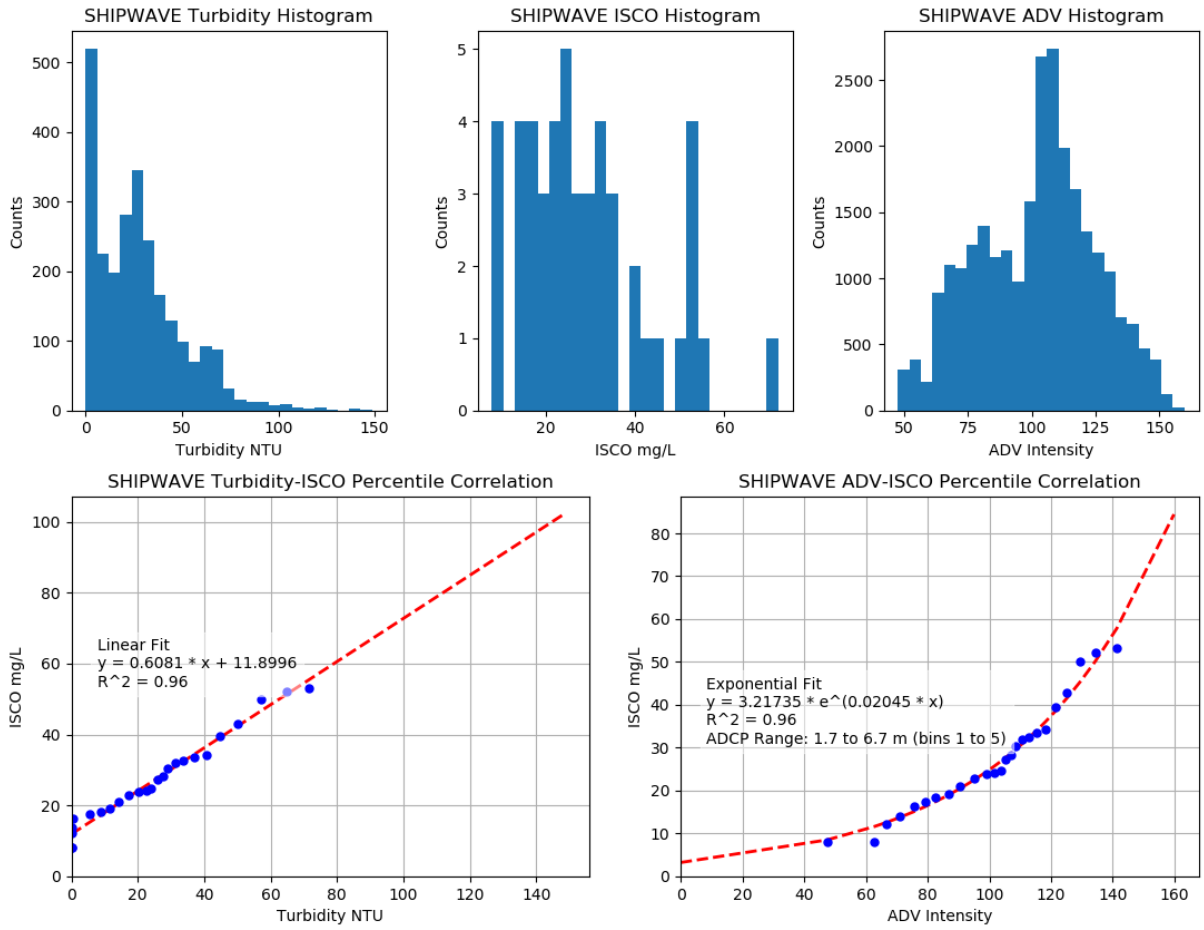

Figure 34. Shipwave Percentile-Based CTD Turbidity and ADV vs. ISCO SSC Calibration.

The percentile calibration method resulted in high correlations for the CTD turbidity data (R^2 = 0.96, linear fit) and ADV data (R^2 = 0.96, exponential fit). The resulting time series from these calibrations (Figure 35) has had many portions of the data removed due to equipment malfunction, but like the one-to-one calibration time series, it appears to track well the conditions observed in late March 2017.

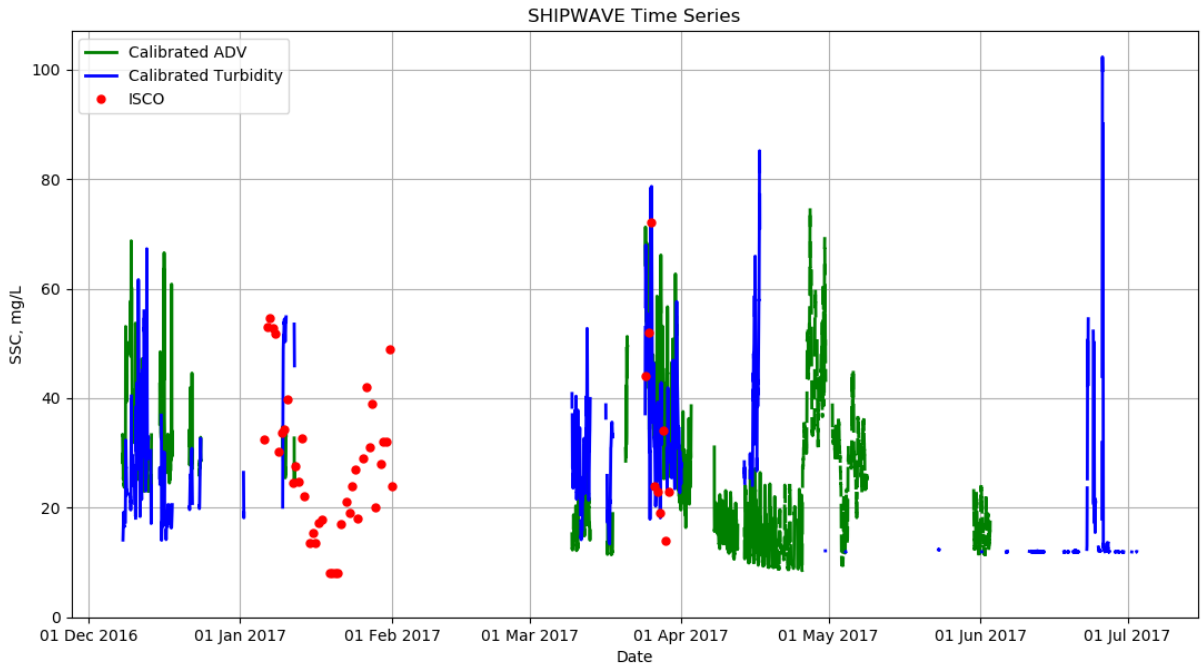

Figure 35. Time series of calibrated CTD turbidity, ADV backscatter, and ISCO suspended sediment concentration at Shipwave site.

Tensaw River at Causeway (TCW)

Location

Data were collected along the east bank of the Tensaw River north of the US Route 98 causeway (TCW Site 30.68N, 88.01W; Figure 36) over the period 18 December 2018 through 1 August 2017. This site was outfitted with CTD (conductivity, temperature, and turbidity), HADCP (water velocity), and ISCO (water samples for suspended sediment concentration) instruments. Periodic boat-based ADCP cross-sectional measurements were collected for calibrating the fixed HADCP instrument.

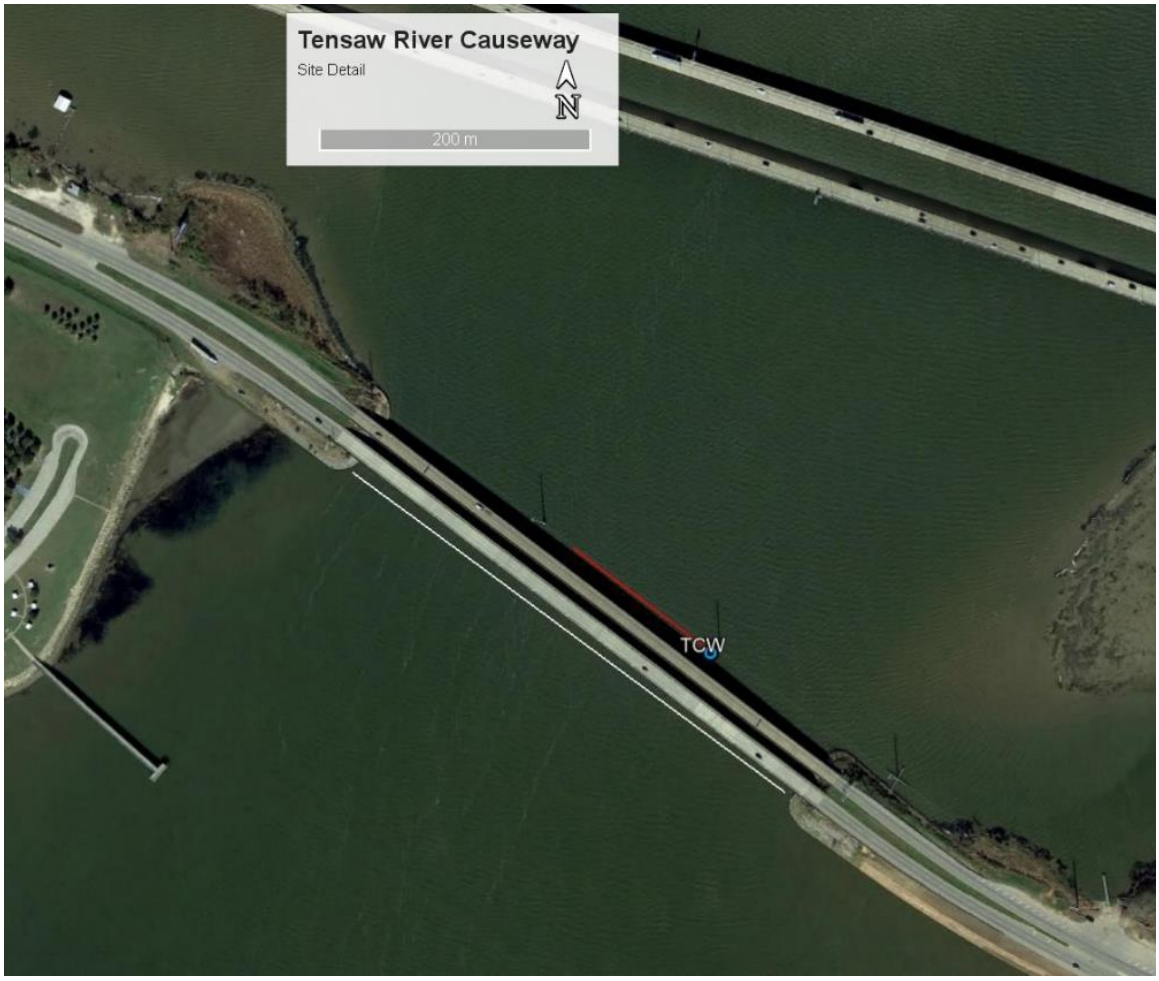

Figure 36. Tensaw River at Causeway (TCW) site detail. The location of the site instrumentation is shown with a blue circle, the location of the boat-based ADCP transect is shown with a white line (just south of bridge), and the extent of the horizontally averaged HADCP beam is shown in red.

Site Instrumentation and Specifications

The TCW site was equipped with a Hydrolab MS5 for measurement of conductivity, temperature, depth, and turbidity. This instrument recorded these data at 15 minute intervals for the study period. A 300 kHz RDI Workhorse horizontal ADCP was deployed at this site. This HADCP was configured to record one ensemble (60 pings) every three minutes. The site was also equipped with an ISCO 6712 automatic water sampler configured to sample every 14 hours for a total of 24 samples per program period, resulting in a service timeline of ~14 days.

Figure 37. Platform setup at Tensaw River at Causeway site.

Site Timeline

This site was installed on 13 December 2016, and serviced on the dates indicated in

Table 6. Servicing dates and notes from the TCW site

Service Date	Servicing Notes	Boat-based measurements
21 December 2016	Replaced charge controller, programmed ISCO	
4 January 2017	Retrieved ISCO samples, restarted ISCO program	ADCP transects (Sontek RiverSurveyor M9)
10 January 2017	Previous ISCO program did not start, restarted ISCO program, calibrated HADCP	
12 January 2017		ADCP transects (Sontek RiverSurveyor M9), ADCP transects (RDI Workhorse 12 kHz), sediment bed sample
18 January 2017	Previous ISCO program did not start, restarted ISCO program, cleaned MS5, ISCO intake, and HADCP	ADCP transects (Sontek RiverSurveyor M9)

1 February 2017	Retrieved ISCO samples, restarted ISCO program, cleaned MS5, ISCO intake, and HADCP	ADCP transects (Sontek RiverSurveyor M9)
14 February 2017	Retrieved ISCO samples, restarted ISCO program, cleaned MS5, ISCO intake, HADCP has no power	ADCP transects (Sontek RiverSurveyor M9)
17 February 2017	Fixed HADCP connection	
27 February 2017	Retrieved ISCO samples, restarted ISCO program, cleaned MS5, ISCO intake, and HADCP	ADCP transects (Sontek RiverSurveyor M9)
16 March 2017	Retrieved ISCO samples, restarted ISCO program, cleaned MS5, ISCO intake, and HADCP	ADCP transects (Sontek RiverSurveyor M9)
29 March 2017	Retrieved ISCO samples, restarted ISCO program, unable to service sensors due to high water	ADCP transects (Sontek RiverSurveyor M9)
10 April 2017	Retrieved ISCO samples, restarted ISCO program, cleaned MS5, ISCO intake, and HADCP	ADCP transects (Sontek RiverSurveyor M9)
25 April 2017	Retrieved ISCO samples, removed ISCO from platform, cleaned MS5, HADCP is stuck on beam and cannot be serviced	ADCP transects (Sontek RiverSurveyor M9)

Discharge Time Series

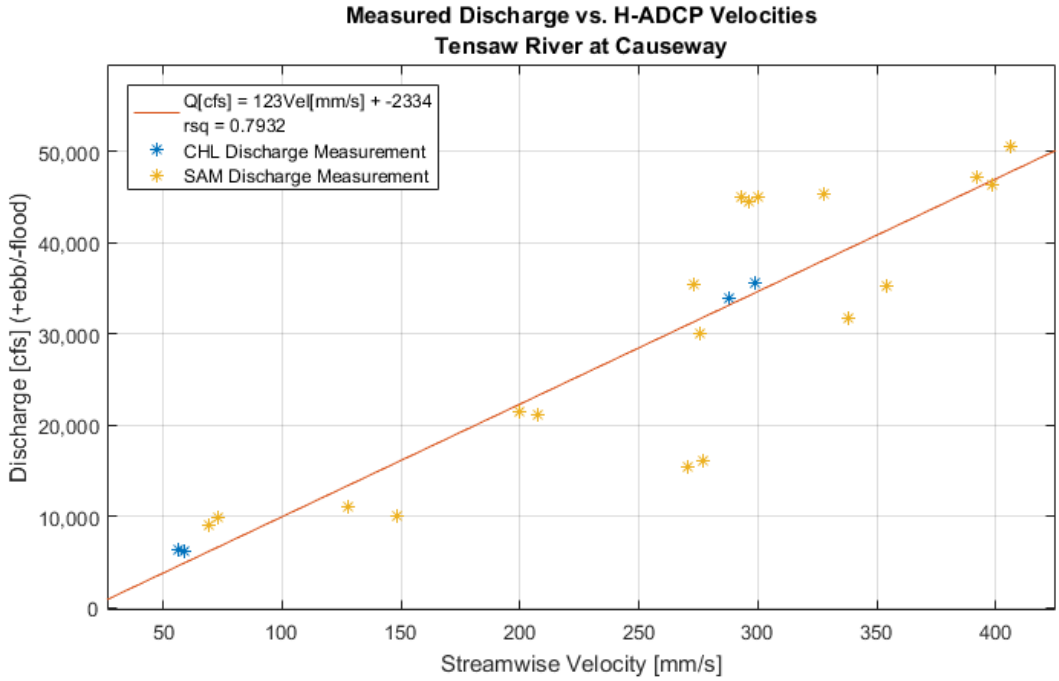

Figure 38. Tensaw River at Causeway (TCW) Measured Discharge vs. H-ADCP Velocities

The average streamwise water velocities measured by the stationary HADCP correlated well ($R^2 = 0.79$) with the periodic discharge measurements collected with boat-based ADCP (Figure 38). Calibration of these cross-sectional ADCP measurements to the observed horizontal water velocities allows the calculation of a continuous synthetic discharge time series.

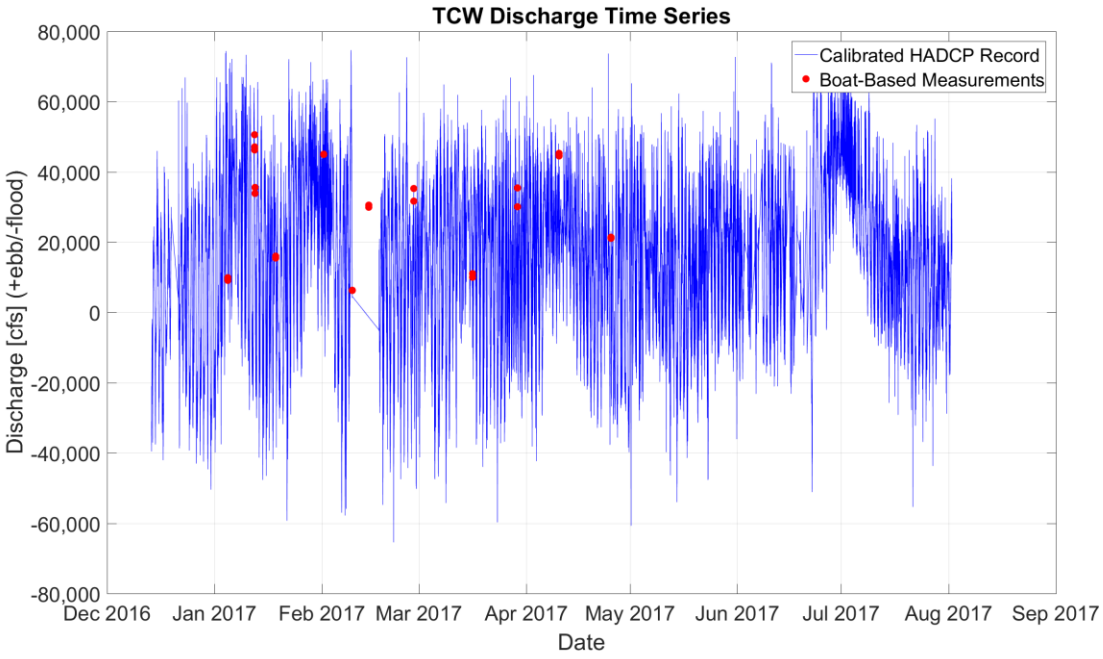

Figure 39. Time series of HADCP-calculated discharge at Tensaw River at Causeway (TCW) site.

The time series of water discharge at the TCW site shows a higher degree of tidal variability than that of the TR site, which is 12 miles upstream, evidence of its more distal location. This site (TCW) exhibits both spring-neap and diurnal tidal cycles, and its discharge modulates about 0 cfs as the tide comes in and out each day. The only period of record where the discharge remained consistently unidirectional was in July 2017, a tropical storm which was also observed in the records at the North Mobile River (NMR) and Tensaw River (TR) sites.

Suspended Sediment Time Series

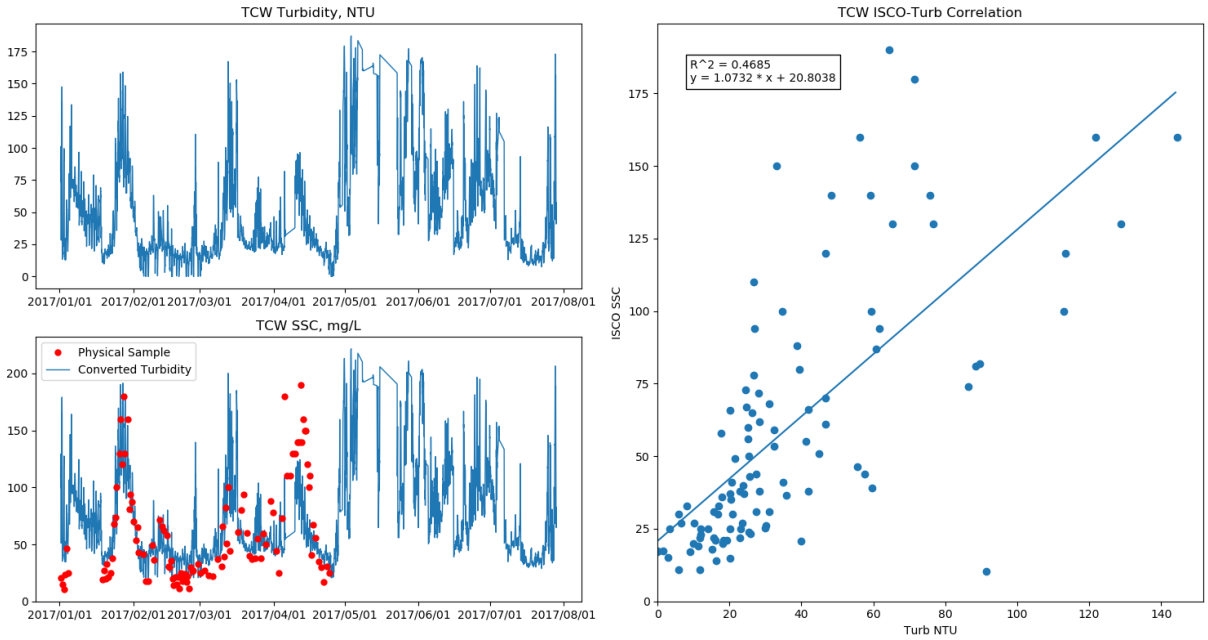

Figure 40. Tensaw River at Causeway (TR) Turbidity vs. ISCO SSC Calibration.

The one-to-one (time based) calibration of turbidity and ISCO suspended sediment concentration at the Tensaw River Causeway site showed a positive correlation ($R^2 = 0.47$). The resulting time series (Figure 40, bottom left) shows that the turbidity record for the most part is predicts the ISCO samples, with the exception of several samples collected in April 2017, which had higher suspended sediment concentrations than predicted by the turbidity. A pulse of high sediment concentration can be observed in this record associated with the tropical storm event in July 2017, mentioned above in the discharge record.

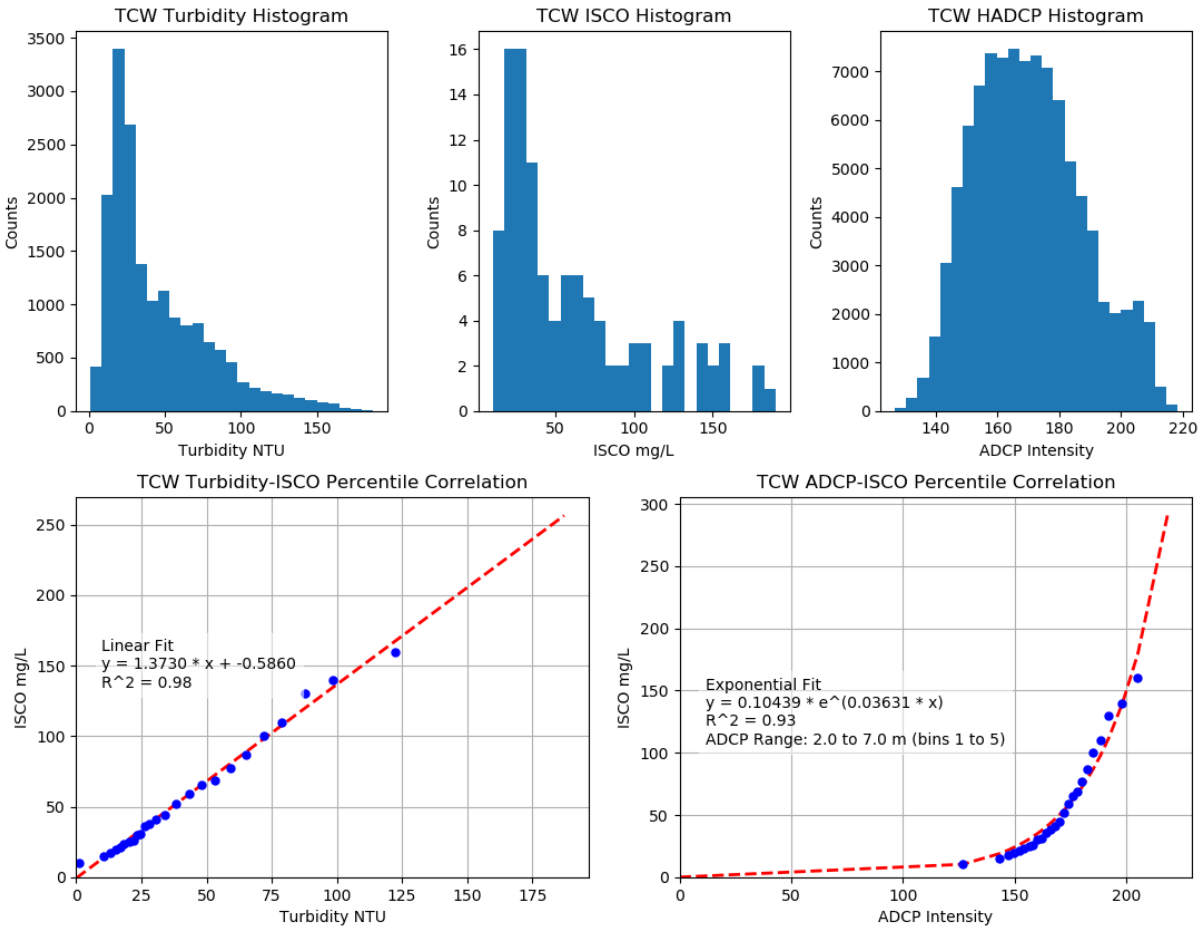

Figure 41. Tensaw River at Causeway (TCW) Percentile-Based CTD Turbidity and HADCP vs. ISCO SSC Calibration.

The percentile calibration method resulted in high correlations for the CTD turbidity data (R^2 = 0.98, linear fit) and HADCP backscatter data (R^2 = 0.93, exponential fit). The resulting time series from these calibrations (Figure 42) track the turbidity time series well. While the HADCP-derived time series exhibits more noise than the turbidity-derived time series, it follows the same general time trends. Notably, both records predict high sediment concentrations for the July 2017 flood.

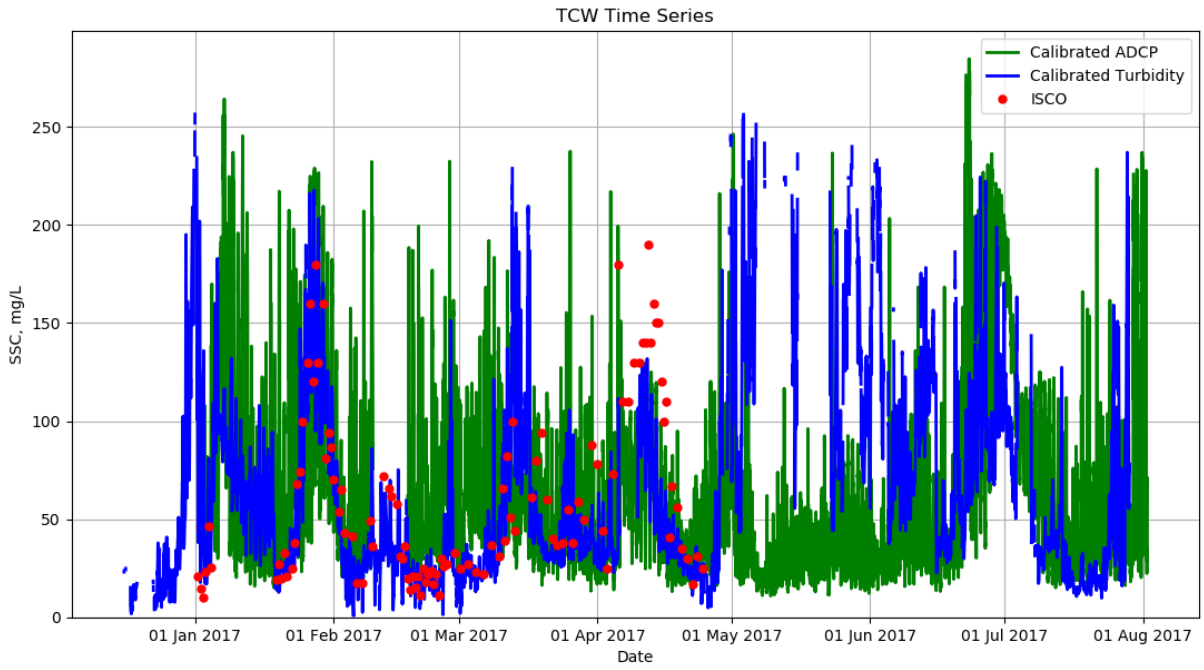

Figure 42. Time series of calibrated CTD turbidity, HADCP backscatter, and ISCO suspended sediment concentration at Tensaw River at Causeway site.

Full Time Series

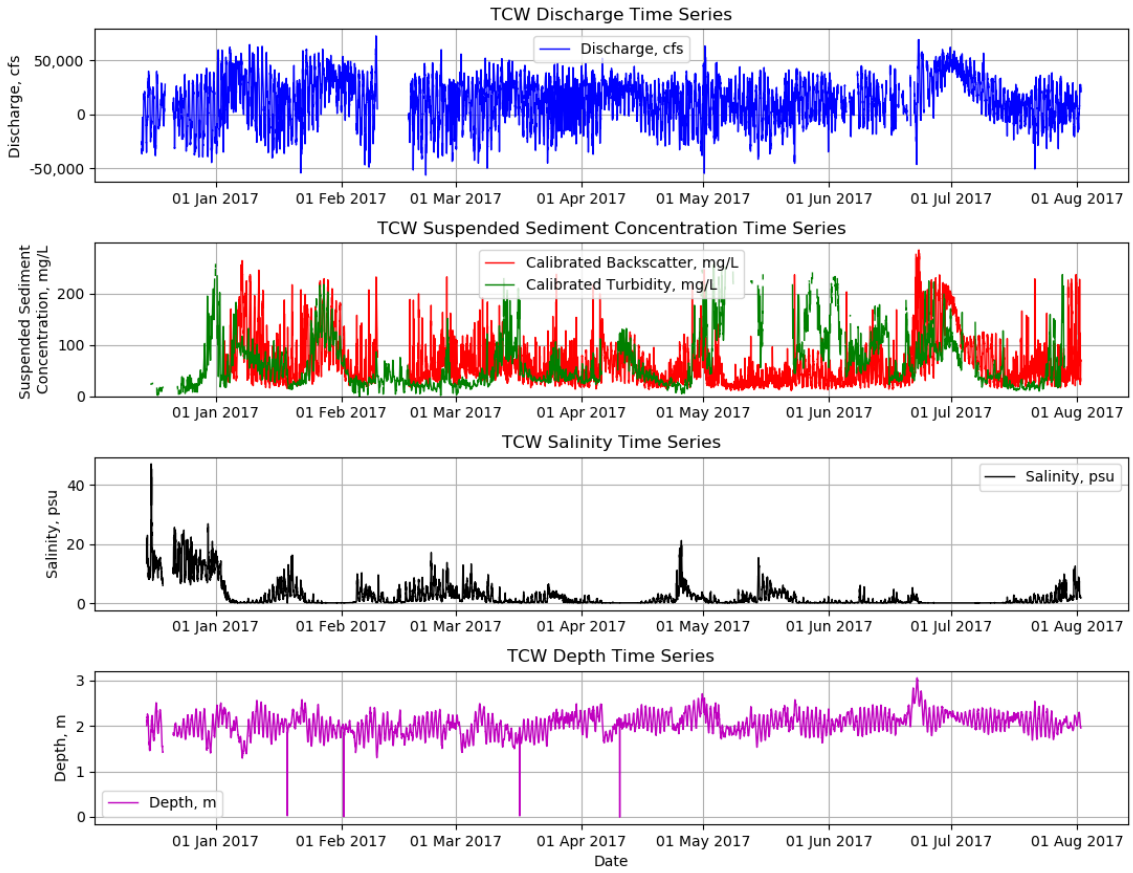

Figure 43. Full Time Series of Discharge, Suspended Sediment Concentration, Salinity, and Water Depth for the Tensaw River at Causeway Site.

The full 15 minute-interval time series (Figure 43) for the Tensaw River at Causeway station showed a hydrograph with a mixture of tidal- and river-dominated intervals. For the majority of the time series, the diurnal and spring-neap tides were observed, punctuated by moderate river floods in January, March, April, and July. Each river flood was associated with a peak in suspended sediment concentration during the rising limb of the flood, indicating a possible supply limit on sediment for this area, which becomes exhausted early in the flood. These river flood events are also associated with salinity minima, punctuated by salinity peaks between floods.

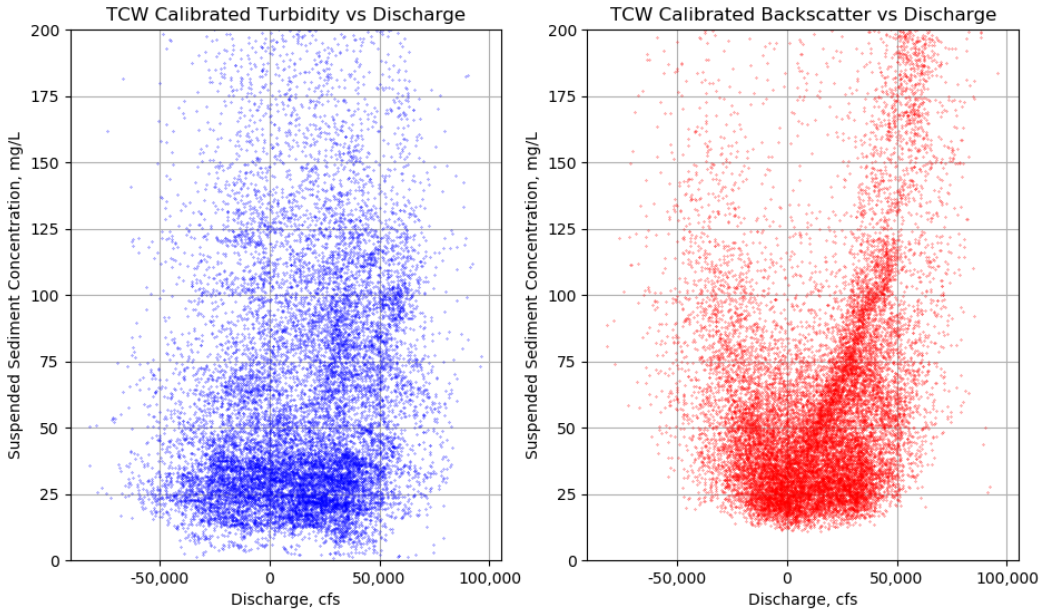

Figure 44. Relationships between water discharge and suspended sediment concentrations calculated from turbidity and ADCP backscatter.

The relationship between suspended sediment concentrations and water discharge at the Tensaw River at Causeway site (Figure 44) exhibited a similar bimodal distribution to that of the South Mobile River site, particularly in the sediment concentrations calculated from the HADCP backscatter data. This may be related to the dominance of tidal variability over much of the time series, however the highest sediment concentrations were observed for the highest water discharge, during the July 2017 river flood.

Apalachee River (AR)

Location

Data were collected in the Apalachee River from a transmission line pole north of US Route 98 causeway (AR Site 30.67N, 87.95W; Figure 45) over the period 12 January 2017 through 1 August 2017. In this location the river thalweg tracks towards the west bank of the river, so the site was placed to record the conditions in the river thalweg, rather than the relatively flat shallow channel area east of the transmission line pole. This site was outfitted with CTD (conductivity, temperature, and turbidity), HADCP (water velocity), and ISCO (water samples for suspended sediment concentration) instruments. Periodic boat-based ADCP cross-sectional measurements were collected for calibrating the fixed HADCP instrument.

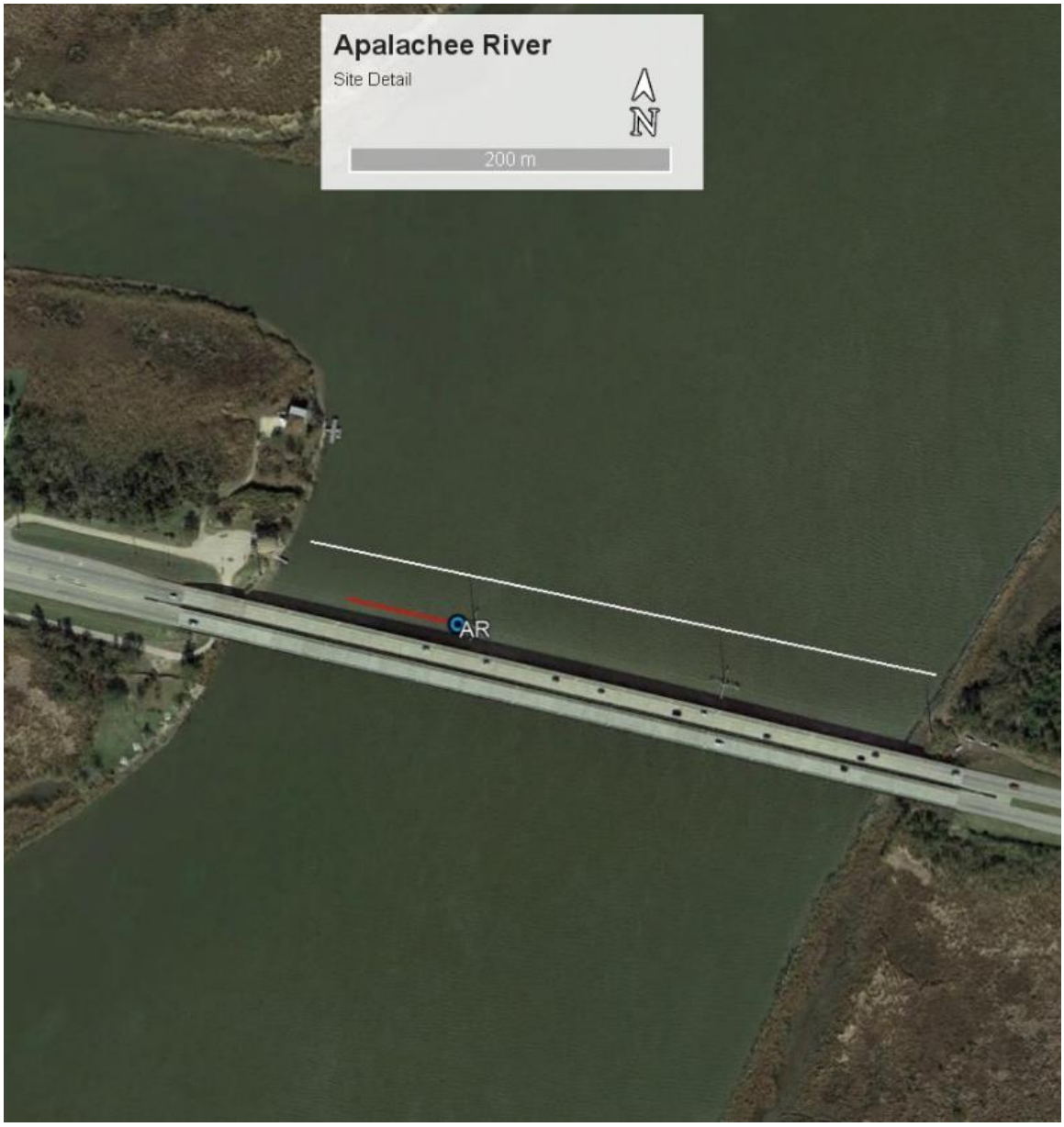

Figure 45. Apalachee River (AR) site detail. The location of the site instrumentation is shown with a blue circle, the location of the boat-based ADCP transect is shown with a while line, and the extent of the horizontally averaged HADCP beam is shown in red.

Site Instrumentation and Specifications

The AR site was equipped with a YSI multiparameter sonde for measurement of conductivity, temperature, and turbidity. This instrument was configured to record these parameters every one minute for the study period. As the YSI sonde does not have a vented pressure sensor, and additional Druck pressure sensor was added at this station. This sensor recorded water depth at 10 second intervals. A 600 kHz RDI Workhorse horizontal ADCP was deployed at this site. The HADCP was configured to record one ensemble (60 pings) every 5 minutes, with a bin size of 1 m. This site was also equipped with an ISCO 6712 automatic water sample configured to sample every 14 hours for a total of 24 samples per program and a service timeline of one fortnight.

Figure 46. Platform setup at Apalachee River site.

Site Timeline

This site was installed on 14 December 2016, and serviced on the dates indicated in Table 7. The ISCO water sampler was removed on 25 April 2017 to save money by requiring less frequent servicing of the station. Dates of boat-based ADCP transects are also given in Table 7. The Druck sensor was incorrectly wired until 16 March 2017, and therefore recorded no valid data prior to that date.

Table 7. Servicing dates and notes from the AR site

Service Date	Servicing Notes	Boat-based Measurements
20 December 2016	Started ISCO program	
4 January 2017	Retrieved ISCO samples, restarted ISCO program	ADCP transects (Sontek RiverSurveyor M9)
10 January 2017	Previous ISCO program did not start, restarted ISCO program, computer system not working, computer system removed (for later replacement)	
11 January 2017	Installed new computer system, reconfigured sensors (HADCP, YSI, Druck)	
12 January 2017		ADCP transects (RDI 1200 kHz Workhorse), one bed sample, one sediment profile (no sediment in sample)
18 January 2017	Retrieved ISCO samples, restarted ISCO program, cleaned YSI, ISCO intake, and HADCP	ADCP transects (Sontek RiverSurveyor M9)

1 February 2017	Retrieved ISCO samples, restarted ISCO program	ADCP transects (Sontek RiverSurveyor M9)
14 February 2017	Retrieved ISCO samples, restarted ISCO program	ADCP transects (Sontek RiverSurveyor M9)
6 March 2017	Retrieved ISCO samples, restarted ISCO program, cleaned YSI, Druck, ISCO intake, and HADCP	ADCP transects (Sontek RiverSurveyor M9)
8 March 2017	Replaced computer battery backup, diagnosed faulty Druck signal connection	
16 March 2017	Retrieved ISCO samples, restarted ISCO program, cleaned YSI, Druck, and ISCO intake, corrected Druck wiring	ADCP transects (Sontek RiverSurveyor M9)
29 March 2017	Retrieved ISCO samples, restarted ISCO program, unable to service sensors due to high water	ADCP transects (Sontek RiverSurveyor M9)
10 April 2017	Retrieved ISCO samples, restarted ISCO program, cleaned YSI, Druck, ISCO intake, and HADCP	ADCP transects (Sontek RiverSurveyor M9)
25 April 2017	Retrieved ISCO samples, removed ISCO from platform, cleaned YSI and HADCP	ADCP transects (Sontek RiverSurveyor M9)

Discharge Time Series

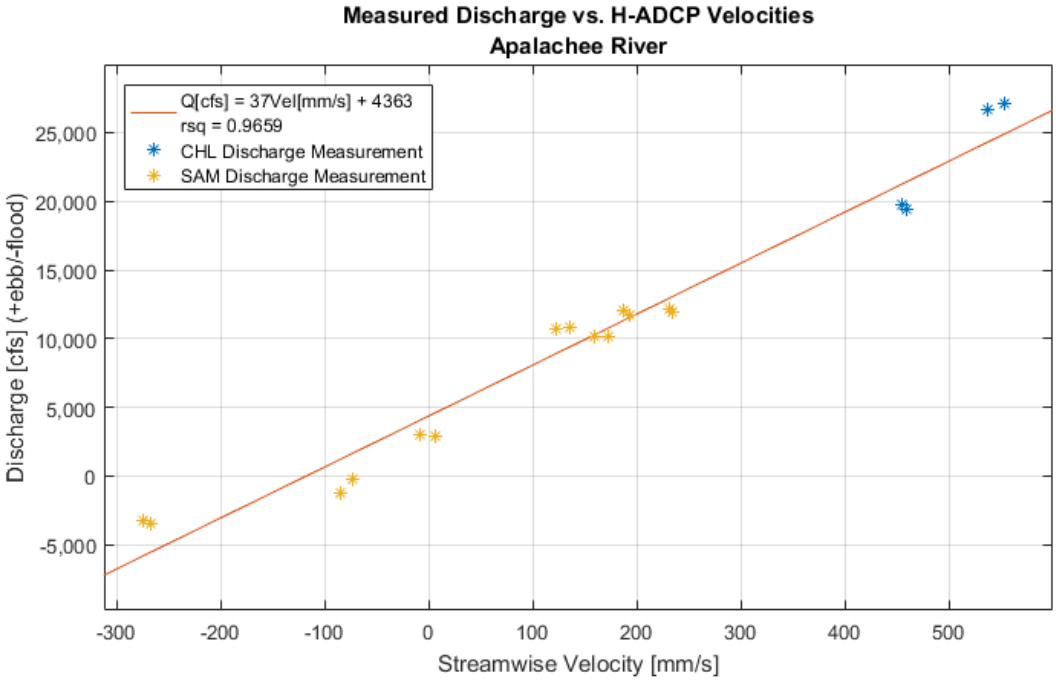

Figure 47. Apalachee River (AR) Measured Discharge vs. H-ADCP Velocities

The average streamwise water velocities measured by the stationary HADCP correlated well ($R^2 = 0.97$) with the periodic discharge measurements collected by boat-based ADCP (Figure 47). Calibration of these cross-sectional ADCP measurements to the observed horizontal water velocities allows the calculation of a continuous synthetic discharge time series.

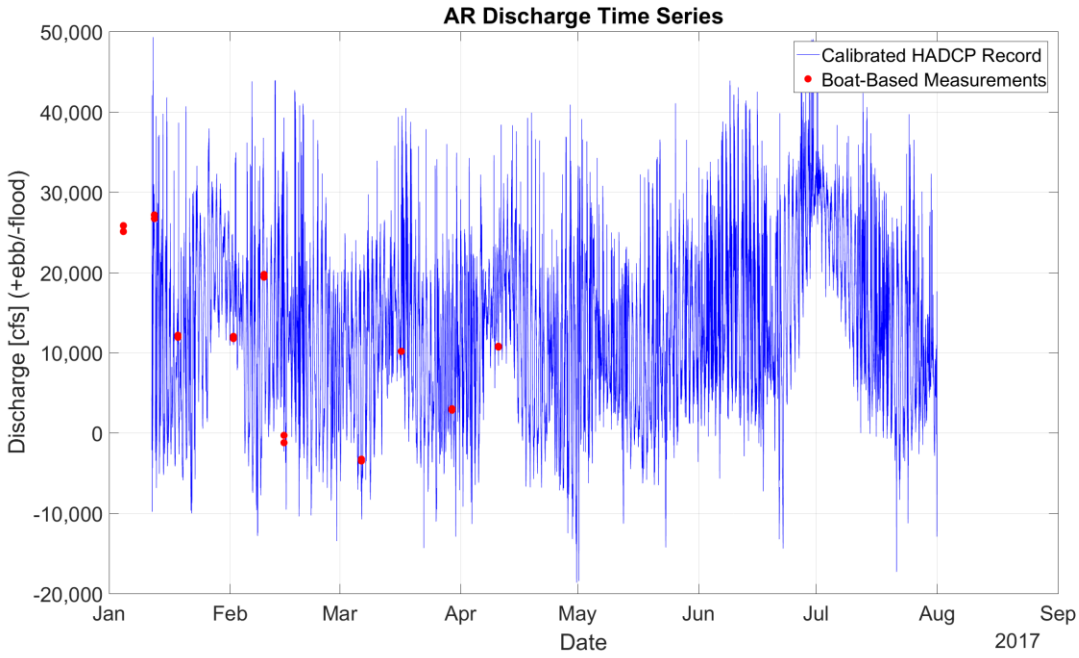

Figure 48. Time series of HADCP-calculated discharge at Apalachee River (AR) site.

Like the time series at TCW, the time series of water discharge at the AR site (Figure 48) shows a higher degree of tidal variability than that of the TR site, which is 10 miles upstream. This site (AR) exhibits less tidal variability than the TCW site, but still shows both spring-neap and diurnal tidal cycles, and its discharge occasionally modulates below 0 cfs during low flow periods. This site also shows a consistently unidirectional flow during the July 2017 Flood, as observed at several of the stations.

Suspended Sediment Cross-Section Calibration

One profile of suspended sediment was attempted at this site; however, the water samples contained no measurable sediment so the calibration was not possible.

Suspended Sediment Time Series

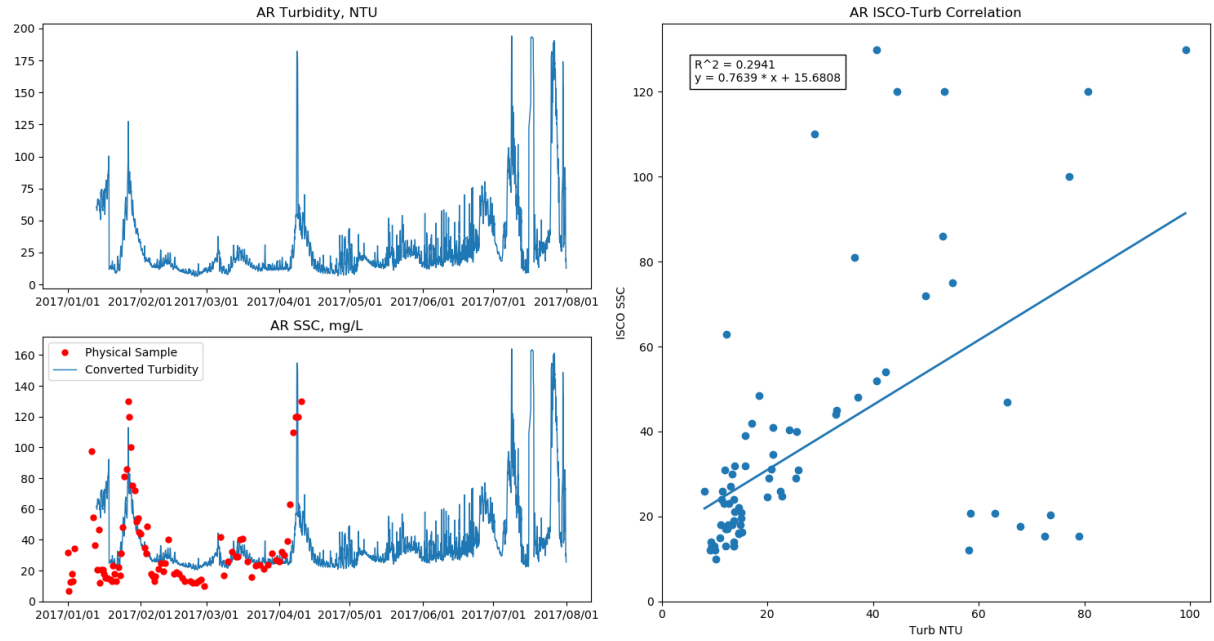

Figure 49. Apalachee River (AR) Turbidity vs. ISCO SSC Calibration.

The one-to-one (time based) calibration of turbidity and ISCO suspended sediment concentration at the Apalachee site showed a weak positive correlation ($R^2 = 0.29$). The resulting time series (Figure 49, bottom left) shows that the turbidity record for the most part predicts the ISCO samples, with several time periods where the suspended sediment concentration was overestimated by turbidity time series.

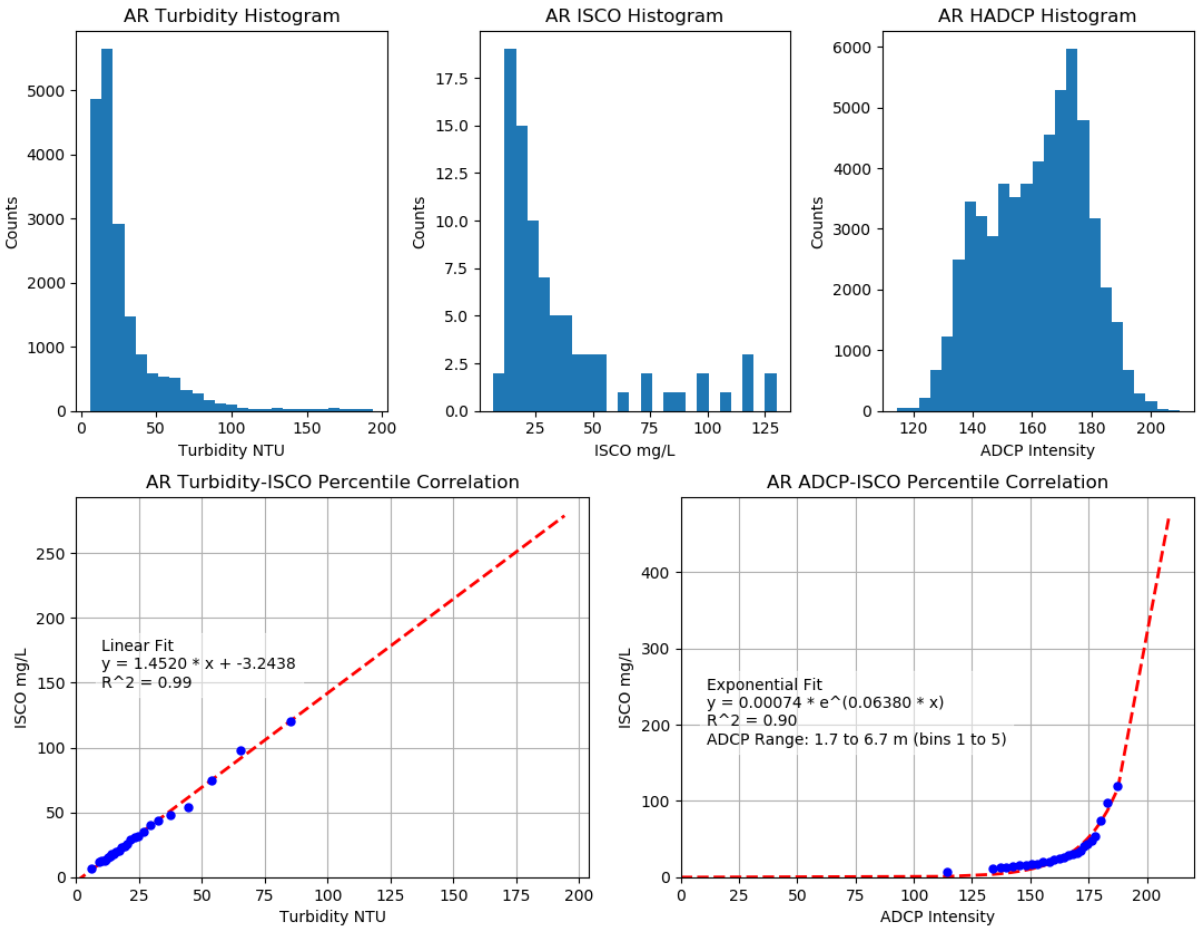

Figure 50. Apalachee River (AR) Percentile-Based CTD Turbidity and HADCP vs. ISCO SSC Calibration.

The percentile calibration method resulted in high correlations for the CTD turbidity data (R^2 = 0.99, linear fit) and HADCP backscatter data (R^2 = 0.90, exponential fit). The resulting time series from these calibrations (Figure 51) track the ISCO time series well. The HADCP-derived time series exhibits more noise than the turbidity time series (particularly during the January-April 2017 interval), it follows the same general time trends. Like the time series at the TCW station, both records predict high sediment concentrations for the July 2017 flood.

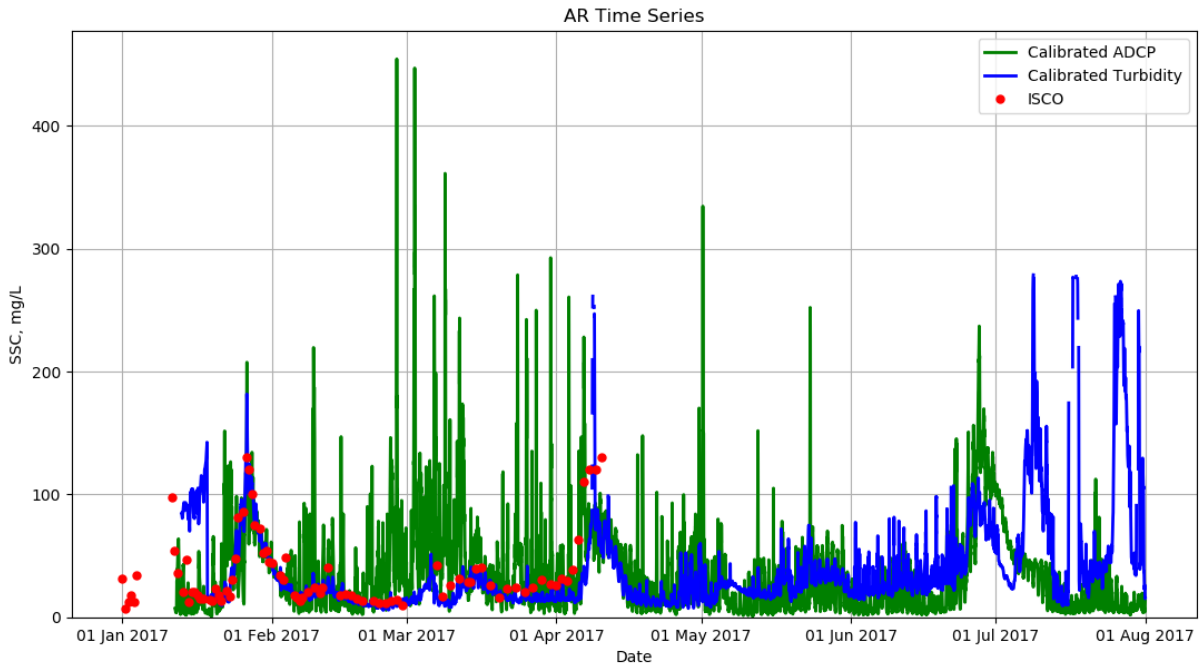

Figure 51. Time series of calibrated CTD turbidity, HADCP backscatter, and ISCO suspended sediment concentration at Apalachee River site.

Full Time Series

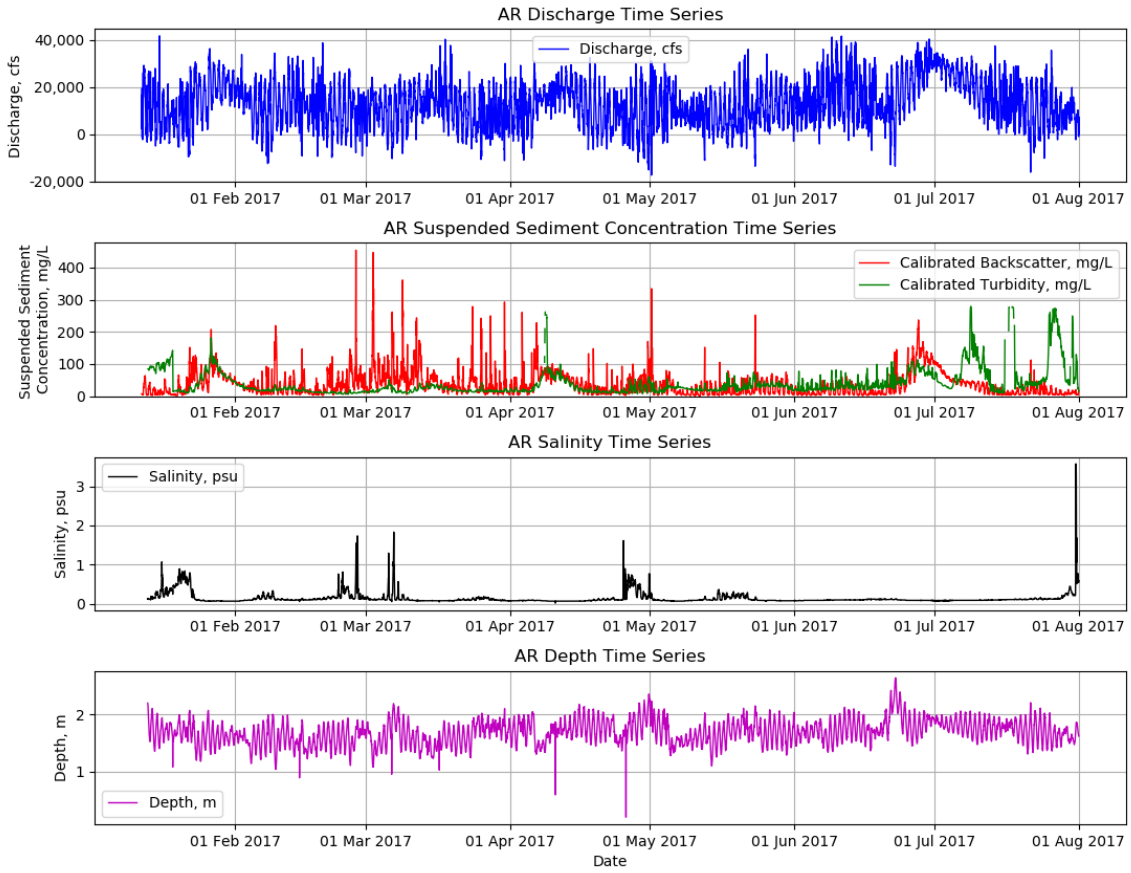

Figure 52. Full Time Series of Discharge, Suspended Sediment Concentration, Salinity, and Water Depth for the Apalachee River Site.

The full time series for the Apalachee River Site (Figure 52) showed a mixed signal, with a river flood hydrograph that has diurnal tidal variability overprinted. The largest pulses of suspended sediment were associated with the onset of periodic river floods; however, this site also exhibited several suspended sediment concentration peaks during regular tidal flows. The salinity record suggests that the tidal influence, while effective in modulating the water level and water discharge is not great enough to appreciably enhance the salinity, except for a few brief low-flow periods.

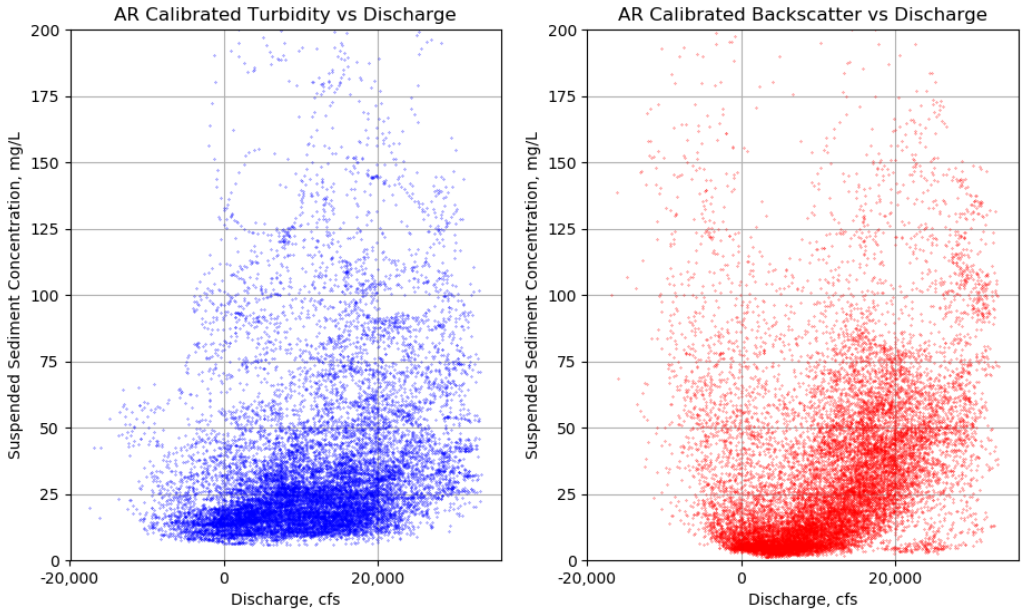

Figure 53. Relationships between water discharge and suspended sediment concentrations calculated from turbidity and ADCP backscatter.

The Apalachee River site exhibited a positive correlation between suspended sediment concentration and water discharge (Figure 53), with a generally exponential rise in suspended sediment concentration for increasing positive water discharge (this is the river flood signal, seen best in the HADCP backscatter-calibrated sediment data). The tidal signal at this site could be best observed in the negative discharge interval (flood-tidal flows), where there was a sparse-but-present population of high suspended sediment concentrations.

Blakely River (AR)

Location

Data were collected in the Blakely River from a transmission line pole north of US Route 98 causeway (BR Site 30.67N, 87.92W; Figure 54) over the period 11 January 2017 through 1 August 2017. Like at the Apalachee River site, here the river thalweg tracks towards the west bank of the river, so the site was placed to record the conditions in the river thalweg, rather than the relatively flat shallow channel area east of the transmission line pole. This site was outfitted with CTD (conductivity, temperature, and turbidity), HADCP (water velocity), and ISCO (water samples for suspended sediment concentration) instruments. Periodic boat-based ADCP cross-sectional measurements were collected for calibrating the fixed HADCP instrument.

Figure 54. Blakely River (BR) site detail. The location of the site instrumentation is shown with a blue circle, the location of the boat-based ADCP transect is shown with a white line, and the extent of the horizontally average HADCP beam is shown in red.

Site Instrumentation and Specifications

The BR site was equipped with a YSI multiparameter sonde for measurement of conductivity, temperature and turbidity. This instrument was configured to record these parameters every one minute for the study period. As the YSI sonde does not have a vented pressure sensor, and additional Druck pressure sensor was added at this station. This sensor recorded water depth at 1 minute intervals. A 600 kHz RDI Workhorse horizontal ADCP was deployed at this site. The HADCP was configured to record one ensemble (60 pings) every 5 minutes from 11 January 2017 through 28 March 2017. At this time the HADCP was reconfigured to record one ensemble (60 pings) every 10 minutes. HADCP profiles were configured with a bin size of 1 m throughout the study period. This site was also equipped with an ISCO 6712 automatic water

sample configured to sample every 14 hours for a total of 24 samples per program and a service timeline of one fortnight.

Figure 55. Platform setup at Blakely River site.

Site Timeline

This site was installed 13 December 2016, and serviced on the dates indicated in Table 8. The ISCO water sampler was removed on 25 April 2017 to save money by requiring less frequent servicing of the station. Dates of boat-based ADCP transects and sediment profiles are also indicated in Table 8. The Druck sensor was incorrectly wired until 17 March 2017, and therefore recorded no valid data prior to that date.

Table 8. Servicing dates and notes from the BR site.

Service Date	Servicing Notes	Boat-based measurements
20 December 2016	Installed cellular antenna, started ISCO program	
3 January 2017	Previous ISCO program malfunctioned, restarted ISCO program	ADCP transects (Sontek RiverSurveyor M9)
10 January 2017	ISCO confirmed working, repositioned HADCP	ADCP transects (RDI 1200 kHz Workhorse), sediment profiles
12 January 2017		ADCP transects (RDI 1200 kHz Workhorse)
18 January 2017	Retrieved ISCO samples, ISCO not working, cleaned YSI and ISCO intake	ADCP transects (Sontek RiverSurveyor M9)
1 February 2017	ISCO still not working, observed solar panel needs to be remounted	ADCP transects (Sontek RiverSurveyor M9)

14 February 2017	Replaced ISCO, started ISCO program, cleaned YSI, Druck, and ISCO intake	ADCP transects (Sontek RiverSurveyor M9)
6 March 2017	Retrieved ISCO samples, restarted ISCO program	ADCP transects (Sontek RiverSurveyor M9)
8 March 2017	Cleaned YSI, Druck, ISCO intake, and HADCP, replaced computer system battery backup, diagnosed incorrect signal wiring for Druck	
16 March 2017	Retrieved ISCO samples, restarted ISCO program, cleaned YSI, Druck, ISCO intake, and HADCP	ADCP transects (Sontek RiverSurveyor M9)
17 March 2017	Corrected Druck wiring	
29 March 2017	Retrieved ISCO samples, restarted ISCO program, unable to service sensors due to high water	ADCP transects (Sontek RiverSurveyor M9)
10 April 2017	Retrieved ISCO samples, restarted ISCO program, cleaned YSI, ISCO intake, and HADCP	ADCP transects (Sontek RiverSurveyor M9)
25 April 2017	Retrieved ISCO samples, removed ISCO from platform, cleaned YSI and HADCP	

Discharge Time Series

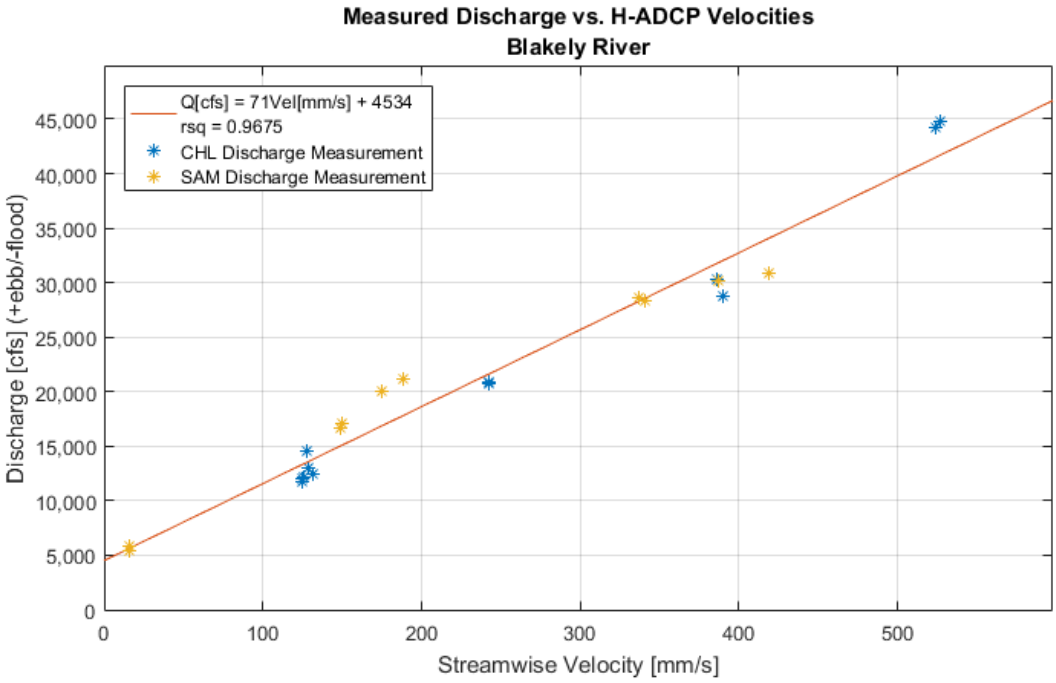

Figure 56. Blakely River (BR) Measured Discharge vs. H-ADCP Velocities

The average streamwise water velocities measured by the stationary HADCP correlated well ($R^2 = 0.97$) with the periodic discharge measurements collected with boat-based ADCP (Figure 56). Calibration of these cross-sectional ADCP measurements to the observed horizontal water velocities allows the calculation of a continuous synthetic discharge time series.

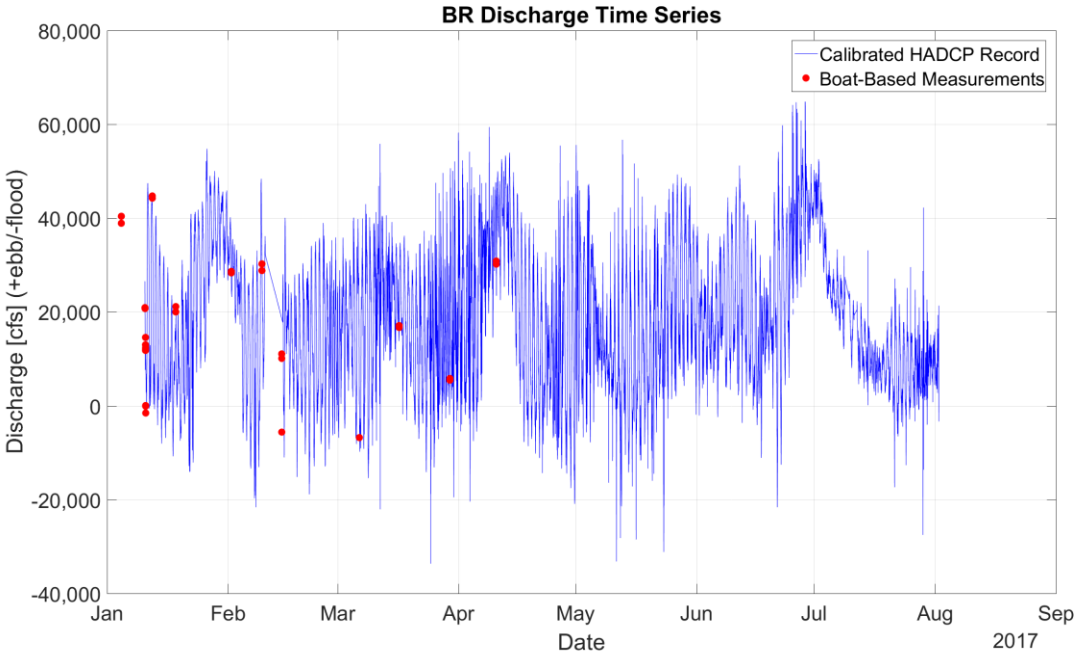

Figure 57. Time series of HADCP-calculated discharge at Blakely River (BR) site.

The time series of water discharge at the BR site (Figure 57) is almost identical to the time series calculated for the AR site, as the two distributaries diverge from the Apalachee River 2 miles upstream. Both records show spring-neap and diurnal tidal cycles, but the discharge at the Blakeley River Site is approximately twice that of the Apalachee River site.

Suspended Sediment Cross-Section Calibration

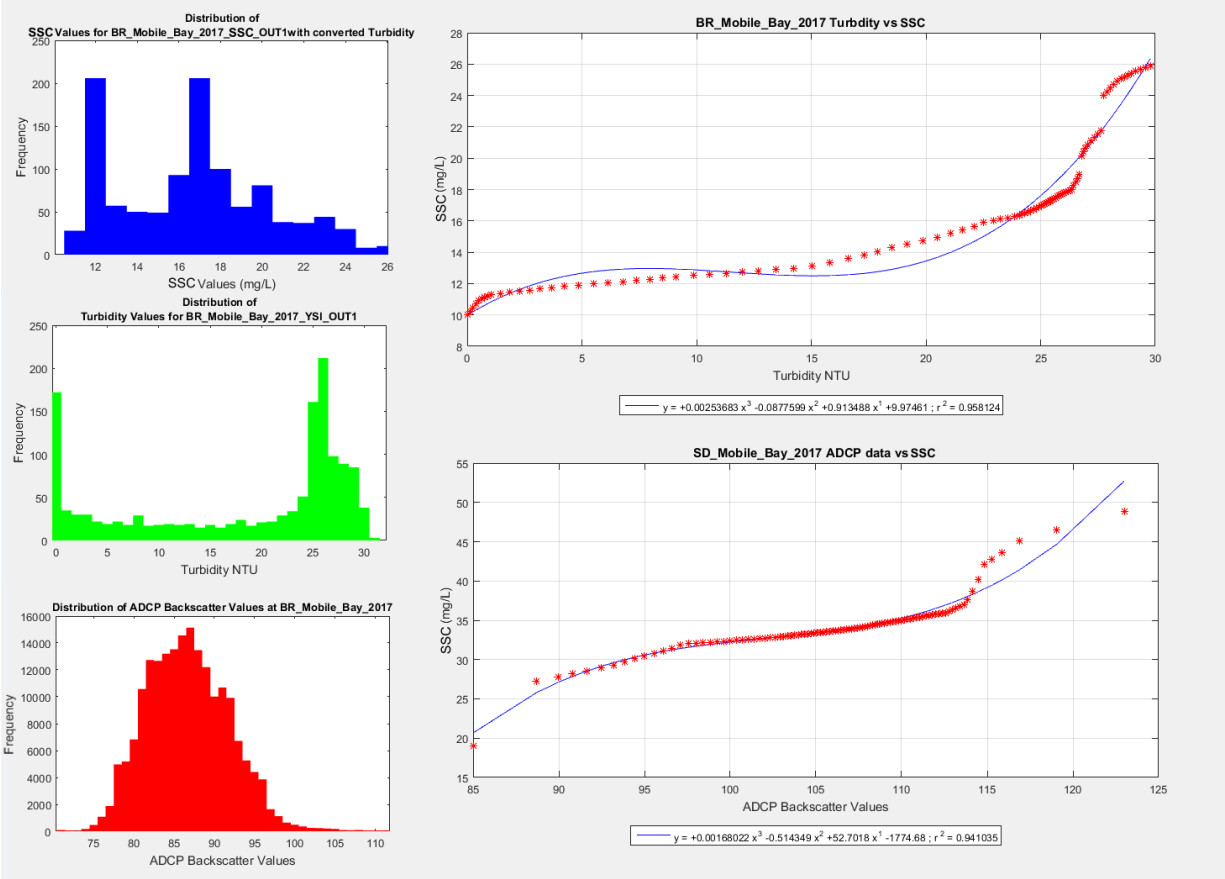

Figure 58. Blakely River (BR) Boat Mounted ADCP vs. SSC Calibration.

Strong correlations were observed between the three boat-based measurements of suspended sediment (Figure 58): suspended sediment concentration (SSC) from the water samples, turbidity from the vertical CTD profiles, and acoustic backscatter from the ADCP cross sections. From these calibrations, snapshots of suspended sediment concentration can be calculated from the ADCP cross-sectional data.

Suspended Sediment Time Series

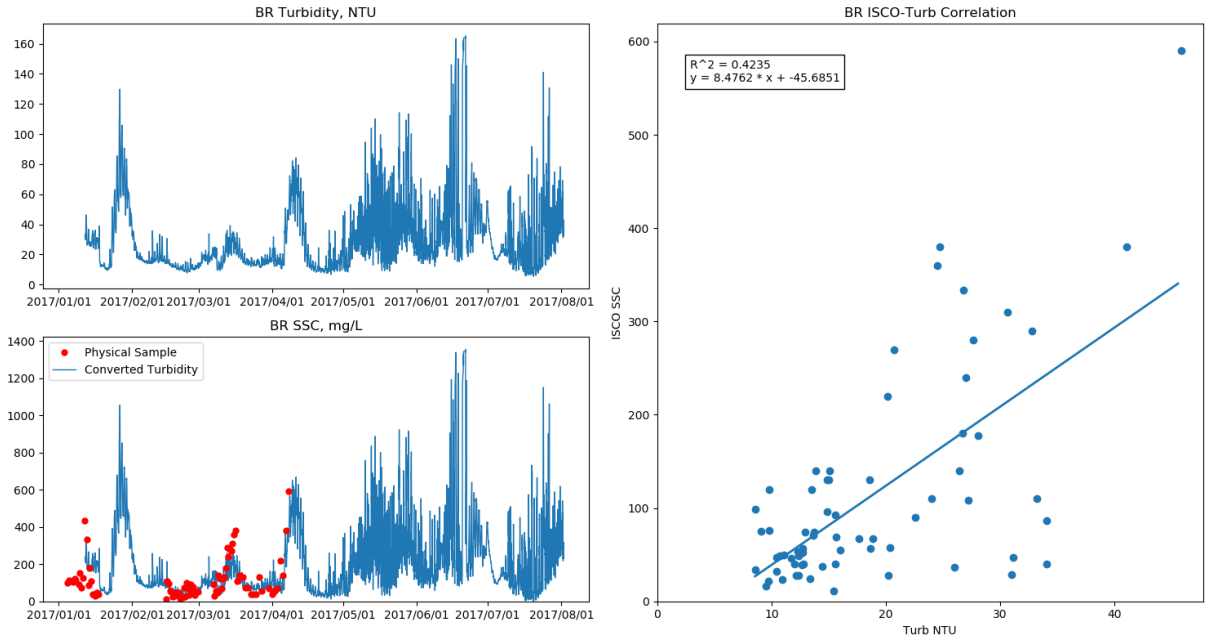

Figure 59. Blakely River (BR) Turbidity vs. ISCO SSC Calibration.

The one-to-one (time based) calibration of turbidity and ISCO suspended sediment concentration at the Blakely River site showed a weak positive correlation ($R^2 = 0.42$). The resulting time series (Figure 59, bottom left) of turbidity predicts the ISCO samples well, with substantially more noise in the signal for the May-August 2017 interval. Site maintenance had ceased during this period, and the high noise level is likely associated with biofouling.

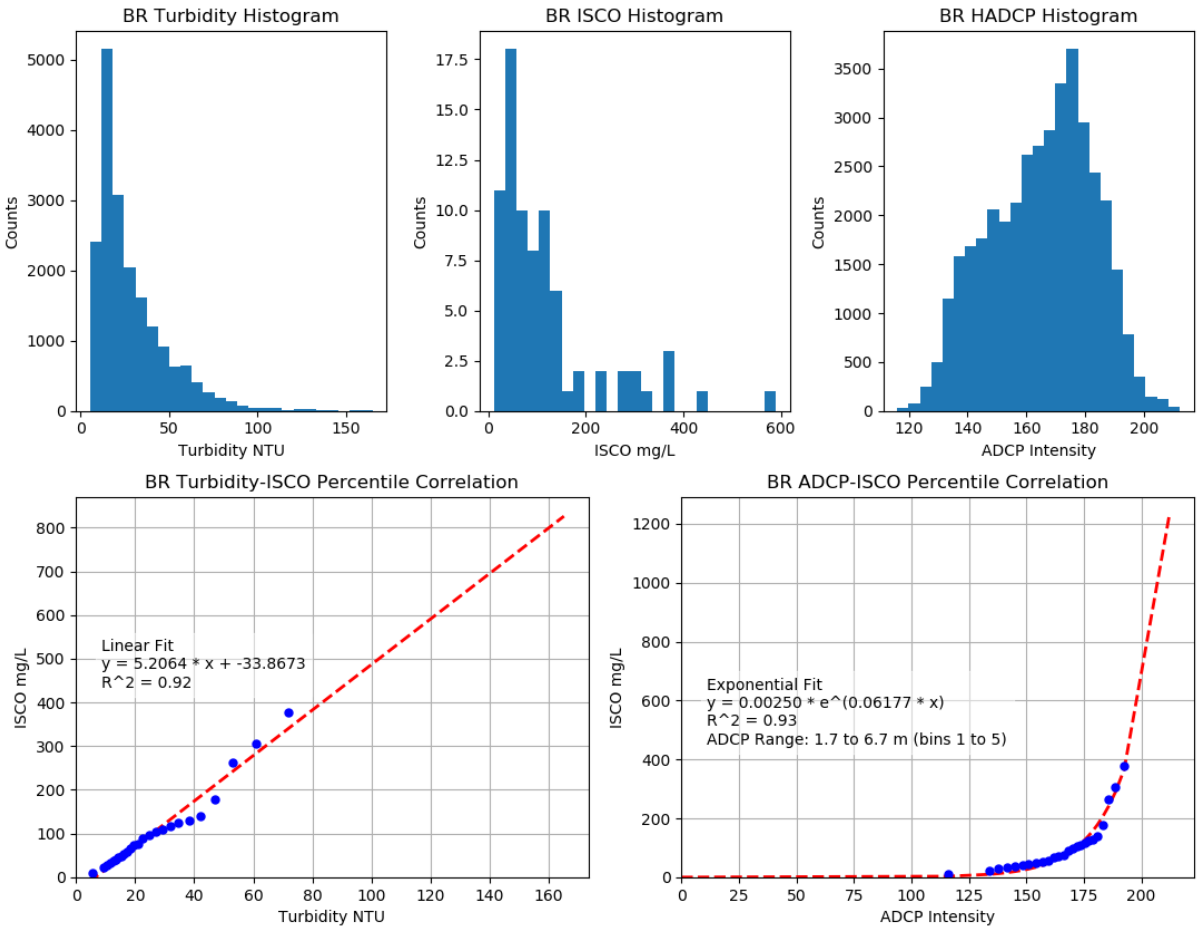

Figure 60. Blakely River (AR) Percentile-Based CTD Turbidity and HADCP vs. ISCO SSC Calibration.

The percentile calibration method resulted in high correlations for the CTD turbidity data (R^2 = 0.92, linear fit) and HADCP backscatter data (R^2 = 0.93, exponential fit). The resulting time series from these calibrations (Figure 61) tracked the ISCO time series well. The HADCP-derived time series exhibited more noise than the turbidity time series during the January-April 2017 interval, while the turbidity time series exhibited more noise during the May-August interval.

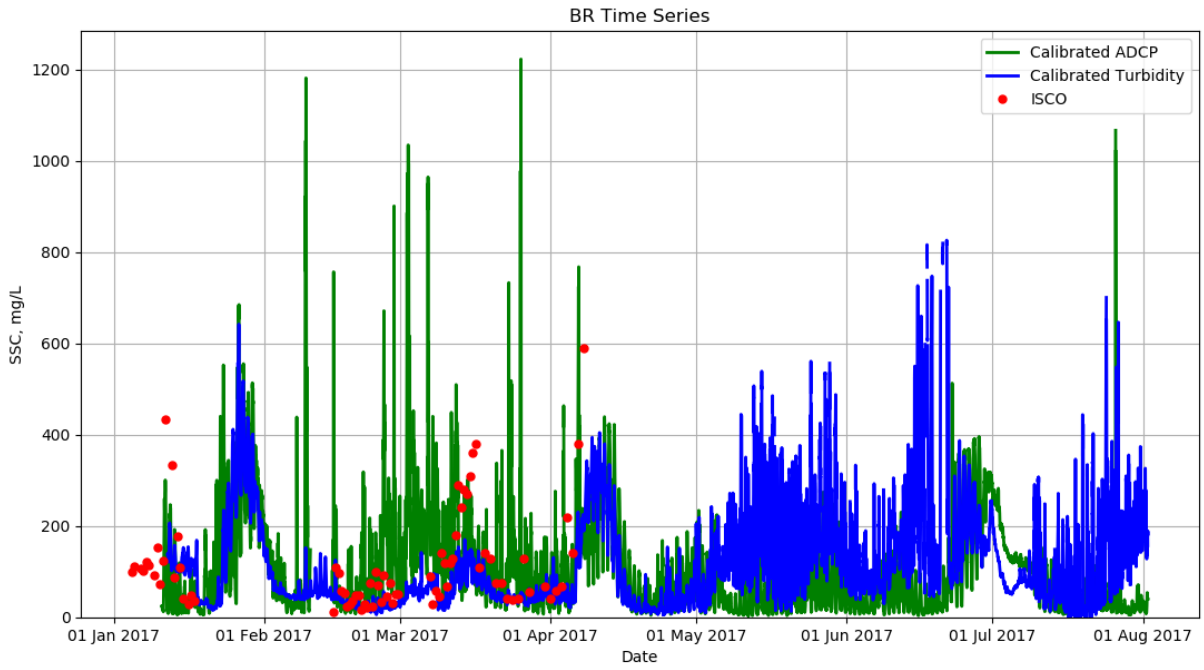

Figure 61. Time series of calibrated CTD turbidity, HADCP backscatter, and ISCO suspended sediment concentration at Blakely River site.

Full Time Series

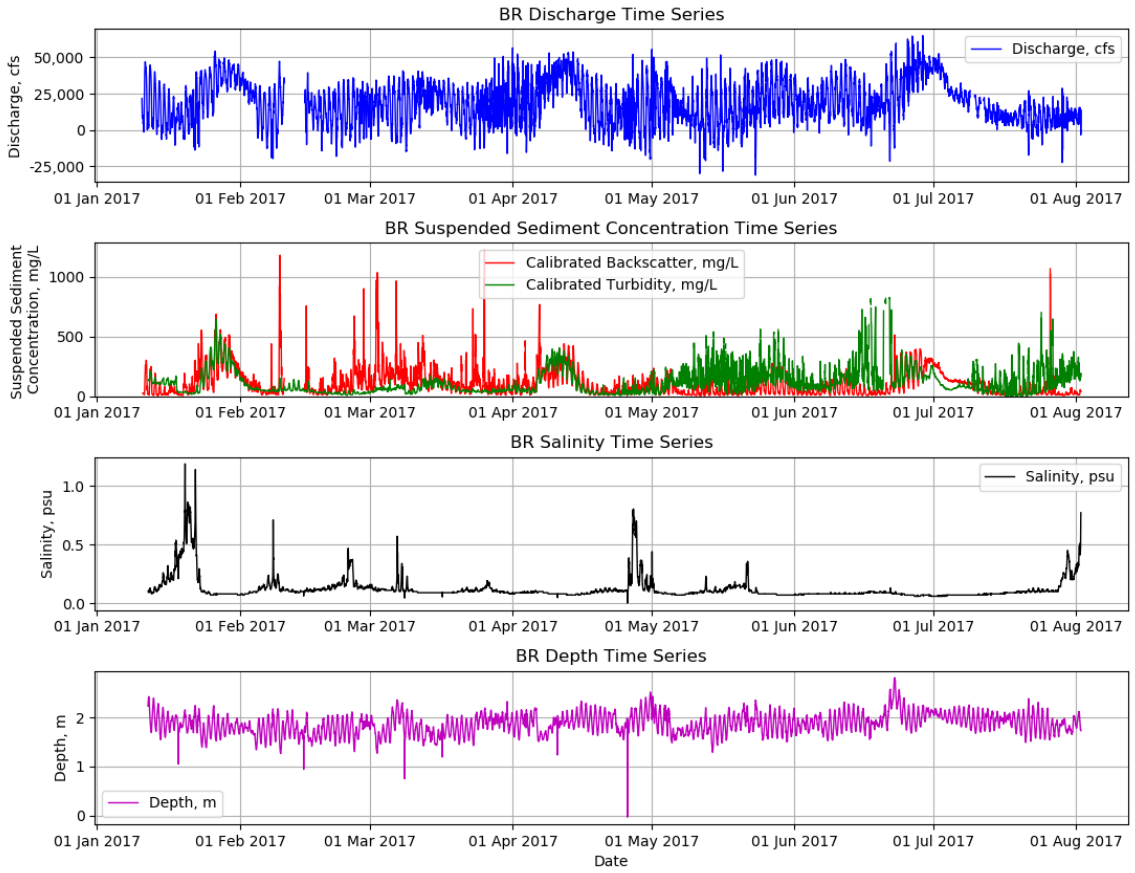

Figure 62. Full Time Series of Discharge, Suspended Sediment Concentration, Salinity, and Water Depth for the Blakely River Site.

The Blakely River site hydrograph (Figure 62) was river-dominated for the majority of the study period, however brief periods between river floods displayed a tidal signal with water discharges dipping below 0, indicating upstream-directed flow. The river floods were associated with peaks in the suspended sediment concentration during the rising limbs of the floods, however the tidally-dominated periods between floods also show some small increases in suspended sediment concentration. The salinity record shows the low tidal influence at this site.

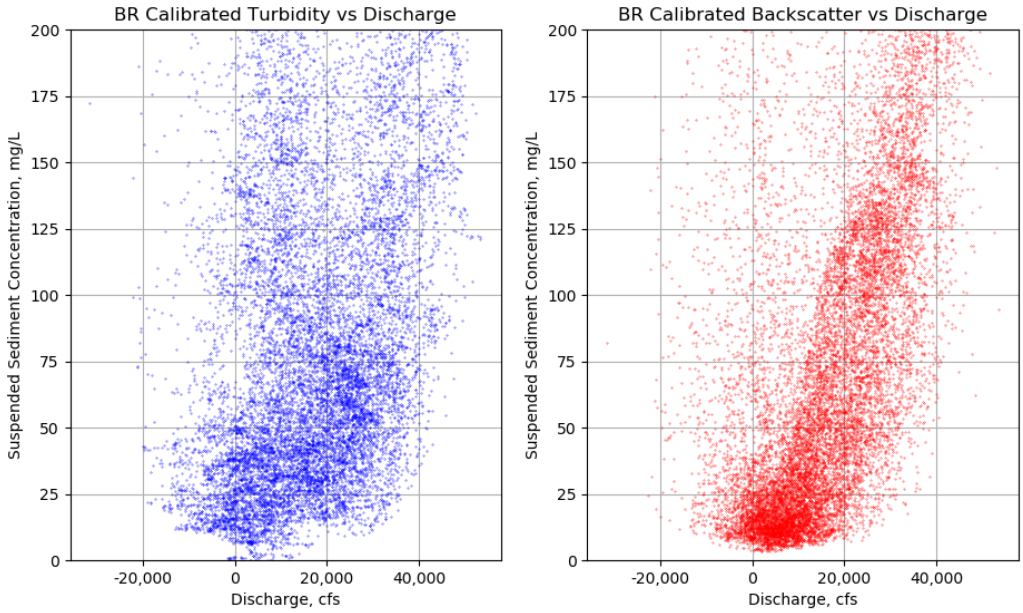

Figure 63. Relationships between water discharge and suspended sediment concentrations calculated from turbidity and ADCP backscatter.

Water discharge and suspended sediment concentration showed a positive correlation (Figure 63) at the Blakely River site. The strong river-dominated signal was evidenced by the dense population of rapidly rising suspended sediment concentrations with increasing water discharge.

State Docks (SD)

Location

Data were collected at State Docks on the Mobile River co-located with the NOAA PORTS gage (mb0301) on the north end of the Alabama State Docks Pier E (SD Site 30.70N, 88.04W; Figure 64) over the period 16 December 2016 through 13 June 2017. This site was outfitted with CTD (conductivity, temperature, and turbidity), HADCP (water velocity), and ISCO (water samples for suspended sediment concentration) instruments. Periodic boat-based ADCP cross-sectional measurements were collected for calibrating the fixed HADCP instrument.

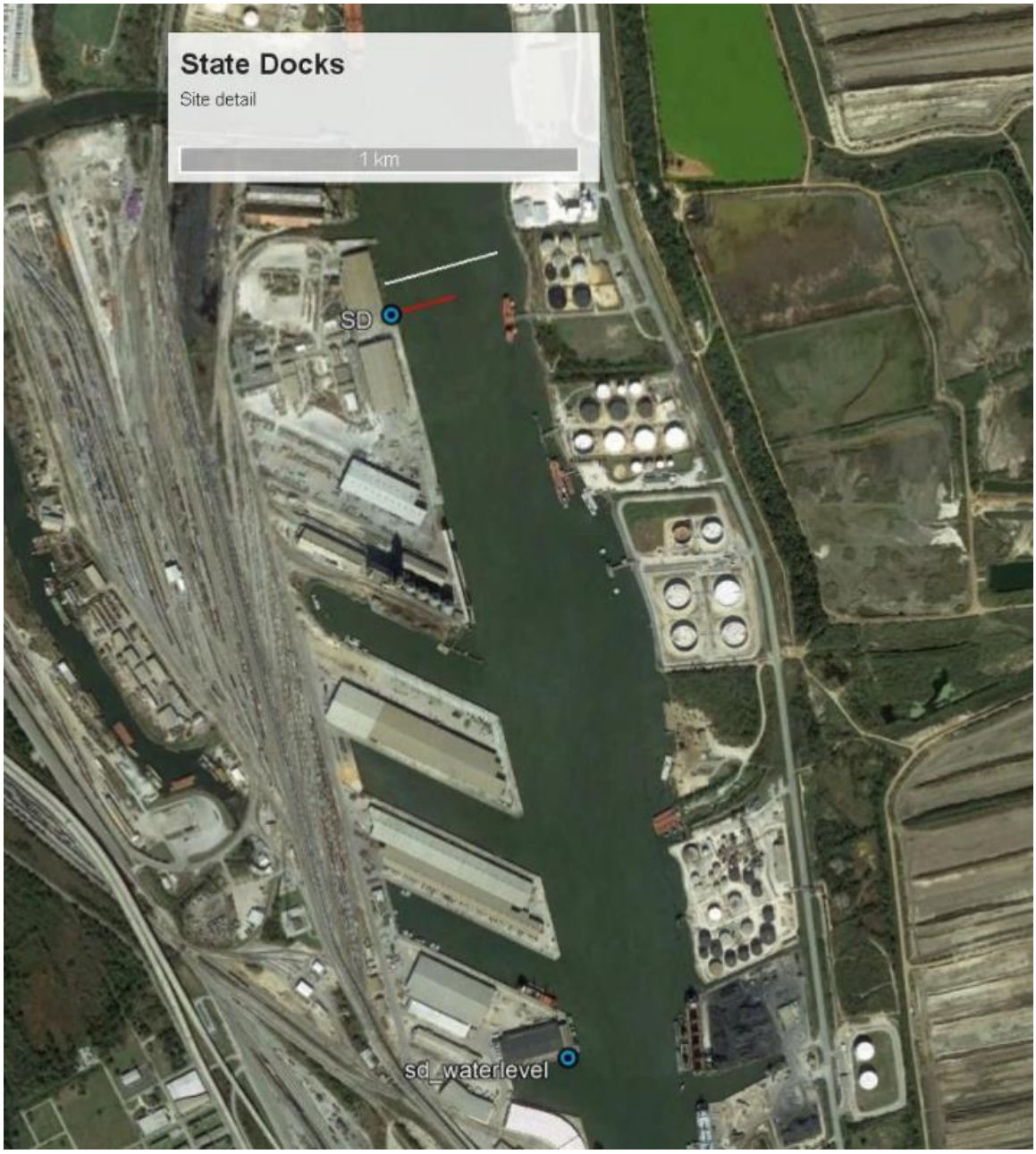

Figure 64. State Docks (SD) site detail. The location of the primary site instrumentation as well as the location of the water-level gage are shown with blue circles, the location of the boat-based ADCP transects is shown with a white line, and the extent of the horizontally averaged HADCP beam is shown in red.

Site Instrumentation and Specifications

The SD site was equipped with a YSI multiparameter sonde for measurement of conductivity, temperature, and turbidity. These quantities were measured at 15 minute intervals throughout the study period. Because the YSI sonde does not have a vented pressure sensor, water level data from the nearby NOAA 8737048 Mobile State Docks, AL gage were used. These data were recorded at 6 minute intervals. The NOAA Ports gage mb0301 is equipped with a NOAA-operated Sontek 250 kHz ADP for measuring water velocities. These data were recorded every 6 minutes with a bin size of 4.5 m. A USACE-operated ISCO 6712 automatic

water sampler was also used at this site to collect a water sample every 14 hours for a total of 24 samples per program period, resulting in a service timeline of 14 days.

Site Timeline

This site was installed 16 December 2016, and serviced on the dates indicated in Table 9. The ISCO water sampler was removed on 25 April 2017 to save money by requiring less frequent servicing of the station. Dates of boat-based ADCP transects and sediment profiles are also indicated in Table 9.

Table 9. Servicing dates and notes from the SD site

Service Date	Service notes	Boat-based Measurements
21 December 2016	Started ISCO program	
4 January 2017	Retrieved ISCO samples, restarted ISCO program, cleaned YSI and ISCO intake	
12 January 2017		ADCP transects (RDI Workhorse 1200 kHz), sediment profile
18 January 2017	Retrieved ISCO samples, restarted ISCO program, cleaned YSI and ISCO intake	ADCP transects (Sontek RiverSurveyor M9)
1 February 2017	Retrieved ISCO samples, restarted ISCO program, cleaned YSI and ISCO intake	ADCP transects (Sontek RiverSurveyor M9)
14 February 2017	Retrieved ISCO samples, restarted ISCO program, cleaned YSI and ISCO intake	ADCP transects (Sontek RiverSurveyor M9)
27 February 2017	Retrieved ISCO samples, restarted ISCO program, cleaned YSI and ISCO intake	ADCP transects (Sontek RiverSurveyor M9)
17 February 2017	Retrieved ISCO samples, restarted ISCO program, cleaned YSI and ISCO intake	ADCP transects (Sontek RiverSurveyor M9)
29 February 2017	Retrieved ISCO samples, restarted ISCO program, cleaned YSI and ISCO intake	ADCP transects (Sontek RiverSurveyor M9)
10 April 2017	Retrieved ISCO samples, restarted ISCO program, cleaned YSI and ISCO intake	ADCP transects (Sontek RiverSurveyor M9)
25 April 2017	Retrieved ISCO samples, removed ISCO from platform, cleaned YSI	ADCP transects (Sontek RiverSurveyor M9)

Discharge Time Series

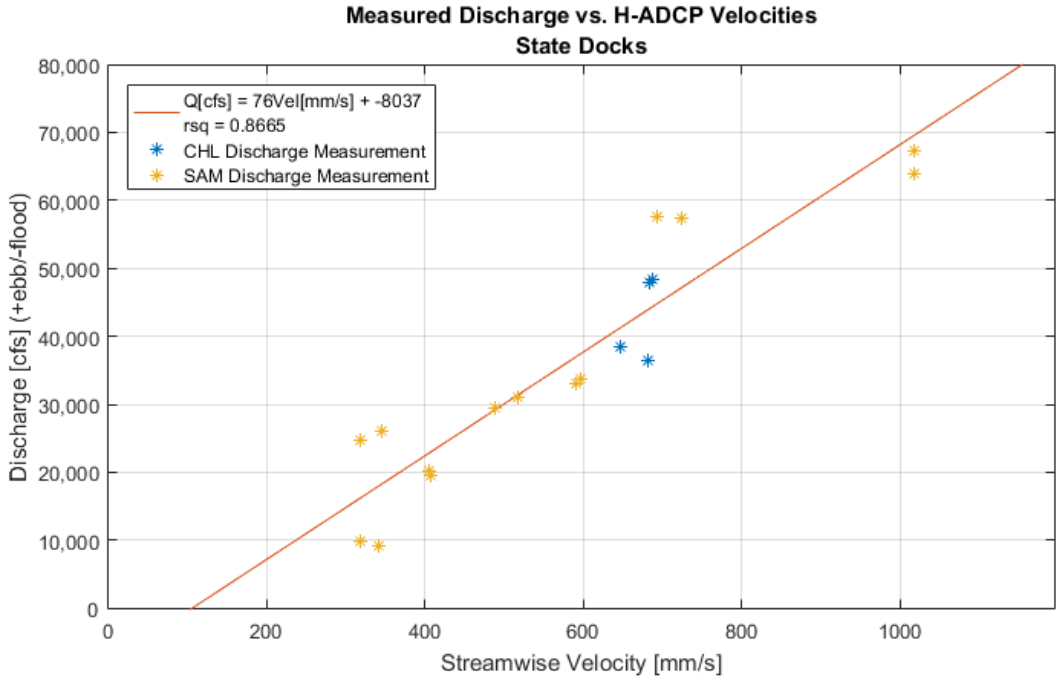

Figure 65. State Docks (SD Measured Discharge vs. H-ADCP Velocities

The average streamwise water velocities measured by the stationary HADCP correlated well ($R^2 = 0.87$) with the periodic discharge measurements collected with boat-based ADCP (Figure 65). Calibration of these cross-sectional ADCP measurements to the observed horizontal water velocities allows the calculation of a continuous synthetic discharge time series.

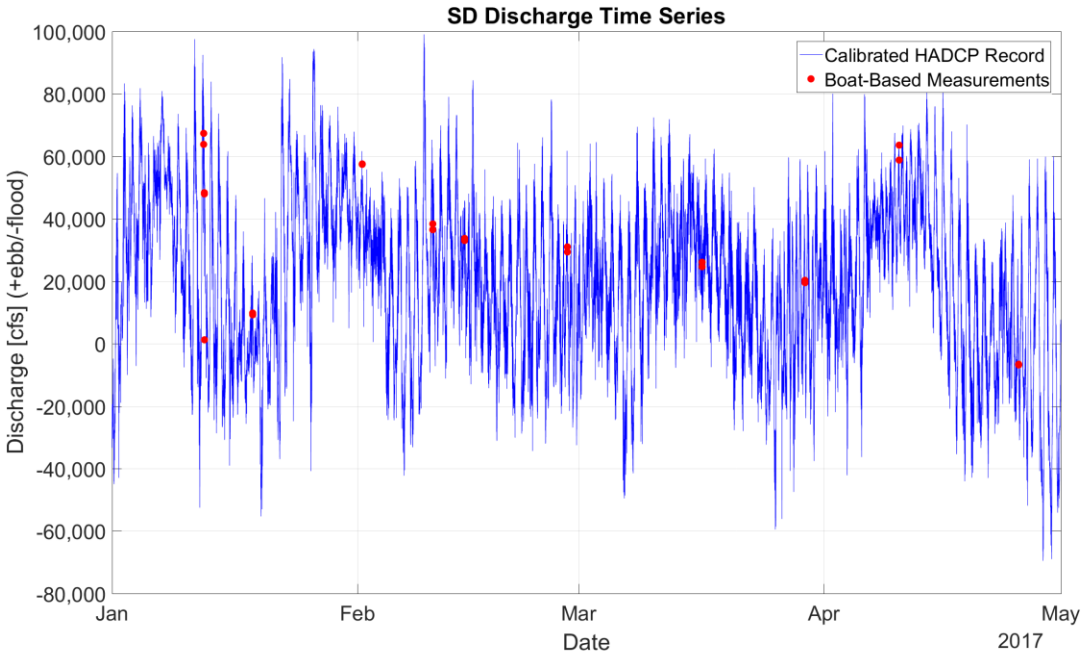

Figure 66. Time series of HADCP-calculated discharge at State Docks (SD) site.

The time series of water discharge at the SD site (Figure 66) shows a strong signal of the discharge of the Mobile River with the overprint of spring-neap and diurnal tidal cycles. At least 4 spring floods can be observed from this record, in January, February, March and April.

Suspended Sediment Cross-Section Calibration

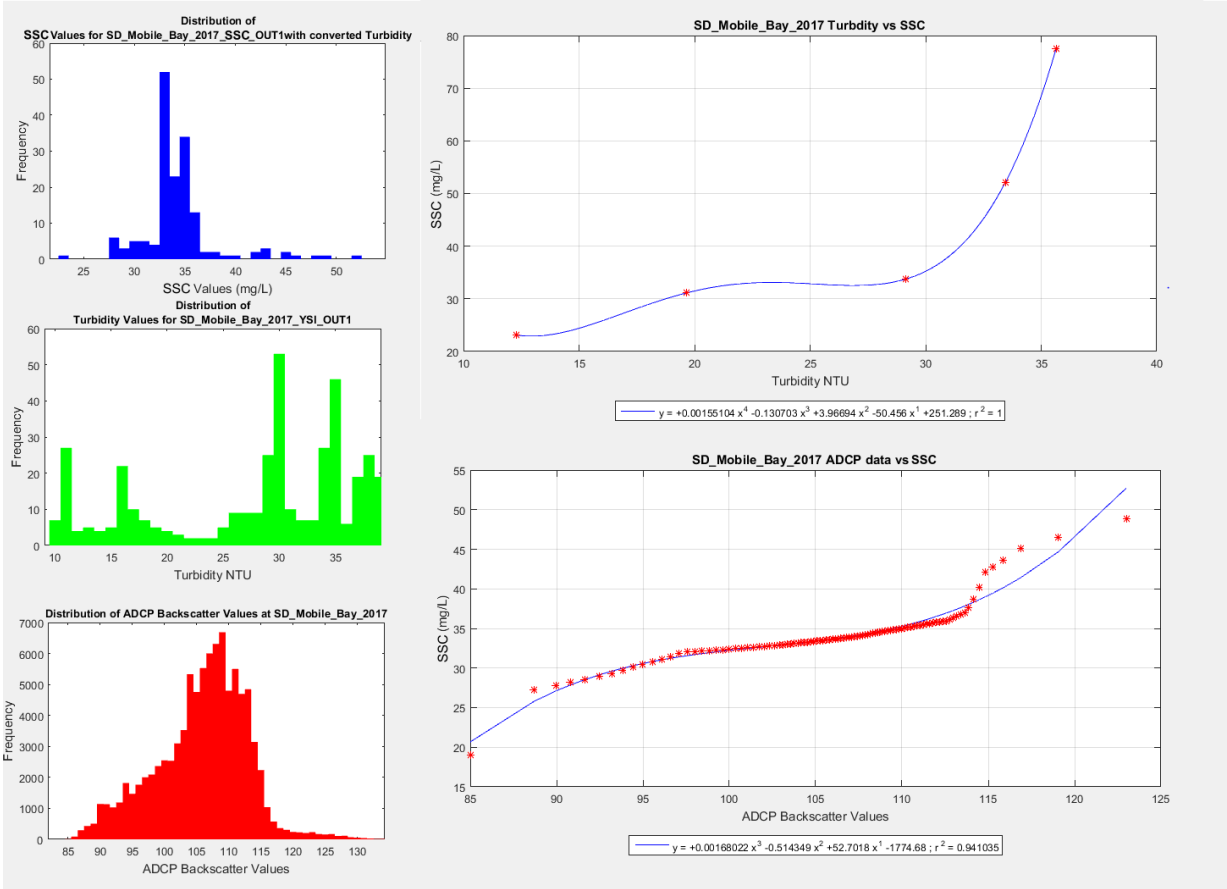

Figure 67. State Docks (SD) Boat Mounted ADCP vs. SSC Calibration.

Strong correlations were observed between the three boat-based measurements of suspended sediment (Figure 67): suspended sediment concentration (SSC) from the water samples, turbidity from the vertical CTD profiles, and acoustic backscatter from the ADCP cross sections. From these calibrations, snapshots of suspended sediment concentration can be calculated from the ADCP cross-sectional data.

Suspended Sediment Time Series

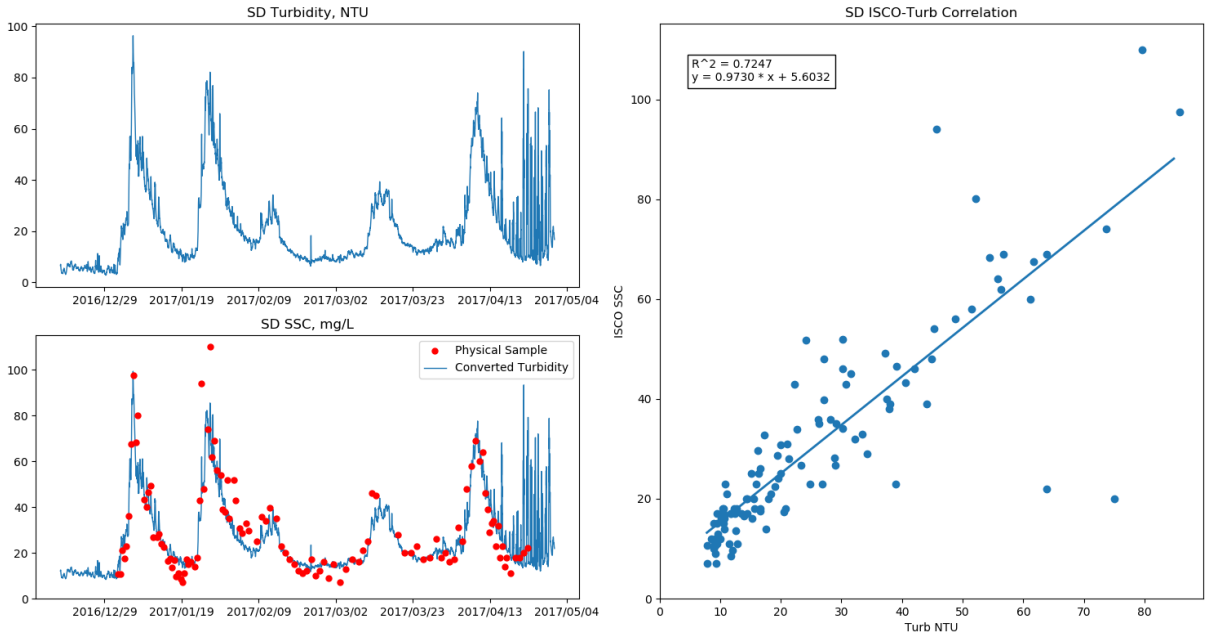

Figure 68. State Docks (SD) Turbidity vs. ISCO SSC Calibration.

The one-to-one (time based) calibration of turbidity and ISCO suspended sediment concentration at the State Docks showed a high positive correlation ($R^2 = 0.72$). The resulting time series (Figure 68, bottom left) turbidity record was very well-matched to the ISCO samples for the interval January-April 2017.

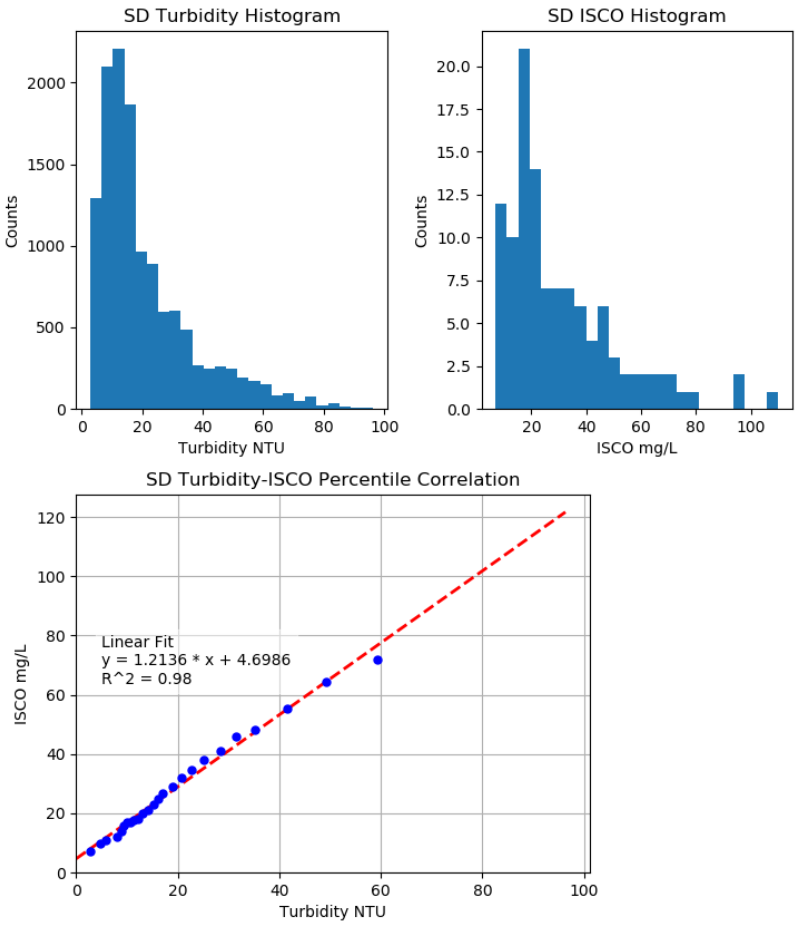

Figure 69. State Docks (SD) Percentile-Based CTD Turbidity vs. ISCO SSC Calibration.

The percentile calibration method resulted in strong positive correlation for the CTD turbidity data (R^2 = 0.97, linear fit). No HADCP backscatter data was available for this site, so only the CTD turbidity calibration could be performed. The resulting time series from these calibrations (Figure 70) tracked the ISCO time series well.

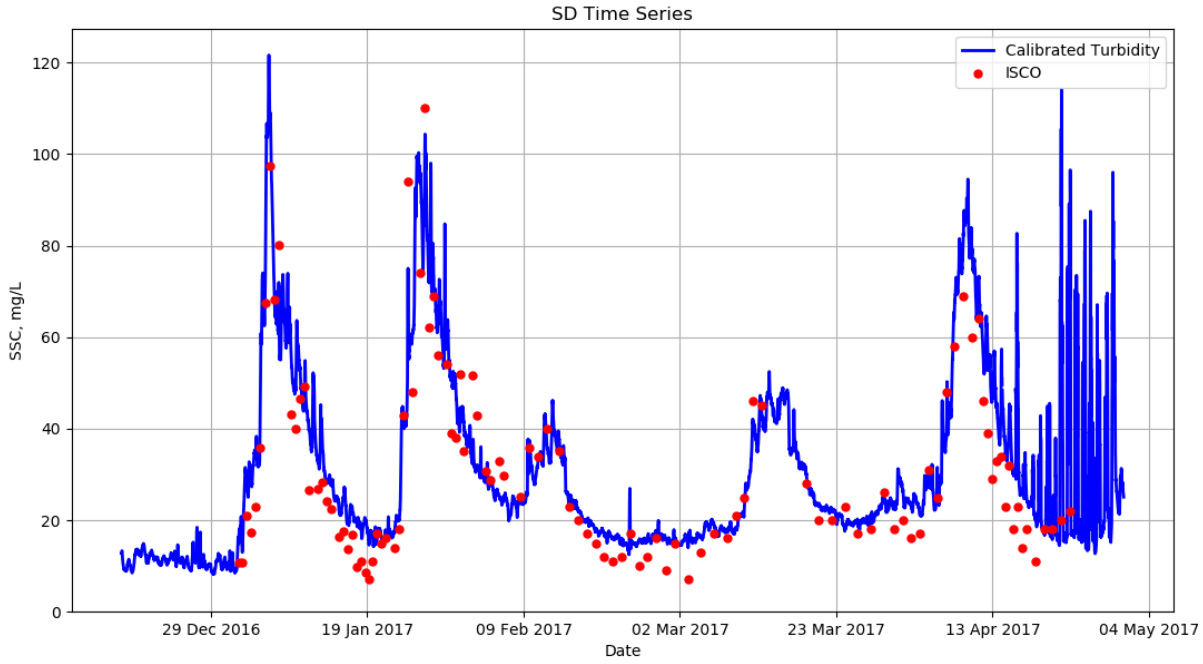

Figure 70. Time series of calibrated CTD turbidity and ISCO suspended sediment concentration at State Docks site.

Full Time Series

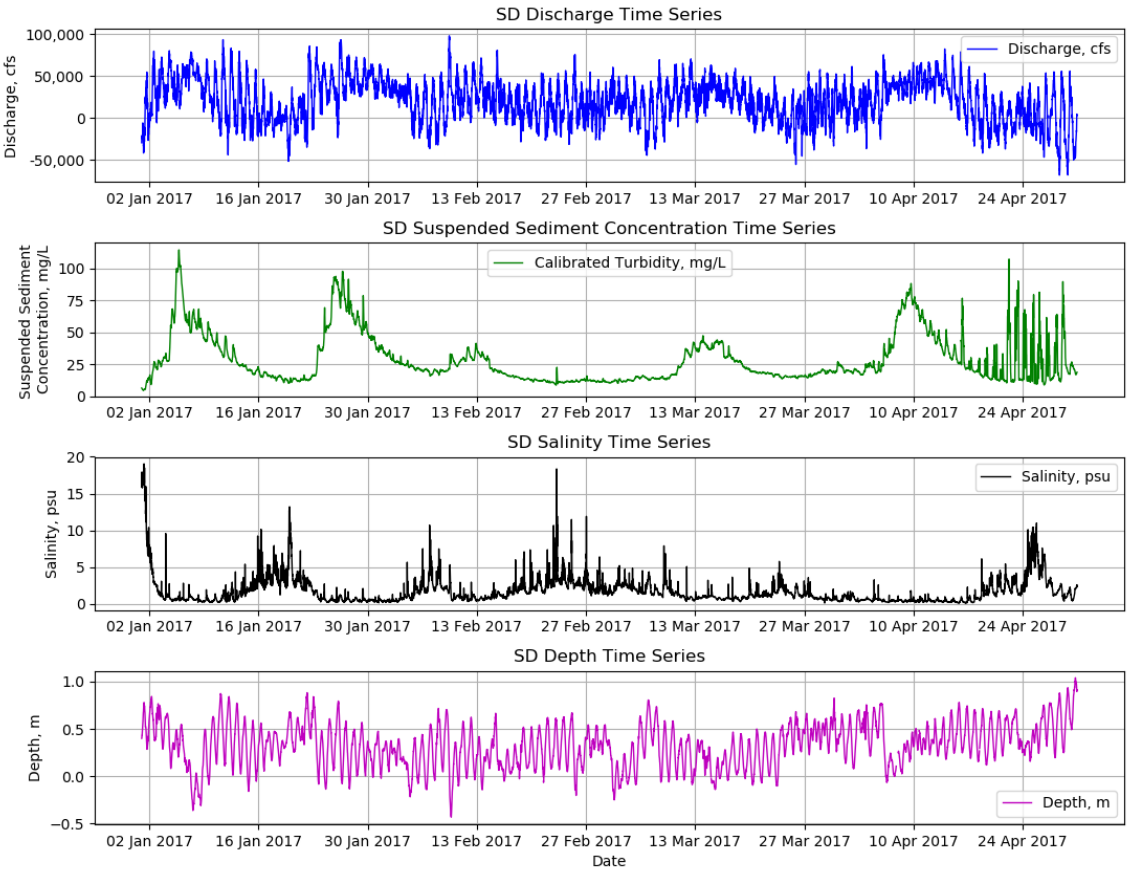

Figure 71. Full Time Series of Discharge, Suspended Sediment Concentration, Salinity, and Water Depth for the State Docks Site.

The full time series of water discharge and suspended sediment concentration (HADCP backscatter data was not available for this site) displayed a strong river-dominant signal, with daily modulation by diurnal tides (Figure 71). Five river floods could be clearly observed in the data: two in January, one in February, one in March and one in April. Each of these floods was accompanied by a corresponding peak in suspended sediment concentrations, preceding the flood discharge peak by several days. The salinity record shows a moderate tidal influence, despite the relatively high discharges at this site compared to the others.

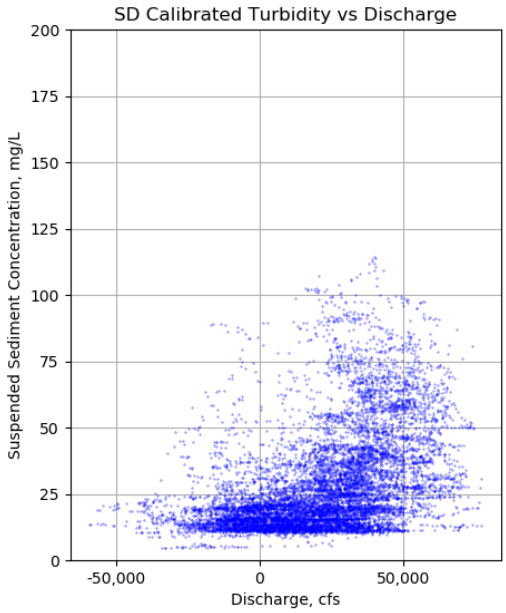

Figure 72. Relationship between water discharge and suspended sediment concentrations calculated from turbidity.

A positive correlation was observed between the calculated suspended sediment concentrations and the water discharge at the State Docks, with very few high sediment concentrations measured for low (or negative) water discharges. These results were indicative of a river-dominant sediment transport regime at this site.

Middle Bay (MB)

Middle Bay was the location of an Aquadopp Wave and Current (AWAC) instrument deployed from 12 May 2016 through 18 July 2016 (MB site 30.62N, 87.99W; Figure 73). The instrument was retrieved on 7 June 2016 for data download and battery replacement and redeployed at the same location.

Figure 73. AWAC Sites Detail. The location of the AWAC deployments at Middle Bay (MB), Fairhope Yacht Club (FYC), and Range Marker (RM) are shown with blue circles.

This instrument was configured for continuous measurement of water currents at 60 second intervals, and burst measurement of waves at 2 Hz for 1024 seconds every hour. Bin size for the current measurements was 0.25 m, and bin size for the wave measurements was 0.5 m.

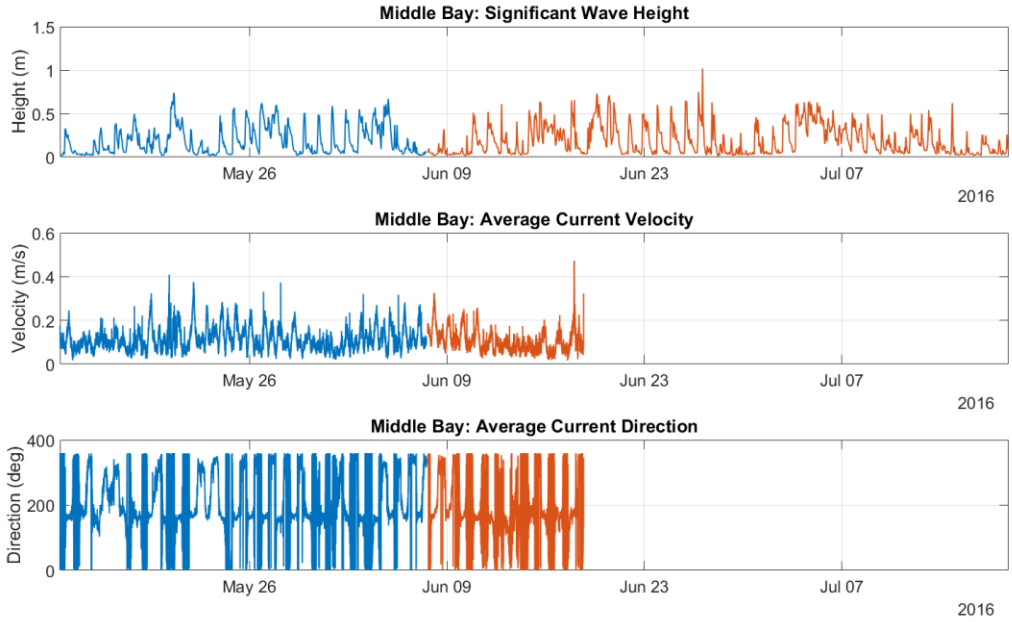

Figure 74. Wave and current time series from AWAC sensor deployed at Middle Bay site. Each color is a separate deployment period.

The wave record at the Middle Bay site shows a largely diurnal signal, with the largest waves occurring in the daytime. Significant wave height is defined as the average height of the highest 1/3 of the wave population, which at this site rarely exceeded 0.5 m. The wave direction, while initially appearing very noisy, is showing a bimodal distribution indicative of waves generated by a daily sea breeze process. The waves during the day are generally from the south (the periods hovering just below 200 degrees), while the nighttime waves are directed from the north (these periods show fluctuations above and below 360 and 0 degrees). It is not clear why the current statistics were not recorded beyond June 18.

Fairhope Yacht Club (FYC)

After two deployments, the AWAC was moved to a location southeast toward the Fairhope Yacht Club (FYC site; 30.56N, 87.95W; Figure 73). The instrument was deployed at this location from 1 July 2016 through 28 July 2016.

This instrument was configured for continuous measurement of water currents at 60 second intervals, and burst measurement of waves at 2 Hz for 1024 seconds every hour. Bin size for the current measurements was 0.25 m, and bin size for the wave measurements was 0.5 m.

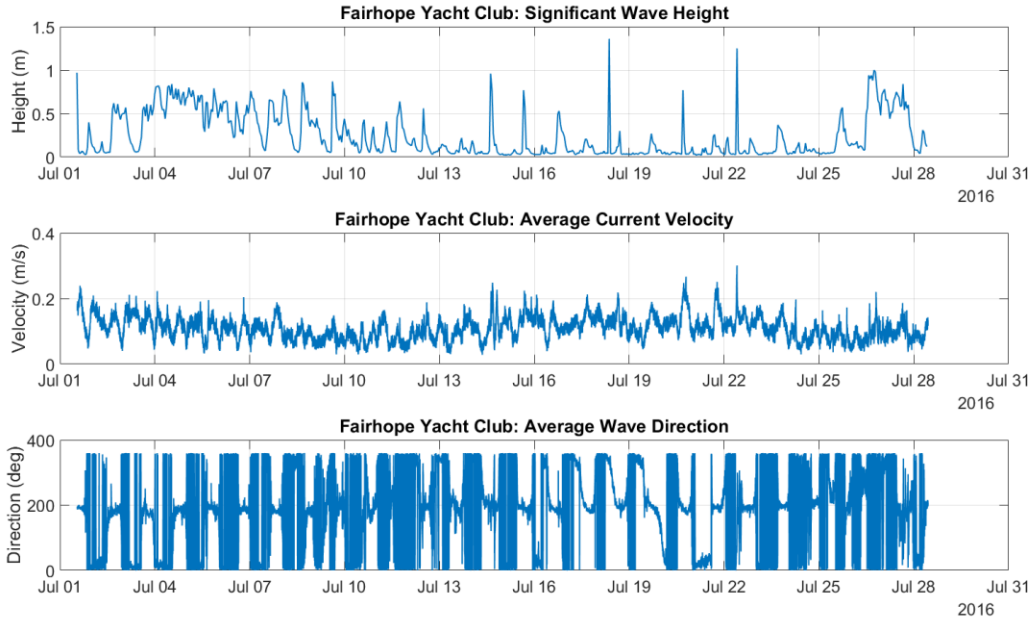

Figure 75. Wave and current time series from AWAC sensor deployed at Fairhope Yacht Club site.

The wave record at Fairhope Yacht Club shows a similar diurnal cycle as at the Middle Bay site, however there appears to be more weekly variability at this site. The first two weeks exhibited several days with significant wave heights greater than 0.5 m, while the second two weeks at this location showed smaller waves. This site showed the diurnal sea-breeze dependence of current direction.

Range Marker (RM)

In July 2016 the AWAC station was moved to the Range Marker near the entrance to the Mobile River (RM site; 30.64N, 88.03W; Figure 73), where it remained for the duration of the study period. The instrument was deployed here five times:

- 29 July 2016 – 12 September 2016
- 22 September 2016 – 3 October 2016
- 11 December 2016 – 26 January 2017
- 10 January 2017 – 23 February 2017
- 23 March 2017 – 1 August 2017

For the first five deployments, the water currents were measured at 1 minute intervals, while the sixth deployment here used a current measurement interval of 5 minutes (this interval was increased to save battery power in order to extend the deployment period). Wave measurements were made at 1 hour burst intervals throughout the study period with a sample rate of 2 Hz and burst length of 1024 seconds.

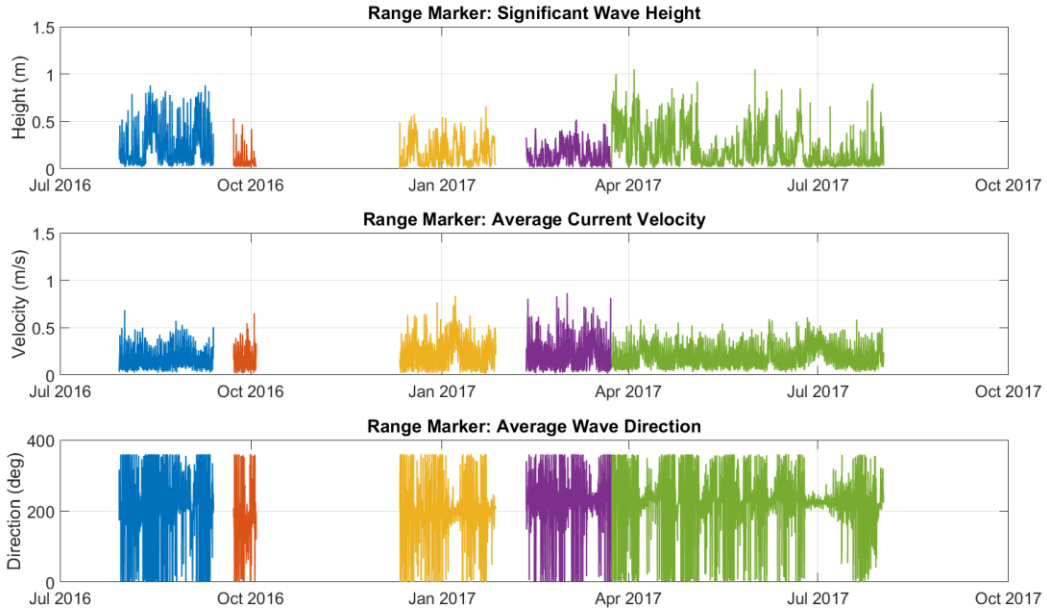

Figure 76. Wave and current time series from AWAC sensor deployed at Range Marker site.

The wave record at the Range Marker site, being the longest record, showed the greatest variability in wave and current conditions. In general, the waves were largest during the Summer 2016 and 2017 deployments, with few periods in the September 2016, December 2016, and January 2016 deployments exceeding 0.5 m significant wave heights. Throughout the record, the wave direction shows the same diurnal dependence on sea breeze direction as the other sites.

Conclusions

The long-term remote instrumentation and periodic boat-based survey efforts of this study were used to derive continuous, calibrated time series of water discharge and suspended sediment concentrations at each of the monitoring stations in the complex system of rivers which discharge into northern Mobile Bay. The stations at North Mobile River and Tensaw River collected over one full year of data, while the stations as South Mobile River, Shipwave, Tensaw River at Causeway, Apalachee River, Blakely River, and State Docks each provided 6-8 months of data.

Several of the instrument records were plagued by noise due to biofouling in this active estuarine ecosystem, however the overlapping datasets provided by the CTD and HADCP at each site were able to provide near-continuous datasets in most cases. Data processing methodologies were to calibrate the CTD turbidity and HADCP backscatter data to discrete sediment samples collected at each site to calculate time series of suspended sediment concentrations, while HADCP water velocities were calibrated to boat-based measurements of river cross-sectional discharge to calculate a time series of water discharge.

As is typical of an estuarine system, most of the sites exhibited a mixture of hydrographic and sediment influences from both upstream river forcing and downstream tidal forcing. In

particular, the North Mobile River, Tensaw River, and State Docks sites exhibited primarily riverine hydrographs with overprinted tidal variability. These sites generally showed positive correlations between water discharge and suspended sediment concentration, higher water discharges on average, and a strong signal of river floods during the spring hydrograph.

The Apalachee River, Blakely River, and Tensaw River at Causeway, all being situated at river mouths displayed a mixture of river and tidal influence. Each site had a strong tidal signal which was observed to reverse flow direction almost daily throughout the study period, but these sites still showed high discharge unidirectional flow during significant flooding events. The Blakely River site had a stronger river signal in its hydrograph despite being in close proximity to the Apalachee River site, as the Blakely River distributary captures the majority of the flow from its partner Apalachee River distributary. These sites exhibited bimodal relationships between sediment concentrations and water discharge, indicating that both river flow and diurnal tidal flows were responsible for sediment transport in these locations at the interface between river and bay.

The South Mobile River site showed a strong dependence on tidal flow for sediment transport, with suspended sediment concentrations peaking primarily during flood tides, however this site was only operational during the low-river-flow Summer-Autumn of 2016, when river influence was expected to be the least. The Shipwave site had the most problems with biofouling resulting in invalid data, but this site—being in the open water of Mobile Bay—could be expected to exhibit the greatest tidal influence.

In the time domain, all of the sites showed some degree of lag between the highest flood-related sediment concentrations and the peak river flow associated with the flood. This is a common feature of fluvial sediment transport, particularly in rivers with smaller watersheds, and is indicative of upstream controls on sediment supply: available sediment within the river basin is quickly washed into the during the onset of flood conditions, and is largely exhausted before the peak of river flood discharge (Williams, 1989).

References

Goring, D. G., and V. I. Nikora (2002). Despiking acoustic Doppler velocimeter data, *Journal of Hydraulic Engineering* 128. doi :10.1061/(ASCE)0733-9429(2002)128:1(117)

Wahl, T. L. (2003). Discussion of "Despiking acoustic Doppler velocimeter data" by Derek G. Goring and Vladimir I. Nikora, *Journal of Hydraulic Engineering* 128, doi: 10.1061/(ASCE)0733-9429(2003)129:6(484)

Williams, G. P. (1989). Sediment concentration versus water discharge during single hydrologic events in rivers, *Journal of Hydrology* 111, doi: 10.1016/0022-1694(89)90254-0